

Final Report - Ike Dike Concept for Reducing Hurricane Storm Surge in the Houston-Galveston Region

Bruce A. Ebersole, Thomas C. Massey, Jeffrey A. Melby,
Norberto C. Nadal-Caraballo, Donald L. Hendon, Thomas W.
Richardson, Robert W. Whalin

April 2018

Contents

1	Overview	6
2	Storm Surge Model Validation for Hurricane Ike.....	11
	Introduction	11
	Computed Maximum Water Surface Elevations for Hurricane Ike.....	13
	Comparison with High Water Marks	14
	<i>High Water Marks from Gage Measurements of Water Surface Elevation</i>	15
	<i>Visually Estimated High Water Marks</i>	19
3	Texas Coast Historic Hurricanes	24
	Intensity of Historic Hurricanes.....	24
	The September 1900 Galveston Hurricane	25
	Hurricane Carla	31
	Hurricane Ike.....	34
4	The “Bracketing” Set of Hypothetical Synthetic Storms	35
5	Hurricane Surge Generation on the Open Coast – Causative Factors.....	41
	What Causes a Storm Surge?.....	41
	<i>Wind</i>	41
	<i>Atmospheric Pressure</i>	42
	<i>Waves</i>	42
	Storm Surge along the Texas Coast	44
	<i>Surge Forerunner</i>	44
	<i>Surge Generation by the Core Winds</i>	54
6	Hurricane Surge Generation within Galveston Bay – Causative Factors.....	58
	Introduction	58
	Existing Conditions	59
	Surge Generation in Galveston Bay - With the Ike-Dike Concept.....	68
7	Influence of Storm Track on Surge Development.....	79
	Introduction	79
	Forerunner Surge Development as a Function of Storm Track	80
	Development of Surge within the Bays Due to Forerunner Propagation and Winds	92
	Galveston Bay Storm Surge Response to the Hurricane’s Core Winds.....	106
8	Reduction in Flooding Achieved with the Ike Dike – Initial Assessment.....	123
	Introduction	123
	The Long Dike or Levee Effect.....	124
	Hurricanes of Varying Intensity - The Direct-Hit Set.....	125
	Major Hurricanes Approaching from the South.....	134
	Major Hurricanes Approaching from the South-Southeast	143

Major Hurricanes Approaching from the Southeast	154
9 Placing Hurricane-Induced Water Levels in a Probabilistic Context.....	161
Introduction	161
Approach for Statistical Analysis of Water Surface Elevation	162
<i>Joint Probability Analysis</i>	163
<i>Joint Probability Method</i>	163
<i>Joint Probability Method with Optimal Sampling</i>	166
<i>JPM-OS-BQ Implementation for the Present Study</i>	167
<i>Probability Distributions of Tropical Storm Parameters</i>	176
<i>Estimation of Errors and Other Secondary Terms</i>	177
<i>Summary of Differences in JPM-OS Studies for the Houston-Galveston Region</i>	181
Existing Condition Water Surface Elevation Statistics	182
Probabilistic Context for Hurricane Ike's Maximum Water Surface Elevations	190
The Proxy Storm Concept.....	191
Identification and Selection of Proxy Storms	193
10-yr Proxy Storm.....	196
100-yr Proxy Storm.....	198
500-yr Proxy Storm.....	200
10 Storm Surge Simulations with an Extended Ike Dike	203
Introduction	203
Effect of the Extended Ike Dike for Hurricane Ike	205
<i>Effect of the Extended Ike Dike for the 10-yr Proxy Storm</i>	209
<i>Effect of the Extended Ike Dike for the 100-yr Proxy Storm</i>	212
<i>Effect of the Extended Ike Dike for the 500-yr Proxy Storm</i>	216
11 Influence of Sea Level on Storm Surge	221
Recent Historic Changes in Sea Level for the Region.....	221
Effects of Sea Level Rise on Storm Surge and Wave Processes	224
Past Relevant Work by ARCADIS (2011).....	227
Storm Surge for Present and Future Sea Level Scenarios	228
<i>Hurricane Ike Peak Surge for Present and Future Sea Levels</i>	231
<i>Storm 535 (10-yr Proxy Storm) Peak Surge for Present and Future Sea Levels</i>	239
<i>Storm 033 (100-yr Proxy Storm) Peak Surge for Present and Future Sea Levels</i>	247
<i>Storm 036 (500-yr Proxy Storm): With and Without Sea Level Rise</i>	255
12 Exposure to Inundation, Residual Flood Risk, and Implications for Secondary Lines of Defense	265
Introduction	265
Galveston Island.....	269
<i>City of Galveston</i>	269
<i>Galveston Island (central portion)</i>	275
<i>Galveston Island (western end)</i>	278
Bolivar Peninsula	281
<i>Bolivar Peninsula (western end)</i>	281

<i>Bolivar Peninsula (central portion)</i>	284
<i>Bolivar Peninsula (eastern end)</i>	286
Galveston Bay	288
<i>Texas City (south)/La Marque/Bayou Vista</i>	288
<i>San Leon/Texas City (north)/Bacliff/Dickinson</i>	295
<i>Clear Lake/Bayport/La Porte</i>	301
Houston Ship Channel.....	306
<i>Upper Houston Ship Channel (eastern portion)</i>	306
<i>Upper Houston Ship Channel (western portion)</i>	310
13 Examination of Alternate Ike Dike Configurations	314
Introduction	314
Alignment 1a – A Modification of the Extended Ike Dike	315
Alternate Alignment 1b – Alignment 1a with Lowered Gate Elevations	317
Alternate Alignment 2.....	319
Alternate Alignment 3.....	320
Storm Surge Simulations Made for the Alternate Dike Alignments.....	322
<i>Peak Surge Maps for Each Dike Alignment/Storm Simulation</i>	322
<i>Extraction of Peak Storm Surge Values for Analysis</i>	331
Comparison of Two Different Alignments for an Eastern Termination Section.....	332
Surge Reduction in the Houston-Galveston Region with and without an Eastern Termination Section	337
<i>Analysis of Peak Surge Elevations</i>	337
<i>Analysis of Water Surface Elevation Time Series</i>	339
Storm Surge Reduction Benefits of a Western Termination Section	347
<i>Analysis of Temporal Changes in Water Surface Elevation and Velocity</i>	350
Influence of Lowered Gate Elevations on Interior Surge Levels.....	356
14 Water Level Considerations for Operating the Ike Dike Storm Surge Gates	358
Introduction	358
Processes that Influence Antecedent Water Levels.....	359
<i>Mean Sea Level</i>	360
<i>Astronomical Tide</i>	362
<i>Wind-Driven Surge Forerunner</i>	365
<i>Volume Mode Forerunner</i>	367
Wind-Driven Forerunner - Proxy Storms and Hurricane Ike	368
<i>10-yr Proxy Storm</i>	368
<i>100-yr Proxy Storm</i>	372
<i>500-yr Proxy Storm</i>	374
<i>Simulated Hurricane Ike</i>	376
<i>Observations of Forerunner Propagation into Galveston Bay during Hurricane Ike</i>	379
Volume Mode Forerunner – Modeling and Analysis Approach	384
<i>Selection of the Storm Set</i>	384
<i>Isolation of the Volume Mode Oscillation</i>	387
Volume Mode Forerunner - Generation Mechanism	389

<i>Water Fluxes Into/Out of the Gulf of Mexico</i>	389
<i>Water Surface Elevation and Velocity Patterns Associated with the Moving Hurricane</i>	393
<i>Water Surface Elevation Changes Induced by the Volume Oscillation</i>	397
<i>Examination of the Shallow Water Anomaly – Far-Field Influence of the Wind-Driven Forerunner</i>	403
<i>Propagation of the Volume Mode Forerunner into Galveston Bay</i>	412
Volume Mode Forerunner – Dependence upon Hurricane Characteristics	413
<i>Influence of Storm Track and Forward Speed</i>	413
<i>Quantitative Analysis of Volume Oscillation Characteristics</i>	422
<i>Discrepancy with the Volume Oscillation Amplitudes Found by Bunpapong et al (1985)</i>	425
<i>Influence of Storm Intensity</i>	426
<i>Influence of Storm Size</i>	427
Influence of Forward Speed on the Wind-Driven Forerunner and Peak Surge Development	429
<i>Selection of a Storm Set for Analysis</i>	429
<i>The Analysis Approach</i>	429
<i>Central Yucatan Storm 01 (6-kt Forward Speed)</i>	432
<i>Central Yucatan Storm 02 (12-kt Forward Speed)</i>	437
<i>Central Yucatan Storm 03 (18-kt Forward Speed)</i>	443
<i>Evolution of the Wind-Driven Forerunner and Interaction with the Hurricane's Core Winds</i>	449
Summary.....	460
15 Nearshore Wave and Water Level Conditions to Consider in	
Design of the Ike Dike	465
Introduction	465
Water Surface Elevation	467
Significant Wave Height	468
Peak Wave Period	470
Mean Wave Period	471
16 Summary of Key Results, Findings, and Recommendations	473
Regional Storm Surge Dynamics	473
<i>Generation of the Open Coast Storm Surge</i>	473
<i>Surge Generation within Galveston Bay</i>	473
<i>Influence of Storm Track on Surge Development</i>	474
<i>Dependence of Peak Surge on Hurricane Intensity</i>	476
<i>Dependence of Peak Surge on Storm Track</i>	477
Putting Storm Surge in the Context of Probability	478
Storm Surge Reduction Achieved with the Ike Dike Concept: Results from Original Bracketing Set of Storms and Initial Modeling Approach	480
Storm Surge Reduction Achieved with the Ike Dike Concept: Results from the Refined Modeling Approach with the Extended Ike Dike.....	481
<i>Reduction in Peak Storm Surge Values</i>	481
<i>Residual Risk with the Ike Dike in Place</i>	487

Consideration of Secondary Lines of Defense and Recommendations.....	489
<i>City of Galveston</i>	489
<i>Galveston Island and Bolivar Peninsula</i>	492
<i>Bayou Vista and Hitchcock areas</i>	492
<i>San Leon, Texas City (north), Bacliff and Dickinson areas</i>	492
<i>Clear Lake, Bayport and La Porte areas</i>	493
<i>Upper Houston Ship Channel</i>	494
Examination of Alternate Ike Dike Configurations	494
<i>The Different Configurations</i>	495
<i>Storms That Were Simulated</i>	497
<i>Merits of an Eastern Termination Section</i>	497
<i>Merits of a Western Termination Section</i>	498
<i>Influence of Lowered Gates at the Passes</i>	499
Water Level Considerations for Operating the Ike Dike Storm Surge Gates	500
Wave Conditions to Consider in Designing the Ike Dike	504
17 References	506
Appendix A: Inundation Maps for the Simulated Hurricane Ike and the 100-yr and 500-yr Proxy Storms	513
Appendix B: Water Surface Elevations at Selected Locations for Different Ike Dike Alignments.....	547

1 Overview

A consortium of universities and other partners, led by Texas A&M University at Galveston, is investigating the feasibility of a coastal barrier to greatly reduce hurricane-induced coastal flooding in the Houston/Galveston region. In 2008 Hurricane Ike produced considerable storm surge and damage in the area, raising awareness of the flooding threat to the region posed by hurricanes. Had Ike tracked and made landfall 20 to 40 miles farther to the southwest, storm surge in the Houston/Galveston region would have been much more devastating. In support of the feasibility study and as members of the study team, Jackson State University and the U.S. Army Engineer Research and Development Center's Coastal and Hydraulics Laboratory (ERDC) are collaborating to quantify the reduction in flooding that can be expected with a long coastal dike and gate system. This protective measure, called the Ike Dike concept, has been proposed and advanced by the Texas A&M University at Galveston (Merrell 2012). This report presents results from the initial assessment of the Ike Dike's flood mitigation benefits.

Utilizing the latest state-of-the-science coupled computer models for hurricane winds, pressures, waves and storm surge, the study compares inundation due to hurricane surge for existing conditions with reduced inundation achieved by a proposed 17 foot high Ike Dike that stretches from Freeport in the west to Sea Pines State Park in the east (at Sabine Pass), which would provide risk-reduction to the entire Galveston Bay area during a severe hurricane. The models were first set up and applied as part of the Federal Emergency Management Agency's (FEMA) Region VI Risk MAP study to update coastal flood risk maps for the Texas coast, then adapted and modified for use in the present feasibility study (USACE 2011). These are the same models that have been developed and applied by the U.S. Army Corps of Engineers in their recent assessments of coastal flood risk done for FEMA, the Nuclear Regulatory Commission, and in their internal design of flood-risk-reduction measures, including measures constructed in the New Orleans area.

Initial results documented in this report were derived from a total of 50 hypothetical synthetic hurricane simulations. Twenty-five different hurricanes were simulated for both the existing conditions reflecting a post-Ike (2008) condition and the with-Ike-Dike condition. Twenty-one of the storms involved a very intense, rare, but possible storm having a

900-mb central pressure. Each of those 21 storms had a different path, characterized by one of three general approach directions (south, south-southeast, and southeast). The other 4 storms had varying intensities, central pressures of 900 mb, 930 mb, 960 mb, 975 mb, but were all on a “direct-hit” path approaching from the south-southeast. The direct-hit path involved landfall at the City of Galveston and a storm track along the western shoreline of Galveston Bay.

These 25 storms were chosen as a “bracketing set.” They represent a small subset of storms considered in the FEMA Region VI Risk MAP project (USACE 2011). The bracketing set was intended to achieve the following objectives: understanding exactly how hurricane storm surge is generated in the region and in different locations within the region for both the existing and with-dike conditions; quantify how high the storm surge can reach for this severe rare hurricane intensity (900 mb central pressure) in those key areas that have the greatest potential for damage and losses; characterize how the peak surge varies from location to location throughout the region for a particular storm and how storm track influences both the surge development process and peak surge. The “direct-hit” storms were selected to provide insights into how storm surge varied as a function of intensity, primarily. The effectiveness of the Ike Dike in reducing storm surge was examined for all storms.

Results from the “direct-hit” storms were used to assess the reduction in damages/losses associated with the Ike Dike. This economic analysis work is being done by the economics team as part of the feasibility study, work that also is being led by Texas A&M University at Galveston.

Flooding associated with Hurricane Ike and three “proxy” storms was examined. The work included validation of the storm surge modeling approach for Hurricane Ike was performed using available measured water level data including high water marks acquired by the Harris County Flood Control District.

The three proxy storms were selected from among the set of hypothetical storms that were simulated as part of the FEMA Risk MAP study. The proxy storms best approximate peak water surface elevations at a set of locations, that lie along the heavily populated and industrialized western side of the bay, that are associated with the statistical 10-yr, 100-yr and 500-yr average recurrence intervals at these same locations. Examination of proxy storms provides an initial probabilistic assessment of economic

damages and losses. The proxy storm approach was adopted as balance between level of effort, technical rigor, and resources available to perform the work (time and funding).

The influence of sea level rise on storm surge and economic damages/losses was examined for the three proxy storms and Hurricane Ike. A projected contribution to global sea level rise of 1.5 feet over the next 50 years was adopted for this sensitivity study. The subsidence contribution to relative sea level rise, which can have significant local variation, was neglected in this preliminary analysis. The effects of sea level rise was investigated for both existing and with-dike conditions.

A rigorous assessment of flood risk, and the risk of damage/loss with the Ike Dike in place, requires simulation of a much larger set of storms, characterization of the flooding and economic damage/loss for each storm, and estimation of the probability of occurrence of each storm that is simulated. Despite the valuable insights gained from work involving a relatively small set of hypothetical hurricanes, Hurricane Ike, and proxy storms, it does not thoroughly consider the probability, or likelihood, that a particular hurricane will occur (and the spatial variability in flooding and damages/losses it causes). As such, the work described in this report serves a precursor to a more rigorous effort to characterize the probability of flooding for existing conditions and conditions reflecting the dike in place. Such an effort must involve a much larger set of hypothetical synthetic storms (on the order of 200) having a wider range of characteristics such as intensity, track, forward speed and radius-to-maximum winds.

The 17-ft Ike Dike is extremely effective in reducing the peak storm surge around the entire perimeter of the Texas City levee and in the upper reaches of the Houston Ship Channel for all the storms that were considered, including Hurricane Ike and the 100-yr and 500-yr proxy storms. Without the Ike Dike in place these hurricanes produce extremely large storm surges and widespread inundation in key areas (as much as 22.5 ft at the Texas City levee and 25 ft in the upper Houston Ship Channel). For the many areas in the upper ship channel that are home to petro-chemical facilities, as well as the Texas City industrial area, the magnitude of the surge suppression achieved with the Ike Dike is sufficient to reduce the risk of inundation in nearly all of the highly industrialized areas to a very low probability of occurrence. This is a major benefit of the 17-ft Ike Dike; i.e., just how well it protects the vast majority of the

highly industrialized areas from inundation for even very rare hurricane events, like the 500-yr proxy storm, including those with the future sea level scenario.

Even with the Ike Dike in place and despite the high degree of surge reduction it provides, for the higher surge levels generated by the 100-yr and 500-yr proxy storms inundation still occurs in the lower-lying residential areas, particularly for the higher sea level. An analysis of exposure to inundation, residual flood risk, and possibilities for secondary lines of defense are discussed in the report text. The intent of these additional risk-reduction measures is to reduce the residual flood risk that exists in certain areas, even with the 17-ft Ike Dike in place.

The report initially examines the storm surge reduction benefits of the originally envisioned Ike Dike concept, which started at Freeport, ended at Sabine Pass, and which followed the coastline. The report also examines a number of other possible alternate configurations for the Ike Dike, including shorter versions that provide less surge reduction. One of the other alignments examined is quite similar to the coastal spine recommended by the Gulf Coast Protection and Restoration District (GCCPRD) that extends from the western end of Galveston Island to High Island. The merits of adding eastern and western termination dike sections to the alignment recommended by the GCCPRD are examined, as is the influence of adopting lower crest elevations for storm surge gates at Bolivar Roads and San Luis Passes.

Early closure of the storm surge gates at both San Luis and Bolivar Roads Passes is a critical operational feature of the Ike Dike concept. The amount of water within Galveston and West Bays at the time of gate closure influences the peak surge elevation that will be generated by local hurricane force winds that still act on the bays after the gates are closed. A higher antecedent water level in the bays leads to a higher peak surge within the bays, and thus a greater residual flood risk. The following contributors influence the antecedent water level: long-term and seasonal and long-term mean sea level, astronomical tide, wind-driven surge forerunner, and volume mode forerunner. The wind-driven forerunner can cause an increase in water level at Galveston of as much as several feet, one or two days before landfall. Importantly, the wind-driven forerunner that is generated at the coast readily propagates through the passes and open storm surge gates into the bays, with little or no attenuation. Therefore, wind-driven forerunner surge directly increases

residual flood risk inside the bays. The report examines the implications of the various water level contributors on operation of storm surge gates that are built as part of the Ike Dike concept.

Design of the land barrier and navigational/environmental sections of the gate systems, both of which will be constructed as part of the Ike Dike concept, will require nearshore wave information. All components will need to be resilient to overflow and overtopping, which means they will experience minimal damage and no loss of functionality in the event the hydraulic design conditions are exceeded and the Ike Dike is overtopped, even with overflow. There is always some risk of this happening. The report provides preliminary information on the nearshore wave conditions that are generated by severe hurricanes.

2 Storm Surge Model Validation for Hurricane Ike

Introduction

The modeling reflected in this report used state-of-the-science coupled computer models for hurricane winds and pressures, waves and storm surge. These are the same models that have been developed and applied by the U.S. Army Corps of Engineers (USACE) to design flood-risk-reduction measures, including measures constructed in the New Orleans area following Hurricane Katrina. The models also were used by the USACE in recent assessments of coastal flooding risk that have been performed for FEMA and the Nuclear Regulatory Commission. The models are run as a coupled modeling system using the USACE Coastal STORM Modeling System (CSTORM-MS). The system is comprised of the following:

- a) a tropical cyclone Planetary Boundary Layer (PBL) model, Cardone et al. (1992), Cardone et al. (1994), Thompson and Cardone (1996), Cardone and Cox (2009),
- b) a deep water wave model, WAM, WAMDII Group (1988), Komen et al. (1994), Gunther (2005), Smith et al. (2010),
- c) a shallow water wave model, STWAVE, Smith et al. (2001), Smith (2007), Smith et al. (2010), Massey et al. (2011), and,
- d) a storm surge model, ADCIRC, Luetlich et al. (1992), Westerink et al. (1992), Blain et al. (1994), Dietrich et al. (2010a and 2010b).

The models were set up and applied to the north Texas coast as part of the FEMA Risk MAP project to update coastal flood risk maps for the entire Texas coast, then adapted and modified for use in the present feasibility study.

One change was made to the wave modeling approach that was originally adopted in the Risk MAP study. In the Risk Map study, the regional north Texas shallow water wave model domain that included the Houston-Galveston region was first simulated with the half-plane version of STWAVE. The half-plane wave model then provided boundary conditions

to a nested wave model within Galveston Bay which was run with the full-plane version of STWAVE. The half-plane version of STWAVE only considers waves approaching the coast in a 180-degree window relative to the coastline, which is a reasonable approximation for the open coast of Texas. In the full-plane model waves can approach from a full 360-degree window, which is required to accurately simulate wave conditions around the periphery of a fully- or semi-enclosed bay, like Galveston Bay. For this feasibility study, in light of computational efficiency advancements made to the CSTORM-MS modeling system, the wave modeling was improved by simulating shallow water waves for the full north Texas regional domain using the full-plane version of STWAVE.

Storm surge simulations of several extreme 900-mb storms included in the original bracketing set of storms, using the original FEMA Risk Map study grid mesh, became numerically unstable. To stabilize the simulations, global slope limiting was applied to all of the bracketing set of storms, for all time steps, to produce the original bracketing set results.

In an effort to reduce the error associated with applying slope limiting globally, on the entire computational domain, a more localized procedure for applying slope limiting was sought and developed. A polygon was created which encompassed the very shallow nearshore open Gulf region (shallower than approximately 10 m water depth), from Sabine Pass to the south of Texas; and it extended inland to the landward side of the natural dune system, encompassing the jetty systems at the passes, and extending into the throats of the passes. These were the areas where model instabilities tended to develop for several of the most extreme hurricanes in the bracketing set. The application of slope limiting was geographically restricted to those areas within the polygon. A trigger also was applied to restrict application of slope limiting to those time steps when the water surface slope exceeded a threshold value.

One other change was made to the model set-up that was applied in the original bracketing set of storm simulations. The bottom friction coefficient on the Louisiana and Texas continental shelves was reduced to enable a better simulation of the wind-driven hurricane surge forerunner that can occur along the Texas shelf for approaching hurricanes. The reduced bottom friction enabled higher along-shelf water velocities to develop under wind forcing, which in turn produced a greater Coriolis-driven Ekman setup at the coast, i.e. the surge forerunner. Bottom friction on the continental shelf was reduced to levels that were quite similar to

those used in the FEMA study; and the level of accuracy of forerunner simulation achieved with this revised modeling procedure is quite similar to that achieved in the original FEMA study.

The change in wave modeling approach, while improving the quality of the wave computations, was not expected to significantly alter the computed storm surge. To verify this, and as a check of the revised coupled modeling system's capability to replicate the accuracy of results obtained in the original FEMA Risk Map study, the modeling system was rerun for Hurricane Ike. The re-validation also provided a check on the performance of and influence of the polygon-based application of slope limiting.

Extensive verification of the coupled models was performed in the original Risk MAP study for several historic hurricanes, including Ike. Verification included comparisons between ADCIRC results and high water marks collected by different agencies as well as comparisons between water surface elevation hydrographs computed using ADCIRC and hydrographs measured by the U.S. Geological Survey (USGS), see East et al (2009), by the National Oceanic and Atmospheric Administration (NOAA), by the Texas Coast Ocean Observing Network (TCOON) and by Kennedy et al (2010, 2011).

At present, the economic analysis of damage/losses prevented by the Ike Dike concept relies solely on maximum water surface elevations (still-water elevations) that are simulated with the ADCIRC storm surge model. In light of this fact, the re-evaluation of model accuracy for Hurricane Ike only considered a comparison of computed and measured high water marks.

Computed Maximum Water Surface Elevations for Hurricane Ike

The maximum water surface elevation field (in feet) computed for Hurricane Ike using the ADCIRC model, with the modified modeling procedure, is shown in Figure 2-1. At each computational node of the ADCIRC grid mesh, the maximum water surface elevation is recorded as the simulation progresses and saved to an output file. At the conclusion of the simulation, the maximum elevation file reflects the maximum water surface elevation reached at each and every grid node in the active model domain, regardless of when the maximum occurred during the simulation. Figure 2-1 graphically displays the maximum water surface elevation

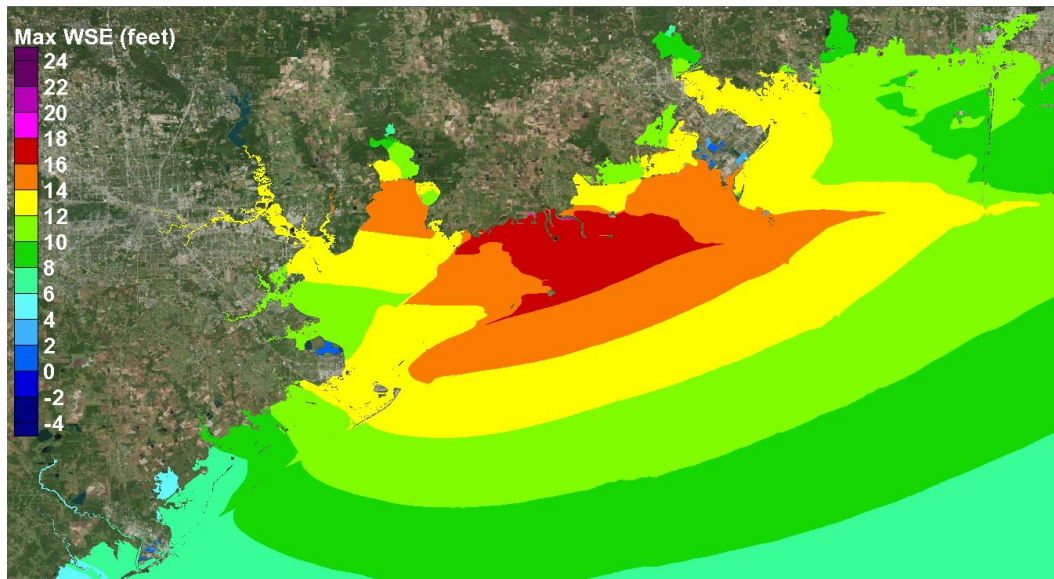


Figure 2-1. Map of computed maximum water surface elevations for Hurricane Ike

(WSE) field for the entire model domain. The maximum WSE computed using ADCIRC is directly comparable to those high water marks that reflect a still water level.

The zone of maximum computed peak storm surge occurs to the northeast of Galveston Bay, between the Bay and Port Arthur, with peak surges slightly exceeding 17 ft. Computed peak surges near the City of Galveston were 13 to 14 ft. From the City of Galveston moving north, peak surge values decrease along the western shoreline of Galveston Bay to values of 11 to 13 ft along Texas City, and 11 to 12 ft in the vicinity of Clear Lake. Peak surges then increase along the western shoreline to values of 13 to 14 ft in the upper reaches of the Houston Ship Channel. Peak surge along Galveston Island decreases from 13 to 14 ft at its northern end to 8 to 9 ft at the southern end. Peak surge along Bolivar Peninsula is 14 to 16 ft. All elevations are relative to NAVD88, the vertical datum used in the storm surge modeling.

Comparison with High Water Marks

A set of measured high water marks were derived from the same data sources that were considered in the original Risk MAP study: 1) high water marks extracted from recorded water surface elevation hydrographs that were measured with pressure gages deployed by the USGS, and reported by East et al (2009), 2) high water marks extracted from recorded hydrographs that were measured with permanent pressure gages which

are maintained by TCOON and NOAA, and reported on the NOAA Tides and Currents web site, 3) high water marks estimated from graphical plots of water surface elevation hydrographs that were measured with gages deployed by Kennedy et al (2011) ; and 4) a set of visually identified high water marks taken from FEMA's Texas Hurricane Ike Rapid Response Coastal High Water Mark Collection (2008) effort. Even though these same data sets were included in the original Risk Map model validation work, the exact data set which was adopted for each of the various data sources might be slightly different than the data set used here due, for example, to different decisions on which data were included/excluded from the analysis for various reasons.

An additional set of high water marks that were acquired within Galveston Bay by the Harris County Flood Control District (HCFCD), immediately following Hurricane Ike, that were not considered in the original Risk Map study, were considered in this re-evaluation. These data were acquired via personal communication with Mr. Steven Fitzgerald, Chief Engineer with HCFCD.

Only visually identified high water marks that reflect still-water elevations were considered in the analysis. These are the only types of high water marks that are appropriate for direct comparison with water surface elevations computed with ADCIRC. Only high water marks that were rated by the collectors as being of good or excellent quality were retained in the analysis. High water marks that were acquired at locations which did not fall within the computational grid mesh or were located a significant distance away from the inundated parts of the model domain were excluded from the analysis.

High Water Marks from Gage Measurements of Water Surface Elevation

High water marks from NOAA/TCOON maintained pressure gages were extracted by first displaying the water surface elevation hydrograph within the NOAA tides and currents web site (<http://tidesandcurrents.noaa.gov/stations.html?type=Water+Levels>), scrolling the cursor over the water surface elevation hydrograph to the time of maximum elevation and reading the maximum value directly from the screen.

The high water marks from gages deployed by the USGS were derived from hydrographs comprised of measured pressures every minute that

were subsequently converted to water surface elevation. See East et al (2009) for details of the data processing. Time series at perhaps a third of the locations showed data-point-to-data-point variability in water surface elevation due to the influence of short-period wind waves that were reflected in the pressure measurements. The degree of wave-induced variability varied for different gages.

The type of modeling being done here to simulate storm surge does not compute water surface elevation changes on time scales of seconds and fractions of a second, which occur for short-period wind waves. Instead a “mean”, in the time sense, or much more slowly varying water surface elevation (often called the still water level) is computed by the ADCIRC model.

In an attempt to filter out these higher-frequency fluctuations, or “noise,” from the measured data and develop an estimate of the still water level that is consistent with the water surface elevation, or storm surge, being computed with the models, a 20-min average was computed at approximately the time of maximum water level. The 20-min average value was used as the measured high water mark for that location.

The quality of the measured hydrographs was good, and high water marks derived from the measured hydrographs are considered to be the most accurate data which are available, more so than high water marks that are not based on measured data but rather reflect some other type of marking left behind by the elevated surge and waves such as the FEMA and HCFCD high water marks.

USGS/NOAA/TCOON gage-based high water marks from Matagorda, Brazoria, Galveston, Harris, Chambers, and Jefferson counties in Texas, and Cameron parish in Louisiana, were considered in the analysis. All high water marks that were located within the model domain were retained in the analysis; whereas, other marks that fell outside the model domain or fell outside the region of simulated inundation were not considered in the analysis.

The locations of 41 USGS gages, whose data were retained in the analysis, are shown as yellow dots in Figure 2-2. Locations of the 6 NOAA-TCOON gages are shown as magenta dots, and locations of the 5 Kennedy et al

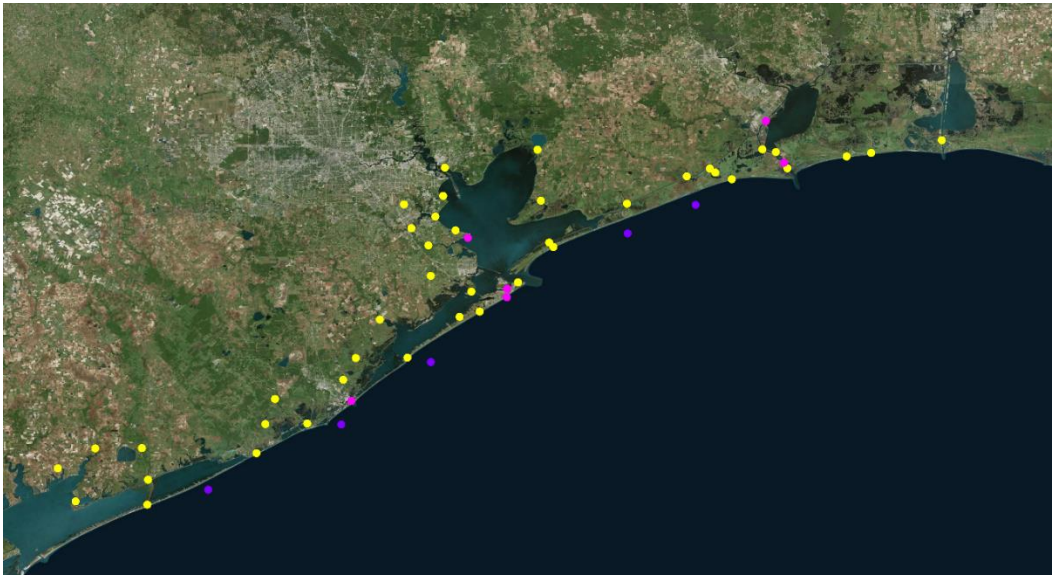


Figure 2-2. Locations of USGS (yellow), NOAA/TCOON (magenta) and Kennedy (purple) gages.

gages are shown with purple dots. The Kennedy et al gages were deployed along the open coast, in relatively shallow water, at fairly regular alongshore spacing; although, data from the gage located closest to the City of Galveston were not available.. The NOAA/TCOON gages were mostly deployed within the bay systems, except for a single gage along the open coast at Galveston Pleasure Pier.

This set of gage-derived high water marks reflects a broad regional coverage, centered about the Houston-Galveston area which is of prime interest. Comparisons between surge model maximum water surface elevations and this measured data set best illustrates model accuracy for the entire region, with gages distributed rather uniformly throughout the region.

A scatter plot of the comparison between maximum water surface elevations computed with the ADCIRC model and gage-derived high water marks for each of the 52 gages is shown in Figure 2-3. A 45-degree dashed line also is shown in the figure. If there is perfect agreement between measurements and model results, then all points would fall on the dashed line. The distance away from the dashed line indicates the magnitude of error reflected in the model results.

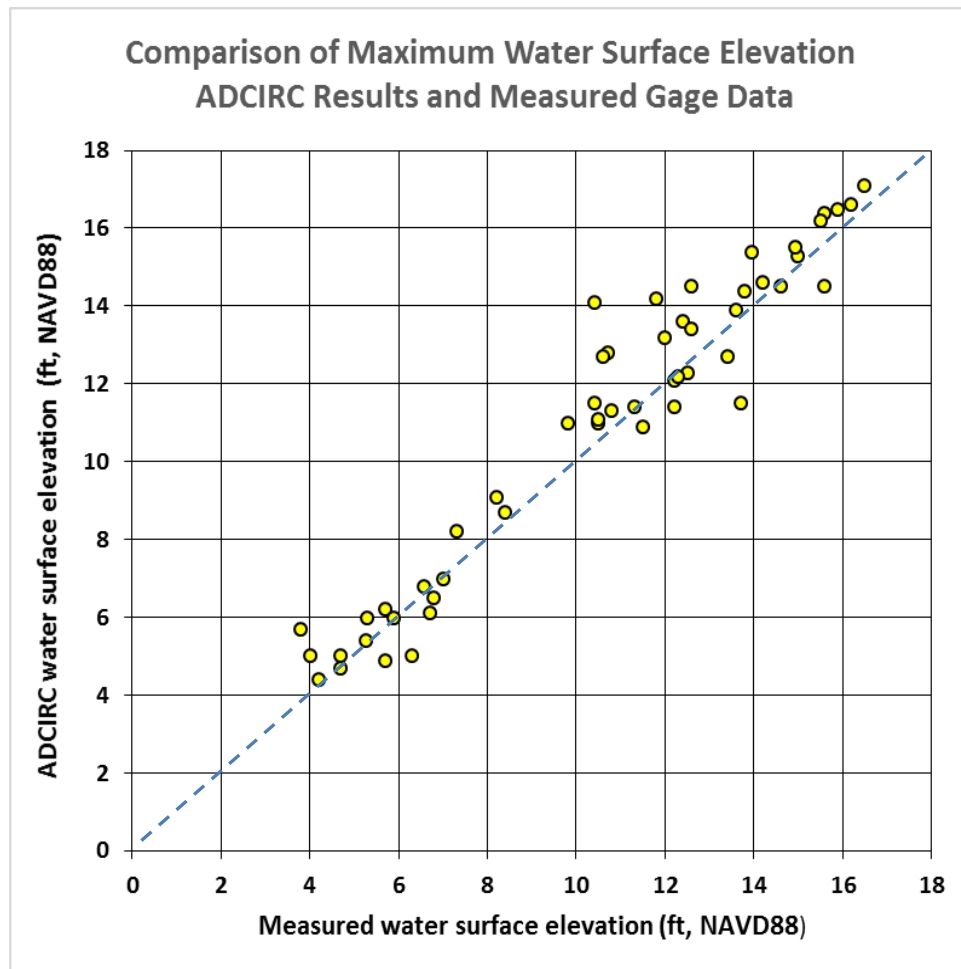


Figure 2-3. Scatter plot of measured and modeled maximum water surface elevations for all hydrograph-derived high water marks.

Average error and average absolute error were computed for all pairs of modeled and measured values, for each gage location. Average error was computed by subtracting the measured water surface elevation from the modeled elevation, and then taking an average. An average error of 0.47 ft was computed using model-measurement data pairs for the 52 gage locations. The positive average value indicates a slight positive bias, i.e., the model results are slightly higher than the measured values. Average absolute error provides a measure of the average magnitude of the difference between measured and modeled values, without regard for whether the modeled value is greater than or less than the measured value. The average absolute error for the entire data set was 0.81 ft. This error measure provides an overall estimate of model skill and accuracy in making peak storm surge estimates as part of the feasibility study, using the current model setup.

The scatter plot also reveals the slight high bias in the modeled high water marks, i.e. on average, modeled high water marks slightly exceed measured values. The modeled/measured high water mark differences and the bias evident in Figure 2-3 for the Houston-Galveston region are quite similar to the results for Hurricane Ike shown in the original FEMA Risk MAP study.

Visually Estimated High Water Marks

The locations of 69 high water marks acquired by FEMA following Hurricane Ike are shown as light blue dots in Figure 2-4. These data also are reasonably well distributed, regionally, to both the northeast and southwest of the Houston-Galveston region. Marks acquired to the northeast of Galveston Bay appear to have been mostly acquired along the inland edge of inundation caused by the hurricane. Coverage is not as uniformly distributed as was coverage of the gage-derived high water marks.

A scatter plot of the comparison between ADCIRC results and 69 FEMA high water marks is shown in Figure 2-5. The plot shows trends that are similar to those seen for the gage-derived high water marks. The average error for this data set was 0.44, and average absolute error was 0.98 ft; both results were similar to results for the previous data set.

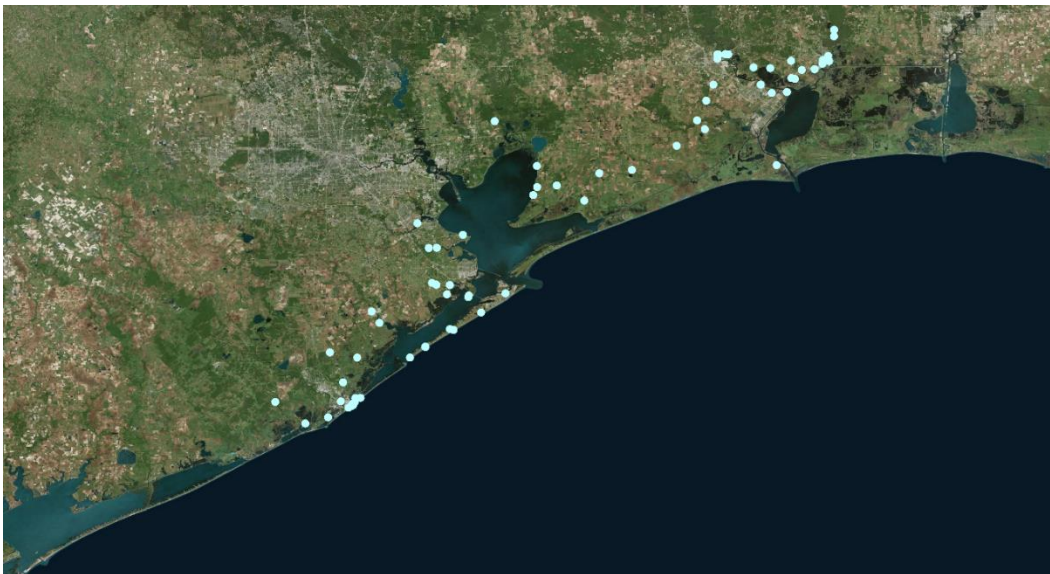


Figure 2-4. Locations of FEMA high water marks.

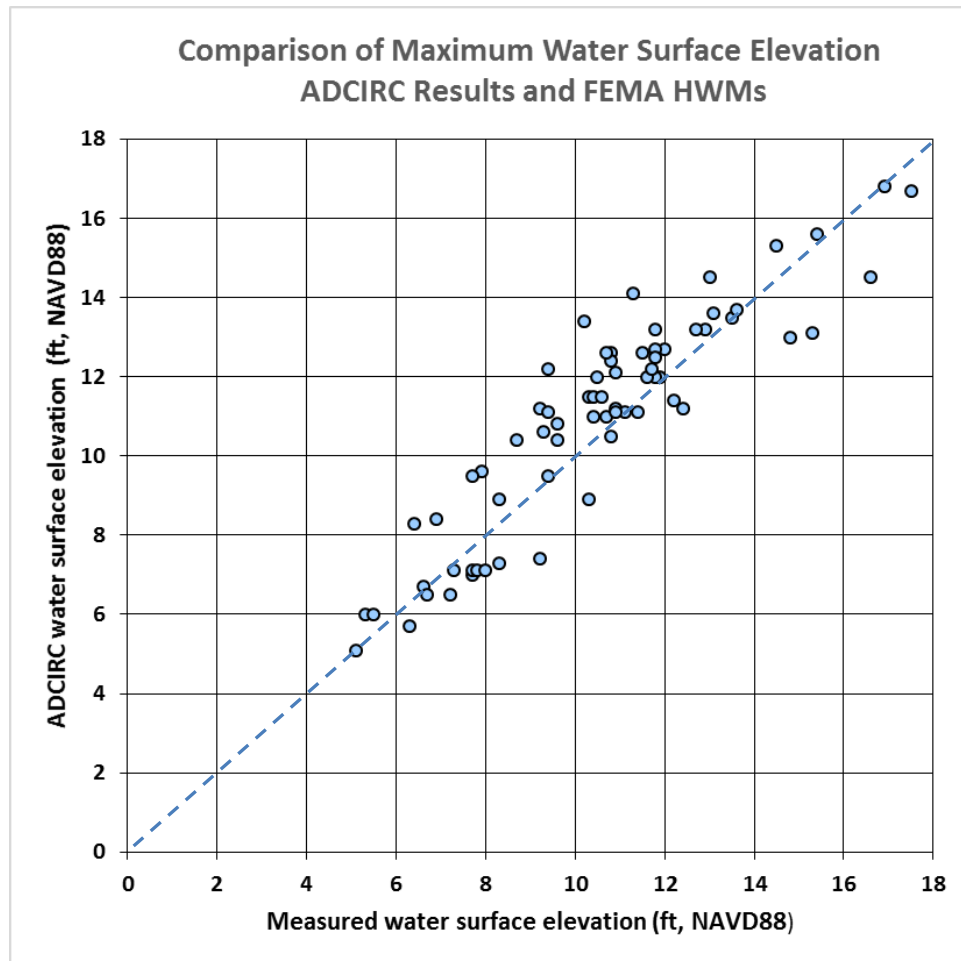


Figure 2-5. Scatter plot of measured and modeled maximum water surface elevations for the FEMA high water marks.

The set of HCFCF high water marks were not included in the validation one as part of the original Risk MAP study. They are included in the analysis reported here because they were all acquired within Galveston Bay, particularly in areas along the western side of the bay and in the upper reaches of the Houston Ship Channel that are of great interest in the economic analysis facet of the feasibility study.

The locations of 69 high water marks acquired by HCFCF are shown as green dots in Figure 2-6. These data were nearly exclusively acquired in the northwest portion of Galveston Bay and the vicinity of the upper reach of the Houston Ship Channel, i.e., in a much smaller area relative to that reflected in the other data sets.

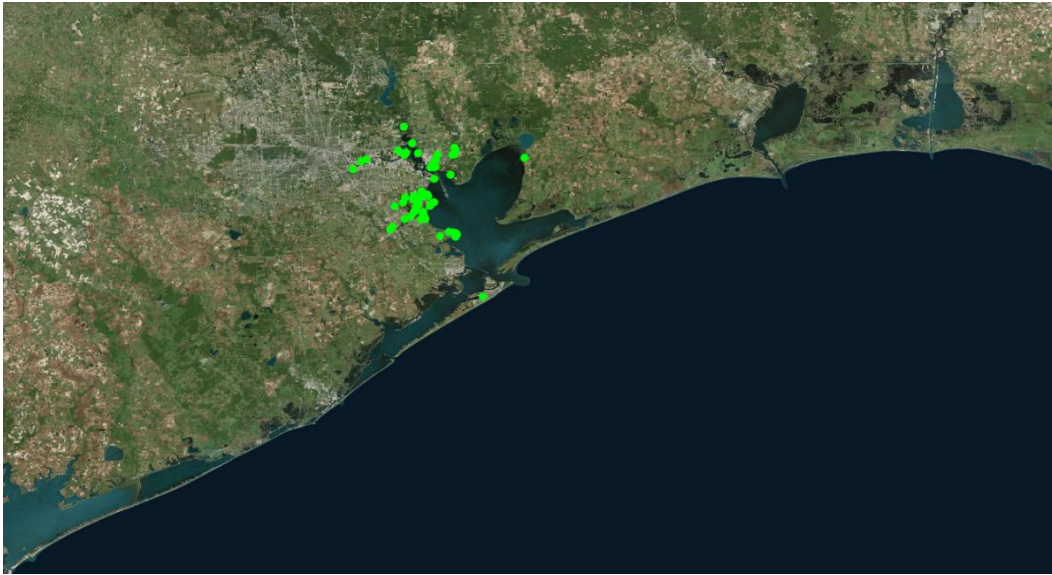


Figure 2-6. Locations of HCFCD high water marks.

A scatter plot of the comparison between ADCIRC results and the 69 HCFCD high water marks is shown in Figure 2-7. The plot shows trends that are similar to those seen for the gage-derived and FEMA high water marks. The average and average absolute errors computed for this data set are 0.42 ft and 1.00 ft, very similar to the values obtained for the other two data sets. The small positive bias of the model results seen in the gage-derived data comparisons and in the FEMA high water mark comparisons also are evident for the HCFCD data set.

Figure 2-8 shows a scatter plot for all the high water mark data sets, combined in a single plot. Not surprisingly, the same consistent trends that are evident for the individual data sets also are evident for the composite data set. The average and average absolute error computed for this entire set of 179 model-measurement data pairs is 0.44 ft and 0.98 ft, respectively.

The slight high bias of the model results is clearly seen in the figure as well. Results shown in Figure 2-8 indicate that the current modeling approach yields maximum water surface elevation results for Hurricane Ike that are very similar to those produced in the Risk MAP study. As a percentage of the peak storm surge of 11-14 feet that was generated by Ike along the western side of Galveston Bay and into the upper reaches of the Houston Ship Channel, the average absolute error reflects an error of 7 to 9%.

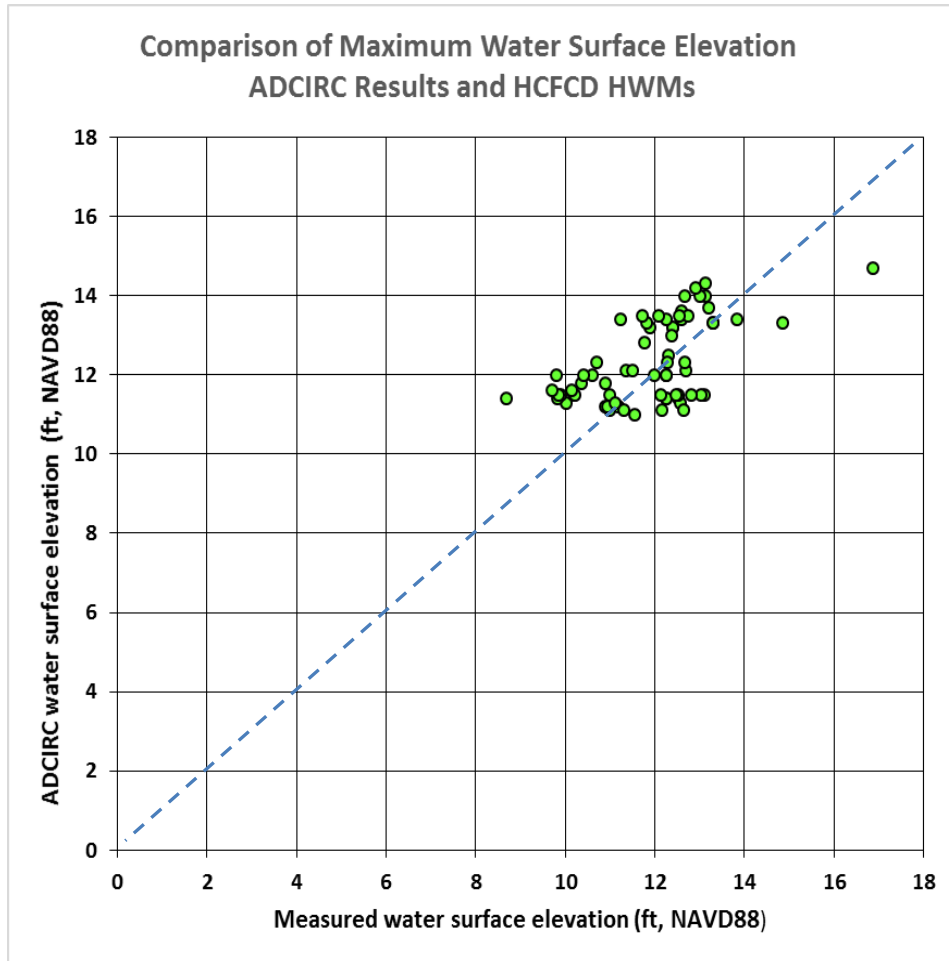


Figure 2-7. Scatter plot of measured and modeled maximum water surface elevations for the HCFCO high water marks.

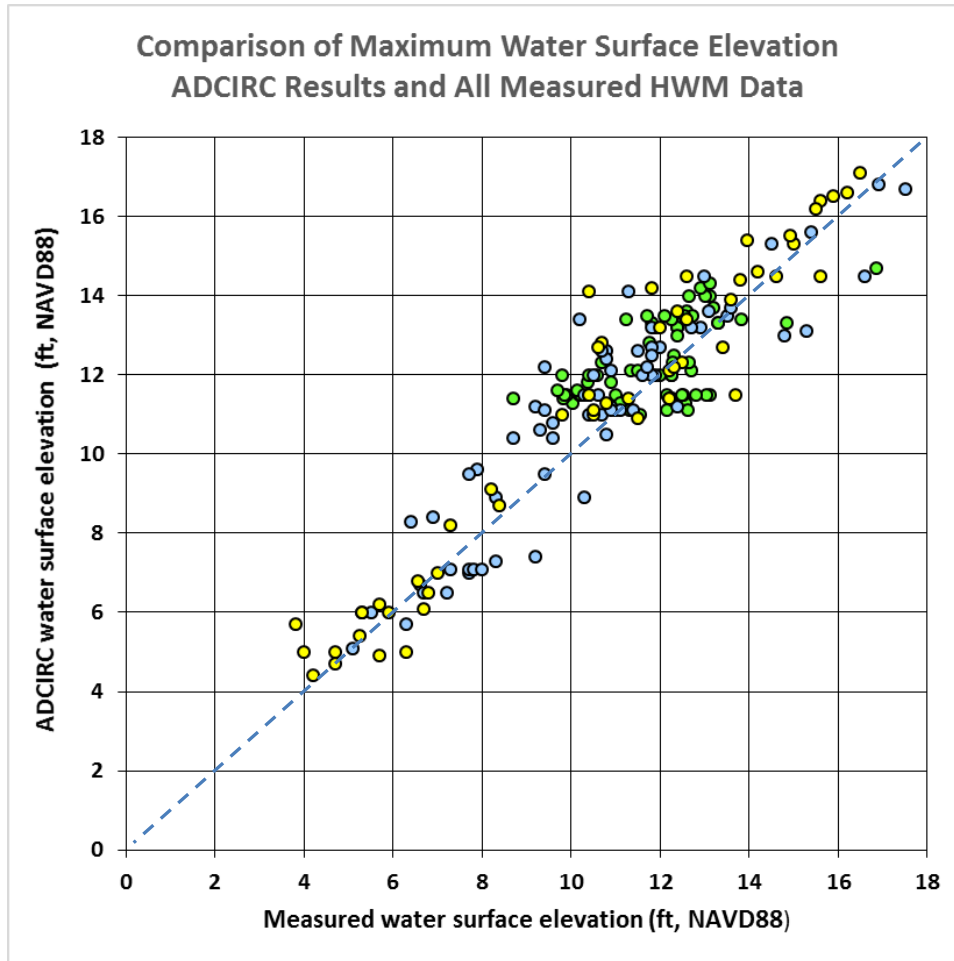


Figure 2-8. Comparison of ADCIRC maximum water surface elevations with high water marks measured by the USGS-NOAA-TCOON-Kennedy (yellow), FEMA (blue), and HCFC (green).

3 Texas Coast Historic Hurricanes

Intensity of Historic Hurricanes

The National Weather Service (Roth) documented historic hurricanes that have impacted the Texas coast. Based on this work, Figure 1 shows the occurrence of Category 3, 4 and 5 hurricanes (the most severe hurricanes) from 1870 through 2010, as indicated by their central pressures (in mb). The National Weather Service defines hurricane categories based on maximum wind speed. However, central pressure is highly correlated to maximum wind speed, so central pressure also is a reasonably good indicator of hurricane intensity. The lower the central pressure the more intense is the hurricane, generally speaking. Hurricane central pressure is used here as the measure of hurricane intensity, for illustrative purposes and to compare the intensity of different historic and synthetic storms.

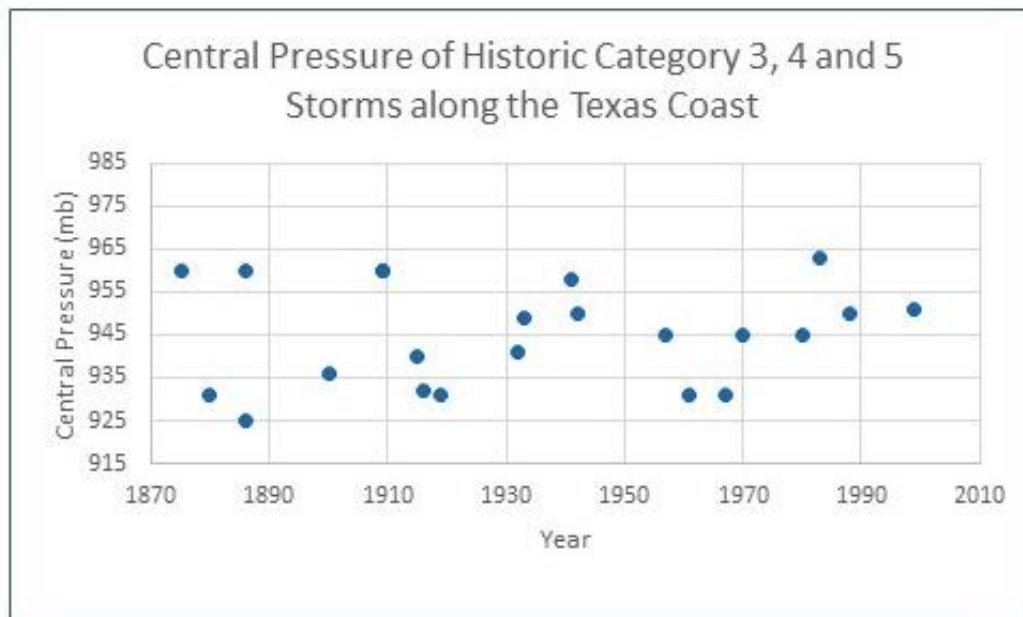


Figure 3-1. Occurrence of severe hurricanes along the Texas coast from the historic record.

Twenty-one hurricanes having intensities of Category 3, 4 or 5 occurred during this 140-year span, roughly once every 7 years on average. These storms generally have central pressures of 960 mb or less. Roth's work indicates that central pressure information for the hurricanes first became available in the 1870's. For three of the of Category 3 storms, central pressure information was not available. So, to still include these storms in

the figure a central pressure of 960 mb was assumed for illustrative purposes.

The historical record shows 7 storms having a central pressure of 935 mb or less during this time span. The occurrence of a storm of this intensity was not uniformly distributed during the 140 years.

The September 1900 Galveston Hurricane

The track and intensity characteristics for the 1900 Galveston Hurricane, based on information contained in the NOAA Hurdatt2 data base, are shown in Table 3-1. Column 1 of the table shows the year, date and time (referenced to GMT) of each set of observations; columns 2 and 3 show the position of the eye of the hurricane, in latitude and longitude, along its path, or track; column 4 shows the maximum sustained 1-minute wind speed; column 5 shows a conversion of this 1-min wind speed to metric units; column 6 shows a conversion of the metric 1-min wind speed to a 10-min wind speed; and column 7 shows the observed central pressure in the eye. Few pressure observations were available for this storm.

The Galveston Hurricane of 1900 had a central pressure of 936 mb at landfall; the minimum central pressure is unknown. So in terms of intensity, the Texas coast has experienced a storm of this, or greater, intensity on a number of occasions during this 140-year period. Because of its notoriety, and fact that its intensity, while extreme, is not rare, the Galveston Hurricane of 1900 was thought to be a reasonable severe hurricane with which to examine the feasibility of the Ike Dike. The NOAA Digital Coast site reports the maximum wind speed for this hurricane to be 125 kts, a Category 4 hurricane.

Figure 3-2, generated using the NOAA Digital Coast web site, shows the track of the 1900 Galveston Hurricane among the tracks of 15 other severe historic hurricanes of Categories 3, 4 and 5. The storm tracked to the southwest of Galveston and landfall occurred to the southwest of Galveston, but this track caused the maximum wind band on the right hand side of the storm to directly impact Galveston. A number of severe historical hurricanes have tracked to the southwest of Galveston Bay.

Table 3-1. Galveston Hurricane of 1900, Track and Intensity Characteristics

Mo/Day/Yr/Hr (GMT)	Lat (deg)	Lon (deg)	Wmax (kt) Max sust.	Wmax (m/sec) Max sust.	Wmax ¹ (m/sec) 10-min	Cp (mb) obs
1900/09/05/0:00	22N	79.5W	35	18.0	16.0	X
1900/09/05/6:00	22.4N	80.1W	35	18.0	16.0	X
1900/09/05/12:00	23N	80.7W	45	23.1	20.6	X
1900/09/05/18:00	23.5N	81.5W	55	28.2	25.2	X
1900/09/06/0:00	24.1N	82.3W	60	30.8	27.5	X
1900/09/06/6:00	24.8N	83.2W	65	33.3	29.8	X
1900/09/06/12:00	25.5N	84.1W	75	38.5	34.4	X
1900/09/06/18:00	26.1N	85.2W	85	43.6	38.9	974
1900/09/07/0:00	26.5N	86.2W	95	48.7	43.5	X
1900/09/07/6:00	26.8N	87.4W	105	53.9	48.1	X
1900/09/07/12:00	27N	88.7W	115	59.0	52.7	X
1900/09/07/18:00	27.2N	89.7W	125	64.1	57.3	X
1900/09/08/ 0:00	27.4N	90.6W	125	64.1	57.3	X
1900/09/08/6:00	27.6N	91.5W	125	64.1	57.3	X
1900/09/08/12:00	27.8N	92.4W	125	64.1	57.3	X
1900/09/08/18:00	28.2N	93.5W	120	61.6	55.0	X
1900/09/09/0:00	28.9N	94.7W	120	61.6	55.0	936
1900/09/09/2:00 ²	29.1N	95.1W	120	61.6	55.0	936
1900/09/09/6:00	29.8N	95.9W	90	46.2	41.2	X
1900/09/09/12:00	31N	96.9W	65	33.3	29.8	X
1900/09/09/18:00	32.2N	97.6W	50	25.7	22.9	X
1900/09/10/0:00	33.4N	97.8W	45	23.1	20.6	X
¹ factor of 0.88 used to convert max sustained wind speed to 10-min wind speed						
² time of landfall						

For the present study, the original plan was to simulate the 1900 Galveston Hurricane on its original track. A Planetary Boundary Layer (PBL) model representation of the storm winds and pressures, with best available information on hurricane parameters and track, was to be used to develop the wind and pressure fields required as input to the storm surge modeling.

However, in light of the lack of available central pressure data prior to landfall, through time, uncertainty in the radius to maximum winds value that was identified in a search for information, and relative lack of any other information for characterizing the spatial structure of the wind fields as the storm approached and crossed the continental shelf, the primary

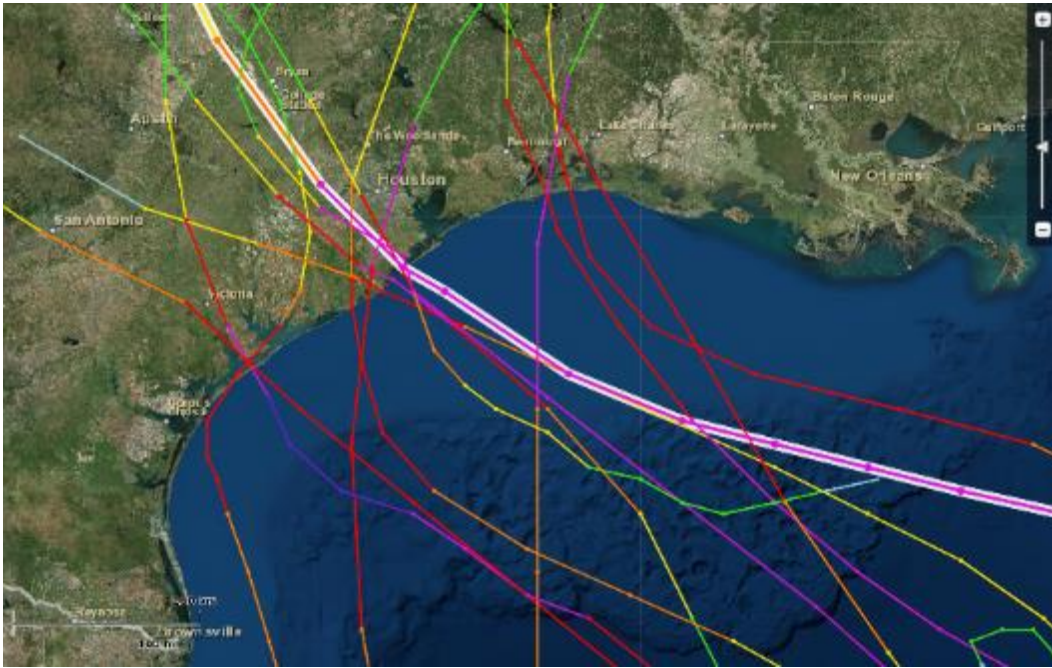


Figure 3-2. Track Galveston Hurricane, among other Category 3, 4 and 5 storms.

storm surge generation zone, a decision was made not to simulate this storm, and instead, compare it to other storms in the FEMA storm set.

Figure 3-3 compares the track for the 1900 Galveston Hurricane and the storm track considered in the FEMA Risk Map study that most closely matches the original the track. The FEMA storm track that is shown is named TXN SE Track 3b. The tracks are similar over the continental shelf, the primary storm surge generation zone. The track general track orientation and landfall location are quite similar; with landfall near San Luis Pass.

Table 3-3 compares various storm characteristics for the 1900 Galveston Hurricane with those for three FEMA Risk Map study storms, Storm 128, Storm 147, and Storm 158, which were all simulated for track TXN SE Track 3b. Column 2 shows that Storm 128 was a 900-mb storm, in terms of minimum central pressure, and Storms 158 and 147 were 930-mb storms. Based on minimum central pressure alone, Storm 128 would be expected to produce greater storm surge than the others, including the 1900 Galveston Hurricane. The first column compares the peak maximum wind speed (10-min wind speed), at any position along the track, and column 3 compares the maximum wind speed (10-min speed) at landfall.

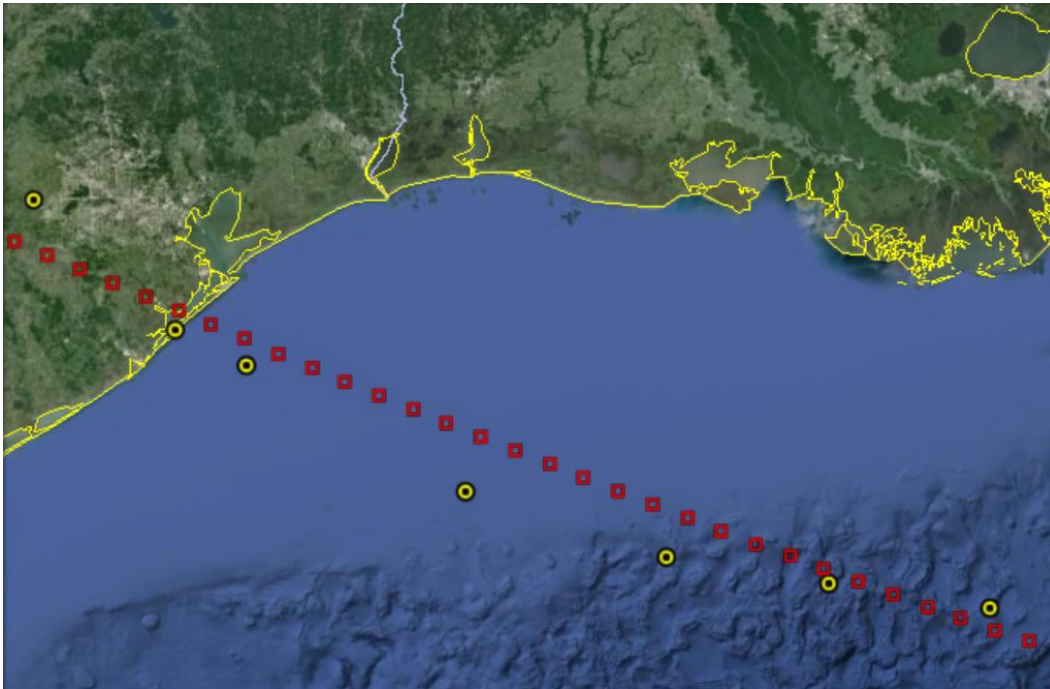


Figure 3-3. Track of the 1900 Galveston Hurricane (yellow symbols) and the closest track from the FEMA storm set (red symbols).

Table 3-2. Comparison of Storm Characteristics, 1900 Galveston Hurricane and Similar storms from the FEMA storm set.

Storm	Peak Wmax (m/sec) 10-min	Minimum Cp (mb)	Wmax at landfall (m/sec) 10-min	Cp at landfall (mb)	Rmax (nm)	Forward speed (kts)
1900 Galveston Hurricane	56.4	?	54.2	936	14	10 to 13
FEMA Storm 128	62.9	900	53.2	912	17.7-25.7	11
FEMA Storm 158	60.6	930	51.0	942	17.7-25.7	17
FEMA Storm 147	52.9	930	42.4	942	17.7-25.7	6

In terms of maximum wind speeds, Storms 128 and 158 are higher than the 1900 Galveston Hurricane; the maximum wind speeds for Storm 147 are less than those for the 1900 Galveston Hurricane. The greater maximum wind speeds for Storms 128 and 158 would tend to produce larger storm surge than for the 1900 Galveston Hurricane. The maximum wind speed at landfall is also an important factor in defining the open coast storm surge, because winds are most effective in generating storm surge in

shallower water. At landfall, the maximum wind speeds for Storms 128 and 158 are both slightly less than the value for the 1900 Galveston Hurricanes; the maximum wind speed for Storm 147 is much less than that for the 1900 Galveston Hurricane. In terms of maximum wind speed, storm 158 seems like it would produce open coast storm surge that is most similar to the 1900 Hurricane compared to the other two storms. The central pressure at landfall for Storm 158 is slightly higher (i.e. less intense) than that for the 1900 Hurricane; the central pressure for Storm 128 is much lower (i.e., more intense) than that for the 1900 Hurricane. In terms of the intensity parameters, central pressure and maximum wind speed; Storm 128 is expected to produce a greater storm surge than the 1900 Galveston Hurricane; Storm 158 is expected to produce a surge that is similar to the 1900 Hurricane; and Storm 147 is expected to produce less storm surge than the 1900 Hurricane.

The single radius-to-maximum-winds value for the 1900 Hurricane (14 n mi) is less than the values for Storms 128, 158 and 147 (17.7 to 25.7 n mi). Also, the track for the three FEMA storms was displaced a few miles to the northeast compared to the 1900 Hurricane track. Both the larger radius-to-maximum winds and the displacement in track would suggest that the zone of maximum surge will be displaced further to the north for the three FEMA storms, compared to the location of maximum surge for the 1900 Galveston Hurricane. In general, larger Rmax values also tend to produce larger open coast storms surges than smaller Rmax values.

The forward speed for the 1900 Galveston Hurricane is similar to that for Storm 128; but quite different from the forward speeds for Storms 158 and 147. In light of the work by Bunpapong and Reid (1985) for the Galveston area, the higher forward speed of Storm 158 is expected to increase the storm surge relative to the storm surge for a slower moving storm like Storm 147.

The peak storm surge at Galveston during the 1900 Galveston Hurricane was reported to be 15.2 ft (U.S. Weather Bureau, 1900), referenced to an unknown datum. The peak storm surge maps for the three FEMA storms, Storm 128, Storm 158 and Storm 147 are shown in Figure 3-4.

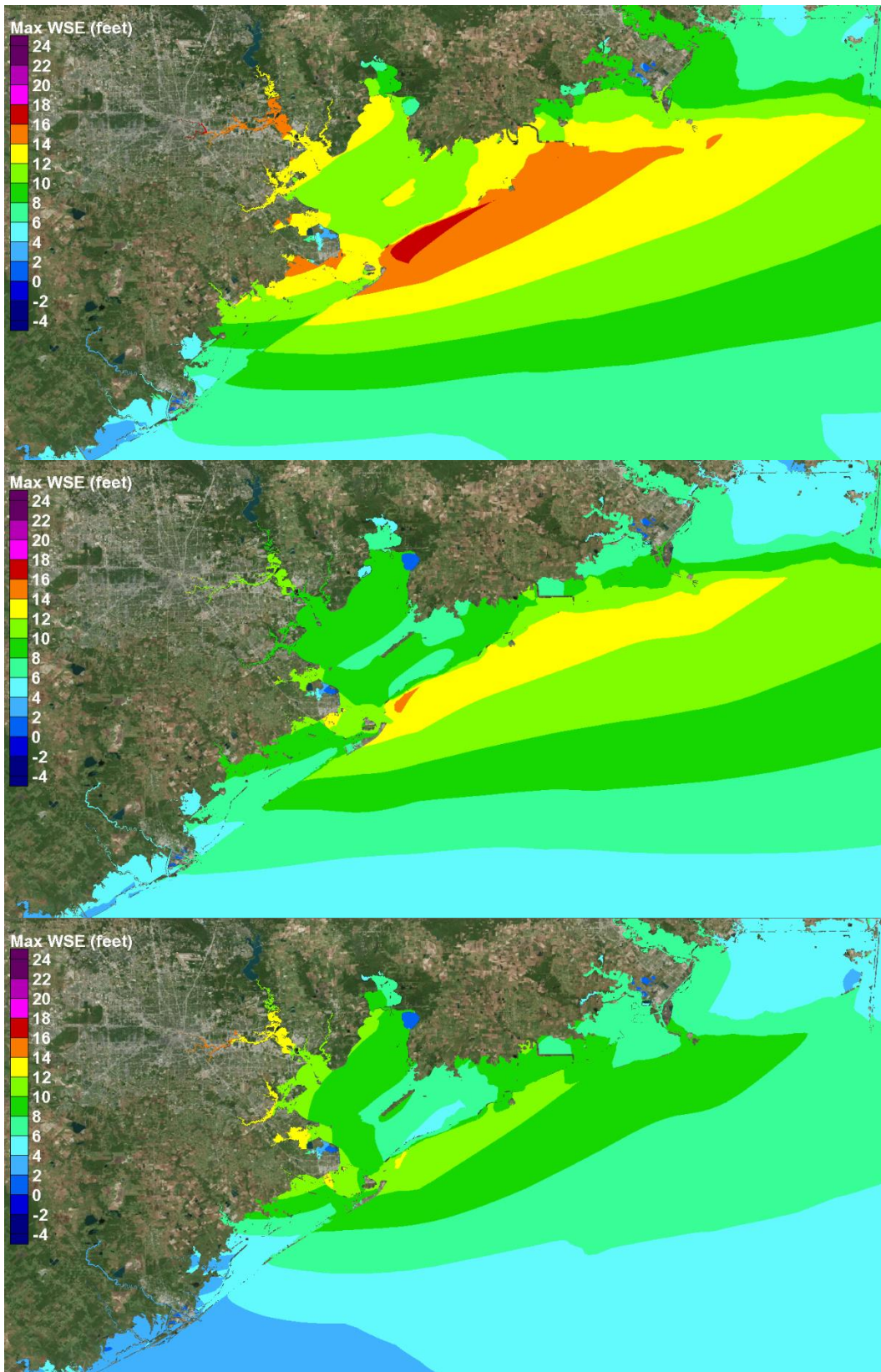


Figure 3-4. Maximum water surface elevation map for Storms 128 (upper), 158 (middle) and 147 (lower).

The zone of maximum storm surge for Storm 128 lies along Bolivar Peninsula, reaching a maximum value of 16 to 17 ft NAVD88. For Storm 158, the zone of peak surge also lies along the southern end of Bolivar Peninsula, with a maximum of just over 14 ft NAVD88. For Storm 147, the zone of peak surge also lies along the southern end of Bolivar Peninsula, with a maximum of just over 12 ft NAVD88. For reasons discussed earlier, the zone of maximum surge for the three FEMA storms is displaced further to the northeast than what would have been expected for the 1900 Galveston Hurricane. For the 1900 Hurricane, the zone of maximum surge would probably have been closer to the City of Galveston.

These peak storm surge results are consistent with the earlier discussion comparing intensity and the other parameters. The peak storm surge for Storm 128 (16 to 17 ft) was expected to be greater than the maximum observed during the 1900 Galveston Hurricane (approximately 15 ft), primarily because of its greater intensity offshore, similar intensity at landfall, and larger R_{max} . The peak surge for Storm 158 (14 ft) was expected to be most similar to the 1900 Hurricane (15 ft) because of its slightly higher intensity offshore and slightly lower intensity at landfall. The maximum for Storm 147 (12 ft) was expected to be less than the observed value for the 1900 Hurricane (15ft) because of its lower intensity offshore and much lower intensity at landfall.

These results suggest that the modeling is producing results consistent with those that were observed during the 1900 Galveston Hurricane, for storms having similar tracks and intensity characteristics.

Hurricane Carla

Another more recent severe hurricane from the historic record is Hurricane Carla, in 1961. Figure 3-5 shows the track of Hurricane Carla. Hurricane Carla had a minimum central pressure of 931 mb and maximum wind speed of 155 kts. Hurricane Carla was a Category 5 storm offshore, with Category 5 strength winds occurring over the continental shelf, the zone where coastal storm surge and waves are effectively generated by the wind. The time during which Hurricane Carla reached Category 5 intensity is shown as the blue portion of the track in Figure 3-5. As it approached landfall, its intensity decreased to Category 4 strength. Storm parameters, as a function of time, for Hurricane Carla are shown in Table 3-3.

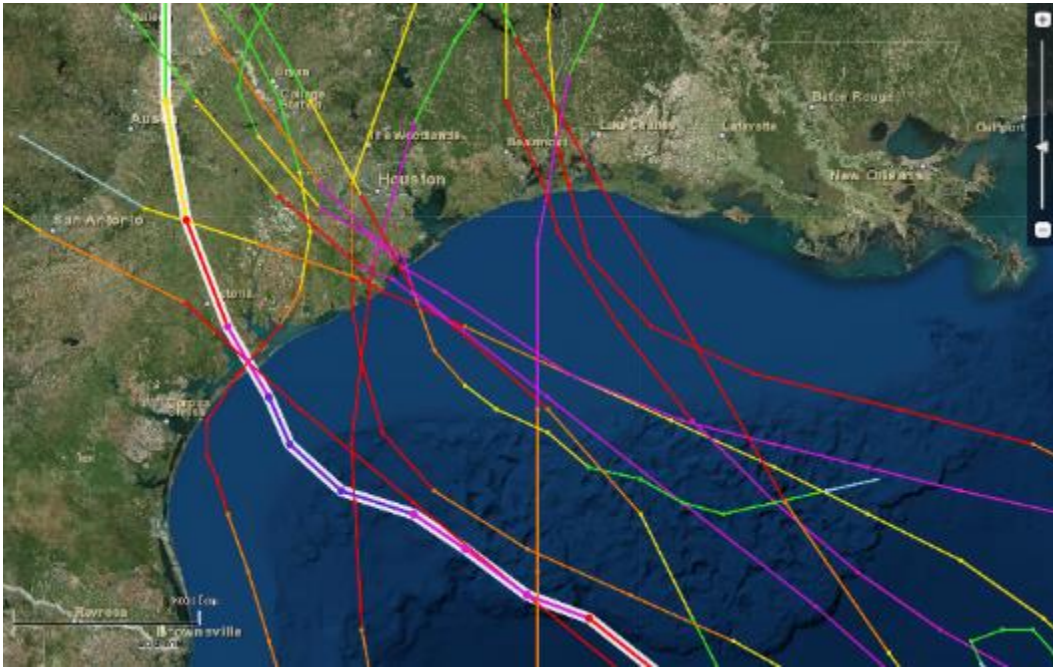


Figure 3-5. Track of the Hurricane Carla in 1961, among other Category 3, 4 and 5 storms.

The track of Hurricane Alicia (1983) is shown in Figure 3-6, along with the track of Carla. The track of Alicia is nearly parallel to the track of Carla, at least over the continental shelf where storm surge is primarily created.

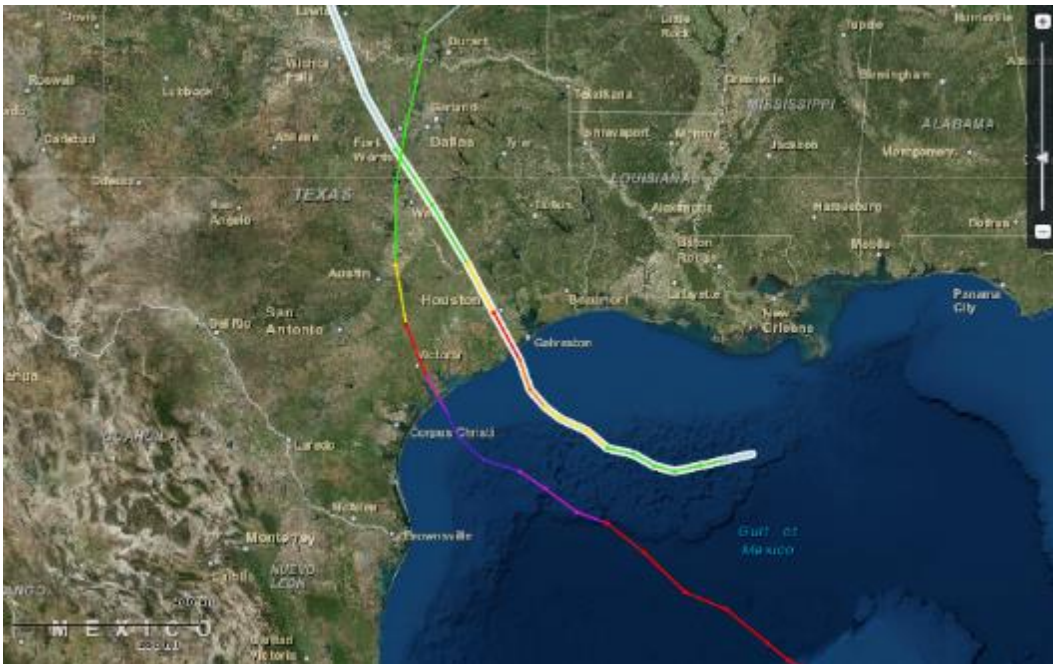


Figure 3-6. Tracks of Hurricanes Carla (1961) and Alicia (1983). Alicia is highlighted.

Hurricane Ike

Hurricane Ike (2008) was considered in the feasibility study. Hurricane Ike is the most recent major hurricane to strike the Texas coast, most people remember it and relate to it. The track for Hurricane Ike is shown in Figure 3-7, among other Category 2 storms in the NOAA Digital Coast data base.

Hurricane Ike was only a Category 2 intensity hurricane (central pressure of 950 mb and a maximum wind speed of 95 kts) as it made landfall and tracked up the center of Galveston Bay. Its maximum winds were around 95 kts for the entire transit across the continental shelf. However its large size was a strong contributor to the high coastal storm surge that was generated. Storm size and intensity are the two most important factors in dictating the magnitude of the open coast storm surge. Hurricane Ike was considered in the storm surge model validation conducted as part of the FEMA flood risk remapping study, so the highest quality wind fields available for the storm will be used.

Hereafter in this document, the 1900 Galveston Hurricane, Hurricane Carla, and Hurricane Ike will be referred to as “historic” storms or hurricanes, in contrast with hypothetical synthetic hurricanes.

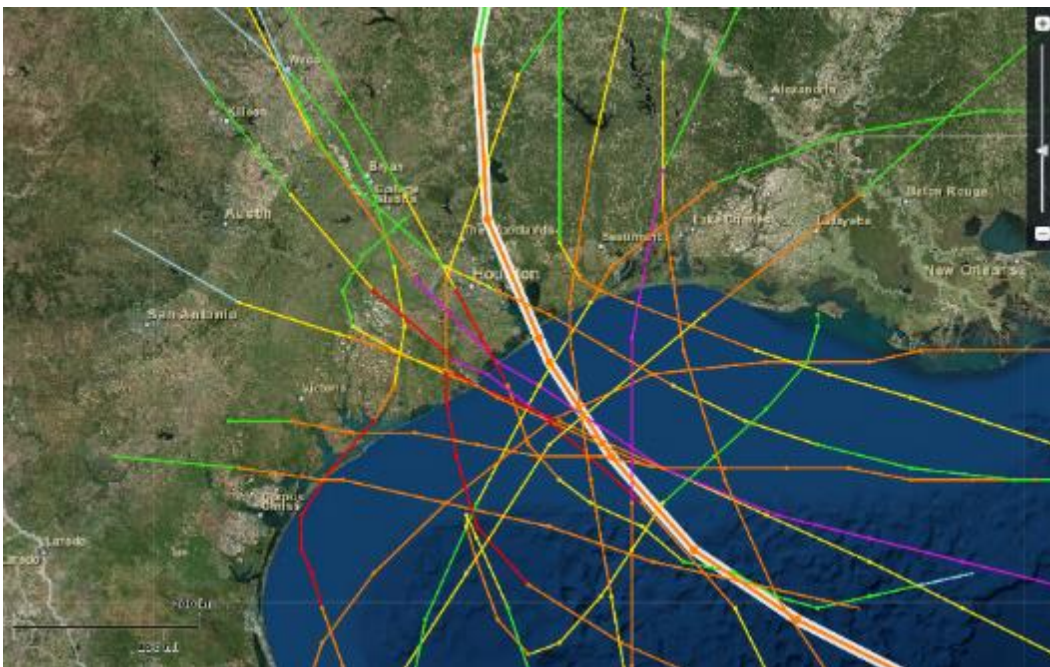


Figure 3-7. Track of the Hurricane Ike in 2008, among other Category 2 storms.

4 The “Bracketing” Set of Hypothetical Synthetic Storms

Initially, a set of 25 hypothetical synthetic hurricanes was simulated. The set includes 21 storms, each on a unique storm track, or trajectory, selected from among those tracks that were considered in the original FEMA Risk MAP studies (FEMA 2011) to update flood insurance rate maps for the Texas and Louisiana coasts. The trajectories at which these storms approach the coast can be divided into three categories.

The first category is the “direct-hit” category. These storms follow the same path and have the same landfall angle of approach, but are of differing central pressures and forward speeds. The radius-to-maximum winds is the same for all four storms. The direct-hit track, shown in Figure 4-1, runs along the western shoreline of Galveston Bay. The direct-hit set was selected to examine the storm surge within the region as a function of primarily intensity, for existing and with-dike conditions. Characteristics of the direct-hit storm set are given in Table 4-1.

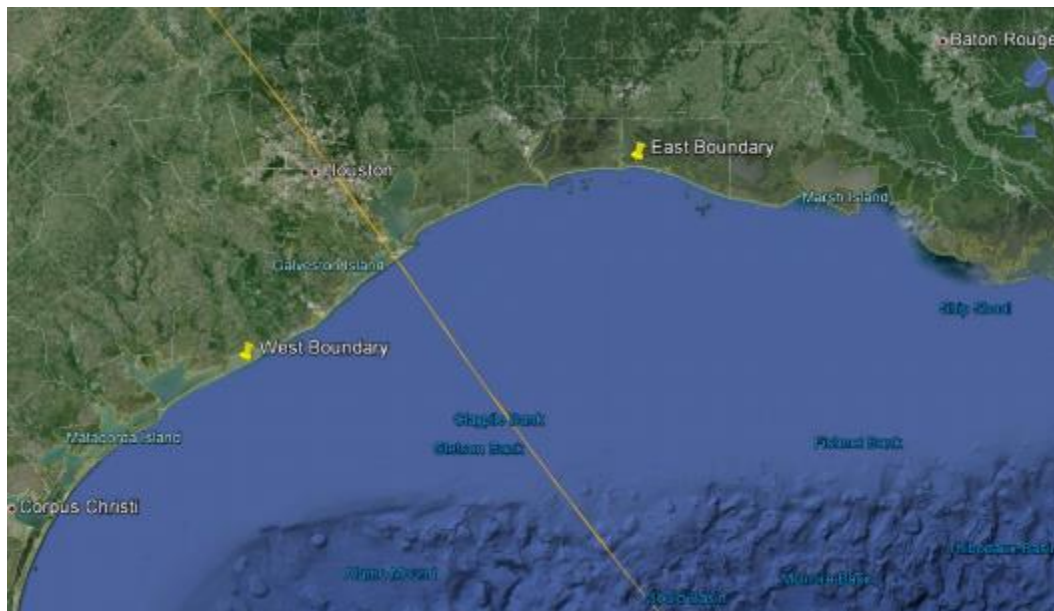


Figure 4-1. Track for all storms in the “direct-hit” storm set

Table 4-1. Characteristics of the direct-hit set.

Storm ID	Landfall		Heading (deg)	CP (mb)	Vf (kn)	Rmax (nmi)
	Lat	Lon				
TEX_FEMA_RUN122.TROP	29.27	-94.84	-35	900	11	17.7
TEX_FEMA_RUN155.TROP	29.27	-94.84	-35	930	17	17.7
TEX_FEMA_RUN121.TROP	29.27	-94.84	-35	960	11	17.7
TEX_FEMA_RUN561.TROP*	29.27	-94.84	-35	975	11	17.7

The second category consists of 12 synthetic storms making landfall at varying locations on Texas' northeastern coast, shown in Figure 4-2. Known as the North Texas set or the TX-12, three originate in the northern Gulf of Mexico off the western coast of Florida, five originate outside the Gulf of Mexico and enter the Gulf of Mexico through the Yucatan Straits between Mexico and Cuba, and the final four originate in the southwestern Gulf of Mexico. The storms all have an identical central pressure of 900 mb, but differ in other parameters, such as the forward speed, radius-to-maximum-winds, and angle (heading) at which the storm makes landfall varying from -41° to 11° . Characteristics of the 12 storms in the North Texas set are given in Table 4-2.

The third and final category of synthetic hurricanes consists of 9 storms making landfall in the vicinity of the north Texas and western Louisiana coast (shown in Figure 4-3). Known as the West Louisiana set or the LA-9, three originate off the coast of southern Florida near the Florida Strait, four originate outside the Gulf and enter the Gulf through the Yucatan Straits between Mexico and Cuba, and two originate in the south central Gulf of Mexico and head west, then take a sharp turn in the northern direction. Like the second category, the North Texas set, these storms all have the same central pressure of 900 mb with other parameters, such as the angle at which the storm makes landfall, varying from -57° to 11° . Characteristics of the 9 storms in the West Louisiana set are given in Table 4-3.

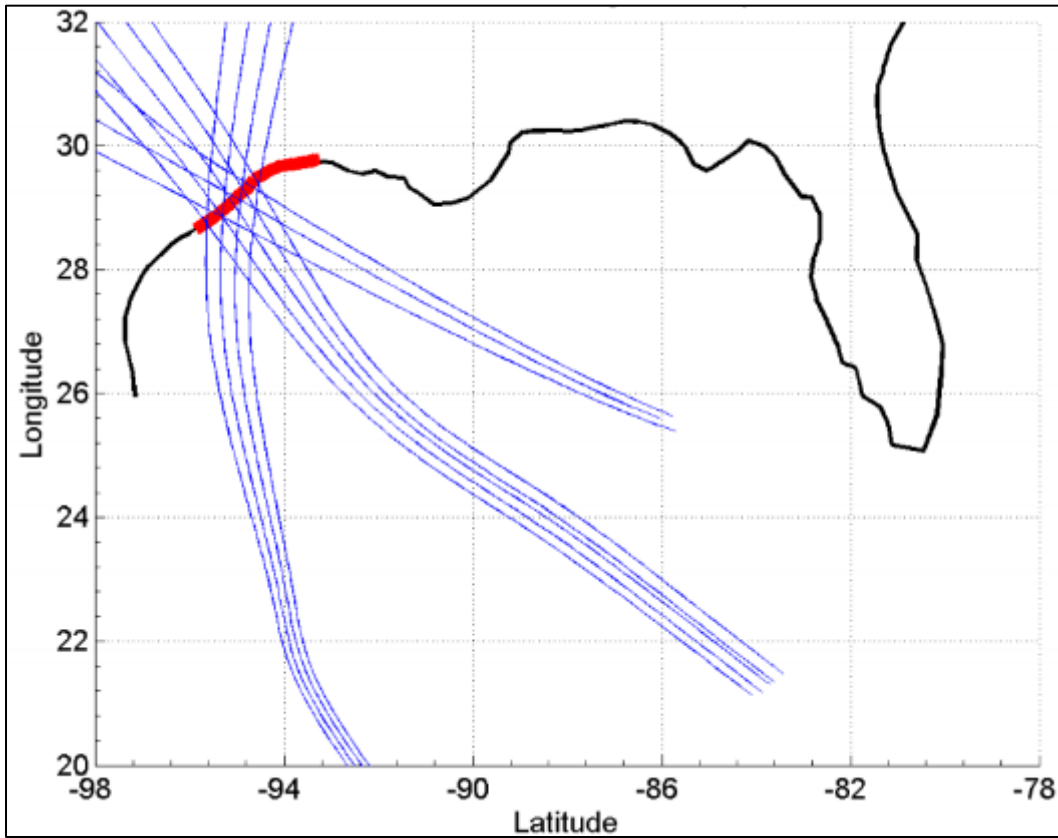


Figure 4-2. Tracks for the 12 storms from the North Texas set

Table 4-2. Characteristics of the 12-storm North Texas set.

Storm ID	Landfall		Heading (deg)	CP (mb)	Vf (kn)	Rmax (nmi)
	Lat	Lon				
TEX_FEMA_RUN027.TROP	28.75	-95.65	-41	900	11	21.8
TEX_FEMA_RUN036.TROP	29.09	-95.09	-37	900	11	21.8
TEX_FEMA_RUN045.TROP	29.46	-94.61	-35	900	11	21.8
TEX_FEMA_RUN057.TROP	28.89	-95.40	-64	900	11	18.4
TEX_FEMA_RUN061.TROP	29.35	-94.72	-64	900	11	18.4
TEX_FEMA_RUN077.TROP	28.96	-95.28	6	900	11	18.4
TEX_FEMA_RUN081.TROP	29.51	-94.50	11	900	11	18.4
TEX_FEMA_RUN128.TROP	29.16	-95.01	-63	900	11	17.7
TEX_FEMA_RUN134.TROP	28.76	-95.64	3	900	11	17.7
TEX_FEMA_RUN136.TROP	29.23	-94.90	8	900	17	17.7
TEX_FEMA_RUN142.TROP	28.91	-95.36	-37	900	6	17.7

TEX_FEMA_RUN144.TROP	29.27	-94.84	-37	900	6	17.7
----------------------	-------	--------	-----	-----	---	------

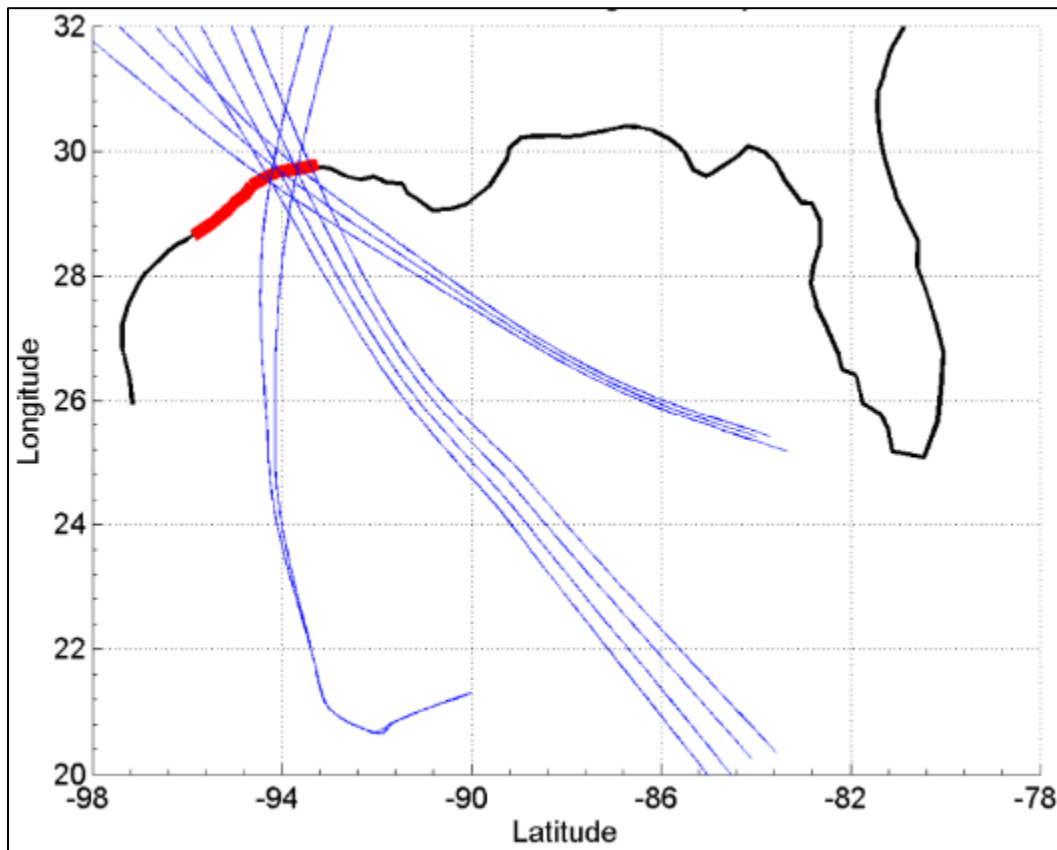


Figure 4-3. Tracks for the 9 storms from the West Louisiana set

Table 4-3. Characteristics of the 9-storm West Louisiana set.

Storm ID	Landfall		Heading (deg)	CP (mb)	Vf (kn)	Rmax (nmi)
	Lat	Lon				
JPM_FEMA_RUN209.TROP	29.59	-94.29	-35	900	11	21.8
JPM_FEMA_RUN218.TROP	29.71	-93.69	-28	900	11	21.8
JPM_FEMA_RUN249.TROP	29.56	-94.37	-57	900	11	18.4
JPM_FEMA_RUN253.TROP	29.72	-93.63	-53	900	11	18.4
JPM_FEMA_RUN269.TROP	29.61	-94.22	11	900	11	18.4
JPM_FEMA_RUN326.TROP	29.68	-94.04	-57	900	11	17.7
JPM_FEMA_RUN332.TROP	29.72	-93.67	11	900	11	17.7
JPM_FEMA_RUN338.TROP	29.67	-94.05	-30	900	6	17.7
JPM_FEMA_RUN340.TROP	29.76	-93.39	-26	900	6	17.7

The twelve storms comprising the North Texas set are shown with pink tracks in Figure 4-4; the nine storms comprising the West Louisiana set are shown with green tracks in Figure 4-4. The spacing between tracks, at landfall, is approximately 20 miles. Figure 4-4 shows the storm numbering scheme that is used throughout this report. The storm numbers are also indicated in the storm ID, which is the first column of Tables 4-1, 4-2 and 4-3.

Most of the storms in the bracketing set have central pressures of 900 mb. The hurricane wind and pressure model using in this feasibility study simulates a decrease in storm intensity and an increase in the radius to maximum winds just before landfall (a process call storm filling). This filling process has been observed for severe storms. As a result of storm filling, the central pressure at landfall for these 900-mb storms ranges from approximately 910 mb to 920 mb. These are severe hurricanes, all having maximum wind speeds of about 125 kts, or of Category 4 intensity on the Saffir-Simpson wind intensity scale. Central pressure is highly correlated to maximum wind speed. In terms of intensity, these storms are generally more severe than those that have occurred along the Texas coast over the

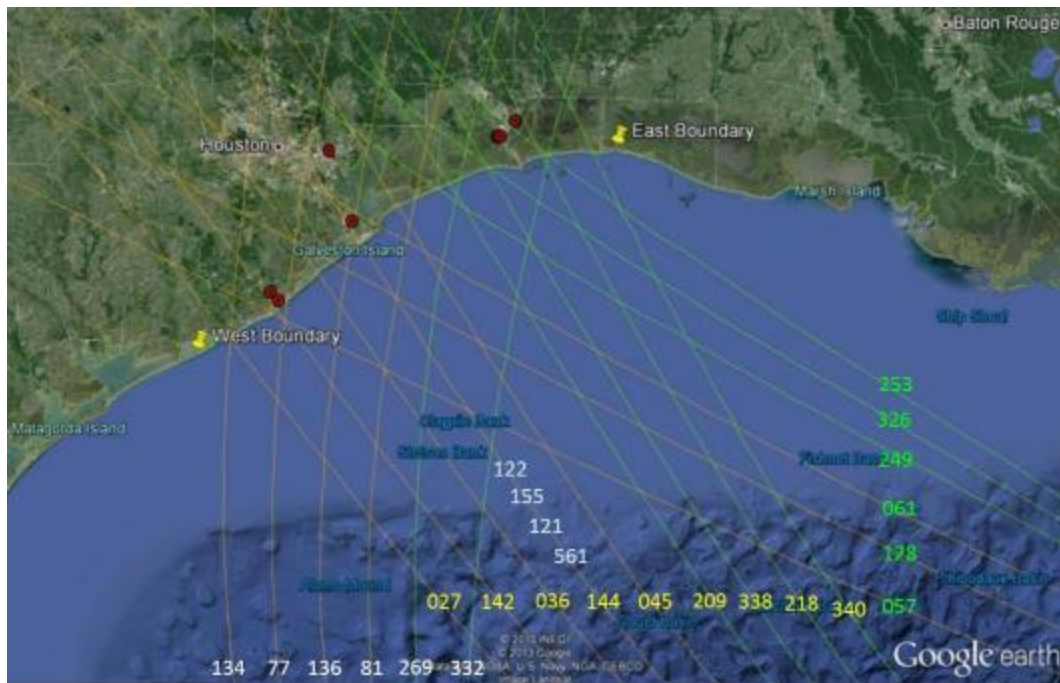


Figure 4-4. Storm tracks for the Texas set (In pink) and the Louisiana set (In green).

past 140 years (see Figure 1), with the notable exception of Hurricane Carla in 1961, which reached Category 5 as it moved across the continental shelf then weakened to Category 4 intensity at landfall.

5 Hurricane Surge Generation on the Open Coast – Causative Factors

What Causes a Storm Surge?

Hurricanes are intense storms that originate in tropical waters and derive their energy from warm water. They weaken in intensity when the heat source is diminished or removed, which occurs when the storm passes over cooler water or when winds are blowing over land. Hurricanes also can be weakened by vertical wind shear. Hurricanes are low-pressure systems, in which winds spin counterclockwise (in the northern hemisphere) around the storm's center, or eye. A hurricane's intensity is measured by its maximum wind speed and central pressure; the two are strongly correlated. Hurricane intensity, size, path, and speed of movement all change with time during any particular event. Hurricane characteristics can vary widely from storm to storm.

Storm surge is defined here as an anomalous increase in the water level associated with a coastal storm. Storm surge is a long wave that is primarily forced by wind and to a lesser degree by spatial gradients in atmospheric pressure and momentum fluxes associated with waves, particularly in the surf zone.

The modeling being used in this feasibility study to simulate the development of storm surge treats each of these contributions to storm surge, as described below.

Wind

Wind exerts a shear stress on the water surface, which acts to push water in the direction of the wind. Shear stress is a nonlinear function of the wind speed, i.e., it is related to wind speed raised to the second or third power, depending on the formulation of wind drag coefficient used to calculate surface stress for different wind speeds. For example, an increase in wind speed by a factor of 2 will increase the surface shear stress by a factor of 4 to 8. The contribution to storm surge caused by wind stress is called wind set-up.

Wind is most effective in creating a set-up (increase) in the water level when it blows over shallow water because, in the balance of momentum, the effective wind stress is inversely proportional to water depth. Therefore storm surge is mostly generated on the continental shelf, in the shallow nearshore coastal region and in shallow bays and estuaries. Wind is much less effective in creating wind set-up in deep water. The magnitude of wind set-up depends on the fetch, or the distance over which a wind blows, in addition to the duration or persistence of winds.

Atmospheric Pressure

An elevated water surface dome is created under the center of a low pressure storm system, which contributes to the storm surge. Atmospheric pressure is the weight of air above the water. In regions of high pressure (at the storm periphery), the force pushing down on the water is greater than the force over regions of low pressure (storm center). This horizontal gradient in atmospheric pressure forces water to move from regions of higher pressure toward regions of lower pressure. Water is forced toward the eye of the hurricane, which creates the dome of water. The amplitude of this contribution to storm surge is dependent upon the magnitude of the difference between the peripheral and central pressures; but it can be as much as several feet for a major hurricane. This pattern of water movement is not static; instead, it moves with the translating hurricane.

Waves

Storm winds also result in the generation of energetic short-period waves, which at elevated water levels can pose a significant coastal flood hazard and cause structural damage. Similar to the generation of wind set-up, storm wave characteristics (height, period, and direction) are strongly influenced by wind speed and direction, fetch, and the persistence of wind from a particular direction. Higher wind speed, greater fetch distance and longer duration generally lead to greater wave energy (higher wave height) and longer wave periods. However, unlike storm surge, waves are very effectively generated in deep water and the most energetic waves are usually found in deeper water. Waves generated by a hurricane propagate outward away from the storm in all directions. Along the open coast, severe hurricanes typically generate significant wave heights of 15 to 30 ft, with typical peak wave periods of 10 to 15 sec. In more sheltered areas, storm wave heights and wave periods are generally smaller.

As obliquely incident wind waves propagate into shallow water their propagation speed slows, they begin to “feel” the bottom, turn and seek to align themselves in such a way that wave crests approach in a direction increasingly more parallel to the shoreline. In the absence of wind energy input this refraction process generally causes a decrease in wave height, although complex irregular bathymetry can create patterns of locally increased and decreased wave height. Some wave energy is dissipated due to bottom friction and white-capping. But generally during hurricanes, strong onshore winds continue to act as an energy source offsetting energy losses associated with these other processes.

As waves propagate into even more shallow water, they shoal, steepen and eventually break, dissipating energy much more strongly. In response to this depth-induced dissipation, significant wave height decreases. In the inner surf zone, despite the presence of high winds, wave energy becomes saturated and the local significant wave height is generally limited to values of 0.4 to 0.6 times the local water depth. Wave height can be smaller if wind input is reduced and energy is dissipated by vegetation or diminished in some other way due to sheltering or disruption of wave propagation by buildings, other landscape features, or by debris.

Wave transformation and breaking is strongly dependent upon the local water depth. If the storm surge significantly changes the local water depth, wave transformation and breaking processes will be altered accordingly. Increases in water depth associated with increases in storm surge generally enable greater wave energy (height) to be present locally.

As waves break on a beach in very shallow water, wave heights decrease and the flux of wave momentum in the onshore direction is reduced. This change in wave momentum is balanced by an increase in the mean water level, a contribution to the storm surge called wave setup. Wave setup is usually treated in engineering analysis as a “mean” (in time) quantity that varies every half hour or hour as the incident wave conditions change.

The magnitude of wave setup is greatest right at the shoreline, and the maximum value is roughly 10 to 20% of the incident significant wave height at the seaward edge of the surf zone, i.e., the breaking wave height. For example, incident waves having a significant height of 20 ft can force a maximum wave setup at the shoreline of 2 to 4 ft. Wave setup produces an additional increase in the storm surge elevation, which in turn exacerbates

wave runup on beaches and structures and increases the potential for inundation and subsequent propagation of waves over inundated terrain.

Storm Surge along the Texas Coast

In addition to atmospheric pressure and wave effects, storm surge along the north Texas coast is strongly influenced by two wind-forced contributors. One is the development of a wind-driven surge forerunner, an Ekman wave that develops as along-shore moving water on the continental shelf forced by the hurricane's peripheral winds which is then directed onshore by the Coriolis force even while the storm is well offshore. The second contributor is the direct effect of the highest winds in the core of the hurricane as it crosses the continental shelf and approaches landfall, pushing the shelf waters toward the coast and into the bay.

Within Galveston Bay, storm surge is highly dependent upon infilling that occurs due to surge propagation over the low barrier islands and through the passes linking the Gulf of Mexico to Galveston Bay and West Bay, and by local wind-set up. For the bracketing set of 25 storms, the maximum simulated water surface elevation was 25 ft NAVD88 in the upper reaches of the Houston Ship Channel. Peak surge can vary significantly within Galveston Bay, depending on storm track and location.

Surge Forerunner

In a broad sense, a hurricane forerunner is a rise in the water surface elevation at the coast when the eye of the hurricane is far offshore in very deep water, and which is not directly attributable to the strong core winds closer to the eye of the storm. Several contributors to the forerunner have been identified, including the hurricane's far-field winds as well as other wave dynamics associated with the fact the Gulf of Mexico is a nearly enclosed basin, but forced by the flux of water through the Florida Straits and the Yucatan Straits. The Coriolis force, which acts on moving water and is associated with the rotation of the earth, is a critical factor in development of the forerunner.

Ekman Wave Formation

Kennedy et al (2011) described and documented well what appears to be the most significant contribution to the forerunner, or mechanism driving the forerunner, along the northwest Texas Gulf coast. They identified the forerunner during Hurricane Ike through measurements, and verified it using modeling and analysis. This mechanism is the development of a

wind-driven surge forerunner, an Ekman wave, that develops as along-shore moving water on the continental shelf forced by the hurricane's peripheral winds, then directed onshore by the Coriolis force (to the right in the northern hemisphere) even while the storm is well offshore. Kennedy et al (2011) found that this contribution to the water surface elevation steadily increased over a period of several days before Ike's landfall and reached approximately 6 feet in amplitude.

Figure 5-1, from Kennedy et al (2011), shows the measured water surface elevation during Hurricane Ike which was recorded at a gage located on the open coast, in shallow water, just east of Bolivar Peninsula. Measured water surface elevations are shown in black, results of a storm surge model simulation with the Coriolis force turned on are shown in red, and results from a model simulation without Coriolis forcing are shown in blue. Measured data show a steady rise in water level beginning 2 days prior to landfall, when the storm was located in the deep water region of the Gulf. The forerunner gradually increased to an elevation of approximately 6 ft (2 meters) at a time 12 hours prior to landfall, after which the core winds of the storm began to dominate the surge response along the coast. Without Coriolis forcing included in the model, the forerunner could not be simulated at all.

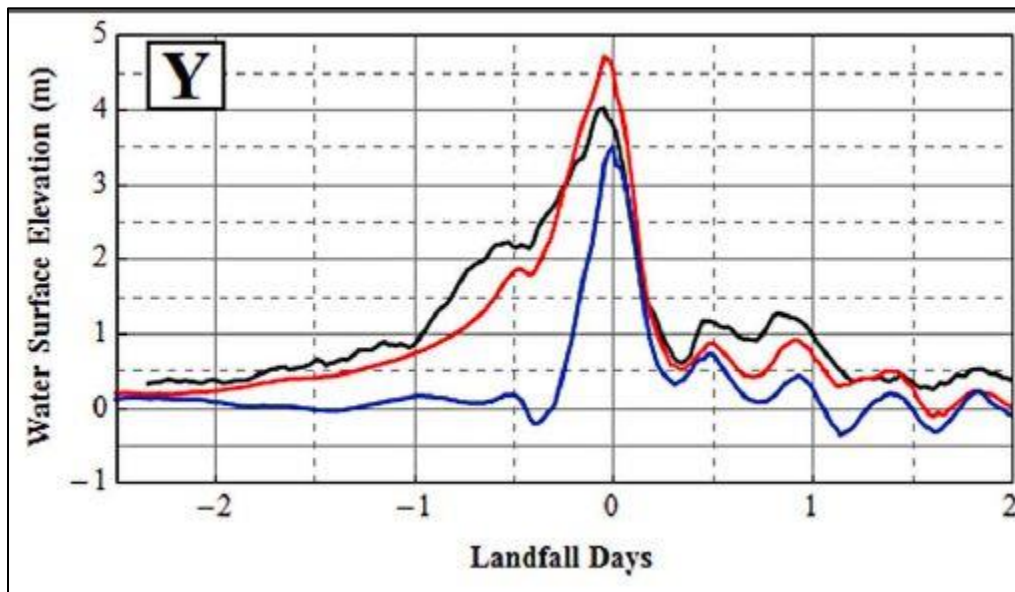


Figure 5-1. Water surface elevation measurements made during Hurricane Ike that show the wind-driven forerunner, from Kennedy et al (2011)

The work of Kennedy et al (2011) showed the importance of the wide continental shelf off the Louisiana-Texas coast in development of the Ekman wave, forced initially by the wind, which then propagates along the shelf to the south as a free wave once the wind forcing subsides. Because of the generation mechanism involved, the counterclockwise rotation of winds about the hurricane eye, and the wide continental shelf along the Louisiana and north Texas coasts, conditions are generally favorable to force a significant forerunner for all major hurricanes that approach the coast along the northwest Gulf of Mexico.

Figure 5-2 shows the Gulf of Mexico bathymetry, where the shallower depths on the shelf are shown as the color-shaded contours. The shallow areas with colored contours reflect the location and varying width of the continental shelf around the periphery of the Gulf. The very deep portion of the Gulf, beyond the continental shelf, is indicated by the monochrome maroon colored area. As stated previously, winds are only important in generating a storm surge on the shelf and in adjacent shallow coastal and bay waters. The extensive shelf situated along the northwestern Gulf coast is a critical factor in the development of the forerunner, and storm surge in general, in the Houston-Galveston region.

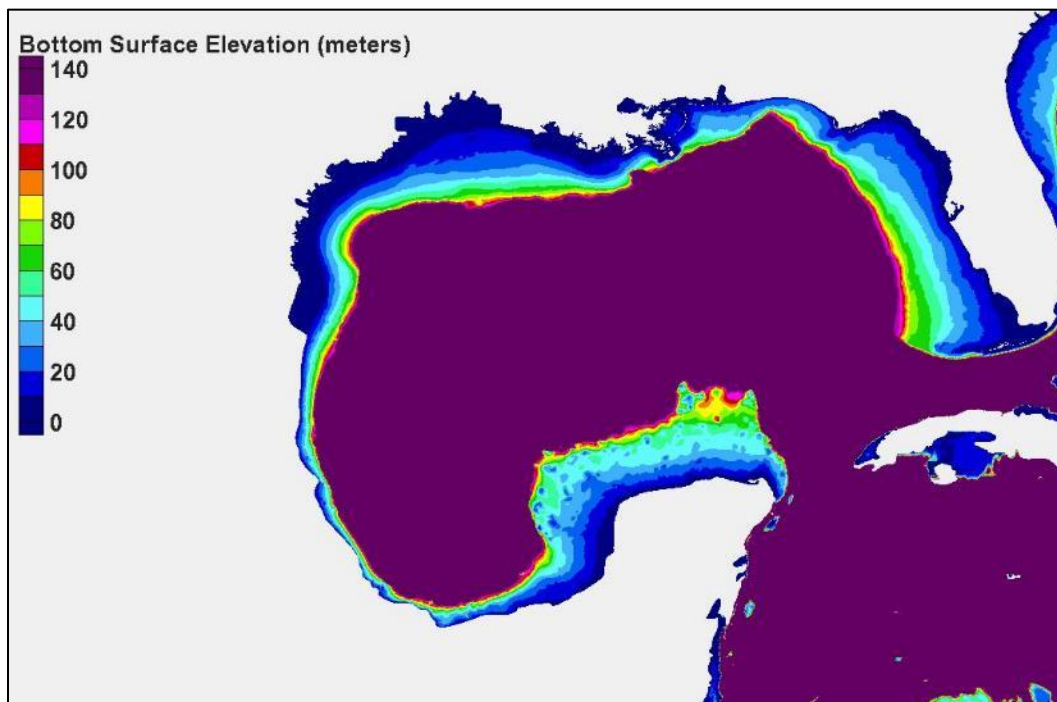


Figure 5-2. Bottom surface elevation in the Gulf of Mexico

Volume Mode Oscillation

In a study funded by the U.S. Army Corps of Engineers, Bunpapong et al (1985) identified other contributors to the forerunner in the Gulf of Mexico, arising from physical processes other than far-field winds blowing along the shelf. For the Texas coast near Galveston, they found one mechanism in particular to be more significant than several others they identified.

Using model simulations and measured water surface elevation data from tide measurement stations located around the periphery of the Gulf, for Hurricanes Carla (1961) and Allen (1980), they showed that as a hurricane enters the Gulf of Mexico, an in-phase difference in the magnitude of the volume of water entering/leaving the Florida and Yucatan Straits (both in or both out), a volume mode or Helmholtz type of oscillation is excited throughout the entire Gulf. For this mode of oscillation, the water surface of the entire Gulf rises and falls in phase, with a nearly uniform amplitude throughout the Gulf. The flux of water through the Straits is driven by both wind and the atmospheric pressure gradient associated with the storm, with the latter forcing water from regions of high atmospheric pressure toward the low-pressure center of the hurricane. They found that the effect of wind-driven transport was the most important.

Bunpapong et al (1985) found that for hurricanes, having a central pressure deficit of 80 mb and a radius to maximum winds of 16 n mi, which entered the Gulf through the Yucatan Straits on a straight track resulting in landfall on the Texas coast, a forerunner was generated at Galveston that had an amplitude of approximately 0.7 ft. A hurricane with an 80-mb pressure deficit is akin to a hurricane having a central pressure of approximately 930 mb and a far-field pressure of 1010 mb. They found that for larger storms, having the same pressure drop of 80 mb but radius to maximum winds of 32 n mi, the amplitude of the volume mode oscillation doubled to 1.3 ft. For pressure drops of 40 mb and 120 mb, and the larger radius to maximum winds of 32 n mi, they found amplitudes of 0.7 and 2 ft, respectively. They found that the hurricane path and evolution play important roles in dictating the amplitude of the forerunner.

A significant forerunner was not always generated; the amplitude depended on storm track, intensity and size. They showed that for hurricanes of lesser intensity when entering the Gulf through the Florida

Straits, and for hurricanes originating within the Gulf, the amplitude of this volume mode along the Texas coast was less than when an intense storm enters through the Yucatan Straits.

For this particular contribution to the forerunner, the timing between this volume mode oscillation and the primary wind induced surge generated at the coast determines whether or not this mode oscillation contributes to the peak surge or detracts from it. This will depend upon the relative timing of the two contributors, which is strongly influenced by the hurricane's forward speed. Bunpapong et al (1985) found that increasing forward speed produced a significant increase in peak open coast surge along the Texas coast, but that different forward speeds had little effect on the amplitude of the volume model oscillation.

The follow-on work plan proposes to further examine the effect of this forerunner mechanism on peak surge in the Houston-Galveston region, confirming the maximum amplitude of this mechanism for intense storms that enter the Gulf, examining sensitivity of the amplitude to location of entry into the Gulf (which influences the Strait fluxes driven by the wind), the prevalence of this phenomenon, the likelihood that it can be an additive effect to the open coast surge, and the influence of forward speed on peak surge.

An Example of Forerunner Development: Direct-hit Storm 122

The model simulation for Storm 122, a direct-hit storm having central pressure of 900 mb at its most intense stage, a forward speed of 11 kts, and a radius to maximum winds of 17.7 n mi, is used to illustrate development of the hurricane surge forerunner. This storm originated outside the Gulf and entered through the Yucatan Straits, at its northernmost point. However, its central pressure as it entered the Gulf through the Yucatan Straits was not very intense, only 980 mb with a far field pressure of 1013 mb; i.e., a pressure deficit of only 33 mb.

The modeling of surge being done in this feasibility study should be able to simulate the volume mode oscillation identified by Bunpapong et al (1985). Both the wind and atmospheric pressure gradient forcing are being simulated in the storm surge modeling and water flux through both Straits is being well simulated since the surge model's open water boundaries are located in the middle of the Atlantic Ocean. Because Storm 122 is not very intense as it enters the Gulf, and because the wind-driven water flux is directed out of one Strait and into the other as a result of its

entry location, the amplitude of the volume mode contribution to the forerunner is expected to be small for this storm, on the order of a few tenths of a foot at most, based on the results of Bunpapong et al (1985).

Figure 5-3 shows the simulated Gulf-wide field of water surface elevation and wind vectors for Storm 122 just before its entry into the Gulf, almost 3 days before making landfall at Galveston. At this point in time the central pressure of the storm is 980 mb. The initial water surface elevation for this simulation is about 0.9 ft NAVD88, or approximately 0.4 ft above mean sea level to account for steric increases in Gulf water levels during the summertime hurricane season. The very small circular light blue area just south of Cuba reflects a small dome of water beneath the eye of the hurricane that is forced by atmospheric pressure gradients which push water toward the storm center.

Figure 5-4 shows the water surface elevation and wind vectors for Storm 122, about a day later, 2 days prior to landfall. At this point in time the storm's central pressure is 942 mb. The counterclockwise rotation of wind vectors about the eye of the storm is quite evident. The dome of water under the eye of the storm has grown, having a maximum water surface elevation of more than 3 ft NAVD88, 2 to 2.5 feet above mean sea level. The dome is following the eye of the storm as it transits across the Gulf toward the Texas coast.



Figure 5-3. Water surface elevation and wind vectors in the Gulf of Mexico nearly 3 days before landfall for Storm 122 (direct-hit track, 900 mb)

Also evident are increasing water surface elevation along sections of the Gulf coast where the winds are blowing along the continental shelf, the shelf is widest, and a Kelvin wave is being forced. The figure clearly shows the development of this wind driven contribution to the forerunner, along the Louisiana-Texas coast; it's also evident along other regions of the Gulf having a wider continental shelf where winds blow along the coast. Along the north Texas coast, the increase in water surface elevation is approximately 1 ft. Also note the near uniform increase in water surface elevation through the Gulf, compared with the elevation in the previous figure. This appears to be associated with the volume model of oscillation, forced by entry of the storm into the Gulf about a day earlier.

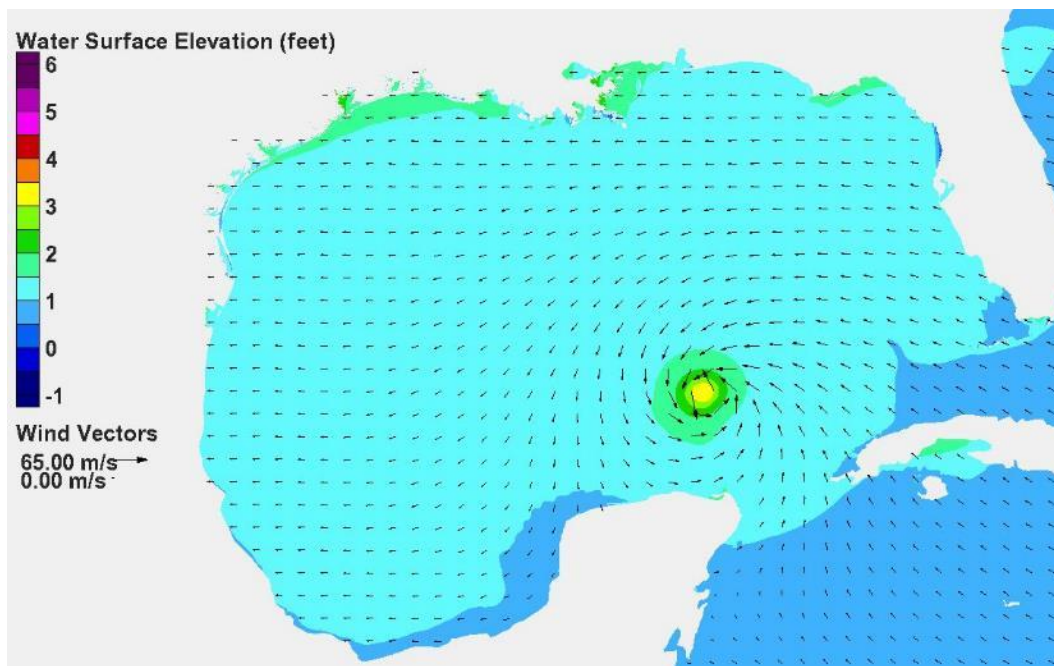


Figure 5-4. Water surface elevation and wind vectors in the Gulf of Mexico 2 days before landfall for Storm 122 (direct-hit track, 900 mb)

It should be noted that in these idealized synthetic hurricane simulations the hurricane is the only meteorological system in the Gulf; there are no other weather systems. So winds throughout the Gulf are only influenced by the hurricane and its forward speed as calculated by the planetary boundary layer wind model being used in the simulations. Along the northern Gulf coastline, winds blow along the coast from the east due to the counterclockwise wind circulation about the eye and its forward speed.

Figure 5-5 shows the water surface elevation and wind vectors for Storm 122, one day prior to landfall. The dome of water under the eye of the storm has grown as the storm intensifies to its minimum central pressure

of 900 mb. The maximum water surface elevation within this dome is greater than 4 ft NAVD88, 3 to 3.5 feet above mean sea level. Along the north Texas coast, due to the wind-driven forerunner, the increase in water surface elevation is approximately 1.5 to 2 ft above mean sea level.

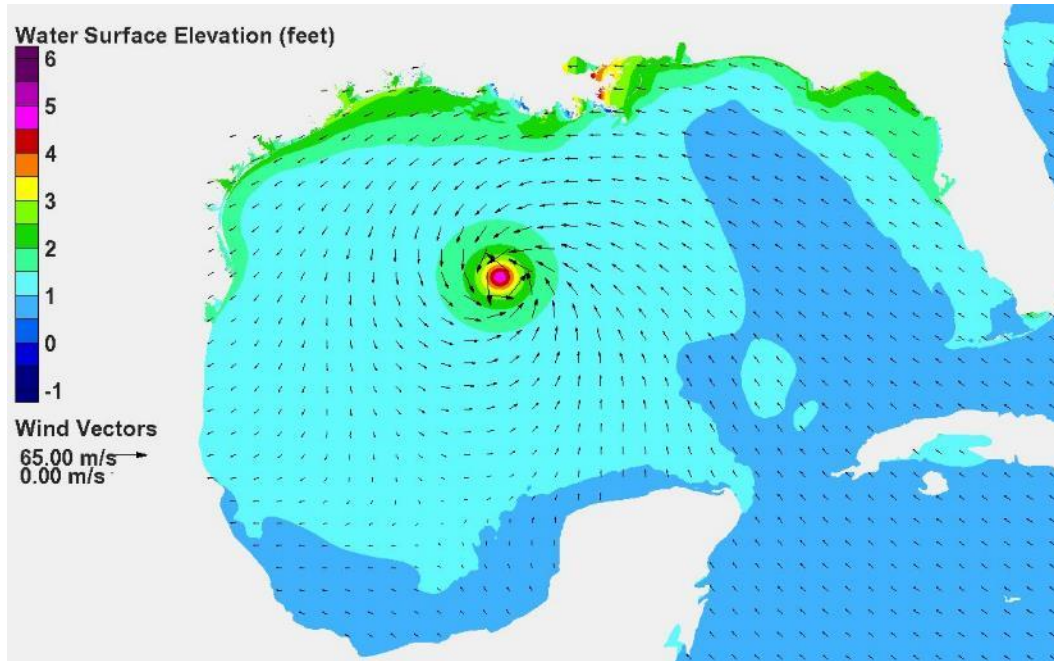


Figure 5-5. Water surface elevation and wind vectors in the Gulf of Mexico one day before landfall for Storm 122 (direct-hit track, 900 mb)

Figure 5-6 shows the water surface elevation and wind vectors for Storm 122, 12 hours after landfall. The hurricane has moved inland, the wind forcing is diminished and changed in direction, yet the water surface remains elevated along many coastal areas where the shelf is wide. This observation is consistent with the finding of Kennedy et al (2011) that the Kelvin wave becomes a free wave, moving along the shelf, after the wind forcing diminishes.

Figure 5-7 shows the water surface elevation and wind vectors for Storm 122, one day after landfall. The hurricane has moved well inland, and the wind forcing has decreased further. Evidence of the forerunner along the coast where the shelf is widest persists.

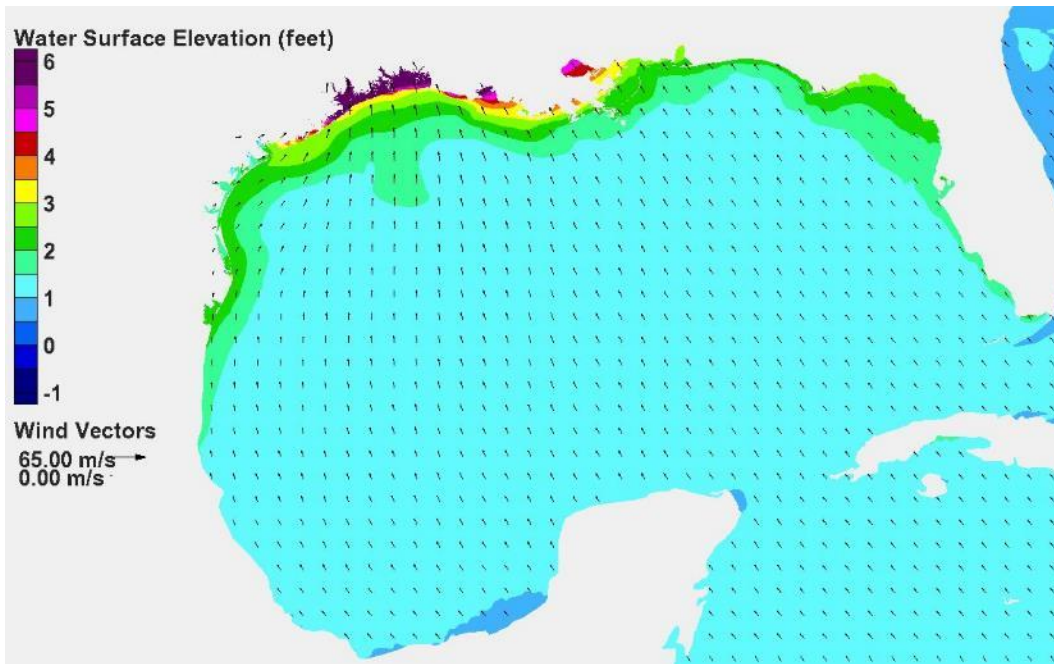


Figure 5-6. Water surface elevation and wind vectors in the Gulf of Mexico 12 hours after landfall for Storm 122 (direct-hit track, 900 mb)

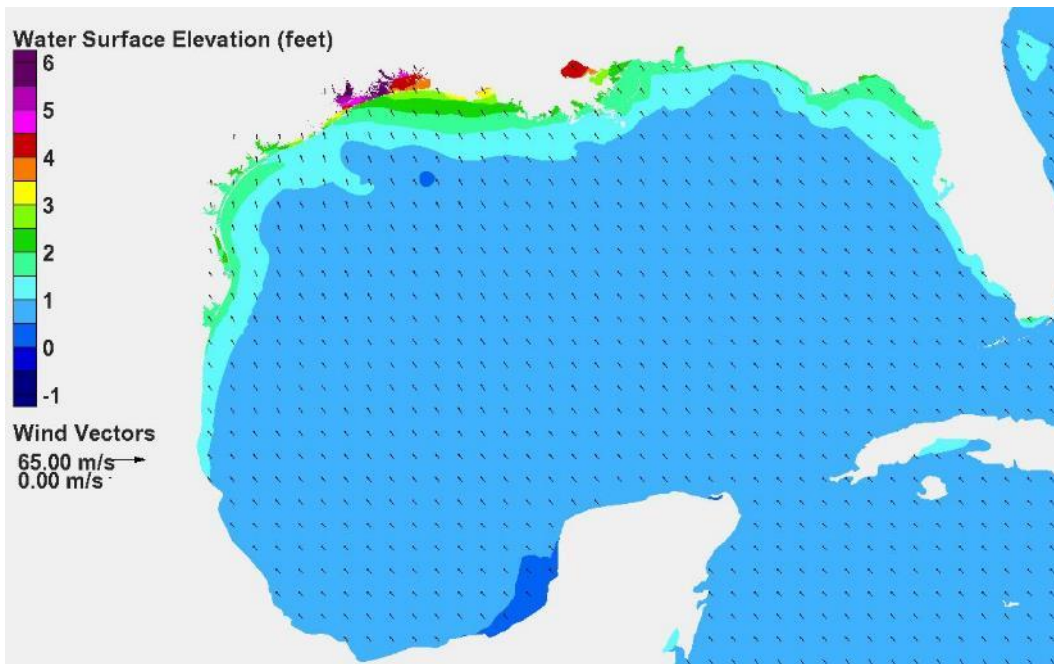


Figure 5-7. Water surface elevation and wind vectors in the Gulf of Mexico one day after landfall for Storm 122 (direct-hit track, 900 mb)

Comparing Figure 5-7 with Figure 5-6, snap-shots in time separated by 12 hours, a nearly uniform change in water surface elevation throughout the entire Gulf is evident. The entire Gulf water surface has decreased during this 12-hour period of time. Comparing Figure 12 prior to the hurricane entering the Gulf, with Figure 13 reflecting conditions a day later, a uniform increase in water surface elevation Gulf-wide also is evident. The color changes suggest an increase and decrease of about the same magnitude. This type of change is consistent with the volume mode, or Helmholtz, type of oscillation identified by Bunpapong et al (1985).

To further illustrate the development of the forerunner, Figure 5-8 shows the temporal variation of water surface elevation through time, during the first 60 hours of the simulation, at three locations: the open coast at Galveston (Pleasure Pier), inside Galveston Bay near the Clear Lake area along the western shoreline, and well into the Houston Ship Channel. The figure shows a slow steady increase in water surface elevation associated with the wind-driven Ekman wave, an increase of about 2 ft during the first 2 days, then nearly another foot of rise over the next 10 hours. The rate at which the surge builds noticeably increases at hour 50 as the storm winds over the continental shelf increase. Landfall occurs at hour 70. Also evident is the penetration of the forerunner into Galveston Bay for this storm. Elevations are higher inside the Bay due to an additional contribution of wind setup, where winds from the northeast set up the western side of the Bay by an additional 0.5 ft.

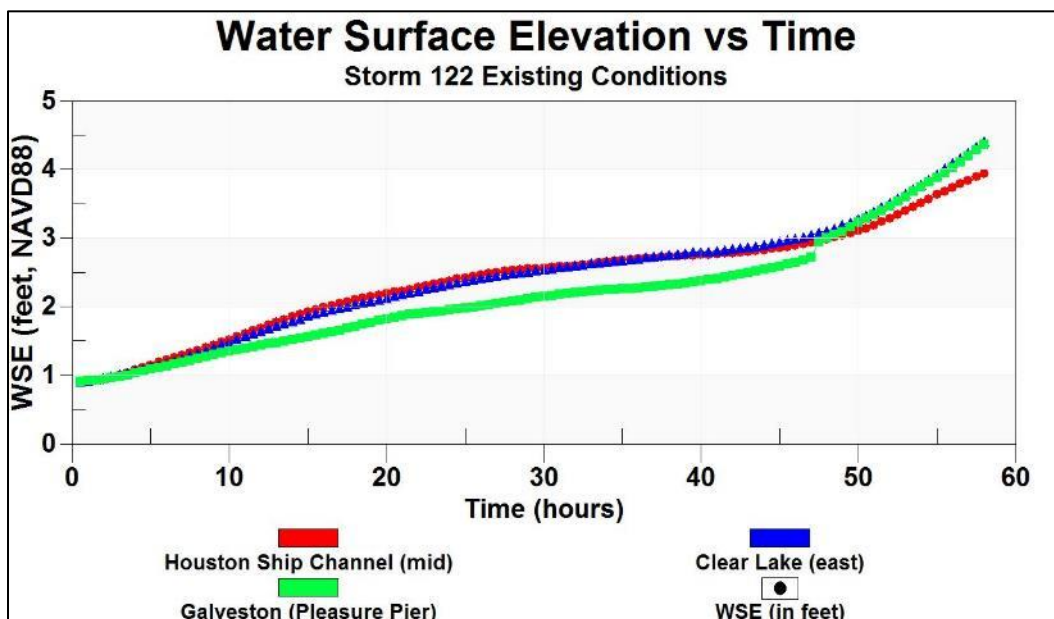


Figure 5-8. Temporal variation of water surface elevation showing forerunner development.

Surge Generation by the Core Winds

As the eye of the storm approaches the continental shelf, the stronger winds in the core of the storm, closest to the eye, begin to dominate the generation of the surge on the shelf. Winds are most effective in pushing water in the relatively shallow depths on the shelf, and, since the relationship between wind speed and surface wind stress is highly nonlinear, they become increasingly more effective as the hurricane moves toward shore into shallower and shallower water. . The increasing wind speed and resulting surface stress, and the presence of increasingly more shallow water causes the effect of the wind stress on the shelf and near the coast to increase dramatically as the hurricane moves towards the coastline. These processes are illustrated via the series of water surface elevation-wind snapshots for Storm 122 in Figures 5-9 through 5-13, which show the developing storm surge for the 12-hour period prior to landfall.

Figure 5-9 shows conditions 12 hours prior to landfall. The forerunner effect on the shelf and at the coastline are evident. The forerunner has increased the water surface elevation to nearly 4 ft NAVD88 along the coastline. Also evident is the effect of wind in the very shallow Galveston and West Bays, setting up the water surface on the downwind side (southwest side) of each bay due to winds blowing from the northeast.

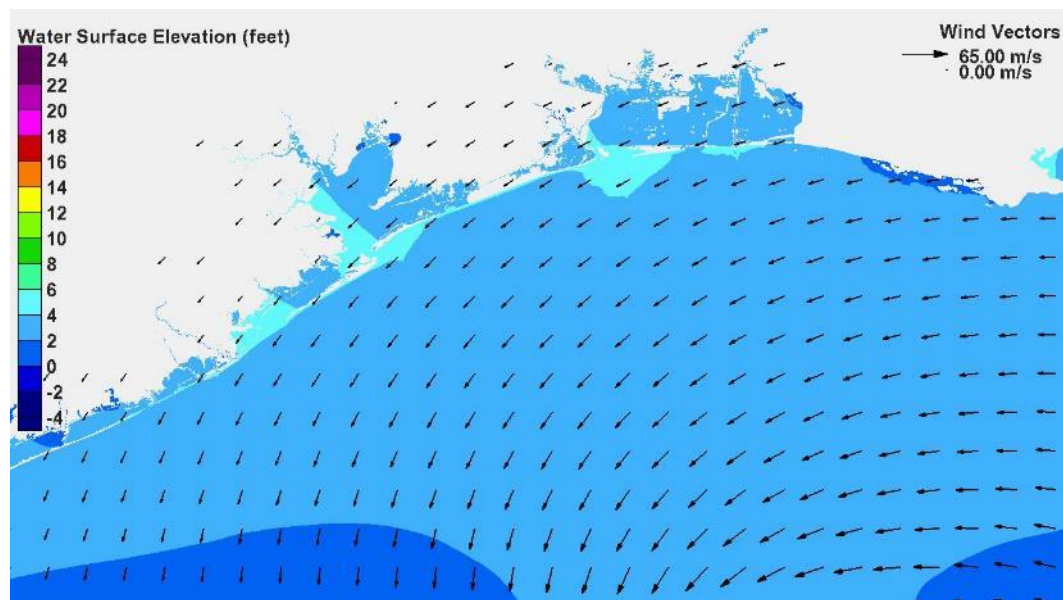


Figure 5-9. Water surface elevation and wind vectors 12 hours before landfall for Storm 122 (direct-hit track, 900 mb)

Figure 5-10 shows conditions 3 hours later, at a time 9 hours prior to landfall at Galveston. The eye of the hurricane is clearly visible, as evidenced by the counterclockwise wind circulation around the eye. The dome of water beneath the eye which is forced by the atmospheric pressure gradients is visible. Also evident is the increase in surge in the right front quadrant of the storm (viewed relative to the direction of storm advance). This is the zone where the surface winds have their maximum speed and greatest surge building capacity. Surge is building farther out on the shelf due to the higher core winds and decreasing water depth. The wind-driven surge on the shelf associated with the core winds is beginning to merge with the surge that has been forced as a forerunner closer to the shore.

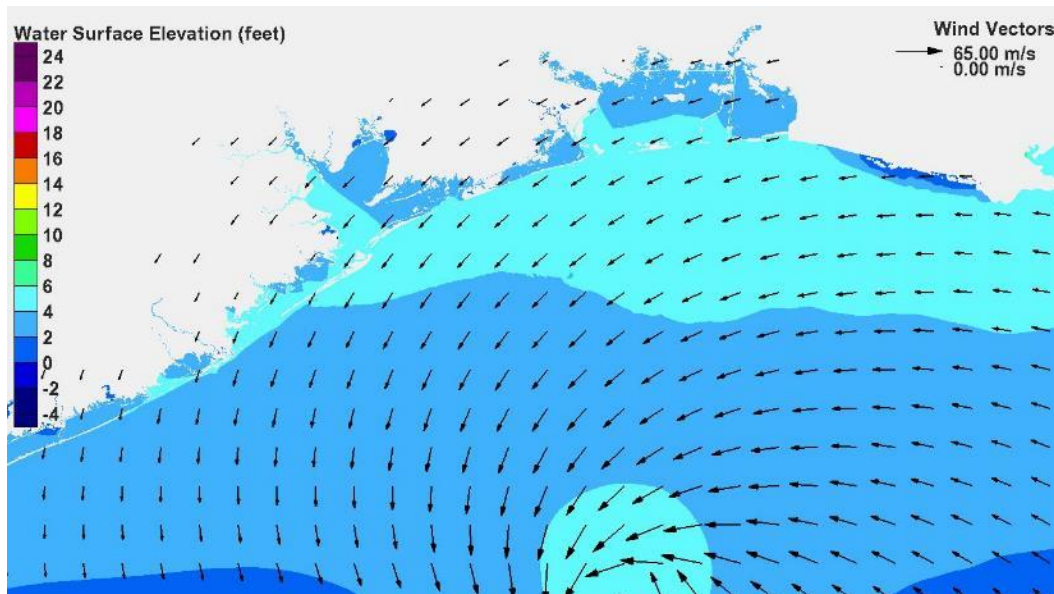


Figure 5-10. Water surface elevation and wind vectors 9 hours before landfall for Storm 122 (direct-hit track, 900 mb)

Figure 5-11 shows conditions 3 hours later at a time 6 hours before landfall. As the core winds move into increasingly more shallow water, surge on the shelf is increasing. The surge generated by the core winds is merging with the forerunner surge.

The same pattern of surge evolution is shown in Figure 5-12, three hours later, at a time 3 hours prior to landfall. The surge associated with the core winds and the forerunner have now merged. The core winds are producing waves, and have been even when the storm center was in deep water. The wave setup created by breaking waves is also contributing to

the storm surge, but the storm surge is now primarily being forced by the core winds.

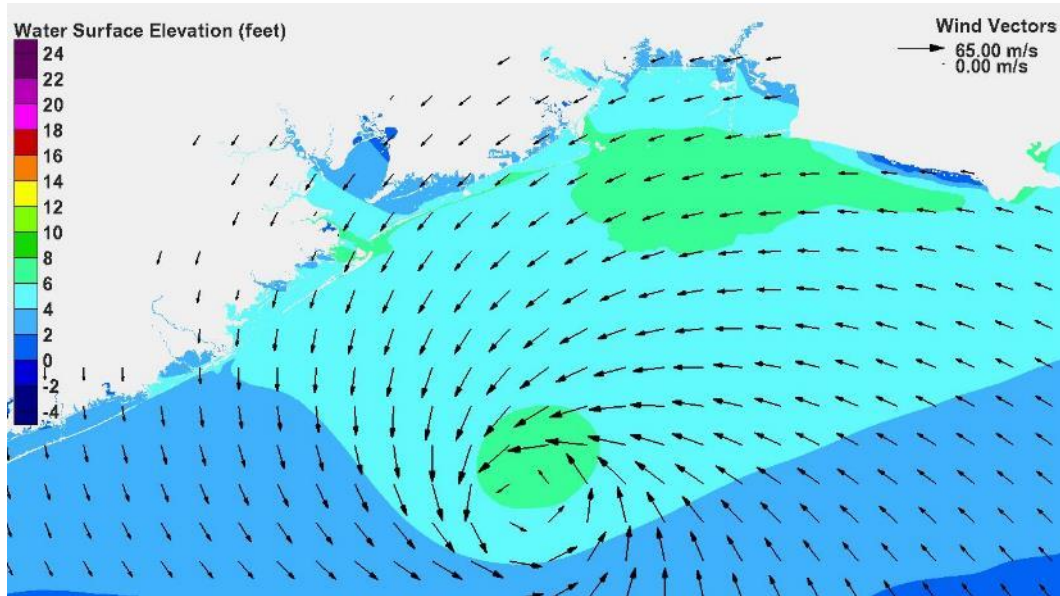


Figure 5-11. Water surface elevation and wind vectors 6 hours before landfall for Storm 122 (direct-hit track, 900 mb)

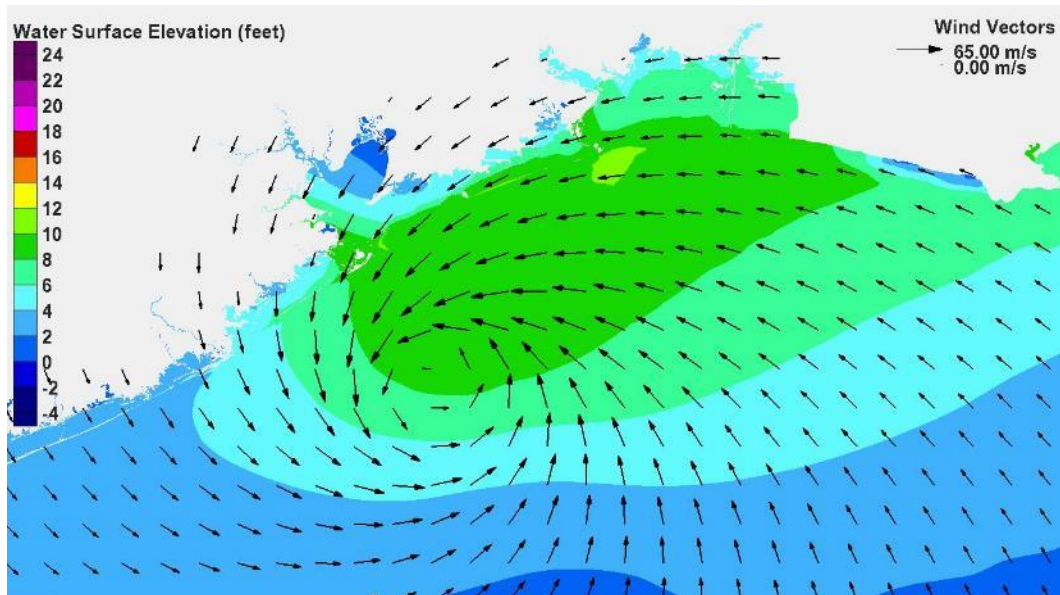


Figure 5-12. Water surface elevation and wind vectors 3 hours before landfall for Storm 122 (direct-hit track, 900 mb)

Figure 5-13 shows conditions at landfall. The surge at the coast has rapidly increased to levels in excess of 18 ft along Bolivar Peninsula. The onshore-directed winds have pushed the water that was accumulating on the shelf up against the coastline, with even greater force and effectiveness because of the very shallow water depths.

The focus of this chapter was the development of storm surge on the open coast. The following chapter will focus on surge development within Galveston Bay.

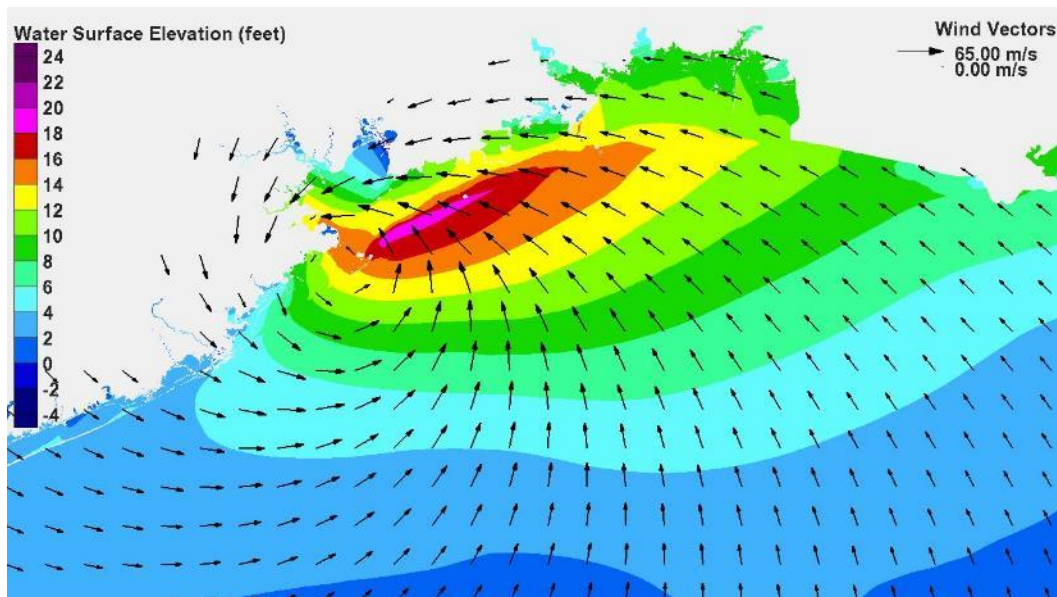


Figure 5-13. Water surface elevation and wind vectors at landfall for Storm 122 (direct-hit track, 900 mb)

6 Hurricane Surge Generation within Galveston Bay – Causative Factors

Introduction

In a semi-enclosed shallow water body like Galveston Bay (having an average water depth of approximately 10 ft), water levels will respond to both a filling action and a tilting of the water surface. Lake Pontchartrain near New Orleans, which also is semi-enclosed and has a water depth similar to Galveston Bay, responded to Hurricane Katrina with both filling and tilting of the water surface as the storm's eye moved through the region.

Filling arises from several sources. Filling occurs in response to water surface elevation differences (or head differences) between the ocean and bay at each of the passes that connect the two water bodies. Filling also occurs in response to overflow of adjacent barrier islands during extreme surge levels. Head differences are primarily caused by the surge forerunner and increased ocean surge associated with arrival of the storm's core winds. The tilting of the water surface within the bay occurs in response to local wind speed and direction, with a setup in water surface on the downwind side of the bay and possibly a set-down in water surface on the upwind side.

There is feedback between filling and tilting of the water surface, and the interactions are complex. Set-down is reduced within the bay if the filling rate is large enough to fill the area where wind is acting to set down the water surface. Also, the wind-induced tilting of the water surface within the bay can influence the head difference between ocean and bay, thereby affecting flow through the inlets, which in turn influences the filling rate. The greater the head difference, the faster the rate of filling. The magnitude of the water surface slope within the bay, i.e. the degree of tilting, is dependent upon the amount of filling. The greater the water depth in the bay, the less is the water surface slope induced by a certain wind speed. Filling acts to increase water surface elevations throughout the bay system, which reduces the degree of tilting of the water surface. The tilting of the water surface within the bay responds rather quickly to

changes in wind direction and therefore the tilting can be quite sensitive to storm track and position of the storm center relative to the bay. The modeling done in this feasibility study simulates well this complex interaction between filling and tilting of the water surface slope within Galveston Bay.

Surge generation within the Bay will be discussed for both the existing and with-dike conditions. In general the dike eliminates or dramatically reduces the filling action, which is substantial for existing conditions. The dike does not eliminate local tilting of the water surface within the bay. But by eliminating or reducing filling, the dike has a substantial beneficial effect on surge conditions within the Bay.

Existing Conditions

Previous sections of the report covered storm surge development during the several days prior to landfall, and development of the open coast surge. The focus here is on surge development within Galveston Bay. Surge development is once again illustrated via a series of water surface elevation-wind vector snapshots in time, one hour apart, spanning the time period from 6 hours before landfall to 10 hours after landfall. These are shown in Figures 6-1 through 6-15.

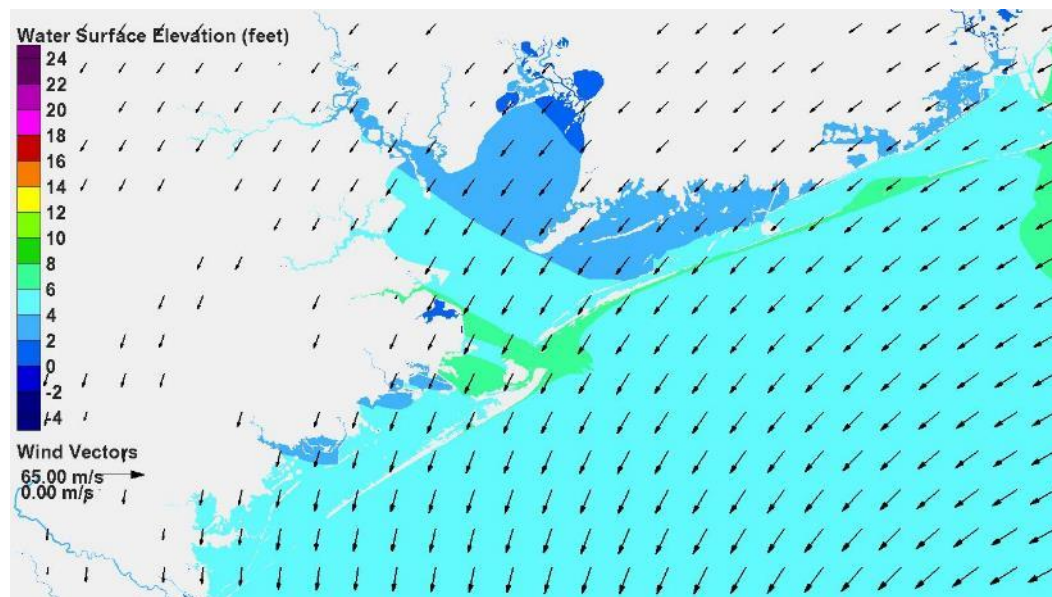


Figure 6-1. Water surface elevation and wind vectors 6 hours before landfall for Storm 122 (direct-hit track, 900 mb)

Figures 6-1 through 6-3 show the water surface slope within the bay, or tilt, increasing as the storm moves closer and wind speeds increase. Wind sets up the water surface in the southwest corner of the bay. Filling of the bay through the passes by the forerunner has raised the water surface throughout the entire bay. Flow over the low barrier islands has begun.

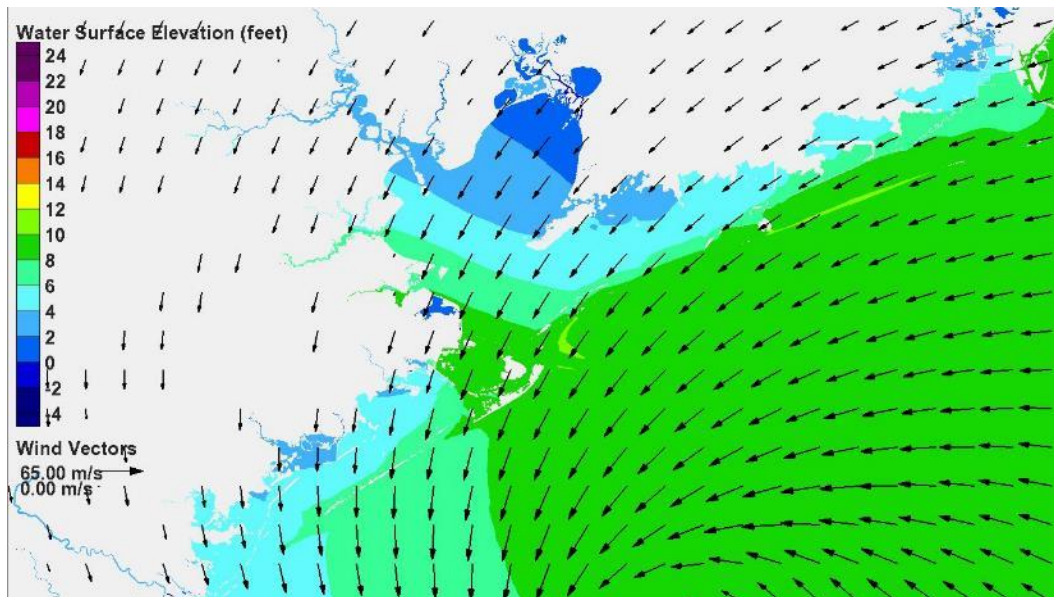


Figure 6-2. Water surface elevation and wind vectors 3 hours before landfall for Storm 122 (direct-hit track, 900 mb)

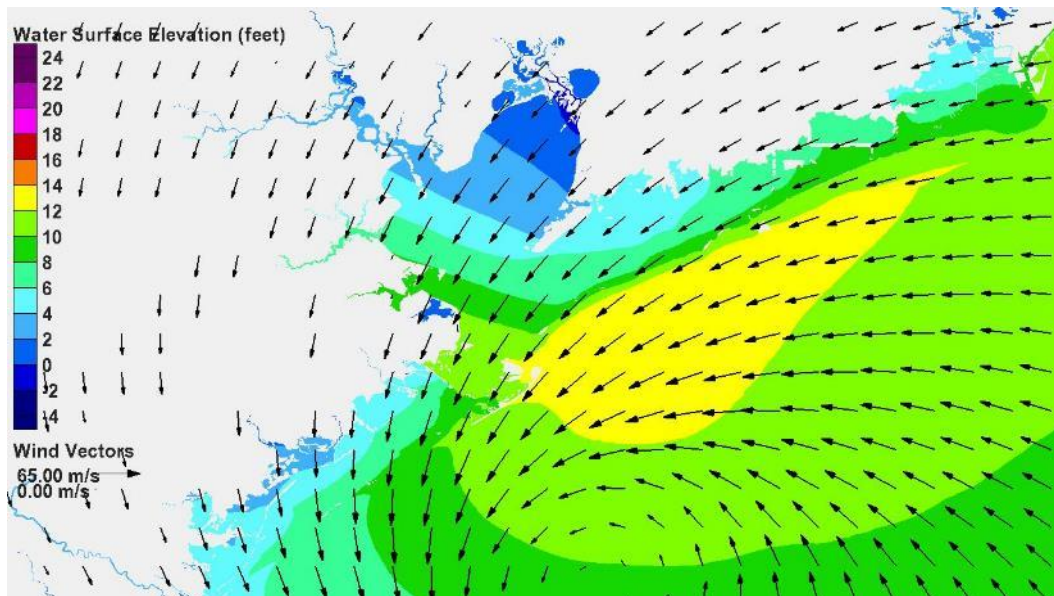


Figure 6-3. Water surface elevation and wind 2 hours before landfall for Storm 122 (direct-hit track, 900 mb)

In Figures 6-4 and 6-5, near landfall, filling due to barrier island overflow continues. The open coast surge of 18 ft has overwhelmed Bolivar Peninsula; surge of 8 to 14 ft has overwhelmed most of Galveston Island. Once overtopped, barrier island overflow is the predominant source of bay filling. Local wind setup continues, building surge at Texas City and Galveston.

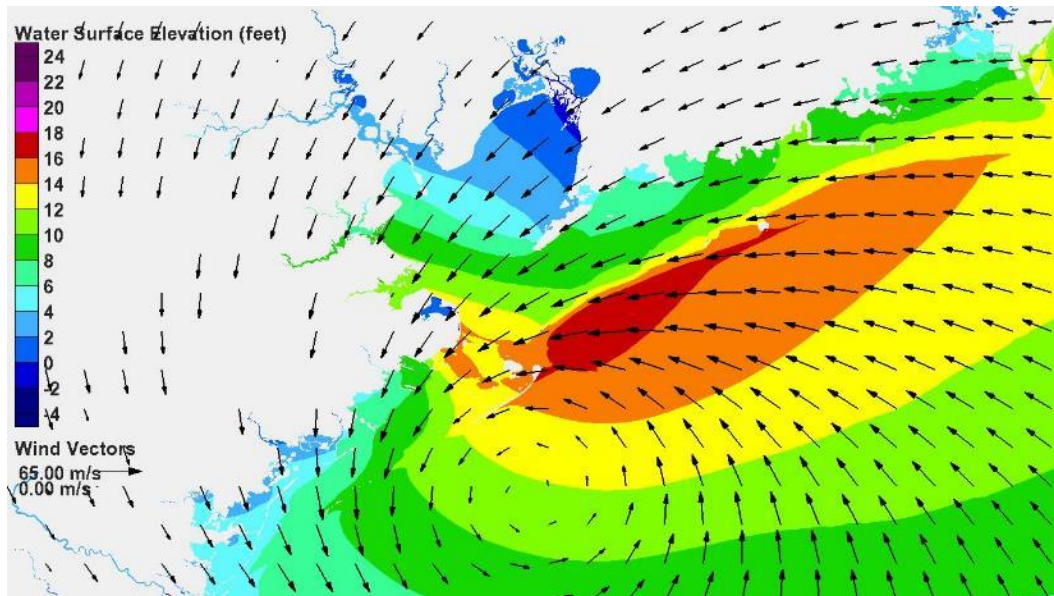


Figure 6-4. Water surface elevation and wind vectors 1 hour before landfall for Storm 122 (direct-hit track, 900 mb)

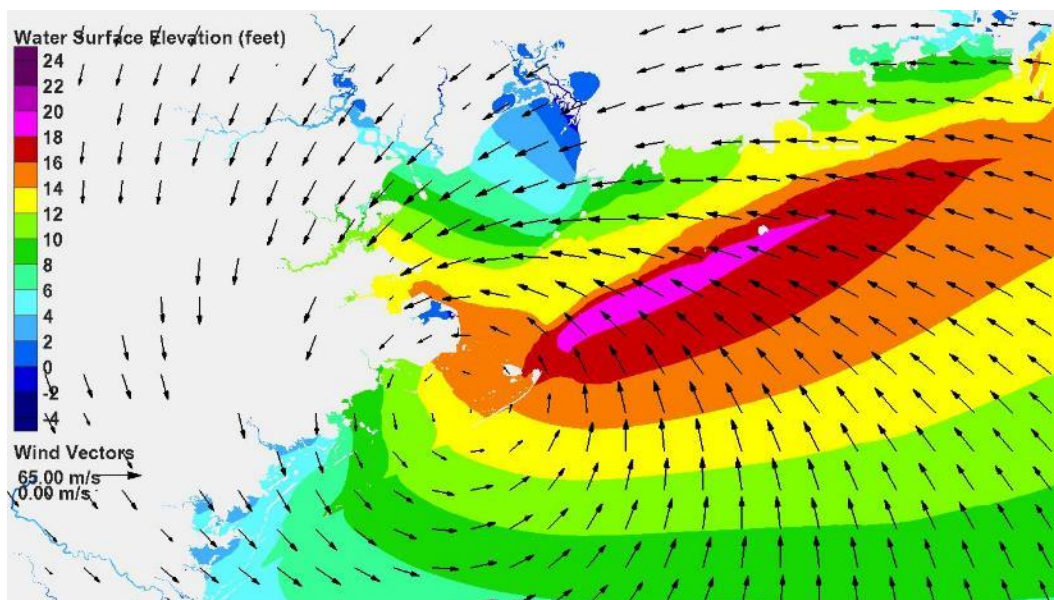


Figure 6-5. Water surface elevation and wind vectors at landfall for Storm 122 (direct-hit track, 900 mb)

The water surface slope within the Bay is changing. Figures 6-6 through 6-7 show the shifting wind pattern. In a matter of hours, winds have quickly shifted from the northeast, then from the east, then the southeast, then from the south. Winds are blowing onshore, strongly driving the water farther inland, toward the northwest inside the bay. Surge is 13 to 15 feet along the western shoreline of the Bay and at Galveston.

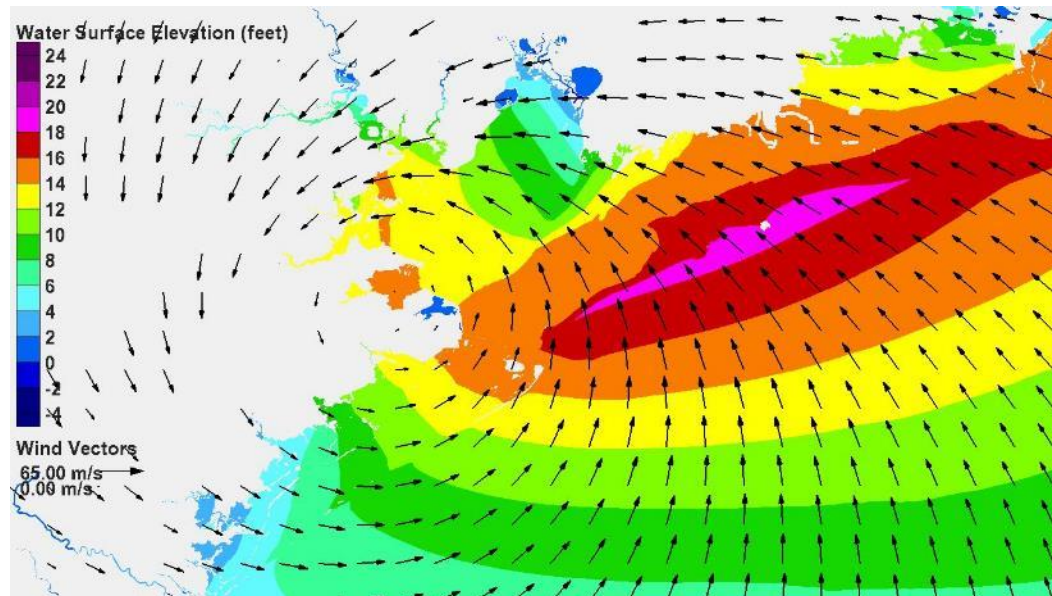


Figure 6-6. Water surface elevation and wind vectors 1 hour after landfall for Storm 122 (direct-hit track, 900 mb)

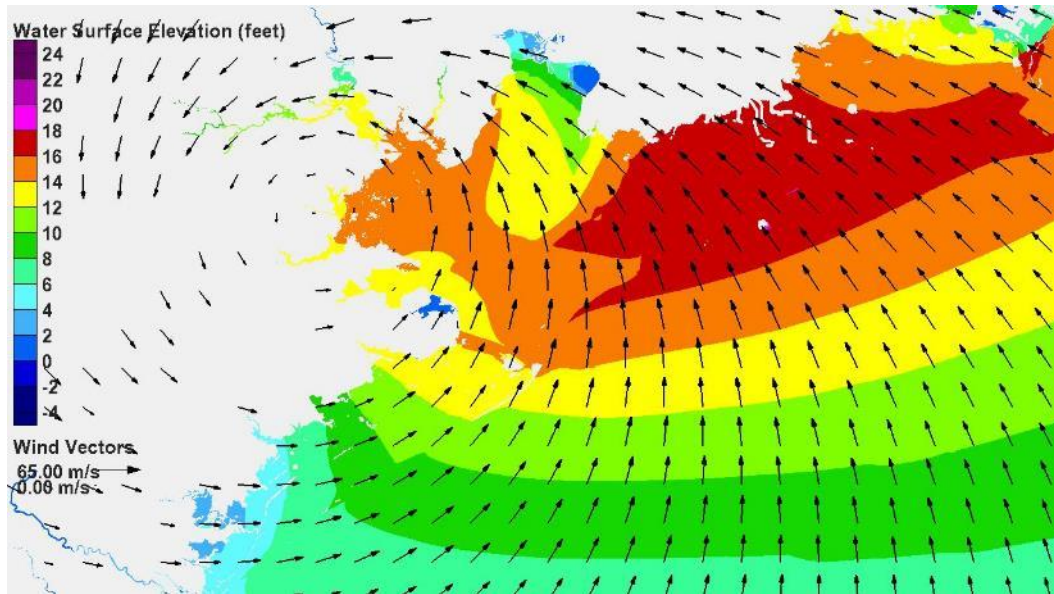


Figure 6-7. Water surface elevation and wind vectors 2 hours after landfall for Storm 122 (direct-hit track, 900 mb)

Figures 6-8 and 6-9 show the surge 3 to 4 hours after landfall. The eye is moving through the Houston area. Winds from the south persist, pushing water that has accumulated within the Bay to the north. Surge is building in the upper reaches of Galveston Bay and the Houston Ship Channel. Surge is already subsiding at the coast and lower parts of the Bay.

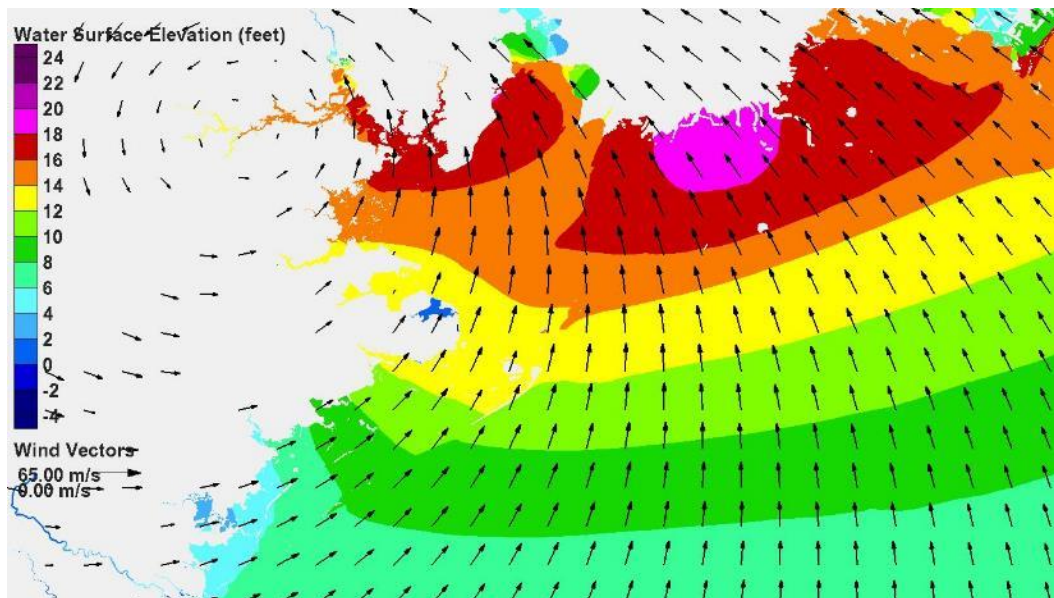


Figure 6-8. Water surface elevation and wind vectors 3 hours after landfall for Storm 122 (direct-hit track, 900 mb)

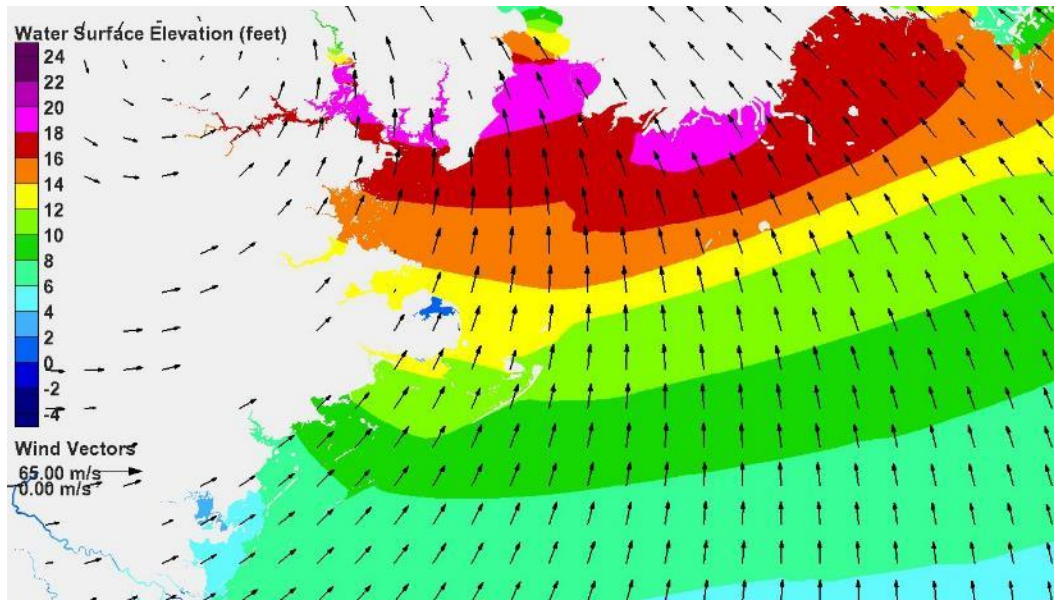


Figure 6-9. Water surface elevation and wind vectors 4 hours after landfall for Storm 122 (direct-hit track, 900 mb)

In Figures 6-10 and 6-11, the pattern of winds from the south continues, increasing the surge in the upper reaches of Galveston Bay. While surge levels at Galveston continue to decrease to 10 ft, surge in upper reaches of the Houston Ship Channel is approaching its maximum value of 19 ft. Surge levels in the middle of the Bay remain steady, at 13 to 17 ft.

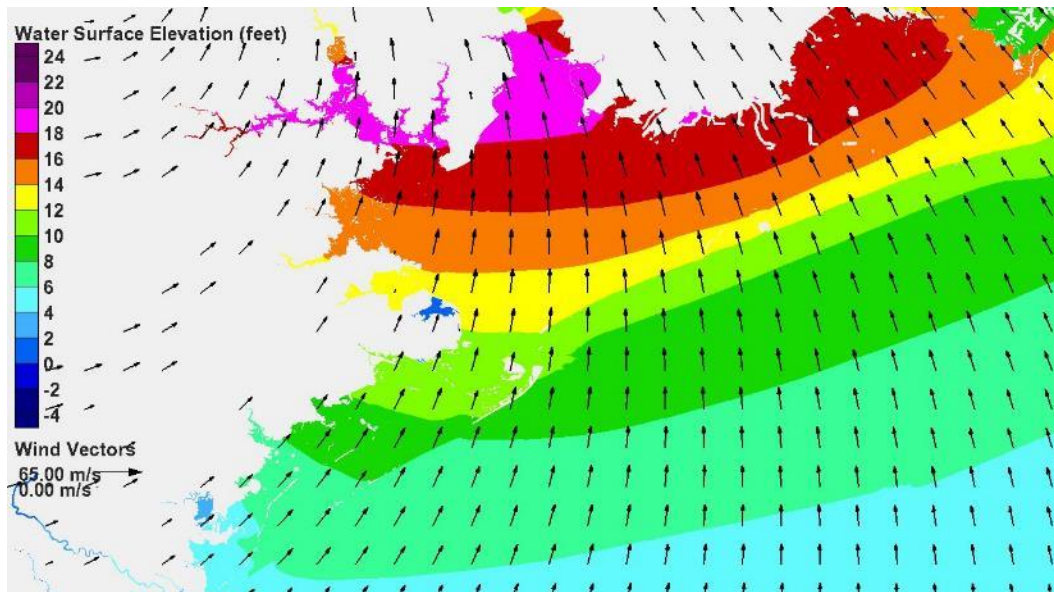


Figure 6-10. Water surface elevation and wind vectors 5 hours after landfall for Storm 122 (direct-hit track, 900 mb)

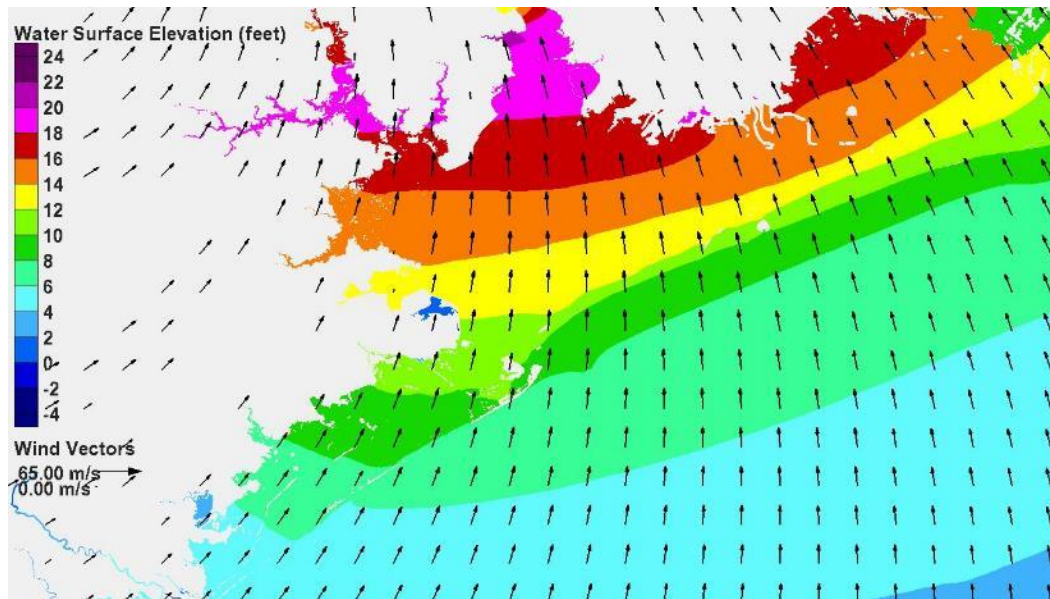


Figure 6-11. Water surface elevation and wind vectors 6 hours after landfall for Storm 122 (direct-hit track, 900 mb)

Figures 6-12 and 6-13 show the storm surge field 7 and 8 hours after landfall, respectively. Surges in the upper reaches of the Houston Ship Channel have reached their peak and are beginning to subside. Winds remain from the south but they are diminishing in strength. Surge within the whole Houston-Galveston area is beginning to recede back over the barrier islands and through the passes. Surge along the western bay is 11 to 15 ft.

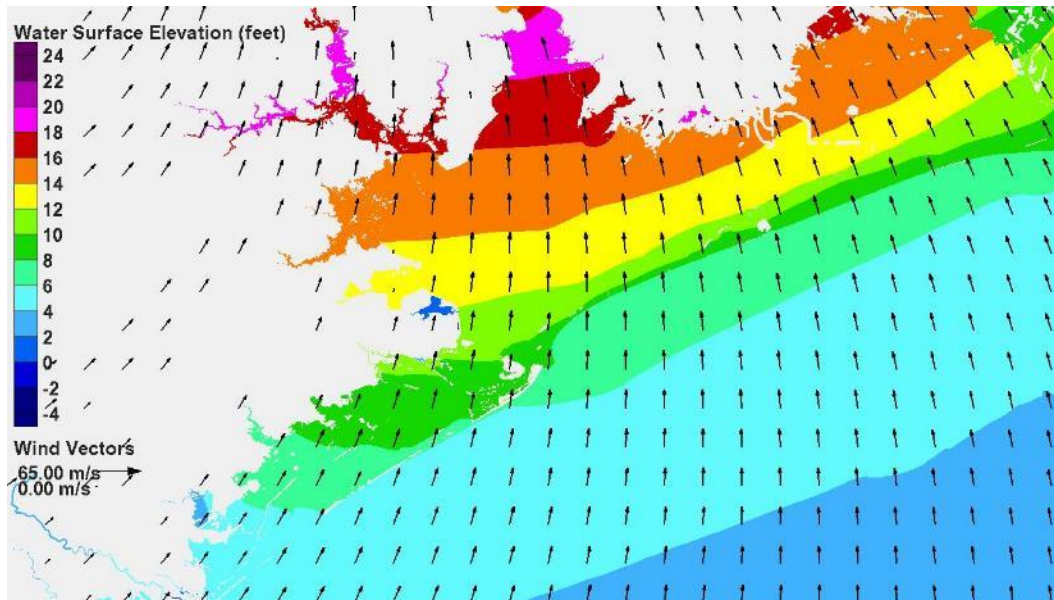


Figure 6-12. Water surface elevation and wind vectors 7 hours after landfall for Storm 122 (direct-hit track, 900 mb)

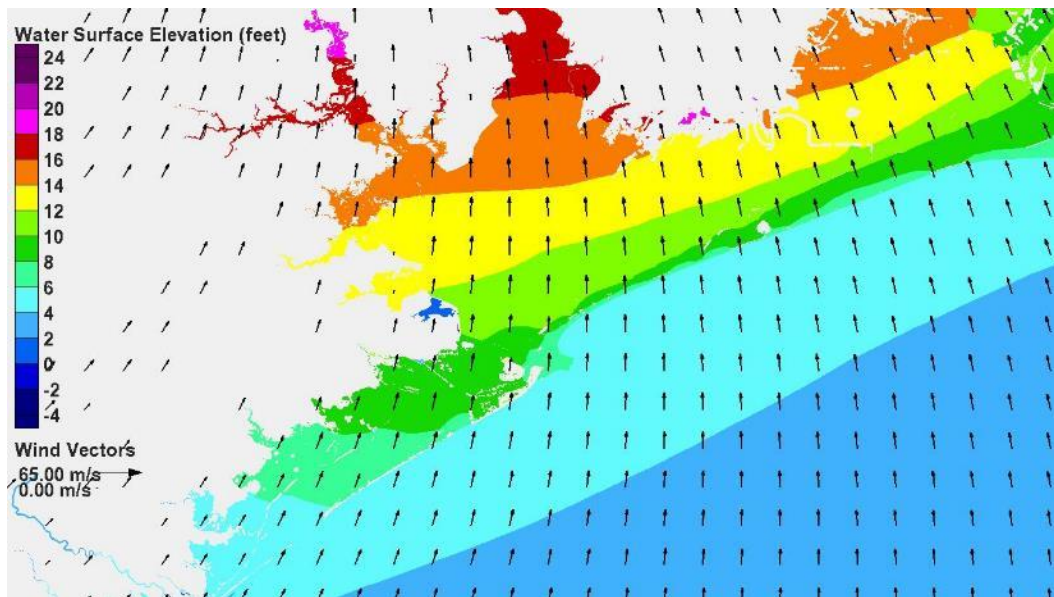


Figure 6-13. Water surface elevation and wind vectors 8 hours after landfall for Storm 122 (direct-hit track, 900 mb)

Continued recession of the surge is shown in Figures 6-14 and 6-15, 9 and 10 hours after landfall, respectively. Surges in the upper Bay and Houston Ship Channel still exceed 14 ft. Surge along the west shoreline of the Bay are 9 to 14 ft. Surge levels along the open coast have receded to 5 ft, facilitating flow of water from the Bay back to the Gulf.

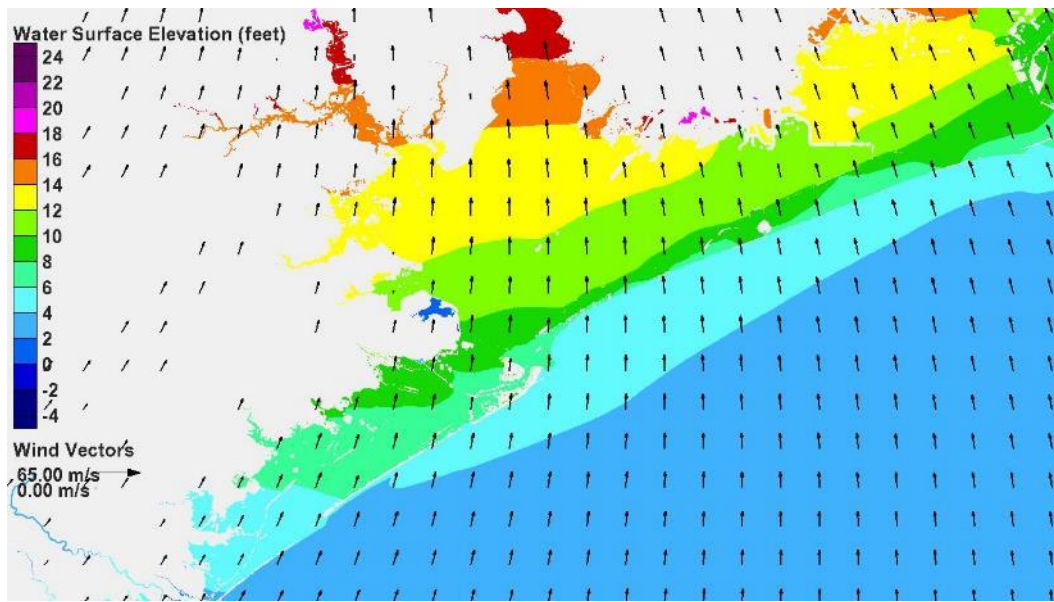


Figure 6-14. Water surface elevation and wind vectors 9 hours after landfall for Storm 122 (direct-hit track, 900 mb)

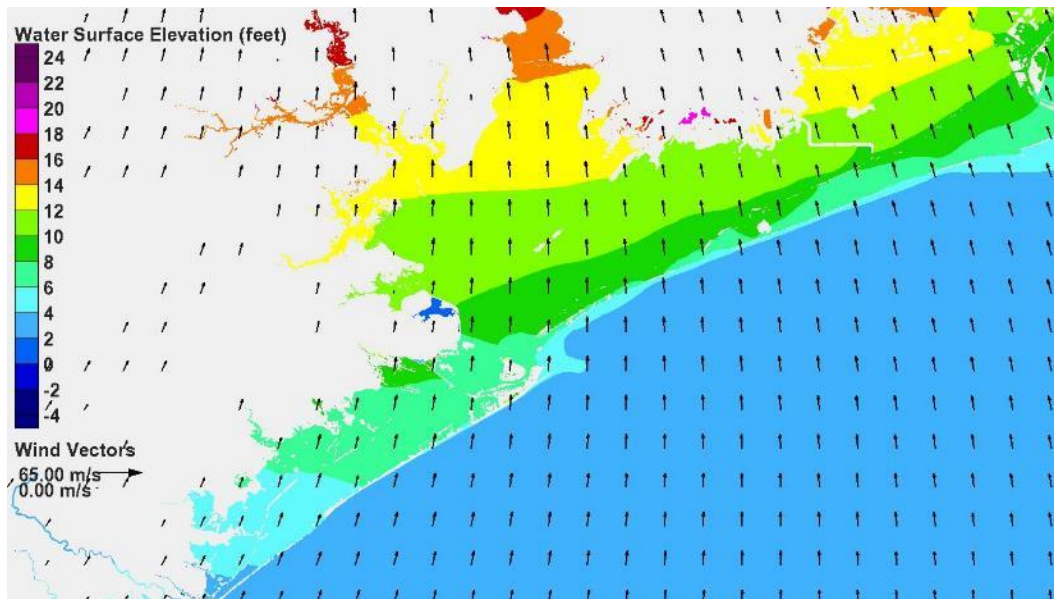


Figure 6-15. Water surface elevation and wind vectors 10 hours after landfall for Storm 122 (direct-hit track, 900 mb)

Figure 6-16 shows the temporal variation of storm surge at five locations: Galveston (Pleasure Pier) on the open coast, the Bay side of the City of Galveston, just north of Texas City along the western Bay shoreline, the Clear Lake area along the Bay shoreline, and in the upper reach of the

Houston Ship Channel. Storm surge at the Pleasure Pier and the Bay side of Galveston rose rapidly, from 7 ft to a peak of about 15 feet, in 3 to 4 hours. A similar rate of rise is seen at other locations along the western Bay shoreline. The hydrographs at Texas City and Clear Lake show persistent surge levels of 13 to 15 ft for about 7 hours, following slightly higher peak surges, after the eye moves through and winds blow steadily from the south. At Galveston, surge decreases relatively quickly after the time of peak surge. The hydrograph shape in the Houston Ship Channel is quite different. There is actually a decrease from 4 ft to 3 ft when other locations are experiencing a rapid increase in surge. This occurs as strong local winds set up the southwest part of the Bay, drawing water from the upper parts, as landfall is nearing. But as the eye moves through and wind direction changes rapidly, storm surge in the upper reaches of the Houston Ship Channel changes dramatically, increasing from 3 ft to 19 ft in the span of only 6 hours. Peak surge occurs about 7 hours after landfall, much later than at the other locations. The rates at which surge falls following passage of the hurricane through the region are much less than the rates of rise as the surge was building. Even 20 hours after landfall, surge levels in the Bay vary from 3 ft (lower Bay) to 10 ft (upper Bay).

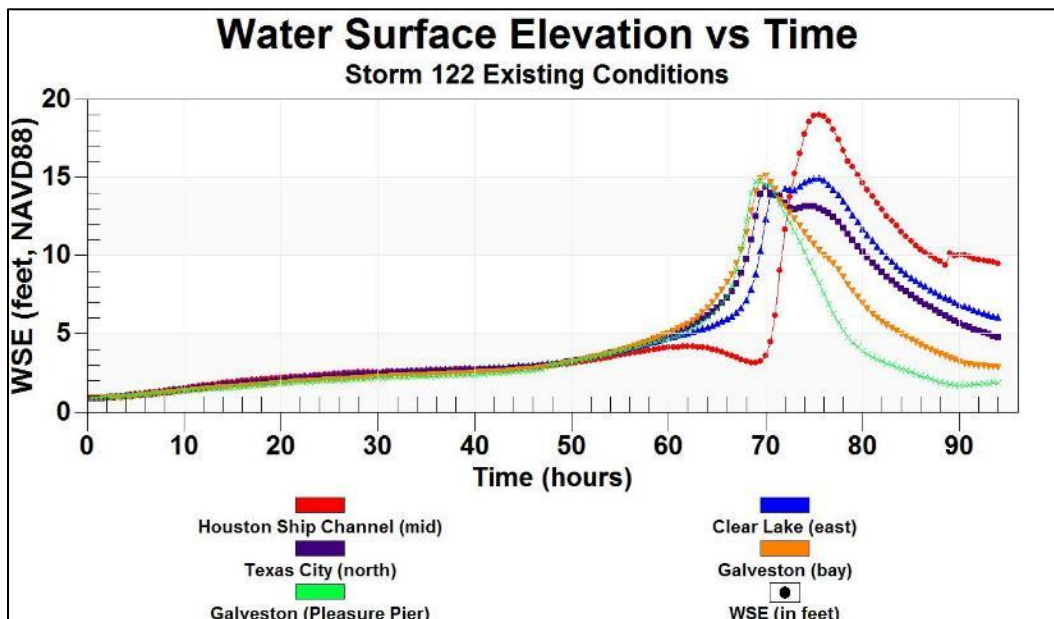


Figure 6-16. Temporal variation of water surface elevations within Galveston Bay for Storm 122 , existing conditions

Surge Generation in Galveston Bay - With the Ike-Dike Concept

Figures 6-17 to 6-31 show snapshots of water surface elevation and wind vectors for with-dike conditions. Snapshots in time are shown for the

same times prior to, at, and after landfall as were shown in the previous section. In general, the dike greatly reduces or eliminates flow over the barrier islands, resulting in a significant reduction in storm surge within the Bay. Barrier island overflow is the dominant contributor to filling within the Bay for the existing condition. Some major storms overtop the dike that is being considered at present, but that volume is considerably less than the volume that can flow over the low barrier islands. The dike does not alter wind fields within the Bay, however, so tilting of the water surface by the wind within the Bay is not affected very much by the presence of the dike.

Figure 6-17 shows conditions within the Bay 6 hours before landfall. Persistent winds from the northeast set up the southwest corners of Galveston and West Bays, as they have been doing prior to this time. In the absence of a source of water to raise the Bay's water level, the northeast corner is being set down by the wind, i.e., negative water surface elevations. Water is being pushed from Galveston Bay into West Bay, subject to constrictions that impede the water from doing so.

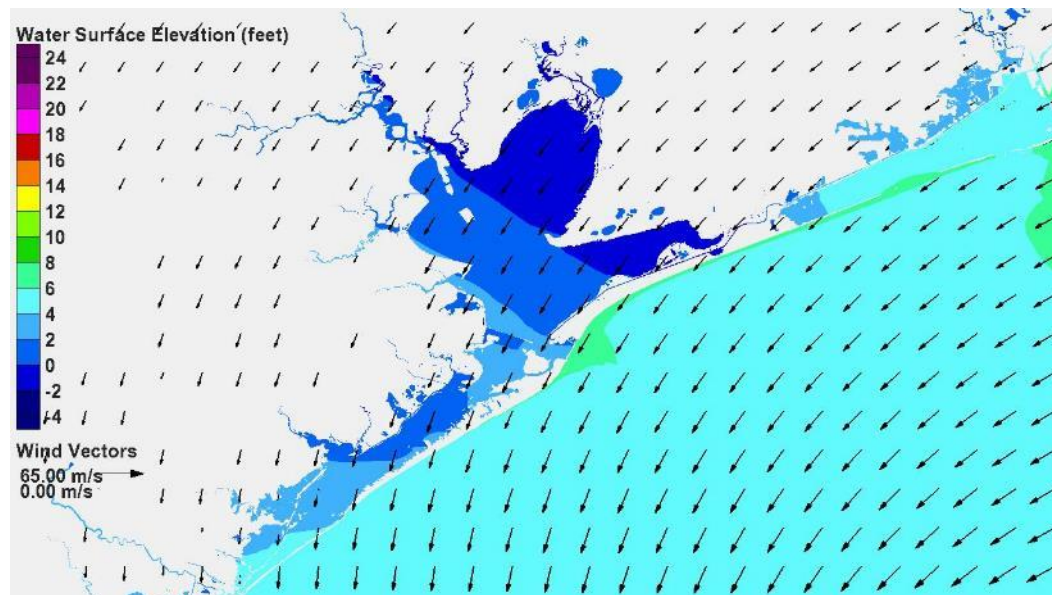


Figure 6-17. Water surface elevation and wind vectors 6 hours before landfall for Storm 122 (direct-hit track, 900 mb)

Figures 6-18 and 6-19 show the storm approaching and wind speeds within the Bay increasing. The increase in speed increases the water surface slope, or tilt, within the Bays forcing water from the northeast

parts of Galveston Bay to the southwest part and then into West Bay. The tilting action is drawing water out of the upper reaches of the Houston Ship Channel.

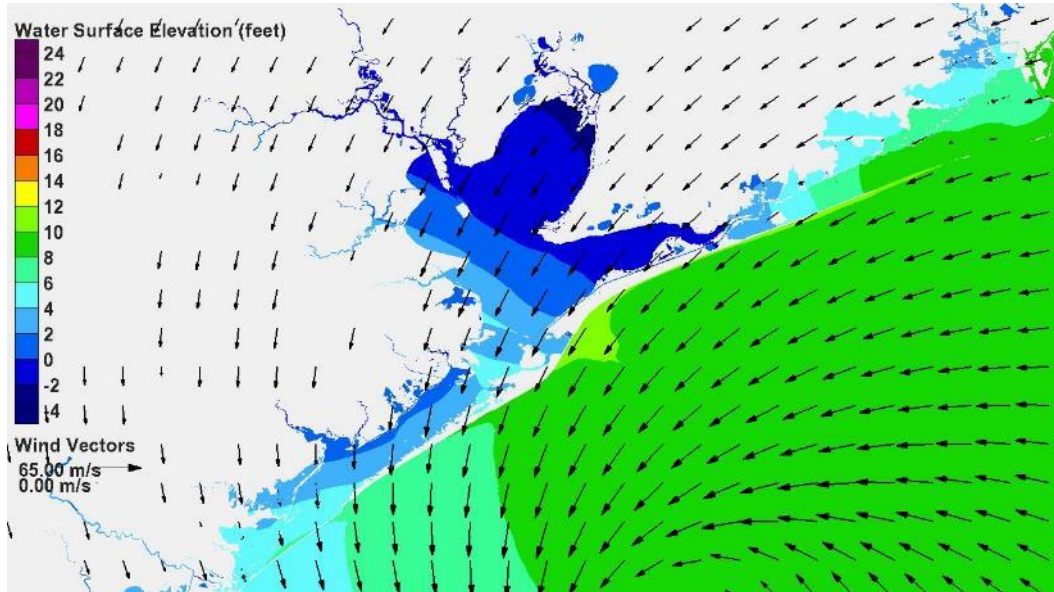


Figure 6-18. Water surface elevation and wind vectors 3 hours before landfall for Storm 122 (direct-hit track, 900 mb)

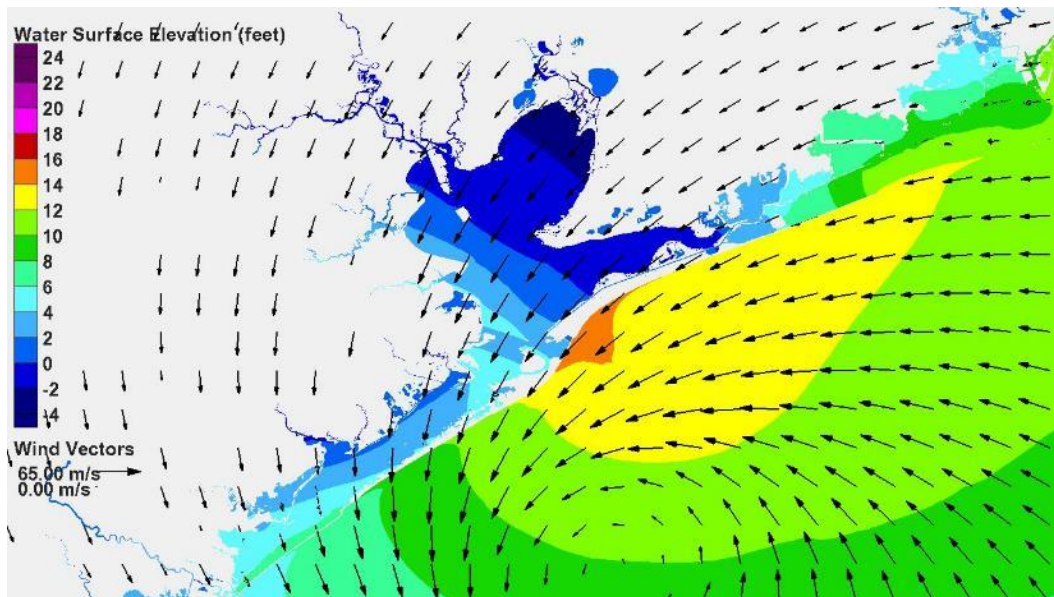


Figure 6-19. Water surface elevation and wind vectors 2 hours before landfall for Storm 122 (direct-hit track, 900 mb)

Figures 6-20 and 6-21 show conditions near landfall. The tilting action is exacerbated by the higher wind speeds in the Bay. The surge at the

southwest corner of Galveston Bay reaches 8 to 9 ft, some 7 ft less than for existing conditions. The dike is being overtopped along Galveston Bay.

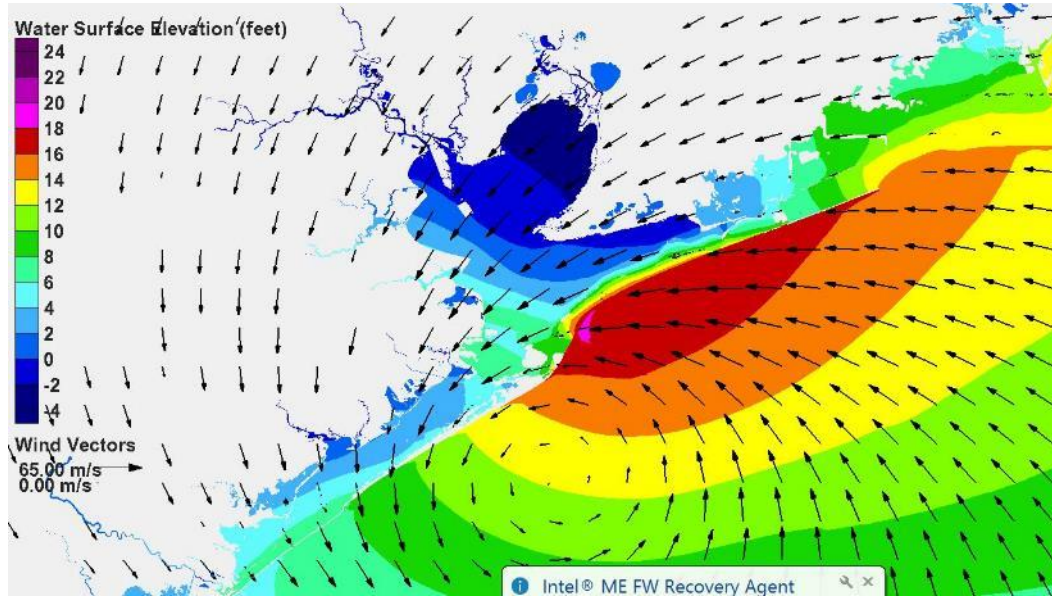


Figure 6-20. Water surface elevation and wind vectors 1 hour before landfall for Storm 122 (direct-hit track, 900 mb)

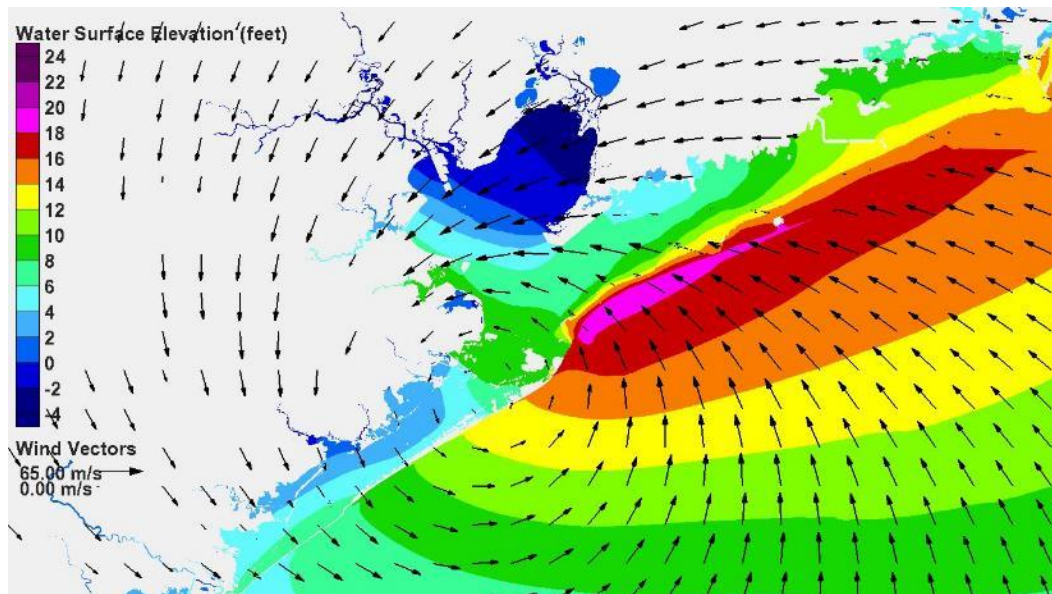


Figure 6-21. Water surface elevation and wind vectors at landfall for Storm 122 (direct-hit track, 900 mb)

Figures 6-22 and 6-23 show conditions just after landfall. Overflow continues along Bolivar Peninsula; no overflow is occurring along Galveston Island. Winds are shifting rapidly, and water is being driven to the northern parts of the Bay and into the upper reaches of the Houston Ship Channel. Surge on the Bay side of Galveston has reached its peak of 8 to 10 ft.

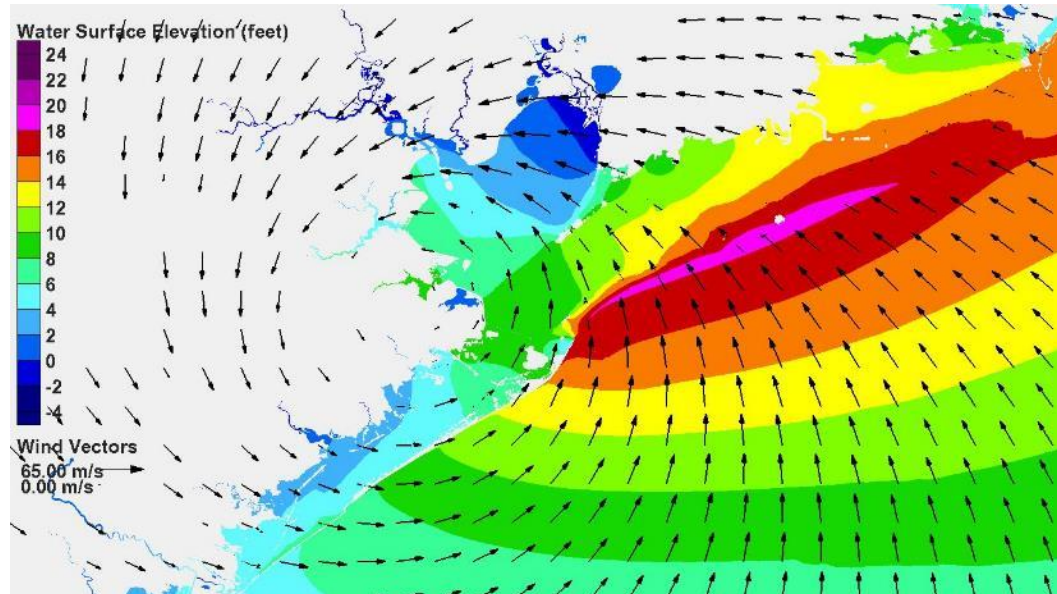


Figure 6-22. Water surface elevation and wind vectors 1 hour after landfall for Storm 122 (direct-hit track, 900 mb)

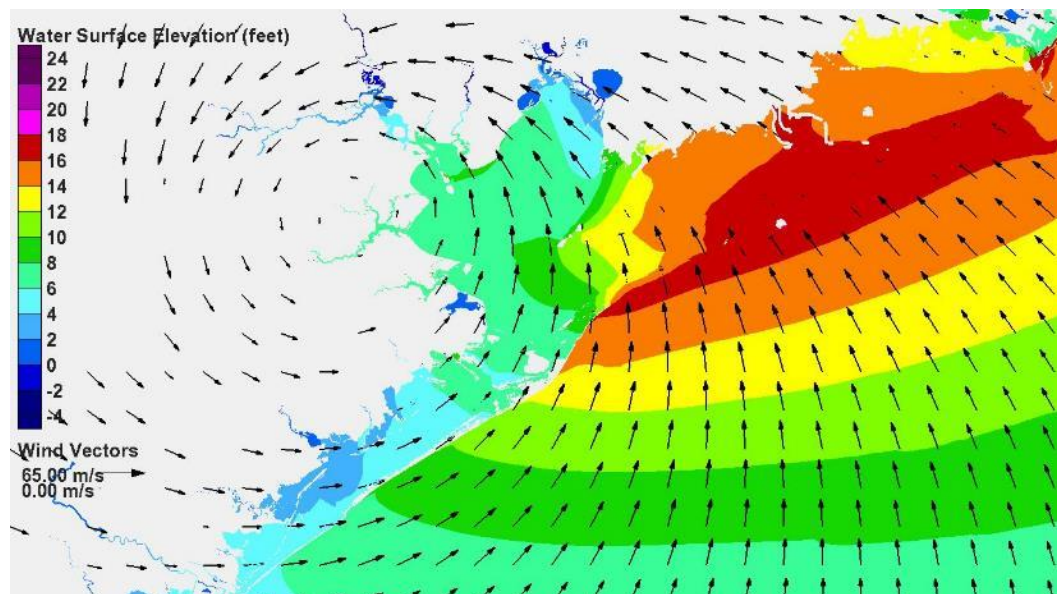


Figure 6-23. Water surface elevation and wind vectors 2 hours after landfall for Storm 122 (direct-hit track, 900 mb)

Figures 6-25 and 6-26, 4 and 5 hours after landfall, respectively, show persistent winds from the south as the hurricane moves out of the region. Surge has reached its maximum in the upper Houston Ship Channel, nearly 13 ft, some 6 feet less than for existing conditions. Surges along the western shoreline of Galveston Bay also have peaked but are stationary.

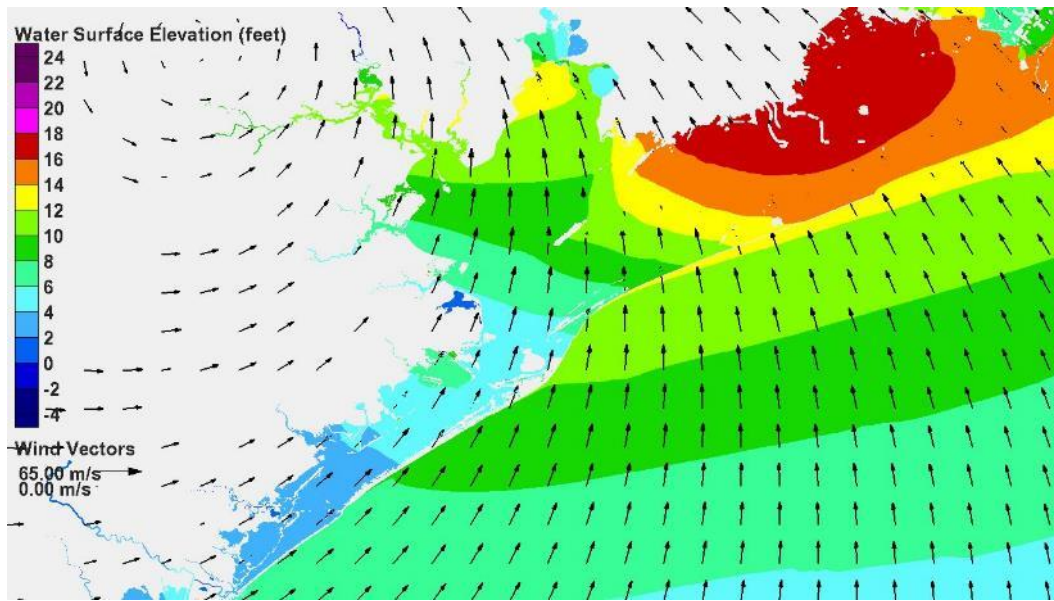


Figure 6-25. Water surface elevation and wind vectors 4 hours after landfall for Storm 122 (direct-hit track, 900 mb)

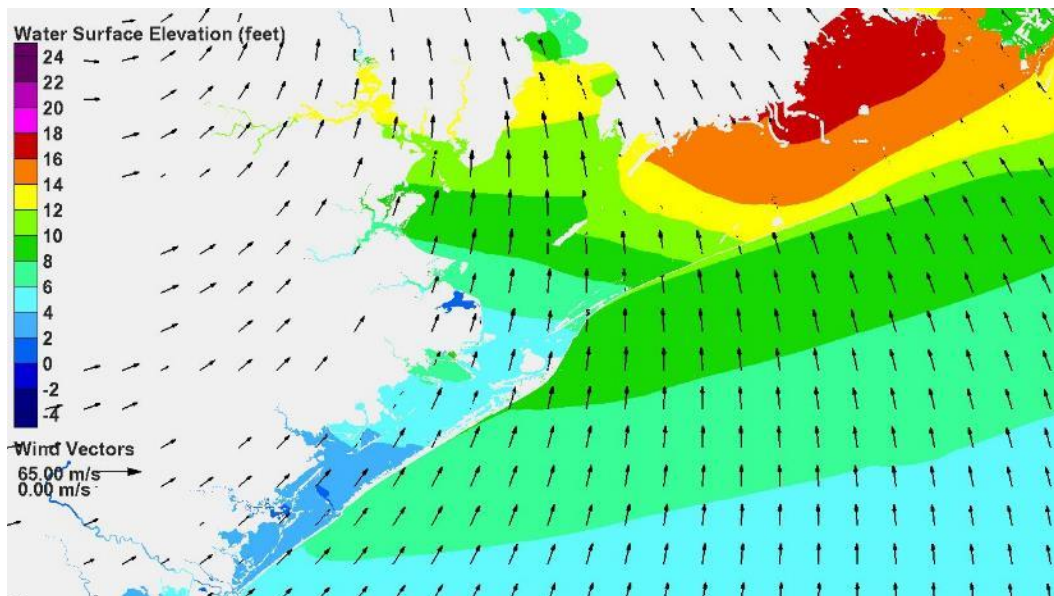


Figure 6-26. Water surface elevation and wind vectors 5 hours after landfall for Storm 122 (direct-hit track, 900 mb)

Figures 6-27 through 6-31 show persistent surge levels along the western shoreline of the Bay, and decreasing surge in the upper Houston Ship Channel. Water that encroached around the northern extent of the dike is moving into the Bay and acting to fill it. This is an artifact of not having tie-ins of the dike to higher ground.

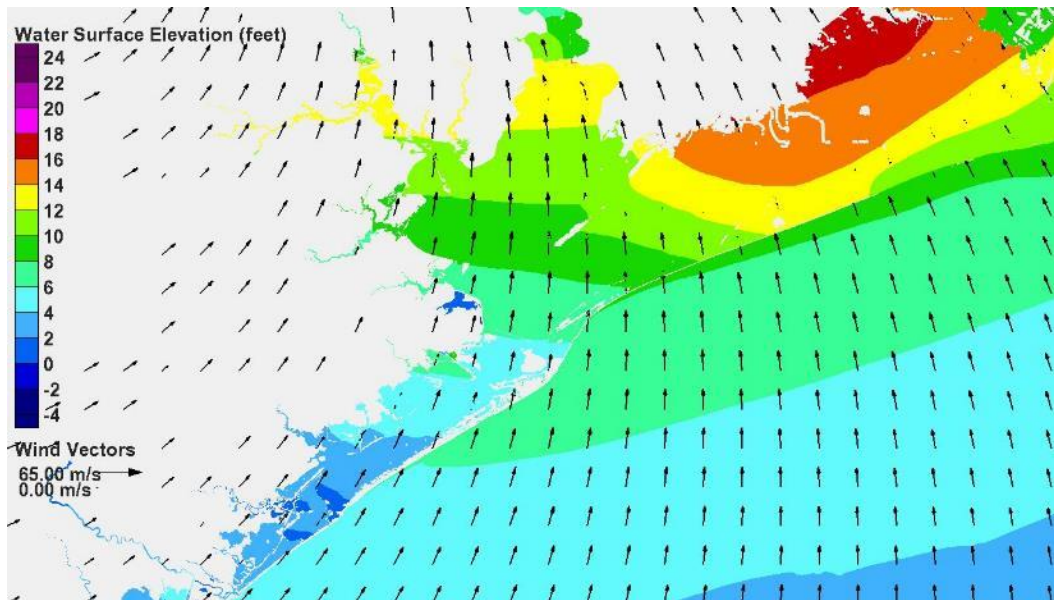


Figure 6-27. Water surface elevation and wind vectors 6 hours after landfall for Storm 122 (direct-hit track, 900 mb)

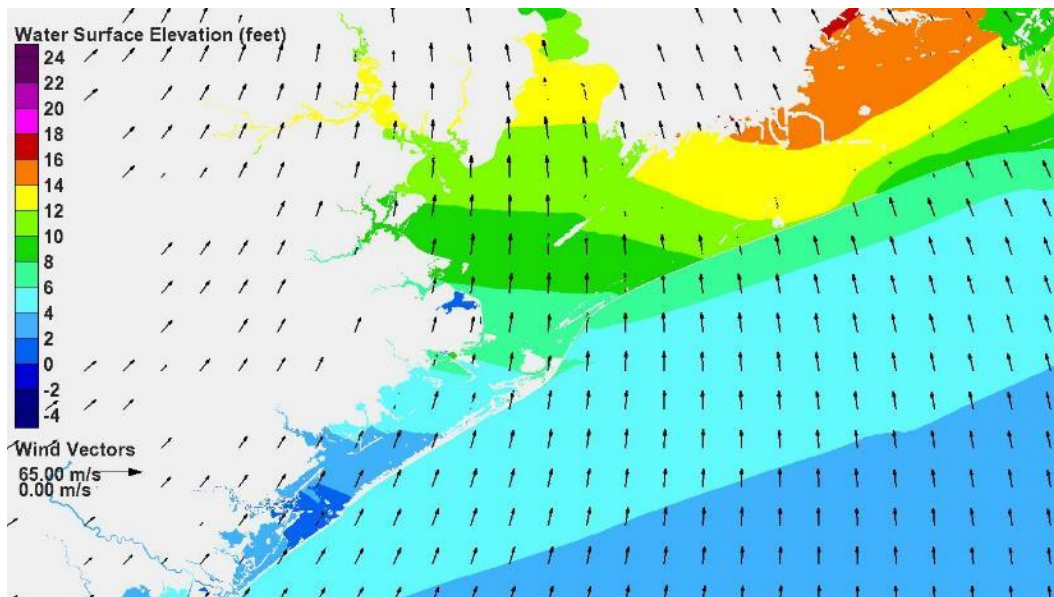


Figure 6-28. Water surface elevation and wind vectors 7 hours after landfall for Storm 122 (direct-hit track, 900 mb)

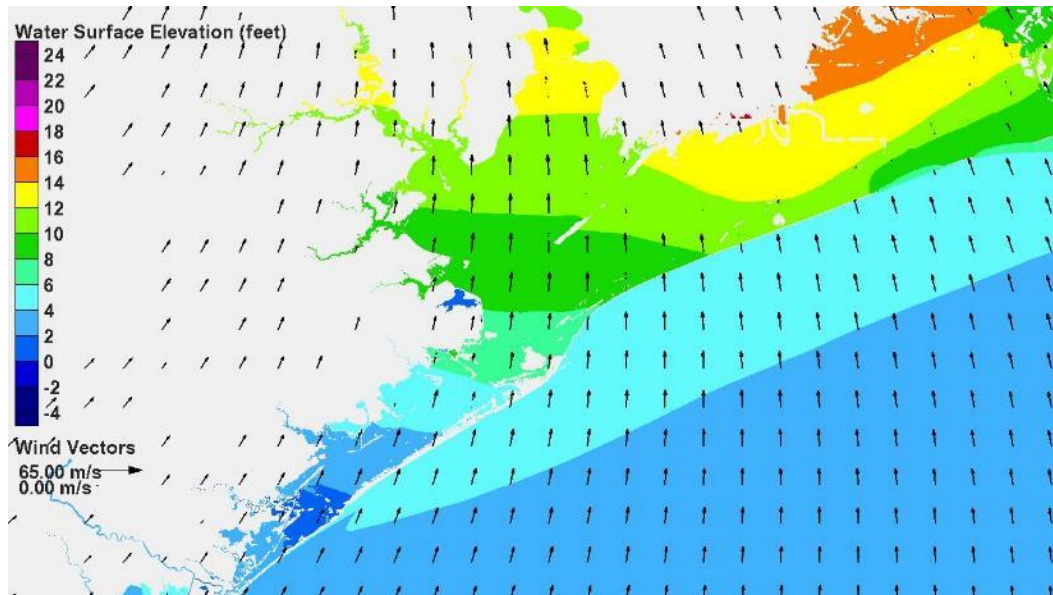


Figure 6-29. Water surface elevation and wind vectors 8 hours after landfall for Storm 122 (direct-hit track, 900 mb)

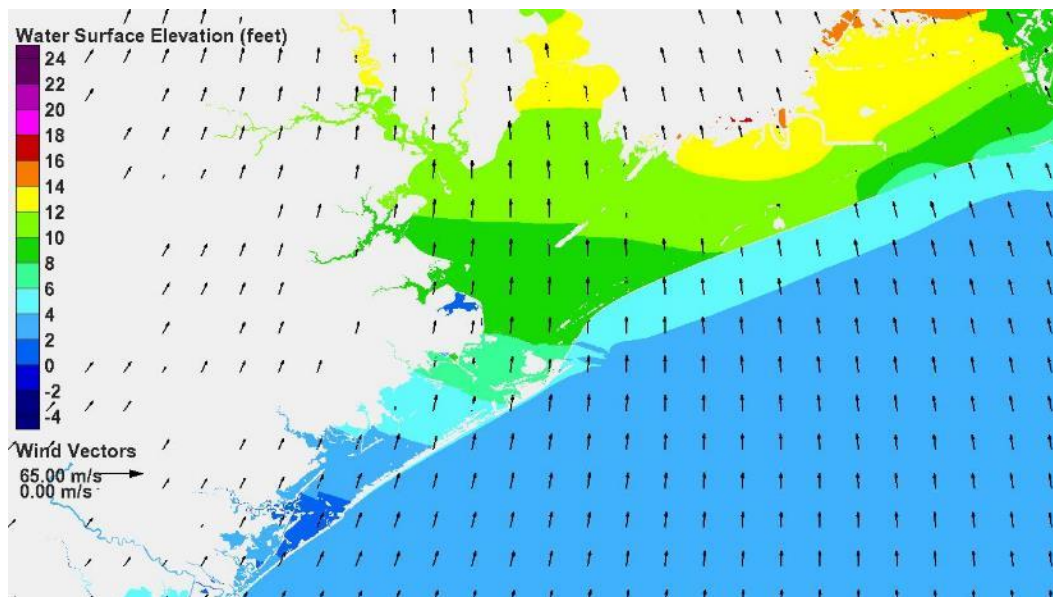


Figure 6-30. Water surface elevation and wind vectors 9 hours after landfall for Storm 122 (direct-hit track, 900 mb)

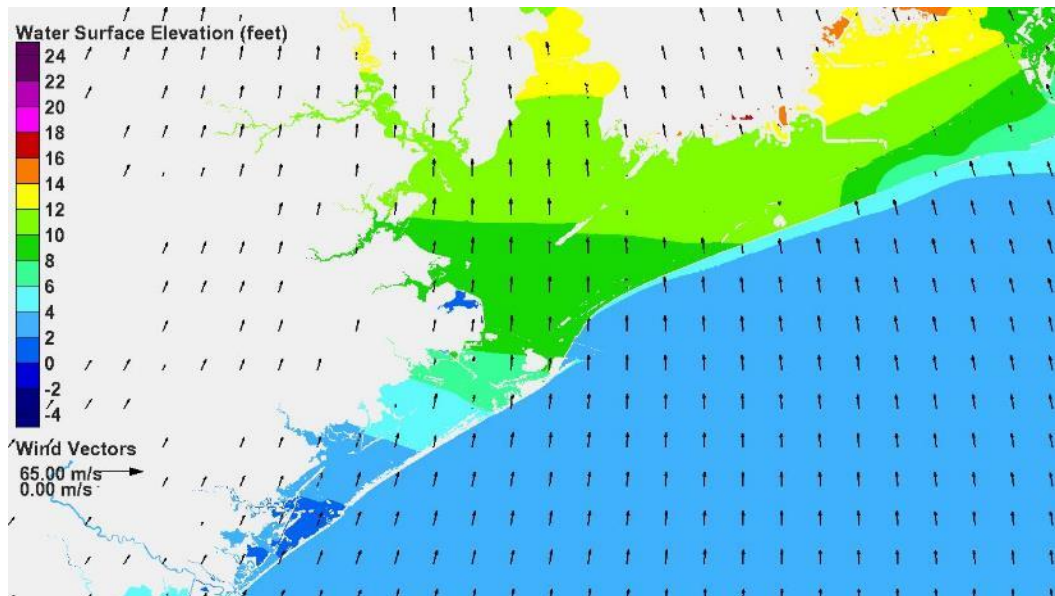


Figure 6-31. Water surface elevation and wind vectors 10 hours after landfall for Storm 122 (direct-hit track, 900 mb)

Figure 6-32 shows computed water surface elevation as a function of time for the with-dike condition for Storm 122. Results are shown for the same 5 locations that were shown in Figure 6-16 for existing conditions.

At Galveston Pleasure Pier, the hydrograph shape is nearly identical to the shape for existing conditions. The surge forerunner on the open coast is unchanged by the dike. With a dike in place, peak surge on the ocean side of Galveston is about 15.5 ft, 0.5 feet more than for existing conditions. This small increase is expected. A substantial dike, levee or floodwall will allow surge to be stacked against it by the wind instead of overtopping a lower barrier island. This increase must be accounted for in any final design of the Ike dike concept.

Inside the Bay, at Galveston, the timing of the peak surge is the same as for existing conditions, but the peak surge is reduced from 15 ft to 9 ft, a decrease of 6 ft. At Texas City, the timing of peak surge is the same as for existing conditions, but the peak surge is reduced from 14 ft to 8 ft, also a 6 ft decrease. At Clear Lake the timing of peak surge is the same, but the peak surge is reduced from 14 to 7 feet, a decrease of 7 feet. In the upper reach of the Houston Ship Channel the initial drawdown of water is greater for the with-dike condition, compared to the existing condition. The peak surge is reduced from 19 ft to 12.5 ft, a decrease of 6.5 ft. As with

the existing condition, the rate of rise in surge in the upper Houston Ship Channel is rapid, increasing from -2 ft to +13 ft, a change of 15 ft, in only 2 to 3 hours. The timing of peak surge is the same.

The elevated water levels evident late in the hydrograph are primarily an artifact due to encroachment of the surge around the north end of the dike, allowing a large amount of water to enter the bay. The dike, as it's initially represented and implemented in the modeling, holds the water inside the Bay. In actuality the dike would be built with lateral terminations, or tie-ins to higher ground, that would prevent or substantially reduce surge encroachment around the end of the dike. Gates would be built in the passes and opened following passage of the storm to allow water to leave the Bay and return to the ocean.

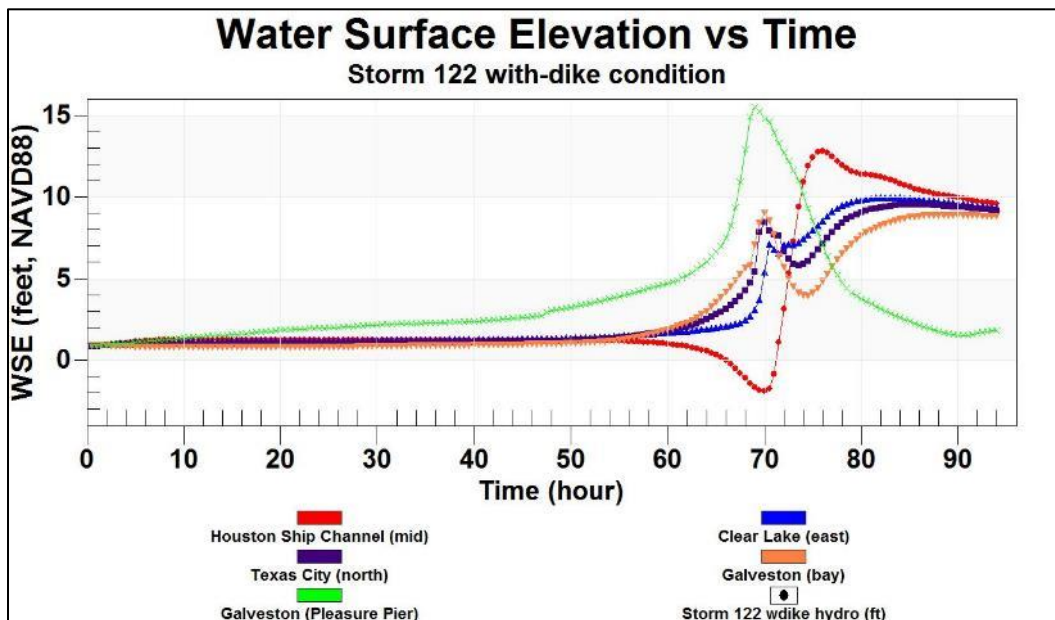


Figure 6-32. Temporal variation of water surface elevations within Galveston Bay for Storm 122, with-dike condition

7 Influence of Storm Track on Surge Development

Introduction

The influence of hurricane track on storm surge development was examined by comparing surge generation for a single severe hurricane approaching from each of three different approach directions: from the south, from the south-southeast, and from the southeast. First, the development of the surge forerunner was examined as a function of track, then development of the surge associated with arrival of the storm's stronger core winds was examined.

For the forerunner analysis, three storms were selected from the bracketing set that had the same values of minimum central pressure, forward speed, and radius to maximum winds. Central pressure and radius to maximum winds are generally considered to be the two most important parameters that determine open coast surge amplitude and peak surge for a particular coastal setting like the north Texas coast. Bunpapong et al (1985) found that forward speed was important for this region. One storm was selected from each of the three track groups represented in the bracketing set; the three were chosen to have as similar a landfall location as possible, subject to the constraint of having the same hurricane parameters. The three storms selected were Storms 134, 122 (extensively described previously in this report) and 128. The forerunner analysis considered the time period when the hurricane was well offshore and the forerunner surge was building, up until a time that is 12 hours before landfall.

Development of the storm surge associated with arrival of the core winds, as a function of storm track, also was examined for each of the three approach directions. For this analysis, three storms were selected that had approximately the same landfall location, the same minimum central pressure and the same radius to maximum winds. The storms selected for this analysis were Storms 136, 122 and 128. Storm 136 has a different forward speed compared to the others; however, the landfall location for storm 136 is approximately 50 miles north of the landfall location for Storm 134 and closer to the landfall location of the other two. The three chosen storms make landfall along the upper half of Galveston Island.

Forerunner Surge Development as a Function of Storm Track

Storms 134 (south), 122 (south-southeast) and 128 (southeast) were compared to examine forerunner development. Each has a minimum central pressure of 900 mb, a radius-to-maximum-winds of 17.7 n mi, and a forward speed of 11 kts, and the same value of the Holland B parameter, 1.27, which controls the radial distribution of wind speed. The paths through the Gulf for storms in each of the three directional groupings were shown in Figure 7, and their individual paths in the Houston-Galveston Region were shown in Figure 9.

Storm 128 originates within the Gulf, in deep water, west of the Florida peninsula. From its time of origin, the storm immediately begins to move across the Gulf until it makes landfall just south of Bolivar Roads 45 hrs after its initiation. The storm had an initial central pressure of 980 mb, and it begins to intensify immediately after its origin. Its central pressure decreases rapidly to 960 mb after 3 hours, decreases to 930 mb during the next 9 hrs, and then decreases to its minimum of 900 mb during the following 9 hours. The storm maintains its minimum central pressure until just before landfall, 24 hours later, when storm filling occurs the storm weakens and central pressure increases.

Storm 122 originates just outside the Gulf, south of Cuba, and it enters the Gulf near the northern limit of the Yucatan Straits. Its central pressure at the time of origin is 980 mb. It starts moving on its track for 8 hrs while maintaining the initial central pressure of 980 mb, before it begins to intensify. Once intensification begins, the central pressure decreases to 960 mb over the next 7 hours, decreases to 930 mb over the ensuing 12 hrs, and decreases to its minimum pressure of 900 mb during the following 12 hrs. The storm maintains its minimum central pressure until just before landfall, 31 hours later.

Storm 134 originates on land near the Yucatan peninsula, with an initial central pressure of 980 mb. For 28 hrs the hurricane remains stationary with a central pressure of 980 mb. For the next 18 hours, while the storm moves to the north, the central pressure remains at 980 mb. Then the storm begins to intensify over the next 5 hours, with the central pressure decreasing to 960 mb. During the next 6 hours the central pressure decreases to 930 mb, and then 7 hours later decreases to its minimum central pressure of 900 mb. The storm maintains its minimum pressure until just before landfall, 31 hours later.

From the time all three storms commence movement along their respective tracks, Storm 122 is in motion for 70 hours and it has the longest path to landfall. Storm 134 has a slightly shorter path, compared to Storm 122, and it is in motion for 67 hours. Storm 128 takes the shortest path to landfall, and it is in motion for 45 hours. Prior to landfall, the durations for which each storm has a central pressure of 900 mb are: 31 hours for Storm 122, 31 hours for Storm 134, and 24 hours for Storm 128.

Figures 7-1 through 7-5 show snap-shots in time of water surface elevation and wind vectors at different times prior to landfall. The snap-shots are used to illustrate position of the storm and the evolution of the surge forerunner. Forerunner amplitudes cited in the following discussion are estimated visually from the graphical images. Computed time series of water surface elevation, which characterize the forerunner amplitude more accurately, are presented and discussed later.

Figure 7-1 shows results for Storms 134 and 122 60 hrs prior to each storm's landfall. Results are not shown for Storm 128, since its time of origin was later and there is no snap-shot for this storm 60 hrs before landfall. Storm 134 is just beginning its movement into the Gulf, and it is undergoing intensification. Storm 128 has recently entered the Gulf and also is experiencing intensification.

For both storms, the wind-induced surge forerunner has already started to develop along the Louisiana and north Texas coasts. The magnitude of the forerunner surge along the Louisiana and north Texas coasts is similar. Near Galveston, the water surface elevation is approaching between 1 and 1.5 ft NAVD88 for both storms. The NAVD88 datum is the vertical datum used for all references to water surface elevation; for the rest of this chapter, the datum will be omitted from water surface elevation references. Since the initial water surface elevation for all the hypothetical storm simulations is 0.9 ft (about 0.4 ft above mean sea level), the amplitude of the forerunner, relative to mean sea level, is between 0.1 and 0.6 ft.

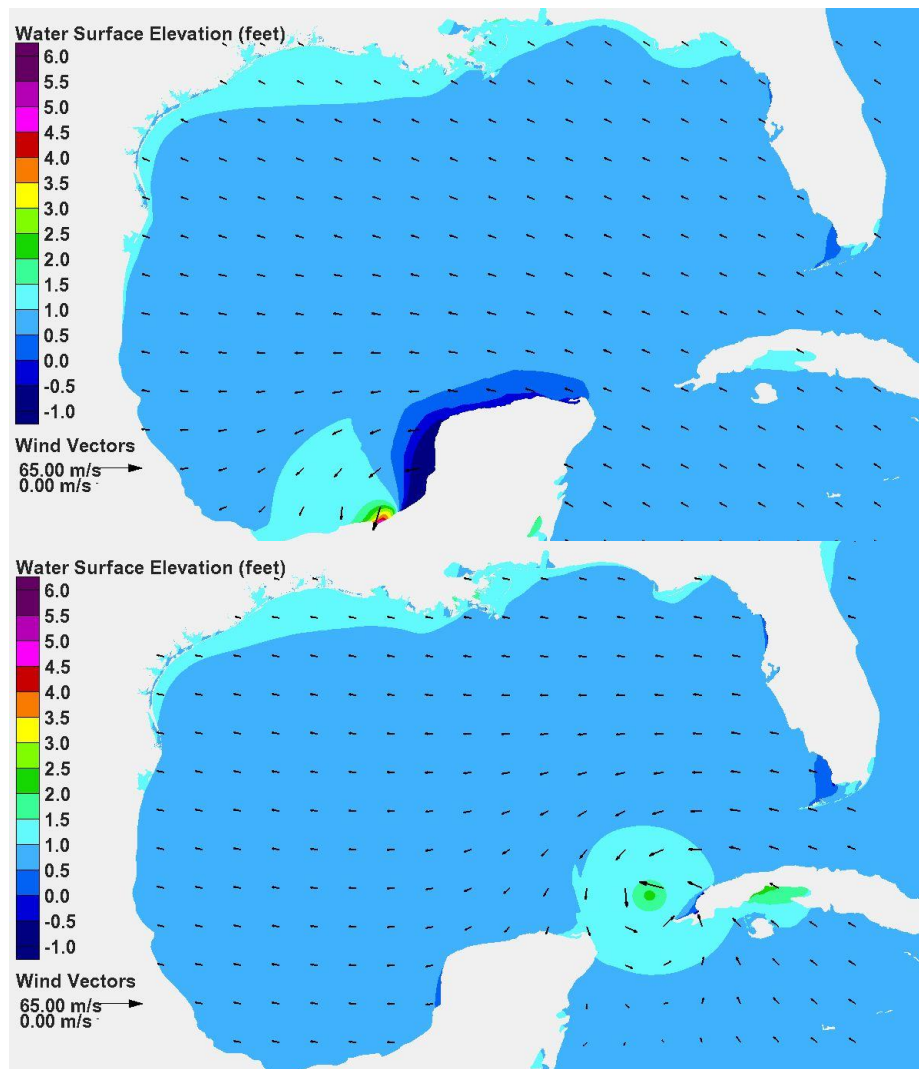


Figure 7-1. Water surface elevation and wind vectors 60 hours before landfall, Storm 134 (upper panel), Storm 122 (lower panel).

Along both the Louisiana and Texas coasts, the area reflecting the presence of the surge forerunner correlates well with the location of the continental shelf, which indicates the importance of wind forcing on the shelf in forerunner development.

In some places along the Texas shelf the wind has a significant onshore component. Along the north Texas shelf, winds are directed primarily onshore for both storms, but slightly more onshore for Storm 134. Along the Louisiana shelf the wind is directed more along the shelf. For Storm 122, along the Louisiana coast, wind sets in motion a current that is moving to the west along the continental shelf which is then directed to the right, or toward shore, by the Coriolis force, forming the forerunner. Along the Louisiana coast the winds for Storm 134 are directed slightly

more onshore than they are for Storm 122, but they also have an alongshore component. Onshore-directed winds of the same speed are more effective in building the surge at the coast than are along-shore directed winds of the same speed. However, the alongshore blowing winds also set in motion a movement of water along the shelf from Louisiana toward Texas which eventually increases the amount of water on the Texas shelf that can be blown toward shore by the core winds of the hurricane. Far-field winds that blow directly onshore would not tend to produce this alongshore moving water. The amplitude of the surge forerunner along the Texas coast is slightly larger for Storm 134 compared to Storm 122 because the winds are directed more onshore and because the alongshore moving water on the shelf has not yet moved from Louisiana toward Texas.

It is worth noting that in these simulations there is only one contributor to winds in the Gulf, the hurricane itself, as simulated by the PBL model which is an idealized wind model. In real situations, other weather systems would be present and influence winds in the Gulf and on the shelf as the hurricane either forms within the Gulf or enters the Gulf. These other weather systems, and how they interact with an approaching hurricane, will influence winds over the shelf (both speed and direction); and therefore, they can influence development of the forerunner. Generation of the forerunner by wind along the Louisiana and Texas continental shelves will be strongly influenced by the local wind conditions on these two shelves.

Figure 7-2 shows snap-shots for all three storms 48 hrs prior to landfall for Storms 134 and 122. The snap shot for Storm 128 is actually taken slightly later, 45 hours prior to landfall; it has just originated in the Gulf. All three storms are intensifying at this stage in time. Storm 122 is the most intense of the three, so its far field winds along the Texas and Louisiana coasts are slightly greater. Winds along the Louisiana and Texas coasts are directed more onshore for storm 134 compared to Storm 122. Wind is pushing water along the coast, from Louisiana toward Texas, for both storms. The amplitude of the surge forerunner along the north Texas coast, above the initial mean water surface elevation used in the modeling, is similar for Storm 122 compared to Storm 134, approximately 1 ft, but seemingly slightly larger for storm 122. For Storm 128, which is the least intense storm of the three at this time, the forerunner surge along the Louisiana and Texas coasts is quite small.

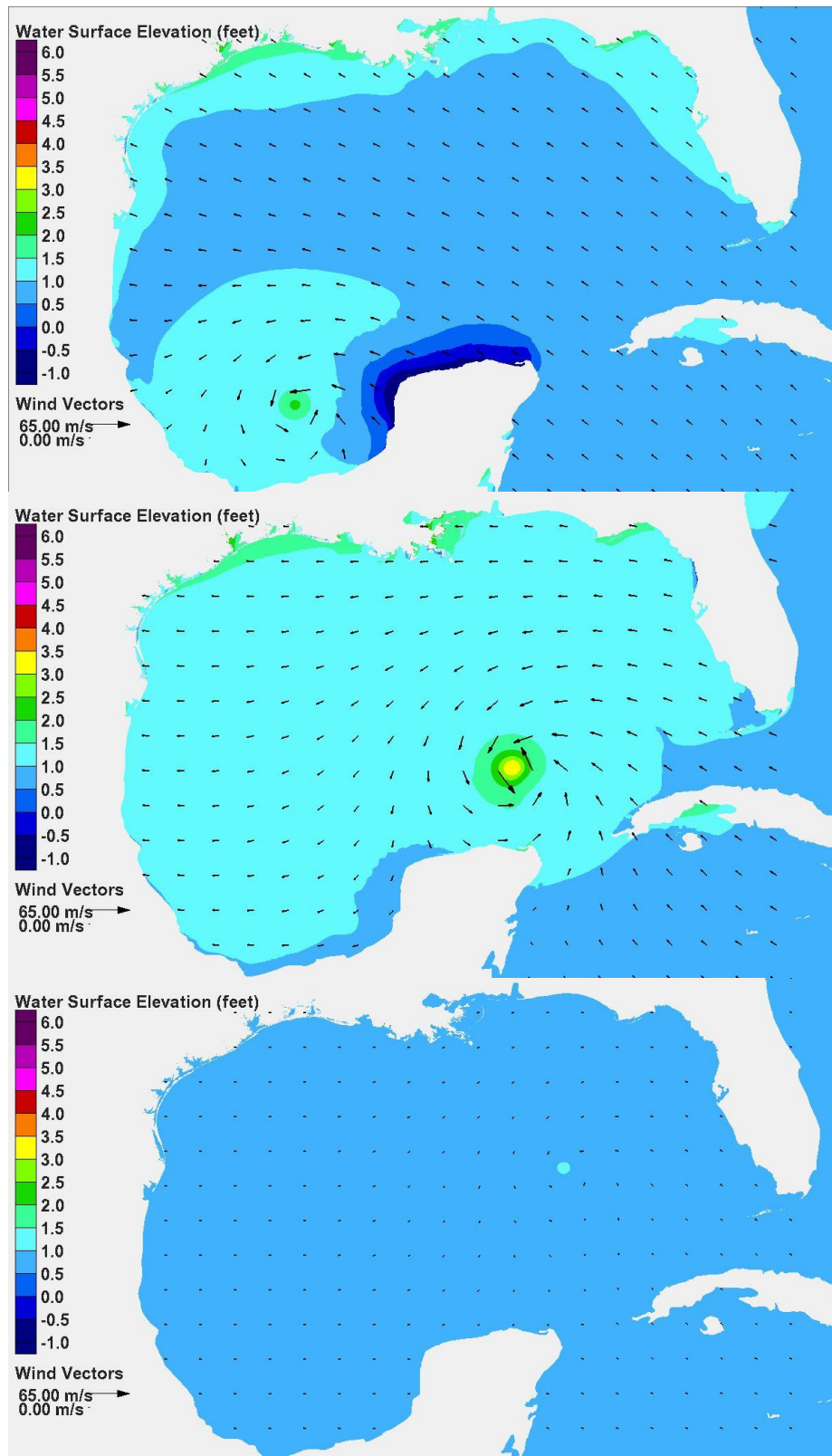


Figure 7-2. Water surface elevation and wind vectors 48/45 hours before landfall, Storm 134 (upper panel), Storm 122 (middle panel), Storm 128 (lower panel).

The snap-shot for Storm 122 shows evidence of the volume-mode contribution to the forerunner investigated by Bunpapong et al (1985); the entire water surface within the Gulf is elevated for this storm, which was not evident in results for the other two storms. Because they do not pass through the ports leading to the Gulf, the volume mode contribution to the forerunner for Storms 134 and 128 is expected to be less than the volume model oscillation for Storm 122. Because Storm 122 is relatively weak when it enters the Gulf, its volume model oscillation is expected to be small.

Figure 7-3 shows snap-shots for all three storms 36 hrs prior to landfall for each storm. Storm 122 is the most intense of the three at this stage as well; Storm 128 is the least intense. The amount of water building beneath the eye of the storm is a measure of storm intensity. The bulge of water under the eye develops because of atmospheric pressure gradients. The lower the central pressure in the eye the larger the spatial pressure gradients that act to push water toward the eye from all directions. Of the three storms the bulge for Storm 122 is greatest, indicating its greater intensity (i.e., its lower central pressure). None of the storms has yet reached its minimum central pressure (or strongest winds).

Intensity affects the magnitude of the simulated far field winds as well as the core winds. Winds for Storms 122 and 128 continue to be directed more parallel to shore along the north Texas and Louisiana coasts, pushing water along the shelf and toward the coastline by the Coriolis force. Winds for Storm 134 are directed much more onshore, directly pushing water up against the coastline. Both alongshore winds/water movement (because of the Coriolis force) and onshore winds/water movement act to increase the water surface elevation at the coast

At the time shown in Figure 7-3, Storm 122 has the largest surge forerunner. The forerunner amplitude for Storm 134 is only slightly less and the forerunner for Storm 128 is the smallest but is developing. The forerunner amplitude near the Galveston region is between 1 and 1.5 ft for Storms 122 and 134. Even though Storm 122 is more intense and has been since its inception, creating stronger winds along the shelves, the onshore directed far field winds of Storm 134 still produces a significant forerunner.

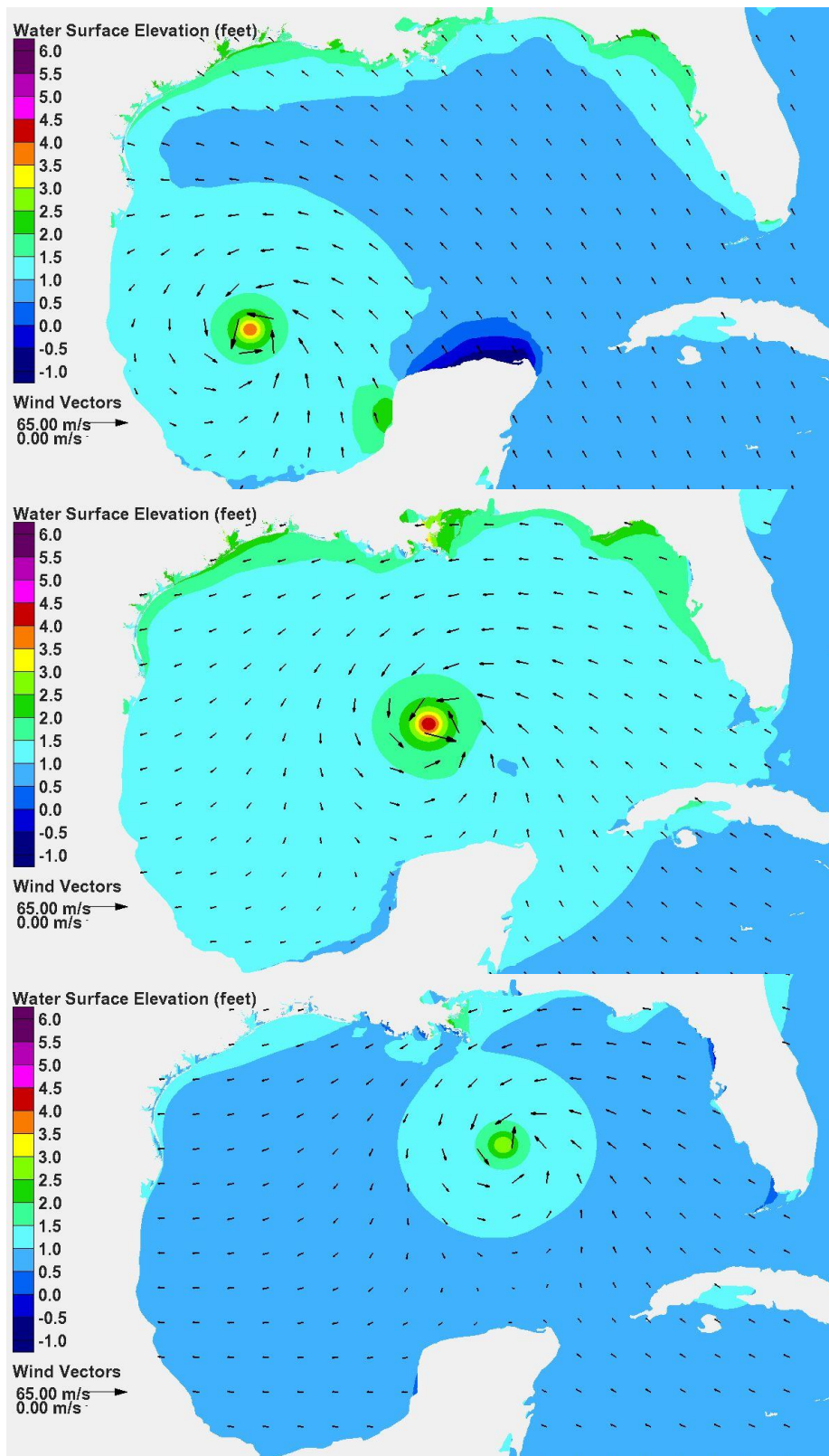


Figure 7-3. Water surface elevation and wind vectors 36 hours before landfall, Storm 134 (upper panel), Storm 122 (middle panel), Storm 128 (lower panel).

For Storm 128, a change is taking place along the Louisiana coast. Winds there are becoming increasingly directed more toward the offshore as the eye of the hurricane moves to the west and closer to landfall. The offshore directed winds are reducing the water surface elevation along the Louisiana coast and the along-shelf movement of water from the Louisiana shelf toward the north Texas shelf. The smaller surge forerunner for Storm 128 at this point in time is attributed to its lower intensity, its lag in time of intensification relative to the other two storms, and offshore directed winds.

For all three storms the wind-driven forerunner is present along the entire Texas shelf, and the width of the zone of highest forerunner surge is strongly correlated to the width of the shelf.

This snapshot for Storm 122, again, also reflects a uniform increase in water surface elevation, throughout the Gulf, indicative of the volume mode oscillation.

Figure 7-4 shows snap-shots for all three storms 24 hrs prior to landfall for each storm. At this point, all three storms have reached their most intense stage, a minimum central pressure of 900 mb. The water surface elevation increase under the eye of each storm is similar because the central pressure is the same. The amplitude of this bulge in the water surface is approximately 4 ft for each storm.

Wind speeds on the Texas and Louisiana shelves are now increasing as a result of the intensification and increasing proximity of the eye to the shelf. Winds for Storms 122 and 128 continue to have greater along-shelf components along the entire Texas coast, which are acting to build the forerunner. For Storm 134 winds are still directed somewhat onshore along the Texas coast, which is quite effective in developing the forerunner. It is noteworthy that the south Texas shelf is not nearly as wide as the north Texas and Louisiana shelves. Therefore, wind forcing along the south Texas shelf is not expected to develop as much of a forerunner. For Storms 122 and 134, winds along the Louisiana shelf have a significant alongshore component, pushing water to the west and onto the north Texas shelf.

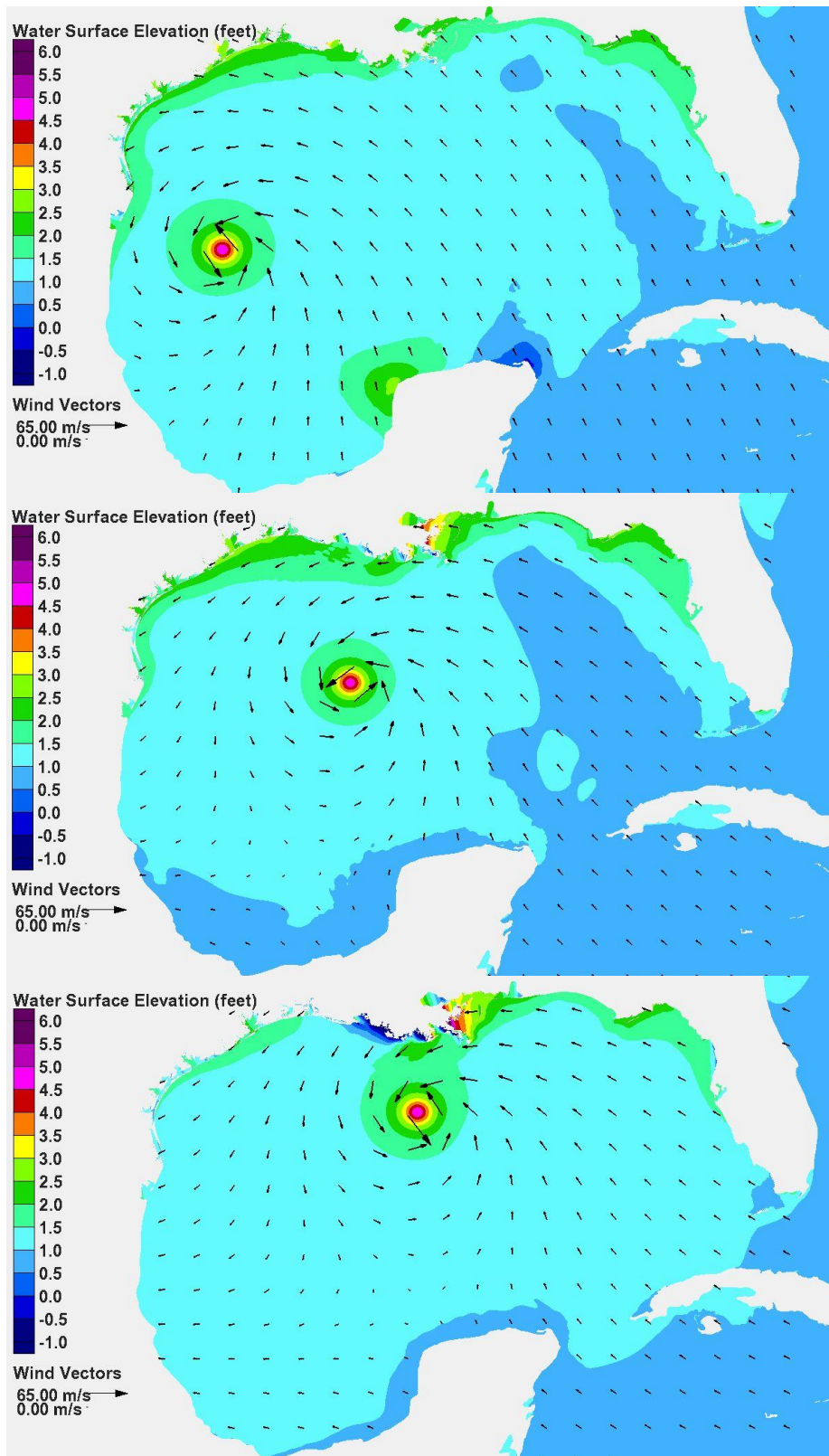


Figure 7-4. Water surface elevation and wind vectors 24 hours before landfall, Storm 134 (upper panel), Storm 122 (middle panel), Storm 128 (lower panel).

For Storm 128, winds are becoming stronger over the Louisiana shelf and continue to be directed toward the offshore as the eye of the hurricane moves to the west. Storm 128 winds are directed along the Texas shelf. Since both onshore and alongshore winds act to develop the forerunner on the Texas coast, all three storms are having this effect.

The closer proximity of Storm 134 to the south Texas coast, and the higher winds over the Texas shelf, is resulting in a larger forerunner there compared to the other storms. Storm 122 has the largest surge forerunner along the Louisiana coast. Both Storms 122 and 134 have generated a forerunner having a similar amplitude along the north Texas coast. The forerunner for Storm 134 is only slightly less in these areas. The forerunner amplitude near Galveston is between 1.5 and 2.0 ft for Storms 122 and 134.

The forerunner amplitude at the north Texas coast is smallest for Storm 128, approaching 1 ft. The offshore directed winds for Storm 128 are setting down the water surface (negative water surface elevations) in places along the Louisiana coast. Compared to Storms 122 and 134, the wind pattern for Storm 128 significantly reduces the amount of water that moves along the Louisiana and Texas shelves, which in turn reduces the amplitude of the surge forerunner along the north Texas coast by reducing the along-shelf movement of water from the Louisiana shelf toward the Texas shelf.

For all three storms the wind-driven forerunner is present along the entire Texas shelf, and the width of the zone of highest forerunner surge continues to be strongly correlated to the width of the shelf. The close proximity of Storm 134 to the south Texas coast means the surge forerunner is most pronounced there due to the higher alongshore and onshore winds.

Figure 7-5 shows snap-shots for all three storms 12 hrs prior to landfall for each storm. All three storms are at their most intense state in terms of central pressure and wind speeds.

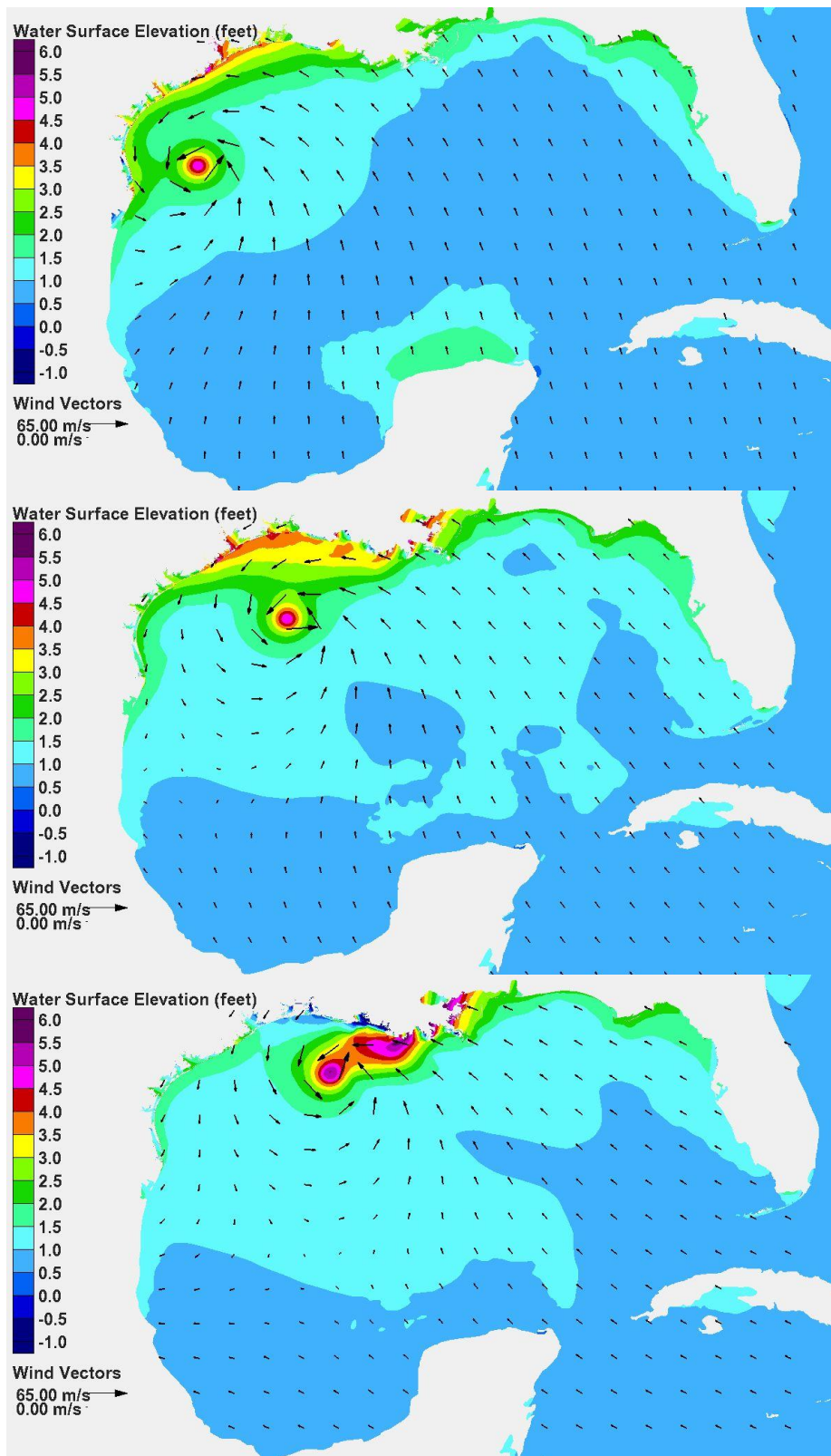


Figure 7-5. Water surface elevation and wind vectors 12 hours before landfall, Storm 134 (upper panel), Storm 122 (middle panel), Storm 128 (lower panel).

At this point, with the eyes closer to landfall, wind directions along the north Texas coast are becoming different for each storm. For Storm 134, winds are directed more onshore, winds for Storm 122 are directed more alongshore, and winds for Storm 128 are directed more offshore.

Forerunner amplitude is increasing for Storms 134 and 122 along the Louisiana and Texas coasts. Storm 122 has the largest surge forerunner along the open coast, with considerable water being pushed from the Louisiana shelf onto the Texas shelf. The forerunner amplitude near Galveston is between 2.5 and 3.0 ft for Storms 122 and 134. For Storm 122, the along-shelf movement of water from Louisiana to Texas is greatest and contributes to the higher forerunner surge along the north Texas coast. Storms 122 and 134, and to a lesser degree Storm 128, are creating a forerunner surge along the south Texas coast driven by the alongshore movement of water and the Coriolis force. Again, because of the close proximity of Storm 134 to the south Texas coast and the resulting higher wind speeds, the surge forerunner there is most pronounced.

The forerunner amplitude for Storm 128 has reached its maximum near Galveston and is beginning to decrease due to the pattern of offshore-directed winds as the eye approaches. As Storm 128 moves closer to the Houston-Galveston region, the offshore-directed winds begin to decrease the forerunner surge along the north Texas coast. That trend will continue until the core winds arrive on the shelf and increase the storm surge.

The surge response along the open north Texas coast is beginning to change from forerunner dominance (caused by far field winds) to dominance of the hurricane's core winds. The close proximity of the eye of Storm 122 to the shelf is beginning to force a much greater surge response on the Louisiana shelf, pushing a considerable amount of water toward the north Texas shelf. The eye from Storm 134 is farther from the wider Louisiana and north Texas shelves, but the onshore directed winds continue to build the forerunner. For Storm 128, winds along the north Texas shelf are directed offshore, decreasing forerunner development.

At 12 hours prior to landfall, the eyes of the three hurricanes are still in deep water but about to enter onto the continental shelf. Storm 128 is closest, and strong winds are beginning to force a much greater surge response on the Louisiana shelf.

Development of Surge within the Bays Due to Forerunner Propagation and Winds

Discussion now shifts to forerunner propagation through the passes that connect the Gulf with the bays, and how surge response within the bays develops as a function of bay filling associated with forerunner penetration and local wind conditions. As was the case for the open coast, bay surge response is strongly influenced by storm track because of the dependence of wind direction on track. Figures 7-6 through 7-9 show the surge forerunner response and wind conditions in the immediate Houston-Galveston region for the same three storms (Storms 134, 122 and 128), zooming in on the bays and nearshore coastal region. The figures show snap-shots of water surface elevation (as color-filled contours) and wind (as vectors) at times 48/45, 36, 24 and 12 hrs prior to landfall (45 for Storm 128 which originated later than the others).

The snap-shots in Figure 7-6 are 48/45 hrs prior to landfall. Water surface elevation along the open coast at the entrance to Galveston Bay is between 1.5 and 2 ft for Storms 134 and 122, and a negligible amount for Storm 128. Elevations inside both Galveston and West Bays are similar to those in the Gulf, suggesting effective penetration of the forerunner into both bays at this time. For Storm 134, winds are blowing approximately onshore from the southeast, and for Storm 122 winds are blowing from slightly south of east. Inside the bay, local winds are setting up the water surface from southeast to northwest for Storm 134 and from east to west for Storm 122, creating a tilt to the water surface in both cases. In response to the local wind, water moves within the bays such that water surface elevation contours are generally perpendicular to the wind direction. A sloping water surface is evident having an increase from one side of the bay to the other in the wind direction of approximately 1 ft.

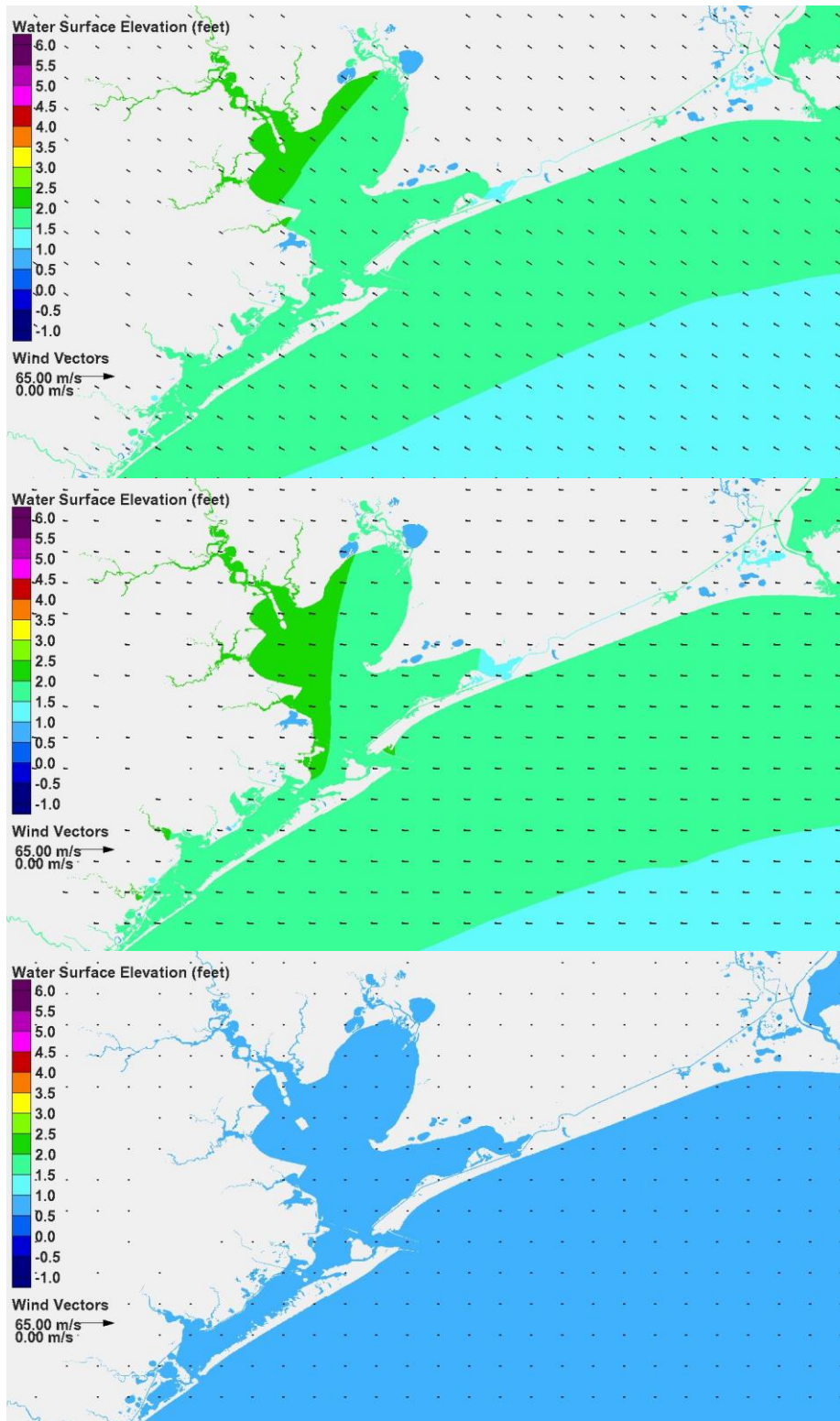


Figure 7-6. Water surface elevation and wind vectors 48/45 hours before landfall, Storm 134 (upper panel), Storm 122 (middle panel), Storm 128 (lower panel).

A point at the center of Galveston Bay is reasonably indicative of the Bay's overall water surface elevation in that it removes the effect of the tilting water surface. The water surface elevation in the middle of the bay is between 1.5 and 2 ft for Storm 134 and nearly 2 ft for Storm 122, indicating that the surge forerunner has effectively propagated into the bay and raised the entire water level through this filling action. The forerunner amplitude within the Bay is slightly greater for Storm 122, compared to Storm 134. The local wind imposes a tilt to the water surface (setting it up on downwind side and setting it down on the upwind side) that is superimposed on the raised water level.

For Storm 134 in particular, winds blowing from the southeast tend to set up the water surface along the open coast and the northwest part of Galveston Bay and set down the water surface along the southeast side of the Bay. This pattern of water surface elevation, for this wind direction, will create a water surface elevation gradient, or head difference, across the entrance pass at Bolivar Roads which will enhance propagation of the forerunner into the Bay, i.e., it will enhance filling of the Bay. The same process can occur at San Luis Pass.

For Storm 128, winds are still quite small within the Bay, so tilting of the water surface is evident in Figure 7-6. The degree of tilting is a function of the local wind speed within the Bay.

Figure 7-7 shows results for all three storms 36 hrs prior to landfall. Within the Bay, winds for Storms 134 and 122 are still from different directions. Wind direction for each storm is similar to what it was 12 hours earlier, so the general patterns of water surface tilting remain the same as the previous snap-shot, although the magnitude is slightly greater.

For Storm 134, the open coast water surface elevation is a slightly greater than 2 ft. The elevation in the middle of the bay appears to be about the same or slightly higher. As discussed for the previous snap-shots, southeasterly winds which are directed onshore give a "boost" to filling by setting down the lower part of the Bay, which increases the head difference across the pass.

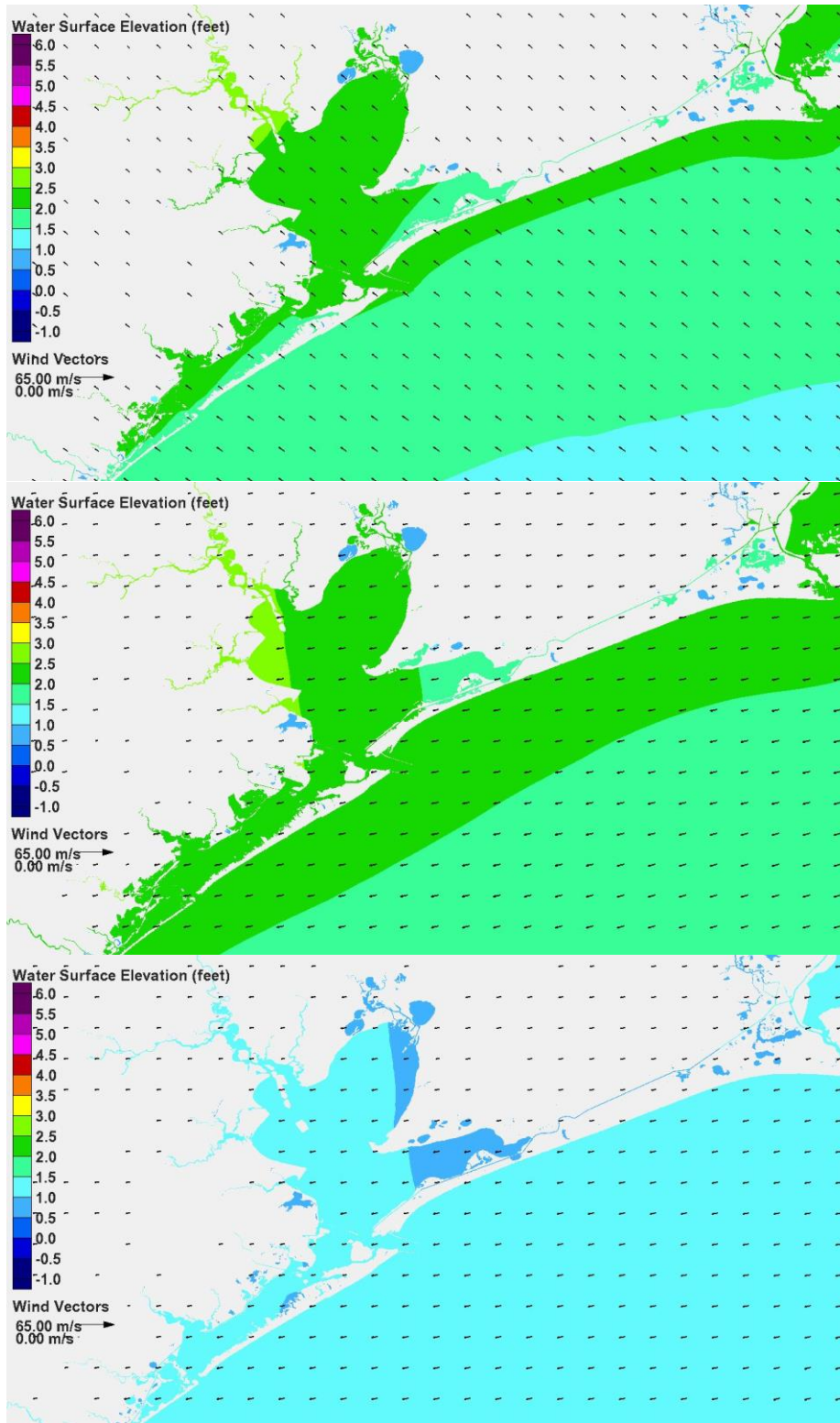


Figure 7-7. Water surface elevation and wind vectors 36 hours before landfall, Storm 134 (upper panel), Storm 122 (middle panel), Storm 128 (lower panel).

For Storm 122, the open coast water surface elevation at the entrance to the Bay is greater than for Storm 134, closer to 2.5 ft. The water surface in the middle of the Bay appears to be about the same for Storm 122, about 2.5 ft. The wind direction for Storm 122, winds from the east, does not produce the same degree of enhanced filling as Storm 134. Winds from the east tend to set up the western side of the Bay. Since Bolivar Roads is situated closer to the west side of Galveston Bay, a higher wind setup there reduces the head difference across Bolivar Roads pass, which in turn reduces the filling rate. If the wind were blowing from the north the wind setup on the south side of the Bay would be maximized, the head difference across the pass would be minimized, and the filling rate through the pass would be minimized.

For Storm 128, winds are also from the east, similar to Storm 122, and the pattern of water surface tilt is similar. The higher winds for Storm 122 create a greater degree of tilt within the Bay. At this time before landfall, Storms 122 and 134 have a greater intensity, i.e., higher wind speeds, than Storm 128. The forerunner amplitude on the open coast is lower for Storm 128, so the degree of filling within the Bay is expected to be less.

Figure 7-8 shows results for each of the three storms 24 hrs prior to landfall. The storms are closer to the coast so winds within the Bay are stronger. Storm 128 has just reached its minimum central pressure of 900 mb, while the other two storms have been at their minimum central pressure for 7 hours. Wind speeds in the Bay for the three storms are similar and are shifting in the counterclockwise direction. For Storm 134, winds are now blowing from the east-southeast; winds for Storm 122 are blowing from the east-northeast; and winds for Storm 128 are blowing from the northeast.

For all three storms, in response to the change in wind direction, the pattern of water surface tilt has also changed. In each case, the contours of constant water surface elevation within the Bay remain nearly perpendicular to the wind direction. Water is moving within the bay in response to the wind to create the water surface elevation gradient, or tilt.

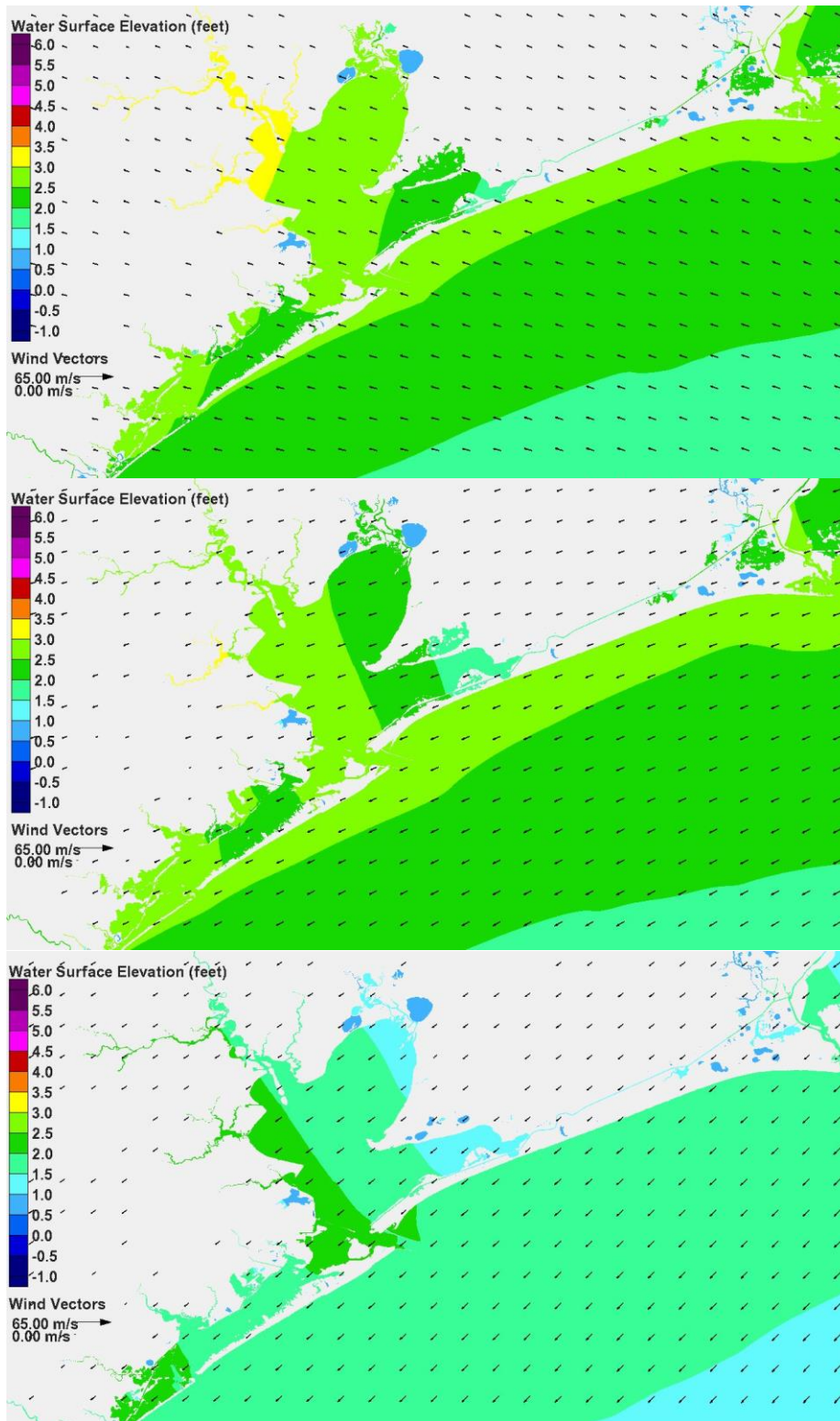


Figure 7-8. Water surface elevation and wind vectors 24 hours before landfall, Storm 134 (upper panel), Storm 122 (middle panel), Storm 128 (lower panel).

It is important to note that wind effectively establishes the water surface tilt throughout Galveston Bay, projecting the same tilting pattern into the upper reaches of the Houston Ship Channel and into other estuaries. This is the case for all three storms, and is seen in the water surface elevation fields for all three.

The amplitude of the forerunner on the open coast is slightly greater for Storm 122 than for Storm 134. The amplitude of the forerunner at the coast for Storm 128 is 0.5 to 0.75 ft lower than for the other storms. The water surface elevation in the middle of the Bay is still greatest for Storm 134, slightly more than the elevation for Storm 122. Storms approaching from the south tend to increase propagation of the forerunner surge into the Bay compared to tracks from the south-southeast and southeast.

The magnitude of the water surface tilt (the difference between water surface elevations on opposite sides of the bay in the direction of the wind) is similar for Storms 122 and 134, approximately 1.5 ft. However, the water surface elevations are higher for Storm 134, compared to Storm 122, because of the higher degree of Bay filling. The magnitude of the tilt for Storm 128 is about 1 ft across the Bay, which is larger than the previous snap-shot.

These snap-shots also illustrate a feature in the water surface slope within West Bay that is worth noting. West Bay has been filling, just as Galveston Bay has been filling, due to the open coast forerunner surge driving the filling action. At this point, winds in West Bay have a significant easterly component, more so for Storms 122 and 128, and less so but still present for Storm 134. This easterly wind component is acting to set up the west end of West Bay. It is also acting to enhance water movement from Galveston Bay into West Bay, particularly for Storms 122 and 128, where winds are blowing in the direction of the long axis. For all three storms, there is some indication that the water surface elevation on the Bay side of San Luis Pass is nearly the same or greater than the water surface elevation on the Gulf side. Once the water surface elevation is greater on the Bay side, water will actually start to flow back toward the Gulf through San Luis Pass. This flow reversal might have implications for design and operation of any gate at San Luis pass that is a structural component of the Ike Dike concept.

Figure 7-9 shows snapshots 12 hrs prior to landfall. At this point all three storms have been at their most intense stage for 12 hrs for Storm 128 and approximately 18 hrs for the other two storms. Winds are continuing to shift direction with a counterclockwise rotation; winds are now blowing from the east, northeast, and north-northeast for Storms 134, 122 and 128, respectively.

The water surface in Galveston Bay responds predictably to the shift in winds, moving quickly to establish contours of constant water surface perpendicular to the wind direction. Wind speed is increasing as is the magnitude of water surface slope in response to the higher winds.

The magnitude of the water surface tilt from one side of the bay to the other, in the direction of the wind, is approximately 2 ft for Storms 134 and 122. The tilt for Storm 128 is now nearly the same as it is for the other two storms, approximately 2 ft, because winds within the Bay are quite similar for all three storms. For Storm 128, the northeast-most portion of Galveston Bay (in Trinity Bay) is set down by the wind. The water surface elevation here is approaching 0 ft NAVD88 which is about 0.5 ft below mean tide level.

The degree of Bay filling, as estimated by the water surface elevation in the middle of the Bay, is between 3.5 and 4 ft for Storm 134, approximately 3.5 ft for Storm 122, and between 1 and 1.5 ft for Storm 128. For Storm 128, winds were blowing from the northeast 12 hrs earlier and are now blowing from the north-northeast. Recall from the previous report section that this wind direction is decreasing the amplitude of the surge forerunner along the open coast. This trend is seen in the lower panel of Figure 7-9. Winds from northerly directions set up the lower, or southern, portion of Galveston Bay. The decreased open coast water surface elevation and the higher elevation on the Bay side at Bolivar Roads due to wind setup both act together to reduce filling of the Bay by reducing the head difference across Bolivar Roads. These processes are key factors in reducing forerunner penetration into Galveston Bay for storms that approach from the southeast or from more easterly directions.

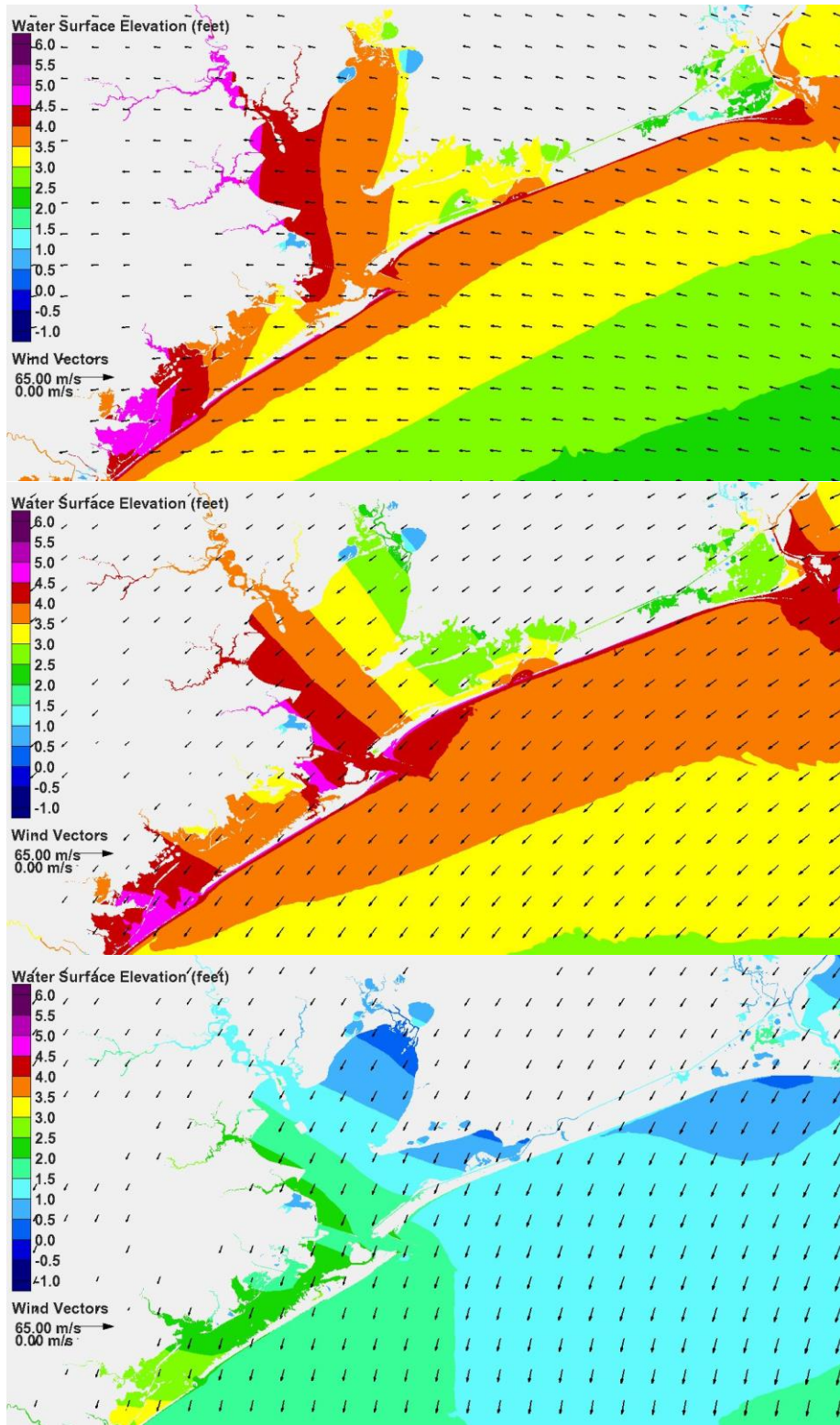


Figure 7-9. Water surface elevation and wind vectors 12 hours before landfall, Storm 134 (upper panel), Storm 122 (middle panel), Storm 128 (lower panel).

For all three storms, in response to the wind direction, the pattern of water surface tilt in the coupled system is forcing water from Galveston Bay into West Bay, and wind is setting up the west end of West Bay. The mean water surface in West Bay is as high, or higher, than it is in Galveston Bay, particularly for Storm 128. For all three storms, the water surface elevation on the Bay side of San Luis Pass is higher than the elevation on the Gulf side, causing water to flow toward the Gulf through the Pass.

To further support this surge forerunner analysis and to provide more quantitative information on water surface elevations and forerunner amplitude, water surface elevation time series were generated for all three storms at the six locations shown in Figure 7-10. The six locations are: 1) the open Gulf coast at Galveston Pleasure Pier, 2) the bay side of the City of Galveston where West Bay meets Galveston Bay, which is also indicative of the bay side of Bolivar Roads, 3) Texas City, 4) the entrance of the tidal channel that leads to the Clear Lake area, 5) the upper Houston Ship Channel, and 6) a point in the middle of Galveston Bay called Trinity Bay (central). Trinity Bay is the large embayment on the northeast side of Galveston Bay.

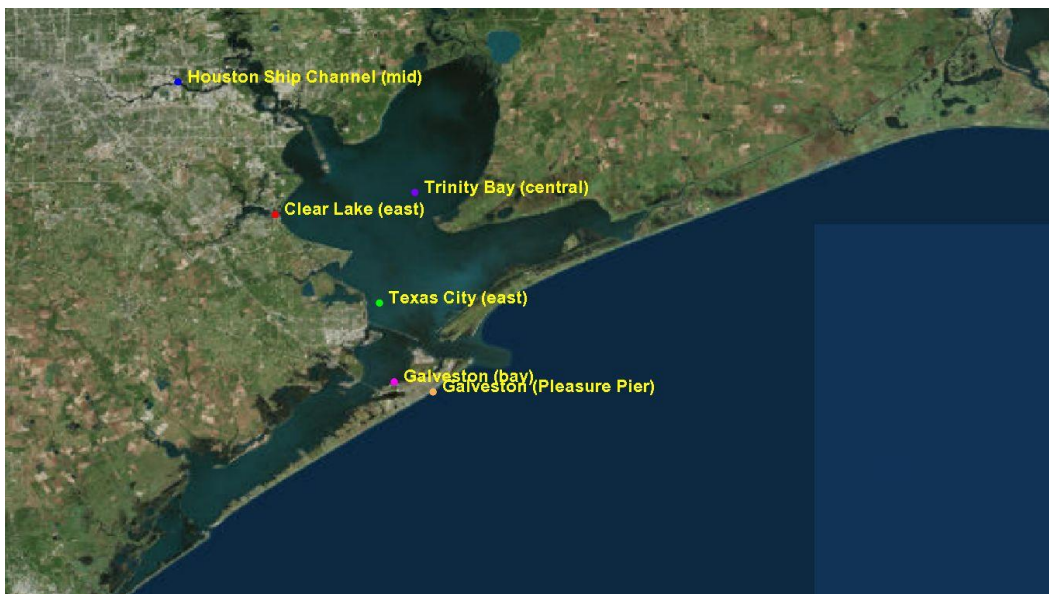


Figure 7-10. Locations of hydrographs considered in the analysis of forerunner development as a function of storm track.

Figures 7-11 through 7-13 show times series at the six locations for Storms 134, 122 and 128, respectively. The vertical axis for each graph is water surface elevation, in feet, NAVD88. The horizontal axis is time, in hours, from the beginning of the simulation. The last point in time shown in each graph is 12 hours prior to landfall for that particular storm. For example, in Figure 7-11, hour 83 on the horizontal axis corresponds to a time 12 hours prior to landfall. Hour 71 on the horizontal axis is 24 hours before landfall, and so on.

Figure 7-11, for Storm 134, shows that the water surface elevation time series at all five locations inside the bay equal or exceed the open coast time series at Galveston Pleasure Pier. This indicates that the open coast surge forerunner effectively propagates into the Bay through the passes, i.e. fills the Bay, for this general storm track. At the Trinity Bay (central) location, which approximates the average water surface elevation within the Bay, the time series lies consistently above the open coast time series for most of the time shown. This reflects the “boost” to the filling rate described previously that arises because the far field winds are primarily directed onshore as the storm approaches.

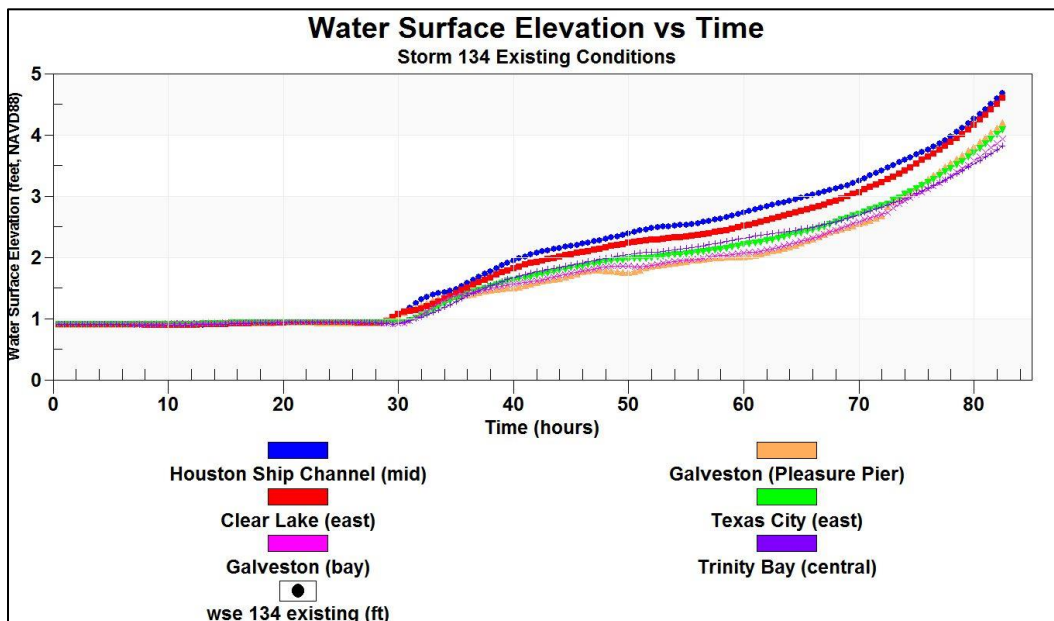


Figure 7-11. Temporal variation of storm surge for Storm 134.

Twelve hours prior to landfall, the open coast surge forerunner at Galveston Pleasure Pier has an amplitude of nearly 3.5 ft relative to mean sea level, which corresponds to the water surface elevation of nearly 4 ft NAVD88 seen at the end of the time series. This amplitude is nearly identical to that in the middle of the bay at Trinity Bay (central). At 24 hours prior to landfall, the open coast forerunner has a smaller amplitude of 2.1 ft, while the amplitude in the middle of the bay is about 0.2 ft higher, 2.3 ft.

Within the Bay, both the filling action and tilting action caused by local wind contribute to the water surface elevations. Higher water surface elevations are evident for locations in the upper parts of the Bay (including the upper Houston Ship Channel and Clear Lake), with the highest being in the upper reaches of the Channel. Lower water surface elevations are seen for locations in the lower parts of the Bay (bay side of Galveston and Texas City). This pattern is consistent with winds blowing from the southeast, which occurred during much of the forerunner development period of time.

Figure 7-12, for Storm 122, shows similar trends. The water surface elevation time series at all five locations inside the Bay equal or exceed the open coast time series at Galveston Pleasure Pier. For Storm 122 the open coast surge forerunner also effectively propagates into the Bay through the passes. For this and other storms on this general track, effective propagation of the forerunner into the Bay is expected.

Within the Bay, both the filling action and tilting action caused by local wind contribute to the water surface elevations. Higher water surface elevations are evident for locations in the northwestern parts of the Bay (including the upper Houston Ship Channel and Clear Lake), with those two locations having nearly the same water surface elevations for much of the forerunner development period. Compared to Storm 134, there is less variation in the time series along the western side of the Bay. This tendency is due to the prevalence of easterly winds, which tend to set up the western side of the Bay where most of the monitoring locations are situated.

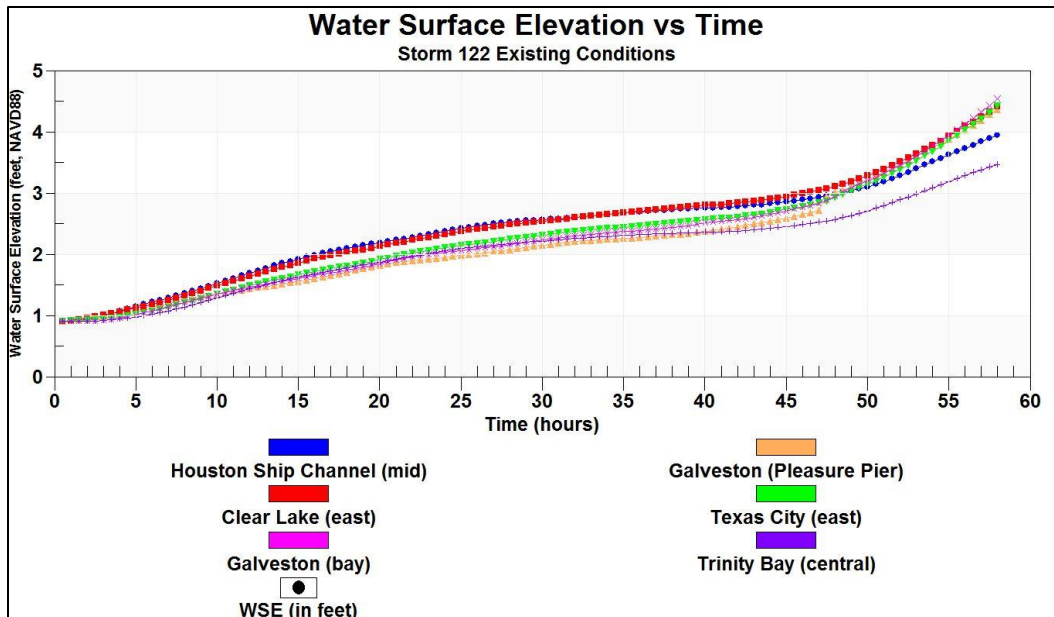


Figure 7-12. Temporal variation of storm surge for Storm 122.

In the middle of the Bay, the Trinity Bay (central) time series is very similar to the open coast time series at Galveston Pleasure Pier. Storms on this track do not appear to produce the “boost” in forerunner propagation into the Bay that was observed for Storm 134.

For Storm 122, twelve hours prior to landfall, the open coast surge forerunner at Galveston Pleasure Pier has an amplitude of 3.9 ft relative to mean sea level (elevation of 4.4 ft NAVD88). This amplitude is approximately 0.9 ft higher than the forerunner amplitude at Trinity Bay (central). At 24 hours prior to landfall, the open coast forerunner has a smaller amplitude of 2.1 ft, while the amplitude in the middle of the bay is about 0.1 ft lower, 2 ft.

Figure 7-13, for Storm 128, shows very different trends in forerunner propagation into the bay and evolution compared to Storms 134 and 122. All the time series for Storm 128 show an initial build-up of the surge forerunner, as did the other two storms. However, the trend of increasing forerunner amplitude changes to a trend of decreasing amplitude about 20 hours prior to landfall. The exact time of change is a function of the storm’s forward speed. As the storm on this track moves closer to shore, winds begin to shift to northerly directions, diminishing the surge forerunner amplitude and pushing water way from the coast.

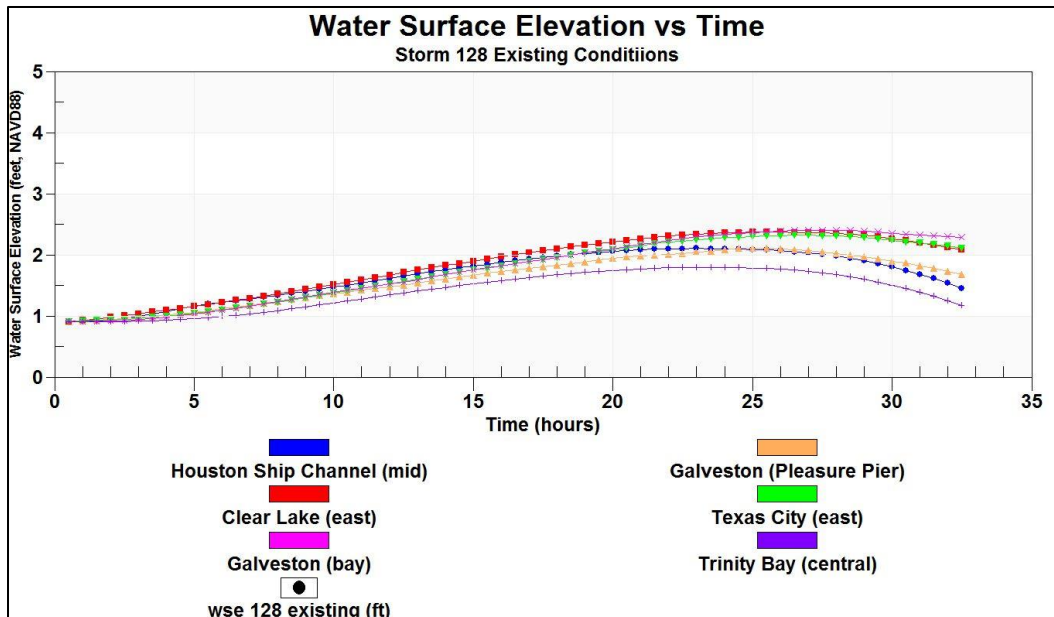


Figure 7-13. Temporal variation of storm surge for Storm 128.

For Storm 128 the forerunner amplitude on the open coast is greater than the amplitude in the middle of the Bay for the entire duration of the storm. This indicates a reduced capacity of the forerunner to penetrate into the Bay through the passes. This behavior is caused by the easterly winds (early) and northeasterly winds (later) which tend to set up the western side of the Bay (early) and southwesterly side (later), where most of the monitoring locations are situated. For this storm there is also much less variation in the time series along the western side of the Bay, due to the same prevailing wind directions. In the latter stages of forerunner development, when winds are blowing more out of the north, water is pulled from the upper reaches of that part of the Bay system.

Twelve hours prior to landfall, the open coast surge forerunner at Galveston Pleasure Pier has an amplitude of 1.2 ft relative to mean sea level. This amplitude is approximately 0.6 ft higher than the forerunner amplitude at Trinity Bay (central) at the same time. At 24 hours prior to landfall, the open coast forerunner has a higher amplitude of 1.4 ft, while the amplitude in the middle of the bay is about a 0.2 ft lower, 1.2 ft.

Galveston Bay Storm Surge Response to the Hurricane's Core Winds

For these three storms, until 12 hours prior to landfall, the surge forerunner dictates surge development along both the open coast and within Galveston and West Bays. As the storms move onto the continental shelf the storm's core winds, i.e., those winds closer to the eye particularly on the right hand side where wind speeds are generally highest, begin to dominate the surge development process. The temporal rate of change in water surface elevation begins to increase; because, as the eye moves into shallower water, winds become increasingly more effective in pushing water. The effective surface wind stress in the water momentum balance is inversely related to water depth. Therefore, for the same wind speed, the effective wind stress is less in deeper water and greater in shallower water; and it is greatest in the very shallow water of the nearshore coastal zone and in the shallow bays.

Figures 7-14 through 7-22 show snap-shots in time for three storms from the bracketing set. Storm 136 approaches from the south, Storm 122 approaches from the south-southeast, and Storm 128 approaches from the southeast. Storm 136 was selected to represent storms approaching from the south, instead of Storm 134 which was selected previously, because the landfall location for storm 136 is closer to the landfall locations of the other two storms. All three storms have the same minimum central pressure (900 mb) and the same radius to maximum winds (17.7 n mi). Storm 136 has a faster forward speed, 17 kts. Forward speeds for the other two storms are 11 kts.

The snap-shots show the water surface elevation field as filled color contours and the wind field as black vectors, for the immediate Houston-Galveston region. Note the change in water surface elevation scale for this series of figures, compared to that used in the previous discussion of the forerunner. A color bar scale that ranges from -4 to +24 ft is used in this report section. Each figure contains three images. The top panels show results for Storm 136, results for Storm 122 are shown in the middle panel, and results for Storm 128 are shown in the bottom panel. Each figure reflects a different point in time as the hurricane approaches the coast, makes landfall, and then moves out of the Houston-Galveston region. This analysis advances the progression in time from the point where it ended in the previous report section, 12 hours before landfall. The first figure shows results 6 hours prior to landfall and the last figure shows results 9 hours

after landfall. The time increments between snap-shots are variable; they are concentrated on times around landfall.

Figure 7-14 shows results 6 hrs prior to landfall. Wind speeds are increasing as the eye moves closer to shore. For each of the storms, wind directions are similar to what they were 6 hrs earlier; but they continue to shift, rotating in the counterclockwise direction. At this point, in Galveston Bay, winds for Storm 136 are blowing from the east-northeast, winds for Storm 122 are blowing from the northeast, and winds for Storm 128 are blowing from the north-northeast.

For all three storms the higher wind speeds are creating a larger gradient, or tilting, in the water surface. For Storm 136 the region of highest surge within Galveston Bay is along the western shoreline, and the zone of highest surge extends into the upper reaches of the Houston Ship Channel. In West Bay the east-northeasterly winds set up the western side of the bay and push water from Galveston Bay into West Bay. For the other two storms, the zone of highest surge is at the southwest corner along the bay side of the City of Galveston. This water surface pattern also acts to push water from Galveston Bay into West Bay. For Storms 136 and 122, local winds having a significant northerly component and they set down the water surface in the upper reaches of the Channel. For all three storms, the northeast part of Galveston Bay is being set down by the wind.

Figure 7-15 shows snap shots 3 hrs prior to landfall. The eye of the hurricane is beginning to enter the image for all three storms. The curvature of the wind field about the eye, associated with the counterclockwise wind circulation in a hurricane, is evident for all three storms. For Storm 136 (upper panel), winds in Galveston Bay are still blowing from the east-northeast, which is producing the highest surges within Galveston Bay along its western shoreline. Along this side of the Bay, easterly winds are forcing a higher surge into the western reaches of the Clear Lake and Dickinson areas, where wind is pushing water up into the channels and estuaries, establishing the same water surface gradient that is evident throughout the rest of the Bay. Increasing wind speeds within the Bay are increasing the magnitude of the water surface elevation gradient.

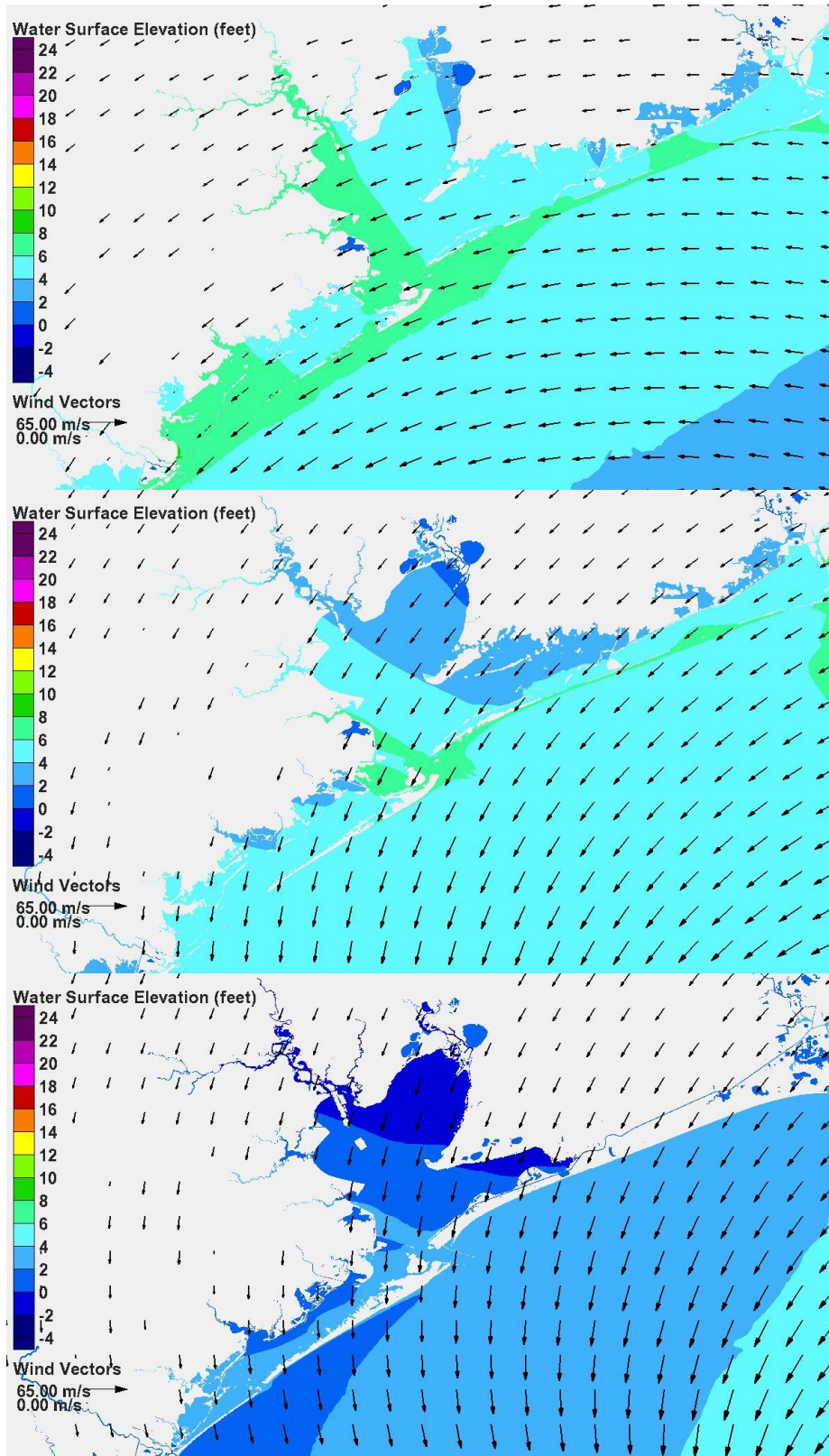


Figure 7-14. Water surface elevation and wind vectors 6 hours before landfall, Storm 136 (upper panel), Storm 122 (middle panel), Storm 128 (lower panel).

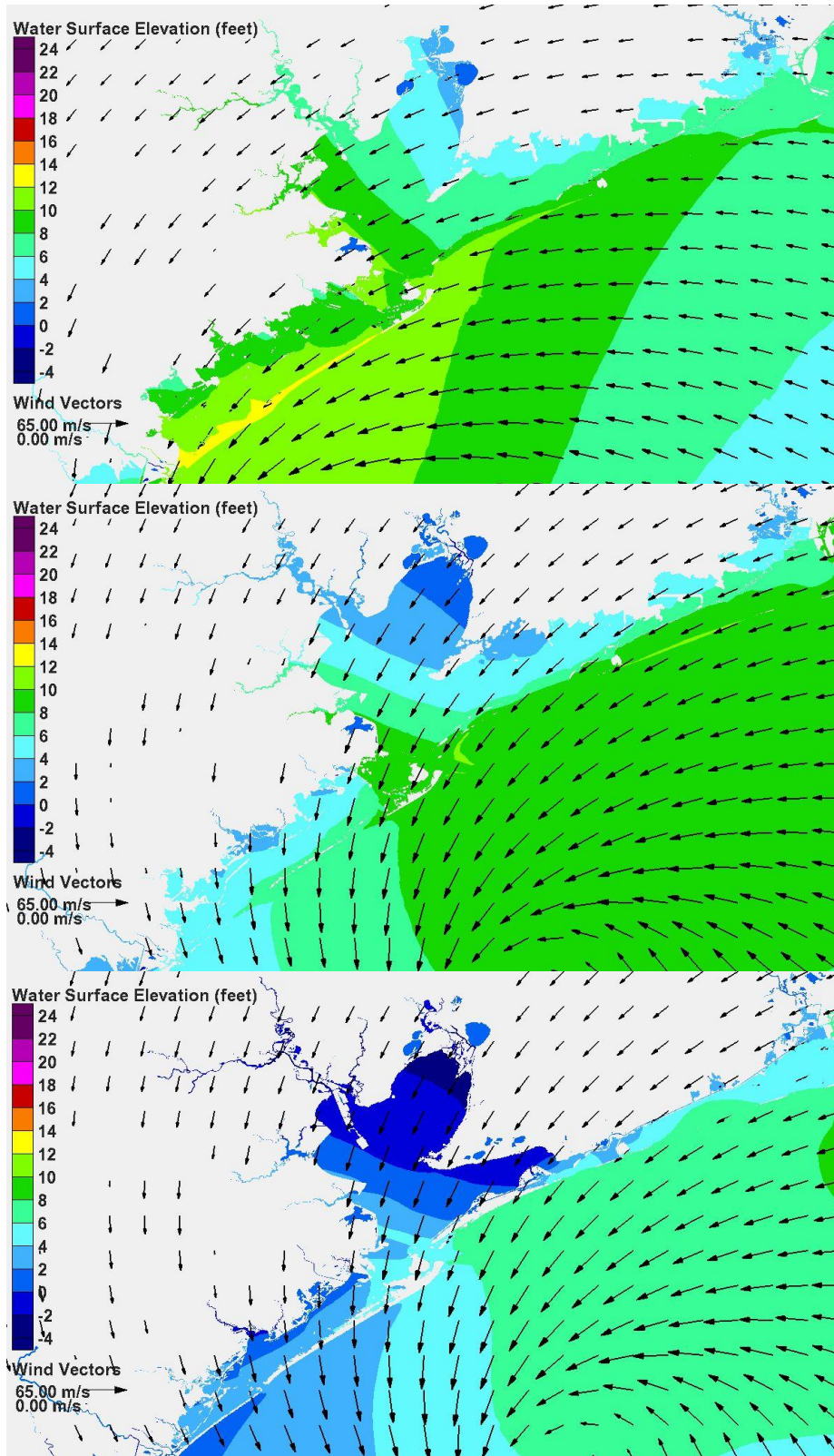


Figure 7-15. Water surface elevation and wind vectors 3 hours before landfall, Storm 136 (upper panel), Storm 122 (middle panel), Storm 128 (lower panel).

Along the open coast, the zone of highest surge for Storm 136 is near San Luis Pass, and it is moving to the northeast as the storm advances toward the northeast. This is a different direction of peak surge migration compared to the other two storms, which are moving into the region from the east and northeast.

In West Bay for Storm 136, winds are blowing from the northeast in the direction of the long axis of the Bay, due to the curvature in the core hurricane winds. This wind direction acts to set up the western side of the Bay, which continues to force water from Galveston Bay into West Bay. The highest surge in West Bay at this point in time is at its western end. Along the open coast, winds also are pushing water into the region from the east. Considerable flow over Galveston Island and Bolivar Peninsula is taking place.

For Storm 122, along the coast, surge is growing and developing from the east and northeast, and moving into the Houston-Galveston region from that direction. In response, the largest surges are along the Gulf side of Bolivar Peninsula. Within Galveston Bay winds are blowing from the northeast to north-northeast directions, setting up the southwest corner of the Bay. The largest surge at this point within Galveston Bay is at this corner, near the bay side of the City of Galveston. Within West Bay, due to curvature of the hurricane wind field, winds are blowing from the north-northeast and setting up the water surface on the bay side of Galveston Island. Water is moving from Galveston Bay into West Bay due to the gradient in water surface elevation between the two bays. Surge on the Gulf and bay sides of Galveston Island are nearly the same. Considerable flow over the barrier islands is taking place.

The pattern of storm surge development for Storm 128 is similar to that for Storm 122. The coastal surge is building and moving into the region from the east and northeast. Winds within Galveston Bay are nearly the same as for Storm 122. In response, a similar water surface elevation gradient is established within the Bay, although absolute elevations are greater for Storm 122 because of the greater forerunner penetration. The maximum surge within the Bay at this time is also on the bay side of the City of Galveston. Some flow over Bolivar Island is occurring; little flow is apparent over Galveston Island at this point because of lower water surface elevations.

Figure 7-16 shows conditions approximately 1 hr before landfall. The wind fields are fairly similar for all three storms because the eyes have similar positions, and the counterclockwise wind circulation about the eye is similar for all three storms. In the previous set of snap-shots (see Figure 7-15) 3 hrs before landfall, because of the counterclockwise wind circulation, winds were blowing more or less along the coast for Storms 122 and 128, pushing water into the nearshore coastal region from the east. As these storms approach landfall winds will become directed more onshore, like Storm 136 shows for this time. In response to onshore winds, surge that has been building from the east is driven toward shore. As the storms move into shallower water the highest core winds to the right hand side of the eye become increasingly more effective in pushing the water in the direction of the wind and building the storm surge against the coastline.

Along the open coast, the zone of peak surge for Storm 136 continues to move to the northeast and is now situated at the City of Galveston. For both Storms 122 and 128, surge continues to build from the east and the zone of peak surge is positioned along Bolivar Peninsula. For all three storms, Galveston Bay is filling because of the large volume of water that is flowing over Bolivar Peninsula into the bay, which is then pushed by the wind toward the Bay. The high open coast surge also is propagating into the bay through Bolivar Roads.

Flow over Galveston Island is occurring for all three storms. Winds in West Bay are directed offshore along the western portion of Galveston Island, on onshore along the eastern portion, for all three storms. Offshore-directed winds act to push water against the back side of Galveston Island and drive flow over the inundated barrier island.

Within Galveston Bay, winds are from the east-northeast for Storm 136 and from the northeast for the other two storms. These wind directions continue to set up the water surface along the western shoreline of the Bay for Storm 136, and along the southwestern shoreline of the Bay for Storms 122 and 128. The higher wind speeds are increasing the degree of tilt, or the gradient, in the water surface. The highest surge remains along the bay side of the City of Galveston and the Texas City area at this point for all three storms. The surge at this location also is influenced by the propagation of coastal surge through the pass at Bolivar Roads.

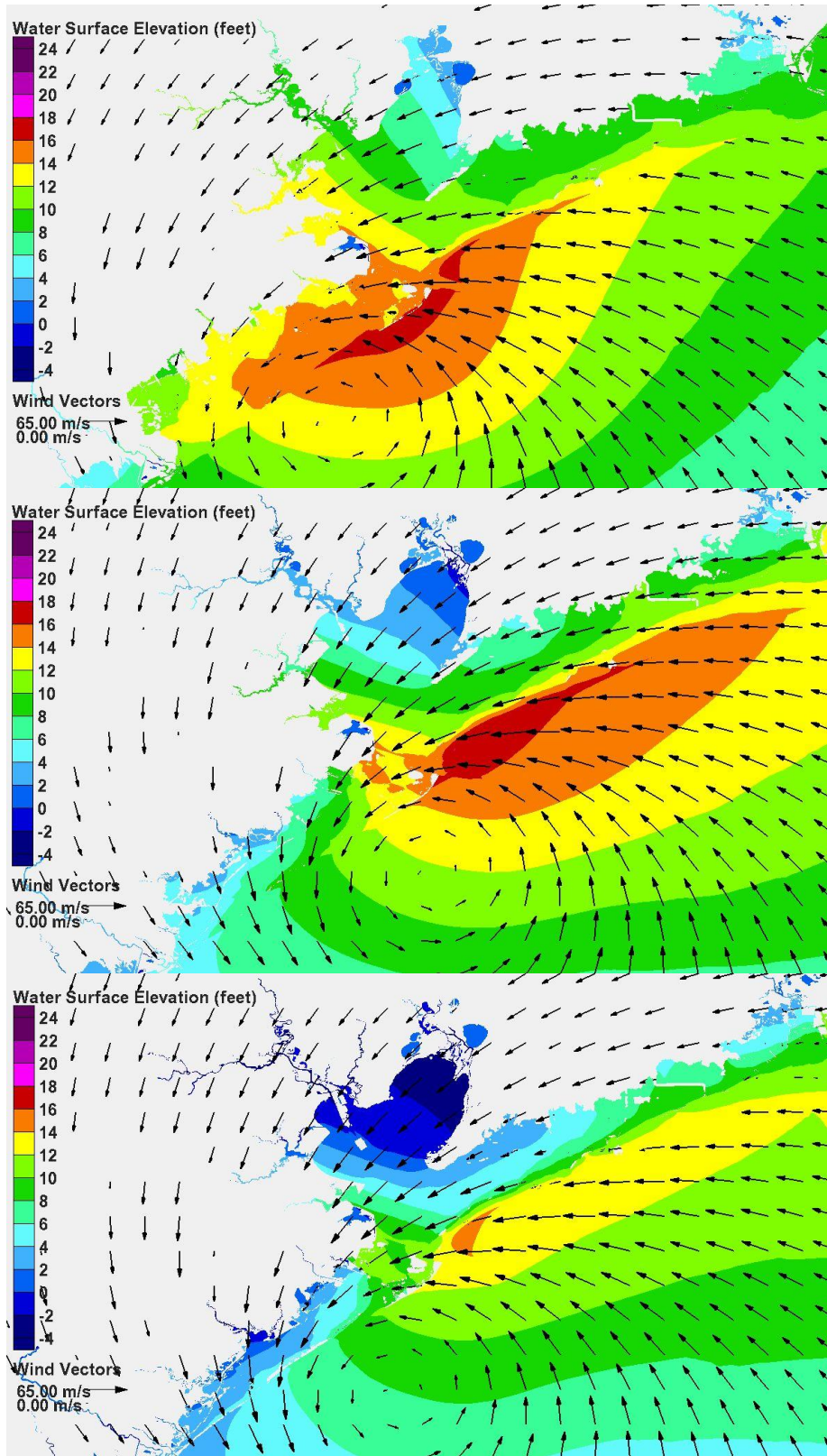


Figure 7-16. Water surface elevation and wind vectors 1 hour before landfall, Storm 136 (upper panel), Storm 122 (middle panel), Storm 128 (lower panel).

Figure 7-17 shows the storm surge and wind fields at landfall. Winds are directed onshore to the east of the eye for all three storms. For Storm 136, the zone of peak surge continues to move toward the northeast and is now situated at the western end of Bolivar Peninsula. For Storms 122 and 128, the zones of peak surge persist along Bolivar Peninsula. Winds to the east of the eye continue to push surge over Bolivar Peninsula and into the Bay. Winds in West Bay are directed offshore along those parts of the island to the left, or west, of the eye. The offshore-directed winds continue to stack water against the Bay side of Galveston Island and push water over the inundated island.

At this time, wind conditions within the Bay are quite similar for all three storms, blowing from the east, and forcing a similar water surface tilt. Differences in absolute elevation between storms are due to different forerunner penetration and differing amounts of filling by flow over the barrier islands. Winds in the Bay are shifting rapidly, and the water surface elevation field responds quickly to the wind shift. Water is moving rapidly to establish the primary momentum balance between wind shear stress and water surface slope.

Figure 7-18 shows conditions 1 hr after landfall. The eyes of the storms are moving inland; as they do so, winds are rapidly shifting within Galveston and West Bays. The curvature in wind fields produces considerable variation in wind direction for all the storms, but less so for Storm 128 since its eye is the farthest away from the Bay. With the eye being farther away, the curvature of the wind fields in the Bay is less. For all three storms, water that has been pushed into Galveston Bay is now starting to be driven to the north and northwest sides. Water also is filling the northeast parts of the Bay that previously had been p set down by the wind. In West Bay the winds are shifting rapidly, blowing from the northwest for Storms 136 and 122. For Storm 128, winds are now blowing from the south in the eastern portion of the Bay, setting up the north side. The water surface is responding quickly to the shifts in wind conditions in these shallow bays.

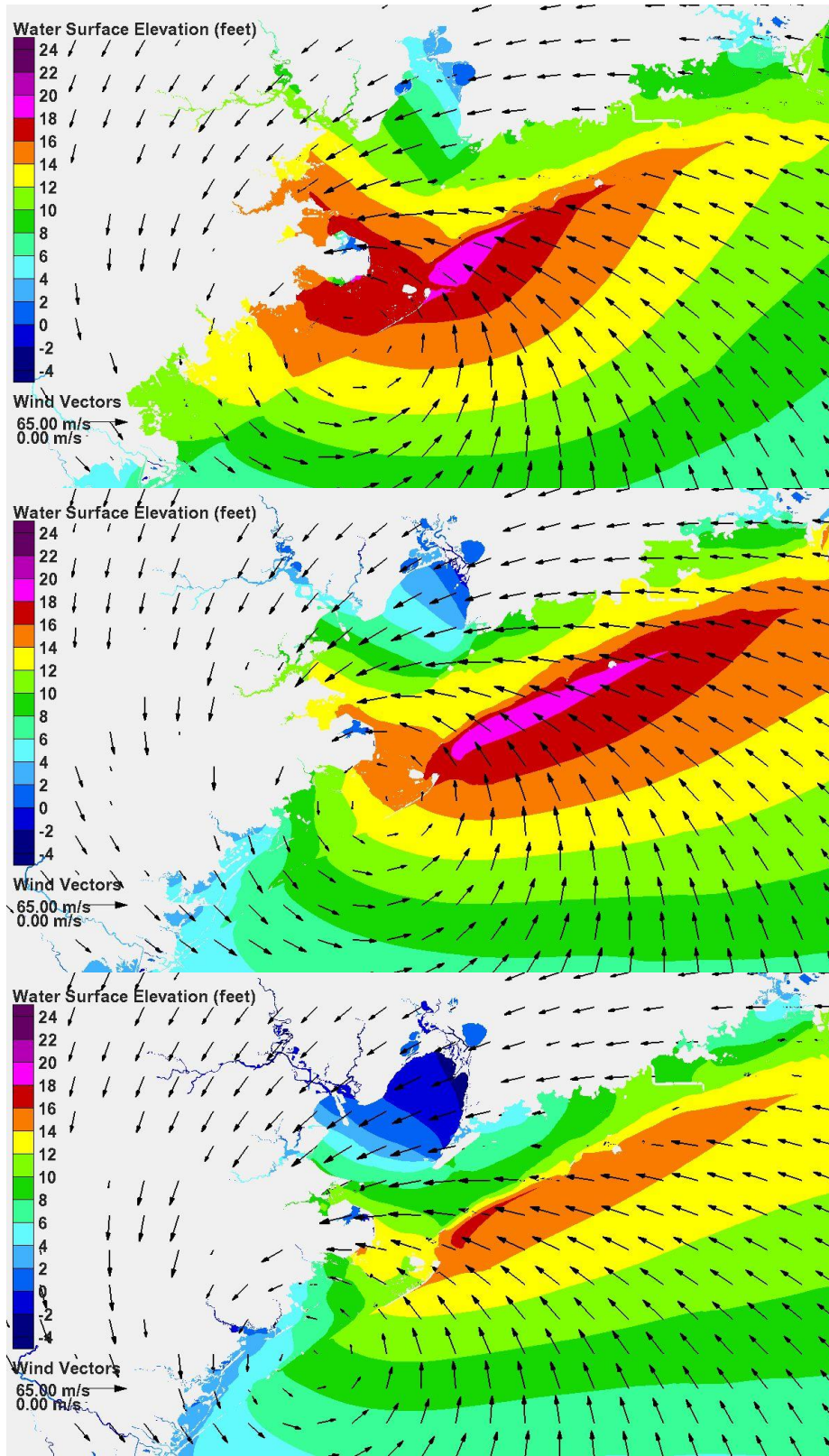


Figure 7-17. Water surface elevation and wind vectors at landfall, Storm 136 (upper panel), Storm 122 (middle panel), Storm 128 (lower panel).

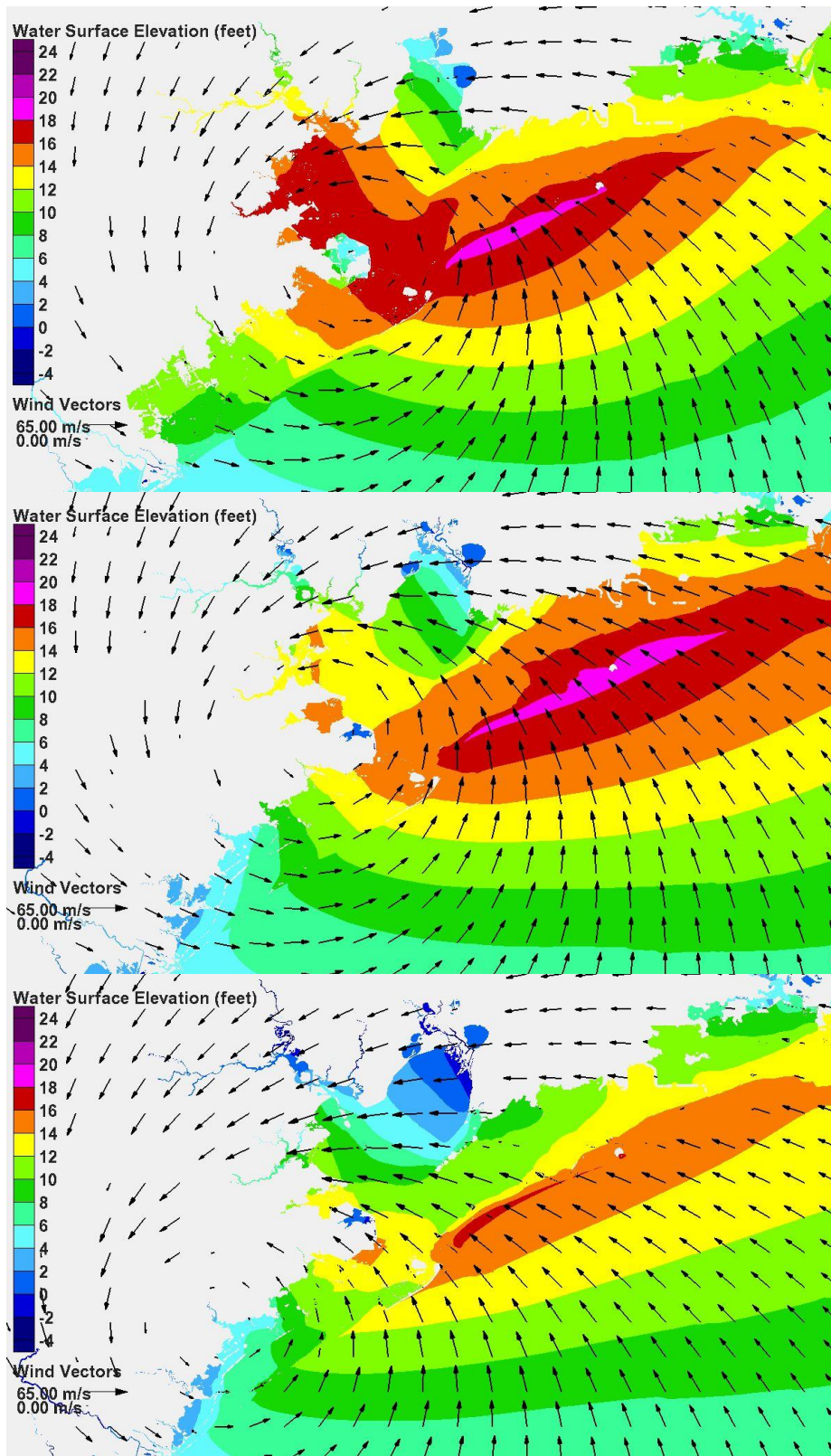


Figure 7-18. Water surface elevation and wind vectors 1 hour after landfall, Storm 136 (upper panel), Storm 122 (middle panel), Storm 128 (lower panel).

Along the open coast, the zone of highest surge for Storm 136 continues to move to the northeast and is situated along the middle and eastern portions of Bolivar Peninsula. For Storms 122 and 128, the zone of highest surge persists along Bolivar Peninsula. The onshore winds along Bolivar Peninsula, for all three storms, continue to build surge against the coastline and push water across the inundated barrier island.

Figure 7-19 shows water surface elevation and wind fields 2 hrs after landfall. Along the open coast, persistent onshore winds for all three storms push water against the coast, across the inundated Bolivar Peninsula, and then into Galveston Bay.

For Storm 136, the eye of the storm is positioned directly over Galveston Bay and moving toward the north. Winds throughout the Bay are quite variable in direction, with no persistent direction, and are characterized by relatively lower wind speeds because of the presence of the eye. In response, water surface elevations throughout much of the Bay are somewhat uniform at this time. The northeast part of the Bay continues to fill. In West Bay winds are blowing from the west and west-northwest, setting up the eastern side.

The eye for Storm 122 is moving along the western shoreline of Galveston Bay toward the north-northwest, and is positioned near the northwest corner at this time. Winds in Galveston Bay are generally blowing to the north, pushing water toward the north. Winds in West Bay are blowing from west and southwest, depending on location within the Bay, and are setting up the eastern.

The eye of Storm 128 made landfall farthest to the west of the three storms. It is moving toward the northwest, and this movement is increasing its distance from the Bay. Winds within Galveston Bay are all directed to the northwest, pushing water in that direction and setting up the northwest corner. The northeast corner also is filling due to water surface elevation gradients that force water from areas of high surge to areas of lower surge. Winds in West Bay are blowing from the south, setting up the north side and pushing water inland. Water is being pushed across the inundated Galveston Island toward the north.

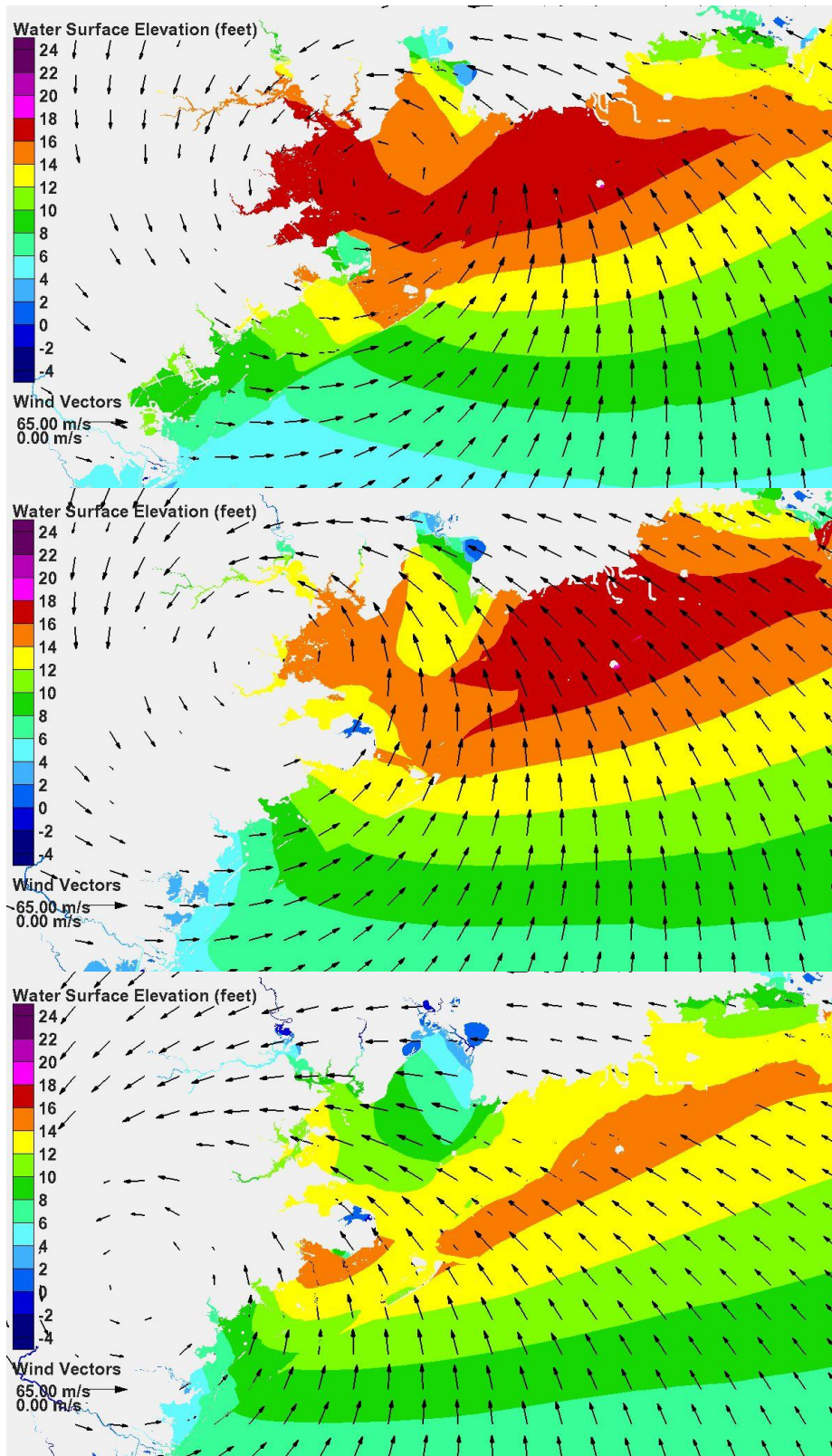


Figure 7-19. Water surface elevation and wind vectors 2 hours after landfall, Storm 136 (upper panel), Storm 122 (middle panel), Storm 128 (lower panel).

Figure 7-20 shows conditions 3 hrs after landfall. Along the open coast, persistent onshore winds for all three storms continue to push water against the coast and across the inundated Bolivar Peninsula. For Storms 122 and 128, the water being pushed across Bolivar Peninsula continues to flow into Galveston Bay, toward the north for Storm 122 and toward the northwest for Storm 128. However, the eye of Storm 136 has moved north of Galveston Bay, and strong winds on the back side of the eye are now directed toward the east. Those winds push water toward the east side of Galveston Bay.

Figure 7-21 shows winds and water surface elevation fields 6 hours after landfall. Along the open coast winds have an onshore component for all three storms, but more so for Storms 122 and 128 than for Storm 136. Winds for Storm 136 are blowing more from the southwest. Within Galveston Bay, winds for Storm 136 are from the west-southwest throughout the region. Winds for Storms 122 and 128 are from the south and south-southeast, respectively, throughout the region. As the eye of the storm moves farther away, the winds become more uniform in direction because the degree of curvature of the wind fields lessens with distance away from the eye.

The open coast storm surge is subsiding for all three storms, most rapidly for Storm 136. For this storm and at this time, the water surface elevation is higher in Galveston Bay than along the open coast; and in response, water is flowing from the Bay back to the Gulf. This same process is occurring in West Bay, where water is flowing back over Galveston Island toward the Gulf. For Storms 122 and 128, the response along the barrier islands is quite different. Southerly winds continue to push water toward the coast, across the inundated Bolivar Peninsula and Galveston Island, and into Galveston Bay and West Bay, respectively.

Different water surface responses also are occurring within the Bays. For Storm 136 winds in Galveston Bay are directed toward the east. In response, the water surface is set up on the east side of the Bay and set down along the western shoreline. Westerly winds in West Bay set up the east end and set down the west end. For Storm 122, persistent southerly winds continue to push water that has accumulated in Galveston Bay to the north, setting up the water surface in the northern parts of the system and pushing water into the channels and estuaries. The persistent southerly wind is establishing a large south-to-north water surface

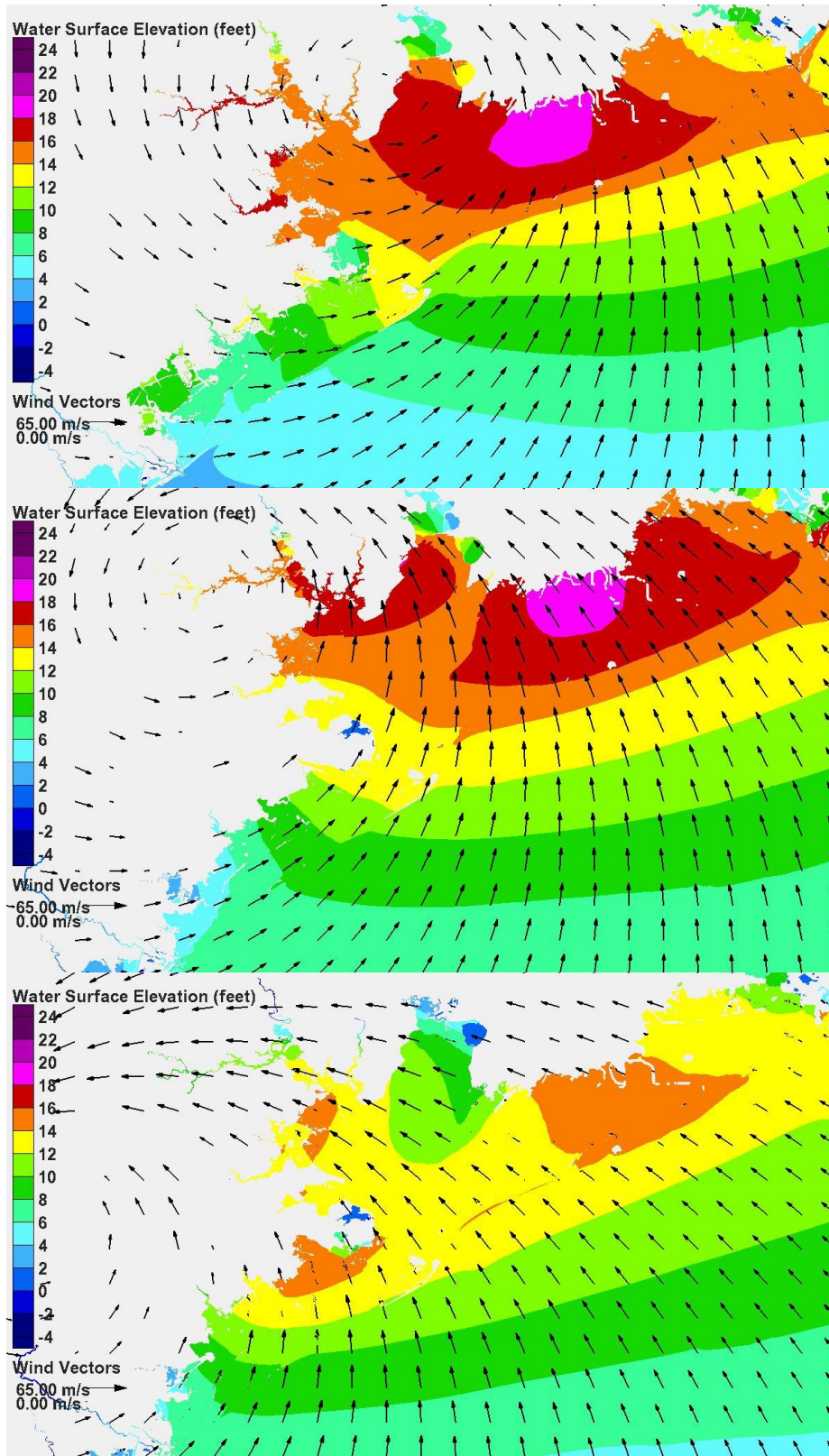


Figure 7-20. Water surface elevation and wind vectors 3 hours after landfall, Storm 136 (upper panel), Storm 122 (middle panel), Storm 128 (lower panel).

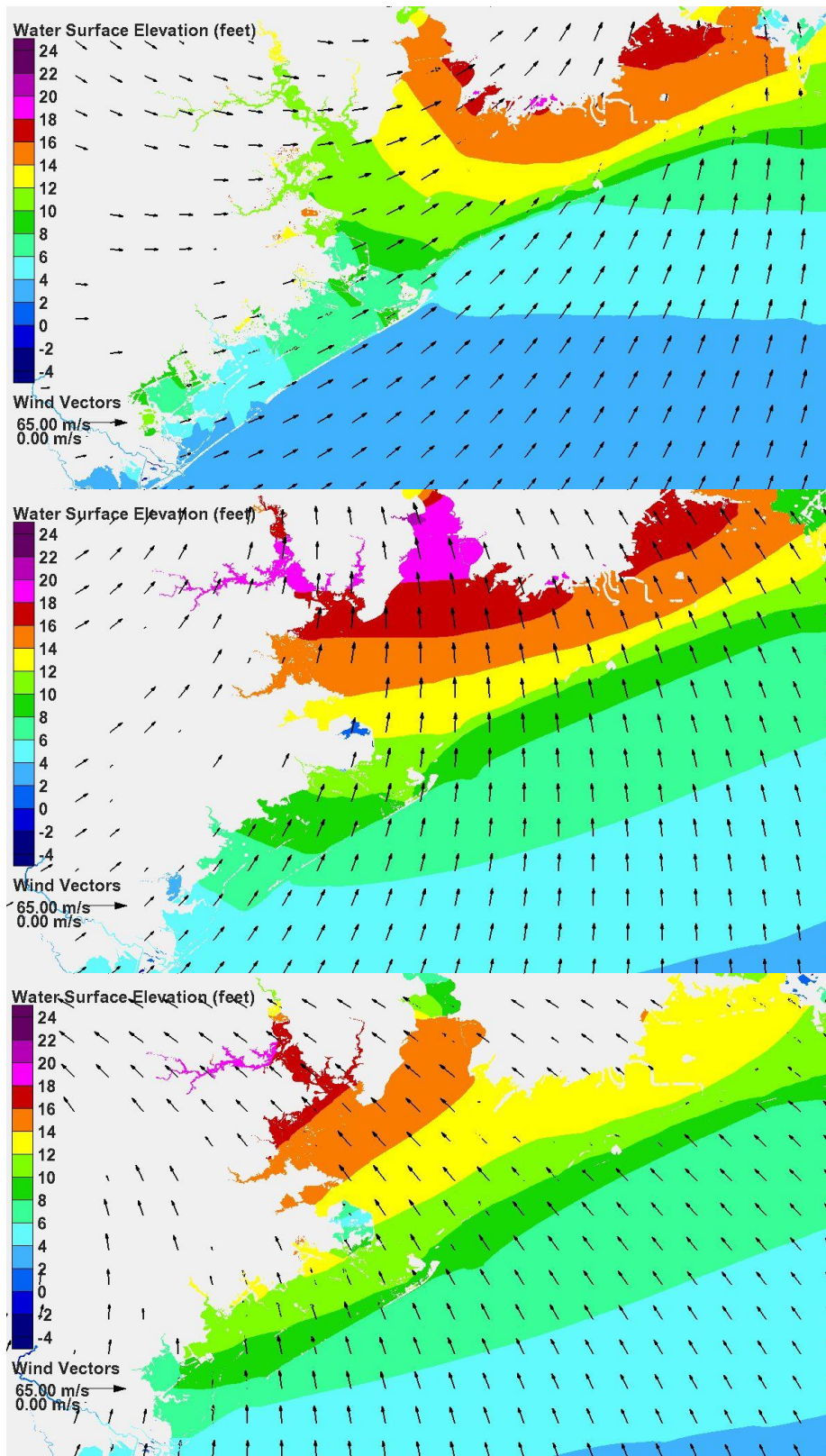


Figure 7-21. Water surface elevation and wind vectors 6 hours after landfall, Storm 136 (upper panel), Storm 122 (middle panel), Storm 128 (lower panel).

gradient throughout the Bay. In West Bay, southeasterly winds set up the northeast corner.

The surge development process within the Bay at this time is similar for Storm 128, compared to Storm 122. Uniform winds from the south-southeast set up the north-northwest parts of the Bay, pushing water in that direction and into channels and estuaries, and establishing a persistent water surface gradient throughout the Bay. In West Bay southerly winds set up the north side and push water inland.

Figure 7-22 shows conditions 9 hours after landfall. At this time the storm eyes have moved well away from the Houston-Galveston region and winds are rather uniform in direction throughout the region for each storm. Wind directions for each storm are quite similar to what they were 3 hrs earlier. Wind speeds are decreasing for each storm as the eye moves farther away from the region.

Within the Bays, surges have reached their maximum values and are decreasing. However, even 9 hours after landfall, high surges persist throughout the system and in particular the northern parts of the system.

For all three storms, the open coast storm surge is subsiding, water is draining from the Bays and flowing back to the Gulf. This draining takes place much more slowly than the filling did. As water surface elevations decrease to values lower than crest elevations of the degraded barrier islands, draining will be restricted to flow through passes and any breach channels that formed on the eroded barrier islands during the storm.

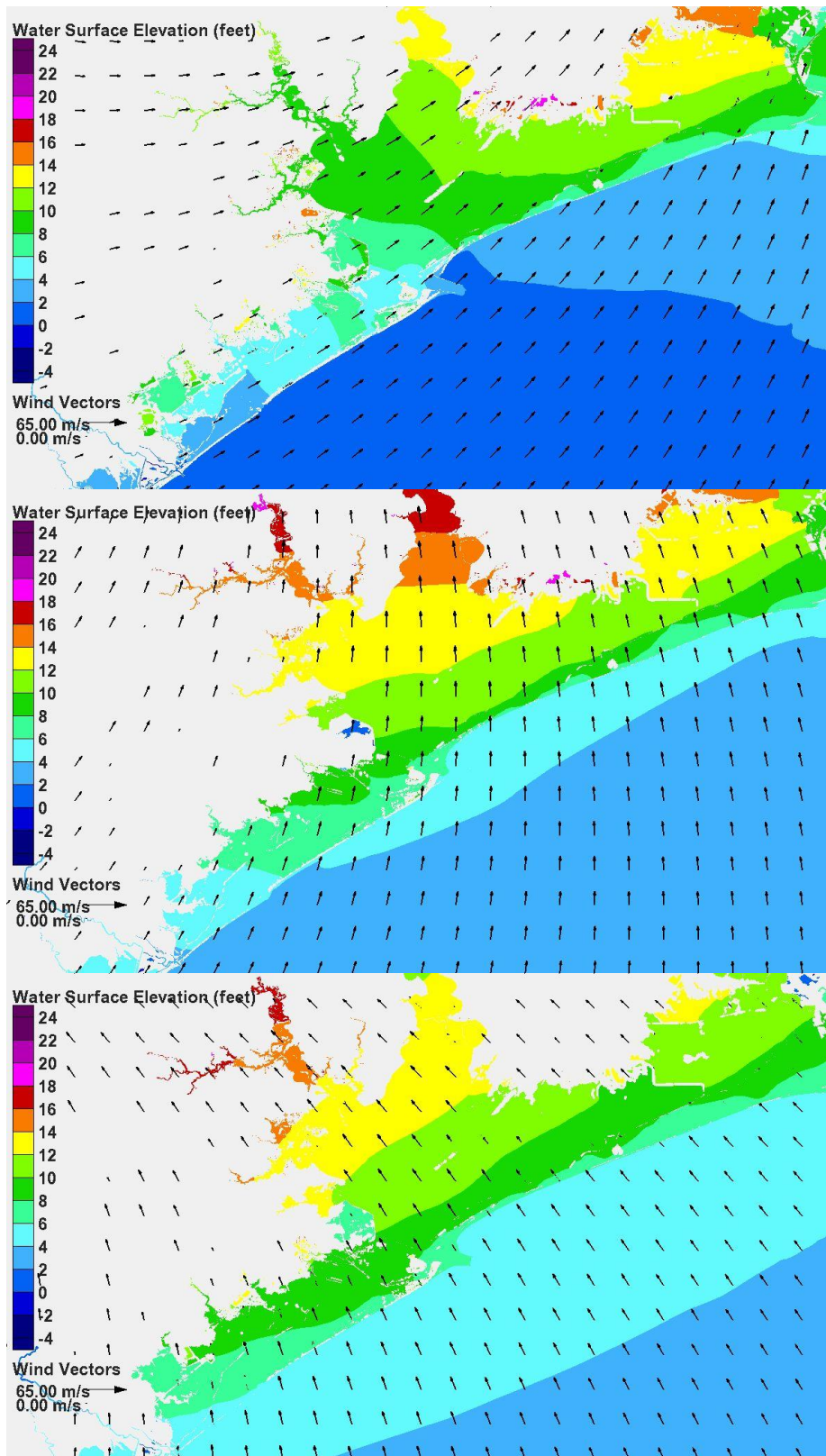


Figure 7-22. Water surface elevation and wind vectors 9 hours after landfall, Storm 136 (upper panel), Storm 122 (middle panel), Storm 128 (lower panel).

8 Reduction in Flooding Achieved with the Ike Dike – Initial Assessment

Introduction

Reduction in flooding achieved by the Ike Dike concept was initially examined by comparing maximum water surface elevation maps for existing conditions with maximum water surface elevation maps for with-dike conditions. The maximum water surface elevation maps were computed for each storm in the following way: at every grid node of the computational mesh used in the storm surge modeling, the maximum water surface elevation is recorded, regardless of when it occurred during the hurricane simulation. The water surface elevation maxima at every grid mesh node are then used to develop the maximum water surface elevation map. A difference map was computed by subtracting the with-dike map from the existing condition map for each storm. All water surface elevations are relative to the NAVD88 vertical datum, which is about 0.5 ft below the mean sea level tidal datum.

For each storm a figure is provided which shows three maps, one for existing conditions (top panel), one for with-dike conditions (middle panel), and the difference map (bottom panel). The water surface elevation color bar scale used for each map is shown in each panel. The same scale is used throughout this chapter. Following the figure showing the maps, storm surge information for existing conditions, with-dike conditions, and the difference, is shown in tabular and descriptive form for each of 9 locations in the Houston-Galveston region: Galveston (Gulf side), Galveston (Bay side), rest of Galveston Island west of the City of Galveston, Bolivar Peninsula, the Texas City area, Clear Lake area, Bayport Area, and the upper reaches of the Houston Ship Channel. The tables help quantify reduction in surge achieved with the dike. The reduction is generally not uniform throughout the Houston-Galveston region for a particular storm, and the reductions at each location vary from storm to storm.

Storms are divided into four groupings, and results provided below are grouped in the same way. The first group is the direct-hit set of four

storms, all on the same track, with varying intensity (900 mb, 930 mb, 960 mb and 975 mb). The other groupings are based on storm track, one group for each of the three main approach directions, south, south-southeast and southeast. All storms in the three track groups were 900 mb storms. The storms in each grouping have the same heading but they differ in their landfall location.

Landfall location has great influence on the storm surge that is experienced in the Houston-Galveston region. Storms that make landfall at a distance of one radius-to-maximum-winds to the west of Bolivar Roads tend to produce the largest storm surge in the most economically sensitive areas. For the storms simulated here, one radius-to-maximum-winds distance to the west of Bolivar Roads is approximately at San Luis Pass. So the storm(s) in each track grouping that make(s) landfall nearest San Luis Pass tends to produce the largest storm surge in the Houston-Galveston region for that group of storm tracks.

As the landfall location moves east of Bolivar Roads, the maximum surge will be located well to the east of Galveston Bay. For these storms, as the distance between landfall position and Bolivar Roads increases, the region of maximum surge will occur farther and farther way from the Houston-Galveston region and storm surge within the region will decrease. This trend is evident in the results shown below. Storms in the West Louisiana set tended to make landfall well to the east of Galveston Bay, and the surges they generated in the area of interest tended to be much less than surge generated by the storms in the North Texas set. Therefore this report will only show results for the North Texas set.

The Long Dike or Levee Effect

When a long coastal dike, seawall or levee is constructed to reduce the risk of storm flooding, it can result in a local increase of storm surge compared to surge that would have occurred at that same location had the dike or other structure not been present. The structure provides a barrier for the wind-driven water to stack up against, and it restricts the ability of the water to move elsewhere away from the structure. This increase in surge occurs for the Ike Dike concept and is seen in the results that follow. Surge is generally increased by amounts of up to 1.5 ft for the 900 mb storms that have been simulated. The maximum increase tends to occur where the storm surge is greatest. If flow over the dike commences, as it does for a number of the storms, this will tend to mask the amount of the

increased surge had the dike been higher and prevented overflow from occurring. This effect and the surge increase must be recognized and factored into the design of the risk reduction measure.

Hurricanes of Varying Intensity - The Direct-Hit Set

Results for the direct-hit set of four storms illustrate the benefits of the Ike Dike concept in reducing storm surge for hurricanes of varying intensity. The four storms have the same track, shown in Figure 8-1, but different central pressures: Storm 122 (900 mb), Storm 155 (930 mb), Storm 121 (960 mb) and Storm 561 (975 mb).

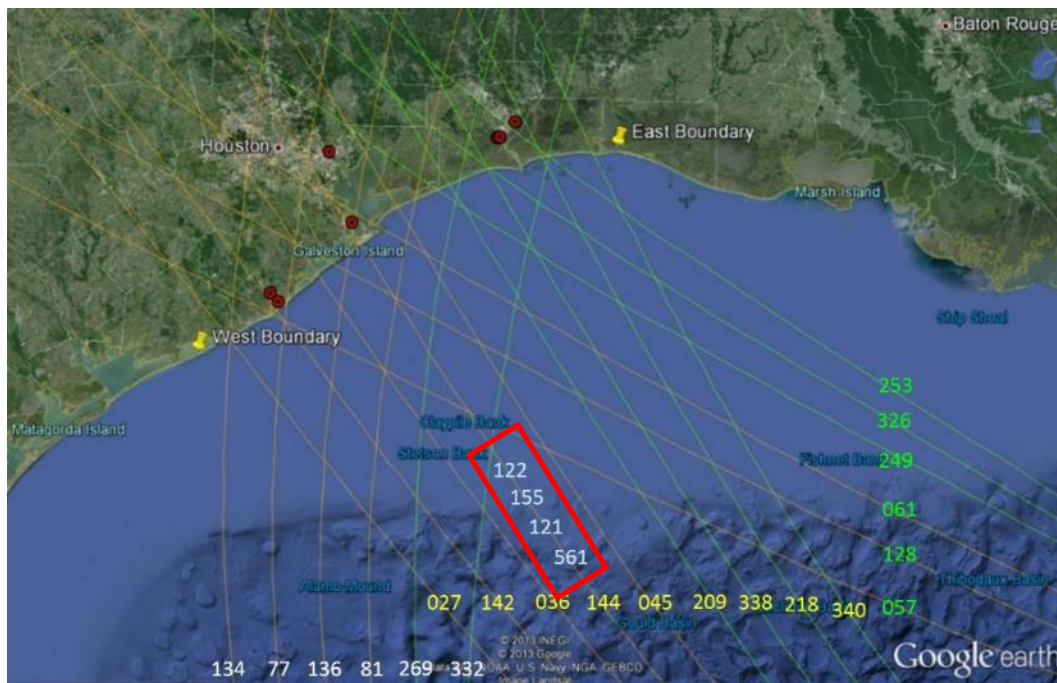


Figure 8-1. Direct-hit group of hurricanes approaching from the southeast (storms 122 (900 mb), 155 (930 mb), 121 (960 mb), 561 (975 mb))

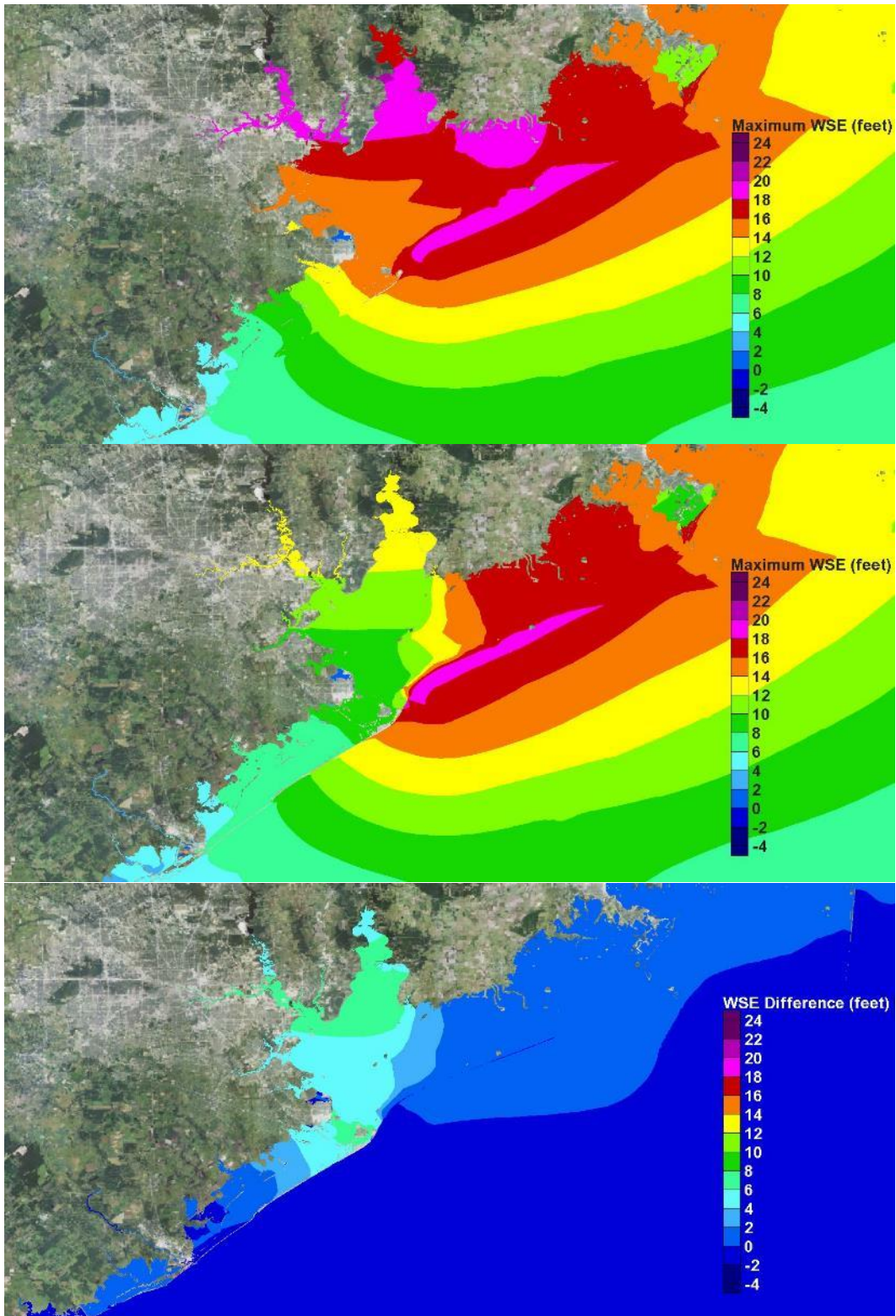


Figure 8-2. Maximum water surface elevation maps for Storm 122 (900 mb). Existing conditions (top); With-dike conditions (middle); Difference in maximum water surface elevation (bottom)

Table 8-1. Summary of Maximum Storm Surge Conditions for Storm 122.

Location	Existing Condition	With-Dike Condition	Changes
Galveston (Gulf side)	13.5 to 16.5 ft	14 to 17.5 ft	The dike causes surge by 0.5 to 1 ft in front of the seawall. Overtopping and overflow expected.
Galveston (Bay side)	14 to 16 ft	8.5 to 11 ft	Reduction of 5.5 ft to 6 ft
Rest of Galveston Island	7 to 14 ft, increasing from west to east	6.5 to 8.5 ft	Reductions of 0 ft in the west to 5.5 ft in the east.
Bolivar Peninsula	18 to 18.5 ft	14 to 17 ft	0 to 2 ft. Overflow and overtopping along most/all of the dike. No significant change
Texas City area	11 to 15 ft	8.5 to 9.5 ft	Reduction of 4.5 to 5.5 ft
Clear Lake Area	15 to 15.5 ft	9.5 to 10.5 ft	Reduction of 5 to 5.5 ft
Bayport Area	15.5 to 16.5 ft	10.5 to 11.5 ft	Reduction of 5.5 to 6 ft
Upper reaches of Houston Ship Channel	19 to 20 ft	13 to 14 ft	Reduction of 6 to 7 ft

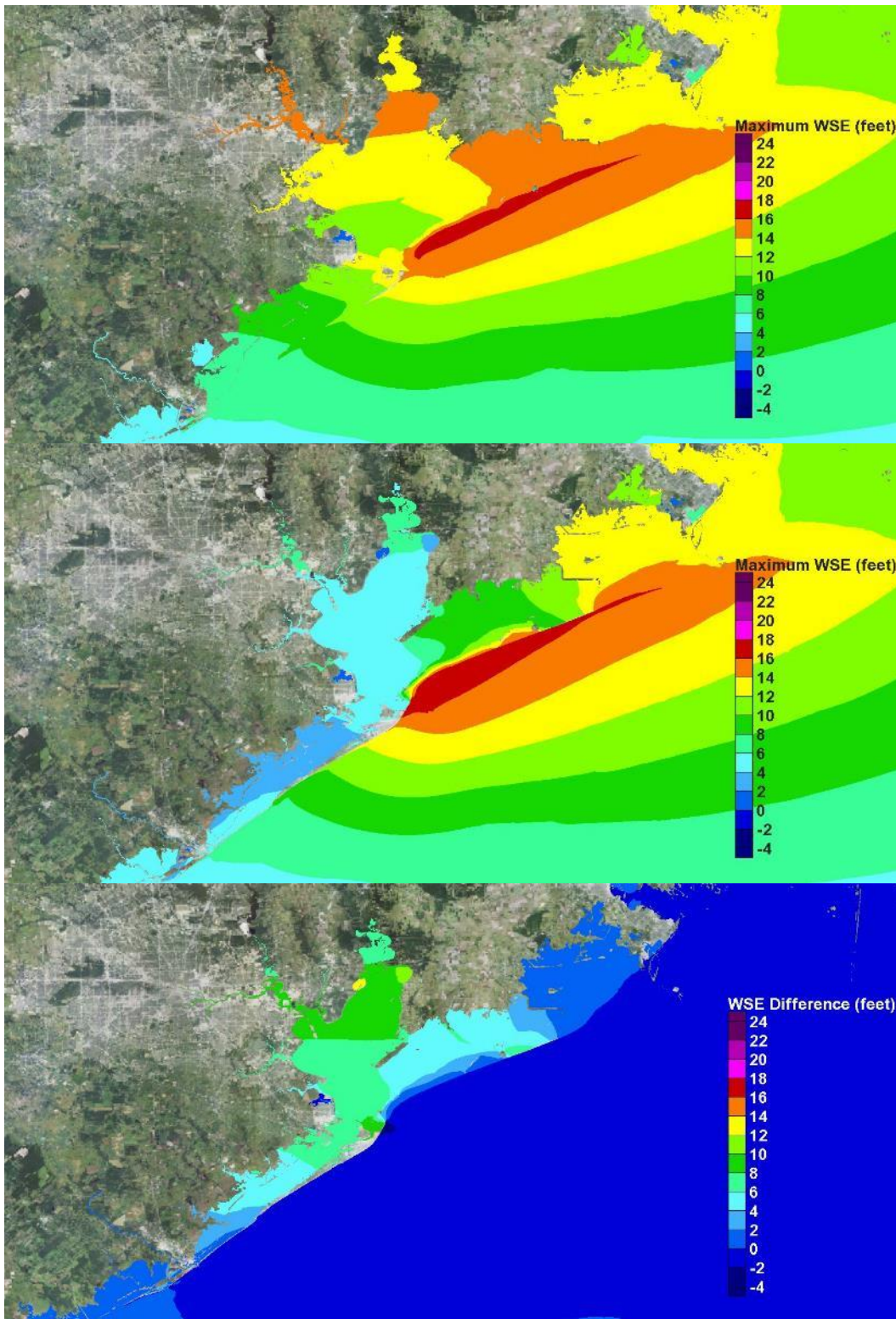


Figure 8-3 Maximum water surface elevation maps for storm 155 (930 mb). Existing conditions (top); With-dike conditions (middle); Difference in maximum water surface elevation (bottom)

Table 8-2. Summary of Maximum Storm Surge Conditions for Storm 155.

Location	Existing Condition	With-Dike Condition	Changes
Galveston (Gulf side)	11 to 15 ft increasing from west to east	12 to 16 ft	Increase of 1 ft. Increase in overtopping is expected.
Galveston (Bay side)	11 to 14 ft increasing from west to east	4 to 5.5 ft	Reduction of 7 to 10 ft
Rest of Galveston Island	7 to 11 ft, increasing from west to east	4 to 4.5 ft	Reductions of 2 ft in the west to 6 ft in the east.
Bolivar Peninsula	16 to 17 ft	10 to 16 ft	0 to 4 ft. Presence of the dike increases surge in front of dike by 1 ft. Overflow along most/all of the dike
Texas City area	11.5 to 12.5 ft	4 to 5 ft	Reduction of 7 to 8 ft
Clear Lake Area	13 ft	4 to 5 ft	Reduction of 7.5 to 8.5 ft
Bayport Area	13.5 ft	5 to 5.5 ft	Reduction of 8 to 8.5 ft
Upper reaches of Houston Ship Channel	15 ft	7 ft	Reduction of 8 ft

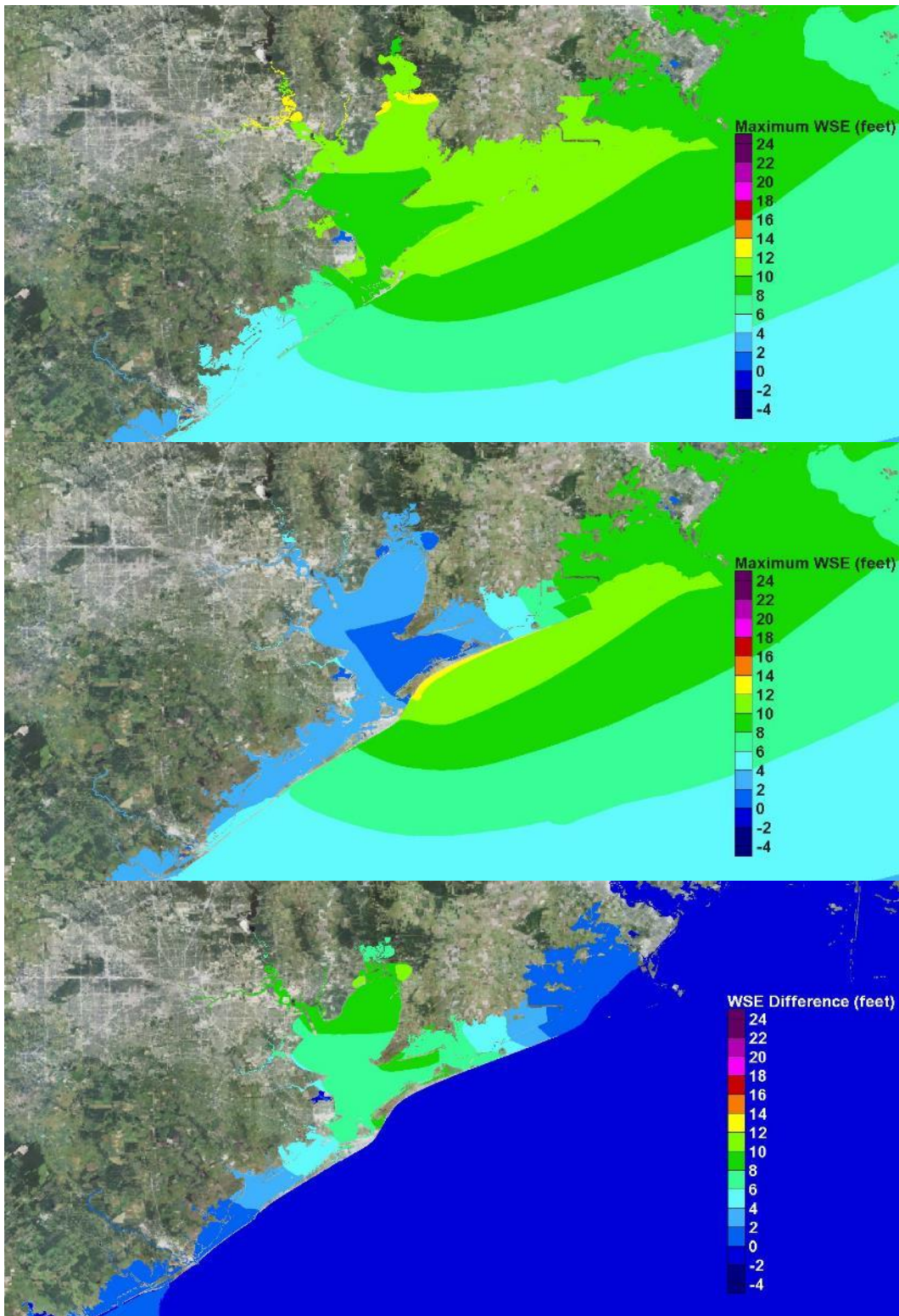


Figure 8-4. Maximum water surface elevation maps for storm 121 (960 mb). Existing conditions (top); With-dike conditions (middle); Difference in maximum water surface elevation (bottom)

Table 8-3. Summary of Maximum Storm Surge Conditions for Storm 121.

Location	Existing Condition	With-Dike Condition	Changes
Galveston (Gulf side)	7.5 to 10.5 ft	8 to 10.5 ft	Increase of 0 to 0.5 ft. No significant change.
Galveston (Bay side)	8.5 to 10.5 ft	2.5 to 3 ft	Reduction of 6 to 8 ft
Rest of Galveston Island	5 to 8 ft, increasing from west to east	3 to 4 ft	Reductions of 1 ft in the west to 5 ft in the east.
Bolivar Peninsula	11 to 11.5 ft	2 to 2.5 ft	Presence of the dike increases surge by 1 ft on ocean side. Reduction in bay of 9 ft
Texas City area	8.5 to 11 ft	2 to 4 ft	Reduction of 6 to 7 ft
Clear Lake Area	10 ft	3 to 4 ft	Reduction of 7 ft
Bayport Area	10 to 10.5 ft	3 to 4 ft	Reduction of 7 to 7.5 ft
Upper reaches of Houston Ship Channel	12 to 12.5 ft	3 to 4 ft	Reduction of 8 to 9 ft

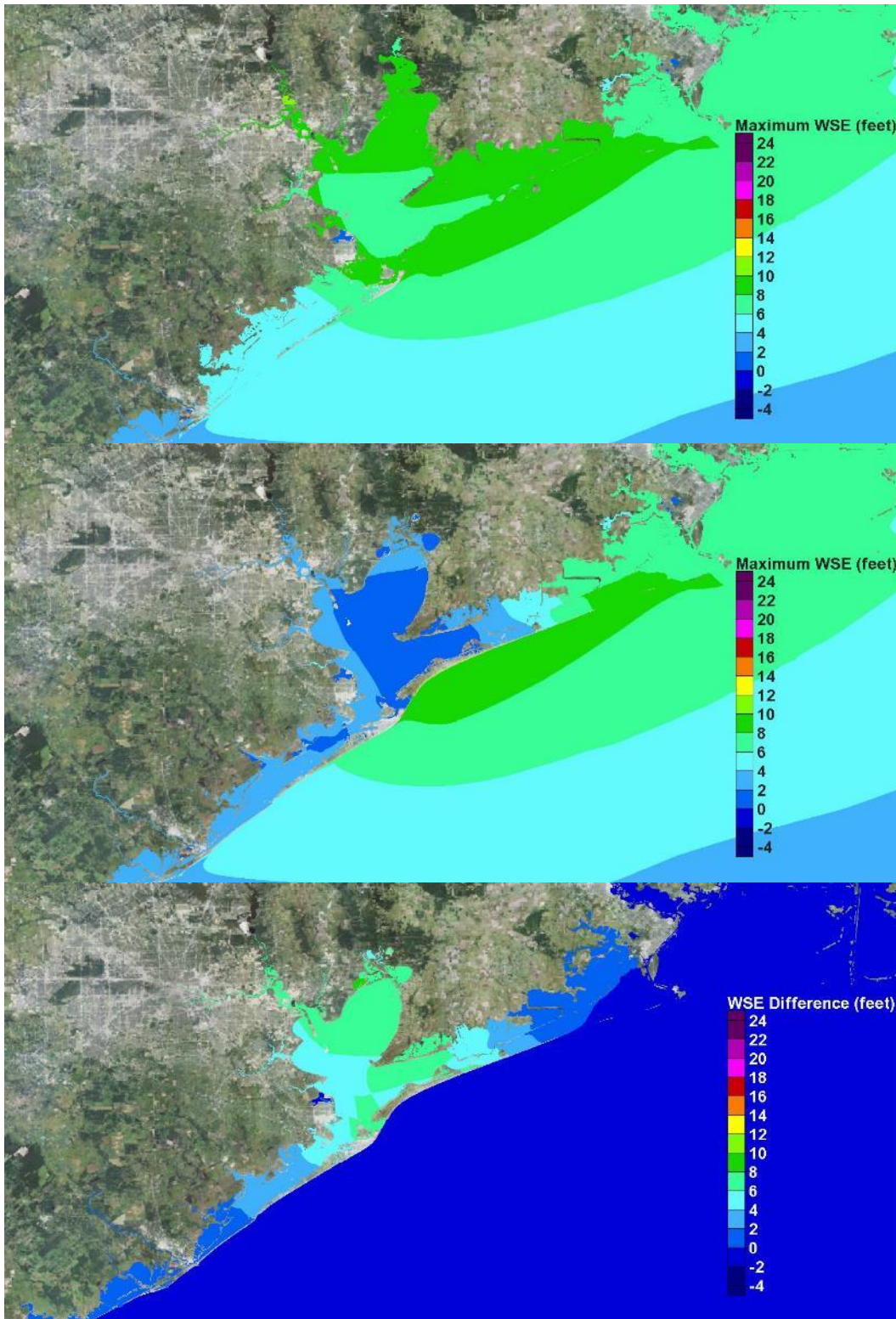


Figure 8-5. Maximum water surface elevation maps for storm 561 (975 mb). Existing conditions (top); With-dike conditions (middle); Difference in maximum water surface elevation (bottom)

Table 8-4. Summary of Maximum Storm Surge Conditions for Storm 561.

Location	Existing Condition	With-Dike Condition	Changes
Galveston (Gulf side)	7 to 8.5 ft	7 to 8.5 ft	No change
Galveston (Bay side)	7.5 to 8.5 ft	2 to 2.5 ft	Reduction of 5 to 6.5 ft
Rest of Galveston Island	4.5 ft in the west to 6.5 ft in the east	2 to 3 ft	Reductions of 1.5 ft in the west to 4 ft in the east.
Bolivar Peninsula	9 ft	2 to 3 ft	Reduction of 6 to 7 ft
Texas City area	8 to 8.5 ft	2.5 to 3 ft	Reduction of 5 to 6 ft
Clear Lake Area	8 ft	3 ft	Reduction of 5 ft
Bayport Area	8.5 ft	2 to 3 ft	Reduction of 6 ft
Upper reaches of Houston Ship Channel	9 to 10 ft	3 to 4 ft	Reduction of 6 to 7 ft

Major Hurricanes Approaching from the South

The following results are for the group of four North Texas storms that approached from the south. The influence of landfall position on maximum storm surge in Galveston Bay is evident. Storm 077 produces the maximum surge in the region, followed by Storm 134, Storm 136 and Storm 081, in order of decreasing maximum surge in the Houston-Galveston region.

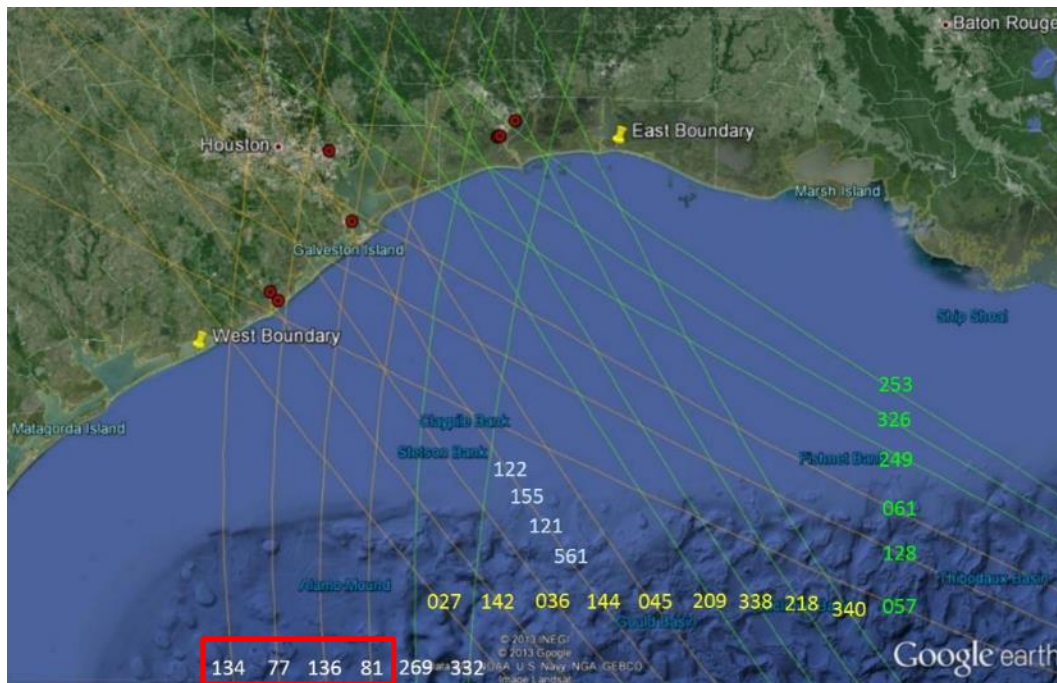


Figure 8-6. Group of hurricanes approaching from the south (storms 134, 77, 136, 81)

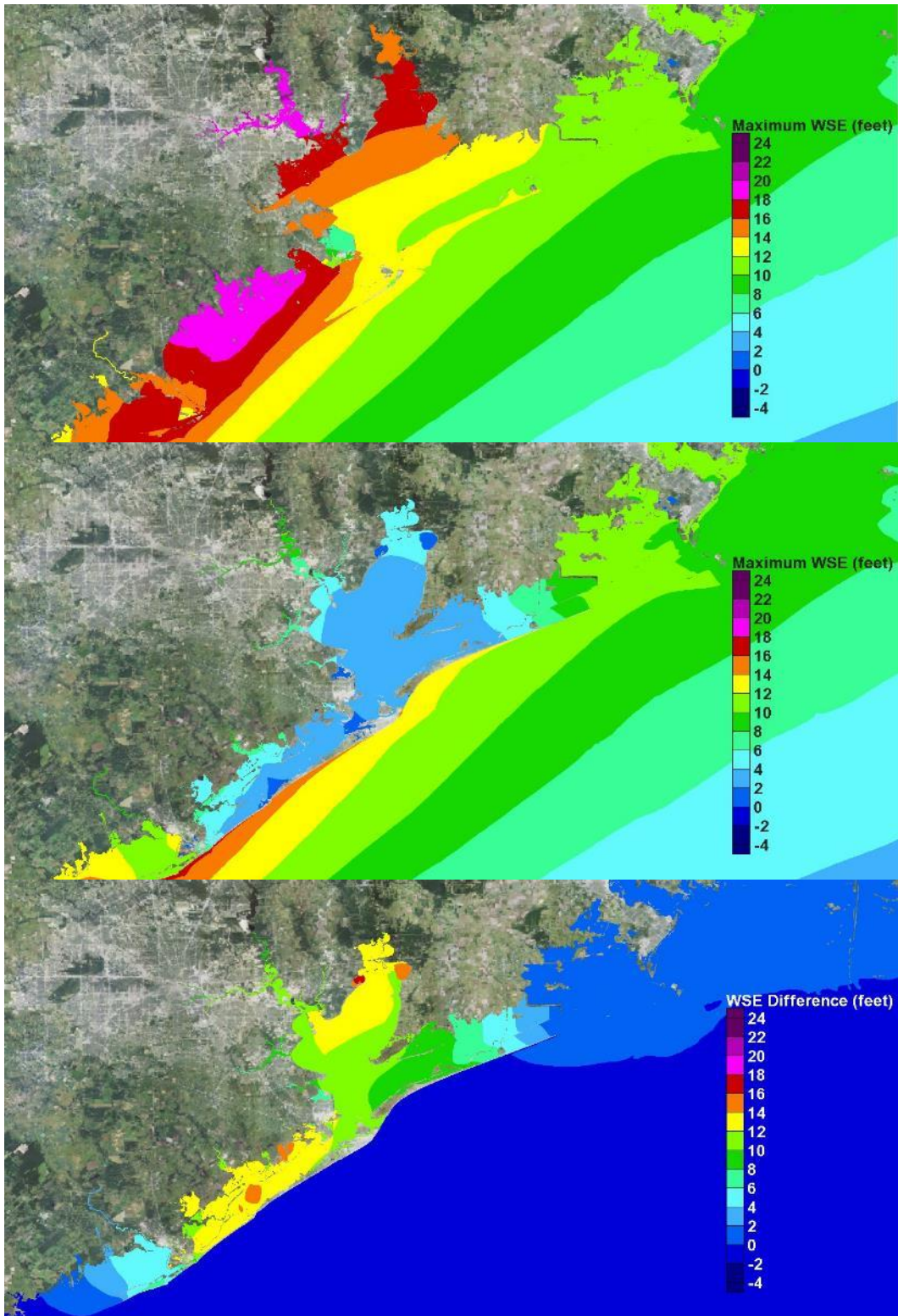


Figure 8-7. Maximum water surface elevation maps for storm 134. Existing conditions (top); With-dike conditions (middle); Difference in maximum water surface elevation (bottom)

Table 8-5. Summary of Maximum Storm Surge Conditions for Storm 134.

Location	Existing Condition	With-Dike Condition	Changes
Galveston (Gulf side)	13 to 14 ft	13 to 14 ft	No change
Galveston (Bay side)	13 ft	2 to 3 ft	Reduction of 11 ft
Rest of Galveston Island	14 to 16 ft	2 to 4.5ft	Reductions of 12 to 14 ft
Bolivar Peninsula	12 to 13 ft	3 to 4 ft	Reduction of 8 to 10 ft
Texas City area	13 to 16.5 ft	2.5 to 3 ft	Reduction of 12 ft. Prevented interior flooding.
Clear Lake Area	15 to 16.5 ft	4 to 5 ft	Reduction of 11 to 12 ft
Bayport Area	17 to 18 ft	4 to 5 ft	Reduction of 12 ft
Upper reaches of Houston Ship Channel	19 to 20 ft	8 to 9 ft	Reduction of 11 to 12 ft

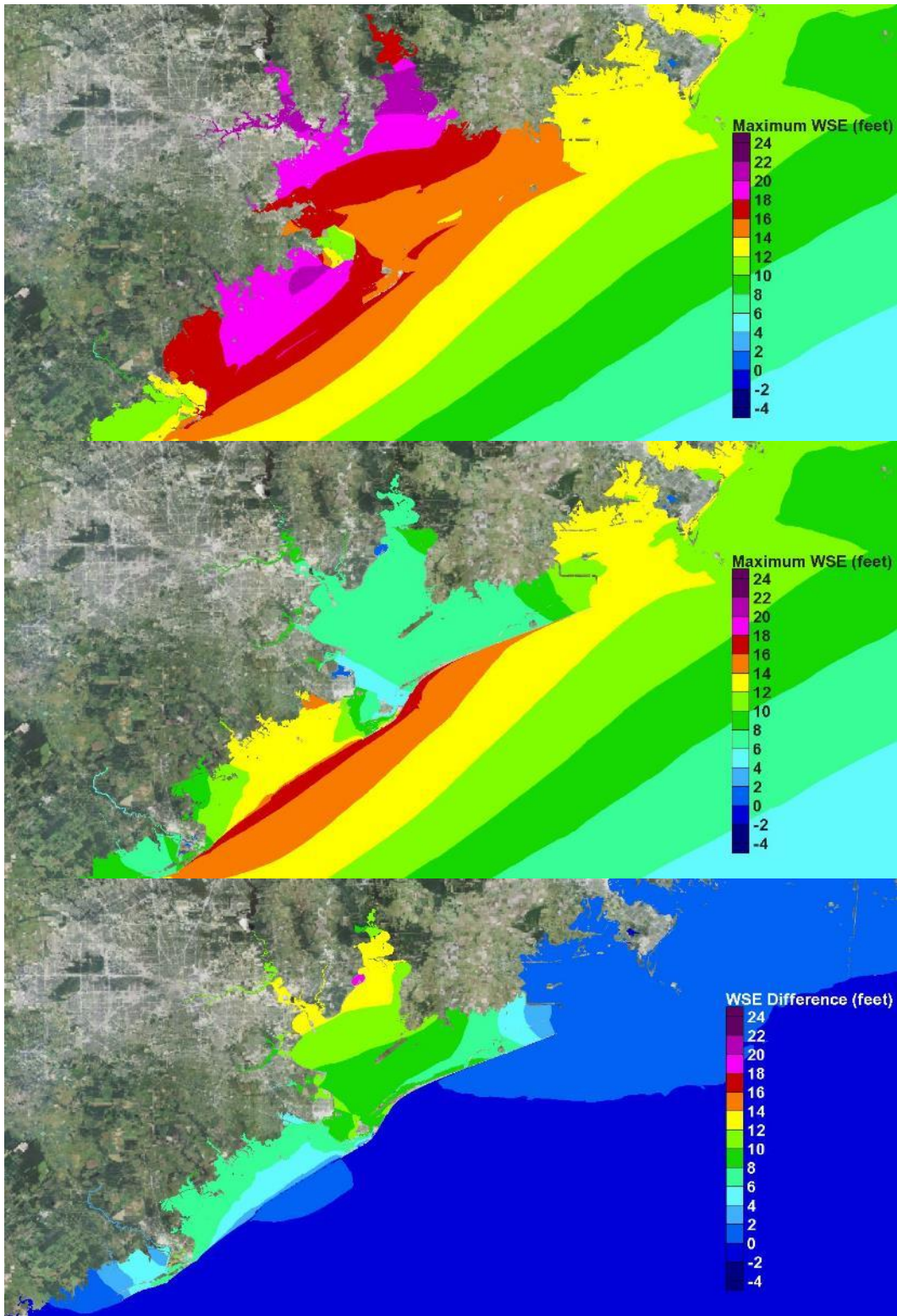


Figure 8-8. Maximum water surface elevation maps for storm 077. Existing conditions (top); With-dike conditions (middle); Difference in maximum water surface elevation (bottom)

Table 8-6. Summary of Maximum Storm Surge Conditions for Storm 077

Location	Existing Condition	With-Dike Condition	Changes
Galveston (Gulf side)	16 ft	16 to 16.5 ft	0 to 0.5 ft increase. Increase in overtopping expected.
Galveston (Bay side)	16 ft	6 to 10 ft	Reduction of 6 to 10 ft
Rest of Galveston Island	16.5 to 17 ft	10 to 16 ft	Overtopping/overflow of the dike. Reduction of 4 to 6 ft.
Bolivar Peninsula	13 to 16 ft	6 to 8 ft	Reduction of 6 to 9 ft
Texas City area	16 to 22 ft	7 to 13 ft	Reduction of 8 to 11 ft. Prevented interior flooding.
Clear Lake Area	17 to 19 ft	7 ft	Reduction of 10 to 12 ft
Bayport Area	19 ft	7 ft	Reduction of 12 to 12.5 ft
Upper reaches of Houston Ship Channel	21 to 22 ft	9 to 10 ft	Reduction of 11 to 12 ft

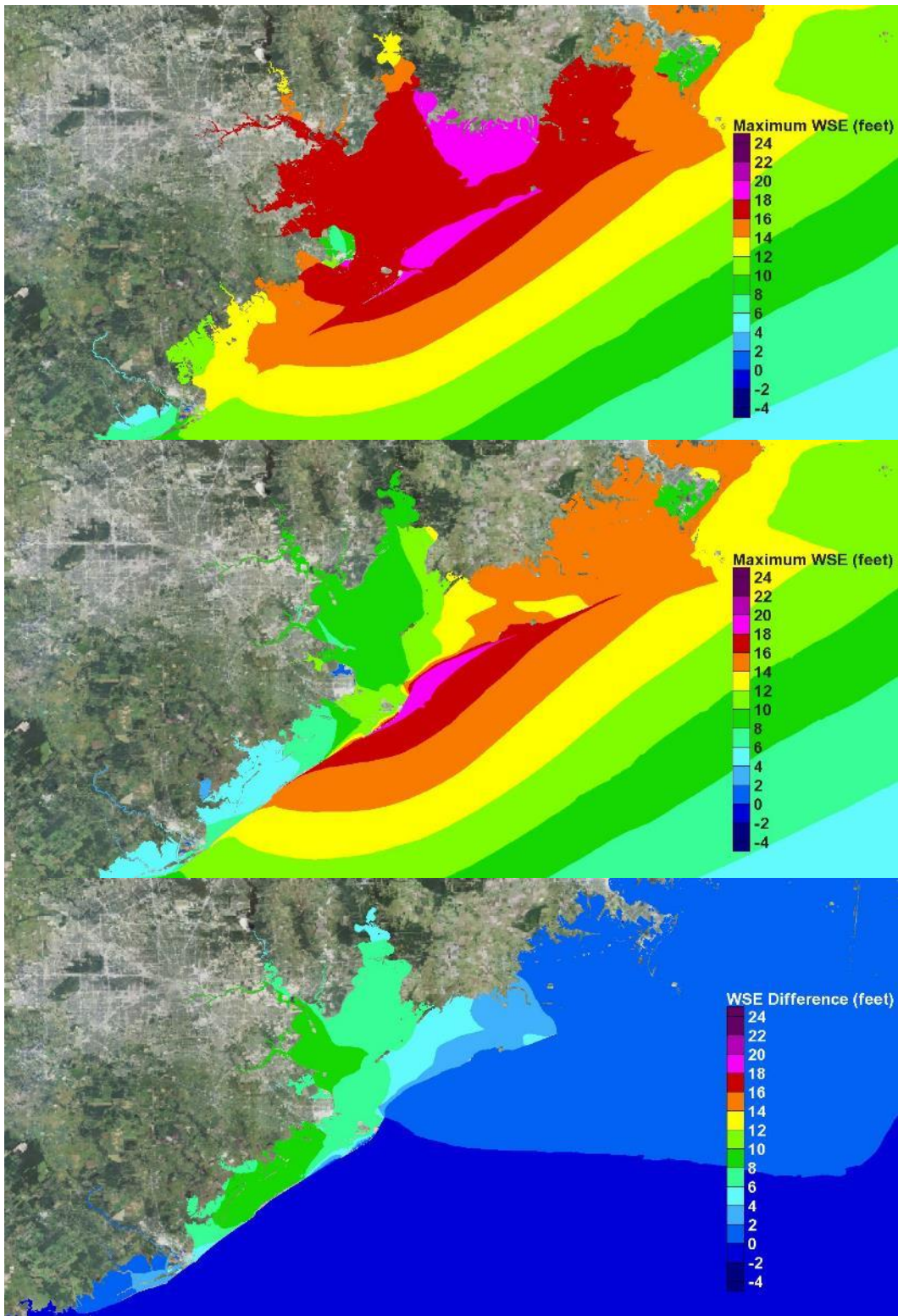


Figure 8-9. Maximum water surface elevation maps for storm 136. Existing conditions (top); With-dike conditions (middle); Difference in maximum water surface elevation (bottom)

Table 8-7. Summary of Maximum Storm Surge Conditions for Storm 136

Location	Existing Condition	With-Dike Condition	Changes
Galveston (Gulf side)	18 ft	18 to 19.5 ft	0 to 1.5 ft increase. Increase in overtopping and overflow is expected.
Galveston (Bay side)	18 ft	12 ft	Reduction of 6 ft
Rest of Galveston Island	12 to 17 ft, increasing from west to east	5 to 10 ft	Some overtopping and overflow of the dike. Reduction of 7 to 10 ft.
Bolivar Peninsula	16 to 19 ft	12 to 17 ft	Overtopping/overflow of the dike. Reduction of 3 to 4 ft
Texas City area	18 to 19 ft	9 to 10 ft	Reduction of 8 to 9 ft. Significantly reduced interior flooding.
Clear Lake Area	17 ft	7.5 to 9 ft	Reduction of 8 to 9 ft
Bayport Area	18 ft	10 ft	Reduction of 8 to 9 ft
Upper reaches of Houston Ship Channel	17 to 18 ft	10 ft	Reduction of 7 to 8 ft

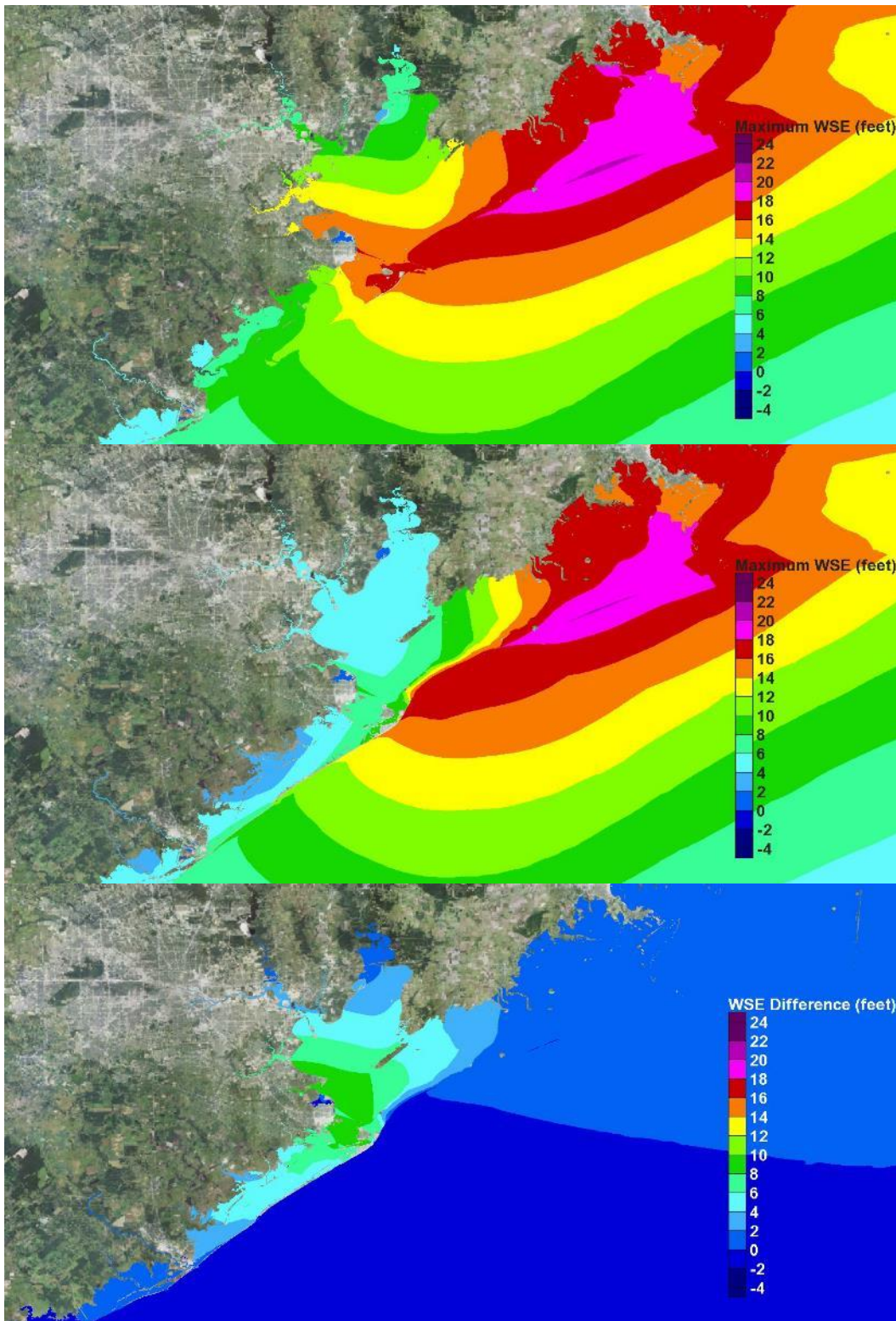


Figure 8-10. Maximum water surface elevation maps for storm 081. Existing conditions (top); With-dike conditions (middle); Difference in maximum water surface elevation (bottom)

Table 8-8. Summary of Maximum Storm Surge Conditions for Storm 081

Location	Existing Condition	With-Dike Condition	Changes
Galveston (Gulf side)	13 to 16 ft	13 to 16 ft	No change
Galveston (Bay side)	14 to 16 ft	8 ft	Reduction of 6 to 8 ft
Rest of Galveston Island	8 to 13 ft, increasing from west to east	5 to 6 ft	Reduction of 3 to 7 ft.
Bolivar Peninsula	17 to 19 ft	12 to 18 ft	Overtopping/overflow of the dike. Reduction of 1 to 4 ft
Texas City area	11 to 16 ft	6 to 8 ft	Reduction of 7 to 10 ft.
Clear Lake Area	12 to 14 ft	5 to 6 ft	Reduction of 6.5 to 8.5 ft
Bayport Area	11 ft	5 to 6 ft	Reduction of 5 to 6 ft
Upper reaches of Houston Ship Channel	7 to 8 ft	4 to 5 ft	Reduction of 3 ft

Major Hurricanes Approaching from the South-Southeast

The following results are for the group of five North Texas storms that approach from the south-southeast. The influence of landfall position on maximum storm surge in Galveston Bay is again evident. Storms making landfall to the west of Bolivar Roads tended to produce larger surges in the region than storms making landfall very close to, or to the east of, Bolivar Roads. Storm 036 produces the maximum surge in the region, followed by Storm 027, Storm 142, Storm 144 and Storm 045, in order of decreasing maximum surge. Based solely on track, with other storm parameters being the same, Storm 142 would be expected to produce a larger surge in the region compared to Storm 027. Storms 027 and 142 have different radii to maximum winds. The radius for Storm 027 is 21.8 n mi; the radius for Storm 142 is 17.7 n mi. The forward speed for Storm 027 is 11 kts, whereas for storm 142 it is slower, 6 kts. Intensity and storm size are the two factors that tend to influence peak surge the most. Bunpapong et al (1985) also found that forward speed is important along the Texas coast; the faster the forward speed the greater the peak surge. The larger radius to maximum winds and the faster forward speed combine to create the larger surge for Storm 027 compared to the surge for Storm 142 which makes landfall closer to Bolivar Roads.

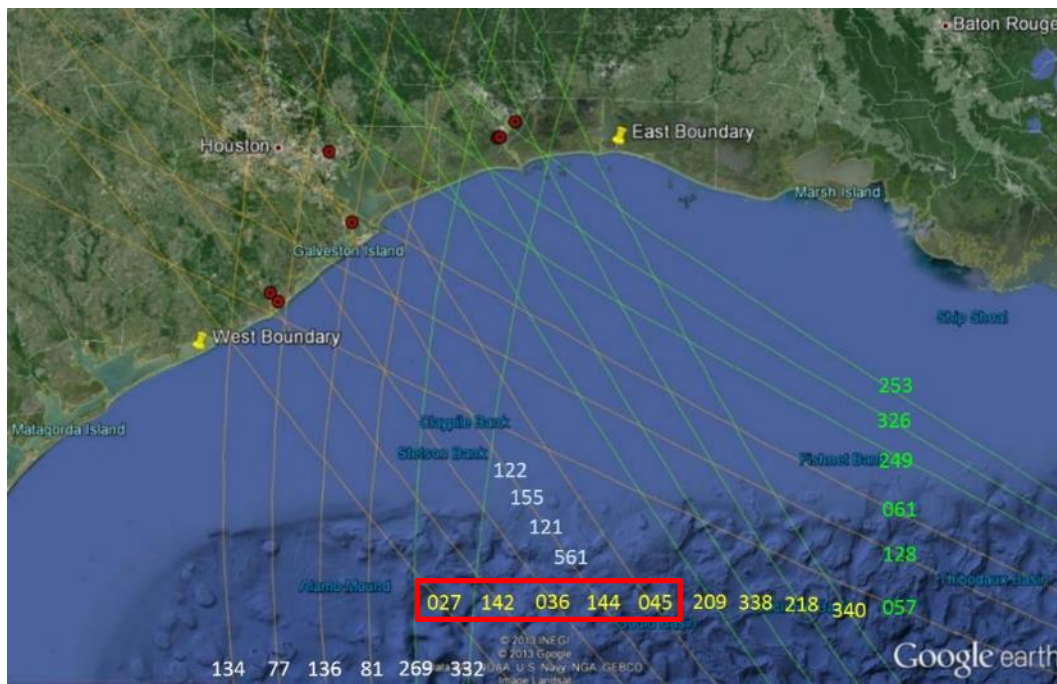


Figure 8-11. Group of hurricanes approaching from the south-southeast (storms 027, 142, 036, 144, 045)

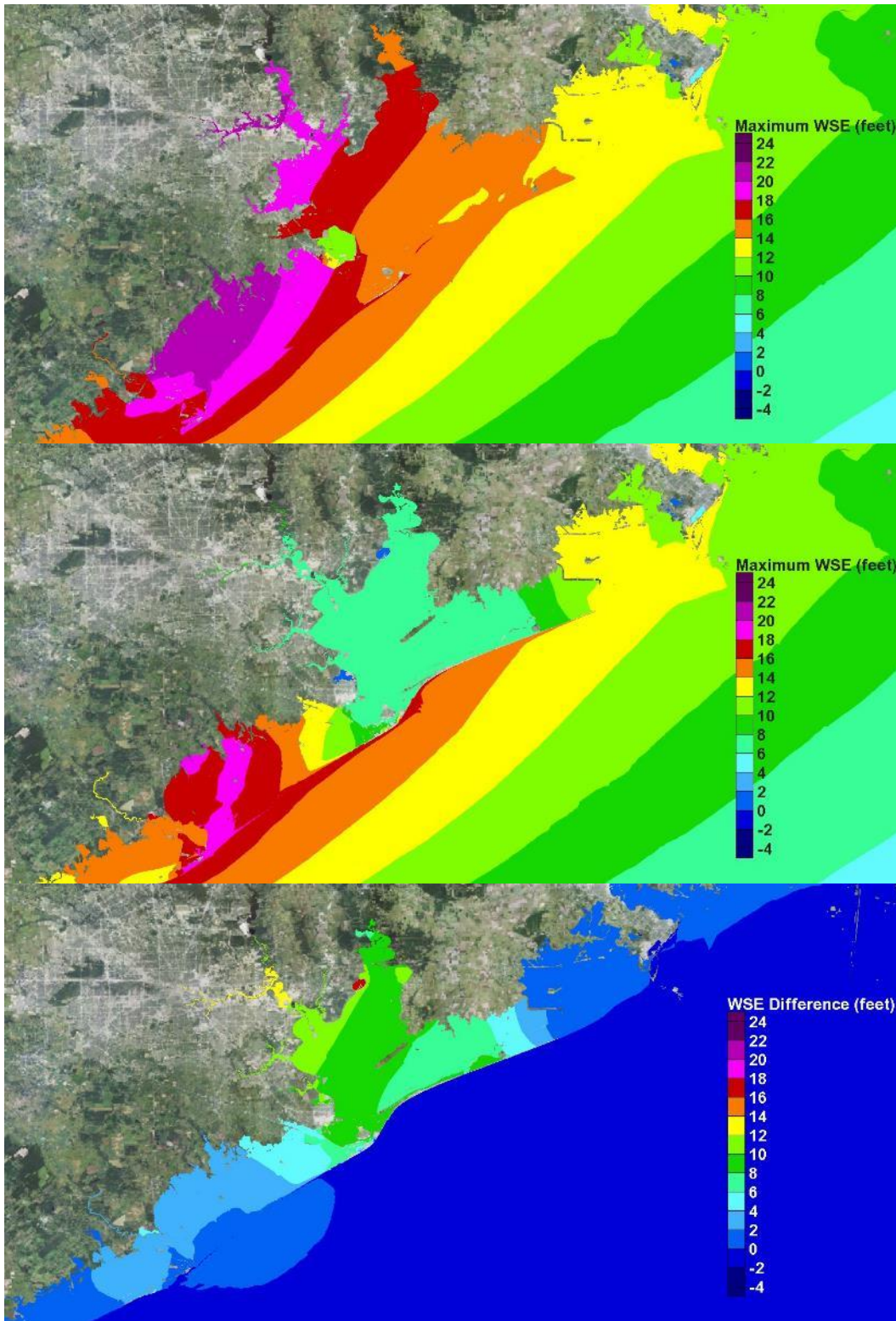


Figure 8-12. Maximum water surface elevation maps for storm 027. Existing conditions (top); With-dike conditions (middle); Difference in maximum water surface elevation (bottom)

Table 8-9. Summary of Maximum Storm Surge Conditions for Storm 027

Location	Existing Condition	With-Dike Condition	Changes
Galveston (Gulf side)	16 ft	16 ft	No change
Galveston (Bay side)	15 to 16 ft	8 to 10 ft	Reduction of 7 to 8 ft
Rest of Galveston Island	16 to 18.5 ft, decreasing from west to east	12 to 18.5 ft	Overtopping/overflow of the dike. Reduction of 1 to 6 ft.
Bolivar Peninsula	13 to 16 ft	7 to 10 ft	Reduction of 6 to 8 ft
Texas City area	15 to 19 ft	7 to 13 ft	Reduction of 5 to 10 ft. Eliminated interior flooding.
Clear Lake Area	18 to 19 ft	7 ft	Reduction of 11 to 12 ft
Bayport Area	19 ft	7 ft	Reduction of 12 ft
Upper reaches of Houston Ship Channel	21 ft	7 ft	Reduction of 13 to 14 ft

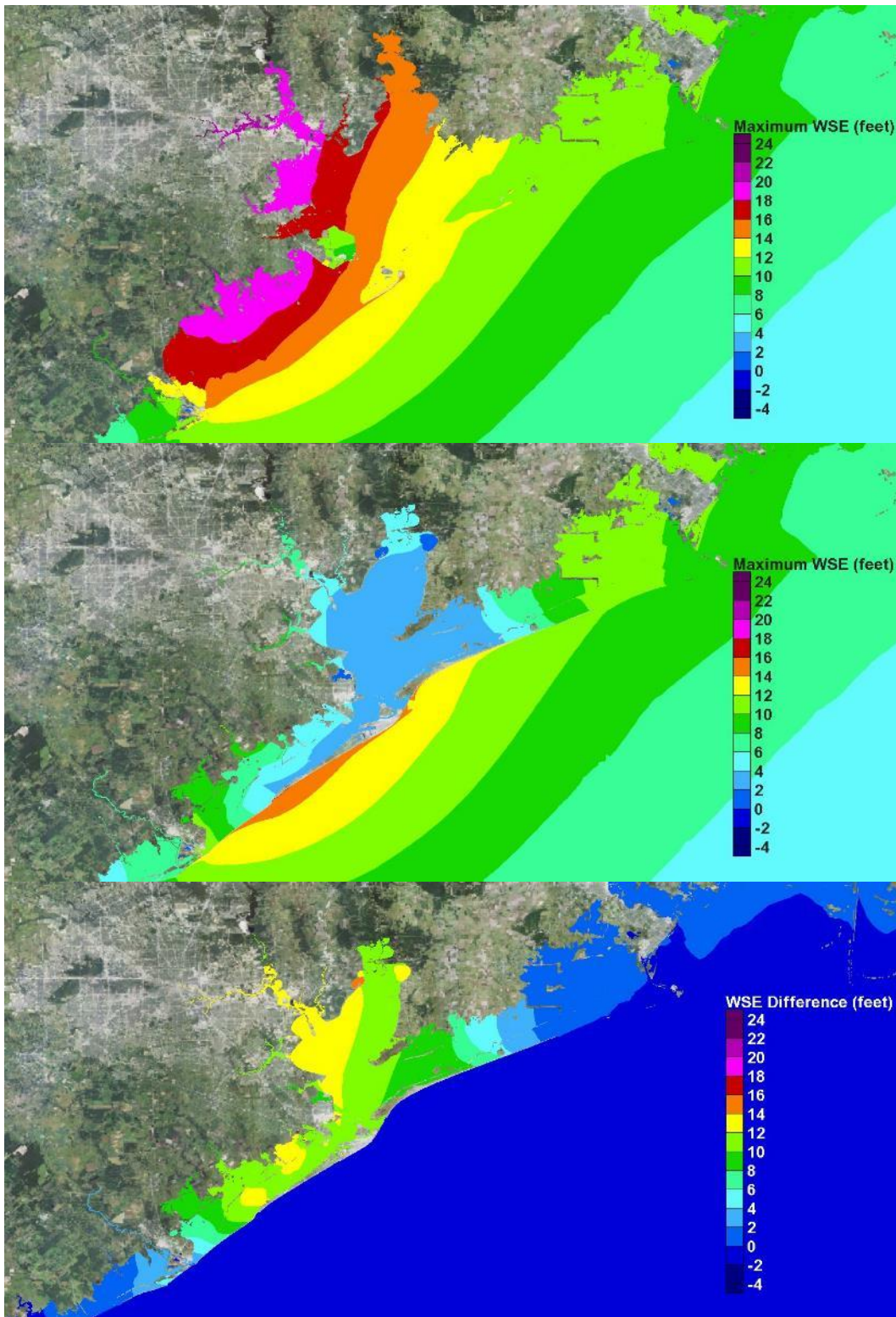


Figure 8-13. Maximum water surface elevation maps for storm 142. Existing conditions (top); With-dike conditions (middle); Difference in maximum water surface elevation (bottom)

Table 8-10. Summary of Maximum Storm Surge Conditions for Storm 142

Location	Existing Condition	With-Dike Condition	Changes
Galveston (Gulf side)	14 ft	14 ft	No change
Galveston (Bay side)	13 to 14 ft	3 ft	Reduction of 10 to 11 ft
Rest of Galveston Island	14 ft	3 to 6 ft	Reduction of 10 to 12 ft.
Bolivar Peninsula	11 to 13 ft	3 to 8 ft	Reduction of 5 to 10 ft
Texas City area	15.5 to 17.5 ft	4 to 5 ft	Reduction of 11 to 12 ft. Eliminated interior flooding.
Clear Lake Area	18 to 19 ft	6 ft	Reduction of 12 to 13 ft
Bayport Area	19 ft	5ft	Reduction of 13 to 14 ft
Upper reaches of Houston Ship Channel	20-21 ft	7 ft	Reduction of 13 to 14 ft

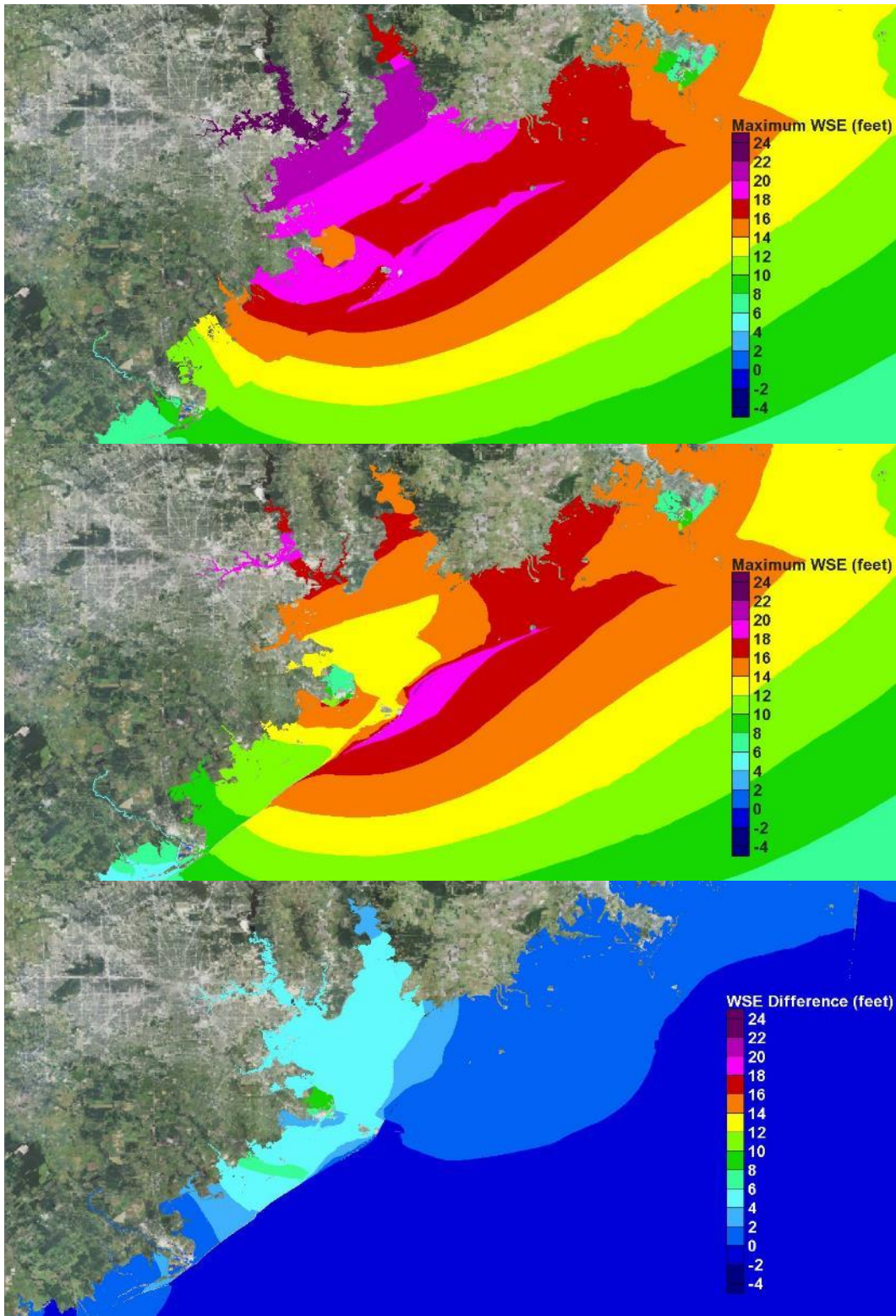


Figure 8-14. Maximum water surface elevation maps for storm 036. Existing conditions (top); With-dike conditions (middle); Difference in maximum water surface elevation (bottom)

Table 8-11. Summary of Maximum Storm Surge Conditions for Storm 036

Location	Existing Condition	With-Dike Condition	Changes
Galveston (Gulf side)	18 to 19 ft	18 to 19 ft	No change. Overflow and overtopping of the seawall
Galveston (Bay side)	18 ft	13 to 15 ft	Reduction of 3 to 5 ft
Rest of Galveston Island	12 to 18 ft increasing from west to east	10 to 17 ft	Some overflow and overtopping of the dike. Reduction of 2 to 6 ft.
Bolivar Peninsula	18 to 20 ft	14 to 17 ft	Overflow and overtopping of the dike. Reduction of 1 to 4 ft
Texas City area	18 to 20 ft	13 to 16 ft	Reduction of 4 to 5 ft. Reduced interior flooding.
Clear Lake Area	19 ft	14 to 15 ft	Reduction of 4 to 5 ft
Bayport Area	21 ft	15ft	Reduction of 4 to 5 ft
Upper reaches of Houston Ship Channel	24-25 ft	19 to 20 ft	Reduction of 5 ft

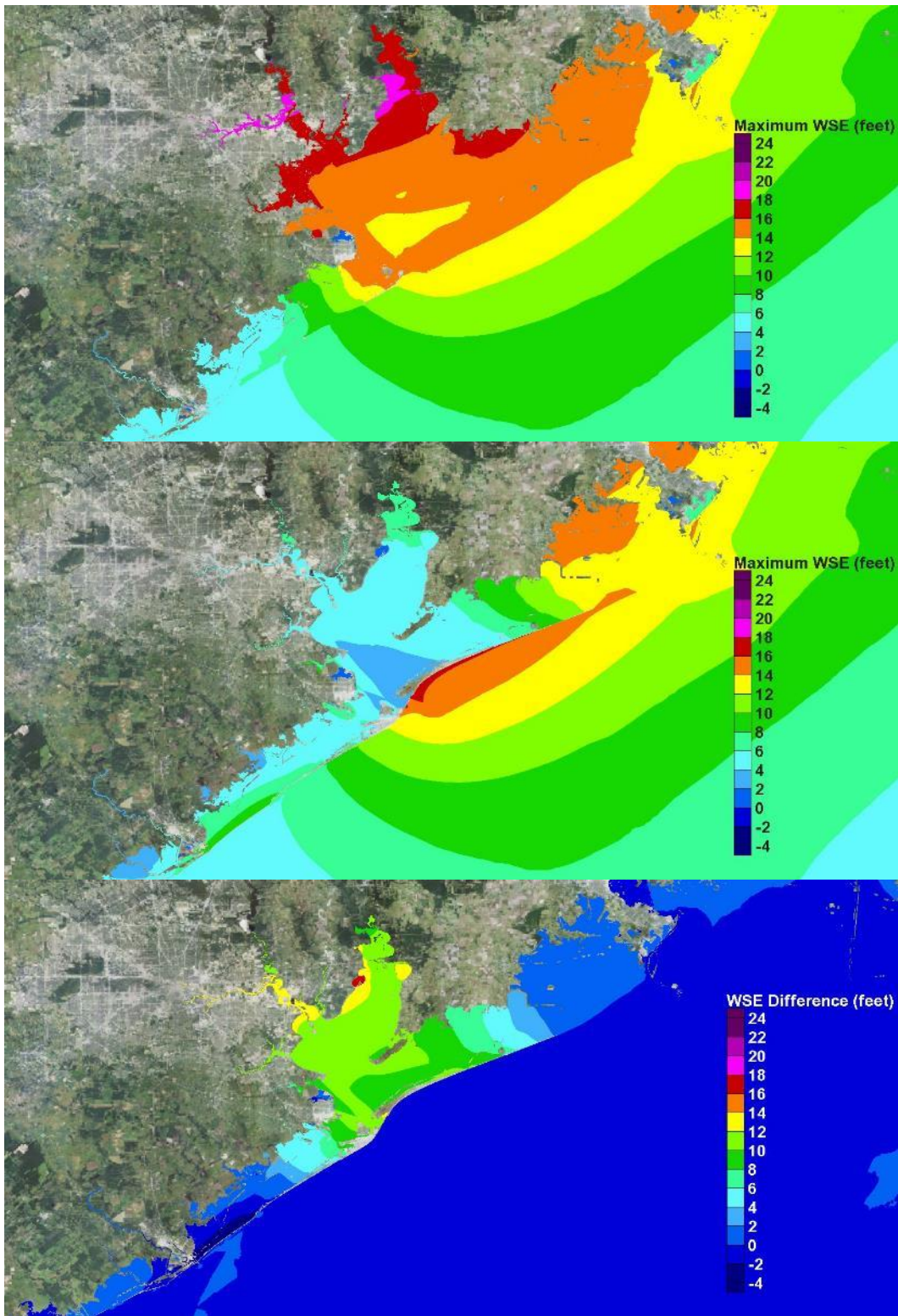


Figure 8-15. Maximum water surface elevation maps for storm 144. Existing conditions (top); With-dike conditions (middle); Difference in maximum water surface elevation (bottom)

Table 8-12. Summary of Maximum Storm Surge Conditions for Storm 144

Location	Existing Condition	With-Dike Condition	Changes
Galveston (Gulf side)	11 to 14 ft	11 to 14 ft	No change.
Galveston (Bay side)	13 to 14.5 ft	4 to 5 ft	Reduction of 8 to 11 ft
Rest of Galveston Island	5 to 11 ft increasing from west to east	5 to 8 ft	Reduction of 0 to 7 ft on the east; increase of 2 to 3 ft on the west.
Bolivar Peninsula	14 to 15.5 ft	3 to 12 ft	Increase of 0 to 0.5 ft at the dike. Reduction of 4 to 10 ft
Texas City area	11 to 15 ft	5 to 6.5 ft	Reduction of 6 to 9 ft
Clear Lake Area	16 to 16.5 ft	4 to 5 ft	Reduction of 11 ft
Bayport Area	16.5 to 17 ft	5ft	Reduction of 11.5 to 12 ft
Upper reaches of Houston Ship Channel	18 to 19 ft	6 ft	Reduction of 12 to 13 ft

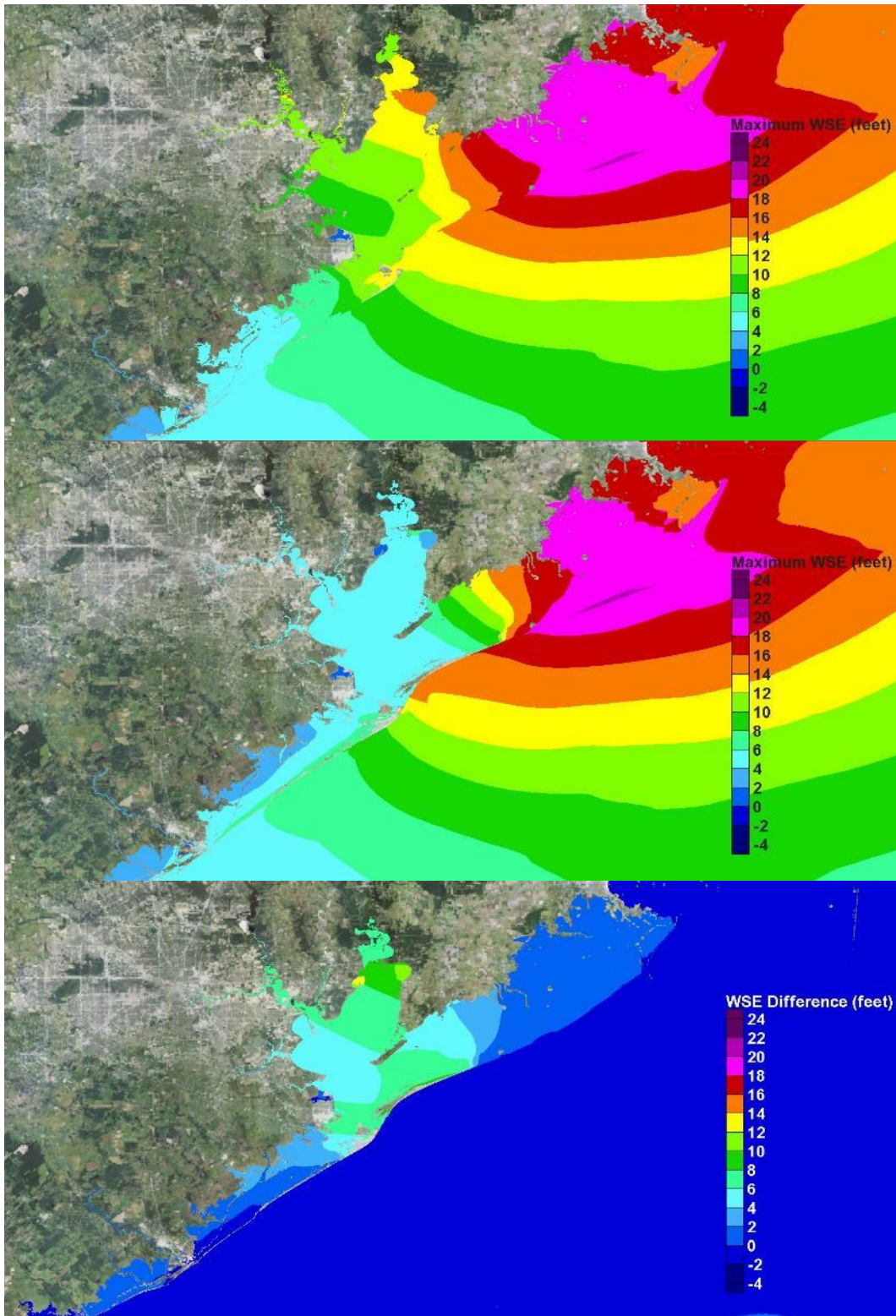


Figure 8-16. Maximum water surface elevation maps for storm 045. Existing conditions (top); With-dike conditions (middle); Difference in maximum water surface elevation (bottom)

Table 8-13. Summary of Maximum Storm Surge Conditions for Storm 045

Location	Existing Condition	With-Dike Condition	Changes
Galveston (Gulf side)	9 to 12 ft	9 to 12 ft	No change.
Galveston (Bay side)	11 to 12 ft	5 to 7 ft	Reduction of 5 to 6 ft
Rest of Galveston Island	5 to 8 ft increasing from west to east	5 to 6 ft	Reduction of 0 to 4 ft on the east. Increase of 0 to 1 ft on the west.
Bolivar Peninsula	13 to 18.5 ft	4 to 18.5 ft	Increase of 0.5 to 1 ft at the dike. Overflow and overtopping of the dike. Reduction of 0 to 7 ft
Texas City area	8 to 11 ft	4 ft	Reduction of 4 to 7 ft
Clear Lake Area	9 ft	4 ft	Reduction of 5.5 ft
Bayport Area	10.5 ft	4.5 ft	Reduction of 6 ft
Upper reaches of Houston Ship Channel	11 to 11.5 ft	5 ft	Reduction of 6 to 6.5 ft

Major Hurricanes Approaching from the Southeast

The following results are for the group of three North Texas storms that approach from the southeast. Storm 057 produces the greater surge in the region, followed closely by Storm 128 and Storm 061, in order of decreasing maximum surges. The peak surges for Storms 057 and 128 are similar. Storm 057 makes landfall to the west of San Luis Pass, Storm 128 to the east of San Luis Pass, both approximately equidistant from the pass. Storm 061 makes landfall at Bolivar Roads. Storm 057 has a radius to maximum winds that is lightly larger (18.4 n mi) than the radius for Storm 128 (17.7 n mi), which contribute to its slightly greater surge in the Bay.

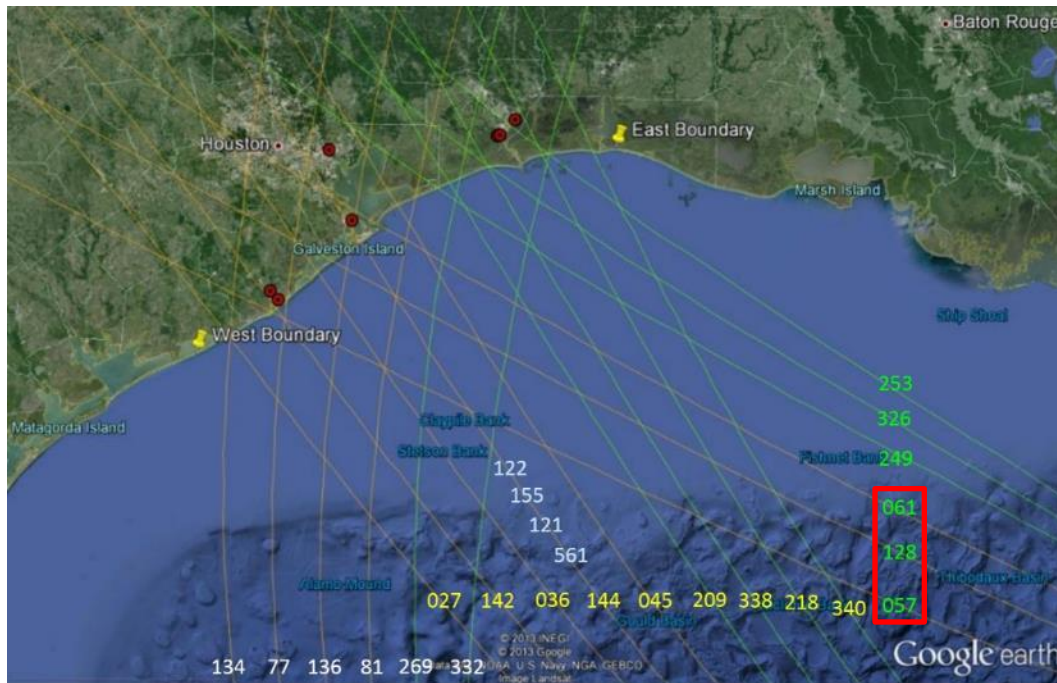


Figure 8-17. Group of hurricanes approaching from the southeast (storms 057, 128, 061)

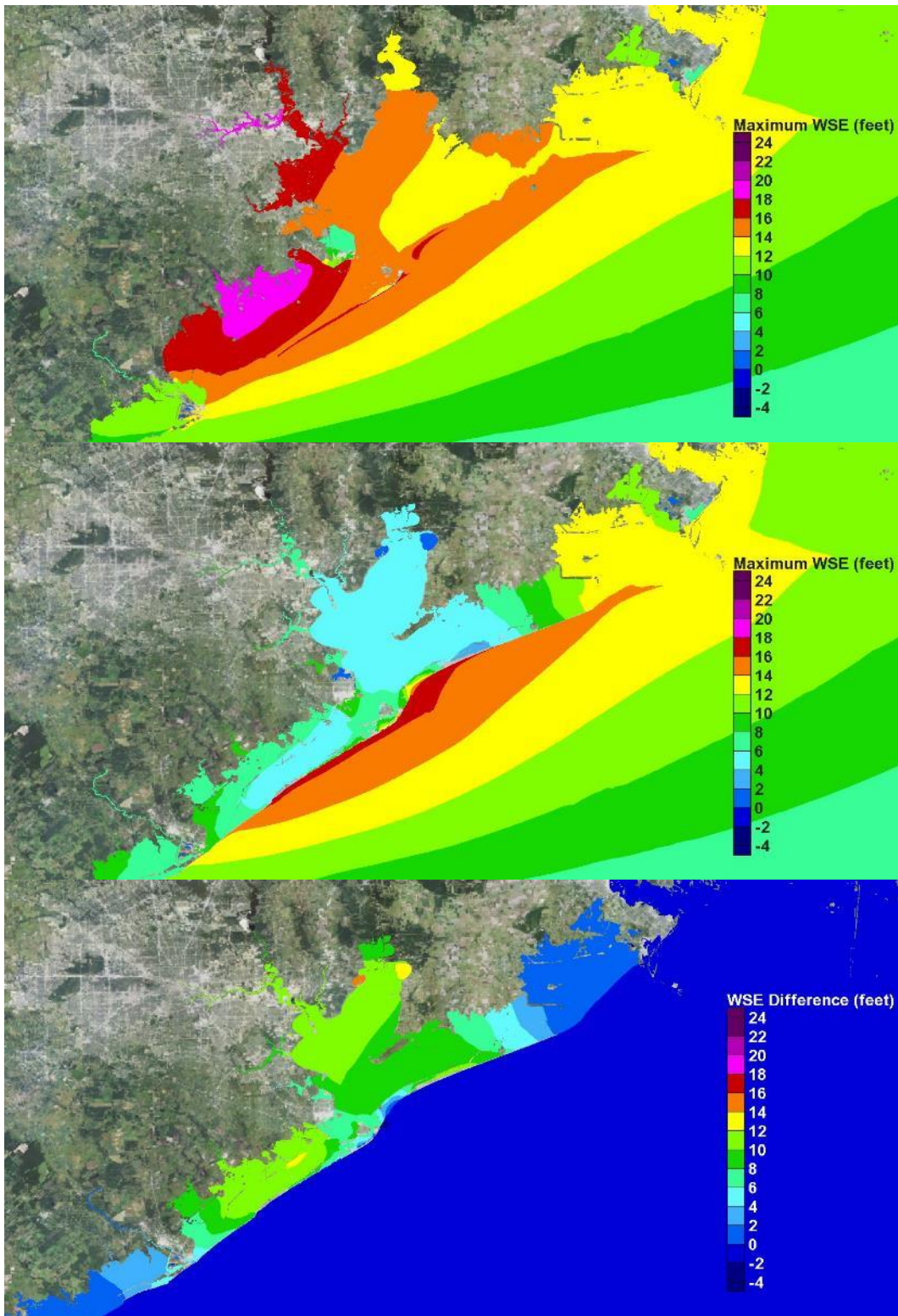


Figure 8-18. Maximum water surface elevation maps for storm 057. Existing conditions (top); With-dike conditions (middle); Difference in maximum water surface elevation (bottom)

Table 8-14. Summary of Maximum Storm Surge Conditions for Storm 057

Location	Existing Condition	With-Dike Condition	Changes
Galveston (Gulf side)	16 ft	16.5 ft	Increase of 0 to 0.5 ft. Increase in overtopping of the seawall expected.
Galveston (Bay side)	14 to 15 ft	6 to 7 ft	Reduction of 7 to 8 ft
Rest of Galveston Island	15.5 to 16 ft	5 to 6.5 ft	Reduction of 8 to 11 ft
Bolivar Peninsula	14.5 to 16 ft	6 to 13 ft	Increase of 0.5 to 1 ft at the dike on west end. Overflow and overtopping of the dike. Reduction of 2 to 8 ft
Texas City area	15 to 17.5 ft	7 to 8.5 ft	Reduction of 7 to 9 ft. Eliminates interior flooding.
Clear Lake Area	16.5 ft	6 ft	Reduction of 10.5 ft
Bayport Area	17 ft	6 ft	Reduction of 11 ft
Upper reaches of Houston Ship Channel	18 to 19 ft	6 to 7 ft	Reduction of 11.5 ft

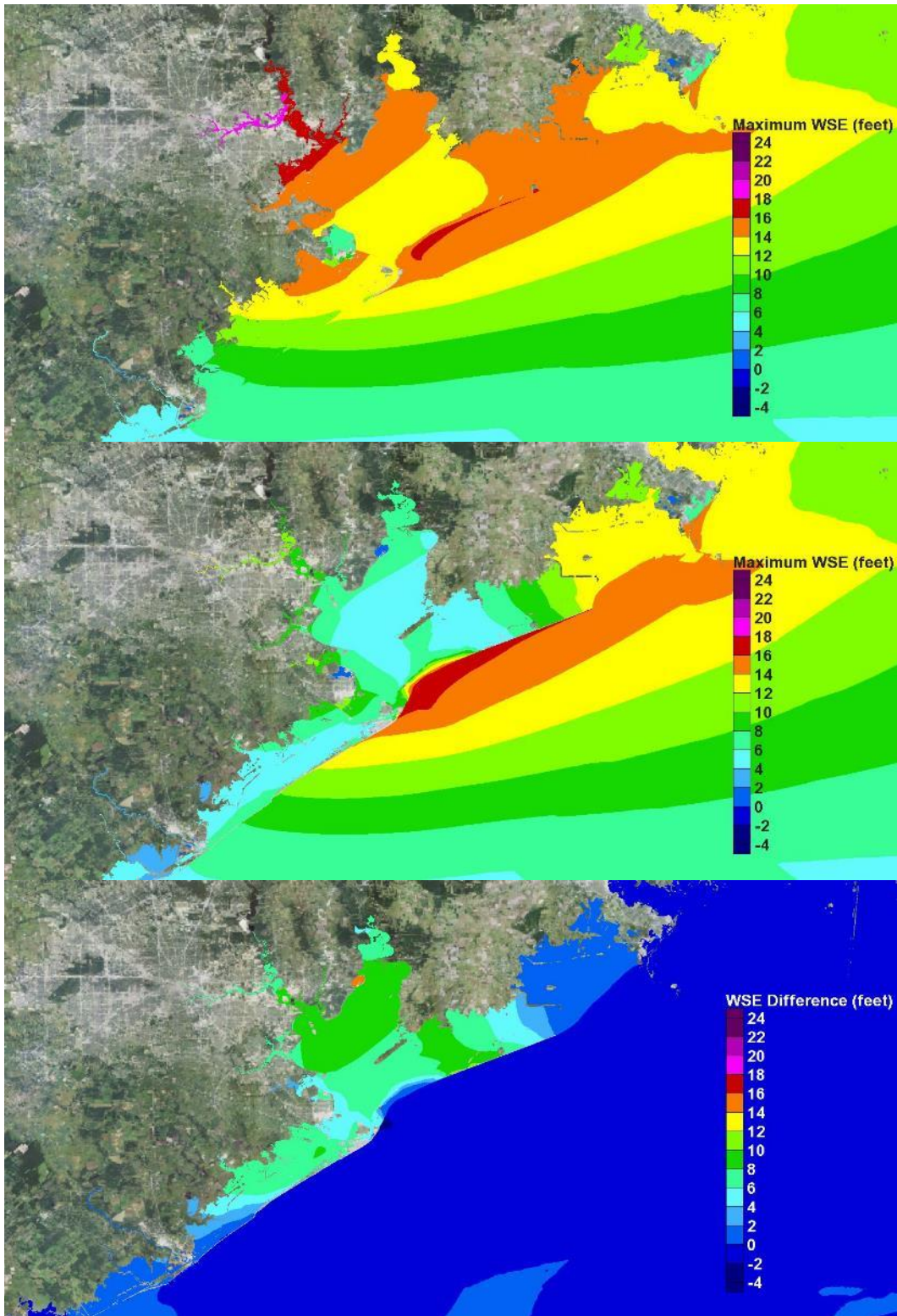


Figure 8-19. Maximum water surface elevation maps for storm 128. Existing conditions (top); With-dike conditions (middle); Difference in maximum water surface elevation (bottom)

Table 8-15. Summary of Maximum Storm Surge Conditions for Storm 128

Location	Existing Condition	With-Dike Condition	Changes
Galveston (Gulf side)	14 to 14.5 ft	14 to 16.5 ft	Increase of 0 to 2 ft. Increase in overtopping of the seawall expected.
Galveston (Bay side)	13.5 to 14 ft	7 to 12 ft	Reduction of 4 to 7 ft
Rest of Galveston Island	8 to 13.5 ft, increasing from west to east	6 to 7 ft	Reduction of 1 to 7 ft
Bolivar Peninsula	15 to 16.5 ft	6 to 13 ft	Increase of 1 ft at the dike. Overflow and overtopping of the dike. Reduction of 2 to 10 ft
Texas City area	13 to 15.5 ft	7 to 9 ft	Reduction of 6 to 7 ft. Eliminates interior flooding.
Clear Lake Area	15 to 16 ft	7 to 7.5 ft	Reduction of 7.5 to 8 ft
Bayport Area	16 ft	7 ft	Reduction of 8 ft
Upper reaches of Houston Ship Channel	18 to 19 ft	10 to 11 ft	Reduction of 8 ft

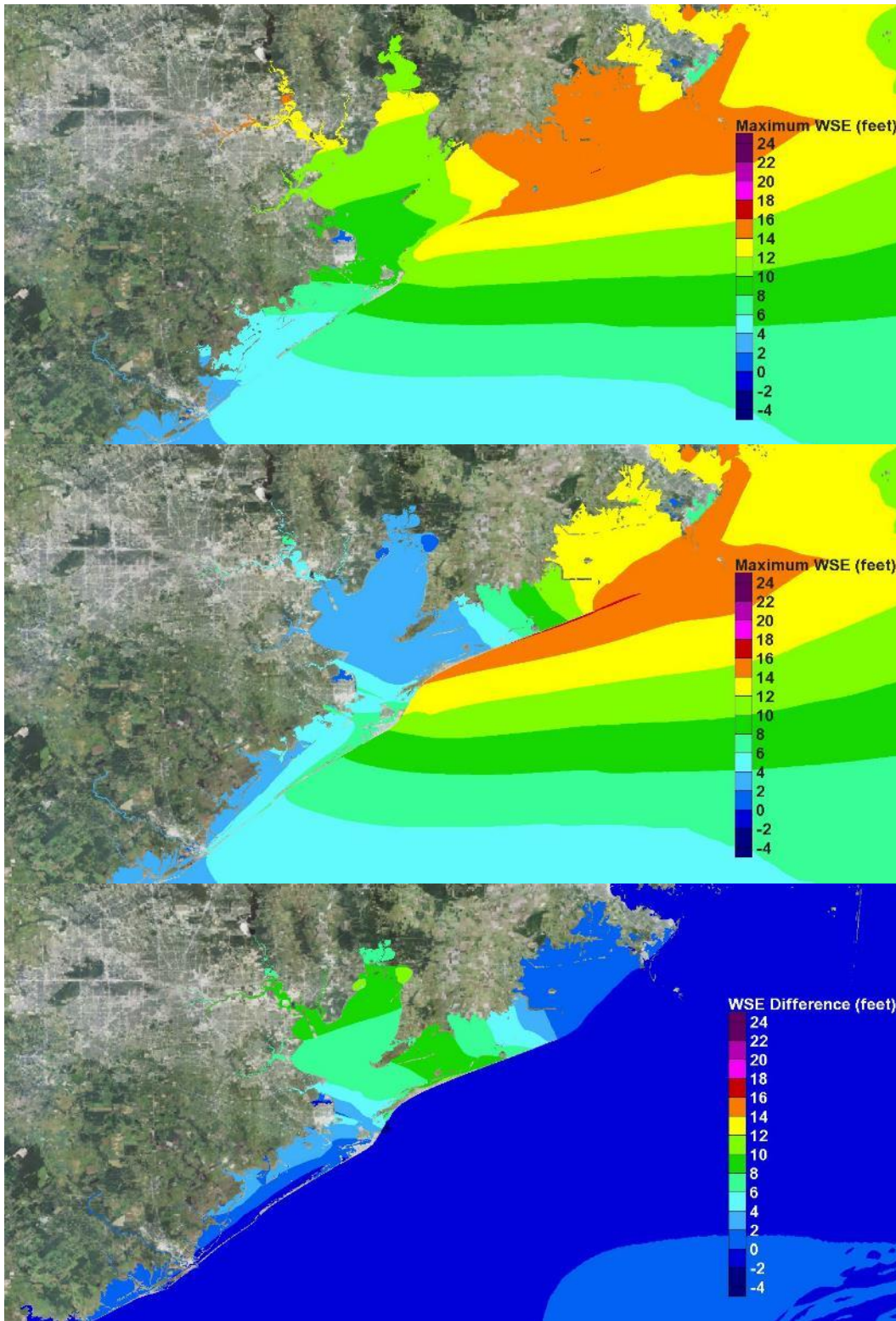


Figure 8-20. Maximum water surface elevation maps for storm 061. Existing conditions (top); With-dike conditions (middle); Difference in maximum water surface elevation (bottom)

Table 8-16. Summary of Maximum Storm Surge Conditions for Storm 061

Location	Existing Condition	With-Dike Condition	Changes
Galveston (Gulf side)	8 to 11 ft	9 to 12 ft	Increase of 1 ft
Galveston (Bay side)	8 to 10 ft	6 to 7 ft	Reduction of 2 to 4 ft
Rest of Galveston Island	4 to 7 ft	4 to 7 ft	Increase of 0 to 0.5 ft
Bolivar Peninsula	14 to 16 ft	3 to 10 ft	Reduction of 4 to 9 ft
Texas City area	8.5 to 9.5 ft	6 to 7 ft	Reduction of 2 to 4 ft
Clear Lake Area	10 to 11 ft	3 ft	Reduction of 7 to 8 ft
Bayport Area	11 to 11.5 ft	3 ft	Reduction of 8 to 8.5 ft
Upper reaches of Houston Ship Channel	14 ft	6 ft	Reduction of 8 ft

9 Placing Hurricane-Induced Water Levels in a Probabilistic Context

Introduction

The 25-storm bracketing set of tropical cyclones (TCs) was mostly comprised of very severe hurricanes having extremely low minimum central pressures of 900 mb and different land-falling tracks. Hurricanes that have a central pressure of 900 mb and make landfall in the Houston-Galveston region, like many of the bracketing set of storms, are exceedingly rare events. The Houston-Galveston region has not experienced a 900-mb hurricane in the most recent 140 years; however, the possibility exists that such a severe hurricane can directly impact the region. The probability of peak storm surge produced by such an occurrence is of great interest, with and without the proposed Ike Dike.

A few less intense storms also were considered in the bracketing storm set, having minimum central pressures of 930-, 960-, and 975-mb, all on a single direct-hit track. The 1900 Galveston Hurricane had a central pressure of 936 mb at landfall. Hurricane Ike had a central pressure of 950 mb at landfall. Both of these storms directly and adversely impacted the Houston-Galveston area. The probabilities of peak surge that produced these types of less intense, but more likely, events also is of great interest.

The Ike Dike concept reduced storm surge throughout Galveston Bay for all the bracketing-set TCs, including the very severe 900-mb storms. The dike showed considerable reduction in storm surge for the 930-mb storms and even more reduction for the less intense 960 and 975-mb storms, all of which have a much greater probability of occurrence compared to 900-mb storms. However, several of the 900-mb TCs, and the 930-mb direct hit storm, produced very high storm surge which overtopped the proposed Ike Dike at various locations. These extreme storms still produced substantial surge and inundation within Galveston Bay as a result of both overtopping and the effect of strong winds within the Bay. It is important to determine the frequency of occurrence of water levels for these types of rare TCs as well as the more likely storms. A full probabilistic approach is

essential for accurately determining the risk of both flooding and damage/losses associated with TCs for the existing condition and for determining the reduction in risk associated with the Ike Dike concept.

An initial approach, which is informative, relatively simple and much less resource intensive than a full probabilistic approach, was taken to gain insight on the inundation and damage/losses prevented by the dike in a probabilistic context. Although simple and not rigorous from a probability and statistics perspective, it sheds some initial light for TCs that produce water levels having certain frequencies of occurrence. This approach is based on the idea of a proxy storm, in which a single storm is selected to best represent a certain annual exceedance probability (AEP), or alternatively the average recurrence interval (ARI), water surface elevation throughout the corridor of greatest potential economic damage/loss. This corridor encompasses the City of Galveston, follows the western shoreline of Galveston Bay including Texas City and the Clear Lake area, and extends into the upper reaches of the Houston Ship Channel. The process for selecting proxy storms and results from the proxy storm analysis are presented later in this chapter.

A final approach will involve simulation of a large set of TCs for both existing conditions and with Ike Dike conditions, to assess risk of flooding and economic damages, without and with the proposed project.

Approach for Statistical Analysis of Water Surface Elevation

To provide a basis for proxy storm selection and to fully and accurately characterize the probability of extreme water surface elevations for existing conditions, a full joint probability analysis was conducted by the U.S. Army Engineer Research and Development Center (ERDC) using joint probability methods. The analysis produced water surface elevation statistics for a set of points, or save locations, in the Houston-Galveston region, including the key corridor for potential economic damage and losses, for existing conditions. The approach used by the ERDC differs slightly, in some aspects, from the approach used in the FEMA Region VI Risk Map study of the Texas coast (FEMA 2011). Differences in the joint probability analyses are noted later in this chapter.

Joint Probability Analysis

To quantify and estimate probabilities of hurricane-induced water levels, a probabilistic model of TCs was first built based on the historical storm climatology; and then the model was used to determine the probability of previously simulated synthetic tropical cyclones. For the present study, a new Joint Probability Analysis (JPA) was applied which takes advantage of more rigorous methods recently developed by the ERDC, which were applied to a recent study of the coastal storm hazard for the northeast United States, the North Atlantic Coast Comprehensive Study (Nadal-Caraballo, et al. 2015).

The present JPA model was built based on the historical storm climatology of tropical cyclones developed in the FEMA Region VI Risk MAP study (FEMA 2011). It also utilized high fidelity hydrodynamic modeling of TCs which was done as part of the Risk MAP study (FEMA 2011), in which the wind, pressure, surge and waves were modeled for each cyclone. The Risk MAP study included specification and modeling of 223 tropical cyclones for the northern Texas region, comprised of 152 high-intensity cyclones and 71 low-intensity cyclones. All hydrodynamic responses were stochastic because storms are random in both recurrence and intensity.

The statistical analysis of the storm surge responses of the 223 simulated TCs produced response statistics including average recurrence interval (ARI) water surface elevations. In addition, epistemic uncertainty was quantified and represented as confidence limits.

Joint Probability Method

Statistical analysis of water level response resulting from TCs in most cases suffers from a lack of historical observations, which results in a small sample size. Moreover, some of the characteristics of the TCs that impact a particular area may make it necessary to consider them as belonging to different populations, further reducing the sample sizes. Storm intensity has been identified as such a characteristic (Resio et al., 2007) since intense TCs tend to behave differently from weak ones.

The Joint Probability Method (JPM) overcomes this problem by focusing on the forcing instead of the response. In broad terms, TCs are defined by a number of forcing parameters which are used to generate the corresponding wind and pressure fields required for the simulation of

storm water level and waves. Therefore, the JPM has become the dominant probabilistic model used to assess the coastal storm hazard in hurricane-prone areas.

Although the details in the application of the JPM can vary significantly by study, the different approaches typically follow a common general methodology, depending on the dominant processes and respective solution strategies.

The JPM methodology generally includes the following steps:

- Characterization of historical storm climatology.
- Computation of historical spatially-varying storm recurrence rate (SSR).
- Storm parameterization and development of probability distributions of historical storm parameters.
- Discretization of probability distributions of storm parameters.
- Development of a synthetic storm set.
- Meteorological and hydrodynamic simulation of synthetic storms.
- Estimation of errors and other secondary terms.
- Integration of joint probability of storm responses (e.g., storm surge or waves)

The AEP of coastal storm hazards at a given site is a function of three main components: the storm recurrence rate (SRR), the joint probability of characteristic storm parameters, and the storm responses (e.g., water surface elevation in the present study).

The JPA of coastal storm hazards can be summarized by means of the JPM integral:

$$\lambda_{r(\hat{x})>r} = \lambda \int P[r(\hat{x}) + \varepsilon > r | \hat{x}, \varepsilon] f_{\hat{x}}(\hat{x}) f_{\varepsilon}(\varepsilon) d\hat{x} d\varepsilon \approx \sum_i^n \lambda_i P[r(\hat{x}) + \varepsilon > r | \hat{x}, \varepsilon] \quad (9-1)$$

where $\lambda_{r(\hat{x})>r}$ = AEP of storm response r due to forcing vector \hat{x} ; ε = unbiased error or epsilon term; $P[r(\hat{x}) + \varepsilon > r | \hat{x}, \varepsilon]$ = conditional probability that storm i with parameters \hat{x}_i generates a response larger than r . The storm parameters commonly used in a JPM for the characterization of TCs and included in the forcing vector \hat{x} are: track location (x_0), heading direction (θ), central pressure deficit (Δp), radius of

maximum winds (R_{max}), and translational speed (V_t). Secondary parameters may include: epsilon, or error, term (ϵ); Holland B , which characterizes the peakedness or radial shape of the wind field; and astronomical tide.

In order to develop the set of synthetic storms, each parameter is treated as a correlated random variable and either a marginal or a conditional probability density function (PDF) is sought for each parameter based on the TCs observed in the historical record. The probability distributions are then discretized and the corresponding weights are assigned to the range of discrete values. Synthetic storms are developed as possible combinations of samples from the marginal or conditional distributions. Each synthetic storm must consist of a physically- and meteorologically-realistic combination of the aforementioned parameters. The parameterized TCs are used as inputs to the PBL wind/pressure model. This model is used as part of the JPM methodology to estimate the time-histories of the wind and pressure fields that drive high-fidelity storm surge and wave numerical hydrodynamic models such as ADCIRC and WAM/STWAVE, respectively.

A central issue surrounding application of the JPM is the number of storm parameters required to adequately represent TCs and their forcing. In current practice, it has been shown that the five parameters listed above are sufficient to characterize TCs and their wind and pressure fields for the purpose of quantifying coastal storm hazards. Sources of epistemic uncertainty often accounted for in the JPM include:

1. Hydrodynamic modeling errors potentially arising from unresolved physical processes, inadequate grid resolution, and bathymetry inaccuracy.
2. Meteorological modeling errors due to use of idealized wind and pressure fields, and wind variations not captured by the PBL model.
3. Track variations not captured in the synthetic storm set.
4. Random variations in the peakedness of the wind fields represented by the Holland B parameter.

The AEP of a particular storm hazard is computed by integration of Equation (9-1). Epistemic uncertainty is quantified and incorporated in the JPM as confidence limits (e.g., 84%, 90%, 95%, and 98% are considered in the present study).

Joint Probability Method with Optimal Sampling

Although the JPM approach has been implemented since the 1970s, recent advancements in sampling techniques and the development of the JPM with Optimal Sampling (JPM-OS) have made it possible to reduce the necessary number of synthetic storms, more efficiently characterizing the parameter and probability spaces. The main accomplishment of these new developments was the reduction in number of storms required for populating the parameter space, from thousands, or even tens of thousands, down to hundreds of storms. This reduction was accomplished by optimizing the sampling of the storm parameters (Resio et al. 2007; Toro 2008; Vickery and Blanton 2008).

Different implementations of the JPM-OS methodology emerged as a result of several studies done in the aftermath of Hurricane Katrina after 2005, which led to the proliferation of surge hazard studies that brought further improvements to the JPM. Different approaches include the JPM-OS by Bayesian Quadrature (JPM-OS-BQ), the JPM with augmented sampling by means of Response Surface (JPM-OS-RS), and other JPM applications that use hybrid optimal sampling techniques.

Of particular importance was the work done by the Interagency Performance Evaluation Taskforce (IPET 2009) in which JPM-OS methods were developed for the statistical analysis of water level extremes to evaluate the performance of the Southeast Louisiana hurricane surge reduction system. This study provided the basic framework for the storm surge and modeling approaches used in later works, including the Texas Risk MAP study (FEMA 2011). This effort, led by a team of USACE, FEMA, NOAA, and private sector and academic researchers, was documented in the IPET (2009) report.

Regional studies conducted after Hurricane Katrina that stood out included the Louisiana Coastal Protection and Restoration (LACPR) (USACE 2009a), the Mississippi Coastal Improvements Program (MSCIP) (USACE 2009b), the Mississippi Coastal Analysis Project (FEMA 2008a) and the Risk MAP Study for the Coastal Counties in Texas (FEMA 2011). The JPM-OS-RS approach was applied in the Texas Risk MAP study (FEMA 2011).

The JPM-OS-BQ was adopted as part of FEMA's National Flood Insurance Program Risk MAP program best practices, as documented in the

Operating Guidance No. 8-12 (FEMA 2012). The JPM-OS-BQ approach was adopted for the present analysis.

JPM-OS-BQ Implementation for the Present Study

Tropical Cyclone Data Sources

The first step in implementing a JPA is characterization of the historical storm climatology, TCs in this case. Characterization requires identification of a TC data source and selection of a period of record for which the analysis will be performed.

For TCs, the main data source was HURDAT2 (Landsea and Franklin, 2013). HURDAT2 is a product of NOAA's National Hurricane Center (NOAA-NHC) and consists of the reanalysis of all historical TCs recorded in the North Atlantic basin (i.e., North Atlantic Ocean, Gulf of Mexico, and the Caribbean Sea) from 1851 to the present. This same basic data source was used in the Texas Risk MAP study (FEMA 2011).

The JPA performed in this study focused on TCs with $\Delta p \geq 28$ hPa. The Δp were computed as the difference between a far-field atmospheric pressure of 1,013 hPa and central pressure (c_p). TCs of this intensity are expected to be classified, on average, as category 1 hurricanes based on the Saffir-Simpson hurricane wind scale (SSHWS), but generally fall within the tropical storm to category 2 range.

Period of Record

Prior to the selection of historical TCs, the specific period of record to be used for the JPA must be defined. The SRR and the marginal distributions of storm parameters are sensitive to the historical record length. The 1940s decade marked the dawn of modern aircraft reconnaissance missions to measure hurricane parameters, resulting in much more reliable estimates of storm characteristics, including frequency and intensity.

Prior to 1944, the main data sources were land stations and ship reports (Jarvinen et al. 1984). During this period it was typical for relatively weak storms to go undetected and for the intensity of strong storms to be underestimated. After 1944 and as a consequence of World War II, aerial reconnaissance led to increased data collection incidence and

measurement accuracy, including storm position, track, wind speed and pressure. The use of satellite imagery was introduced during the 1964 hurricane season (Neumann et al., 1985) and was considered one of the major advances in TC tracking (Jarvinen et al., 1984).

The high frequency of unsampled TCs prior to the 1940s has been well documented. Mann et al. (2007) estimated an undercount in the pre-aircraft reconnaissance era (1870–1943) ranging from 0.5 to 2.0 TC/yr, with a mean of 1.2 TC/yr. Landsea et al. (2010) discussed that the increase in reported TCs during the 1940s and until about 1960 had been interpreted as a result of climate change. This increase, however, is likely to be a consequence of improved observing and recording of short-lived TCs coinciding with the advent of aircraft reconnaissance and satellite imagery.

Worley et al. (2005) identified spikes in the number of unrecorded moderate to long-lived TCs during the 1910s and 1940s as due to reduced ship observations during World War I and World War II, respectively. Vecchi and Knutson (2011), after adjusting HURDAT data for unrecorded TCs, concluded that the mid-twentieth century was a high activity period that extended from the 1940s to the 1960s.

In recent flood hazard studies where the JPM-OS methodology has been used, the period of record that was considered started in the early 1940s (FEMA 2008a, 2012; Resio et al., 2007). For the present study, the period of record was 1940-2013. For the Texas Risk Map study (FEMA 2011), the period of record considered was 1940-2007.

Computation of Spatially-Varying Storm Recurrence Rate

A second step in conducting a JPA is computation of the historical spatially-varying storm recurrence rate (SSR) for the area of interest. Calculation of the SRR requires sampling of historic TC occurrences for the region. The computation method adopted in the present study is different from that used in the Texas Risk MAP study (FEMA 2011), and slightly different rates are calculated.

Efficient storm sampling from the historical record and statistical computation of the SRR can be achieved using several different approaches. In recent studies some of the approaches used to compute the spatial variation of SRR have included: area-crossing, line-crossing,

Gaussian Kernel Function (GKF), and other combined methods. Both area-crossing and line-crossing are examples of capture zone methods. In the area-crossing approach only storms passing through a particular area are counted in the computation of the SRR. The line-crossing approach usually consists of an idealized coastline, or a reference line representing a segment of coastline. Only storms making landfall along the chosen segment of coastline are captured and counted towards the computation of the SRR.

Capture zones can also be defined in other ways, such as a rectangular or circular window, or any other finite spatial region. In past studies, the standard had been to apply any of the capture zone methods in order to count the storms and to assign uniform weights to all captured storms. The main limitation of the capture zone approach is that, while all storms within the chosen capture zone are given uniform weights, storms outside this zone are given a weight of zero. The conundrum lies in establishing a capture zone large enough to reduce the uncertainty associated with sample size by capturing an adequate number of storms from which significant statistics can be derived, but small enough to balance the uncertainty associated with spatial variability and population heterogeneity.

The use of the Gaussian Kernel Function (GKF) method, developed by Chouinard and Liu (1997), can overcome the main limitations of capture zone approaches. The standard application of the GKF consists of establishing a grid of nodes where estimates of the SRR are sought. All storms within this gridded space can be counted at any given node, but the weight assigned to each storm decreases with increasing distance from storm to node. The distance-adjusted weights are computed using a Gaussian probability density function (PDF) with an optimal kernel size.

The GKF equations are as follows:

$$\lambda = \frac{1}{T} \sum_i^n w(d_i) \quad (9-2)$$

$$w(d_i) = \frac{1}{\sqrt{2\pi}h_d} \exp \left[-\frac{1}{2} \left(\frac{d_i}{h_d} \right)^2 \right] \quad (9-3)$$

where, λ = SRR in storms/yr/km; T = record length in (yr); $w(d_i)$ = distance-adjusted weights from the Gaussian PDF (km^{-1}); d_i = distance

from location of interest to a storm data point (km); h_d = optimal kernel size (km). Use of the GKF weights minimizes sample size uncertainty by taking full advantage of all available storm data, while significantly reducing the uncertainty associated with spatial variability and potentially heterogeneous populations.

Optimal Gaussian Kernel Size

For purposes of this study, the optimal kernel size was determined from a series of sensitivity analyses performed using all tropical cyclones in the HURDAT2 database with $\Delta p \geq 28$ hPa within the 1940–2013 period. For validation purposes, the SRR computed from the GKF were compared to the observed SRR estimated using the capture zone approach. The analysis consisted of first estimating the observed SRR using circular capture zones with radii ranging from 100 km to 500 km, and then computing the mean observed SRR corresponding to this range of radii; second, the squared error of the GKF results was computed from the difference between the mean observed SRR and GKF estimates using kernel sizes from 100 km to 500 km. For each cyclone, only track data points with $\Delta p \geq 28$ hPa were accounted for in this analysis.

Figure 9-1 shows the variation of SRR as a function of capture zone radius (blue curve), as well as the mean observed SRR (red line), for a coastal reference location in Galveston, Texas. The observed SRR for Galveston varied from roughly $4.5\text{E-}4$ to $7.0\text{E-}4$ storms/year/km, depending on the capture zone radius, and had a mean of $5.5\text{E-}4$ storms/year/km.

The squared error of the difference between the GKF and the observed SRR for Galveston is presented in Figure 9-2. This difference decreases to almost zero for kernel sizes between 150 km and 200 km, and remains close to zero for the remaining of the evaluated kernel sizes (up to 500 km). While the optimal kernel size for the Galveston location evidently lies within the 150-200 km range, it reaches a plateau after roughly 250 km. For this study, an optimal kernel size of 200 km was adopted for the Galveston, TX and surrounding area.

This optimal kernel size is in agreement with the kernel size of 200 km selected in a FEMA study of coastal Mississippi (FEMA 2008a; Toro 2008). A 200-km kernel size was found to be optimal by Nadal-Caraballo et al. (2015) in the North Atlantic Coast Comprehensive Study.

The weights computed using the GKF with a kernel size of 200 km are illustrated in Figure 9-3. These weights are shown relative to the weight of a storm track point located right on the coastal reference line (CRL), ($d_i = 0$ km), or

$$\text{Relative weight} = \frac{w(d_i)}{w(d_i=0)} \quad (9-3)$$

Data from such a storm track point would have a relative weight of 1.0, whereas, a track point located at a distance 200 km away from the CRL would have a relative weight of 0.6. The weights decrease as distance from the CRL increases, based on the Gaussian pdf, until becoming negligible. The relative weight of track points located at 600 km and 850 km from the CRL, for example, will have relative weights of roughly $1.0\text{E-}2$ and $1.0\text{E-}4$, respectively.

For the present study, further analyses were performed to determine the SRR corresponding to both high intensity ($\Delta p \geq 48$ hPa) and low intensity ($28 \text{ hPa} \leq \Delta p < 48$ hPa) storms for the 1940-2013 period. The SRR of high intensity storms computed for locations in the Galveston region varied from $1.6\text{E-}4$ to $2.2\text{E-}4$ storms/year/km. For low intensity storms in the same area, the computed SRR ranges from $4.2\text{E-}4$ to $5.1\text{E-}4$ storms/year/km.

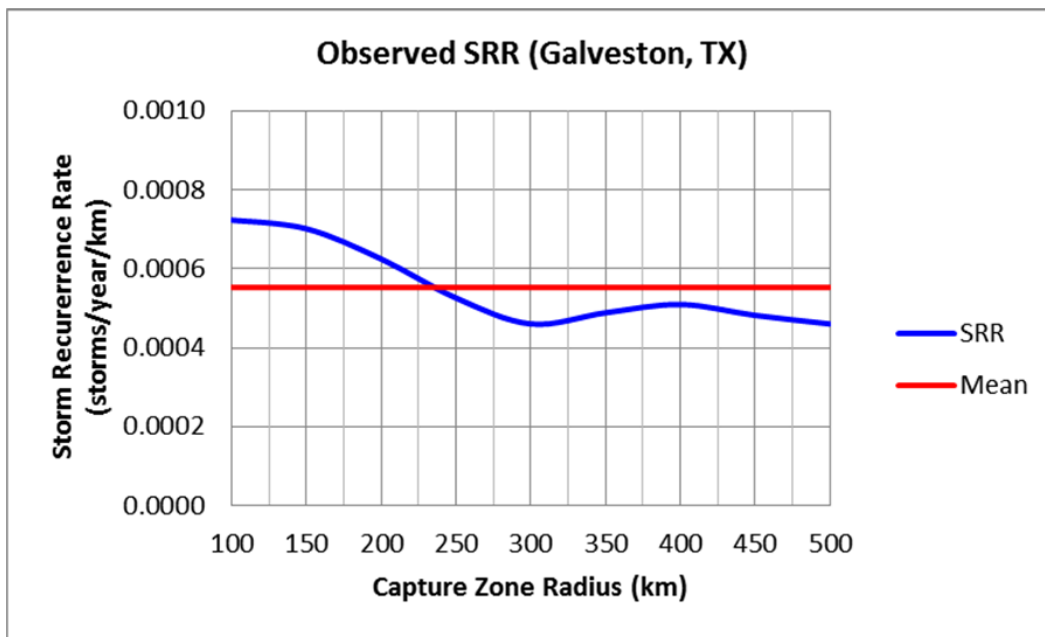


Figure 9-1. Observed SRR for Galveston, Texas.

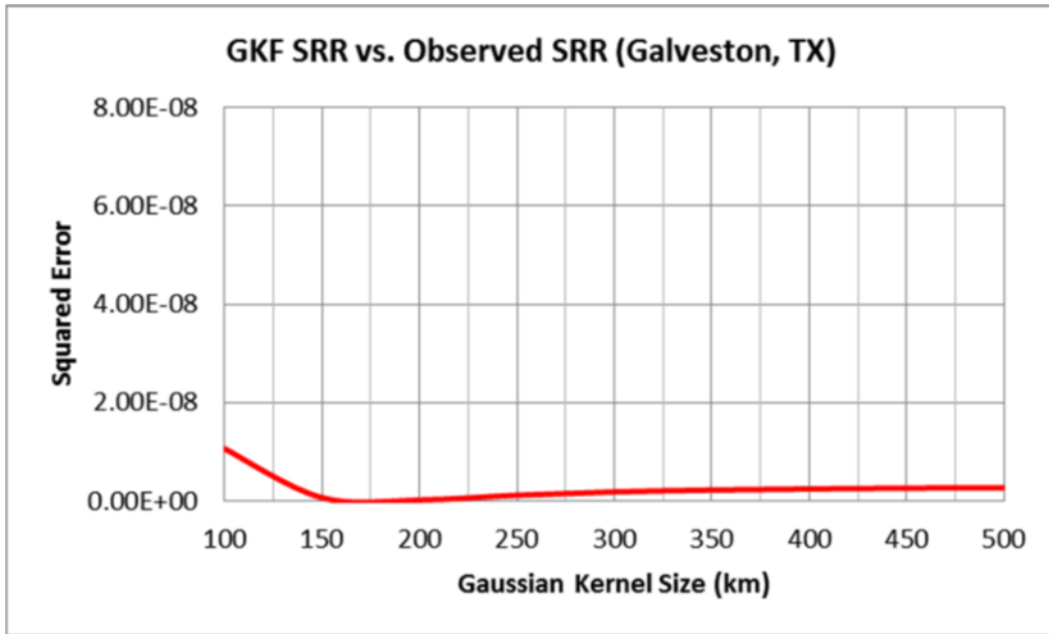


Figure 9-2. Comparison of GKF SRR vs. Mean Observed SRR for Galveston, Texas.

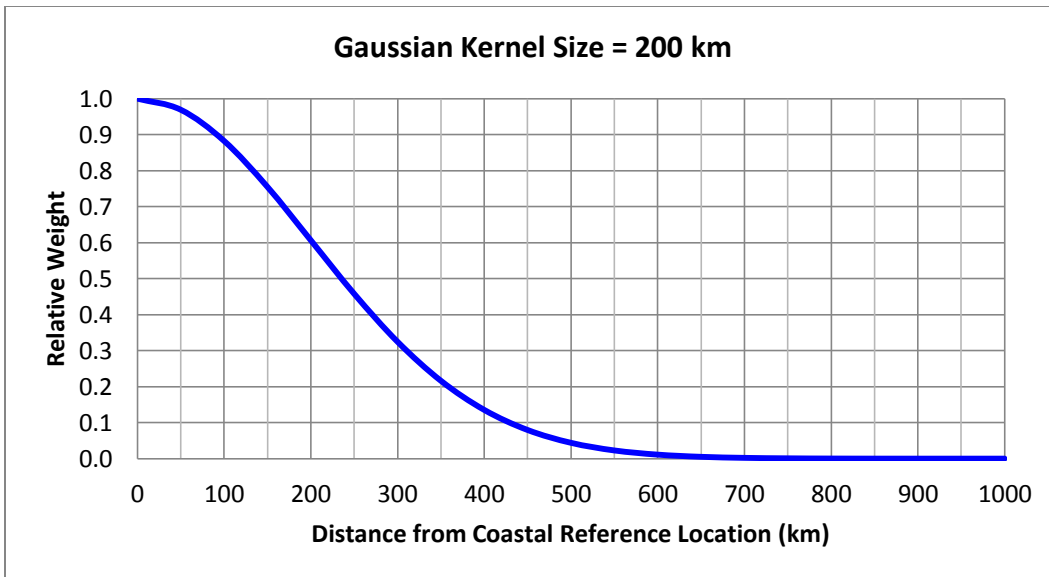


Figure 9-3. Relative weight of storm parameters as a function of distance from CRL.

The GKF SRR results corresponding to high intensity storms ($\Delta p \geq 48$ hPa) in the entire Atlantic basin for the 1940–2013 period are shown in Figure 9-4. SRR of low intensity storms ($28 \text{ hPa} \leq \Delta p < 48 \text{ hPa}$) for the same period are presented in Figure 9-5. The Δp values were determined based on a far-field pressure of 1,013 hPa. The SRR depicted in these figures is $\text{SRR}_{200\text{km}}$, with units of storms/yr, and represents the annual chance of a TC passing within 200 km.

Estimates of SRR from Other Studies

For comparison purposes, the SRR of high intensity storms in previous FEMA studies (Resio et al., 2007; FEMA, 2009a, 2009b; FEMA, 2011) for the Galveston area have been determined to be around 0.02 storms/year/deg, or roughly $2.0\text{E-}4$ storms/year/km.

The SRR analyses in the present study were performed using the standard GKF method developed by Chouinard and Liu (1997) with an optimal kernel size of 200 km. However, in the Resio et al. (2007) work, the SRR was estimated using a hybrid method which employed a line-crossing approach to sample only landfalling storms, then using GKF weights with kernel size of 250 km for the actual computation of SRR. Figure 9-6 shows the coastal reference line that was used. The Resio et al. (2007) results are shown in Figure 9-7 with units of storms/year/deg.

In FEMA (2008a) and Toro (2008), another hybrid method was used that included a rectangular window capture zone. The results, which were based on a kernel size of 160 km, are illustrated in Figure 9-8 with units also in storms/year/deg.

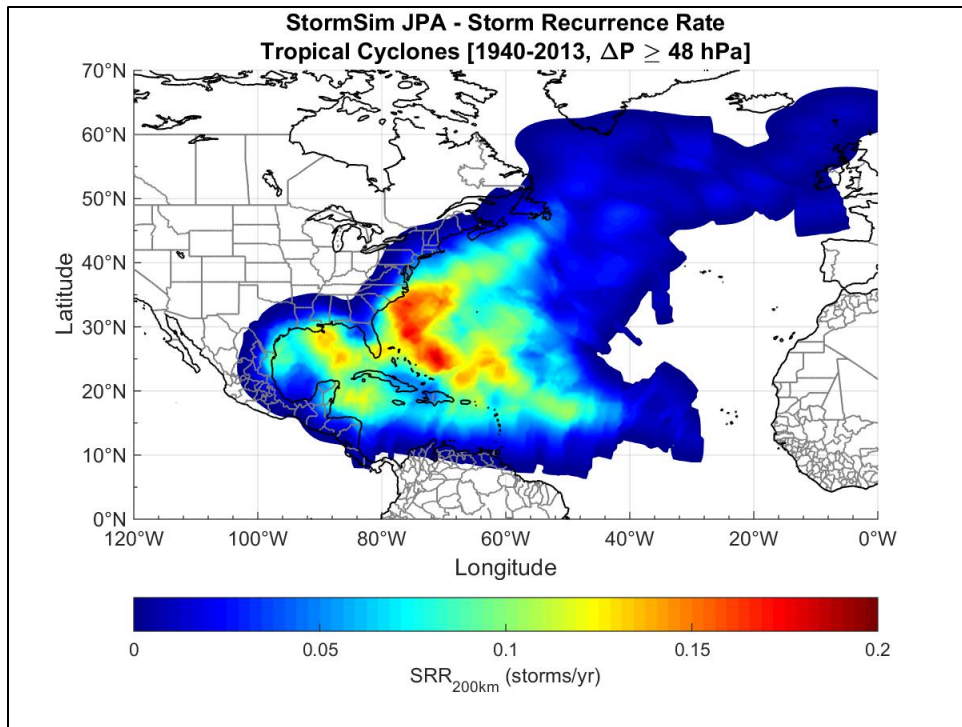


Figure 9-4. SRR for high intensity tropical cyclones recorded in the Atlantic basin from 1940–2013.

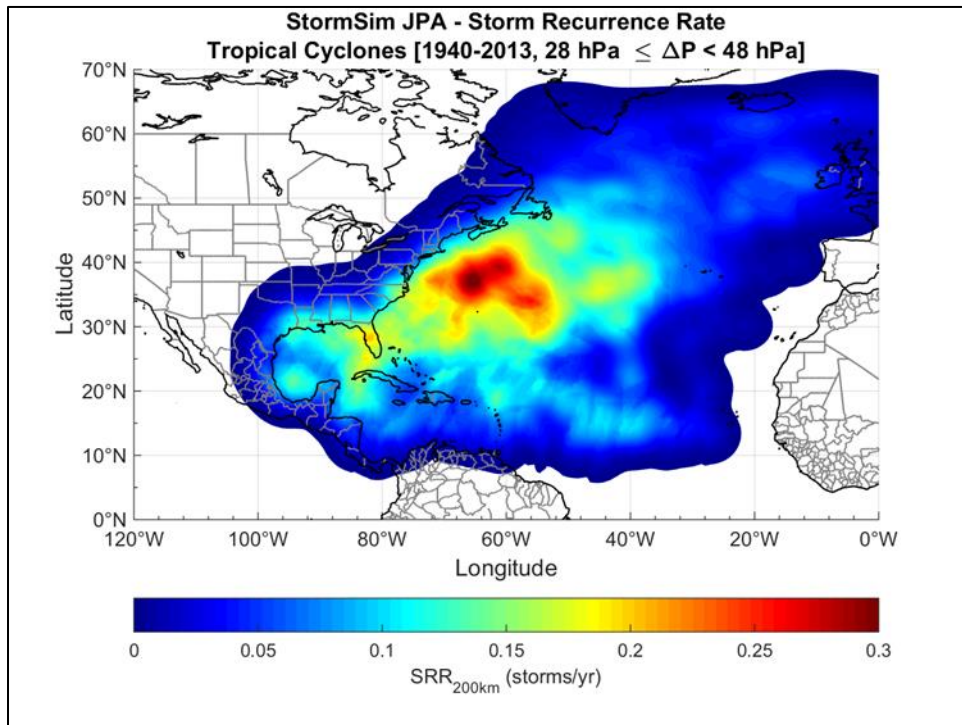


Figure 9-5. SRR for low intensity tropical cyclones recorded in the Atlantic basin from 1940–2013.

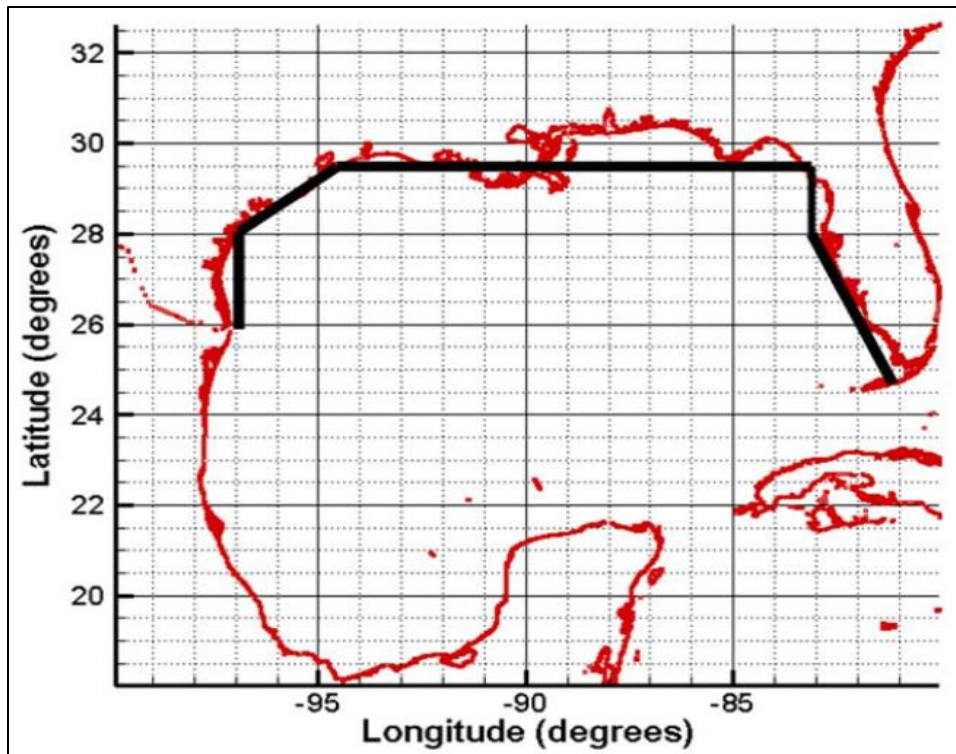


Figure 9-6. Coastal reference line used by Resio (2007) in determining the SRR

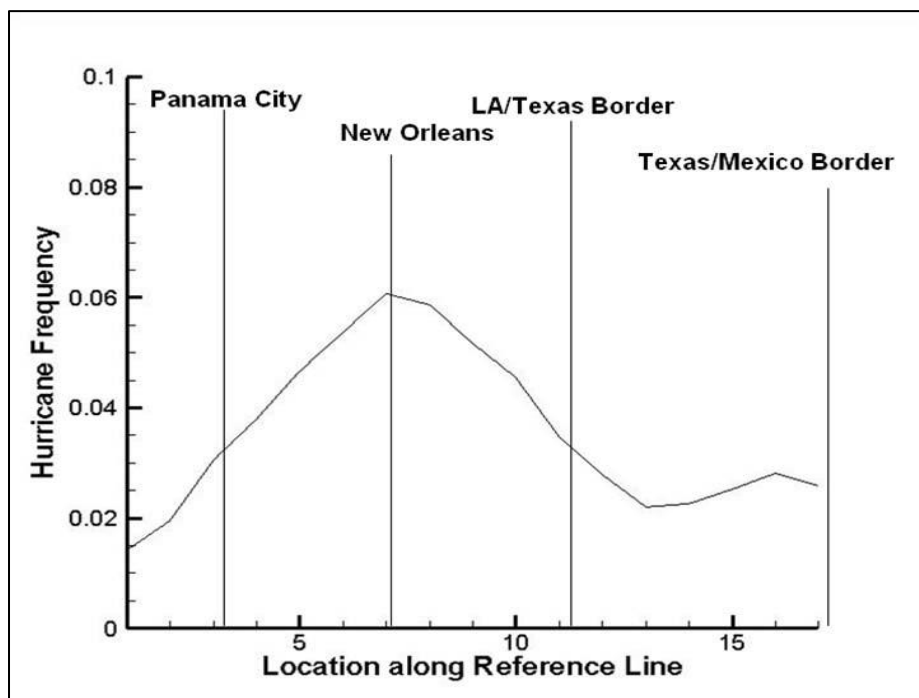


Figure 9-7. SRR estimated for the Gulf coast region by Resio et al (2007).

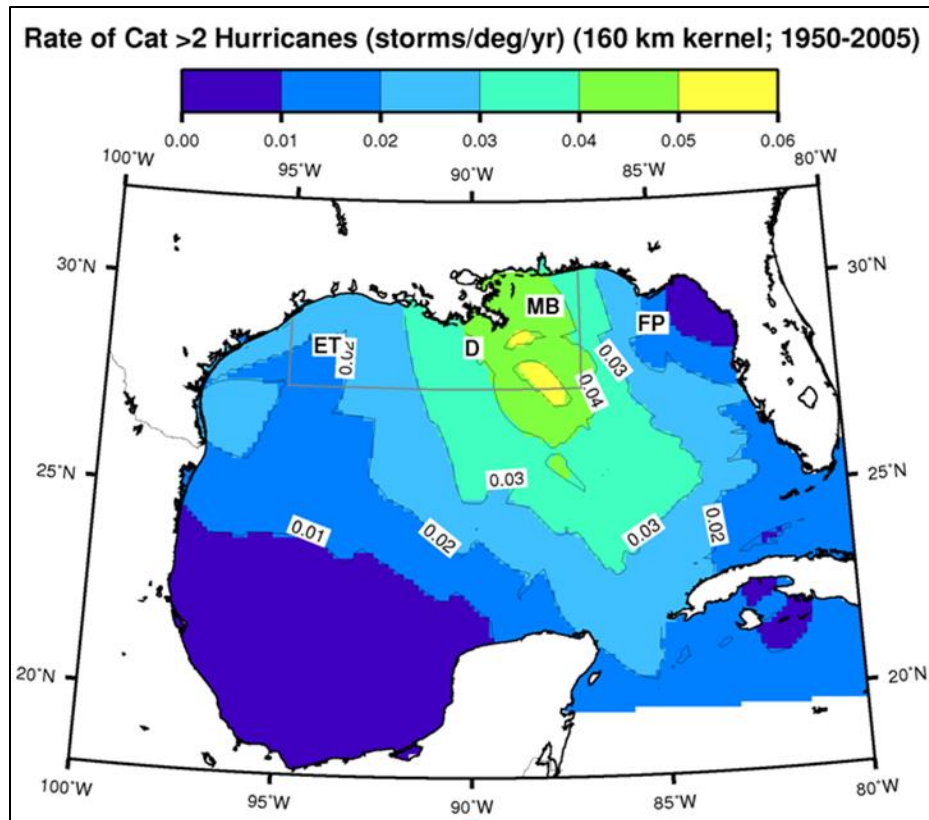


Figure 9-8. SRR computed from GKF for the Gulf of Mexico in FEMA (2008a).

Probability Distributions of Tropical Storm Parameters

In general, the next steps in conducting a JPA are: storm parameterization and development of probability distributions of historical TC parameters, discretization of probability distributions of TC parameters, and development of a synthetic storm set. The storm set adopted for use in the present study is the same storm set that was developed for the FEMA Risk MAP study of the Texas Coast (FEMA 2011). Compared to the method used in the Texas Risk MAP study (FEMA 2011), the present study adopted a different approach for discretizing probability distribution of storm parameters and optimizing the discrete weights assigned to each TC parameter combination.

Most recent FEMA studies of hurricane-prone coastal areas have been based on some implementation of JPM-OS methodology for sampling distributions of TC parameters. The two most well established JPM-OS methods are the JPM-OS Response Surface approach (Resio et al., 2007) and the JPM-OS Bayesian Quadrature approach (Toro et al., 2010). The Response Surface approach (JPM-OS-RS) has been used in studies

throughout the Gulf Coast, including Louisiana (IPET 2009) and Texas (FEMA 2011). The Bayesian Quadrature Approach (JPM-OS-BQ) has been used in areas of the Gulf Coast region such as Mississippi (FEMA 2008a).

The focus of the JPM-OS-RS is to augment the storm sampling by interpolating intermediate parameter values from response surfaces. The interpolated values have been shown to introduce additional uncertainty in water surface elevations with root-mean-square deviation on the order of 0.70 m (CPRA 2013). The added uncertainty is seldom quantified in these studies. The JPM-OS-RS also requires expert judgment for the selection of the storm parameters and associated discrete weights.

The JPM-OS-BQ approach employs a quadrature scheme that selects the optimal storm parameters and assigns the appropriate discrete weights. The JPM-OS-BQ was adopted as part of FEMA's Risk MAP program best practices, as documented in the Operating Guidance No. 8-12 (FEMA 2012). In the present study, the Bayesian Quadrature (Diaconis 1988; O'Hagan 1991; Minka 2000; Toro 2008, Toro et al., 2008) algorithm was used to optimize the discrete weights assigned to each parameter combination corresponding to the synthetic storm set developed as part of the Texas Risk MAP study (FEMA 2011).

Estimation of Errors and Other Secondary Terms

The error or epsilon (ϵ) term that is considered in the JPM integral (Equation 9-1) is a combination of multiple epsilons that are considered to be probabilistically independent and aggregated accordingly. Following is a list of epsilons that have been estimated and accounted for in recent JPM-OS studies:

- 1) Errors in hydrodynamic modeling and grids associated with epistemic uncertainty.
- 2) Errors in meteorological modeling associated with simplified PBL winds.
- 3) Random variations in the Holland B parameter.
- 4) Storm track variations not captured in synthetic storm set.
- 5) Random astronomical tide phase.

The uncertainty associated with each epsilon is assumed to be unbiased and normally distributed. This allows the epsilons to be represented as standard deviations and their effects to be combined additively. The total uncertainty associated with the combined epsilon (σ_ϵ) is computed as the square root of the sum of the squares of the standard deviations of each individual epsilon (σ_i):

$$\sigma_\epsilon = \sqrt{\sum_i^n (\sigma_i^2)} \quad (9-4)$$

where σ_ϵ is the total standard deviation of errors and σ_i is the standard deviation of error i .

Errors in Hydrodynamic Modeling

The epsilon related to hydrodynamic modeling errors, σ_{hyd} , has been estimated in substantially different ways in recent FEMA studies. For example, in FEMA (2008), σ_{hyd} was computed as follows:

$$\sigma_{hyd} = \sqrt{\sigma_{cal}^2 - \sigma_{meas}^2} \quad (9-5)$$

where σ_{cal} = calibration error; σ_{meas} = measurement error. The calibration error was estimated as the standard deviation of the difference between simulated and measured storm surge elevations. The measurement error was estimated as a standard deviation representing the variability in high water marks. The epsilons σ_{cal} and σ_{meas} were estimated to be 0.46 m and 0.40 m, respectively, resulting in $\sigma_{hyd} = 0.23$ m. Other studies (Resio et al. 2007; FEMA 2011) have estimated σ_{hyd} for the Louisiana-Mississippi coast to be in the range of 0.53–0.76 m. This same range for σ_{hyd} , 0.53–0.76 m (mean of 0.645 m), was adopted in the present study.

Errors in Meteorological Modeling

The epsilon associated with errors in meteorological modeling, σ_{met} , is estimated from the variability in water levels when comparing levels simulated using best winds to those simulated with PBL winds. The wind and pressure fields derived from “best winds” employs techniques that combine inputs from a variety of meteorological sources. In Resio et al. (2007) and FEMA (2011) values of σ_{met} are not explicitly provided. However, it is stated that the range of $\sigma_{hyd+met}$ for the Louisiana-Mississippi coast is estimated to be 0.61–1.07 m. In FEMA (2008a), σ_{met}

for coastal Mississippi was estimated at 0.36 m. For the present study, values of 0.07 to 0.30 (mean of 0.185 m) were adopted, the same as values adopted in FEMA (2011).

In the Texas Risk MAP study (FEMA 2011), regional biases were evident in comparisons that were made between maximum water surface elevation results from historic storms run using handcrafted Oceanweather “best winds” and runs using a PBL-model representation of the same historic storms. The same bias correction adopted by FEMA (2011) for the region encompassing Galveston Bay was applied in the present study.

Variations in Holland B Parameter

Regarding the epsilon associated with random variations in the Holland B parameter, σ_B , the storm surge elevation has been found to vary almost linearly with changes in the Holland B parameter. The epsilon σ_B is typically assumed to be in the range of 10–20% of the storm surge (Resio et al. 2007). More recent studies have adopted $\sigma_B = 0.15 \times$ storm surge elevation FEMA (2008a, 2011). This same epsilon term was adopted in the present study, $\sigma_B = 0.15 \times$ storm surge elevation.

Storm Track Variations

The epsilon related to storm track variations not accounted for in the synthetic storm set, σ_{track} , was estimated to be 0.20% of the wave setup contribution to the storm surge elevation (Resio 2007; FEMA 2011). The wave setup is estimated to be roughly 15–30% of the storm surge (Resio 2007; FEMA 2011). Other FEMA (2008a) studies have not explicitly accounted for σ_{track} .

Errors due to track variation were excluded from the present study. The way it was computed in FEMA (2011) resulted in a fairly insignificant magnitude.

Random Astronomical Tide Phase

There are locations where the magnitude of the astronomical tide is small enough that it can be treated as an uncertainty associated with the total water level response. This has been the approach followed for the Gulf of Mexico (e.g., FEMA 2008a, FEMA 2011). In cases where the tide amplitude is relatively small compared to the storm surge, the purpose of

this uncertainty is to capture the aleatory variability arising from the fact that the arrival of a TC can occur at any tide phase. This uncertainty is sometimes computed as the standard deviation of the predicted tide at any given location. FEMA (2008a) estimated the uncertainty associated with the astronomical tide to be 0.20 m for coastal Mississippi. In FEMA (2014), the adopted approach differed and consisted of simulating each storm with a random tide phase.

In the present study, the maximum surge values for each of the 223 FEMA North Texas storms, which were each modeled on a mean sea level with wave effects but without astronomical tides, was linearly superimposed with 96 random tide values. The tide values were obtained from NOAA gage 8771450 (<http://tidesandcurrents.noaa.gov/stationhome.html?id=8771450>). The period of record considered for the tide was '1904 Jan 01' to '2013 Dec 31'. Only tide values corresponding to hurricane season months (June-November) were used. This approach followed that taken in the North Atlantic Coast Comprehensive Study, NACCS, (Nadal-Caraballo et al., 2015)

Summary of Estimated Errors

The values of the error terms used in the present study along with the previous JPM-OS studies for Mississippi (FEMA 2008a), Texas (FEMA 2011), New York/New Jersey (FEMA 2014) and the NACCS, (Nadal-Caraballo et al., 2015) are listed in Table 9-2.

Table 9-2. Comparison of uncertainty estimates in JPM studies.

Uncertainty	Present Study	FEMA 2008a (m)	FEMA 2011 (m)	FEMA 2014 (m)	NACCS (m)
Hydrodynamic modeling	0.53 to 0.76	0.23	0.53 to 0.76	0.39	0.48
Meteorological modeling	0.07 to 0.30	0.36	0.07 to 0.30	0.54	0.38
Storm track variation	n/a	n/a	0.20* x wave setup	n/a	0.25
Holland B	0.15* x surge elevation	0.15* x surge elevation	0.15* x surge elevation	n/a	0.15* x surge elevation
Astronomical tide	variable	0.20	0.20	n/a	variable

*Factor on storm surge elevation is dimensionless.

Summary of Differences in JPM-OS Studies for the Houston-Galveston Region

For the present study, the JPM of hurricane parameters was recomputed and the probabilities of each of the previously modeled storms were recomputed in order to take advantage of new, more rigorous methods recently developed by the ERDC. The joint probability of coastal storm hazards was performed following a methodology similar to that described in FEMA (2011), but using a revised probabilistic model based on Bayesian Quadrature techniques (FEMA 2012). A re-analysis of the joint probability statistics was done using the new probabilistic model, which also incorporates additional data from tropical cyclones that have affected the Gulf of Mexico coast since 2007, including Hurricane Isaac in 2012. As part of the present study, storm recurrence rates, storm parameter statistics, and the probabilities of extreme water levels were recomputed.

The main differences between the FEMA (2011) JPM effort and the present JPM study are the following:

- 1) Period of record – FEMA (2011) considered the period of record 1940-2007. The present study considered the period 1940-2013.
- 2) Storm population – FEMA (2011) only considered landfalling hurricanes. The present study accounted for bypassing tropical storms as well.
- 3) Storm Recurrence Rate (SRR) – FEMA (2011) used a hybrid approach consisting of land-crossing sampling of storms and GKF weights to compute the SRR. The present study used a standard GKF approach that accounted for all tropical cyclones in the NOAA-HURDAT historical record within a given range of intensity and a limited time period (e.g. 1940–2013).
- 4) Storm frequency – FEMA (2011) estimated frequency of landfalling hurricanes at 1-degree increments of longitude starting at latitude 29.5. For the present study, all statistics including SRR were individually computed at 200 locations along the Gulf of Mexico U.S. coastline, for increased spatial coherence and fidelity.
- 5) Discretization method for storm parameters– The discretization method employed in FEMA (2011) and the weights used for the discrete storm parameter values were based on expert judgment. In the present

study, the weights were assigned to the synthetic storm set which was developed as part of FEMA (2011) in an optimal manner based on the Bayesian Quadrature algorithm.

6) Optimal kernel size – FEMA (2011) settled on a kernel size of 333 km. The present study used a kernel size of 200 km.

7) Epsilon terms – The epsilons used in the present study, shown in Table 9-2, were based on the knowledge gathered from previous FEMA (2008a, 2011) studies and from the USACE NACCS study. Differences in epsilon values between the present study and FEMA (2011) are noted in the table.

Existing Condition Water Surface Elevation Statistics

Based on the JPA approach described above and the maximum water surface elevation fields computed for each of the 223 North Texas storms that were simulated by FEMA (2011), water surface elevation statistics (WSE) were computed for a series of 43 locations that are shown in Figure 9-9 and in Table 9-3. These statistics represent existing conditions. Estimates of WSE having average recurrence intervals of 10, 20, 50, 100, 200, 500 and 1,000 years are shown for the mean value (Table 9-4) and for the upper value associated with the following confidence limits (CL), 84%, 90%, 95% and 98%, which are shown in Tables 9-5, 9-6, 9-7 and 9-8, respectively. At a given location, compared to the mean values, WSE values for successively greater confidence intervals are increasingly higher.

As seen in Tables 9-4 through 9-8, some general spatial patterns are evident in the WSE associated with each ARI. Along the open Gulf coast, WSE for a particular ARI are similar in magnitude along both Galveston Island and Bolivar Peninsula, with values being slightly greater along Bolivar Peninsula compared to those along Galveston Island. WSE on the bay sides of both Galveston Island and Bolivar Peninsula are slightly less than WSE on the open Gulf sides of both barriers.

Along the western shoreline of Galveston Bay, WSE for a particular ARI generally increases from the City of Galveston northward toward the upper reaches of the Houston Ship Channel; and along most of the western Bay shoreline they are higher than WSE along the open Gulf coast. The highest WSE values occur in the upper reaches of the Ship Channel for any particular ARI. This overall trend for increasing WSE along the western Bay shoreline is due to the predominance of onshore-directed core winds

associated with those hurricanes that tend to produce the greatest storm surges in the Houston-Galveston region. Strong winds having an onshore component within the shallow Bay tend to set up the water surface from south to north, or southeast to northwest, which act to increase water surface elevations in the northern and northwestern parts of the bay.

Within the interior tidal channels and creeks of the Clear Lake and Dickinson Bay areas, WSE are generally slightly higher than WSE at the entrances to these same areas. This pattern generally arises due to the prevalence of winds that have an east-to-west component, which are associated with the counterclockwise rotating wind circulation about the eye of those approaching hurricanes that cause the highest surges in the Bay. Winds blowing from the east tend to produce higher surge on the west side of the Bay compared to the east side, establishing a water surface gradient. This gradient also is forced within the creeks and tidal channels, which serve as conduits through which the storm surge can propagate into the more interior parts of the system. This gives rise to slightly higher WSE in the western interior parts of the Clear Lake and Dickinson Bay areas, compared to the WSE at the entrances to these areas.

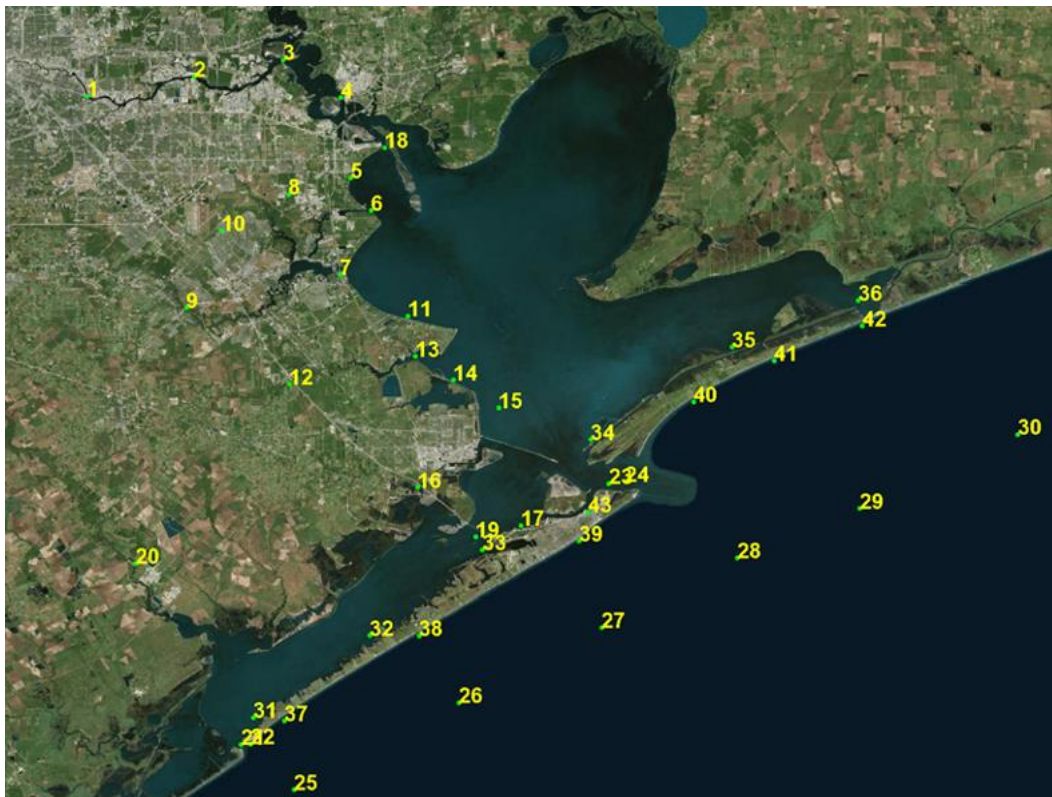


Figure 9-9. Map showing locations where water surface elevation statistics were computed for the present study. Station numbers correspond to the locations listed in Table 9-3.

Table 9-3. Locations where water surface elevation statistics were computed

No.	Location	Latitude (°N)	Longitude(°W)	Bottom Elevation (m, NAVD88)
1	Houston Ship Channel (upper)	29.7275	95.275	-13.3
2	Houston Ship Channel (mid)	29.7469	95.1688	-13.3
3	Houston Ship Channel (lower)	29.7635	95.0801	-15.8
4	Alexander Island	29.7261	95.0228	-15.8
5	LaPorte	29.6461	95.0127	-1.5
6	Bayport	29.6137	94.9925	-13.3
7	Clear Lake (east)	29.5494	95.0233	-6.5
8	Clear Lake (north)	29.6296	95.0743	-1
9	Clear Lake (west)	29.5177	95.1788	-2.7
10	Clear Lake (northwest)	29.5936	95.1414	-0.1
11	San Leon	29.5091	94.9584	-0.6
12	Dickinson	29.4416	95.0763	-0.5
13	Dickinson Bav entrance	29.4692	94.951	-3.5
14	Texas City (north)	29.4456	94.9131	-0.5
15	Texas City (east)	29.4178	94.8679	-2.1
16	Texas City (south)	29.3386	94.9486	-0.4
17	Galveston (bay)	29.3004	94.8458	-1
18	Morgan's Point	29.67603	94.97897	-15.8
19	West Bay (east)	29.2894	94.8908	-4.3
20	West Bay (north)	29.2628	95.2295	-0.6
21	San Luis Pass (throat-bay)	29.08236	95.12465	-4.6
22	San Luis Pass (throat-ocean)	29.08284	95.11508	-4.6
23	Bolivar Roads (throat-bay)	29.34213	94.75846	-15.4
24	Bolivar Roads (throat-ocean)	29.34424	94.74177	-14.6
25	San Luis Pass (offshore)	29.0376	95.0716	-14
26	Galveston Is (offshore mid west)	29.124	94.9075	-14
27	Galveston Is (offshore mid east)	29.1989	94.7654	-14
28	Bolivar Roads (offshore)	29.2684	94.6304	-14
29	Bolivar Pen (offshore mid)	29.3177	94.5085	-14
30	Bolivar Pen (offshore east)	29.3912	94.3511	-14
31	Galveston Is (bay west)	29.1092	95.1121	-0.7
32	Galveston Is (bay mid)	29.1911	94.9963	-0.4
33	Galveston Is (bay east)	29.2763	94.8843	-0.7
34	Bolivar Pen (bay west)	29.3863	94.7761	-0.5
35	Bolivar Pen (bay mid)	29.4785	94.6355	-0.5
36	Bolivar Pen (bay east)	29.5246	94.51	-0.5
37	Galveston Is (nearshore west)	29.106	95.0814	-2.6
38	Galveston Is (nearshore mid)	29.1906	94.947	-2.6
39	Galveston (Pleasure Pier)	29.2853	94.7878	-2.6
40	Bolivar Pen (nearshore west)	29.4236	94.6737	-2.6
41	Bolivar Pen (nearshore mid)	29.4646	94.5936	-2.6
42	Bolivar Pen (nearshore east)	29.4994	94.506	-2.6
43	Univ Texas Medical Branch	29.313816	94.778801	-8

Table 9-4. Average Recurrence Interval WSEs, Mean.

Location		Average Recurrence Interval in years (mean WSE in ft, NAVD88)						
		10	20	50	100	200	500	1,000
1	Houston Ship Channel (upper)	7.0	9.5	12.8	15.2	17.4	19.8	21.3
2	Houston Ship Channel (mid)	6.6	9.0	12.2	14.5	16.5	18.6	20.1
3	Houston Ship Channel (lower)	6.3	8.6	11.7	13.9	15.8	17.9	19.3
4	Alexander Island	6.0	8.2	11.0	13.1	14.8	16.8	18.2
5	LaPorte	6.0	8.1	10.6	12.6	14.3	16.2	17.4
6	Bayport	5.8	7.8	10.1	12.0	13.7	15.6	16.8
7	Clear Lake (east)	5.9	7.9	10.1	11.9	13.6	15.7	16.9
8	Clear Lake (north)	6.4	8.6	11.3	13.3	15.1	16.8	17.9
9	Clear Lake (west)	6.6	8.8	11.3	13.4	15.4	17.6	18.9
10	Clear Lake (northwest)	6.6	8.8	11.5	13.6	15.6	17.7	18.9
11	San Leon	5.4	7.2	9.2	10.8	12.4	14.3	15.5
12	Dickinson	6.9	9.2	11.6	13.3	14.9	16.6	17.6
13	Dickinson Bay entrance	5.8	7.7	10.0	11.7	13.4	15.3	16.5
14	Texas City (north)	5.3	7.1	9.1	10.8	12.4	14.2	15.3
15	Texas City (east)	4.9	6.7	8.8	10.5	12.0	13.8	14.9
16	Texas City (south)	4.4	6.3	8.8	10.9	12.8	15.2	16.8
17	Galveston (bay)	4.8	6.6	8.7	10.5	12.1	14.0	15.1
18	Morgan's Point	5.7	7.8	10.3	12.3	14.0	15.8	17.1
19	West Bay (east)	4.4	6.1	8.1	9.8	11.4	13.2	14.3
20	West Bay (north)	5.3	7.8	10.3	12.5	14.8	17.2	18.7
21	San Luis Pass (throat-bay)	4.3	5.9	8.2	10.0	11.5	13.2	14.6
22	San Luis Pass (throat-ocean)	4.3	6.0	8.4	10.2	11.7	13.4	14.9
23	Bolivar Roads (throat-bay)	4.6	6.5	9.2	10.9	12.4	14.2	15.6
24	Bolivar Roads (throat-ocean)	4.6	6.5	9.3	11.0	12.5	14.4	15.8
25	San Luis Pass (offshore)	4.0	5.6	8.0	9.6	11.0	12.7	14.1
26	Galveston Is (offshore mid west)	4.0	5.8	8.3	9.8	11.2	13.0	14.5
27	Galveston Is (offshore mid east)	3.8	5.4	7.9	9.4	10.7	12.6	14.2
28	Bolivar Roads (offshore)	3.9	5.7	8.4	9.9	11.2	13.0	14.6
29	Bolivar Pen (offshore mid)	3.8	5.6	8.2	9.7	11.1	12.8	14.3
30	Bolivar Pen (offshore east)	3.6	5.3	8.0	9.5	10.9	12.9	14.3
31	Galveston Is (bay west)	3.9	5.1	7.0	8.8	10.4	12.1	13.4
32	Galveston Is (bay mid)	3.8	5.0	7.0	8.8	10.5	12.2	13.3
33	Galveston Is (bay east)	4.2	5.8	7.7	9.5	11.1	12.9	14.0
34	Bolivar Pen (bay west)	4.3	6.0	8.3	9.9	11.3	13.1	14.2
35	Bolivar Pen (bay mid)	2.8	4.2	6.0	7.6	9.0	10.6	11.7
36	Bolivar Pen (bay east)	2.5	4.0	6.2	8.0	9.5	11.4	12.8
37	Galveston Is (nearshore west)	4.4	6.2	8.8	10.6	12.1	14.0	15.4
38	Galveston Is (nearshore mid)	4.4	6.4	9.2	10.9	12.4	14.4	15.9
39	Galveston (Pleasure Pier)	4.4	6.2	8.9	10.6	12.1	14.1	15.9
40	Bolivar Pen (nearshore west)	4.9	7.1	10.2	12.2	13.8	15.7	17.4
41	Bolivar Pen (nearshore mid)	4.6	6.8	9.9	11.7	13.3	15.3	16.9
42	Bolivar Pen (nearshore east)	4.5	6.6	9.7	11.6	13.1	15.1	16.7
43	Univ Texas Medical Branch	4.6	6.5	9.0	10.7	12.3	14.0	15.2

Table 9-5. Average Recurrence Interval WSEs, 84% Confidence Limit.

Location		Average Recurrence Interval in years (84% CL WSE in ft, NAVD88)						
		10	20	50	100	200	500	1,000
1	Houston Ship Channel (upper)	9.2	11.7	15.0	17.4	19.6	22.0	23.5
2	Houston Ship Channel (mid)	8.8	11.2	14.4	16.7	18.7	20.8	22.3
3	Houston Ship Channel (lower)	8.5	10.8	13.9	16.1	18.0	20.1	21.5
4	Alexander Island	8.2	10.4	13.2	15.3	17.0	19.0	20.4
5	LaPorte	8.2	10.2	12.8	14.8	16.5	18.4	19.6
6	Bayport	8.0	10.0	12.3	14.2	15.9	17.8	19.0
7	Clear Lake (east)	8.1	10.1	12.3	14.1	15.8	17.9	19.1
8	Clear Lake (north)	8.5	10.8	13.4	15.5	17.3	19.0	20.1
9	Clear Lake (west)	8.8	11.0	13.5	15.6	17.6	19.8	21.1
10	Clear Lake (northwest)	8.8	11.0	13.7	15.8	17.8	19.9	21.1
11	San Leon	7.6	9.4	11.4	13.0	14.6	16.5	17.7
12	Dickinson	9.1	11.4	13.8	15.5	17.1	18.8	19.8
13	Dickinson Bay entrance	8.0	9.9	12.2	13.9	15.6	17.5	18.7
14	Texas City (north)	7.5	9.2	11.3	13.0	14.6	16.4	17.5
15	Texas City (east)	7.1	8.9	11.0	12.7	14.2	16.0	17.1
16	Texas City (south)	6.6	8.5	11.0	13.1	15.0	17.4	19.0
17	Galveston (bay)	6.9	8.8	10.9	12.7	14.3	16.2	17.3
18	Morgan's Point	7.9	10.0	12.5	14.5	16.2	18.0	19.3
19	West Bay (east)	6.6	8.3	10.3	12.0	13.6	15.4	16.5
20	West Bay (north)	7.5	10.0	12.5	14.7	17.0	19.4	20.9
21	San Luis Pass (throat-bay)	6.5	8.1	10.4	12.2	13.7	15.4	16.8
22	San Luis Pass (throat-ocean)	6.5	8.2	10.6	12.4	13.9	15.6	17.1
23	Bolivar Roads (throat-bay)	6.8	8.7	11.4	13.1	14.6	16.4	17.8
24	Bolivar Roads (throat-ocean)	6.8	8.7	11.5	13.2	14.7	16.6	18.0
25	San Luis Pass (offshore)	6.2	7.8	10.2	11.8	13.2	14.9	16.3
26	Galveston Is (offshore mid west)	6.2	8.0	10.5	12.0	13.4	15.2	16.7
27	Galveston Is (offshore mid east)	6.0	7.6	10.1	11.6	12.9	14.8	16.4
28	Bolivar Roads (offshore)	6.1	7.9	10.6	12.1	13.4	15.2	16.8
29	Bolivar Pen (offshore mid)	6.0	7.8	10.4	11.9	13.3	15.0	16.5
30	Bolivar Pen (offshore east)	5.8	7.5	10.2	11.7	13.1	15.1	16.5
31	Galveston Is (bay west)	6.1	7.3	9.2	11.0	12.6	14.3	15.6
32	Galveston Is (bay mid)	6.0	7.2	9.2	11.0	12.7	14.4	15.5
33	Galveston Is (bay east)	6.4	8.0	9.9	11.7	13.3	15.1	16.2
34	Bolivar Pen (bay west)	6.5	8.2	10.5	12.1	13.5	15.3	16.4
35	Bolivar Pen (bay mid)	5.0	6.4	8.2	9.8	11.2	12.8	13.9
36	Bolivar Pen (bay east)	4.7	6.2	8.4	10.2	11.7	13.6	15.0
37	Galveston Is (nearshore west)	6.6	8.4	11.0	12.8	14.3	16.2	17.6
38	Galveston Is (nearshore mid)	6.6	8.6	11.4	13.1	14.6	16.6	18.1
39	Galveston (Pleasure Pier)	6.6	8.4	11.1	12.8	14.3	16.3	18.1
40	Bolivar Pen (nearshore west)	7.1	9.3	12.4	14.4	16.0	17.9	19.6
41	Bolivar Pen (nearshore mid)	6.8	9.0	12.1	13.9	15.5	17.5	19.1
42	Bolivar Pen (nearshore east)	6.7	8.7	11.9	13.8	15.3	17.3	18.9
43	Univ Texas Medical Branch	6.8	8.7	11.2	12.9	14.5	16.2	17.4

Table 9-6. Average Recurrence Interval WSEs, 90% Confidence Limit.

Location		Average Recurrence Interval in years (90% CL WSE in ft, NAVD88)						
		10	20	50	100	200	500	1,000
1	Houston Ship Channel (upper)	9.8	12.3	15.6	18.0	20.3	22.6	24.2
2	Houston Ship Channel (mid)	9.4	11.9	15.1	17.3	19.3	21.5	22.9
3	Houston Ship Channel (lower)	9.1	11.5	14.5	16.7	18.6	20.7	22.2
4	Alexander Island	8.8	11.0	13.9	15.9	17.7	19.6	21.0
5	LaPorte	8.8	10.9	13.4	15.4	17.2	19.1	20.2
6	Bayport	8.6	10.6	12.9	14.8	16.6	18.4	19.6
7	Clear Lake (east)	8.7	10.7	12.9	14.7	16.5	18.5	19.7
8	Clear Lake (north)	9.2	11.4	14.1	16.1	17.9	19.6	20.7
9	Clear Lake (west)	9.4	11.6	14.1	16.2	18.2	20.4	21.7
10	Clear Lake (northwest)	9.4	11.7	14.3	16.5	18.5	20.5	21.7
11	San Leon	8.3	10.0	12.0	13.6	15.3	17.1	18.3
12	Dickinson	9.7	12.0	14.4	16.1	17.7	19.4	20.5
13	Dickinson Bay entrance	8.6	10.5	12.8	14.5	16.2	18.1	19.3
14	Texas City (north)	8.1	9.9	11.9	13.6	15.2	17.0	18.1
15	Texas City (east)	7.7	9.5	11.6	13.3	14.8	16.6	17.8
16	Texas City (south)	7.2	9.2	11.6	13.7	15.6	18.0	19.6
17	Galveston (bay)	7.6	9.4	11.5	13.3	15.0	16.8	17.9
18	Morgan's Point	8.6	10.6	13.2	15.1	16.8	18.7	19.9
19	West Bay (east)	7.3	8.9	10.9	12.6	14.3	16.0	17.1
20	West Bay (north)	8.1	10.6	13.1	15.3	17.6	20.0	21.5
21	San Luis Pass (throat-bay)	7.1	8.7	11.1	12.8	14.3	16.0	17.4
22	San Luis Pass (throat-ocean)	7.1	8.8	11.3	13.0	14.5	16.3	17.7
23	Bolivar Roads (throat-bay)	7.4	9.3	12.0	13.7	15.2	17.1	18.4
24	Bolivar Roads (throat-ocean)	7.4	9.3	12.1	13.8	15.3	17.2	18.6
25	San Luis Pass (offshore)	6.8	8.4	10.8	12.4	13.8	15.5	16.9
26	Galveston Is (offshore mid west)	6.8	8.6	11.1	12.6	14.0	15.9	17.3
27	Galveston Is (offshore mid east)	6.6	8.2	10.7	12.2	13.6	15.4	17.0
28	Bolivar Roads (offshore)	6.7	8.5	11.2	12.7	14.0	15.8	17.4
29	Bolivar Pen (offshore mid)	6.6	8.4	11.0	12.6	13.9	15.7	17.1
30	Bolivar Pen (offshore east)	6.4	8.1	10.8	12.4	13.8	15.7	17.2
31	Galveston Is (bay west)	6.8	8.0	9.8	11.6	13.2	14.9	16.2
32	Galveston Is (bay mid)	6.6	7.8	9.8	11.7	13.3	15.0	16.1
33	Galveston Is (bay east)	7.0	8.6	10.6	12.3	13.9	15.7	16.8
34	Bolivar Pen (bay west)	7.1	8.9	11.2	12.7	14.2	15.9	17.0
35	Bolivar Pen (bay mid)	5.6	7.0	8.8	10.4	11.9	13.4	14.5
36	Bolivar Pen (bay east)	5.3	6.8	9.0	10.8	12.3	14.2	15.6
37	Galveston Is (nearshore west)	7.2	9.0	11.6	13.4	14.9	16.8	18.2
38	Galveston Is (nearshore mid)	7.2	9.2	12.0	13.7	15.2	17.2	18.8
39	Galveston (Pleasure Pier)	7.2	9.0	11.7	13.5	14.9	17.0	18.7
40	Bolivar Pen (nearshore west)	7.7	9.9	13.1	15.0	16.6	18.6	20.3
41	Bolivar Pen (nearshore mid)	7.4	9.6	12.7	14.5	16.1	18.1	19.7
42	Bolivar Pen (nearshore east)	7.3	9.4	12.5	14.4	15.9	17.9	19.5
43	Univ Texas Medical Branch	7.4	9.3	11.8	13.5	15.1	16.9	18.0

Table 9-7. Average Recurrence Interval WSEs, 95% Confidence Limit.

Location		Average Recurrence Interval in years (95% CL WSE in ft, NAVD88)						
		10	20	50	100	200	500	1,000
1	Houston Ship Channel (upper)	10.6	13.1	16.4	18.8	21.0	23.4	25.0
2	Houston Ship Channel (mid)	10.2	12.7	15.9	18.1	20.1	22.3	23.7
3	Houston Ship Channel (lower)	9.9	12.3	15.3	17.5	19.4	21.5	23.0
4	Alexander Island	9.6	11.8	14.6	16.7	18.5	20.4	21.8
5	LaPorte	9.6	11.7	14.2	16.2	18.0	19.8	21.0
6	Bayport	9.4	11.4	13.7	15.6	17.4	19.2	20.4
7	Clear Lake (east)	9.5	11.5	13.7	15.5	17.3	19.3	20.5
8	Clear Lake (north)	10.0	12.2	14.9	16.9	18.7	20.4	21.5
9	Clear Lake (west)	10.2	12.4	14.9	17.0	19.0	21.2	22.5
10	Clear Lake (northwest)	10.2	12.5	15.1	17.3	19.3	21.3	22.5
11	San Leon	9.1	10.8	12.8	14.4	16.0	17.9	19.1
12	Dickinson	10.5	12.8	15.2	16.9	18.5	20.2	21.3
13	Dickinson Bay entrance	9.4	11.3	13.6	15.3	17.0	18.9	20.1
14	Texas City (north)	8.9	10.7	12.7	14.4	16.0	17.8	18.9
15	Texas City (east)	8.5	10.3	12.4	14.1	15.6	17.4	18.6
16	Texas City (south)	8.0	10.0	12.4	14.5	16.4	18.8	20.4
17	Galveston (bay)	8.4	10.2	12.3	14.1	15.8	17.6	18.7
18	Morgan's Point	9.4	11.4	14.0	15.9	17.6	19.5	20.7
19	West Bay (east)	8.1	9.7	11.7	13.4	15.1	16.8	17.9
20	West Bay (north)	8.9	11.4	13.9	16.1	18.4	20.8	22.3
21	San Luis Pass (throat-bay)	7.9	9.5	11.8	13.6	15.1	16.8	18.2
22	San Luis Pass (throat-ocean)	7.9	9.6	12.1	13.8	15.3	17.1	18.5
23	Bolivar Roads (throat-bay)	8.2	10.1	12.8	14.5	16.0	17.9	19.2
24	Bolivar Roads (throat-ocean)	8.2	10.1	12.9	14.6	16.1	18.0	19.4
25	San Luis Pass (offshore)	7.6	9.2	11.6	13.2	14.6	16.3	17.7
26	Galveston Is (offshore mid west)	7.6	9.4	11.9	13.4	14.8	16.6	18.1
27	Galveston Is (offshore mid east)	7.4	9.0	11.5	13.0	14.4	16.2	17.8
28	Bolivar Roads (offshore)	7.5	9.3	12.0	13.5	14.8	16.6	18.2
29	Bolivar Pen (offshore mid)	7.4	9.2	11.8	13.4	14.7	16.5	17.9
30	Bolivar Pen (offshore east)	7.2	8.9	11.6	13.1	14.6	16.5	18.0
31	Galveston Is (bay west)	7.6	8.8	10.6	12.4	14.0	15.7	17.0
32	Galveston Is (bay mid)	7.4	8.6	10.6	12.5	14.1	15.8	16.9
33	Galveston Is (bay east)	7.8	9.4	11.4	13.1	14.7	16.5	17.6
34	Bolivar Pen (bay west)	7.9	9.6	11.9	13.5	14.9	16.7	17.8
35	Bolivar Pen (bay mid)	6.4	7.8	9.6	11.2	12.7	14.2	15.3
36	Bolivar Pen (bay east)	6.1	7.6	9.8	11.6	13.1	15.0	16.4
37	Galveston Is (nearshore west)	8.0	9.8	12.4	14.2	15.7	17.6	19.0
38	Galveston Is (nearshore mid)	8.0	10.0	12.8	14.5	16.0	18.0	19.5
39	Galveston (Pleasure Pier)	8.0	9.8	12.5	14.3	15.7	17.8	19.5
40	Bolivar Pen (nearshore west)	8.5	10.7	13.9	15.8	17.4	19.4	21.1
41	Bolivar Pen (nearshore mid)	8.2	10.4	13.5	15.3	16.9	18.9	20.5
42	Bolivar Pen (nearshore east)	8.1	10.2	13.3	15.2	16.7	18.7	20.3
43	Univ Texas Medical Branch	8.2	10.1	12.6	14.3	15.9	17.7	18.8

Table 9-8. Average Recurrence Interval WSEs, 98% Confidence Limit.

Location		Average Recurrence Interval in years (98% CL WSE in ft, NAVD88)						
		10	20	50	100	200	500	1,000
1	Houston Ship Channel (upper)	11.4	13.9	17.2	19.6	21.8	24.2	25.7
2	Houston Ship Channel (mid)	11.0	13.4	16.6	18.9	20.9	23.0	24.5
3	Houston Ship Channel (lower)	10.7	13.0	16.1	18.3	20.2	22.3	23.7
4	Alexander Island	10.4	12.6	15.4	17.5	19.2	21.2	22.6
5	LaPorte	10.4	12.4	15.0	17.0	18.7	20.6	21.8
6	Bayport	10.2	12.2	14.5	16.4	18.1	20.0	21.2
7	Clear Lake (east)	10.3	12.3	14.5	16.3	18.0	20.1	21.3
8	Clear Lake (north)	10.7	13.0	15.6	17.7	19.4	21.2	22.3
9	Clear Lake (west)	11.0	13.2	15.7	17.8	19.8	22.0	23.3
10	Clear Lake (northwest)	11.0	13.2	15.9	18.0	20.0	22.1	23.3
11	San Leon	9.8	11.6	13.6	15.2	16.8	18.7	19.9
12	Dickinson	11.3	13.6	16.0	17.7	19.3	21.0	22.0
13	Dickinson Bay entrance	10.2	12.1	14.4	16.1	17.8	19.7	20.9
14	Texas City (north)	9.7	11.4	13.5	15.2	16.8	18.6	19.7
15	Texas City (east)	9.3	11.1	13.2	14.9	16.4	18.2	19.3
16	Texas City (south)	8.8	10.7	13.2	15.3	17.2	19.6	21.2
17	Galveston (bay)	9.1	11.0	13.1	14.9	16.5	18.4	19.5
18	Morgan's Point	10.1	12.1	14.7	16.7	18.4	20.2	21.5
19	West Bay (east)	8.8	10.5	12.5	14.2	15.8	17.6	18.7
20	West Bay (north)	9.7	12.2	14.7	16.9	19.2	21.6	23.1
21	San Luis Pass (throat-bay)	8.7	10.3	12.6	14.4	15.9	17.6	19.0
22	San Luis Pass (throat-ocean)	8.7	10.4	12.8	14.6	16.1	17.8	19.3
23	Bolivar Roads (throat-bay)	9.0	10.9	13.6	15.3	16.8	18.6	20.0
24	Bolivar Roads (throat-ocean)	9.0	10.9	13.6	15.4	16.9	18.8	20.2
25	San Luis Pass (offshore)	8.4	10.0	12.4	14.0	15.4	17.1	18.5
26	Galveston Is (offshore mid west)	8.4	10.2	12.7	14.2	15.6	17.4	18.9
27	Galveston Is (offshore mid east)	8.2	9.8	12.3	13.8	15.1	17.0	18.6
28	Bolivar Roads (offshore)	8.3	10.1	12.8	14.3	15.6	17.4	19.0
29	Bolivar Pen (offshore mid)	8.2	10.0	12.6	14.1	15.5	17.2	18.7
30	Bolivar Pen (offshore east)	8.0	9.7	12.4	13.9	15.3	17.3	18.7
31	Galveston Is (bay west)	8.3	9.5	11.4	13.2	14.8	16.5	17.8
32	Galveston Is (bay mid)	8.2	9.4	11.4	13.2	14.9	16.5	17.7
33	Galveston Is (bay east)	8.6	10.2	12.1	13.9	15.5	17.3	18.4
34	Bolivar Pen (bay west)	8.7	10.4	12.7	14.3	15.7	17.5	18.6
35	Bolivar Pen (bay mid)	7.2	8.6	10.4	12.0	13.4	15.0	16.1
36	Bolivar Pen (bay east)	6.9	8.4	10.6	12.4	13.9	15.8	17.2
37	Galveston Is (nearshore west)	8.8	10.6	13.2	15.0	16.5	18.4	19.8
38	Galveston Is (nearshore mid)	8.8	10.8	13.6	15.3	16.8	18.8	20.3
39	Galveston (Pleasure Pier)	8.8	10.6	13.3	15.0	16.5	18.5	20.3
40	Bolivar Pen (nearshore west)	9.3	11.5	14.6	16.6	18.1	20.1	21.8
41	Bolivar Pen (nearshore mid)	9.0	11.2	14.3	16.1	17.7	19.7	21.3
42	Bolivar Pen (nearshore east)	8.9	10.9	14.1	16.0	17.5	19.5	21.1
43	Univ Texas Medical Branch	9.0	10.9	13.4	15.1	16.6	18.4	19.6

Probabilistic Context for Hurricane Ike's Maximum Water Surface Elevations

Within the Houston-Galveston region, the geographic corridor having the greatest potential for substantial flood-induced economic damages/losses runs from the City of Galveston, northward along the western shoreline of Galveston Bay, and into the upper reaches of the Houston Ship Channel.

Table 9-4 showed expected values for the various ARI water surface elevations. Using these values, the maximum water surface elevations observed during Hurricane Ike can be placed in a probabilistic context, within this corridor having the greatest potential for economic losses that runs along the western shoreline of Galveston Bay and into the upper reaches of the Houston Ship Channel.

At Galveston Pleasure Pier, on the Gulf side, the maximum water surface elevation observed during Ike was 10.6 ft NAVD88. This value is equal to the 100-yr ARI value at this location (10.6 ft) from Table 9-4, i.e., this value has a 1% chance of occurring each and every year. On the bay side of Galveston, the observed maximum water surface elevation reached 10.7 ft, which is also approximately equal to the 100-yr ARI value at this location (10.5 ft).

In the vicinity north of Texas City, near the entrance to Dickinson Bay, and at San Leon, the maximum water surface elevation was slightly higher, approximately 11 ft (11.3 ft was recorded at the Eagle Point gage, and 10.8 ft near San Leon). These values are also approximately equal to the 100-yr ARI values in this vicinity (10.8 ft north of Texas City and at San Leon, and 11.7 ft at the entrance to Dickinson Bay).

At the entrance to Clear Lake and in the vicinity of Morgan's Point, maximum water surface elevations during Ike were slightly higher, 12 to 12.5 ft, NAVD88. These are roughly equal to the expected 100-yr ARI values at the entrance to Clear Lake (11.9 ft) and Morgan's Point (12.3 ft).

In the upper reaches of the Houston Ship Channel, maximum water surface elevations during Ike were higher, approximately 13 to nearly 15 ft, increasing slightly from east to west along the channel. Within the economic corridor, the water surface elevations reached their highest values along this section of the Ship Channel during Ike. The 100-yr ARI values also increase in this section of the channel, from east to west,

ranging from 13.9 ft in the east to 15.2 ft in the west. Conditions during Ike were similar to the expected 100-yr ARI values in the upper reaches of the ship channel.

Throughout this economic corridor, the maximum water surface elevations experienced during Ike were approximately equal to the expected 100-yr ARI values. These conditions have a 1% chance of occurring each and every year.

The Proxy Storm Concept

This economic corridor is generally oriented in a shore-perpendicular direction relative to the open Gulf shorelines of Galveston Island and Bolivar Peninsula. The corridor is relatively narrow in alongshore extent compared to the entire Galveston Bay region.

Because of the corridor's location and orientation, extreme WSEs that can severely impact this area, such as those associated with the 100-yr and 500-yr ARIs, are expected to be principally dictated by the most severe hurricanes which make landfall within a particular stretch of coast. That coastal landfall zone extends from near Bolivar Roads pass (like the "direct-hit" track for some of the bracketing set storms) to a point that is 20 to 30 nm southwest of the pass (like storms 128 and 036 from the bracketing set). The extreme water surface elevation fields associated with the 100-yr and 500-yr ARIs are expected to have a general pattern of variability that is dictated in large part by the extreme bracketing set storms that approach from the south-southeast or southeast directions and make landfall in this critical zone. Tracks from the south-southeast and southeast also are the most common tracks for severe storms that have impacted the Texas coast, historically.

A field of 100-yr WSE (in feet) is shown in Figure 9-10. The figure is based upon the FEMA (2011) JPA approach. To generate this figure, 100-yr ARI WSEs were computed at each node of the storm surge model, color-coded based upon magnitude, and plotted at each model grid node. Elevations shown in Figure 9-10 are draft results from the FEMA (2011) study; and they are considered to be draft results until finalized by FEMA. The "still" WSE in Figure 9-10 only reflect the contributions of storm surge, tide and other sources of uncertainty. It is important to note that these elevations are not FEMA Base Flood Elevations (BFEs); they do not include the

effects of wind wave crests on top of the “still” water surface. The different color contour bands reflect 1-ft changes in WSE.

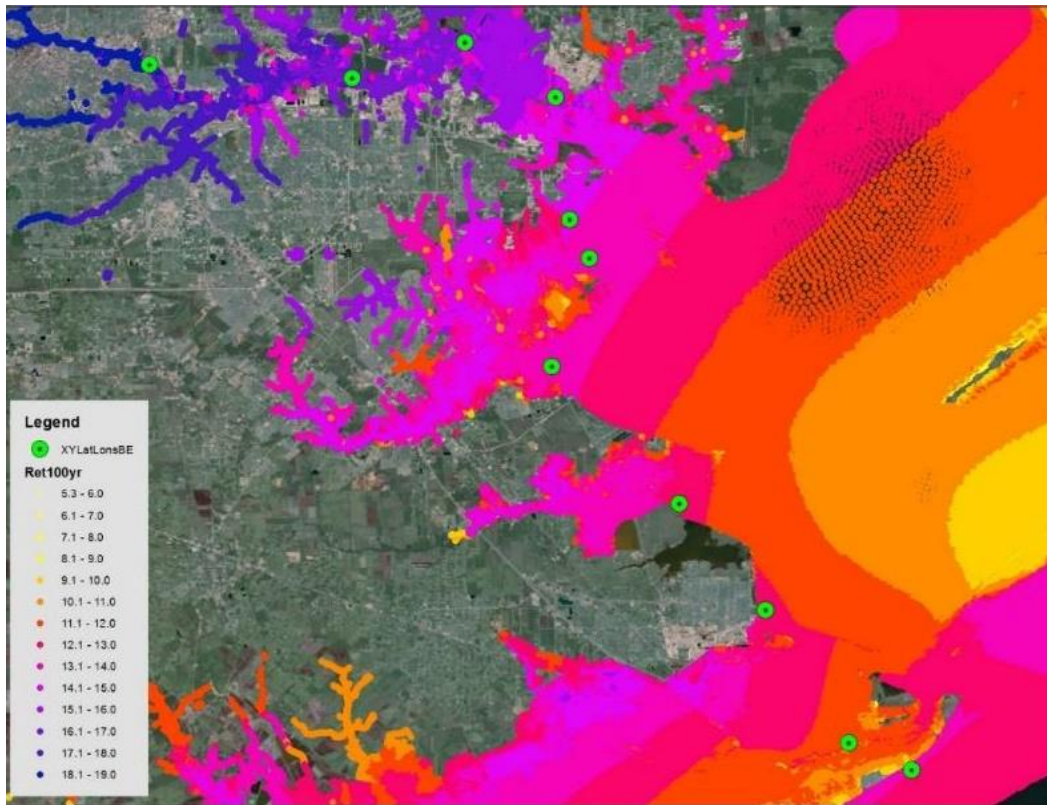


Figure 9-10. Field of water surface elevations (in feet) reflecting the 100-yr average recurrence interval, based on the draft FEMA (2011) results.

Table 9-9 shows the FEMA (2011) “still” WSEs at a few discrete locations within the key economic corridor for both the 100-yr and 500-yr ARIs. These locations are shown as green dots in Figure 9-10. The locations are listed in geographical order, starting with the upper reaches of the Houston Ship Channel, moving toward the south, and ending at the open Gulf coast at Galveston Pleasure Pier.

A sloping water elevation surface, with values increasing from southeast to northwest, is evident in the tabular results for both the 100-yr and 500-yr ARIs. The same pattern also is clearly evident in the graphical results for the 100-yr ARI shown in Figure 9-10; as reflected by the WSE color contours in the Bay which are roughly parallel to the open Gulf shoreline. The sloping surface is evident in the Bay proper, the upper reaches of the Houston Ship Channel, and along the western shoreline of the Bay. This WSE pattern is quite similar to that seen for some of the bracketing set

Table 9-9. 100-yr and 500-yr average recurrence interval “still” water surface elevations at selected locations based upon the JPA approach and North Texas storm simulations from FEMA (2011).

Location	Latitude (N)	Longitude (W)	100-yr ARI WSE (ft)	500-yr ARI WSE (ft)
Houston Ship Channel	29° 44' 52"	95° 17' 12"	18.1	22.7
Houston Ship Channel	29° 44' 20"	95° 09' 14"	16.7	21.2
Houston Ship Channel	29° 45' 44"	95° 04' 48"	15.9	20.5
Alexander Island	29° 43' 35"	95° 01' 15"	14.9	19.2
La Porte	29° 38' 46"	95° 00' 42"	14.1	18.1
Bayport	29° 37' 14"	94° 59' 55"	13.6	17.4
Clear Lake (Seabrook)	29° 32' 59"	95° 01' 24"	13.4	16.8
Texas City levee (north)	29° 27' 35"	94° 56' 24"	12.6	16.1
Texas City levee (east)	29° 23' 24"	94° 53' 00"	12.4	16.2
Galveston (bay side)	29° 18' 10"	94° 49' 44"	11.8	14.8
Galveston (ocean side)	29° 17' 07"	94° 47' 16"	13.1	17.7

storms that approach from the southeast and south-southeast directions and make landfall just to the southwest of the City of Galveston.

Because of the similarity between the ARI WSE pattern and the maximum WSE pattern for individual storms, it was anticipated that there might be a “proxy” storm from among the 223-storm FEMA set, one of the synthetic hypothetical hurricanes that were simulated, which produced a WSE field that was quite similar to the WSE field corresponding to a particular ARI WSE field throughout the key economic corridor. If so, then a with-dike storm simulation could be made for this same FEMA storm and then compared to the FEMA storm that was run for existing conditions as part of the FEMA (2011) study. In this way, without-dike and with-dike results could be compared to assess the effectiveness of the dike in reducing damages/losses for a storm that produces WSEs that have a particular ARI throughout the economic corridor. Based on this preliminary analysis using the FEMA (2011) results, the proxy storm concept seemed to have merit, as a first step to placing water surface elevations and economic damages/losses in a probabilistic context.

Identification and Selection of Proxy Storms

Using the existing condition water surface elevation statistics computed as part of the present study and presented earlier in this chapter, proxy

storms were defined for the 10-yr, 100-yr and 500-yr ARI WSE. With-dike simulations were made for each proxy storm, then the without-dike and with-dike maximum WSE fields were provided to the study economics team for analysis. The following approach, described for the 10-yr ARI proxy storm, was used to identify and select the three proxy storms.

First, based on the statistical analysis results shown in Table 9-8 for the 90% CL WSE values, the 10-yr ARI WSE was identified at each of the eighteen locations within the corridor of high economic value that are shown in Figure 9-11 and listed in Table 9-10. Second, individual storms from the 223-storm FEMA set were examined as potential proxies, based on their track and other hurricane parameters, and on their maximum WSE fields. Third, for each candidate proxy storm, the maximum WSE for that storm was extracted for each of the locations used to make the selection. Fourth, differences and absolute differences were computed between the ARI WSE and the storm-specific WSE at each of the eighteen locations, and average differences were computed for the entire set of locations. Fifth, the proxy storm was selected as the storm that minimized the average differences between it and the ARI WSE values, and minimized any bias.



Figure 9-11. Locations of water surface elevations used to identify and select proxy storms.

Table 9-10. Locations of water surface elevations used to identify and select proxy storms.

	Location	Latitude (°N)	Longitude (°W)
1	Houston Ship Channel (upper)	29.7275	95.275
2	Houston Ship Channel (mid)	29.7469	95.1688
3	Houston Ship Channel (lower)	29.7635	95.0801
4	Alexander Island	29.7261	95.0228
5	LaPorte	29.6461	95.0127
6	Bayport	29.6137	94.9925
7	Clear Lake (east)	29.5494	95.0233
8	Clear Lake (north)	29.6296	95.0743
9	Clear Lake (west)	29.5177	95.1788
10	Clear Lake (northwest)	29.5936	95.1414
11	San Leon	29.5091	94.9584
12	Dickinson	29.4416	95.0763
13	Dickinson Bay entrance	29.4692	94.951
14	Texas City (north)	29.4456	94.9131
15	Texas City (east)	29.4178	94.8679
16	Texas City (south)	29.3386	94.9486
17	Galveston (bay)	29.3004	94.8458
18	Galveston (Pleasure Pier)	29.2853	94.7878

10-yr Proxy Storm

Storm 535 from the original FEMA set was selected to be the 10-yr proxy storm. Storm 535 is a 975-mb storm that approaches from the southeast (TXN Fan set, Track 4, in FEMA storm set jargon) and makes landfall near San Luis Pass. It has the following characteristics:

Minimum central pressure - 975 mb

Central pressure at landfall - 987 mb

Maximum wind speed - 35 m/sec (68 kts)

Max wind speed at landfall - 26 m/sec (50 kts)

Radius to maximum winds - varies from 17.7 to 25.7 n mi

Variable Holland B parameter

Forward speed of 6 kts

The maximum wind speed and wind speed at landfall cited for each of the three proxy storms reflect 30-min average winds at a 10-m elevation.

Results for the 10-yr proxy storm are shown in Table 9-11. Some added precision was retained in the analyses done to identify and select proxy storms, and it is reflected in Table 9-11 and in subsequent tables in this section. However, the added precision is not indicative of overall accuracy of the computed WSEs; the computed WSE are no more accurate than tenths of a foot, at best. In the “Difference” column, green numbers indicate locations where the actual storm maximum WSE exceeded the ARI WSE value; red numbers indicate where the actual storm WSE was less than the ARI WSE value.

In Table 9-11, WSE differences for Storm 535 show a very small negative bias of approximately 0.1 ft; the average absolute difference is about 0.4 ft. The average absolute difference reflects an “error” of about 4% to 6%, in light of the 10-yr ARI WSE range of 7.2 to 9.8 ft.

Table 9-11. Water surface elevations for the 10-yr proxy storm, Storm 535.

	10-yr Proxy Storm Water Surface Elevations	10-yr WSE 90% CL (ft)	Storm 535 WSE (ft)	Difference (ft)	Absolute Difference (ft)
1	Houston Ship Channel (upper)	9.78	10.53	0.75	0.75
2	Houston Ship Channel (mid)	9.42	10.04	0.62	0.62
3	Houston Ship Channel (lower)	9.12	9.61	0.49	0.49
4	Alexander Island	8.86	9.06	0.20	0.20
5	LaPorte	8.83	8.79	-0.03	0.03
6	Bayport	8.63	8.37	-0.26	0.26
7	Clear Lake (east)	8.73	8.50	-0.23	0.23
8	Clear Lake (north)	9.15	9.38	0.23	0.23
9	Clear Lake (west)	9.42	9.48	0.07	0.07
10	Clear Lake (northwest)	9.38	9.65	0.26	0.26
11	San Leon	8.27	7.64	-0.62	0.62
12	Dickinson	9.68	9.55	-0.13	0.13
13	Dickinson Bay entrance	8.63	8.14	-0.49	0.49
14	Texas City (north)	8.10	7.38	-0.72	0.72
15	Texas City (east)	7.74	6.92	-0.82	0.82
16	Texas City (south)	7.19	7.45	0.26	0.26
17	Galveston (bay)	7.58	6.76	-0.82	0.82
18	Galveston (Pleasure Pier)	7.19	6.50	-0.69	0.69
	Average	8.65	8.54	-0.108	0.428

Figure 9-12 shows the maximum WSE field for Storm 525. The WSE pattern is very similar to the pattern shown in Figure 9-10, with highest surges in the northwest part of Galveston Bay and the upper reaches of the Houston Ship Channel.

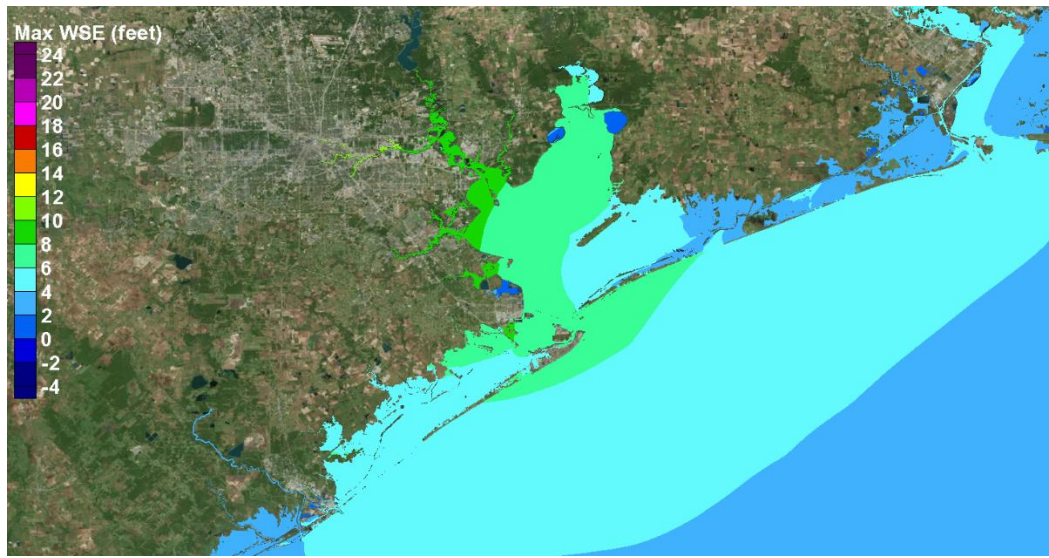


Figure 9-12. Maximum water surface elevation field for Storm 535, from FEMA (2011), the 10-yr proxy storm.

100-yr Proxy Storm

Storm 033 from the original FEMA set was selected to be the 100-yr proxy storm. Storm 033 is a 930-mb storm that approaches from the southeast (also has the TXN Fan set, Track 4) and makes landfall near San Luis Pass. It has the following characteristics:

- Minimum central pressure - 930 mb
- Central pressure at landfall - 948 mb
- Maximum wind speed - 51 m/sec (100 kts)
- Max wind speed at landfall - 40 m/sec (78 kts)
- Radius to maximum winds - varies from 25.8 to 37.4 n mi
- Variable Holland B parameter
- Forward speed of 11 kts

Results for the 100-yr proxy storm are shown in Table 9-12. WSE differences for Storm 033 show no significant bias, overall; however, there are small regional biases, with Storm 033 WSEs being higher than the 100-yr ARI values in the northern and southern portions of the corridor and Storm 033 WSEs being lower than the ARI WSEs in the central portion of the corridor in the Clear Lake and Dickinson Bay areas. The overall average absolute difference is about 0.9 ft. The average absolute difference reflects an “error” of about 5% to 7%, in light of the 100-yr ARI WSE range of 13.3 to 18.1 ft.

Figure 9-13 shows the maximum WSE field for Storm 033. The WSE pattern is very similar to the pattern shown for the 10-yr proxy storm and the 100-yr ARI WSE shown in Figure 9-10, with the highest surges in the northwest part of Galveston Bay and the upper reaches of the Houston Ship Channel. The similarity between the two proxy storms is strongly influenced by the identical track that they both have.

Table 9-12. Water surface elevations for the 100-yr proxy storm, Storm 033.

100-yr Proxy Storm Water Surface Elevations		100-yr WSE 90% CL (ft)	Storm 033 WSE (ft)	Difference (ft)	Absolute Difference (ft)
1	Houston Ship Channel (upper)	18.05	18.34	0.30	0.30
2	Houston Ship Channel (mid)	17.36	18.05	0.69	0.69
3	Houston Ship Channel (lower)	16.70	17.62	0.92	0.92
4	Alexander Island	15.88	16.73	0.85	0.85
5	LaPorte	15.39	15.49	0.10	0.10
6	Bayport	14.80	14.83	0.03	0.03
7	Clear Lake (east)	14.70	13.94	-0.75	0.75
8	Clear Lake (north)	16.14	14.83	-1.31	1.31
9	Clear Lake (west)	16.24	14.34	-1.90	1.90
10	Clear Lake (northwest)	16.47	15.13	-1.35	1.35
11	San Leon	13.65	13.12	-0.52	0.52
12	Dickinson	16.14	14.17	-1.97	1.97
13	Dickinson Bay entrance	14.53	14.44	-0.10	0.10
14	Texas City (north)	13.62	13.48	-0.13	0.13
15	Texas City (east)	13.26	13.88	0.62	0.62
16	Texas City (south)	13.68	15.68	2.00	2.00
17	Galveston (bay)	13.32	13.42	0.10	0.10
18	Galveston (Pleasure Pier)	13.48	15.68	2.20	2.20
Average		15.19	15.18	-0.013	0.880

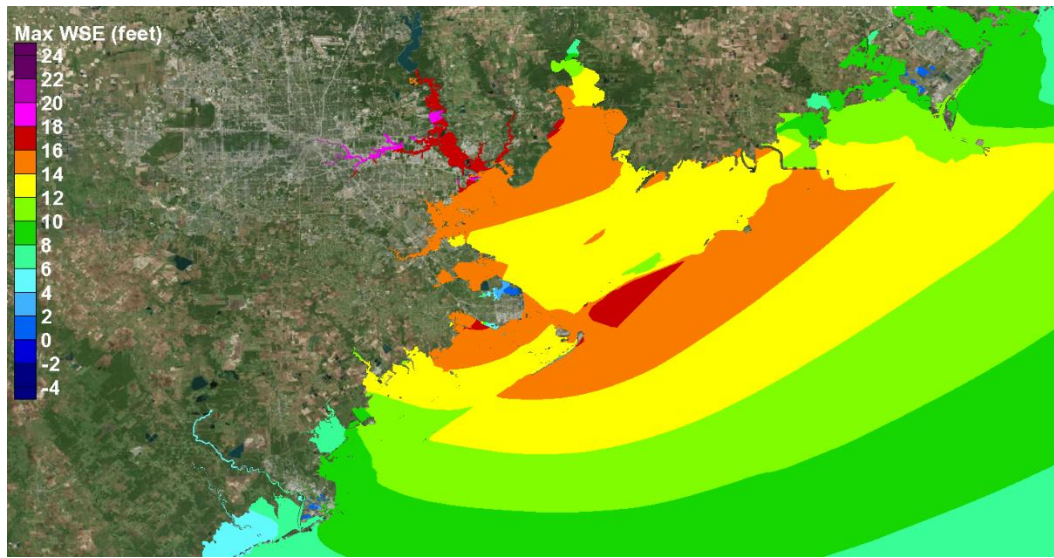


Figure 9-13. Maximum water surface elevation field for Storm 033, from FEMA (2011), the 100-yr proxy storm.

500-yr Proxy Storm

Storm 036 from the original FEMA set was selected to be the 500-yr proxy storm. Storm 036 is a 900-mb storm that approaches from the southeast (it also has the TXN Fan set, Track 4) and makes landfall near San Luis Pass. It has the following characteristics:

- Minimum central pressure - 900 mb
- Central pressure at landfall - 916 mb
- Maximum wind speed – 58 m/sec (112 kts)
- Max wind speed at landfall - 48 m/sec (93 kts)
- Radius to maximum winds - varies from 21.8 to 31.6 n mi
- Variable Holland B parameter
- Forward speed of 11 kts

Results for the 500-yr proxy storm are shown in Table 9-13. WSE differences for Storm 036 show a negative bias of approximately 1 ft, overall, with Storm 036 WSEs being lower than the 500-yr ARI values at most locations. In the Clear Lake and Dickson Bay areas, Storm 036 maximum WSEs are 1 to 4 ft lower than the 500-yr ARI values. Storm 036 produces the largest storm surges in Galveston Bay, among all the 223 FEMA (2011) storms. The overall average absolute difference is about 1.3 ft. The average absolute difference reflects an “error” of about 6% to 8%, in light of the 500-yr ARI WSE range of 16.6 to 22.6 ft.

Figure 9-14 shows the maximum WSE field for Storm 036. The WSE pattern is very similar to the pattern shown for the other proxy storms and the 100-yr ARI WSE shown in Figure 9-10. All three proxy storms had the same track, which contributes to the similarity in maximum WSE patterns exhibited by all three storms. Again, the highest surges occurred in the northwest part of Galveston Bay and the upper reaches of the Houston Ship Channel.

Table 9-13. Water surface elevations for the 500-yr proxy storm, Storm 036.

	500-yr Proxy Storm Water Surface Elevations	500-yr WSE 90% CL (ft)	Storm 036 WSE (ft)	Difference (ft)	Absolute Difference (ft)
1	Houston Ship Channel (upper)	22.64	21.46	-1.18	1.18
2	Houston Ship Channel (mid)	21.46	21.29	-0.16	0.16
3	Houston Ship Channel (lower)	20.74	20.80	0.07	0.07
4	Alexander Island	19.65	19.82	0.16	0.16
5	LaPorte	19.06	18.41	-0.66	0.66
6	Bayport	18.44	17.68	-0.75	0.75
7	Clear Lake (east)	18.50	16.63	-1.87	1.87
8	Clear Lake (north)	19.62	17.68	-1.94	1.94
9	Clear Lake (west)	20.41	16.54	-3.87	3.87
10	Clear Lake (northwest)	20.47	17.88	-2.59	2.59
11	San Leon	17.13	15.65	-1.48	1.48
12	Dickinson	19.39	15.72	-3.67	3.67
13	Dickinson Bay entrance	18.08	17.03	-1.05	1.05
14	Texas City (north)	17.03	16.04	-0.98	0.98
15	Texas City (east)	16.63	16.70	0.07	0.07
16	Texas City (south)	18.01	19.19	1.18	1.18
17	Galveston (bay)	16.80	16.34	-0.46	0.46
18	Galveston (Pleasure Pier)	16.96	18.90	1.94	1.94
	Average	18.95	17.99	-0.959	1.338

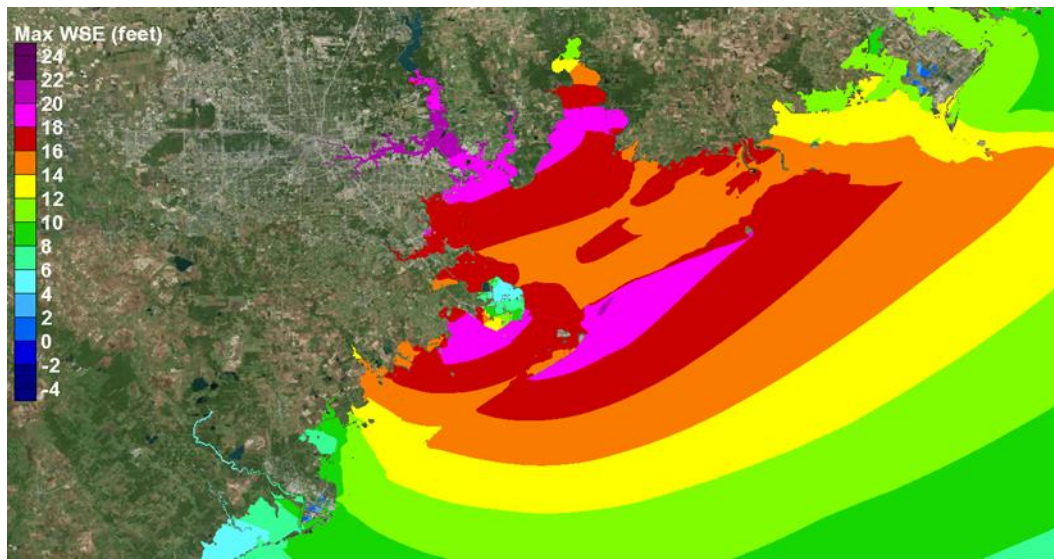


Figure 9-14. Maximum water surface elevation field for Storm 036, from FEMA (2011), the 500-yr proxy storm.

10 Storm Surge Simulations with an Extended Ike Dike

Introduction

The conceptual Ike Dike, as implemented in the original bracketing set of simulations, ended near High Island, close to the northeast end of Bolivar Peninsula. A plan for terminating the dike into higher natural ground, or to some other man-made feature such as an elevated roadway or levee, had not been formulated yet, so the ends of the dike were not transitioned into higher ground in the original model setup.

For some of the severe hurricanes in the bracketing set, model results indicated that a significant amount of water flowed around the northeast end of the unterminated dike. This flanking flow significantly increased storm surge levels within Galveston Bay. These increased water levels were judged to be not indicative of levels that would occur for a dike having an effective termination scheme. To minimize or effectively eliminate the influence of flanking, the with-dike model setup was revised to extend the dike toward the northeast, all the way to Sabine Pass. The southern terminus of the dike, which is located just south of Freeport, was not altered.

In the original modeling approach, the dike was treated as a three-dimensional topographic feature, which led to computational stability issues during some overflow conditions. In addition to these types of instabilities, for a few of the most extreme storms, other instabilities occurred within the open-coast nearshore region near Galveston Bay and within the passes leading to the bays. These instabilities were mitigated in the original modeling approach through the global use of a computational slope-limiting stabilization scheme. The use of slope-limiting created a few undesirable effects in certain areas of the model domain.

To minimize these adverse effects, two other changes were made to the modeling approach. One, the geographical area in which slope-limiting is applied was greatly reduced to a much more localized nearshore region that extends from Sabine Pass to Freeport. The polygon in which slope limiting is applied also extends a short distance into the Bolivar Roads and San Luis passes, covering the areas where instabilities tended to occur.

Second, the manner in which the dike was treated in the model set-up was revised. Instead of treating the dike as a three-dimensional topographic feature, the dike is treated as a single, long, continuous, weir section, an “infinitely thin” barrier. The change to a weir representation was done to promote model stability, avoiding the supercritical flows that would occur on the back side of the three-dimensional dike. The change to a weir representation also allows changes to dike crest elevation to be made with minimal effort. The weir representation allows the dike to be overtopped when the water surface elevation on one side of the dike exceeds the dike’s crest elevation. When overtopping occurs, flow over the dike is computed using a standard weir formula.

These dike modifications required changes to both the storm surge and wave model grid meshes, as well as changes to how the dike alignment was represented within both meshes. The extended dike is a single long, continuous weir section, with no breaks, extending from south of Freeport all the way to Sabine Pass, cutting across all the passes. The dike has a uniform crest elevation of 17 ft NAVD88 along its entire length (the same crest elevation as was used in the original bracketing set of simulations). The seaward-most long green line in Figure 10-1 shows the extended dike alignment.

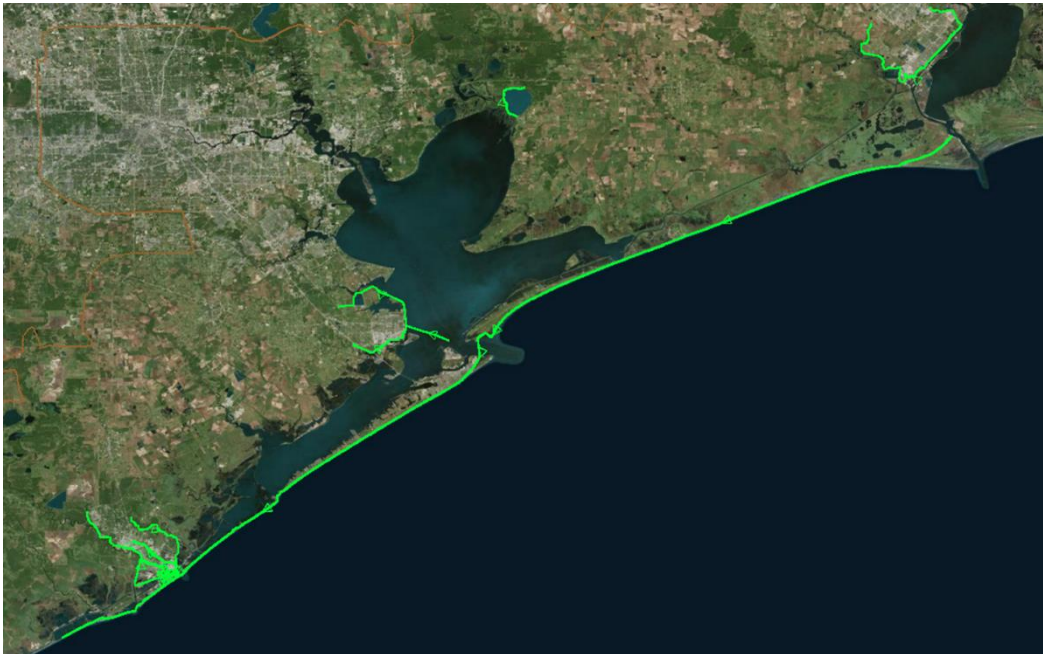


Figure 10-1. Alignment of the extended conceptual Ike Dike (from south of Freeport to Sabine Pass).

Storm surge results using the model set-up with the extended dike are expected to better represent surge conditions within Galveston Bay for a dike having an effective termination scheme. The dike extension greatly reduces the contribution of flanking to water surface elevations within the Bay.

There are other geographic features in the model domain, which also are represented as weir sections. One example is the Texas City levee. The other green lines shown in Figure 10-1 represent such features, and they are part of both the existing condition and the with-extended-dike model grid meshes.

Using the revised modeling approach, the 10-yr, 100-yr and 500-yr proxy storms defined in Chapter 9, and Hurricane Ike, were all simulated with the extended dike, in order to further examine the effectiveness of the conceptual coastal Ike Dike in reducing storm surge levels within the bays. For the three proxy storms, results from the original FEMA study (2011) were used to represent the existing, without-dike, water surface elevation conditions. Existing conditions for Hurricane Ike were simulated using the current modeling approach; and results presented here for Ike are the same as those presented in the model validation chapter, Chapter 2. Maximum water surface elevation results for all simulations were provided to the economics team for further analysis of damages and losses.

Effect of the Extended Ike Dike for Hurricane Ike

Figures 10-2 and 10-3 show the maximum water surface elevation field (in feet), as color-shaded contours, for existing conditions and with-extended-dike conditions, respectively. The figures graphically show the maximum elevation at every storm surge model grid node, without regard to when the maximum occurred during the simulation. In light of the fact that Hurricane Ike is such a recent major hurricane, and the experience was a memorable one, the results for Ike serve as an informative and effective benchmark with which to evaluate results from the existing-condition and with-dike simulations of the proxy storms, particularly the 100-yr and 500-yr storms. Therefore, results for Ike are presented first in this chapter.

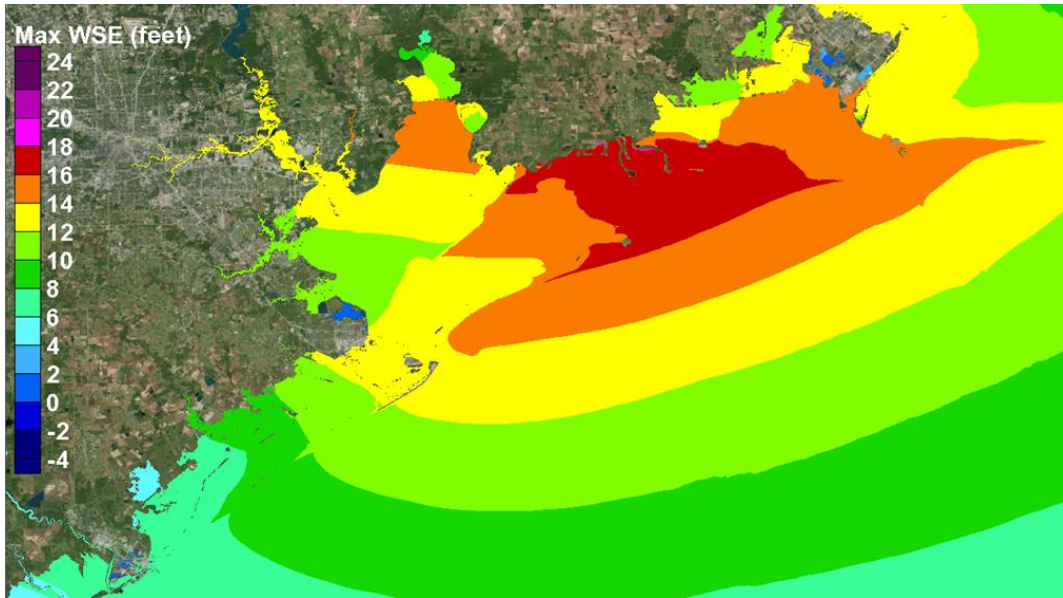


Figure 10-2. Maximum water surface elevation field for Hurricane Ike, existing without-dike conditions.

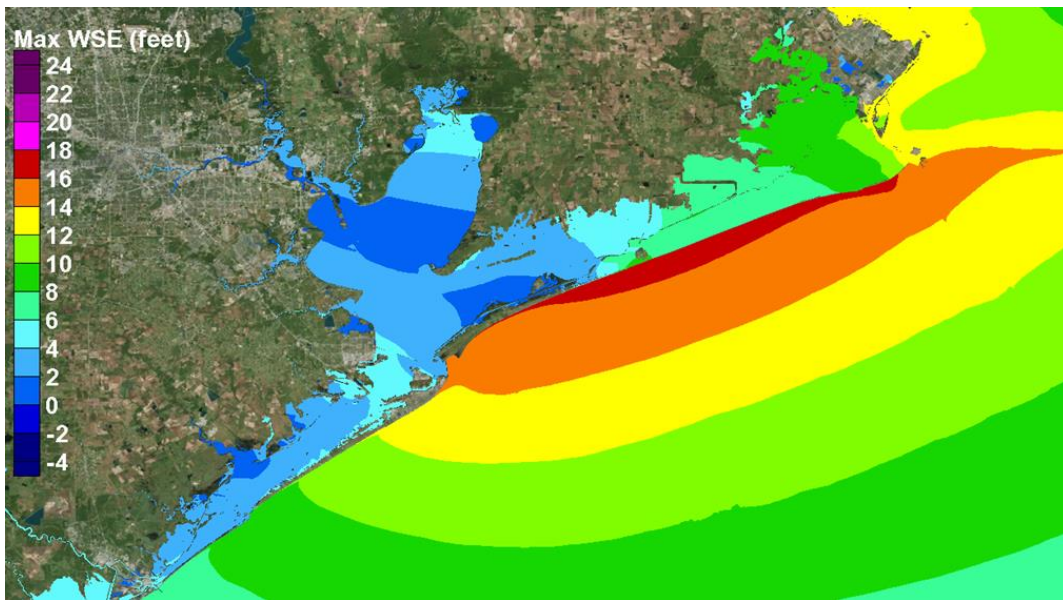


Figure 10-3. Maximum water surface elevation field for Hurricane Ike, extended-dike conditions.

For the existing condition simulation (Figure 10-2), Ike produced rather large maximum water surface elevation values along the north Texas coastline with the overall maximum storm surge (approximately 16.5 ft) occurring between Bolivar Peninsula and Sabine Pass. A peak storm surge of approximately 12 to 13.5 ft was simulated along the Gulf side of the City of Galveston, less than the 17-ft crest elevation of the Galveston Seawall. Similar peak surges were simulated for the bay side of the City of Galveston. Along the rest of Galveston Island, Gulf-side peak surge decreased from 12 ft in the east to 8 ft at the western end, near San Luis Pass. Along Bolivar Peninsula, Gulf-side peak surge reached 16 ft at the eastern end, with a slightly lower peak surge value of 14 ft at the western end, adjacent to Bolivar Roads pass.

Within Galveston Bay for existing conditions, the peak surge reached approximately 12.5 ft along the south side of Texas City. Along the north side of Texas City, peak surges reached approximately 11.5 to 12 ft. No overflow of the levee surrounding Texas City was simulated. From San Leon northward, peak surge along the western shoreline of Galveston Bay increased from south to north, from 11.5 ft to about 12.5 ft at the northern parts of the main part of Galveston Bay, near Bayport. Into the upper reaches of the Houston Ship Channel, peak surges increased slightly, to levels reaching 13 to nearly 14 ft.

A visual comparison of Figures 10-2 and 10-3 clearly shows that the extended conceptual Ike Dike produces a considerable reduction in storm surge throughout the entire bay system for Hurricane Ike. The coastal dike very effectively prevents the storm surge from entering the bay systems via flow over the barrier islands and through the passes. The magnitude of reductions in peak surge levels are quantified below.

Note that Bolivar Roads and San Luis passes are closed from the very beginning of the with-dike simulations. This modeling assumption will slightly understate the amount of hurricane surge forerunner that penetrates into the bays prior to gate closure. An understatement of approximately 1 to 2.5 ft is expected for major hurricanes. The development of the forerunner surge during the early stages of severe hurricanes that move into and through the Gulf of Mexico was discussed in Chapters 5 and 6. Future work should examine the influence that the timing of gate closure has on forerunner propagation into Galveston Bay and its influence on peak surge levels inside the Bay.

Along the Gulf side of the City of Galveston, as well as along Galveston Island and Bolivar Peninsula, the with-dike storm surge is increased slightly compared to the existing condition simulations as a result of the 'long-dike effect'. The amount of increase for Hurricane Ike is 0.5 to 1 ft, resulting in peak surge levels along the Gulf side of Galveston of 13 to 14 ft.

A very long impermeable coastal dike that is built to retard surge penetration will locally increase the surge by a small amount on the open coast side of the dike (usually by amounts of up to 2 ft for extreme storms). The long dike effect is essentially this: the presence of the barrier serves as an obstacle to the wind-driven surge; the barrier represents something for the wind-driven surge to pile up against, which would not occur if the dike were not present. The dike will dramatically reduce the surge for a much larger region behind the barrier by drastically curtailing the storm propagation over/past the dike. The "long dike effect" needs to be recognized and actions to mitigate the effect should be considered.

With the extended dike in place, along the bay side of the City of Galveston, the peak surges were reduced by amounts ranging from 7.5 ft to 9.5 ft. Between the City of Galveston and Texas City, the peak surge only reaches 4 to 5 ft, a reduction of 7.5 to 8 ft. In this region note that there is an area of locally higher surge between Galveston and Texas City (the lightest blue region seen in Figure 10-3). This area of higher maximum surge is a common feature for severe hurricanes that approach from the southeast and make landfall in the region. This storm surge feature is due to the counterclockwise rotating wind fields about the hurricane's eye which act to build surge in the southwest corner of Galveston Bay prior to landfall. As shown more clearly later in this chapter for the more severe proxy storms, the prevalence of this feature suggests that a bayside levee/wall for the city of Galveston, effectively creating a ring around the city, should be considered as a secondary line of defense along with the primary coastal dike.

The extended dike significantly lowered peak surges around Texas City, by approximately 8 ft. At most locations along the western shoreline of Galveston Bay and into the Clear Lake and Dickinson areas, peak surges are generally 8 to 9 ft less than for existing conditions. Peak surges in the upper reaches of the Houston Ship Channel are even more significantly reduced, by amounts of 10 to 11 ft.

Table 10-1. Summary of Simulated Maximum Storm Surge Conditions for Hurricane Ike, With and Without the Extended Dike

Location	Existing Condition	With-Dike Condition	Changes
Galveston (Gulf side)	12 to 13.5 ft increasing from west to east	12.5 to 14 ft increasing from west to east	Slight increase due to "long-dike" effect.
Galveston (Bay side)	12 to 13.5 ft	4 to 5 ft	Reductions of 8 to 9 ft
Rest of Galveston Island	8 to 12 ft, increasing from west to east	3 to 4 ft	Reductions of 5 to 8 ft
Bolivar Peninsula	14 to 16 ft	2 to 6 ft	Reductions of 10 to 12 ft
Texas City area	11.5 to 12.5 ft	3.5 to 5 ft	Reductions of 7 to 8 ft
Clear Lake Area	11 to 11.5 ft	3 to 3.5 ft	Reductions of 8 ft
Bayport Area	13 ft	2 ft	Reduction of 11 ft
Upper reaches of Houston Ship Channel	13 to 14 ft	2 to 4 ft	Reductions of 10 to 11 ft

The peak surge conditions for the without-dike and with-dike simulations of Hurricane Ike are summarized in Table 10-1 for different geographic regions. All cited water surface elevations are relative to the NAVD88 vertical datum. Surge values in the table were estimated from the figures. In an average sense, for Hurricane Ike, the 17-ft high coastal dike reduces maximum surge levels throughout Galveston Bay by approximately 8 to 10 feet.

Effect of the Extended Ike Dike for the 10-yr Proxy Storm

The 10-year proxy storm, Storm 535 (storm number assigned in FEMA study), produces a lower storm surge than Hurricane Ike. Figure 10-4 shows the maximum water surface elevation field (in feet) for Storm 535, existing conditions. The Gulf side peak surge at the City of Galveston is 6

to 7 ft for this less intense storm. Along the bay side of Galveston, peak surges were 6 to 7 ft. Along the western shoreline of Galveston Bay, peak surges range from 6.5 feet at Texas City to 8.5 at Bayport, increasing to 9.5 to 11 feet in the upper reaches of the Houston Ship Channel.

Figure 10-5 shows the maximum water surface elevation field (in feet) for Storm 535 and the with-extended-dike conditions. The Gulf-side peak surge at the City of Galveston (less than 7 ft) is only slightly higher for the with-dike condition, compared to the existing condition, due to the long dike effect. In general, the less intense the storm, the lower the increase in peak storm surge associated with the long-dike effect. On the bay side of Galveston, peak surges with the dike in place were only 1.5 to 2.5 ft. Throughout Galveston Bay, the extended coastal dike reduced peak surges to levels less than 6 ft, even in the upper reaches of the Houston Ship Channel where the surge reached its maximum values of 9.5 to 11 ft for existing conditions.

The extended dike reduces peak surges within Galveston Bay by amounts of 4 to 5 ft throughout Galveston and West Bays, significantly reducing the risk of flooding to all areas behind the dike. High winds that circulate in a counterclockwise rotation about the storm eye at landfall near San Luis Pass set up an east-to-west water surface gradient within the bay, the channels leading to the Dickinson area and into Clear Lake, and in the upper reaches of the Houston Ship Channel. In these channelized areas on the western side of Galveston Bay, peak water levels reach their highest values. The general pattern of maximum water surface elevation within Galveston Bay is nearly the same for without- and with-dike conditions. However, the dike effectively eliminates propagation of surge through the passes and over the barrier islands, significantly reducing the volume of water that enters the bays which would otherwise act to raise surge levels within the bays, as seen for the existing conditions.

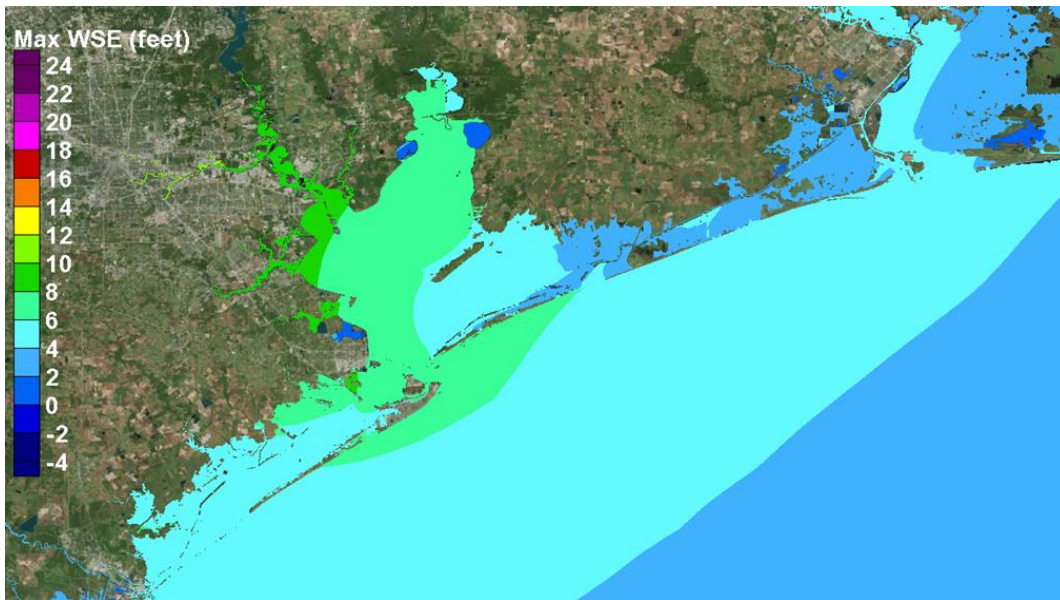


Figure 10-4 Maximum water surface elevation field for the 10-yr proxy storm, from FEMA (2011), representing the existing without-dike conditions.



Figure 10-5. Maximum water surface elevation field for the 10-yr proxy storm, extended-dike conditions.

Table 10-2 summarizes the same peak surge results in tabular form for several important regions of the study area as well as the changes attributed to the presence of the dike, for the 10-year proxy storm. Values listed in the table were visually estimated from the color-shaded contour maps.

Table 10-2. Summary of Maximum Storm Surge Conditions for Storm 535, the 10-yr Proxy Storm, With and Without the Extended Dike

Location	Existing Condition	With-Dike Condition	Changes
Galveston (Gulf side)	6 to 7 ft increasing from west to east	6 to 7 ft increasing from west to east	Slight increase due to "long-dike" effect.
Galveston (Bay side)	6 to 7 ft	1.5 to 2.5 ft	Reductions of 4 to 5 ft
Rest of Galveston Island	5 to 6.5 ft, increasing from west to east	1.5 to 2.5 ft	Reductions of 4 to 5 ft
Bolivar Peninsula	5.5 to 7 ft	Less than 2 ft	Reductions of 4 to 5 ft
Texas City area	6.5 to 8 ft	2.5 to 4 ft	Reductions of 4 to 4.5 ft
Clear Lake Area	8 to 9.5 ft	4 to 5.5 ft	Reductions of 4 to 4.5 ft
Bayport Area	8.5 ft	4 ft	Reduction of 4.5 ft
Upper reaches of Houston Ship Channel	9.5 to 11 ft	5 to 6 ft	Reduction of 4.5 to 5 ft

Effect of the Extended Ike Dike for the 100-yr Proxy Storm

The computed maximum water surface elevation fields for the without-dike and the with-dike conditions, for the 100-yr proxy storm, Storm 033, are shown in Figures 10-6 and 10-7, respectively.

For the existing conditions, a peak storm surge of approximately 14.5 to 16 ft was simulated along the Gulf side of the City of Galveston, increasing from west to east. At this location, the peak surge is approximately 2 ft higher than the peak surge that was computed for Hurricane Ike. Significant wave induced overtopping of the seawall, but no steady overflow, would be expected at this surge level, since levels are below the seawall crest elevation of 17 ft. Peak surges along the rest of Galveston

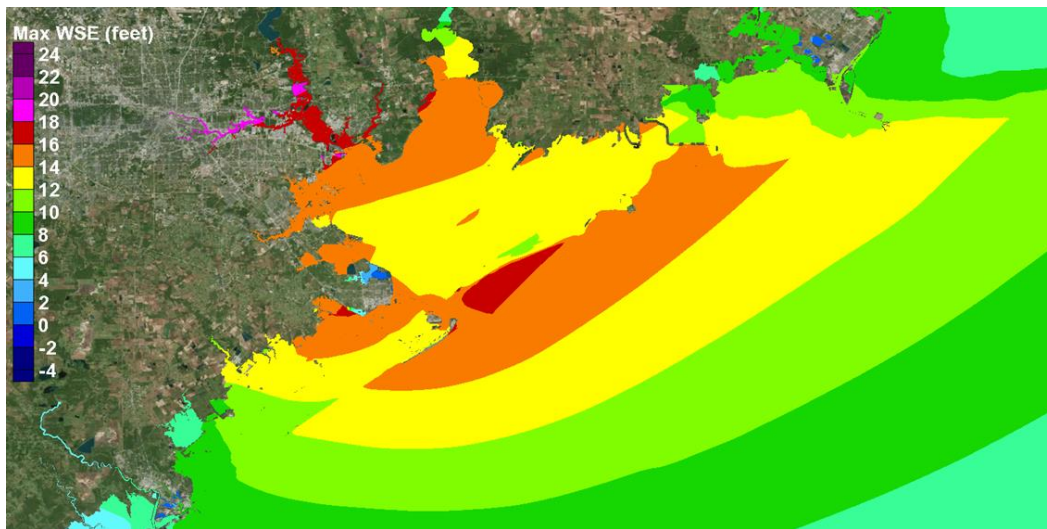


Figure 10-6. Maximum water surface elevation field for the 100-yr proxy storm, from FEMA (2011), representing the existing without-dike conditions.

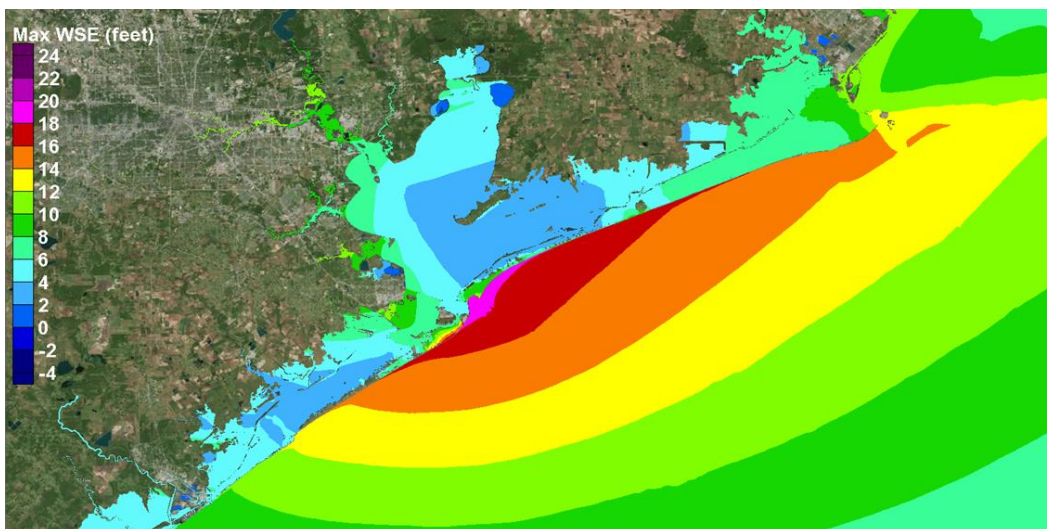


Figure 10-7. Maximum water surface elevation field for the 100-yr proxy storm, extended-dike conditions.

Island were 10 to 14.5 ft, also increasing from west to east along the island. Peak surges of 15 to 17 ft were computed along the open coast of Bolivar Peninsula, with the highest peak surge at the western end, decreasing toward the east end of the peninsula.

In general, the zone of maximum open-coast surge is located where the maximum onshore-directed hurricane winds occur at landfall. All three proxy storms make landfall at San Luis pass, each following the same track; and all three have similar radii-to-maximum-winds as they approach landfall. The location of maximum onshore-directed winds is roughly positioned at one radius-to-maximum winds distance to the

northeast of the landfall location. Therefore, the zone of maximum surge is in roughly location between Bolivar Roads Pass and western Bolivar Peninsula, in light of differences in the radii-to-maximum winds for the three storms as they approach landfall.

For existing conditions within Galveston Bay, from the bay side of the City of Galveston to the north side of Texas City and near San Leon, the peak surge ranged from 14 to 15 ft. From San Leon northward, along the western shoreline of Galveston Bay, peak surge increased from 14 ft to 16 ft near Bayport. Peak surges increased further into the upper reaches of the Houston Ship Channel, approaching maximum values of 19 to 20 ft.

Figure 10-7 shows the maximum water surface elevation field for with-dike conditions. Comparing Figures 10-7 and 10-6, the extended dike produces substantial reductions in peak storm surge levels throughout the interior bay system, in both Galveston and West Bays. The coastal dike prevents a considerable amount of storm surge from entering the bay systems via flow over the barrier islands and through the passes. As was evident for the 10-yr proxy storm, hurricane force winds within the bay still generate a significant east-to-west water surface elevation gradient within the bay, as a result of the counterclockwise rotating wind fields around the eye, as the storm makes landfall. These gradients result in locally higher peak surge levels along the western sides of both bays, but they are significantly less than levels without the dike in place.

Along the Gulf sides of the City of Galveston as well as along Galveston Island and Bolivar Peninsula, the storm surge is increased slightly as a result of the 'long-dike effect,' to maximum values of 17 to 19 ft. This increase results in greater overtopping and steady flow over the Galveston Seawall as is evident in Figure 10-7; the same occurs along the western side of Bolivar Peninsula. For this more intense hurricane, the long-dike effect increases on the open coast side of the dike by 1 to 2 ft. These results suggest that raising of the Galveston Seawall should be considered as an element of the coastal dike, to mitigate the long-dike effect on the existing seawall and provide enhanced risk reduction for the City of Galveston for storms of this intensity and greater.

With the extended dike, along the bay side of the City of Galveston, the peak surges were reduced by amounts ranging from 4 to 5 ft. Between the City of Galveston and Texas City, the peak surge reaches 7 to 10 ft, a

reduction of 6 to 7 ft. As was seen for Hurricane Ike, this area of locally higher surge between Galveston and Texas City is a common feature for hurricanes from the southeast. The prevalence for this feature suggests that a bayside levee for the city of Galveston, effectively creating a ring levee, wall or dike around the city, should be considered as a secondary line of defense along with the coastal dike.

The extended dike greatly reduces the amount of inundation along the western shoreline of Galveston Bay, for the 100-yr proxy storm. The extended dike significantly lowered peak surges around Texas City, by amounts of 6 to 8 ft, in such a way as to reduce overtopping and flow over the protective dike surrounding Texas City on its southern side, compared to the without-dike case. With the dike in place, in most places along the western shoreline of Galveston Bay, peak surges are generally in the 6 to 8 ft range, much less than the 14 to 16 ft surges that occur here without the dike in place. Also note that peak surges with the dike in place are 3 to 5 ft lower than was experienced during Hurricane Ike (10 to 12 ft) in these same areas.

As noted for the other storms considered thus far in this chapter, computed surges for the with-dike conditions are slightly higher, approaching 11 ft, in some of the isolated areas of the interior back channels of Dickinson Bay, compared to surges in the bay proper. This is due to the strong winds from the east at landfall which force east-to-west water surface gradients in the channels leading to Dickinson and into Clear Lake. In light of these gradients, which are a prevalent feature for severe hurricanes that approach from the southeast, secondary lines of defense should be considered within these channels. Secondary lines of defense might be raised topography or roadways, or smaller gates in conjunction with raised topography or roadways, which can provide additional flood risk reduction, if cost-effective.

Peak surges in the upper reaches of the Houston Ship Channel are significantly reduced as a result of the extended dike, to levels less than 12 ft; an 8-ft reduction in peak surge in this area. Peak surge elevations with the dike in place are less than peak surge elevations that were experienced in these same areas during Hurricane Ike.

The peak surge conditions for the without-dike and with-dike simulations are summarized in Table 10-3 for different geographic regions.

Table 10-3. Summary of Maximum Storm Surge Conditions for Storm 033, the 100-yr Proxy Storm, With and Without the Extended Dike

Location	Existing Condition	With-Dike Condition	Changes
Galveston (Gulf side)	14.5 to 16 ft increasing from west to east	16 to 18 ft increasing from west to east	1 to 2 ft increase due to "long-dike" effect.
Galveston (Bay side)	13.5 to 14 ft	8 to 10 ft	Reductions of 4 to 5 ft
Rest of Galveston Island	11 to 14.5 ft, increasing from west to east	4 to 5 ft	Reductions of 7.5 to 9.5 ft
Bolivar Peninsula	15 to 16.5 ft	4 to 9 ft	Reductions of 7.5 to 11 ft
Texas City area	14 to 16 ft	6 to 10 ft	Reductions of 6 to 8 ft
Clear Lake Area	14 to 15 ft	7 to 9 ft	Reductions of 6 to 7 ft
Bayport Area	16 ft	7.5 ft	Reductions of 8.5 ft
Upper reaches of Houston Ship Channel	17.5 to 20 ft	10 to 12 ft	Reductions of 7.5 to 8 ft

Effect of the Extended Ike Dike for the 500-yr Proxy Storm

Figures 10-8 and 10-9 show the computed maximum water surface elevation fields for the existing and with-dike conditions, respectively, for the 500-yr proxy storm, Storm 036. For existing conditions (Figure 10-8), a peak storm surge of approximately 19 ft was generated along the Gulf side of the City of Galveston, higher than the 17-ft crest elevation of the Galveston Seawall. Substantial overflow of the seawall occurs at this surge level, along with widespread inundation of the City of Galveston. Along the rest of Galveston Island, Gulf-side peak surge increased from 14 ft in the west to 19 ft in the east. Gulf-side peak surge approached 19 to 20 ft along the western end of Bolivar Peninsula, decreasing to 18 ft at the eastern end.

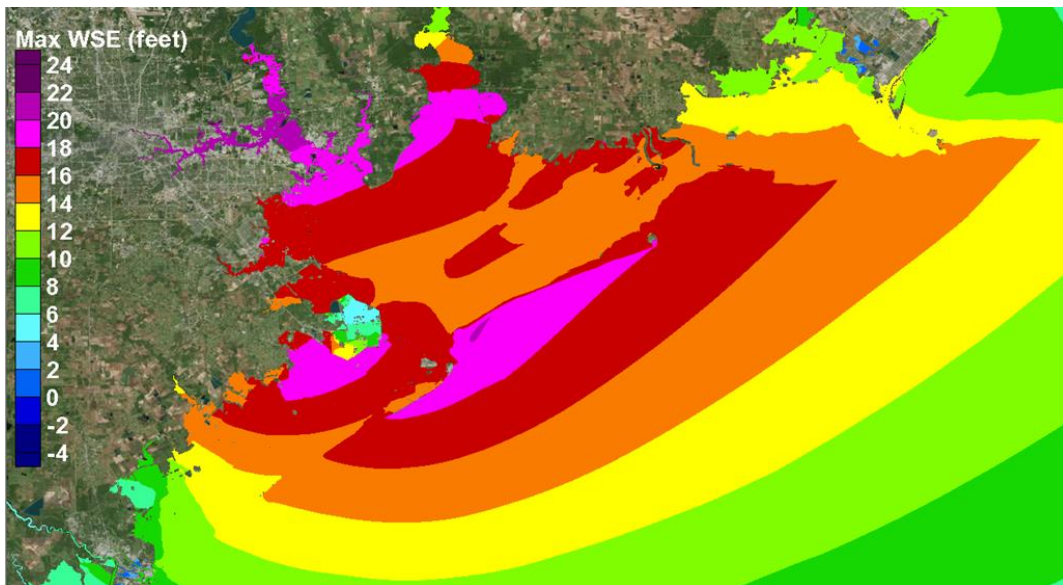


Figure 10-8. Maximum water surface elevation field for the 500-yr proxy storm, from FEMA (2011), representing the existing without-dike conditions.

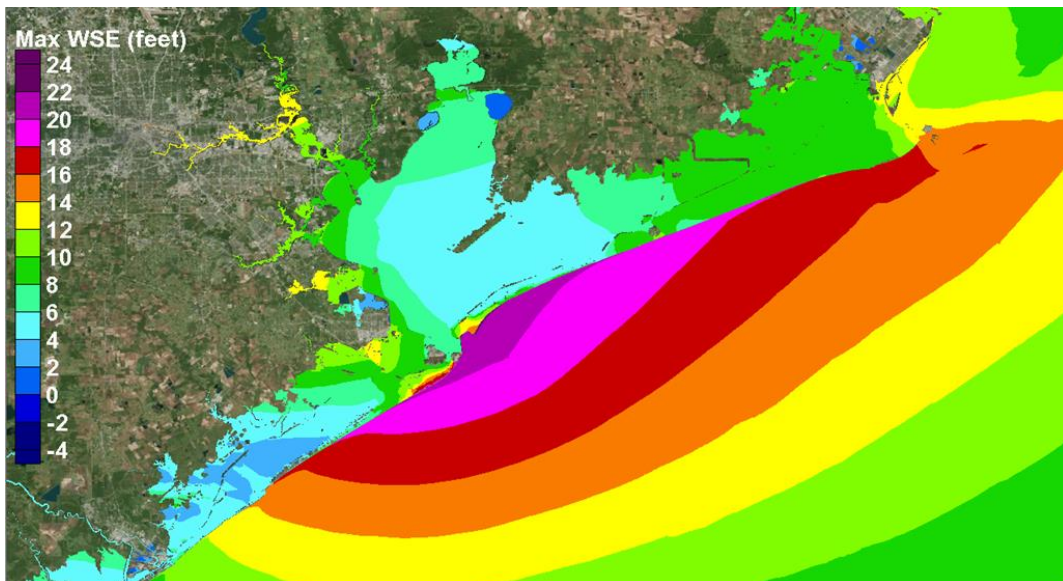


Figure 10-9. Maximum water surface elevation field for the 500-yr proxy storm, extended-dike conditions.

Within the bays for existing conditions, along the south side of Texas City the peak surge reached approximately 18 to 19 ft. Consequently, overflow and overtopping of the levee surrounding Texas City occurred, leading to significant interior inundation within Texas City. North of Texas City, peak surge along the western shoreline of Galveston Bay steadily increased from south to north, from 16 ft to about 18.5 ft at the northern parts of the main part of Galveston Bay, near Bayport. Into the upper reaches of the Houston Ship Channel, peak surges increased further, to levels of 20 to 22 ft.

Even with the extended dike, some flanking flow is evident around the northeast end of the dike for Storm 036. This storm also produces steady flow over the extended dike along the eastern half of Galveston Island, over the Galveston Seawall, and over the entire length of Bolivar Peninsula, albeit for a rather short duration. This overflow contributes to elevated surge levels with the bays.

Even with this overflow of the coastal dike, compared to Figure 10-8, Figure 10-9 shows that the extended dike produces a considerable reduction in storm surge throughout the entire bay system for the 500-yr proxy storm. As was the case for the 100-yr storm, the coastal dike prevents a considerable amount of storm surge from entering the bay systems via flow over the barrier islands and through the passes. As was seen for the 100-yr proxy storm, hurricane force winds within the bay still generate a significant east-to-west water surface elevation gradient within the bay, as a result of the counterclockwise rotating wind fields around the eye, as the storm makes landfall. These gradients result in locally higher peak surge levels along the western sides of both bays; but peak surge levels are significantly less than peak levels without the dike in place. For the 500-yr proxy storm, the pattern of peak surge within the bays is quite similar to the pattern seen for the 100-yr proxy storm (compare Figures 10-9 and 10-7).

Along the Gulf side of the City of Galveston as well as along Galveston Island and Bolivar Peninsula, the storm surge is increased slightly, by amounts ranging from 1 to 2 ft, as a result of the 'long-dike effect,' to peak surge levels of approximately 21 ft at the City of Galveston and western Bolivar Peninsula.

The magnitude of the surge at Galveston for existing conditions, 19 ft, which exceeds the crest elevation of the Galveston seawall (17 ft), and the peak surge level of 21 ft for the with-dike conditions, both suggest that raising of the Galveston Seawall on the Gulf side should be considered as an element of the coastal Ike Dike concept, to mitigate the long-dike effect and provide enhanced flood risk reduction for the City of Galveston.

Along the bay side of the City of Galveston, peak surges are reduced from values of 15.5 to 16.5 to values of 12 to 13 ft, reductions of 3 to 4 ft. The relatively small reductions here are due to the considerable amount of flow over the Galveston Seawall and subsequent inundation of the City of

Galveston, and to the locally higher surge that is created in the southwest corner of Galveston Bay, between Texas City and the City of Galveston. As noted previously for the 100-yr proxy storm, this area of locally higher surge between Galveston and Texas City is a common feature for hurricanes that approach from the southeast along this type of storm track. The occurrence of the locally elevated surge zone for Hurricane Ike and both the 100-yr and 500-yr proxy storms suggests that a bayside levee for the city of Galveston should be considered as a possible feature of the Ike Dike concept, a secondary line of defense. Raising the existing seawall and establishing bay-side protection would create in effect a ring levee/dike/wall around the city. The Gulf-side of the ring levee would be higher than the adjacent sections of the coastal spine. The crest elevation of the bayside portion of the ring dike would need to be optimized through further investigation.

Along the western shoreline of Galveston Bay, peak water surface elevation approached 13 ft in some of the isolated areas of the interior back channels of Dickinson Bay, but peak elevations generally ranged from 10 to 12 ft throughout most of the area. Simulated peak surges in the upper reaches of the Houston Ship Channel for the with-extended dike case are reduced to levels less than 14 ft, roughly an 8-ft reduction in peak surge in this area compared to existing conditions. In general throughout Galveston Bay, for the 500-yr proxy storm, peak surge levels with the Ike Dike concept in place are quite similar to, or slightly less than, peak surge levels that were experienced during Hurricane Ike. The Hurricane Ike experience is a reasonably good overall indicator of the flooding and inundation that would be expected along the western shoreline of Galveston Bay and into the upper reaches of the Houston Ship Channel for the 500-yr proxy storm, with the coastal spine in place as the only flood risk reduction feature, without any secondary lines of defense.

The Ike Dike concept significantly reduced steady flow over the protective levee/dike surrounding Texas City, greatly reducing the depth of inundation for a large portion of Texas City that was inundated by this storm without the coastal dike in place. It appears that even with the coastal dike in place, the 500-yr proxy storm might cause some flow over the Texas City levee. Therefore raising of the Texas City Levee, perhaps only locally, should be examined as an improvement to this flood risk reduction measure, which becomes a secondary line of defense with the coastal dike in place. It could be that with additional forerunner

penetration, under a realistic gate closure scenario, more flow over the Texas City Levee would have been simulated for this storm.

Along most of the eastern shoreline of Galveston Bay, the presence of the dike reduces peak surge levels to elevations of 6 to 8 ft NAVD88.

The peak surge conditions for the without-dike and with-dike simulations are summarized in Table 10-4 for different geographic regions.

Table 10-4. Summary of Maximum Storm Surge Conditions for Storm 036, the 500-yr Proxy Storm, With and Without the Extended Dike

Location	Existing Condition	With-Dike Condition	Changes
Galveston (Gulf side)	18 to 20 ft increasing from west to east	20 to 21 ft increasing from west to east	1 to 2 ft increase due to the "long-dike"
Galveston (Bay side)	15.5 to 16.5 ft	12 to 13 ft	Reductions of 3 to 4 ft
Rest of Galveston Island	13 to 16 ft, increasing from west to east	4 to 10 ft	Reductions of 6 to 9 ft
Bolivar Peninsula	18 to 20 ft	4 to 13 ft	Reductions of 7 to 12 ft
Texas City area	16 to 19 ft	8 to 12 ft	Reductions of 7 to 8 ft
Clear Lake Area	17 to 18 ft	9 to 12 ft	Reductions of 6 to 8 ft
Bayport Area	19 ft	10 ft	Reductions of 9 ft
Upper reaches of Houston Ship Channel	20 to 22 ft	12 to 14 ft	Reductions of 8 ft

11 Influence of Sea Level on Storm Surge

Recent Historic Changes in Sea Level for the Region

Figures 11.1 and 11.2, taken from the NOAA Tides and Currents web site, show the mean sea level changes that have been observed at Galveston. These observations are based on measured water surface elevation data from NOAA tide gages (see <https://tidesandcurrents.noaa.gov/sltrends/>). Figure 11.1 shows the monthly means based on data from the Galveston Pleasure Pier, which is located on the open Gulf side of the city. Figure 11.2 shows the temporal variation of monthly mean sea level at Galveston Pier 21, which is located on the bay side of the City of Galveston. The average annual mean sea level trends at the Pleasure Pier and Pier 21 are similar, 6.62 mm/yr and 6.34 mm/yr, respectively (which correspond to rates of 0.02172 ft/yr and 0.02080 ft/yr, respectively).

As part of this feasibility study, the sensitivity of peak storm surge values to changes in mean sea level was investigated for the Houston-Galveston region. Sensitivity was examined for both the existing condition and for the with-extended-dike condition. A single future sea level scenario was considered in all with-sea-level-rise simulations. Simulations also involved four storms, Hurricane Ike and each of the three proxy storms (10-yr, 100-yr and 500-yr).

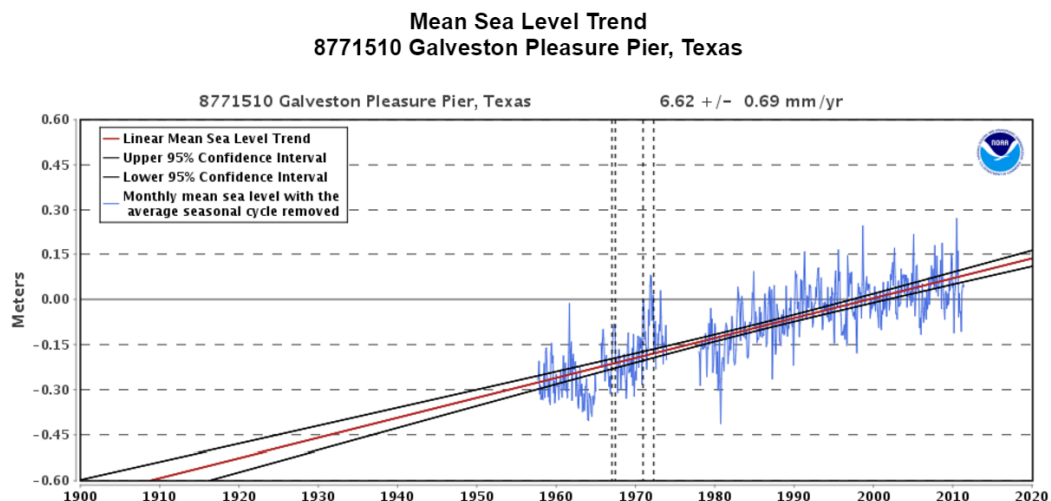


Figure 11-1. Mean sea level trend at Galveston Pleasure Pier, Texas.

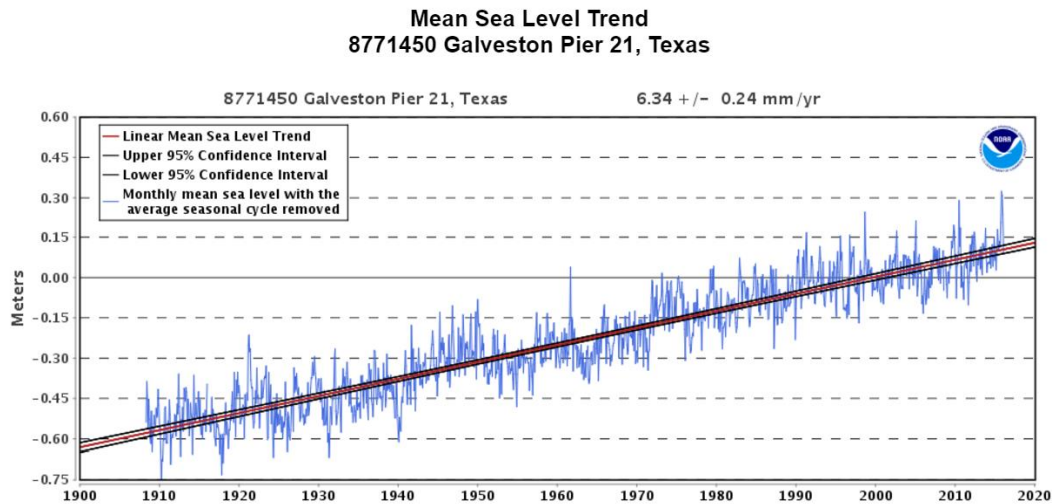


Figure 11-2. Mean sea level trend at Galveston Pier 21, Texas.

The present-day sea level adopted for use in this feasibility study, 0.91 ft NAVD88, reflects 2008 conditions; it is same the value used in the most recent FEMA Risk Map study that was performed for the region.

A future sea level of 3.31 ft NAVD88 was adopted in the with-sea-level-rise analysis, and it is referred to the SLR1 scenario in subsequent discussion. The SLR1 scenario reflects a projected sea level in the year 2085, using the intermediate rate of sea level rise curves from U.S. Army Corps of Engineers (USACE) guidance (see <http://www.corpsclimate.us/ccaceslcurves.cfm>). The future sea level value of 3.31 ft value reflects an increase of +2.4 feet relative to present-day conditions. This future sea level condition was the same as that used by the USACE ERDC in recent flood risk assessment work done to support the Galveston District, USACE. The value is nearly identical to the value used by the Gulf Coast Community Protection and Recovery District (2016) in their work to examine flood risk reduction for the north Texas coast. They used 3.44 ft NAVD88 to represent the 2085 sea level condition.

Figure 11-3 shows three relative sea level change projections for the Galveston Bay vicinity during the period from 2008 to 2085, following the USACE guidance. The upper panel shows curves which utilize the water level data from the Galveston Pleasure Pier gage. The lower panel in Figure 11-3 shows curves which utilize the record of water level data from the Galveston Pier 21 gage. The figures were generated using the USACE

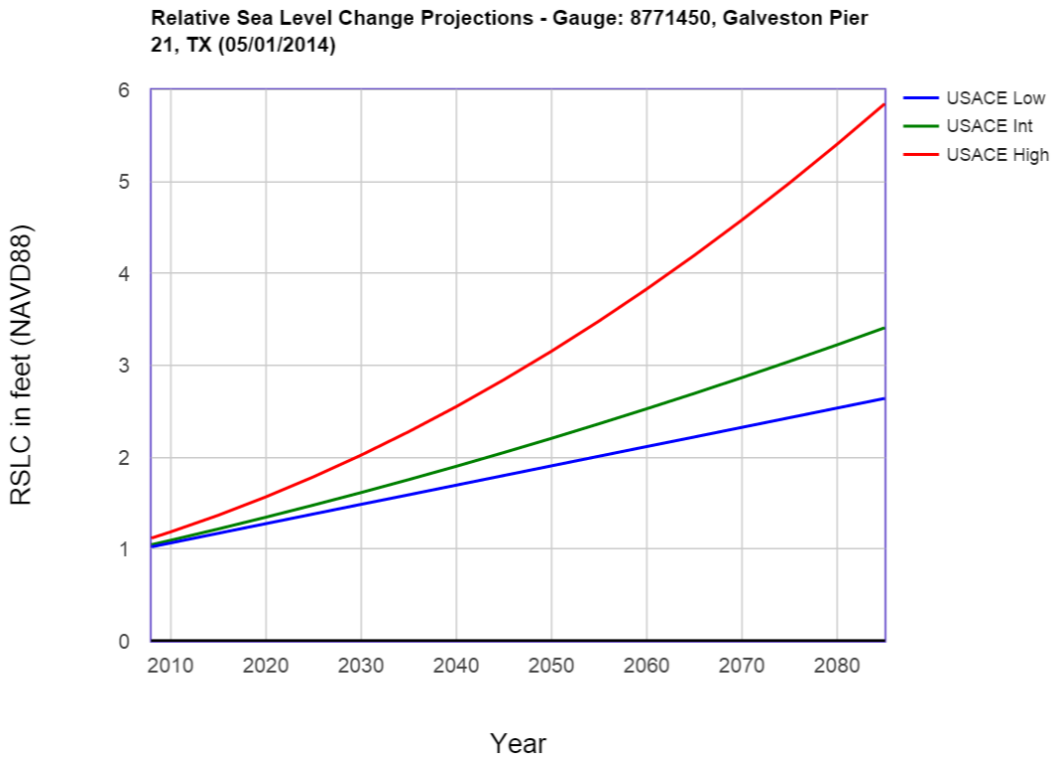
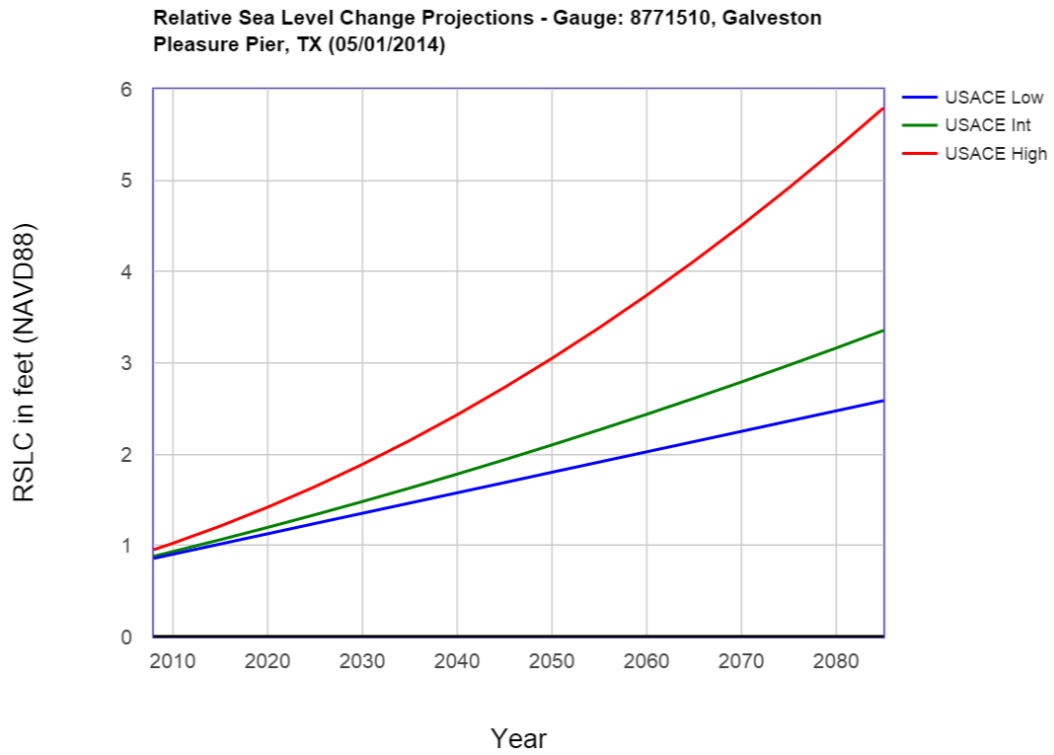


Figure 11-3. Sea level change scenarios for Galveston Bay and vicinity, following USACE guidance (upper panel- based on Galveston Pier 21 gage data; lower panel - based on Galveston Pleasure Pier gage data)

sea level change curve calculator:

<http://www.corpsclimate.us/ccaceslcurves.cfm>.

The “USACE Low” curves in Figure 11-3, reflect a projection of the historic rate of sea level rise into the future, i.e., a projection of the average rates that are shown in Figures 11-1 and 11-2. The “USACE Int” curves in Figure 11-3, which were adopted for this feasibility study, represent an accelerated rate of sea level rise, compared to the recent historic rate. For the year 2085, projection of the historic rate (the “USACE Low” curve) yields a sea level of approximately 1.6 ft, which is 0.8 ft less than the 2.4 ft calculated using the “USACE Int” curve.

A sea level rise of 1.6 ft to 2.4 ft reflects a significant change in the Houston-Galveston region, one that is important to consider in assessing and reducing flood risk for the region in general, and in the design of the Ike Dike concept, in particular. This magnitude of sea level increase represents a 20 to 30% increase in the average, present-day water depth in Galveston Bay.

Effects of Sea Level Rise on Storm Surge and Wave Processes

A rising sea level will lead to greater water depths, which in turn can influence the generation of storm surge and waves. Increases in water depth affect the storm surge and nearshore wave conditions in different ways; they tend to reduce both the effective surface wind stress and reduce the effective bottom shear stress. The former leads to less pushing force on the water; the latter tends to make it easier for the forcing to push the water. Both the reduction in effective wind stress and bottom shear stress exert influence on the storm surge response along the north Texas coast.

A sea level rise that increases water depths will act to slightly reduce the effective surface wind stress in the open Gulf shelf areas near the coast, where winds are most effective in generating storm surge. In terms of the two-dimensional horizontal water momentum balance, the wind stress is divided by the water depth, so the deeper the water the less the effective wind stress is that acts to push the entire water column beneath the surface. The less the effective wind stress, the less the water surface gradient, the less the storm surge amplitude at the upwind side of the basin. So a wind blowing over deeper water will result in a slightly smaller water surface gradient than the same wind blowing over shallower water. A smaller forced water surface gradient leads to a smaller peak surge, in a

general idealized sense. The reduction in effective wind stress will be rather small for most of the open Gulf where the magnitude of sea level rise, the value of 2.4 ft in the year 2085 for example, represents a very small percentage of the total water depth.

However, this effect can be greater in shallow bays like Galveston, West and Trinity Bays where the increase in mean sea level represents a greater percentage of the water depth. In a rather enclosed basin like Galveston Bay, for a momentum balance at steady state, the effective wind stress is balanced by the water surface gradient. In Galveston Bay, assuming an ambient non-storm water depth of 10 ft, a mean sea level increase of 1.6 to 2.4 ft roughly represents a 20% change in water depth, a 20% decrease in water surface gradient, and a 20% reduction in surge amplitude at the downwind side of the bay, for any wind speed. For a depth of 20 ft in the bay, under severe storm conditions (10-ft ambient depth plus a 10 ft storm surge), the 1.6 to 2.4 ft sea level rise roughly represents a 10% change in water depth, water surface gradient, and down-wind surge amplitude.

The increased water depth associated with sea level rise also leads to a reduction in the effective frictional resistance at the bottom/sea bed, in light of how this process is treated in the two-dimensional, depth-averaged momentum balance equations that are solved in the storm surge model. Reduced frictional resistance allows the water column to move more easily in response to the forcing imposed on it. A reduction in bottom frictional resistance associated with a greater water depth is true for all types of bottom roughness, for inundated vegetated terrain as well as open water areas.

An increase in mean sea level can influence the storm surge in other ways. Offshore, reduced frictional resistance allows water to move more easily in response to the wind forcing, perhaps leading to slight increases in the forerunner surge along the north Texas coast. Elevated sea level also leads to earlier onset of overtopping of the barrier islands, and subsequent flow over the barrier islands, leading to an increased flow of water inland and into the interior bay systems. The reduced frictional resistance allows water flowing over the barrier islands and over inundated terrain to move a little faster in response to the forcing.

In terms of surface wind wave generation, deeper water generally leads to more energetic wave conditions (i. e., greater significant wave heights,

with an increase in peak spectral wave period). As a percentage, these changes are expected to be greater in shallow bays like Galveston Bay where the sea level rise represents a much greater change to the water depth, percentage-wise, than in the open Gulf.

Changes in water depth associated with a sea level increase also influence wave conditions in shallow water. In very shallow water, where wave breaking processes are dominant, significant wave height is roughly proportional to the local water depth. Therefore, a 10% or 20% increase in local water depth due to an increase in sea level, such as in Galveston Bay, can lead to a 10% or 20% increase in local significant wave height, respectively. Increases in local wave height can increase the erosive potential of the waves, increase wave forces on structures, and increase the potential for wave run-up and overtopping of dunes, dikes and other man-made or natural flood risk reduction measures.

Sea level rise also can influence the storm surge in other ways, on time scales that are much longer than the hurricane event time scale. As mean sea level increases, the beach and dune system along Bolivar Peninsula and Galveston Island might become more fragile, degrading with time. As sea level rises, the frequency of dune overtopping and overwash, and dune erosion, will increase. If the dunes and beach system are not maintained, the dune crest elevation will probably be lowered on an increasingly more frequent basis. As the dunes degrade, overtopping and overwash will begin to occur during storms of lesser intensity. Without dune maintenance, natural dune building processes associated with wind-blown sand will probably not be able to keep pace with the ever increasing occurrences of overtopping, overwash, and lowering of the crest elevation. The dune degradation process is likely to accelerate in the absence of beach and dune maintenance.

Dune degradation also will probably lead to increased probability of significant breaches forming in the barrier island during hurricanes. As stated earlier, sea level rise by itself will lead to earlier onset of barrier island overflow during storms, leading to more water flowing into the interior bays, contributing to interior flooding. This process is exacerbated by dune degradation.

It is important to note that the Ike Dike coastal spine concept greatly reduces the likelihood of barrier island degradation leading to breaching. It provides integrity to the barrier island.

Changes in the interior bays and wetlands also are expected as a result of sea level rise; which can then, in turn, influence the storm surge. Rising sea level is expected to alter the landscape in the following ways: changes to the type, health and/or density of vegetation due to increased frequency of inundation, permanency of inundation, and changes to the salinity regime; conversion of upland terrain to marshland; conversion of marshland to open water bottom conditions; and, shoreline erosion and changes to sedimentation patterns. Changes to the vegetation canopy also can change the surface roughness that can influence the effective wind stress.

Degradation or loss of vegetation can reduce the frictional resistance of the landscape and allow storm surge to propagate more easily into inland areas, and promote development of storm surge in those areas. For approaching hurricanes that produce high surges and coastal inundation, considerable volumes of water can move across the vegetated barrier islands and wetlands northeast of Galveston Bay, and then into Galveston Bay for certain storms.

Conversion of the landscape to open water, as a result of vegetation loss or erosion, increases wind fetches. Greater fetches can in turn expose ever-expanding open-water areas to the effects of storm surge and more energetic wave conditions. These changes in surge and wave conditions can lead to greater marsh and wetland degradation and/or exacerbate erosion. Loss of vegetation also can reduce the wave energy dissipation benefits of a vegetated landscape when it does become inundated.

Past Relevant Work by ARCADIS (2011)

In support of The Nature Conservancy, ARCADIS (2011) performed an assessment of future landscape changes in the Jefferson County and Galveston Bay areas of north Texas; and they examined the influence of those changes on hurricane storm surge. ARCADIS examined the effects of Hurricane Ike for present-day mean sea level and two future mean sea levels: a sea level of 2.0 ft NAVD88 in the year 2050 and a sea level of 3.9 ft NAVD88 in the year 2100. (For comparison purposes, the present study is considering a sea level of 3.3 ft NAVD88 in the year 2085.) Their work

considered some of the anticipated landscape changes mentioned above: changes to the vegetation canopy which can alter surface wind stress, changes to vegetation that can change the bottom frictional resistance, and increased water depths which tend to reduce frictional resistance in general. ARCADIS (2011) developed two future modified landscapes, which they projected, for the years 2050 and 2100. The modified future landscapes were used to alter the storm surge model input, and Hurricane Ike was simulated for the present landscape scenario (2004) and each of the landscape/sea level scenarios (2050 and 2100).

In general, ARCADIS (2011) showed that the increase in sea level and the corresponding landscape changes both acted to reduce the influence of bottom friction which, in turn, led to greater storm surge penetration and greater storm surge peak amplitude in the inundated areas. They found that for Hurricane Ike, in some areas the peak storm surge increases were much greater than the increase in mean sea level alone, a nonlinear response, with storm surge amplification factors approaching a value of 3 (i.e., increases in peak surge elevations that were 3 times the increase in mean sea level). An amplification factor of 2 indicates an increase in peak surge that is twice the magnitude of the increase in mean sea level. The greatest nonlinear increases were seen for Jefferson County, which is northeast of the Houston-Galveston region, and in the northern end of Trinity Bay, which is in the northeast part of Galveston Bay.

This nonlinear response was not nearly as strong in other areas. For example, along the western shoreline of Galveston Bay, which is an area of great potential for flood damage, they found that the non-linear effect was generally less than in other areas. Amplification factors ranged from 1.0 near the City of Galveston to 1.5 or 1.6 near Morgan's Point, for the year 2050 case. For the 2100 case, amplification factors ranged from 1.0 near the City of Galveston to 1.4 near Morgan's Point. They found that amplification factors were generally less for the higher mean sea level. ARCADIS (2011) only considered Hurricane Ike in their analysis, and they noted that the effects of reduced frictional resistance might be less for Hurricane Ike than for other storms that are smaller and/or had faster forward speeds.

Storm Surge for Present and Future Sea Level Scenarios

Simulations were conducted as part of this feasibility study to further examine the influence of rising mean sea level on storm surge. The

simulations also were done to support an assessment of damages/losses prevented by the Ike Dike concept for a future sea level condition. The analysis presented here does not consider any changes to the landscape, as was done by ARCADIS (2011), some of which would be expected for a future sea level increase of this magnitude (1.6 to 2.4 ft). Instead, a static landscape was assumed: the present-day landscape, as it was treated in the most recent FEMA Risk Map study. As will be discussed and shown below, the assumption of a static landscape is quite reasonable as a first step to examine the effect of a future elevated sea level on storm surge in the Houston-Galveston region.

The static landscape assumption captures the key factors influencing the effect of sea level rise on storm surge in the areas of greatest interest in the Houston-Galveston region: Galveston Island, Bolivar Peninsula, western shoreline of Galveston Bay, and the upper reaches of the Houston Ship Channel. Surge generated in the open Gulf and in Galveston/West Bays is primarily generated by wind blowing over the open water areas, including all areas that are inundated prior to the storm's arrival by the sea level rise. Surge in the interior bays is controlled by the flow of water through Bolivar Roads into the bays, and by water flowing over the barrier islands once they become inundated, a process which occurs earlier in the storm as a result of sea level rise. Changes in water depth in these open water areas is the most important factor in determining the effect of sea level rise on storm surge in the Houston-Galveston region, and those effects are represented in the modeling performed with the static landscape representation. Changes in storm surge attributable to future changes in the landscape vegetation that might occur due to a sea level rise on the order of 2 ft are expected to be of secondary importance in generation of storm surge along the western shoreline of Galveston Bay. The work by ARCADIS (2011) seemed to indicate this as well, for this area.

Using peak water surface elevation fields from surge model simulations for both present-day and future sea level scenarios, a peak surge amplification factor was calculated in the same manner as was done by ARCADIS (2011). The amplification factor was computed for each grid node in the surge model domain as the difference between the maximum water surface elevation for the future SLR1 sea level scenario (a 2.4-ft sea level rise) and the maximum water surface elevation field for the present-day sea level scenario. To normalize the factor, the elevation difference was then divided by 2.4 ft. Therefore, at a particular location, an amplification

factor of 1.0 means that the peak surge response is linear, i.e., the maximum water surface elevation for the SLR1 sea level scenario is exactly 2.4 ft higher than the maximum water surface elevation for the present-day sea level scenario.

Amplification factors other than 1.0 indicate that there is a nonlinear response in peak storm surge at that location. For example, if the maximum water surface elevation at a location for the SLR1 scenario was 4.8 ft greater than the maximum water surface elevation for the present-day sea level scenario, the amplification factor would be 2.0.

Amplification factors greater than 1.0 indicate locations where the increases in maximum water surface elevation, between the two sea level scenarios, are greater than 2.4 ft. If the maximum water surface elevation for SLR1 was only 1.8 ft greater than the maximum water surface elevation for present day sea level, then the amplification factor would be 0.75.

Amplification factors less than 1.0 indicate locations where increases in maximum water surface elevation, between the two sea level scenarios, are less than 2.4 ft.

A series of simulations were made for Hurricane Ike and for the three proxy storms (10-yr, 100-yr and 500-yr); for both the present day sea level scenario (2008) and the SLR1 future sea level scenario (2085, which is 2.4 ft higher than present day sea level); for both the no-dike and with-extended dike conditions. The maximum water surface elevation fields for pairs of simulations, for SLR1 and present-day sea levels, were compared. The sequence of figures shown below for each storm have the following order:

- 1) *maximum water surface elevation field for no-dike conditions, with the present day (2008) sea level scenario*
- 2) *maximum water surface elevation field for no-dike conditions, with the SLR1 scenario*
- 3) *difference in maximum water surface elevation fields for the SLR1 and present-day sea level scenarios, for no-dike conditions (SLR1 minus present-day elevations)*
- 4) *peak surge amplification factor for no-dike conditions*

- 5) *maximum water surface elevation field for with-extended-dike conditions, with the present day (2008) sea level scenario*
- 6) *maximum water surface elevation field for with-extended-dike conditions, with the SLR1 scenario*
- 7) *difference in maximum water surface elevation fields for the SLR1 and present-day sea level scenarios, for with-extended-dike conditions (SLR1 minus present-day elevations)*
- 8) *peak surge amplification factor for with-extended-dike conditions*

Hurricane Ike Peak Surge for Present and Future Sea Levels

The No-dike condition

The group of four figures for Hurricane Ike, no-dike conditions, is shown in Figures 11-4 through 11-7. Figures 11-4 and 11-5 show the maximum water surface elevation fields for the two sea level scenarios, and Figure 11-6 shows the difference between the two. Figure 11-7 shows the amplification factor field. Valuable information about the response of storm surge to rising sea level can be gained by examining the amplification factor fields.

Areas in Figure 11-7 that are colored in white reflect those regions where the increase in storm surge between present-day sea level and the future sea level is approximately equal to the 2.4-ft increase in sea level. This is the linear response that would generally be expected for the deeper coastal waters in the open Gulf. The white areas appear to occur offshore, in the nearshore region that is further removed from the maximum storm surge zone, and in those areas where there is a transition in color from blue to yellow.

In the open Gulf coastal region north of Bolivar Roads, much of the shaded area is blue. This area coincides with the zone of highest peak surge, as seen in Figures 11-4 and 11-5. Amplification factors of 0.85 to 0.95 suggest that the peak surge values in this blue region for the future sea level scenario are 0.1 to 0.4 ft less than values for present-day sea level scenario, a fairly small difference.

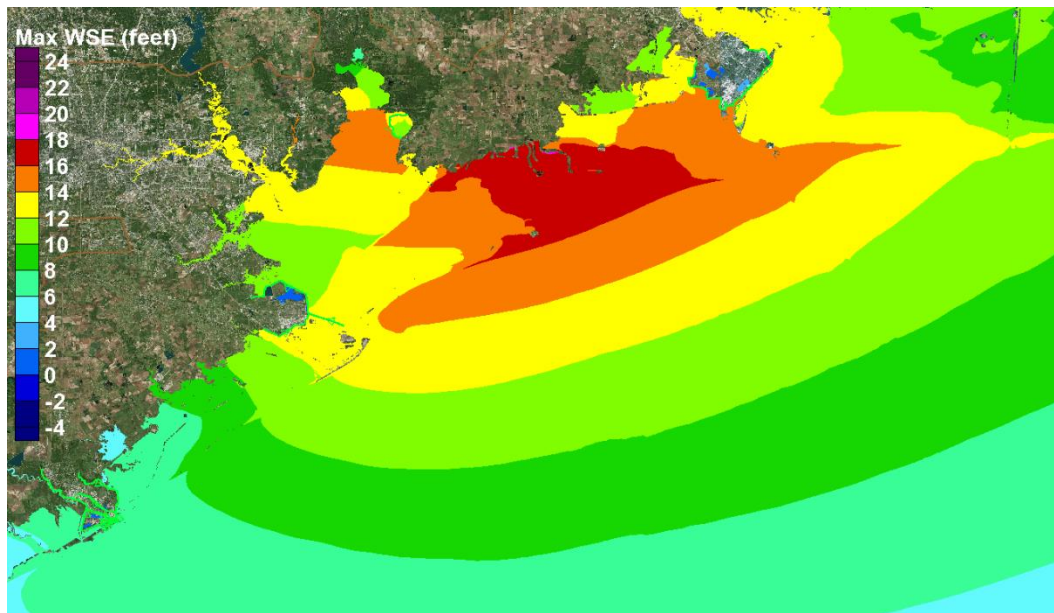


Figure 11-4. No-dike conditions. Hurricane Ike. Maximum water surface elevation field (in feet, NAVD88) for the present-day sea level scenario (+0.91 ft NAVD88)

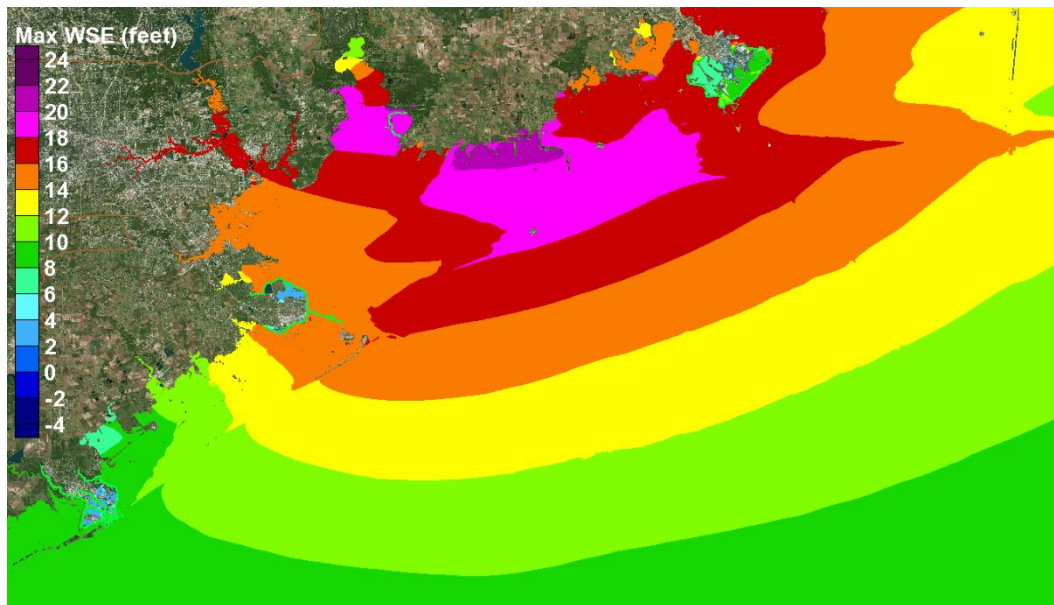


Figure 11-5. No-dike conditions. Hurricane Ike. Maximum water surface elevation field (in feet, NAVD88) for the future sea level scenario (SLR1, +3.31 ft NAVD88)

For the region located landward of the coastline and barrier islands, encompassing the interior bays and inundated wetlands, much of this area is colored in some shade of yellow or orange, i.e., amplification factors are greater than 1.05. Amplification factors along the western shoreline of Galveston Bay, from the City of Galveston to the upper reaches of the Houston Ship Channel range from 1.05 to 1.35 (these factors correspond to peak surge values that are 0.1 to 0.8 ft greater than the magnitude of sea

level increase, 2.4 ft). The nonlinear surge response associated with sea level rise exacerbates flooding in the key areas where flood risk reduction is desired.

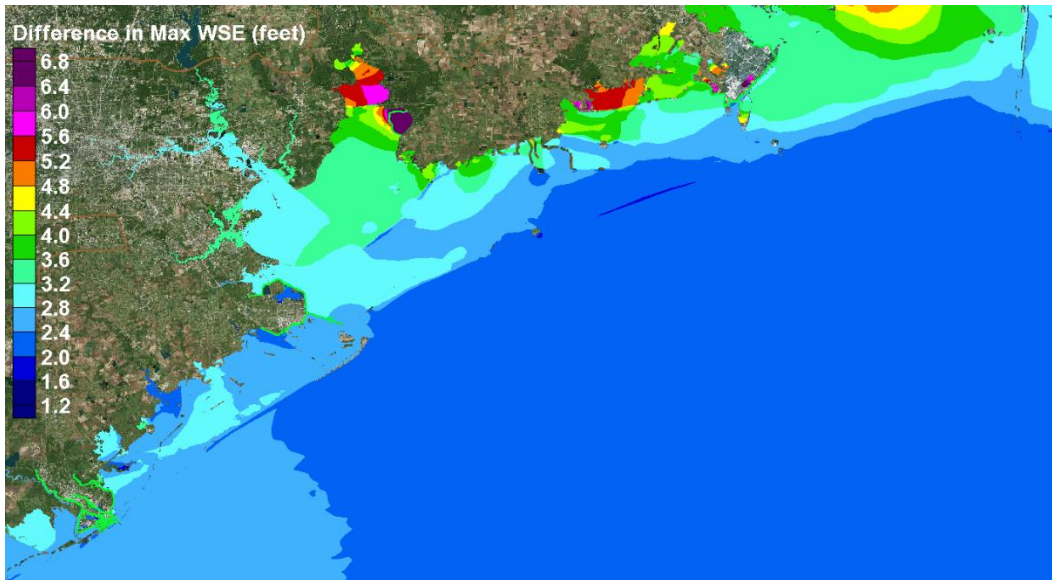


Figure 11-6. No-dike conditions. Hurricane Ike. Change in maximum water surface elevation (wse) fields. Maximum wse for the SLR1 future sea level scenario minus the maximum wse for the present-day sea level scenario.

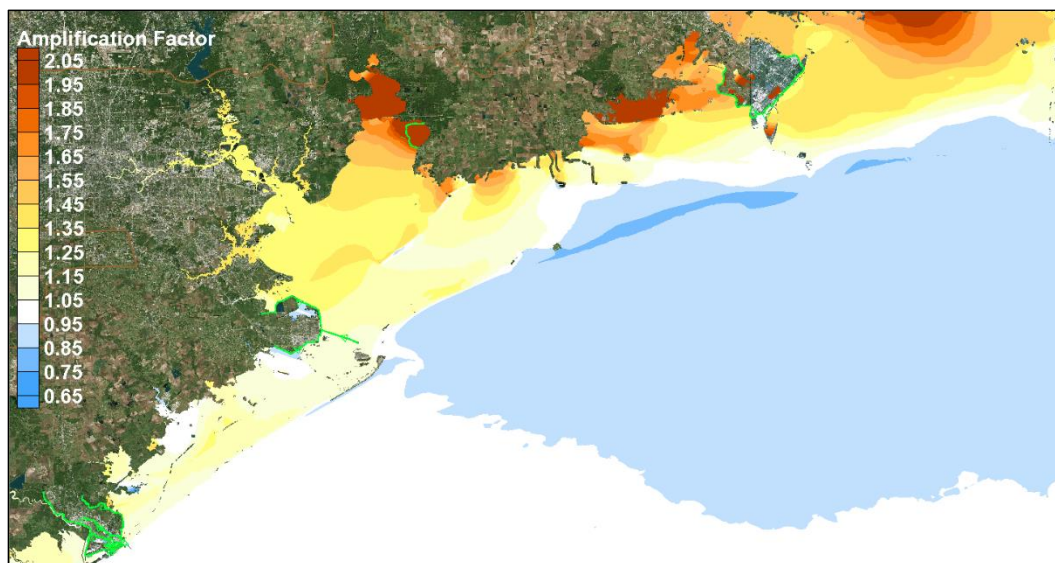


Figure 11-7. No-dike conditions. Hurricane Ike. Peak surge amplification factor.

This overall color pattern of blue offshore and yellow inland was hypothesized by ARCADIS (2011) to be the result of a net movement, or flux, of water from the near coastal region into the interior region as a result of the sea level increase. ARCADIS (2011) attributed this net inland flux of water, in part, to the reduction in bottom frictional resistance, as a result of changes to the landscape as sea level rises. The reduction in frictional resistance makes it easier for storm surge to be pushed inland.

Peak surge amplification factors throughout the region shown in Figure 11-7 are quite similar to the pattern of amplification factors shown in the work by ARCADIS (2011), particularly for their 2100 sea level scenario (a 3-ft rise) which is the more similar of the two sea level scenarios they considered to the one considered here. The areas of highest nonlinear surge amplification seen in Figure 11-7 are identical to those seen in the ARCADIS (2011) result for Hurricane Ike. The similarity in amplification patterns and magnitudes of the amplification factors between the ARCADIS (2011) results and those shown in Figure 11-7 suggests that a reasonable estimate of the effect of sea level rise on storm surge can be obtained in the western Galveston Bay region without considering the effects of sea level rise on the landscape itself. Reasons for the adequacy of the static landscape approach were discussed previously.

The With-dike condition

The group of four figures for Hurricane Ike, for with-dike conditions, is shown in Figures 11-8 through 11-11. Figures 11-8 and 11-9 show the maximum water surface elevation fields for the two sea level scenarios, and Figure 11-10 shows the difference between the two. Figure 11-11 shows the amplification factor field for this case.

Figure 11-11 shows the same blue region offshore that was seen for the no-dike case in Figure 11-7; however, the lighter blue region in the with-dike case is slightly larger than that seen for the no-dike case. The area having the darker blue shade is larger in Figure 11-11 than that seen in Figure 11-7. Following the hypothesis developed by ARCADIS (2011) based on their results for the no-dike case, that the blue region is due to a net flux of water from the open coast to inland areas, then a larger lighter and darker blue area would suggest a greater flux of water moving from offshore to the inland areas for the with-dike case compared to the no-dike case.

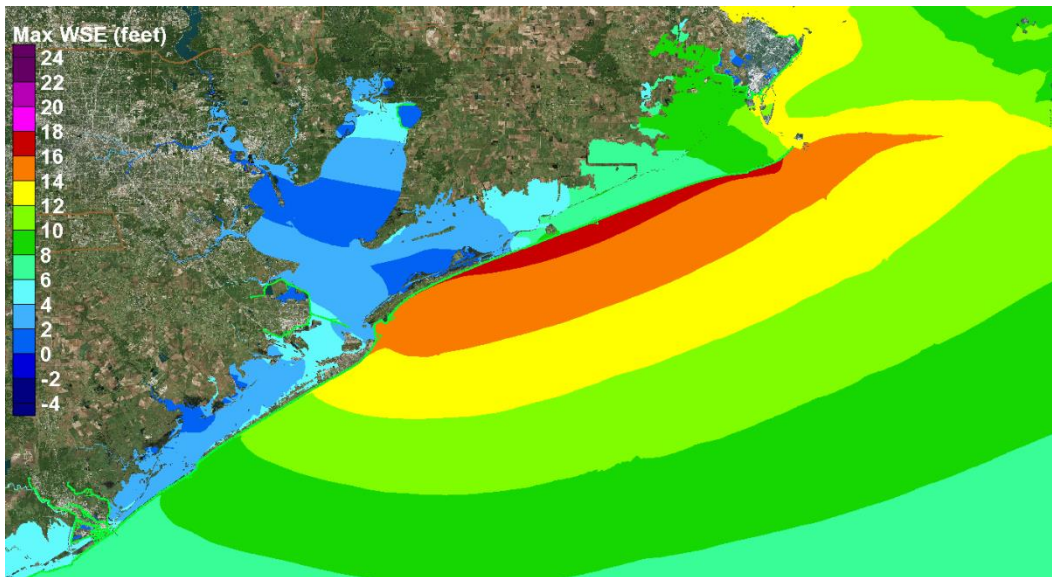


Figure 11-8. With-extended-dike conditions. Hurricane Ike. Maximum water surface elevation field (in feet, NAVD88) for the present-day sea level scenario (+0.91 ft NAVD88).

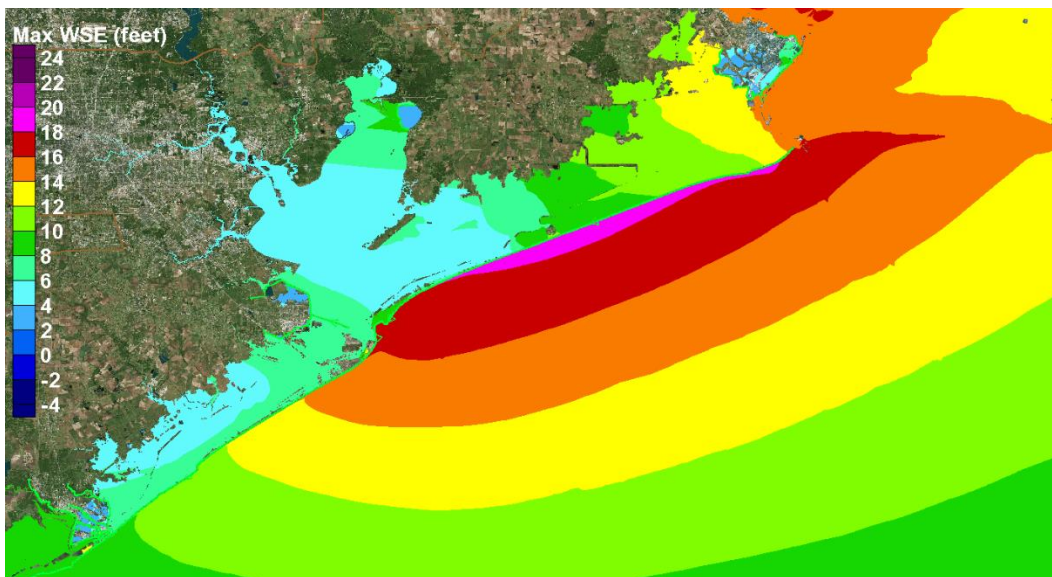


Figure 11-9. With-extended-dike conditions. Hurricane Ike. Maximum water surface elevation field (in feet, NAVD88) for the future sea level scenario (SLR1, +3.31 ft NAVD88).

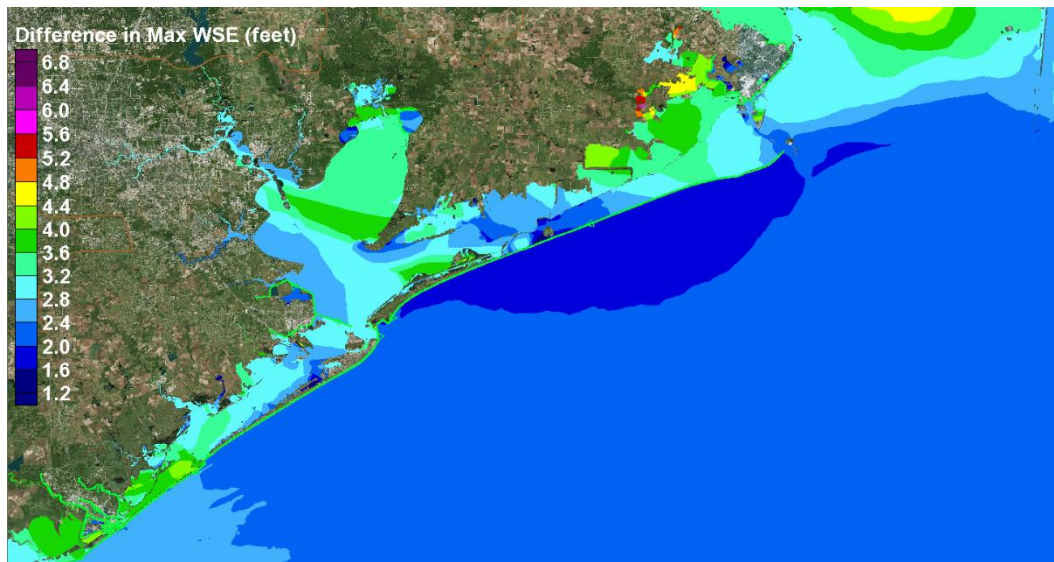


Figure 11-10. With-extended-dike conditions. Hurricane Ike. Change in maximum water surface elevation (wse) fields. Maximum wse for the SLR1 future sea level scenario minus the maximum wse for the present-day sea level scenario.

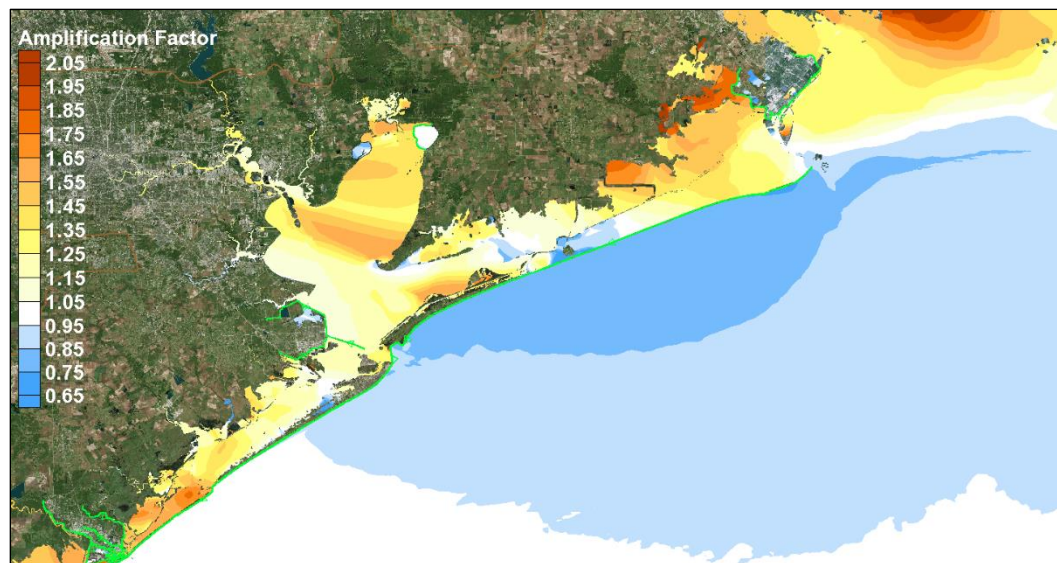


Figure 11-11. With-extended-dike conditions. Hurricane Ike. Peak surge amplification factor.

However the presence of the dike must drastically limit this flux of water from offshore to the inland areas. This result suggests that the blue-shaded region offshore, having amplification factors less than 0.95, is not primarily due to a net inland flux of water.

It seems more likely that the blue region offshore is primarily due to a reduction in the effective wind stress. As sea level increases, the water depth increases, which in turn leads to slight reduction in effective wind

stress. A wind stress decrease would manifest itself in the blue region, due to a lower shear stress piling water against the coastline or against the dike in this case. There is another factor that leads to increased water depth seaward of the dike. With the dike in place, the long-dike effect leads to greater surges on the Gulf side of the dike, which also contribute to a greater water depth. The long-dike effect appears to be the primary contributor to the larger dark blue region shown in Figure 11-11, compared to size of the darker blue region seen in Figure 11-7.

Figure 11-11 shows widespread occurrence of amplification factors greater than 1.0 in areas landward of the dike. What is the source of water that leads to these amplification factors, with the dike in place? The coastal surge, including enhancement of the surge due to the long-dike effect, leads to overflow of the dike, which would be one source. Also, the open coast surge for Ike leads to a strong gradient in water surface elevation at the northeast terminus of the dike. The track of Ike, which crossed Bolivar Peninsula, leads to an open coast surge of 16 ft or more at Sabine Pass. Note that although the dike extends to Sabine Pass, it is not terminated into higher ground elevation. So the large water surface elevation gradient at the eastern end of the dike, drives water toward the west, on the landward side of the dike. Prior to the time of peak surge, the combination of the sea level increase and the large surge forerunner that occurred during Ike also likely contribute to the flanking flow around the eastern terminus of the dike. Water that flanks the dike moves over a less frictionally resistant, inundated, landscape and into Galveston Bay, and, from there, into West Bay and Trinity Bay. These two sources of water, flow over the dike and flanking flow, are apparently enough to offset any effect of reduced wind stress in the bays.

The relative magnitude of both sources of water is unknown. Figure 11-9 suggests that flanking flows are the dominant source, in light of the following: the expanse of the inundated area behind the dike and the gentle slope of the water surface elevation gradient, together with the limited time during the storm (a few hours at most), only near the time of peak surge, that flow over the dike would occur. The duration of flow over the dike is expected to be much less than the duration of flanking flow; and therefore the volume of the overflow source is expected to be much less than the volume of flanking source. A well-terminated dike, tied into ground having an elevation comparable to that of the dike crest, would

drastically reduce or eliminate the flanking flow. However, the lesser quantity of flow over the dike would still occur.

These results for the with-dike case suggest that, for the no-dike case, the prevalence of amplification factors greater than 1.0 in the interior areas are due to earlier overtopping of the barrier islands and to flows moving from northeast to southwest over the inundated landscape. The northeast-to-southwest flows are due to the prevailing counter-clockwise circulating wind fields, and the flows to the southwest are further enhanced by reduced bottom frictional resistance, also noted by ARCADIS (2011).

Summary of Hurricane Ike Peak Surge for Present and Future Sea Levels

Approximate peak storm surge values at a number of key locations, in feet relative to NAVD88, are given in Table 11-1, for the Hurricane Ike simulations. Values are given for both sea level scenarios, and for both no-dike and with-dike conditions. Surge values are estimated from the figures, to the nearest half foot.

Table 11-1. Peak storm surge values for Hurricane Ike (feet, NAVD88), for present-day and SLR1 (+2.4 ft) sea level scenarios

Location	No-dike conditions		With-dike conditions	
	Present	SLR1	Present	SLR1
City of Galveston (Gulf side)	13	15	14	16
City of Galveston (bay side)	13	15	4.5	7
Galveston Island (mid-way)	10.5	13	4	6.5
Bolivar Peninsula (mid-way)	14	17.5	2	5.5
Texas City (south)	12	14	4	6.5
Texas City (east)	12	14.5	4	6.5
Dickinson Bay entrance	11.5	14	3.5	6
Clear Lake entrance	11.5	14.5	2.5	5
Morgan's Point	13	16	2	5
Upper Houston Ship Channel	13.5	16.5	2.5	5

Hurricane Ike was a major hurricane for the Houston-Galveston region. In terms of storm surge generation, it was the worst storm in the region since the devastating 1900 Hurricane, a period of 108 years. The Ike Dike coastal spine concept provides considerable flood risk reduction

throughout the region, for both present-day and the future sea level rise scenario. Considering those locations in Table 11-2 that are inland of the dike, the average surge suppression for the present-day sea level is 9 ft (average peak surge of 12 ft without the dike; 3 ft with the dike), and for the future sea level the average surge suppression is 9 ft (average peak surge of 15 ft without the dike; 6 ft with the dike). These are substantial reductions. Even with the 2.4-ft sea level rise which will, in general, increase the risk of flooding, the presence of the dike greatly reduces coastal flooding for a storm of this magnitude to relatively low levels. A significant attribute of the coastal spine concept is that it provides surge suppression and flood risk reduction benefits for the entire region that is lies behind it.

Storm 535 (10-yr Proxy Storm) Peak Surge for Present and Future Sea Levels

The No-dike condition

The group of four figures for Storm 535, for no-dike conditions, is shown in Figures 11-12 through 11-15. Figures 11-12 and 11-13 show the maximum water surface elevation fields for the two sea level scenarios, and Figure 11-14 shows the difference between the two. Figure 11-15 shows the peak surge amplification factor field for this case, which facilitates examination of any nonlinear surge response to rising sea level.

Figure 11-15 shows a light blue-shaded region offshore, which is characterized by peak surge amplification factors that are less than 1.0, similar to that seen for Hurricane Ike. Compared to Ike, the center of the light blue region is displaced to the southwest. In terms of its alongshore extent, the most pronounced blue region is centered near Bolivar Roads. This location corresponds to the zone of maximum surge, as seen in Figures 11-12 and 11-13. Storm 535, and the other proxy storms, make landfall approximately at the south end of Galveston Island, near San Luis Pass, which places the zone of maximum winds approximately at Bolivar Roads. The zone of maximum surge occurs where the zone of maximum winds occurs. Both the presence of the light blue region, with amplification factors between 0.85 and 0.95, and its location, which is well correlated with the position of the zone of maximum winds, reinforce the thought that this feature is attributed to the reduction in the effective wind stress associated with elevated mean sea level. The expanse of the light blue region is smaller for this storm than it was for Hurricane Ike.

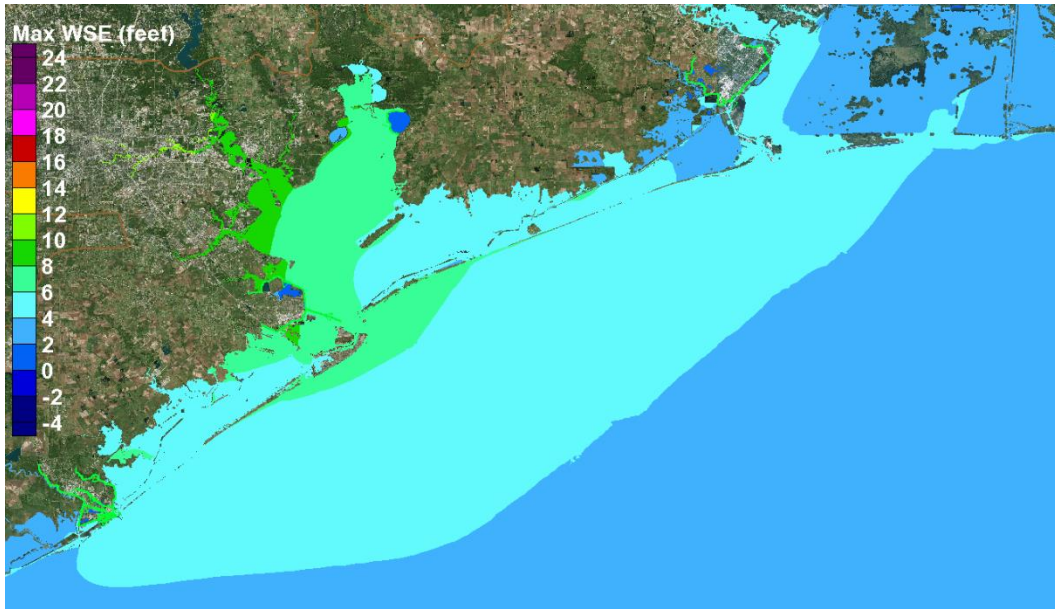


Figure 11-12. No-dike conditions. Storm 535 (10-yr proxy). Maximum water surface elevation field (in feet, NAVD88) for the present-day sea level scenario (+0.91 ft NAVD88)

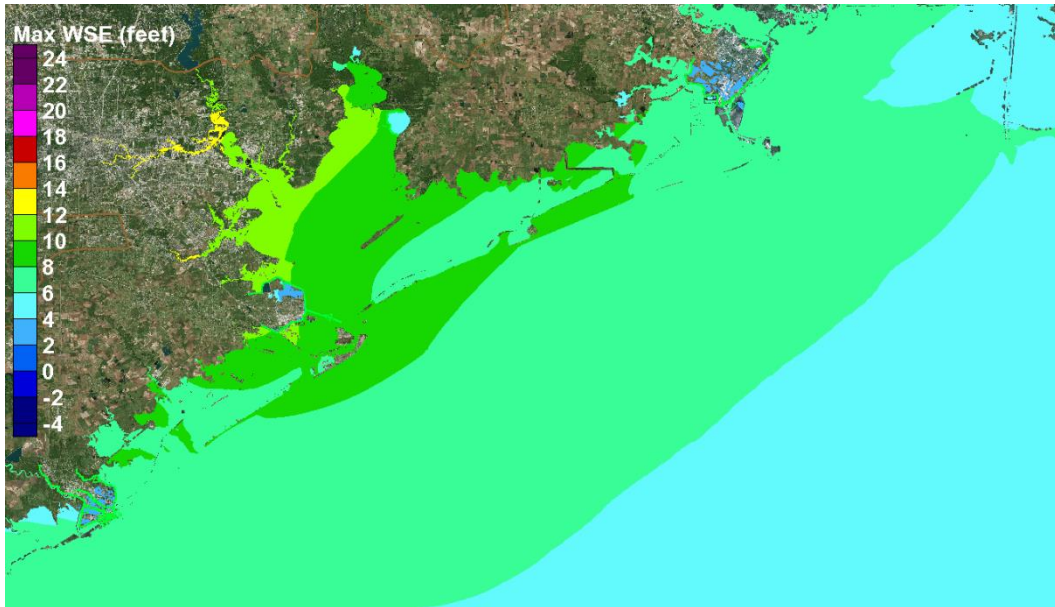


Figure 11-13. No-dike conditions. Storm 535 (10-yr proxy). Maximum water surface elevation field (in feet, NAVD88) for the future sea level scenario (SLR1, +3.31 ft NAVD88)

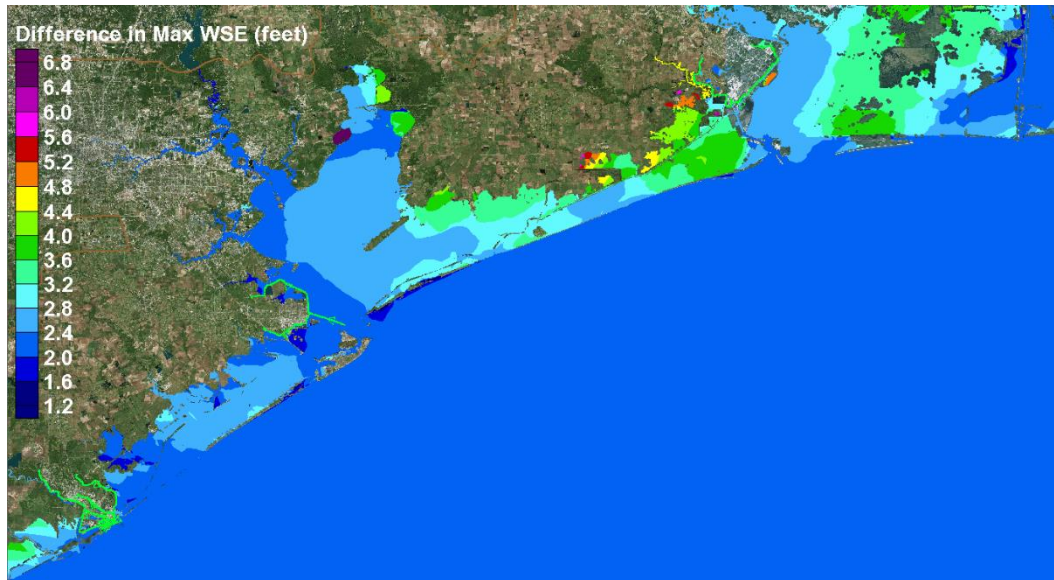


Figure 11-14. No-dike conditions. Storm 535 (10-yr proxy). Change in maximum water surface elevation (wse) fields. Maximum wse for the SLR1 future sea level scenario minus the maximum wse for the present-day sea level scenario.

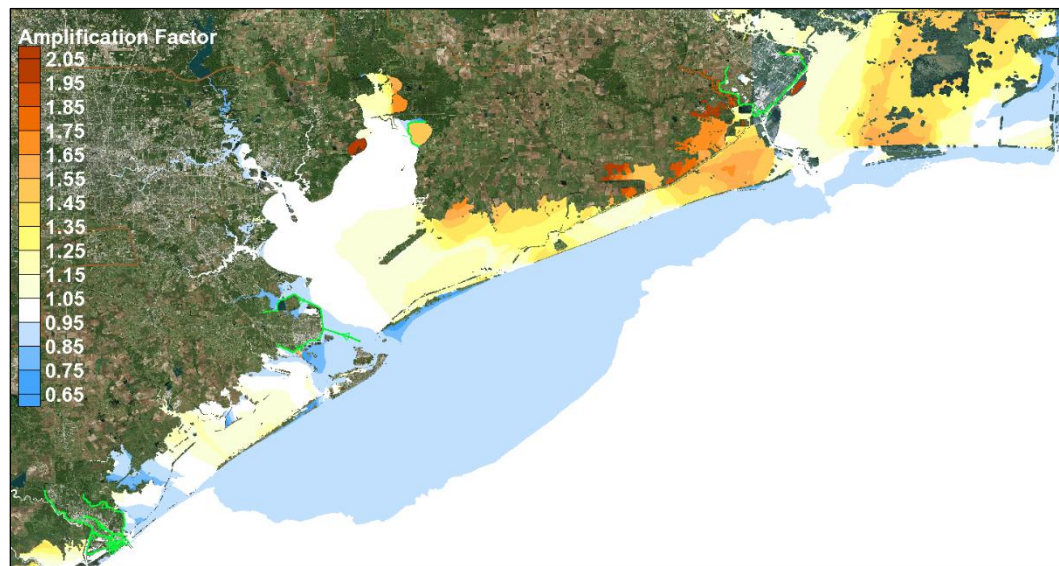


Figure 11-15. No-dike conditions. Storm 535 (10-yr proxy). Peak surge amplification factor.

This is attributed to the lower wind speeds for this storm, which produce smaller water surface elevation gradients and lower peak surges.

The areas where amplification factors are much greater than 1.0, the darker yellow and orange shaded regions, are primarily confined to the inundated wetland areas north and northeast of Bolivar Peninsula, including the easternmost parts of Galveston Bay. The peak surges at the

coast for this storm are significantly less than those for Hurricane Ike, so there is much less water flow over the barrier islands. The effect of reduced bottom friction on these flows is also less significant, in terms of enhancing water movement over the islands and into Galveston Bay. Wind speeds are less for this storm, as well, compared to Ike, which creates a slower northeast-to-southwest movement of water through the inundated wetlands. Reduced speeds of alongshore moving water diminishes the enhancement of flow arising from a reduced effective bottom shear stress. These factors appear to result in less water moving into Galveston Bay from the northeast through the inundated wetlands.

Along the western shoreline of Galveston Bay, from the City of Galveston extending all the way to the north along the bay shoreline and into the upper reaches of the Houston Ship Channel, amplification factors are less than or equal to 1.0 (light blue areas). Factors are significantly less than 1.0 in a number of areas, shown in darker blue. For this storm track, which all the proxy storms follow, winds will be blowing from northeast to southwest as the hurricane approaches landfall, acting to set down the water surface on the eastern side of Galveston Bay and setting up the water surface on the western side of the bay. After landfall, winds will begin to shift and blow toward the north, driving surge into the upper reaches of the ship channel and the northern part of the bay. Amplification factors less than 1.0 along the western bay shoreline and in the northern periphery of the bay and ship channel reflect the reduction in effective wind stress arising from greater water depths in the bay, which are associated with the sea level increase. As discussed previously, the reduced effective wind stress is expected to be greater in the shallow bays than along the open coast. The prevalence of this amplification factor pattern attributed to reduced effective wind stress is not masked by the movement of water into the bay from the northeast and over the barrier islands, as it appeared to be for Hurricane Ike.

The With-dike condition

The group of four figures for with-dike conditions, for Storm 535, are shown in Figures 11-16 through 11-19. Figures 11-16 and 11-17 show the maximum water surface elevation fields for the two sea level scenarios, and Figure 11-18 shows the difference between the two. Figure 11-19 shows the amplification factor field for this case.



Figure 11-16. With-extended-dike conditions. Storm 535 (10-yr proxy). Maximum water surface elevation field (in feet, NAVD88) for the present-day sea level scenario (+0.91 ft NAVD88).

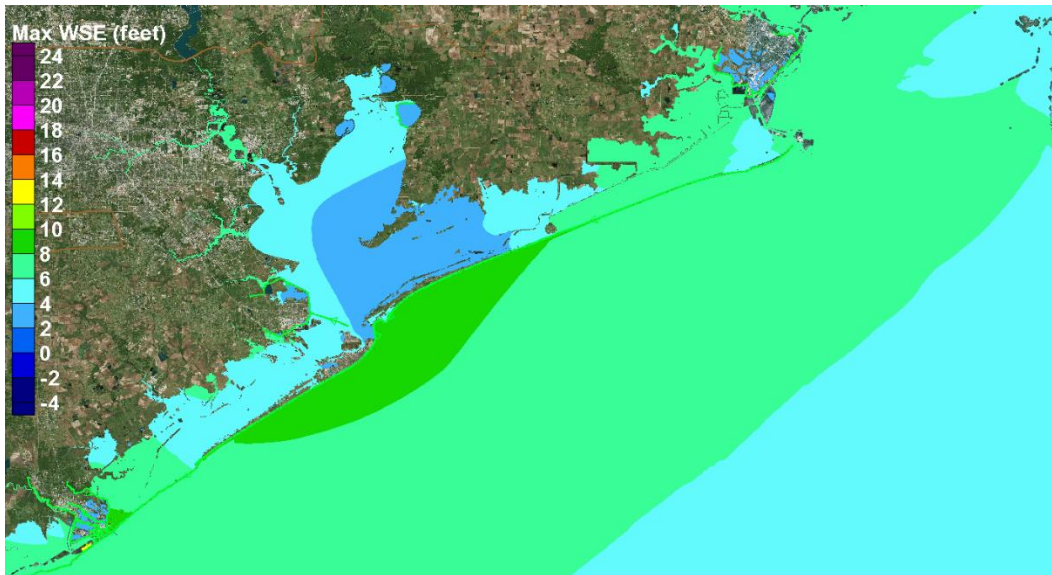


Figure 11-17. With-extended-dike conditions. Storm 535 (10-yr proxy). Maximum water surface elevation field (in feet, NAVD88) for the future sea level scenario (SLR1, +3.31 ft NAVD88).

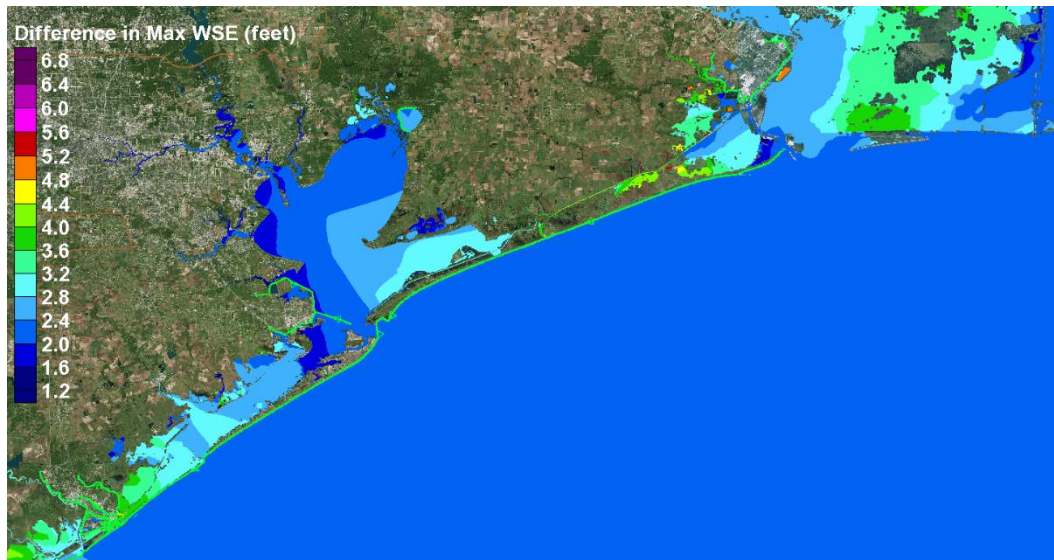


Figure 11-18. With-extended-dike conditions. Storm 535 (10-yr proxy). Change in maximum water surface elevation (wse) fields. Maximum wse for the SLR1 future sea level scenario minus the maximum wse for the present-day sea level scenario.

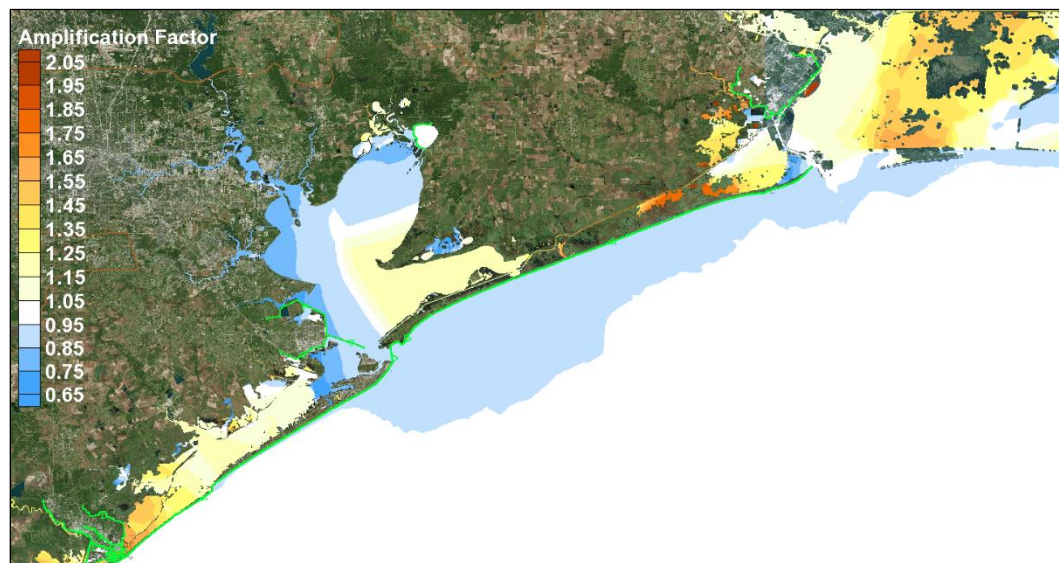


Figure 11-19. With-extended-dike conditions. Storm 535 (10-yr proxy). Peak surge amplification factor.

Figure 11-19 shows the light blue-shaded blue region offshore, as was seen for the no-dike case in Figure 11-15. The long-dike effect is less for less-intense storms, i.e., lower peak surges, so the amplification fields are expected to be nearly the same for the no-dike and with-dike cases, and the same sea level.

For this lower-intensity storm, the sources of water flowing into Galveston Bay are limited by the presence of the dike. No water is entering the bay

system by flowing over the coastal dike, for either the present-day sea level scenario or the future sea level scenario. The only water being introduced into Galveston Bay for the present-day sea level is through the intercostal waterway, driven by the elevated storm surge that exists at the northeastern end of the unterminated coastal dike. There is no large expanse of inundated wetlands behind the dike as there was for Hurricane Ike (see Figure 11-16).

However, for the future sea level scenario (Figure 11-17), there is much more flanking taking place around the northeast end of the dike, and subsequently more movement of water toward the southwest on the inland side of the dike. More water is entering Galveston Bay for the future sea level scenario, compared to the present-day sea level scenario.

Peak surge amplification factors in West Bay are generally greater than 1.0; and, they are much greater than 1.0 in the western end of West Bay. Since there is no flow over the dike, this highly nonlinear surge response at the west end is attributed to water moving through the inundated wetlands behind the dike, due to flanking of its northeast and flow through the Inter-coastal Waterway. For the future sea level scenario, the reduced effective bottom shear stress enhances water movement to the southwest, and it leads to much greater accumulation of that water in the west end of West Bay, compared to the present-day sea level scenario. This area is the farthest downwind area in the combined Galveston-West Bay system for the prevailing wind direction that exists prior to landfall; i.e., winds from the northeast. Water introduced into Galveston Bay tends to move in that direction under the influence of the prevailing winds. However, note that an effective dike termination scheme on its northeast end, tying the dike into a higher ground elevation, would effectively eliminate these flanking flows.

In Galveston Bay the pattern of the amplification factors clearly shows the signature of reduced effective surface wind stress, first apparent on the western side of the bay, which is the downwind side for the prevailing wind direction prior to landfall. The signature also is apparent in the northern parts of the bay, which is the downwind side for the prevailing winds after landfall.

Summary of Storm 535 Peak Surge for Present and Future Sea Levels

Approximate peak storm surge values at the key locations, in feet relative to NAVD88, are given in Table 11-2, for the four Storm 535 simulations. Values are given for both sea level scenarios, and for both no-dike and with-dike conditions. Surge values are estimated from the figures, to the nearest half foot.

Table 11-2. Peak storm surge values for Storm 535, the 10-yr proxy storm, (feet, NAVD88), for present-day and SLR1 (+2.4 ft) sea level scenarios

Location	No-dike conditions		With-dike conditions	
	Present	SLR1	Present	SLR1
City of Galveston (Gulf side)	6.5	9	6.5	9
City of Galveston (bay side)	6.5	9	2	4.5
Galveston Island (mid-way)	5	7.5	2	5
Bolivar Peninsula (mid-way)	5	7.5	1	3.5
Texas City (south)	8	10	3.5	6
Texas City (east)	7	9.5	3.5	5.5
Dickinson Bay entrance	8	10.5	4	6
Clear Lake entrance	8.5	11	4	6
Morgan's Point	8.5	11	4	6
Upper Houston Ship Channel	10	13	5	7

While Storm 535 is a less intense hurricane, some flood damage would be expected for the no-dike surge levels, particularly with the 2.4-ft sea level rise. The Ike Dike coastal spine concept provides flood risk reduction for the Houston-Galveston region, for both present-day and the future sea level rise scenario. Considering the locations that are inland of the dike, the average surge suppression for the present-day sea level is 4 ft (average peak surge of 7 ft without the dike; 3 ft with the dike), and for the future sea level the average surge suppression is approximately 4 ft (average peak surge of 10 ft without the dike; 6 ft with the dike). The greatest surge suppression benefits for this storm are in the northwest parts of the system, with reductions of 6 ft in the upper reaches of the Houston Ship Channel.

Storm 033 (100-yr Proxy Storm) Peak Surge for Present and Future Sea Levels

The No-dike condition

The group of four figures for Storm 033, the 100-yr proxy storm, no-dike conditions, is shown in Figures 11-20 through 11-23. Figures 11-20 and 11-21 show the maximum water surface elevation fields for the two sea level scenarios, and Figure 11-22 shows the difference between the two. Figure 11-23 shows the amplification factor field.

The amplification factor field for Storm 033 is quite similar to that for Hurricane Ike (compare Figures 11-23 and 11-7). In the open Gulf, much of the shaded area is light blue, which is caused by the reduction in effective wind stress resulting in a slightly less open coast storm surge. For the region that is located landward of the coastline and barrier islands, encompassing the interior bays and inundated wetlands, much of this area is colored in some shade of yellow or orange, i.e., amplification factors are greater than 1.05. Amplification factors along the western shoreline of Galveston Bay, from the City of Galveston to the upper reaches of the Houston Ship Channel range from 1.05 to 1.45. There are a few areas northeast of Galveston Bay and in Trinity Bay where amplification factors are approaching 2.0 (darker orange) or are greater than 2.0 (red), as was the case for Hurricane Ike (see Figure 11-7). These occur in the same places, and are strikingly similar to, areas having high amplification factors for Ike.

The close match in peak surge amplification factors between Storm 033 and Hurricane Ike suggests that the same processes are at work, in a similar manner, for both hurricanes. The large area having amplification factors greater than 1.05 indicates that the elevated sea level is causing more water to enter the interior bay systems and the interior wetlands, than occurs for the present day sea level. The increase in water in inland areas is attributed to the following processes: 1) earlier onset of flow over the barrier islands, enhanced by the reduction in effective bottom shear stress associated with deeper water; and 2) north-east to southwest movement of water in the inundated wetlands, which is also enhanced by the reduction in effective bottom shear stress associated with greater depths of inundation. The northeast-southwest movement of water arises due to the prevailing winds from the northeast that are characteristic of the counterclockwise rotating wind fields around the hurricane's eye, prior

to landfall. The maximum storm surge values along the coastline for Storm 033, 16 to 17 ft, are similar to those computed for Hurricane Ike, which lends some support to the similarity in surge amplification patterns.

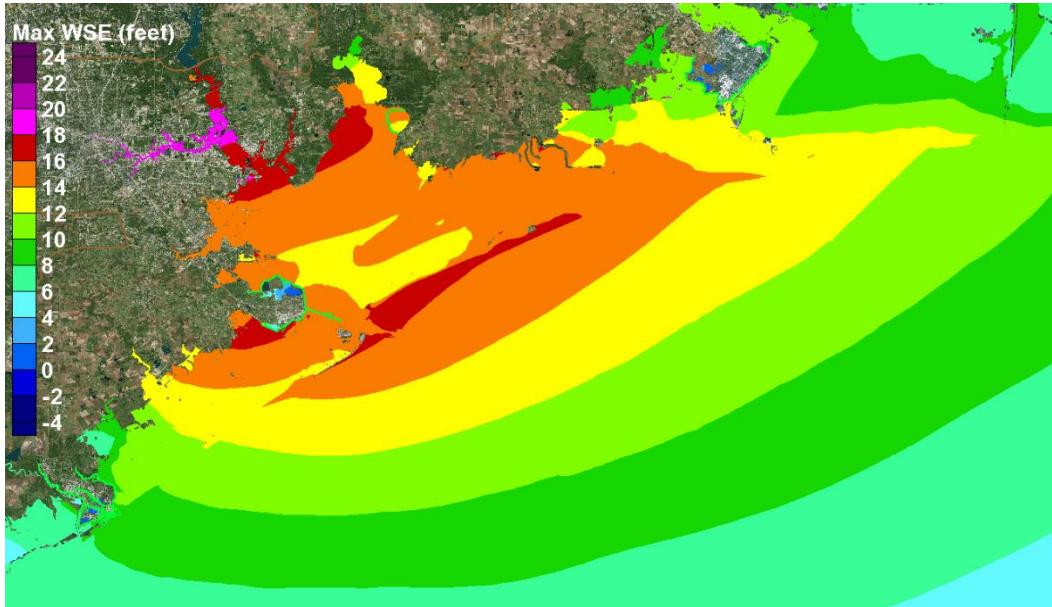


Figure 11-20. No-dike conditions. Storm 033 (100-yr proxy). Maximum water surface elevation field (in feet, NAVD88) for the present-day sea level scenario (+0.91 ft NAVD88)

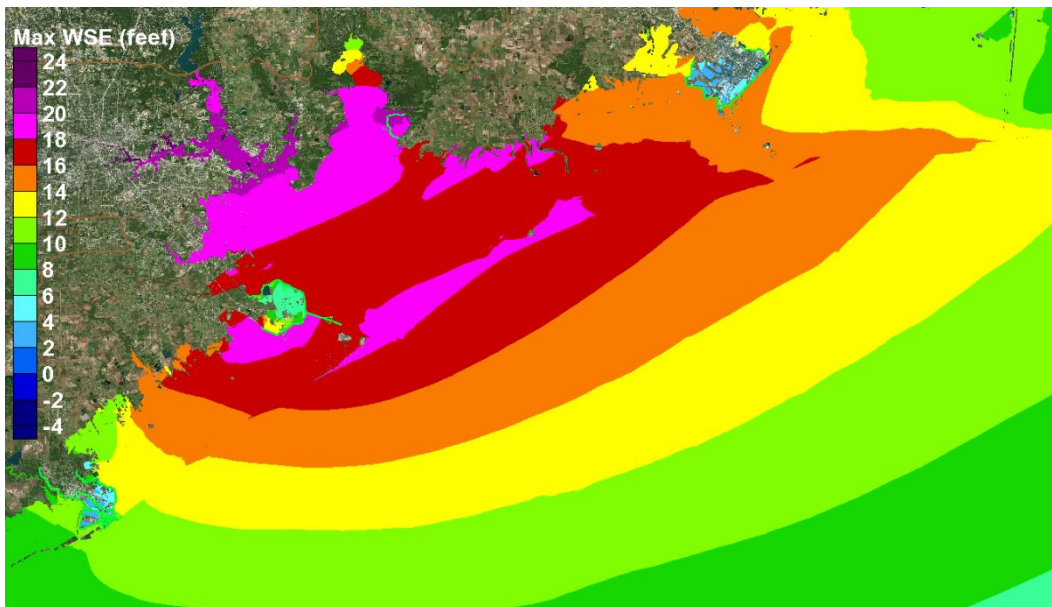


Figure 11-21. No-dike conditions. Storm 033 (100-yr proxy). Maximum water surface elevation field (in feet, NAVD88) for the future sea level scenario (SLR1, +3.31 ft NAVD88)

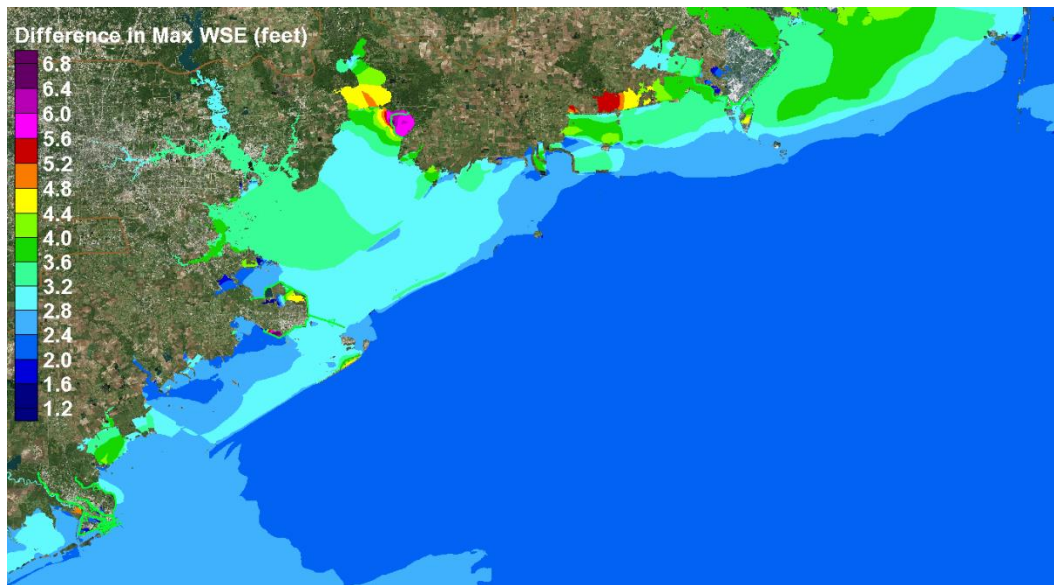


Figure 11-22. No-dike conditions. Storm 033 (100-yr proxy). Change in maximum water surface elevation (wse) fields. Maximum wse for the SLR1 future sea level scenario minus the maximum wse for the present-day sea level scenario.

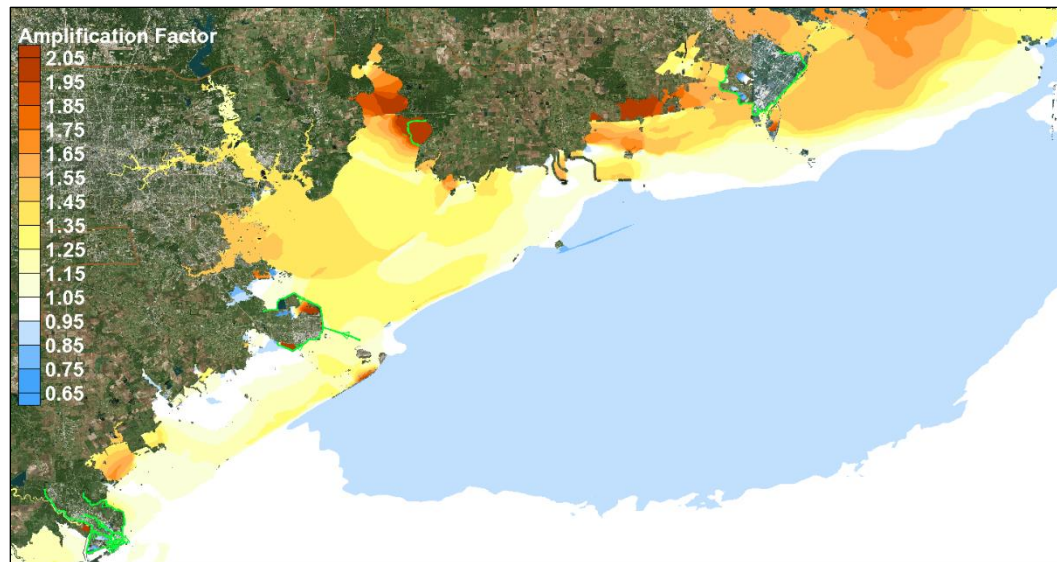


Figure 11-23. No-dike conditions. Storm 033 (100-yr proxy). Peak surge amplification factor.

The With-dike condition

The group of four figures for Storm 033, for with-dike conditions, is shown in Figures 11-24 through 11-27. Figures 11-24 and 11-25 show the maximum water surface elevation fields for the two sea level scenarios, and Figure 11-26 shows the difference between the two. Figure 11-27 shows the amplification factor field for this case.

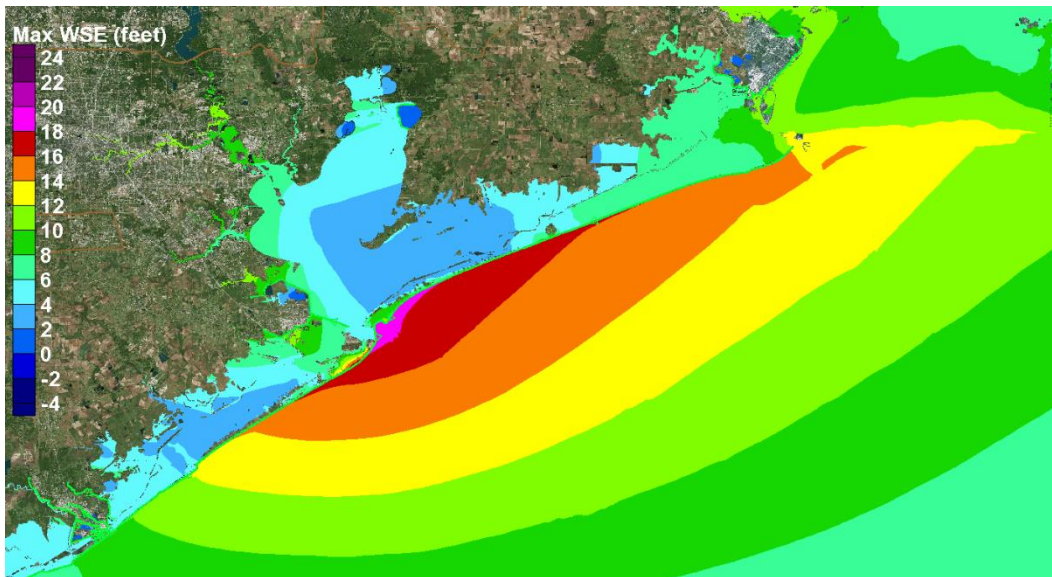


Figure 11-24. With-extended-dike conditions. Storm 033 (100-yr proxy). Maximum water surface elevation field (in feet, NAVD88) for the present-day sea level scenario (+0.91 ft NAVD88).

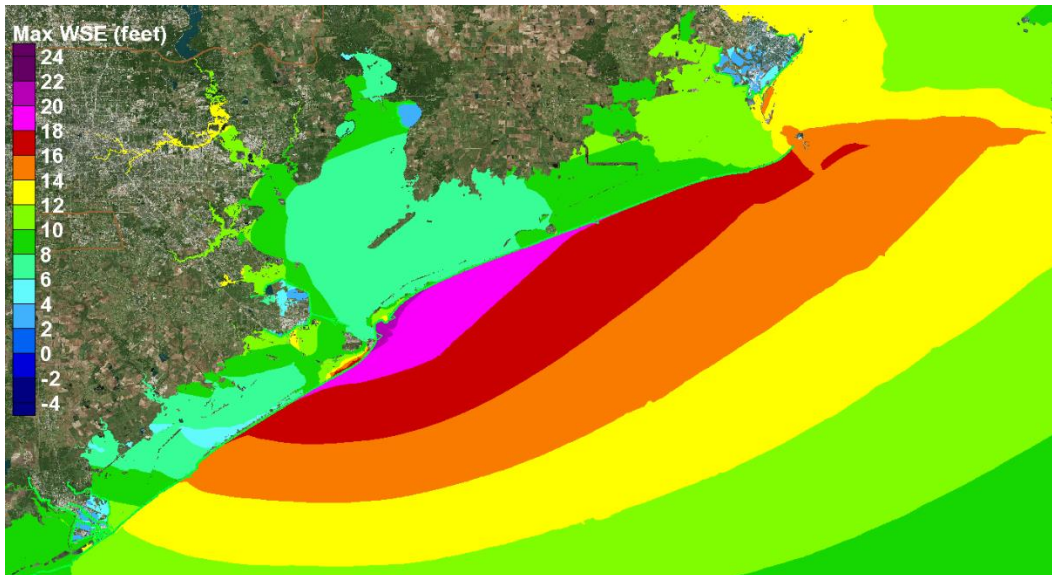


Figure 11-25. With-extended-dike conditions. Storm 033 (100-yr proxy). Maximum water surface elevation field (in feet, NAVD88) for the future sea level scenario (SLR1, +3.31 ft NAVD88).

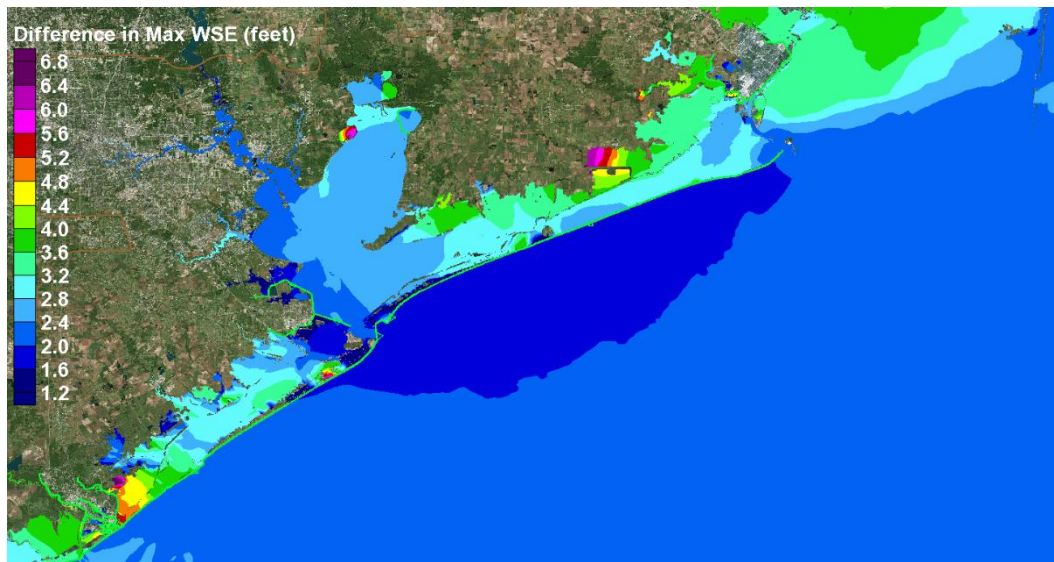


Figure 11-26. With-extended-dike conditions. Storm 033 (100-yr proxy). Change in maximum water surface elevation (wse) fields. Maximum wse for the SLR1 future sea level scenario minus the maximum wse for the present-day sea level scenario.

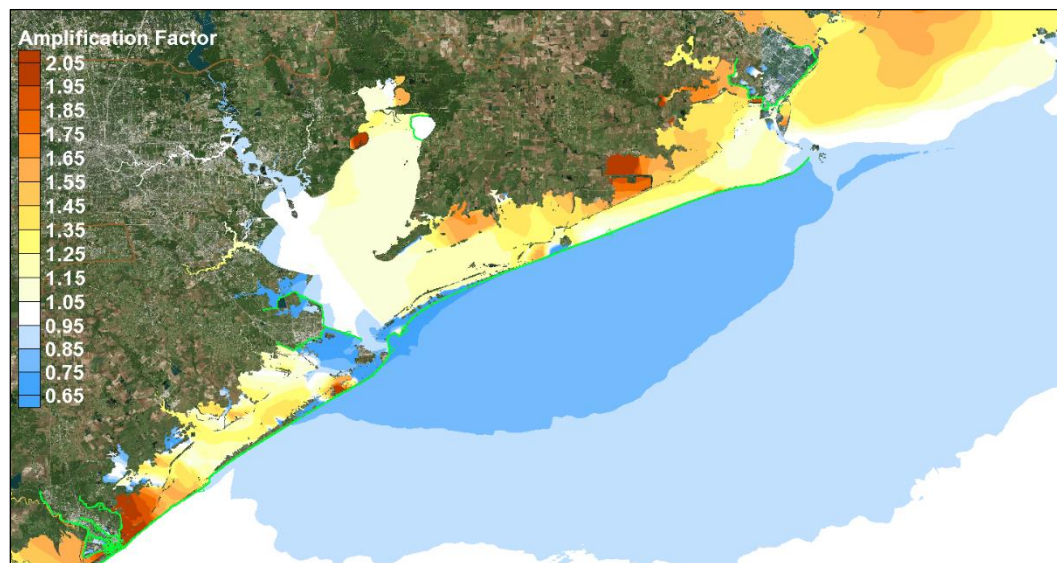


Figure 11-27. With-extended-dike conditions. Storm 033 (100-yr proxy). Peak surge amplification factor.

With the dike in place, in the open Gulf, the surge amplification factor field for Storm 033 is similar to Hurricane Ike (compare Figures 11-27 and 11-11). The shaded blue areas for Storm 033 are shifted to the southwest compared to the shaded areas for Ike. The shift is due to the difference in storm track for the two hurricanes. The track for Storm 033 is shifted 30 to 35 miles to the southwest compared to the track for Ike.

Inside the dike, surge amplification in areas to the northeast of Galveston Bay is similar to amplification for Hurricane Ike in the same areas. Excluding the surge amplification within Galveston Bay, the area to the northeast of Galveston Bay appears to have slightly higher surge amplification for Storm 033, compared to Ike. However, including the surge amplification within Galveston Bay, the amount of surge enhancement is higher for Ike. A higher volume of water in this area for Ike is attributed to higher surge at the northeast end of the dike, compared to Storm 033, driving more flanking flow.

In West Bay, the surge amplification is slightly greater for Storm 033, particularly at the westernmost end of the bay. This is attributed to the slightly higher peak surge in the vicinity of Bolivar Roads for Storm 033 compared to the peak surge in this same area for Hurricane Ike, and resulting higher volume of flow over the dike which occurs there for Storm 033. The amount of overflow at Bolivar Roads is much greater than any amount that might be occurring for Hurricane Ike at this location. The volume of water that flows over the dike in this area is pushed to the west into West Bay by the prevailing winds prior to, and at, landfall. The water ends up at the western end of the bay.

Within Galveston Bay, the amplification factor field for Storm 033 is different from Hurricane Ike. The field for Storm 033 is more similar to that for Storm 535. This is attributed the difference in track and wind fields between Ike and the proxy storms. There is a difference in water volume associated with flanking flow (greater for Ike). Eventually, that water moves first to the southwest through the inundated interior area and then to the north, ending up in the north part of Galveston Bay and Trinity Bay after the storm moves through and winds are predominantly from the southwest and south.

Amplification factors along the western shoreline of Galveston Bay show the signature of a reduced effective shear stress, as was seen for Storm 535 (see Figure 11-19). In Galveston Bay, the presence of the dike greatly reduces, and eliminates in most places, the nonlinear surge amplification that occurs for the no-dike conditions in Galveston Bay, by eliminating earlier flow over the barrier islands, and reducing the flow that moves as flanking flow from the northeast into Galveston Bay through the inundated wetlands. With the dike in place the peak surge amplification field along the western shoreline of the Bay is dominated by the reduction

in effective wind shear stress. This includes the bay side of the City of Galveston, which experiences amplification factors of 0.65 to 0.95. Surge amplification factors less than 1.0 along the western shoreline of Galveston Bay for these “worse-case” track proxy storms is a nuanced benefit associated with the coastal spine concept.

Risk-reduction schemes and measures taken solely inside the bay, without the coastal spine, are subject to the nonlinear surge amplification (amplification factors greater than 1.0) evident for Hurricane Ike and Storm 033, no-dike conditions. These are associated with the earlier onset of barrier island overflow, and flow to the southwest through the inundated wetlands that are enhanced by the reduced effective bottom shear stress.

Summary of Storm 033 Peak Surge for Present and Future Sea Levels

Approximate peak storm surge values at a number of key locations along the western shoreline of Galveston Bay, along Galveston Island, and along Bolivar Peninsula, are given in Table 11-3, in feet relative to NAVD88, for the four Storm 033 simulations. Values are given for both sea level scenarios, and for both no-dike and with-dike conditions. Surge values are estimated from the figures above, to the nearest half foot.

Table 11-3. Peak storm surge values for Storm 033, the 100-yr proxy storm, (feet, NAVD88), for present-day and SLR1 (+2.4 ft) sea level scenarios

Location	No-dike conditions		With-dike conditions	
	Present	SLR1	Present	SLR1
City of Galveston (Gulf side)	16	18	18	20
City of Galveston (bay side)	14	18	6.5	10
Galveston Island (mid-way)	13	15	4	7
Bolivar Peninsula (mid-way)	16	18.5	10	10
Texas City (south)	16.5	19	8	10.5
Texas City (east)	15	17.5	7	9.5
Dickinson Bay entrance	14.5	17.5	8	10
Clear Lake entrance	15	18.5	8	10
Morgan’s Point	17	20	7.5	10
Upper Houston Ship Channel	18.5	21.5	10	12.5

In terms of storm intensity, Storm 033, the 100-yr proxy storm, is a major hurricane for the Houston-Galveston region, which also follows a “worst-case” track for generating storm surge along the western shoreline of Galveston Bay. The central pressure of Storm 033 at landfall was 948 mb (minimum pressure offshore of 930 mb), and the maximum wind speed at landfall was 78 kt (100 kt offshore).

For the no-dike case, and present sea level, the average peak surge is 16 ft for the region represented by the nine locations listed in Table 11-3 that are inland of the dike. This reflects a very damaging storm surge having an average value higher than peak surge conditions observed during Hurricane Ike. For the no-dike case, future sea level scenario, the average peak surge for the entire region is 18 ft. For the with-dike case, present sea level, the average peak surge for the nine locations is 9 ft. For the with-dike case and future sea level, the average peak surge is 10 ft.

Calculating surge suppression as the difference between the averages of peak surge for no-dike and with-dike conditions, the surge suppression for the present-day sea level is 7 ft; and for the future sea level, it is 8 ft. These are substantial reductions in peak surge achieved by the coastal spine concept. Even with the 2.4-ft sea level rise, which will in general increase the risk of flooding, the presence of the dike greatly reduces coastal flooding for a severe storm of this intensity and track. As was the case for Storm 535, on the same worst-case track, the greatest surge suppression occurs in the northern parts of the bay, into the upper reaches of the Houston Ship Channel.

For a storm of this intensity and track, there are areas that remain exposed to flood damage. For the present-day sea level, the City of Galveston seawall would be significantly overtopped, with steady overflow. For this reason, raising of the seawall should be considered as part of the Ike Dike coastal spine concept. To prevent steady overflow for Storm 033, the seawall would have to be raised to accommodate a peak surge level of about 20 ft, NAVD88, with additional elevation of several more feet that would be required to reduce wave-induced overtopping to acceptable levels.

The City of Galveston also can be subjected to flooding from the bay side. Because of its location at the southwest corner of Galveston Bay, and in light of prevailing surge dynamics that occur within the bay for severe hurricanes approaching on a track similar to the Storm 033 path,

significant bay-side flooding would be expected, even if the seawall is raised. As a secondary line of defense for the city, construction of flood risk reduction measures along the bay side should be considered, effectively ringing the city. Assuming the seawall is raised to effectively reduce Gulf-side overtopping to acceptable values, to greatly reduce the risk of flooding from the bay side for this particular storm, the elevation of bay-side risk reduction measures would need to be approximately 12 ft, perhaps plus a few additional feet to reduce the wave-induced overtopping to acceptable amounts and to accommodate a future sea level increase.

With the coastal spine in place, with a crest elevation of 17 ft, and for the present sea level scenario, peak surge levels for Storm 033 were much less than levels experienced during Hurricane Ike, in all areas along the western shoreline of Galveston Bay. With the dike in place, for the future sea level, peak surge levels along the western Galveston Bay shoreline were still less than the hurricane surge experienced during Hurricane Ike, for most locations, perhaps with a few local exceptions.

Secondary lines of defense should be considered for other areas along the western shoreline of the Bay, to further reduce the risk of flooding to acceptable levels. The cost-effectiveness of all secondary lines of defense would need to be examined further. Locations and alignments of possible secondary lines of defense are examined further in the next chapter.

Storm 036 (500-yr Proxy Storm): With and Without Sea Level Rise

The No-dike condition

The group of four figures for Storm 036, the 500-yr proxy storm, no-dike conditions, is shown in Figures 11-28 through 11-31. Figures 11-28 and 11-29 show the maximum water surface elevation fields for the two sea level scenarios, and Figure 11-30 shows the difference between the two. Figure 11-31 shows the amplification factor field.

The amplification factor field for Storm 036 (the 500-yr proxy), which compares peak surge values for the two sea level scenarios, is quite similar to that for Storm 033 (the 100-yr proxy). Compare Figures 11-31 and 11-23. This suggests that similar processes are at work for the future sea level, compared to present-day sea level, for both storms, and that the spatial variability in those processes is similar for both storms.

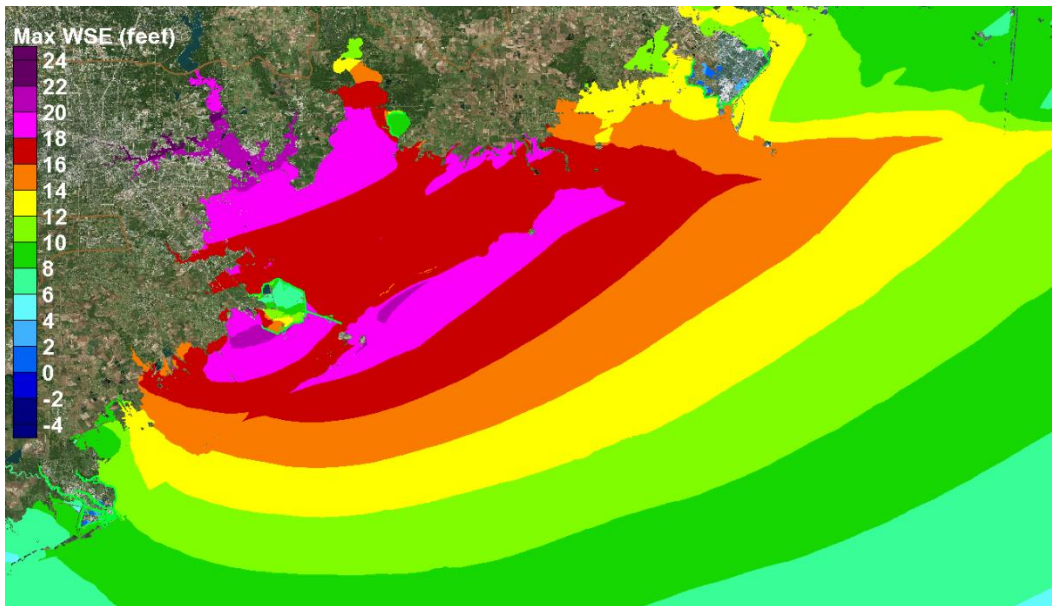


Figure 11-28. No-dike conditions. Storm 036 (500-yr proxy). Maximum water surface elevation field (in feet, NAVD88) for the present-day sea level scenario (+0.91 ft NAVD88)

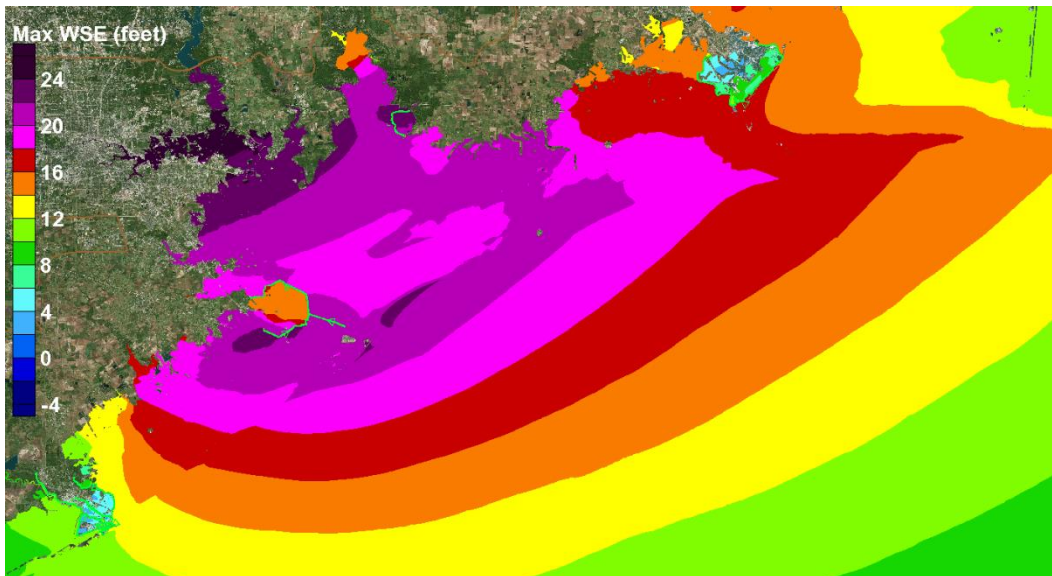


Figure 11-29. No-dike conditions. Storm 036 (500-yr proxy). Maximum water surface elevation field (in feet, NAVD88) for the future sea level scenario (SLR1, +3.31 ft NAVD88)

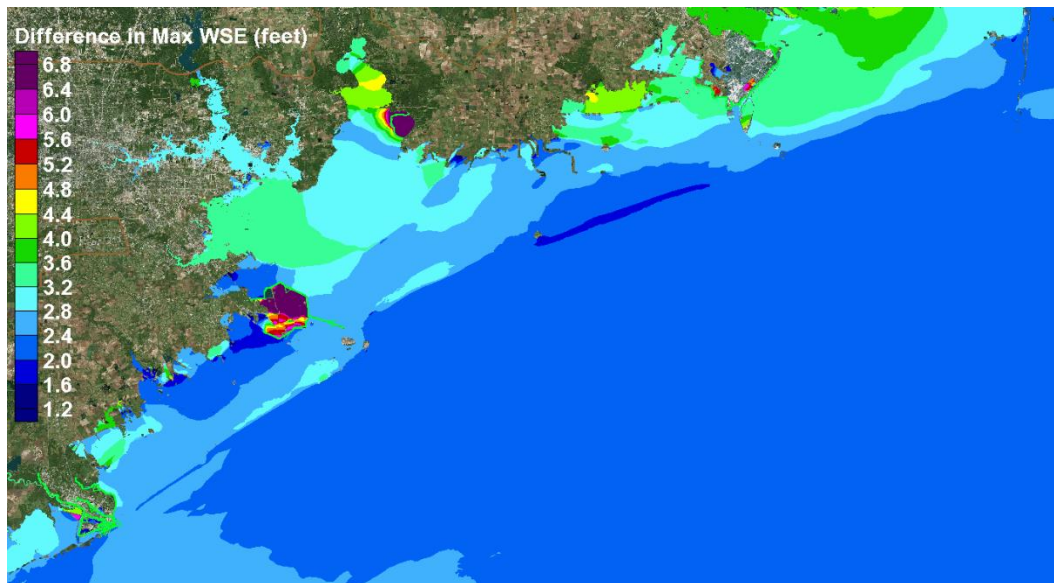


Figure 11-30. No-dike conditions. Storm 036 (500-yr proxy). Change in maximum water surface elevation (wse) fields. Maximum wse for the SLR1 future sea level scenario minus the maximum wse for the present-day sea level scenario.

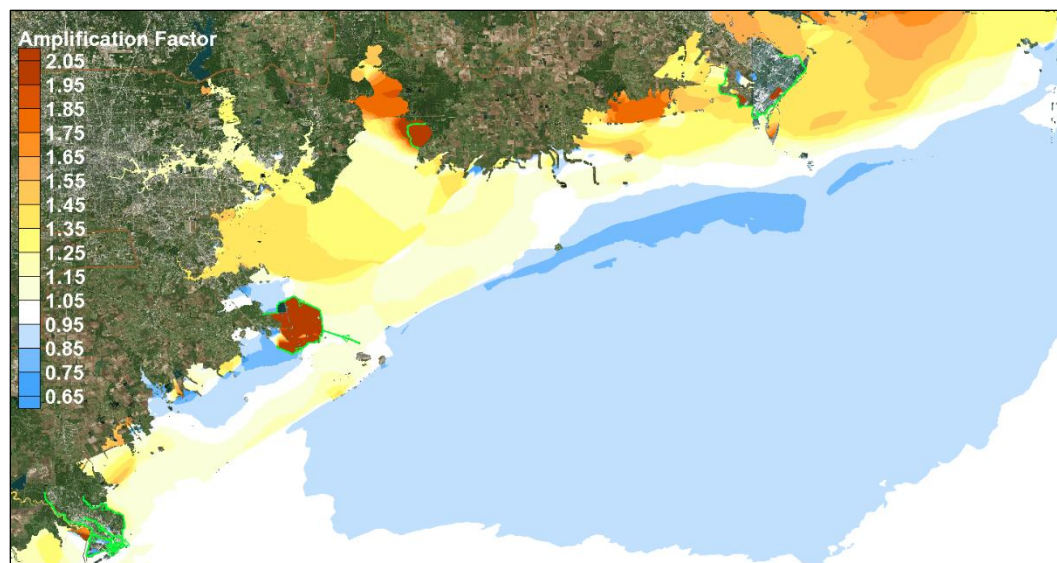


Figure 11-31. No-dike conditions. Storm 036 (500-yr proxy). Peak surge amplification factor.

Both storms follow the same track and they primarily differ in their intensity. Storm 036 is the more intense storm.

There are some small differences in the peak surge amplification fields for Storms 036 and 033. In the open Gulf, much of the shaded area is light blue, as was the case for Storm 033. The area in light blue in Figure 11-31 for Storm 036 is slightly larger than the light blue area for Storm 033

(Figure 11-23). For Storm 036 there is an area of darker blue along the coastline that is not present for Storm 033. The differences in blue-shaded areas for the two storms are attributed to higher wind speeds and greater water surface elevation gradients for Storm 036, compared to Storm 033, which lead to larger reductions in water surface gradient due to greater water depths. The greater water depths are associated with the sea level increase and the greater surge levels associated with Storm 036.

Much of the region located landward of the coastline and barrier islands, encompassing the interior bays and inundated wetlands, is colored in some shades of yellow or orange, as was the case for Storm 033. Yellow and orange areas indicate regions where the peak surge amplification factors exceed 1.05. The pattern of amplification factors in Galveston and West Bays is quite similar for Storms 036 and 033. However, in general peak surge amplification factors are slightly less in Galveston and West Bays for Storm 036, compared to Storm 033. That was also the case for the open Gulf areas. The overall decrease in amplification factors in these inland areas also is attributed to greater surge amplitude and consequently slightly greater water depths for Storm 036 which, in turn, leads to a greater reduction in effective wind stress. The wind stress reduction diminishes slightly the effect of an earlier onset of flow and increased magnitude of flow over the barrier islands as well as water moving alongshore in inundated areas, enhanced by reduced effective bottom shear stress, that occur in the inland areas. The blue shaded regions in West Bay north of Galveston Island also are an indication of the importance of the role of reduced wind stress, associated with greater water depth, in this part of the system.

The red-shaded area inside the Texas City levee system (see Figure 11-31) is a result of the much greater inundation depth in this area for Storm 036, for the future sea level scenario, compared the depth of inundation for the present-day sea level scenario. For both the present-day and future sea level scenarios, inundation inside the Texas City levee is substantial for Storm 036.

The With-dike condition

The group of four figures for Storm 036, for with-dike conditions, is shown in Figures 11-32 through 11-35. Figures 11-32 and 11-33 show the maximum water surface elevation fields for the two sea level scenarios,

and Figure 11-34 shows the difference between the two. Figure 11-35 shows the amplification factor field for this case.

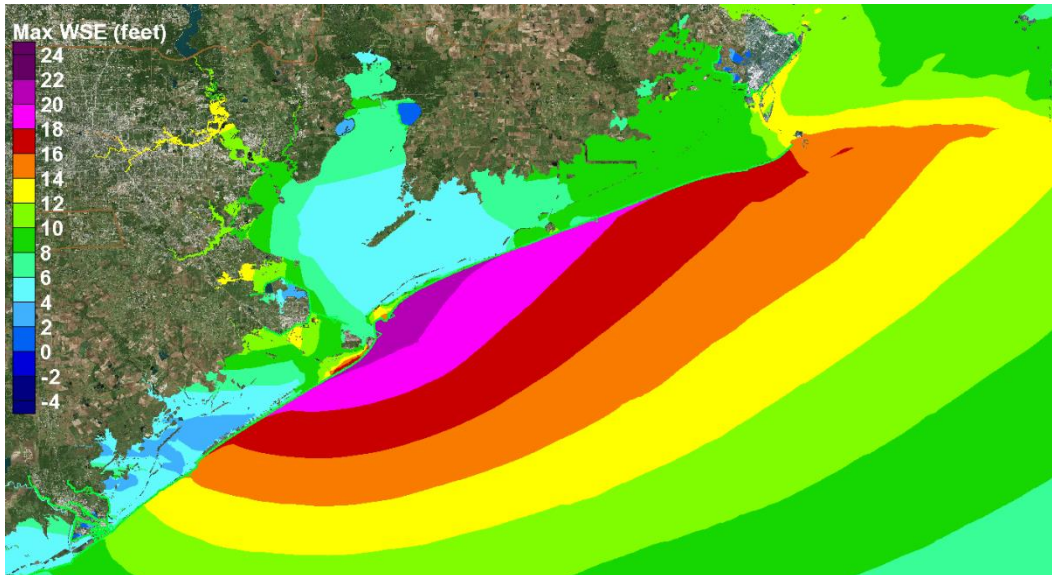


Figure 11-32. With-extended-dike conditions. Storm 036 (500-yr proxy). Maximum water surface elevation field (in feet, NAVD88) for the present-day sea level scenario (+0.91 ft NAVD88).

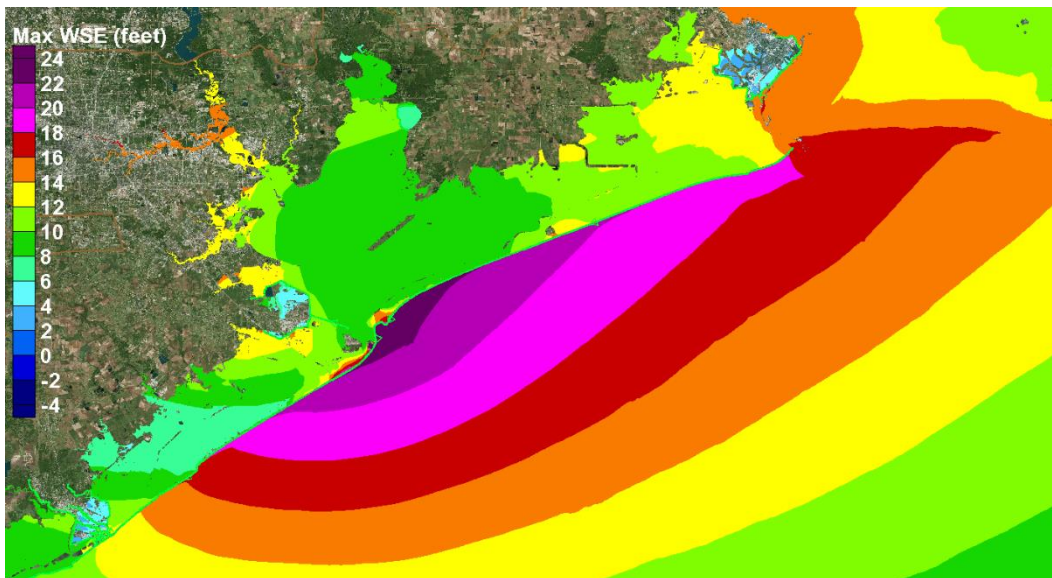


Figure 11-33. With-extended-dike conditions. Storm 036 (500-yr proxy). Maximum water surface elevation field (in feet, NAVD88) for the future sea level scenario (SLR1, +3.31 ft NAVD88).

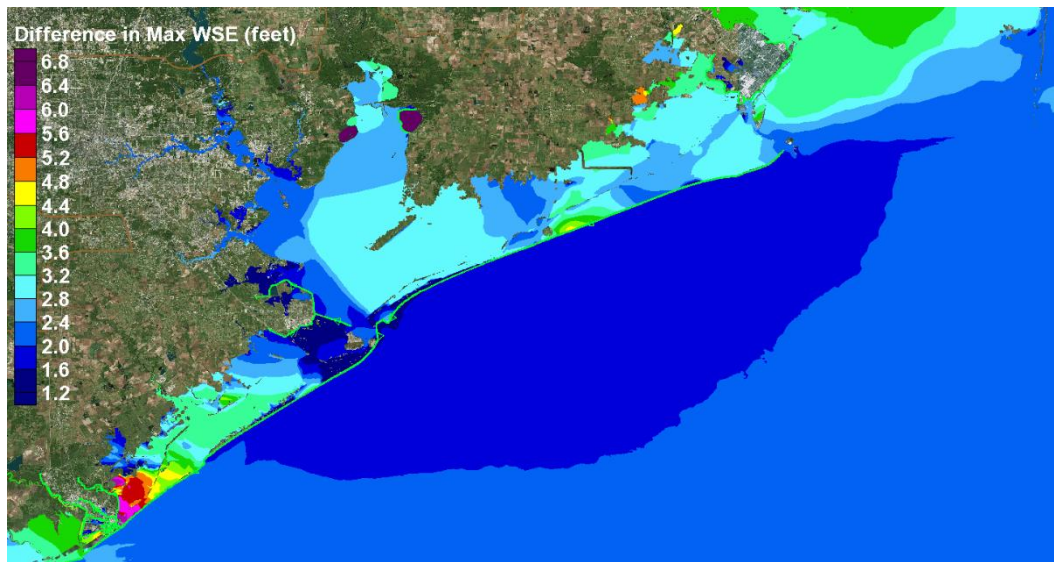


Figure 11-34. With-extended-dike conditions. Storm 036 (500-yr proxy). Change in maximum water surface elevation (wse) fields. Maximum wse for the SLR1 future sea level scenario minus the maximum wse for the present-day sea level scenario.

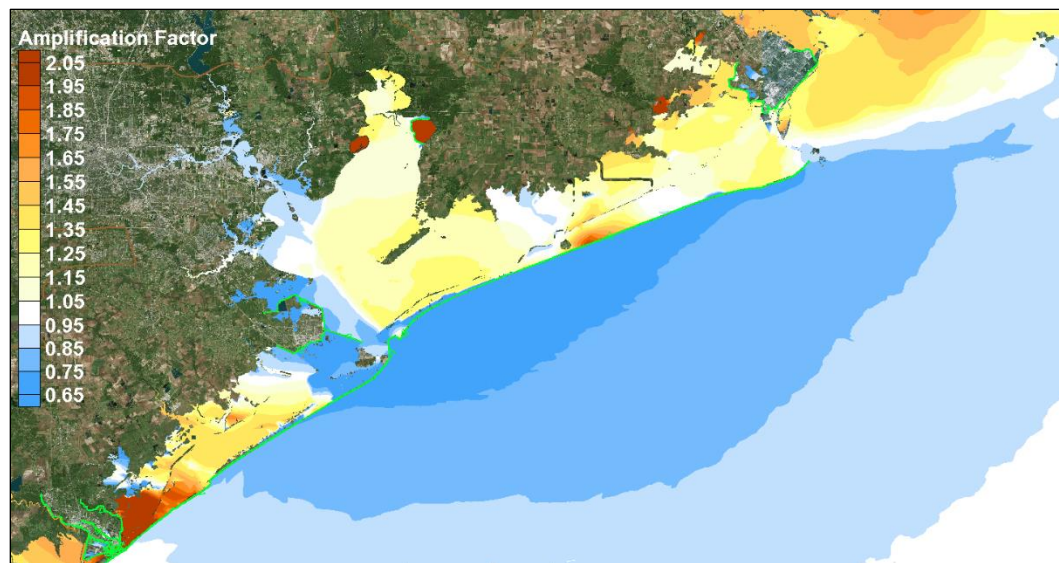


Figure 11-35. With-extended-dike conditions. Storm 036 (500-yr proxy). Peak surge amplification factor.

As was the case of the no-dike condition, the amplification factor field for Storm 036 is quite similar to that for Storm 033. Compare Figure 11-35 with Figure 11-27. Again, this suggests that similar processes are at work for the future sea level, compared to present-day sea level, for both storms, and that the spatial variability in those processes is similar for both storms.

There are some small differences in the peak surge amplification fields for Storms 036 and 033. In the open Gulf, the blue shaded area for Storm 036 is larger than the light blue area for Storm 033. For Storm 036 there are larger and darker blue areas compared to those seen for Storm 033. The differences in blue-shaded areas for the two storms are attributed to higher wind speeds for Storm 036, compared to Storm 033, which lead to larger open-Gulf water surface elevation gradients, which in turn lead to a larger reduction in water surface gradient associated with greater water depth due to sea level increase and the greater surge levels associated with Storm 036. For Storm 036, as was the case for Storm 033, the blue shaded areas are caused by the reduction in effective wind stress resulting associated with greater water depths that arise because of greater storm surge and increased sea level.

For the region that is located landward of coastal spine dike, including interior bays and inundated wetlands, much of this area is colored in some shades of yellow or orange, as was the case for Storm 033. The patterns of amplification factors in Galveston and West Bays are quite similar for Storms 036 and 033.

In general, peak surge amplification factors are slightly greater in eastern Galveston Bay and in West Bay for Storm 036, compared to Storm 033. This is attributed to the greater volume of water that flows over the dike at peak surge levels for Storm 036. For both sea levels, more water flows over the coastal spine for Storm 036, compared to Storm 033. The greater sea level exacerbates flow over the dike, and the higher surge levels for Storm 036 also exacerbate flow over the dike. The peak surge amplification at the west end of West Bay is due to flow over the dike along Galveston Island, and perhaps by flow over the dike along Bolivar Peninsula, which is pushed to the west by prevailing winds. The increased flow over the dike along Bolivar Peninsula might contribute to higher amplification factors in eastern Galveston Bay, compared to Storm 033, or it might be due to enhanced flanking flow for Storm 036 arising from the higher surge levels at the northeastern terminus of the coastal spine. An effectively terminated coastal spine on its northeast end (tied into higher ground elevation) should significantly reduce the amount of flanking flow that moves into Galveston Bay from the northeast.

Amplification factors along the western shoreline of Galveston Bay show the signature of a reduced effective wind shear stress, as was seen for the

other proxy storms, Storm 535 (see Figure 11-19) and Storm 033 (see Figure 11-27). With the dike in place the peak surge amplification field along the western shoreline of the Bay is dominated by the reduction in effective wind shear stress. This includes the bay side of the City of Galveston, which experiences amplification factors of 0.65 to 0.95.

Summary of Storm 036 Peak Surge for Present and Future Sea Levels

Approximate peak storm surge values at a number of key locations along the western shoreline of Galveston Bay, along Galveston Island, and along Bolivar Peninsula, are given in Table 11-4, in feet relative to NAVD88, for the four Storm 036 simulations. Values are given for both sea level scenarios, and for both no-dike and with-dike conditions. Surge values are estimated from the figures above, to the nearest half foot.

In terms of storm intensity, Storm 036, the 500-yr proxy storm, is a rare hurricane for the Houston-Galveston region. The central pressure of Storm 036 at landfall was 916 mb (minimum pressure offshore of 900 mb); and the maximum wind speed at landfall was 93 kt (112 kt offshore). The storm also follows a “worst-case” track for generating storm surge at the City of Galveston and along the western shoreline of Galveston Bay.

Table 11-4. Peak storm surge values for Storm 036, the 500-yr proxy storm, (feet, NAVD88), for present-day and SLR1 (+2.4 ft) sea level scenarios

Location	No-dike conditions		With-dike conditions	
	Present	SLR1	Present	SLR1
City of Galveston (Gulf side)	20	22	21	22.5
City of Galveston (bay side)	18	21	12	13
Galveston Island (mid-way)	16	18.5	10	13
Bolivar Peninsula (mid-way)	19	21.5	10	10
Texas City (south)	20.5	22.5	11	13
Texas City (east)	18	20.5	9	11
Dickinson Bay entrance	17.5	20	10	12
Clear Lake entrance	18	21	10	12
Morgan's Point	20	23	10	12
Upper Houston Ship Channel	22	25	12.5	14.5

For the no-dike case, and for the present-day sea level, the average peak surge is 19 ft for the region represented by the nine locations listed in Table 11-4 that are inland of the dike. This large average surge amplitude reflects a devastating hurricane for the entire Houston-Galveston region, where peak surges are approximately 5 to 8 ft higher than peak surges experienced during Hurricane Ike. For the no-dike case, future sea level scenario, the average peak surge for the entire region is 21 ft. For this sea level scenario, peak surges would be 7.5 to 10.5 ft higher than those experienced during Hurricane Ike.

For the with-dike case, and for present sea level, the average peak surge for the nine locations is 11 ft. This value is approximately a foot less than the values experienced during Hurricane Ike in Galveston Bay for the same areas. For the with-dike case and future sea level, the average peak surge is 12 ft, which is similar to, or slightly greater than, average peak surges experienced within the Bay during Hurricane Ike. This is a useful benchmark for the value of the coastal spine.

Calculating surge suppression as the difference between the averages of peak surge for no-dike and with-dike conditions, the average surge suppression value for the present-day sea level is 8 ft; and for the future sea level, it is 9 ft. These are substantial reductions in peak surge achieved by the coastal spine concept. As was the case for the other proxy storms, the greatest surge suppression occurs in the northern parts of the bay, into the upper reaches of the Houston Ship Channel, where suppression values range from 9 to 10 ft for both sea level scenarios.

For a storm of this intensity and track, even with the 17-ft coastal spine dike in place, Galveston Island and Bolivar Peninsula will experience substantial flooding and damage. For a surge level of 20 ft (present-day sea level) or 22 ft (the future sea level scenario) the City of Galveston seawall would be significantly overtopped, with steady overflow of several feet over the seawall, flooding the city. For present-day sea level, along the eastern half of Galveston Island, steady flow over the Dike would be experienced, as it would be for the entirety of Bolivar Peninsula. For the future sea level scenario, there would be steady flow over most or all of Galveston Island, in addition to all of Bolivar Peninsula. A higher coastal dike should be considered if risk reduction is desired along Galveston Island and Bolivar Peninsula, for a storm of this magnitude. Other measures also should be considered, including raising of the Galveston

seawall and construction of a ring dike/wall system around the entire City of Galveston to provide adequate reduction of risk for flooding from the bay-side.

The 17-ft coastal spine provides much greater risk reduction for the rest of the western shoreline of Galveston Bay, although some areas would still experience flooding and damage. With the 17-ft coastal spine in place, and for the present-day sea level, peak surge levels for Storm 036 were approximately a foot less than levels experienced during Hurricane Ike, all along the western shoreline of Galveston Bay and into the upper reaches of the Houston Ship Channel. For the future sea level, with the dike in place, peak surge levels along the western Galveston Bay shoreline and upper reaches of the Houston Ship Channel were comparable to peak surge levels experienced with the dike. Additional risk reduction measures; i.e., secondary lines of defense, should be considered for areas on the western side of Galveston Bay, and in the upper reaches of the Houston Ship Channel that were severely impacted by Hurricane Ike. For this storm, and for present sea level, the coastal spine limits peak surges to levels that would not result in steady flow over the levee surrounding Texas City. For the future sea level, limited flow over the Texas City levee appears to occur in some areas. For added risk reduction for a storm of this magnitude, raising of the levee surrounding Texas City, in some local areas, should be considered.

To achieve additional flood risk reduction for a storm of this magnitude, the aforementioned secondary lines of defense should be considered to further reduce the risk of flooding to acceptable levels. Locations and alignments of possible secondary lines of defense are examined further in the next chapter.

12 Exposure to Inundation, Residual Flood Risk, and Implications for Secondary Lines of Defense

Introduction

Comparisons of the no-dike and with-dike simulations of Hurricane Ike, and the 100-yr and 500-yr proxy storms, all showed substantial surge suppression benefits associated with the Ike Dike concept. The primary function of the dike is preventing a massive amount of water from entering Galveston Bay over the inundated barrier islands. Averaged along the western shoreline of Galveston Bay, reductions in peak surge range from 7 to 9 ft for these three severe hurricanes, depending on the locations included in the averaging. Slightly greater-than-average surge suppression is achieved in the upper reaches of the Houston Ship Channel.

However, even with the Ike Dike in place, winds during very severe hurricanes can produce a significant storm surge internally, within the bay, along its western shoreline. With the 17-ft Ike Dike in place, and for the present-day and future sea level scenarios, peak surge values along the western shoreline of Galveston Bay ranged from 2 to 7 ft (Hurricane Ike), 8 to 13 ft (100-yr proxy storm) and 10 to 15 ft (500-yr proxy storm). Peak surges of this magnitude can inundate the lower-lying areas within Galveston and West Bays, resulting in some level of residual flood risk. Flow over the Ike Dike, which occurs for the 100-yr and 500-yr proxy storms, also can lead to inundation of the areas that lie directly behind the dike, as the overtopping water flows downslope. The amount of residual risk varies with location.

The 100-yr and 500-yr proxy storms, and Hurricane Ike, were considered in an assessment of residual risk and of possible measures, secondary lines of defense, which can be taken to further reduce flood risk. All three of these hurricanes represent severe hurricanes that produce significant storm surge inside Galveston Bay.

To place residual risk information that is discussed below in a probabilistic context, the encounter probability for a 100-yr water level is approximately 25% over the next 30 years. This means that there is a 25% chance that the 100-yr water level (or something greater) will be encountered during the next 30 years. The encounter probability for a 100-yr water level sometime during the next 50 years is approximately 40%. For the 500-yr water level, the encounter probability is approximately 6% over the next 30 years and approximately 10% over the next 50 years.

Possible additional risk-reduction measures which can be implemented, supplementing the Ike Dike, are discussed in this chapter. Secondary lines are proposed in light of several persistent features of the storm surge dynamics that have been observed within the Galveston Bay system. Possible measures include: 1) raising the Galveston seawall in light of past and future relative sea level increases and of slightly increased surge levels at Galveston as a result of the long-dike effect associated with the Ike Dike, with possible lateral extensions to prevent flanking of the seawall if adjacent areas of the Ike Dike are lower, 2) measures taken on the bay side of Galveston to reduce the risk of flooding from the bay side, 3) use of ring dikes/levees/walls, or elevated roadways or walkways, and 4) elevating the first floor of individual structures. It is unclear how extensively the National Flood Insurance Program maps of flood risk will lead to raising of the first floor elevation of structures throughout the region. This measure seems to be the most suitable and feasible for a number of the lowest-lying areas, in order to reduce residual risk.

One other risk reduction measure that has been proposed is a surge barrier/gate system, the “Centennial Gate”, located in the northwest corner of Galveston Bay, leading to the upper reaches of the Houston Ship Channel. With the 17-ft Ike Dike in place, if the future mean sea level exceeds the +2.4 ft considered here as the future scenario, and if there is significant hurricane surge forerunner penetration into Galveston Bay before the Bolivar Roads surge barrier gate is closed, peak surge levels in the Upper Ship Channel for the 500-yr proxy storm could exceed those experienced during Hurricane Ike by several feet or more. Under these conditions, if the flood risk for many of the industrial areas that lie along the upper ship channel is unacceptable, a “Centennial Gate” gate could be considered as a secondary line of defense.

To facilitate examination of flood risk, residual risk, and possible secondary lines of defense, a set of inundation maps was generated for a number of sub-regions in the Houston-Galveston area that have the greatest potential for flood damages/losses. The sub-regions are located on Galveston Island, Bolivar Peninsula, and along the Galveston Bay shoreline. The examination is documented below, by geographic location; first for three sub-regions comprising both Galveston Island and Bolivar Peninsula, then for three sub-regions encompassing the western shoreline of Galveston Bay, and finally for two regions encompassing the upper reaches of the Houston Ship Channel.

Inundation maps were generated using the peak storm surge fields (model output) and the topographic elevation field used as input to the storm surge model. Maps were generated for the three most severe hurricanes; Hurricane Ike and the 100-yr and 500-yr proxy storms, for both present-day and future sea level scenarios, and for both no-dike and with-dike conditions. Maps were not generated for the 10-yr proxy storm simulations. The Ike Dike is very effective in reducing inundation to negligible levels throughout the Houston-Galveston region for less intense hurricanes like the 10-yr proxy storm. The full set of maps is provided in Appendix A. Selected maps from the appendix are presented in the sections below to facilitate discussion. Inundation for each of the three storms, in each of the following geographic sub-regions, and proposed secondary lines of defense, is discussed below in individual sections, in this order:

Galveston Island

- City of Galveston
- Galveston Island (central portion)
- Galveston Island (western end)

Bolivar Peninsula

- Bolivar Peninsula (western end)
- Bolivar Peninsula (central portion)
- Bolivar Peninsula (eastern end)

Galveston Bay

- Texas City (south)/La Marque/Bayou Vista
- San Leon/Texas City (north)/Bacliff/Dickinson

Clear Lake area/Bayport area/La Porte

Houston Ship Channel

Upper Houston Ship Channel (eastern portion)

Upper Houston Ship Channel (western portion)

Figure 12-1 shows the locations of a number of places along the western shoreline of Galveston Bay that are referenced in the discussion throughout this chapter and in Chapter 14. The section in Chapter 14 titled “Surge and Inundation Suppression Achieved with the Ike Dike Concept: Results from the Refined Modeling Approach and the Extended Dike” contains a much shorter summary of the key points from this chapter.

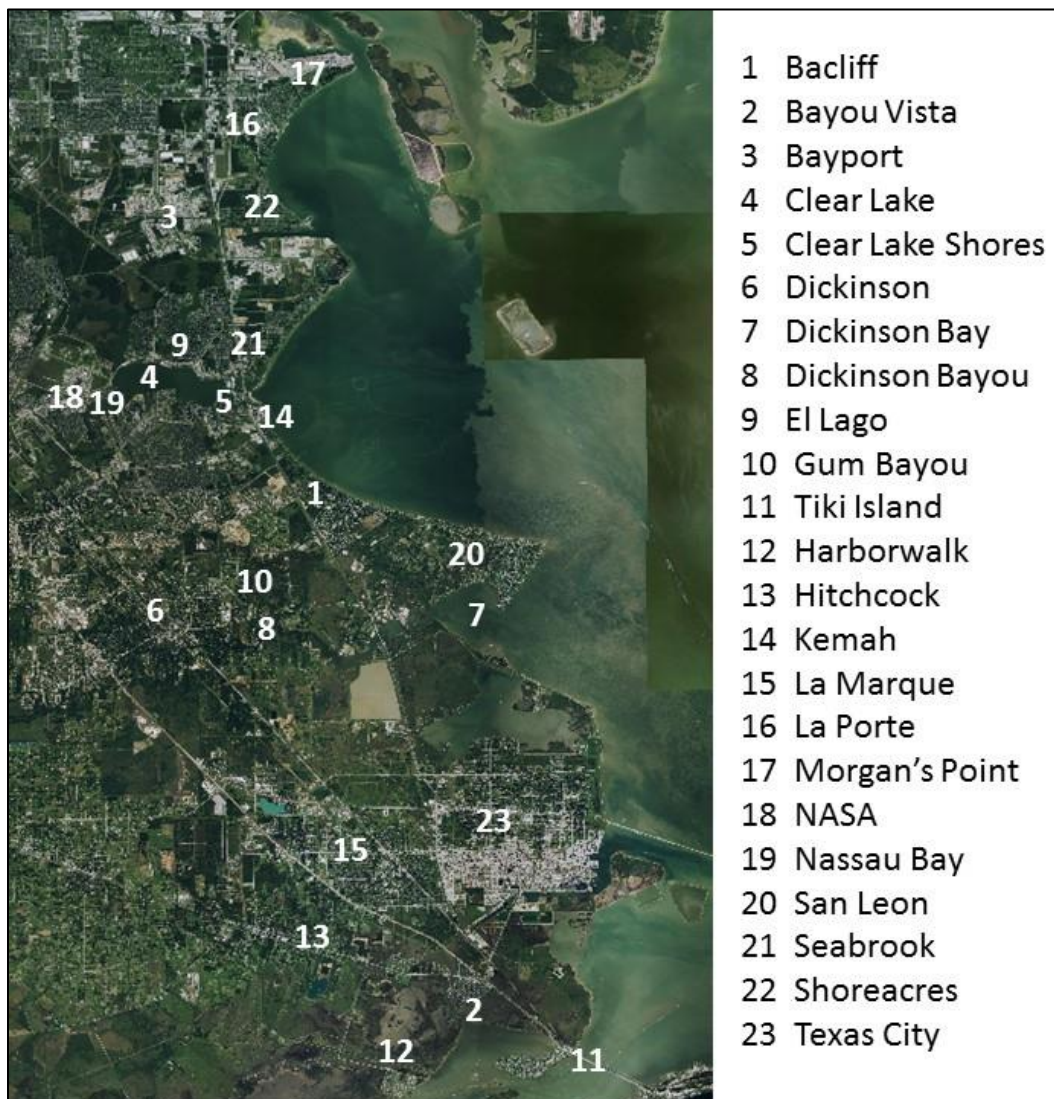


Figure 12-1. Location map for the western shoreline of Galveston Bay.

Galveston Island

City of Galveston

At the Pleasure Pier on the gulf side of Galveston, the 100-yr and 500-yr average recurrence interval (ARI) water levels are 13.5 ft and 17.0 ft NAVD88, respectively (the 90% confidence limit values). These probabilistic values were computed for existing conditions, i.e., present-day sea level with no Ike Dike in place, using the methodology that was described in Chapter 9.

Simulated peak surge levels at the Pleasure Pier for Hurricane Ike and the 100-yr and 500-yr proxy storms are approximately 13 ft, 16 ft and 20 ft, respectively, for the same set of existing conditions. To place these storm surge values in a probabilistic context, the Hurricane Ike simulation resulted in peak surge levels that were most similar to the 100-yr water levels at this same location. The computed peak surge of 13 ft for Hurricane Ike is slightly less than the 100-yr value, by 0.5 ft. The 100-yr proxy storm resulted in a simulated peak surge value of 16 ft at this location, which is 2.5 ft higher than the 100-yr and 1.0 ft less than the 500-yr ARI water levels, respectively.

Due to the long-dike effect, on the gulf side, the Ike Dike increases the peak storm surge compared to peak surge for existing conditions. For the Hurricane Ike simulations, the magnitude of the long dike effect is 1 ft for both sea level scenarios. With the Ike Dike in place, and for present day sea level, the simulated peak surge level at the Pleasure Pier for Hurricane Ike is 14 ft, 1 ft higher than the existing condition peak surge of 13 ft. For the future sea level scenario; the peak surge is 16 ft; also 1 ft higher than the 15 ft peak surge for existing conditions.

With the Ike Dike in place, for the present-day sea level, the Hurricane Ike simulation produced no steady flow over the Galveston seawall, while the proxy storms did produce overflow. For the future sea level scenario, all three of the hurricanes produced steady flow over the seawall. For the Hurricane Ike simulation, overflow occurred at a single location near the northeast end of the original seawall; whereas, both the 100-yr and 500-yr proxy storms caused widespread flow over the seawall along most or all of its length.

The steady flow over the wall for the Hurricane Ike simulation, for the future sea level, prompted a closer look at why this occurred. The peak surge level of 16 ft was presumably less than the 17-ft crest elevation of the seawall. For the with-Ike Dike case, the actual topographic elevations along the Galveston seawall for the existing conditions case were retained in the modeling. The actual elevations vary along the length of the seawall, but they are close to 17 ft along most of its length. For the rest of the Ike Dike implementation, elevations of the extended dike were set to exactly 17 ft NAVD88. At this one location, the existing Galveston seawall appears to be approximately two feet lower than 17 ft NAVD88 elevation. This apparent low point in the sea wall is discussed further below.

Figures A.1 through A.3 in Appendix A show inundation patterns for the City of Galveston, for the simulations of Hurricane Ike and the 100-yr and 500-yr proxy storms. Figure 12-2, inundation for the Hurricane Ike simulation and present-day sea level, shows that the Galveston seawall effectively reduces inundation to a few isolated low-lying areas around the periphery of the city. For the future sea level scenario, shown in Figure 12-3, the Hurricane Ike simulation results in much more widespread inundation, including a large swath in the downtown area having a high density of structures. The flooding originates from both the bay side and from the single area on the gulf side that was identified above.

Figure 12-4 shows topographic elevations in this region from the storm surge model. Displayed elevations are in feet relative to the NAVD88 vertical datum. The negative sign listed in the figure's scale simply indicates elevations that lie above the vertical datum. The bay side of the City of Galveston is characterized by relatively low elevations, less than 6 ft in places. Comparison of the inundation patterns for the two Hurricane Ike simulations with the topographic elevation map suggests that peak surge elevations along the bay side were approximately 4.5 to 5 ft for present-day sea level and 7 to 7.5 ft for the future sea level scenario. The peak storm surge maps for the two simulations confirm this; see Figures 11-8 and 11-9.

The two areas that appear to be the sources for the widespread inundation in the downtown area shown in Figure 12-3 are circled in Figure 12-4. The inundated area downtown is characterized by the rather extensive low-lying region having elevations of 5 to 7 ft. Water that flows downslope from the gulf-side source accumulates in this lower lying area, as does the

water that enters from the bay side. Raising topographic elevations in these two areas would achieve a more consistent level of flood protection in the City of Galveston for the Hurricane Ike simulation, for the future sea level scenario.



Figure 12-2. Inundated areas in the City of Galveston, Hurricane Ike simulation, with-dike condition, present-day sea level.



Figure 12-3. Inundated areas in the City of Galveston, Hurricane Ike simulation, with-dike condition, future sea level scenario which is 2.4 feet higher than present-day sea level.

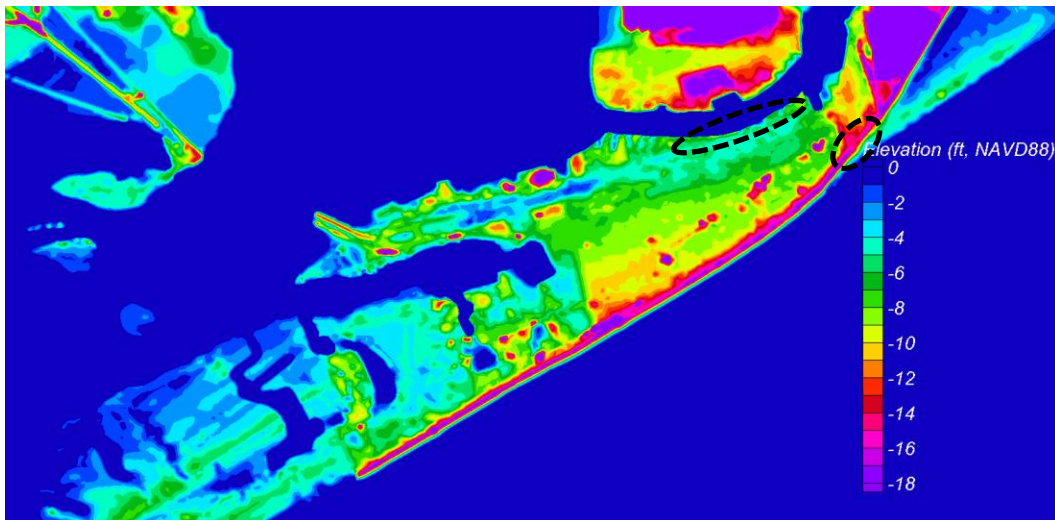


Figure 12-4. Topographic elevations in the City of Galveston, in feet relative to the NAVD88 vertical datum. Negative values indicate elevations that lie above the vertical datum.

As stated earlier, the circled area on the Galveston seawall has model elevations that are approximately 2 ft lower than 17 ft NAVD88. Elevations in this local area should be examined further to make sure the model topography is accurate. If model elevations are correct, and they are several feet lower than 17 ft NAVD88, this area of the seawall constitutes a weak link in the primary line of defense, a deficiency that should be corrected as part of the Ike Dike implementation. Other model elevations along the seawall show more consistent elevations near 17 ft. Actual elevations from a high resolution data source should be examined to identify any other possible areas where elevations are significantly lower than 17 ft.

At the source for flooding from the bay side, these low elevations that are less than 6 ft also appear to constitute a vulnerability that should be addressed. Raising elevations to 8 ft in this area, and in all areas where elevations lower than 8 ft can lead to inundation within the city, should be considered as a secondary line of defense measure. This would seem to provide a consistent elevation for ringing the city against bay-side inundation. This could be achieved by raising a road surface, building a small wall along the side of a road, raising a median between lanes of traffic, or via a wall incorporated into a raised pedestrian walkway.

The extensive elongated area of low-lying elevations in the down town area would tend to accumulate flood water that flows down slope from other sources. Another facet of addressing inundation in this area that should

be considered is a pump station(s) for evacuating accumulating water, and then discharging it back into the bay.

If a higher level of flood risk reduction is desired for the City of Galveston, more extensive risk reduction measures will need to be constructed. Measures would have to include raising the Galveston seawall and construction of much more extensive bay-side measures to raise the bay-side flood defense perimeter to the desired elevation, ringing the city. Pump stations or a structure(s) to facilitate gravity-driven drainage would have to be built to evacuate any water that accumulates inside the ring due to steady overflow and/or wave overtopping in the event that the system is overtopped.

Since construction of the Galveston seawall in the early 1900's, the risk of inundation to the City of Galveston has been increasing because of the rise in relative mean sea level that has occurred (assuming the probabilities of hurricanes are the same, then and now). Based on the long record of measured water level data at Galveston (see Chapter 11, Figures 11.1 and 11.2), the observed change in relative mean sea level at Galveston has been approximately 2 ft over the past 100 years. This relative rise in sea level has increased the risk of flooding to the City of Galveston both from the gulf and the bay sides as is evident from the Hurricane Ike and proxy storm simulations. In light of past sea level rise and a projected rise in the future sea level, and in light of the long-dike effect, raising of the seawall should be considered. To achieve the same level of flood risk that existed when the sea wall was originally built, the seawall should probably be raised by 5 to 6 ft, to a uniform crest elevation of 22 to 23 ft NAVD88. This increase reflects 2 ft of historic relative sea level rise, 2 ft due to the long-dike effect, and 1 to 2 ft of future sea level rise. There might be public opposition to raising the seawall to this elevation, or to raising it at all.

If the Galveston seawall is raised above the crest elevation of the adjacent sections of the Ike Dike, the need for lateral transition sections should be examined and implemented where necessary at the ends of the seawall. Transitions should minimize any negative effect of flanking around the terminal ends of the raised sea wall on the desired level of flood risk within the city.

For the 100-yr proxy storm, peak surge on the bay side of Galveston reached approximately 8 ft (see Figure 11-24) for present-day sea level and 10 to 11 ft (see Figure 11-25) for the future sea level scenario. To accommodate peak surge levels along the bay side for the future sea level scenario of +2.4 ft, the crest elevation of a bay-side ring levee/wall system would need to be approximately 11 ft NAVD88. For risk reduction measures of this elevation, a much more extensive dike/levee/wall system would have to be built to ring the city. This secondary line of defense should be explored further.

Several possible alignments for a more extensive ring dike/levee/wall system are shown in Figure 12-5. The layouts that are shown attempt to maximize use of existing roads, and raising of those roads. Utilization of existing roadways and rights of way, and other public lands such as around the airport, would appear to be among the less costly and less controversial alternatives. One of the alignments encompasses the airport within the ring and would require a gate to support recreational vessels. Certainly, other alignments are possible. Each of them would have different benefits/negatives, costs and pros/cons.

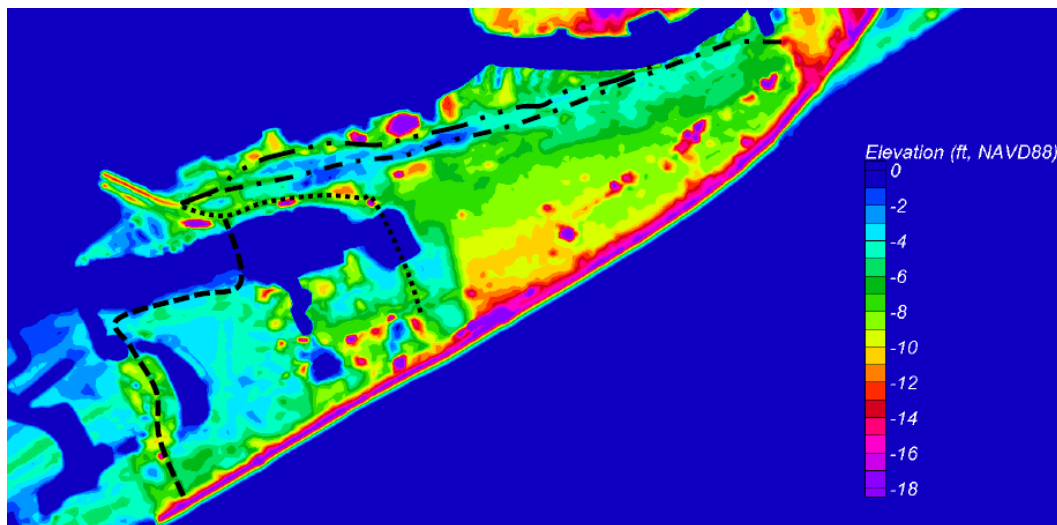


Figure 12-5. Possible alignments for a more extensive dike/levee/wall system that rings the City of Galveston.

There is considerable complexity in integrating a continuous system of levees/dikes, walls, and gates (all having the desired crest elevation, for example, 11 ft NAVD88) to provide risk reduction to the Port of Galveston infrastructure. Complexities involve constructing a system among the many docks, slips, rail lines, roads, buildings, etc., as well as disruption to operation of the port, during and possibly after construction. Other ring

alignments that fully encompass the Port would require construction of deep draft navigation gates, integrated into an open-water wall system. These can be built, but they will be very costly.

There are other issues related to construction of the more extensive ring and its integration into other parts of the city, such as the possible need for multiple pump stations or structures to facilitate gravity-driven drainage to remove water that could accumulate inside the fully ringed polder in the event of significant overflow/overtopping, and other gates needed to provide vehicle and rail access. All would need to be examined as part of the conceptual and detailed design of a bay-side dike/wall system that fully rings the city.

The Gulf Coast Community Protection and Recovery District (2016) study has proposed such a ring dike, although their proposed alignment follows one of the existing roadways and excludes the Port of Galveston. Options for a ring that includes the Port should be examined as well.

Galveston Island (central portion)

Figures A.4 through A.6 in Appendix A show inundation patterns for the simulations of the same three storms for the central portion of Galveston Island. The central portion roughly represents the central third of the barrier island. The 17-ft Ike Dike is very effective in reducing the risk of flooding, as illustrated by the Hurricane Ike simulations. However, even with the dike in place certain areas in this region remain susceptible to flooding from the bay side. The potential for bay-side flooding is dictated by surge levels within West Bay and by the low-lying barrier island topography.

Barrier islands on the upper Texas coast are generally characterized by low topography. They tend to have higher elevations (with or without small dunes) on the gulf side of the island. From the higher gulf side, elevations tend to steadily decrease with increasing proximity to the bay shoreline. The elevation data for the central portion of Galveston Island are shown in Figure 12-6. Examination of the data shows this general pattern of sloping topography from gulf side to bay side. Topographic elevations along the bay shoreline are about 3 ft NAVD88 and they are 7 to 8 ft along much of the gulf side of the island. The very low-lying topography on the bay side of the island strongly contributes to the risk of flooding in these areas, even with the Ike Dike in place.

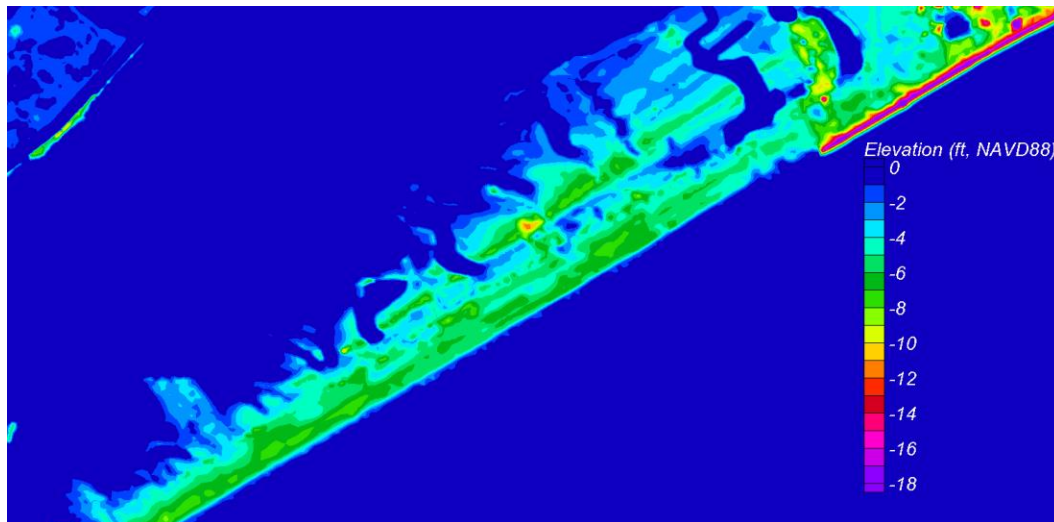


Figure 12-6. Topographic elevations in central portion of Galveston Island, in feet relative to the NAVD88 vertical datum. Negative values indicate elevations that lie above the vertical datum.

The persistent counterclockwise rotation of winds around the center of an approaching hurricane that makes landfall on Galveston Island, or just to the south of it, creates higher storm surge along the western side of Galveston Bay (the downwind side of the bay). This water build-up along the western shoreline leads to locally high surge levels on the bay side of the City of Galveston. This elevated surge level and the prevalence of winds from the northeast also force water from Galveston Bay into West Bay. The same winds act to force a water surface gradient within West Bay, setting down the water surface behind the central part of Galveston Island and then increasing the water surface from east to west, resulting in higher wind set up at the westernmost end of West Bay. The set-down is limited by the high water level in the bay behind the City of Galveston. With the Ike Dike in place, and for storms having tracks like the proxy storms, this is a prevalent storm surge pattern within West Bay. This pattern is seen in Figures 11-24 and 11-32 for the 100-yr and 500-yr proxy storms, respectively.

For Hurricane Ike (see Figure 11-8) the peak surge gradient in West Bay is a little different than the gradient for the proxy storms. Because of the track of Ike and landfall in the Bolivar Roads vicinity, at landfall, winds in West Bay shift rapidly and blow from the north. Strong winds from the north set up the water surface on the downwind or south side of the bay (i.e., the bay side of Galveston Island). This surge dynamic also renders the central portion of Galveston Island susceptible to bay-side flooding for storms that track through Bolivar Roads and to the north of it.

Figure 12-7 illustrates bay-side flooding in the central portion of Galveston Island for the Hurricane Ike simulation with the Ike Dike in place and present-day sea level. Of the three storms, only the Hurricane Ike simulations do not lead to steady flow over the Ike Dike in this region, so the influence of bay-side flooding is most apparent for this simulation. Peak storm surge along the bay side of the island for this simulation is only about 4 ft NAVD88. But in light of the low-lying terrain, inundation of some residential areas occurs, in particular those that are located in the lower-lying areas closest to the bay.



Figure 12-7. Inundated areas for the Hurricane Ike simulation, with-dike condition, present-day sea level, for the central portion of Galveston Island.

For the future sea level scenario, which is 2.4 ft higher than present sea level, all three storms produce nearly complete inundation of this portion of the barrier island, due either due to flooding from the gulf side or from the bay side. Because of the very low topography, inundation is particularly sensitive to an increase in mean sea level.

One measure that can be taken to reduce the risk of flooding from the bay side on Galveston Island, as well as in other low-lying areas, is raising the first floor elevation of individual structures. This measure also can be effective in reducing the risk of flooding associated with flow over the Ike Dike. In the event the crest elevation of the dike is exceeded by the gulf-side surge, the water surface in West Bay will be much lower than the open gulf surge level. Consequently, water flowing over the dike will move rapidly down-slope over the barrier island toward the bay side. The water surface transitions from the higher open gulf side surge level to the lower

water level in West Bay, with much of the transition occurring over a relatively short distance on the bay side of the Ike Dike. Elevating structures to a first floor elevation of 10 to 12 ft NAVD88 would significantly reduce the risk of flooding on the bay side of the 17-ft Ike Dike, even for the future sea level scenario.

Another measure, or secondary line of defense, that can be implemented to reduce flood risk on this portion of the low-lying barrier island is construction of ring dikes or levees around concentrations of structures, perhaps integrated with an access road on top. A ring levee with crest elevation of 10 to 12 ft NAVD88 would significantly reduce the risk of flooding. As is the case with any ring levee/dike that has a residual risk of being overtopped and then having that water trapped within the confines of the ring, a pump station(s) or other structures that would be required to evacuate any accumulating water. A gate or gates might also be required to provide vehicular access to the residential area surrounded by the dike/levee. The benefits and costs of any such secondary lines of defense would need to be examined. Residents are often opposed to such structural measures because they block the view.

Galveston Island (western end)

Figures A.7 through A.9 in Appendix A show inundation patterns for the simulations of Hurricane Ike and the 100-yr and 500-yr proxy storms, respectively, for the western end of Galveston Island. The western end roughly represents the western third of the barrier island.

As was the case for the central portion of the island, the 17-ft Ike Dike is very effective in reducing the risk of flooding from the gulf side, as evidenced by the simulations for Hurricane Ike. However, the low-lying areas in this region also remain susceptible to flooding from the bay side. Figure 12-8 shows the topography for this portion of the barrier island. The range of elevations and patterns of elevation change from the gulf side to the bay side are similar to those found in the central portion of the island. The barrier island is narrower on its western end.

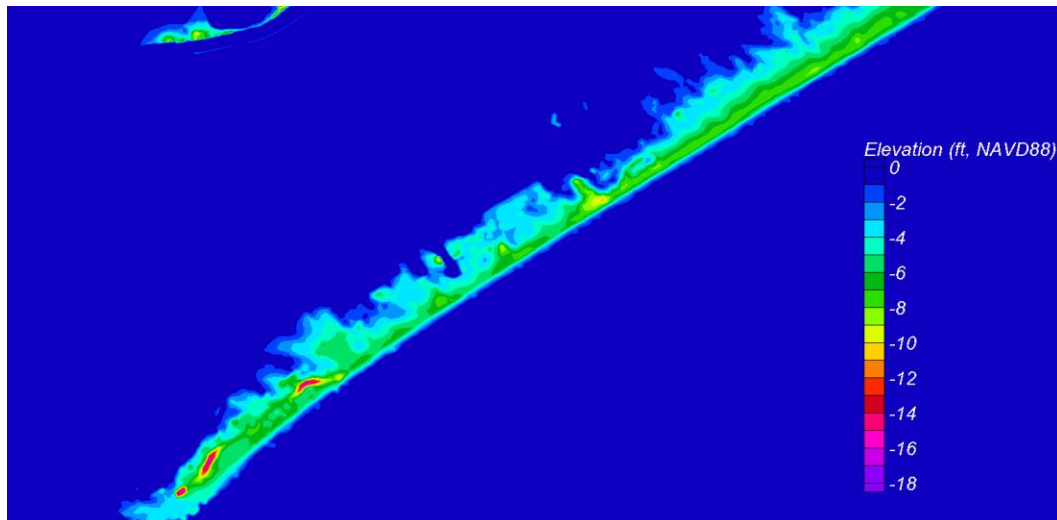


Figure 12-8. Topographic elevations at the western end of Galveston Island, in feet relative to the NAVD88 vertical datum. Negative values indicate elevations that lie above the vertical datum.

Figures 12-9 and 12-10 illustrate inundation in this region for the Hurricane Ike simulation (Figure 12-9) and the 100-yr proxy storm simulation (Figure 12-10), with the 17-ft Ike Dike in place and present-day sea level. Both simulations do not lead to steady flow over the Ike Dike in this region, so the influence of bay-side flooding is most apparent. Peak storm surge for Hurricane Ike is about 4 ft NAVD88 along the bay side of the island, and for the 100-yr proxy storm the peak surge is slightly less. Recall that for Hurricane Ike after landfall, winds set up the southern part of the bay all along the back side of Galveston Island. This leads to slightly higher peak surges for Hurricane Ike in this area, compared to those for the 100-yr proxy storm.

The residential areas that experience inundation for these two storms tend to be those located in the lower-lying areas closest to the bay shoreline. Differences between the two figures illustrate how sensitive inundation from the bay side is to small changes in the peak surge level. The bay sides of barrier islands generally have very gentle slopes, which makes the area of inundation quite sensitive to peak surge elevation.

As was found to be the case for the central portion of Galveston Island, for the future sea level scenario all three storms produce nearly complete inundation of this portion of the barrier island.



Figure 12-9. Inundation pattern for the Hurricane Ike simulation, with-dike condition, present-day sea level, for the western end of Galveston Island.

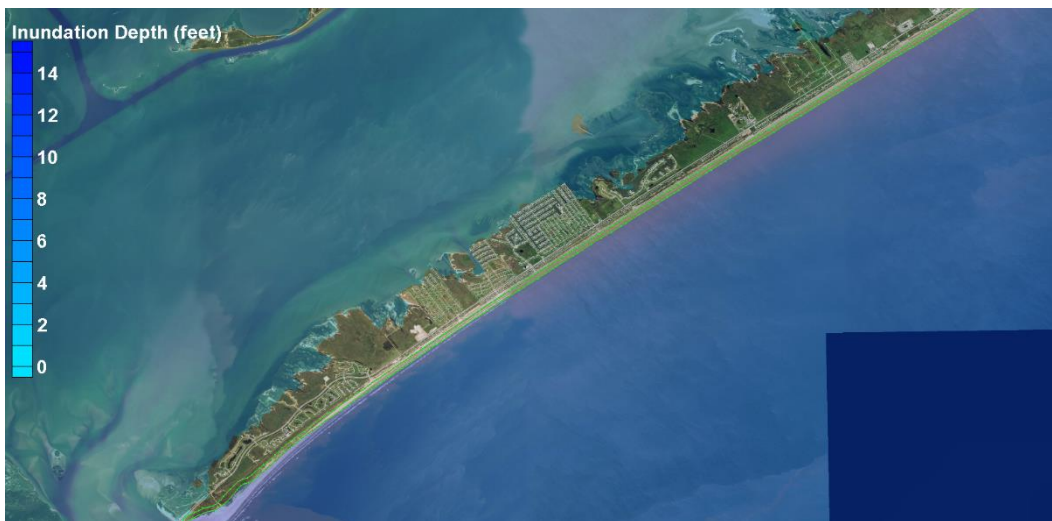


Figure 12-10. Inundation pattern for the 100-yr proxy storm simulation, with-dike condition, present-day sea level, for the western end of Galveston Island.

The same strategies mentioned previously can be adopted here to reduce the risk of flooding, raising the first floor elevations of structures, and/or construction of ring levees/dikes/walls around concentrations of structures. With the 17-ft Ike Dike in place, sea level rise is an important driver of flood risk for these low-lying barrier islands. A long-term plan to reduce the risk of flooding can be focused on either approach to risk reduction. The longer-term nature of sea level rise lends itself to implementation of a longer-term strategy to raise the elevations of individual structures.

Bolivar Peninsula

Bolivar Peninsula (western end)

In some ways, the potential for flooding on Bolivar Peninsula is similar to that on Galveston Island, but, in one important way it differs. Figures A.10 through A.12 in Appendix A show inundation patterns for the three storms, for the western end of Bolivar Peninsula. The western end roughly represents the western third of the peninsula.

As was the case for Galveston Island, the 17-ft Ike Dike is very effective in reducing the risk of flooding from the gulf side. However, as was the case for Galveston Island, even with the dike in place most of this region remains susceptible to flooding from the bay side because of the low-lying topography, particularly for the future sea level scenario. For Bolivar peninsula, the potential for bay-side flooding with the dike in place is dictated by surge levels within southern Galveston Bay and by the low-lying topography on the peninsula. Figure 12-11 shows the topography on the western end of Bolivar Peninsula. The topography is quite similar to that found on Galveston Island, with higher elevations on the gulf side and lower elevations on the bay side.

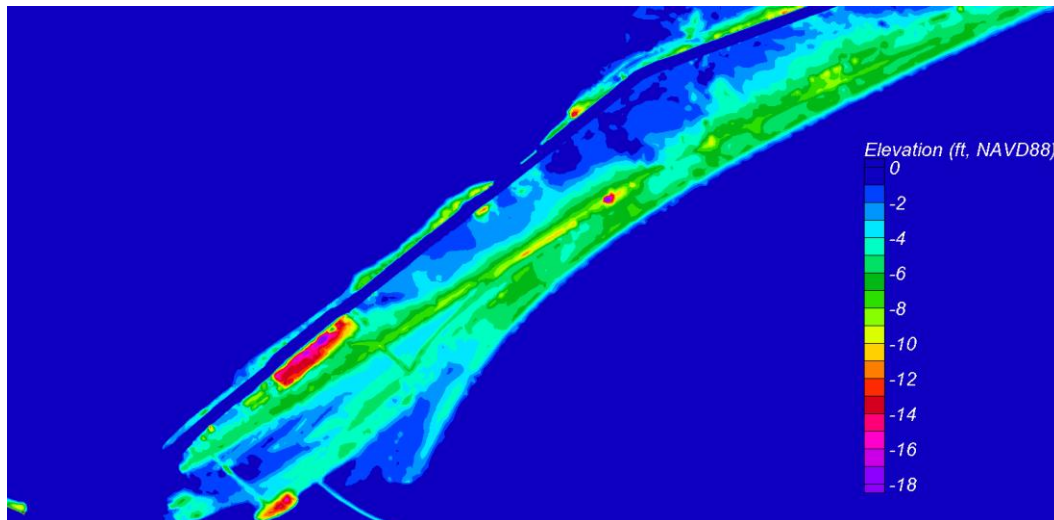


Figure 12-11. Topographic elevations at the western end of Bolivar Peninsula, in feet relative to the NAVD88 vertical datum. Negative values indicate elevations that lie above the vertical datum.

However, even though the topography is similar to Galveston Island, the prevailing storm surge patterns within southern Galveston Bay are quite different from those in West Bay for storms like Hurricane Ike and both proxy storms. In general, this difference reduces the potential for flooding from the bay side on Bolivar Peninsula compared to that for Galveston Island for these three storms and for those that make landfall on Galveston Island.

The persistent counterclockwise rotation of winds around the center of an approaching hurricane creates higher surge levels along the western shoreline of Galveston Bay. With the Ike Dike in place, the storm surge build-up on the western side of the bay is accompanied by a pronounced set-down of the water surface on the eastern side of the bay, which is the part adjacent to Bolivar Peninsula. This water surface gradient, and the set-down behind Bolivar Peninsula, are nicely illustrated in Figures 6-17 through 6-20 for another very severe hurricane that makes landfall in this vicinity, a “direct-hit” storm that was examined earlier in this study.

The signature of this east-west water surface elevation gradient is evident along the western side of Galveston Bay in the peak storm surge map shown in Figure 11-8 (a Hurricane Ike simulation). It is more evident in Figures 11-24 and 11-32, which show the peak surge maps for the 100-yr and 500-yr proxy storms respectively. The set-down in water surface elevation behind Bolivar Peninsula, which occurs before and during the time when the open coast storm surge is at its peak, reduces the potential for bay-side flooding on Bolivar Peninsula.

Even though the Ike Dike extends to Sabine Pass, some flanking flow is occurring for each of these three storms. This is evidenced by the gradient in peak surge within the inundated coastal areas east of Galveston Bay that is seen in each of the figures cited above. The flanking flow tends to reduce the amount of the set-down on the eastern side of the bay; however, the amount of flanking flow is relatively small for this longer, extended configuration of the Ike Dike.

Once the hurricane moves out of the region, and the water surface elevation within the bays levels out after the strong wind forcing has ceased, some bay-side flooding can occur due to the added volume of water that entered the bay, either through Bolivar Roads pass before the surge barrier gates were closed, or via flow over the dike during the peak of

the storm surge or flanking flow around the eastern terminus of the Ike Dike. The peak storm surge maps in Figures 11-8, 11-24, and 11-32 actually mask the amount of the set-down on the eastern side of the bay during the storm, because the peak surge within Galveston Bay behind Bolivar Peninsula occurs after the strong wind forcing has ceased and the water levels within the bays equilibrate.

Figure 12-12 illustrates the bay-side flooding on the western end of Bolivar Peninsula for the Hurricane Ike simulation, with the Ike Dike in place and for the present-day sea level. Of the three storms, only the Hurricane Ike simulation for present day sea level does not lead to appreciable steady flow over the Ike Dike, so the influence of bay-side flooding is most apparent for this simulation. The peak storm surge in the bay for this simulation is less than 2 ft NAVD88 in this region; and it is associated with the equilibrated water levels within the bay. In this model simulation, in which the surge barrier gate is effectively closed at the beginning of the simulation, this peak surge level is indicative of the amount of water that enters the bay due to flanking and flow over the dike in other areas.

None of the residential areas at the western end of Bolivar Peninsula experienced inundation for the Ike simulation at present sea level, despite the low topographic elevations that characterize most the Peninsula.



Figure 12-12. Inundation pattern for the Hurricane Ike simulation, with-dike condition, present-day sea level, for the western end of Bolivar Peninsula.

For the future sea level scenario, which is 2.4 ft higher than present sea level, all three storms produce nearly complete inundation of this portion of the barrier island as well as peak surge levels that exceed the 17-ft Ike Dike throughout this geographic region. Inundation is caused by steady flow over the dike and then down slope over the terrain toward the bay.

The three storms examined here have the distinct surge dynamic of setting down the water surface on the east side of the bay during the event, following by rising water levels as the volume of the water inside the bay equilibrates. A complete assessment of the risk of bay-side flooding on Bolivar Peninsula also must consider other types of storms that have significant surge generating potential in this region. The assessment should consider storms that make landfall to the west of the peninsula, where strong north-to-south blowing winds just prior to landfall, at landfall, and shortly after landfall, blowing over the long north-to-south fetch of Galveston Bay, will set up the south side of Galveston Bay. This wind set-up can cause inundation on the bay side of Bolivar Peninsula, particularly for an elevated future mean sea level. However, the farther a hurricane tracks to the west the lower the potential for flow over the Ike Dike in the Galveston Bay area, and the lower the magnitude of any flanking flow at Sabine Pass.

The same strategies mentioned previously for Galveston Island can be adopted here to reduce the risk of flooding from the gulf and bay sides: raising the first floor elevations of structures, and/or construction of ring levees/dikes/walls around concentrations of structures.

Bolivar Peninsula (central portion)

Figures A.13 through A.15 in Appendix A show inundation patterns for the simulations of Hurricane Ike and the 100-yr and 500-yr proxy storms, respectively, for the central portion of Bolivar Peninsula.

Figure 12-13 shows the topography on the central portion of Bolivar Peninsula. Rollover Pass, which connects the gulf to the bay, is evident on the right side of the figure near the legend. As part of the Ike Dike concept, a gate will be required at Rollover Pass if navigation and water exchange is to be maintained. The peninsula narrows considerably from west to east in this sub-region; and the highest elevations on the peninsula also decrease from west to east. Maximum elevations at the western side of this sub-region are quite low, less than 5 ft NAVD88.

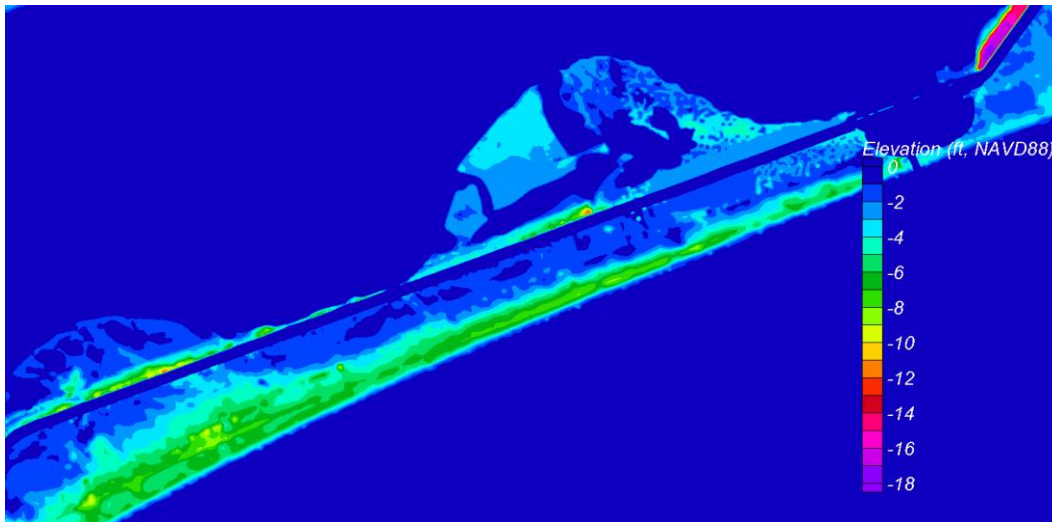


Figure 12-13. Topographic elevations at the central portion of Bolivar Peninsula, in feet relative to the NAVD88 vertical datum. Negative values indicate elevations that lie above the vertical datum.

With the Ike Dike in place, the potential for flooding in the central portion of Bolivar Peninsula is quite similar to that on western end. The terrain is low-lying and the dominant storm surge dynamics are the same. The 17-ft Ike Dike is very effective in reducing the risk of flooding from the gulf side. But even with the dike in place, this region is susceptible to flooding from the bay side because of the low-lying topography, particularly for the future sea level scenario.

Figure 12-14 illustrates the bay-side flooding in this region for the Hurricane Ike simulation, with the Ike Dike in place and present-day sea level. The Hurricane Ike simulation for present day sea level does not lead to steady flow over the Ike Dike in the western (left) side of the figure; however, some overflow is apparent at the eastern (right) side of the figure. Where steady flow over the dike does not occur, little inundation is evident in the areas with the highest concentrations of residences.

For the future sea level scenario, which is 2.4 ft higher than present sea level, all three storms produce nearly complete inundation of this portion of the barrier island. All three storms produce peak surge levels that exceed the 17-ft Ike Dike crest throughout this region with the elevated mean sea level. Inundation is caused by steady flow over the dike and down slope toward the bay. Elevated sea level also leads to greater potential for flooding from the bay side.



Figure 12-14. Inundation pattern for the Hurricane Ike simulation, with-dike condition, present-day sea level, for the central portion of Bolivar Peninsula.

The observations and recommendations regarding measures to reduce the risk of flooding here are the same as those made for the western end of the island.

Bolivar Peninsula (eastern end)

Figures A.16 through A.18 in Appendix A show inundation patterns for the simulations of Hurricane Ike and the 100-yr and 500-yr proxy storms, respectively, for the eastern end of Bolivar Peninsula.

Figure 12-15 shows the topography in this sub-region, which is similar to that found in eastern side of the central sub-region. The peninsula is quite narrow and the highest portions on the gulf side have low maximum elevations. The exception is at High Island, the area of very high topographic elevations clearly seen on the right side of the figure. There are far fewer residences in this sub-region, compared to the others.

With the Ike Dike in place, the potential for flooding in the eastern end of Bolivar Peninsula is quite similar to that elsewhere on the peninsula. The terrain is low-lying and the dominant storm surge dynamics are the same. The 17-ft Ike Dike is very effective in reducing the risk of flooding from the gulf side.

Even with the Ike Dike in place, this region is susceptible to flooding from the bay side because of the low-lying topography, particularly for the future sea level scenario.

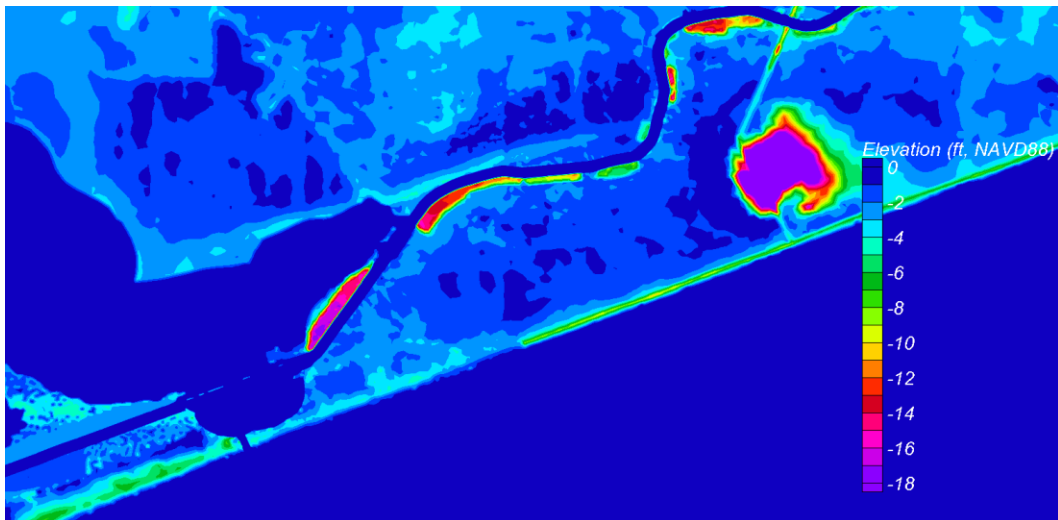


Figure 12-15. Topographic elevations at the eastern end of Bolivar Peninsula, in feet relative to the NAVD88 vertical datum. Negative values indicate elevations that lie above the vertical datum.

Figure 12-16 illustrates the bay-side flooding in this region with the Ike Dike in place, for the Hurricane Ike simulation and present-day sea level. The Hurricane Ike simulation for present day sea level leads to steady flow over the Ike Dike in most places, as do the proxy storms.

The observations and recommendations regarding measures to reduce the risk of flooding here are the same as those made for the rest of Bolivar Peninsula.



Figure 12-16. Inundation pattern for the Hurricane Ike simulation, with-dike condition, present-day sea level, for the eastern end of Bolivar Peninsula.

Galveston Bay

Texas City (south)/La Marque/Bayou Vista

Figures A.19 through A.21 in Appendix A show inundation maps for the sub-region that encompasses the Texas City (south), La Marque, Hitchcock and Bayou Vista areas, all of which are located along the western shoreline of Galveston Bay, across the bay from and north of the City of Galveston. Maps are shown for the simulations of Hurricane Ike and the 100-yr and 500-yr proxy storms.

Texas City/La Marque

Figures 12-17 and 12-18 show the inundated areas for the 100-yr proxy storm and the future sea level scenario, for both the existing, no-dike, condition (Figure 12-17) and for the with-Ike Dike condition (Figure 12-18). The Texas City industrial area and La Marque, which is seen in the upper right corner of both figures, are surrounded by the Texas City levee, which is shown with a thin green line. The Texas City levee has a crest elevation that ranges from 19 to 23 feet.

These two figures provide an indication of the Ike Dike's flood risk reduction benefits in this sub-region. Without the Ike Dike in place, the area inside the levee is subjected to widespread inundation for the 100-yr proxy storm and the future sea level scenario (see Figure 12-17). For these conditions the peak storm surge level on the east side of the Texas City levee is 17.5 ft. On the southwest side of the levee the peak surge level is 19 ft.

The extremely high surge level on the southwest side of the levee, approximately 19 ft, is the source of inundation inside the polder. The western terminus of the levee is flanked in this simulation. This flanking flow appears to be the primary source of water causing inundation inside the polder, although there might be some steady flow over the levee as well. The western terminus of the levee is circled in Figure 12-19, which is a map of the surge model's topographic elevations in this sub-region.

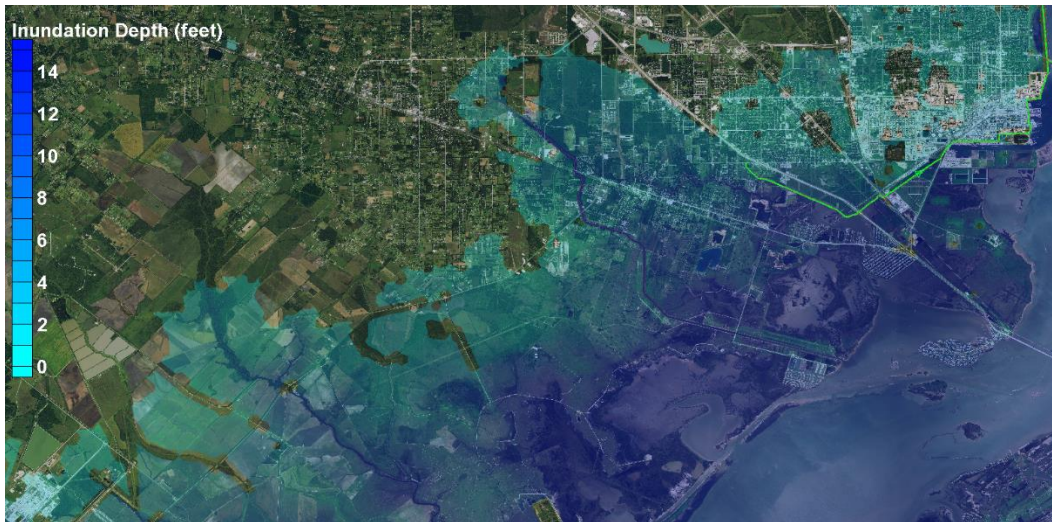


Figure 12-17. Inundation pattern for the 100-yr proxy storm simulation in the Texas City (south)/La Marque/Bayou Vista area, no-dike condition, future sea level scenario..

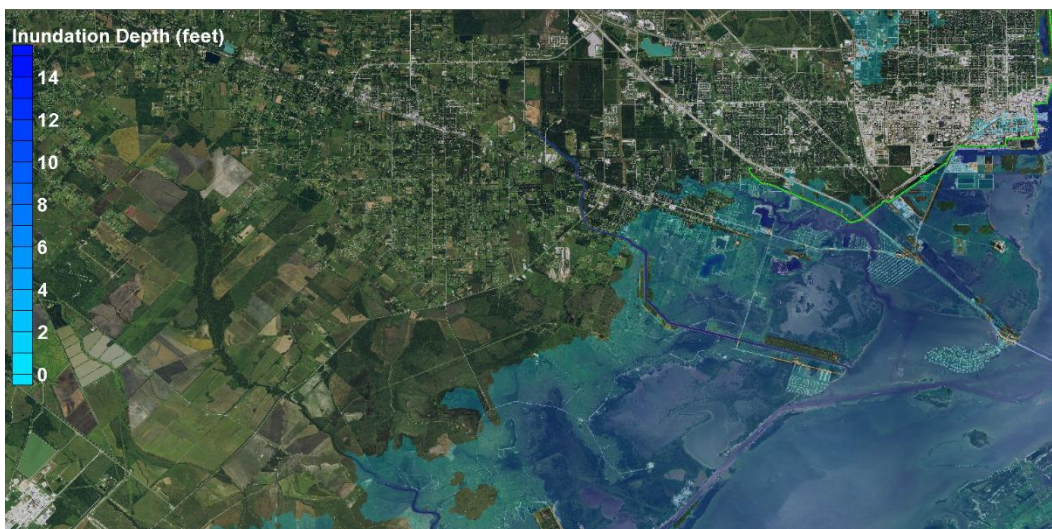


Figure 12-18. Inundation pattern for the 100-yr proxy storm simulation in the Texas City (south)/La Marque/Bayou Vista area, with-dike condition, future sea level scenario.

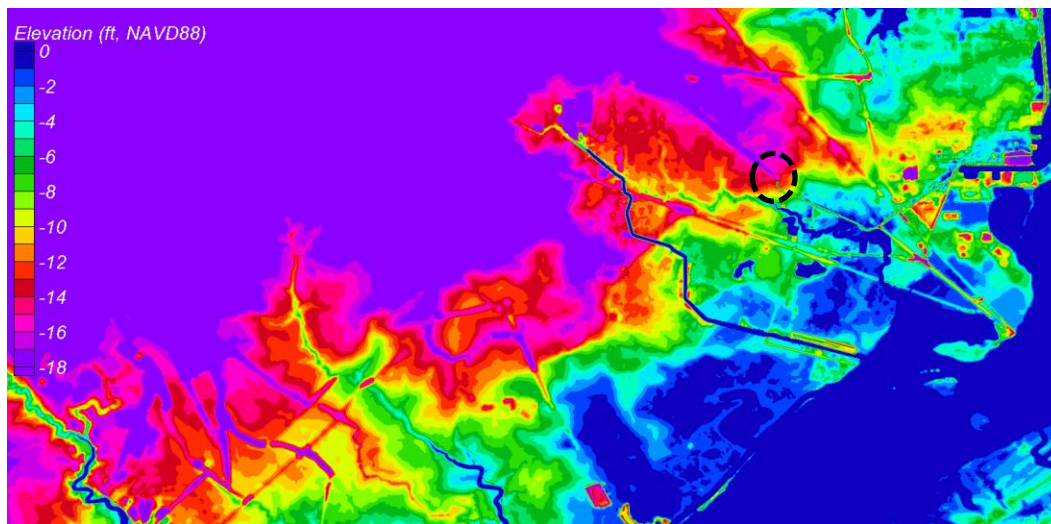


Figure 12-19. Topographic elevations in the Texas City (south)/La Marque/Bayou Vista areas, in feet relative to the NAVD88 vertical datum. Negative values indicate elevations that lie above the vertical datum.

Closer inspection of the model's elevations at this location show much lower topographic elevations than 19 ft (the minimum levee crest elevation) between the western terminus of the levee, as it is represented in the surge model, and an elevated highway embankment nearby, which also is seen in Figure 12-19 as a dark purple linear feature. Inspection of this area using imagery in Google Earth shows that the levee ends short of the elevated highway. The model shows an elevation of 13.6 ft NAVD88 at the levee terminus, and there is a significant distance between the end of the levee and the closest point on the elevated highway where the model elevation is 19 ft NAVD88. The highway elevation is gradually decreasing in this area.

The elevation of the levee at its terminal end, and elevations between the levee terminus and the highway embankment, should be investigated further to ascertain whether or not there is in fact a low spot, or if the surge model representation of this area is inaccurate. A low spot having these elevations and extent would constitute a vulnerability in the levee system which should be addressed.

With the 17-ft Ike Dike in place, the peak surge levels adjacent to the Texas City levee are reduced considerably, to values of 9.5 ft on the eastern side and 10.5 ft on the southern side for the 100-yr proxy storm and the future sea level scenario. These reductions in peak surge prevent the Texas City industrial areas from being inundated for this severe hurricane and sea level conditions (see Figure 12-18).

Figures 12-20 and 12-21 show the inundated areas for the 500-yr proxy storm and the future sea level scenario, for both the existing condition (Figure 12-20) and the with-Ike Dike condition (Figure 12-21).

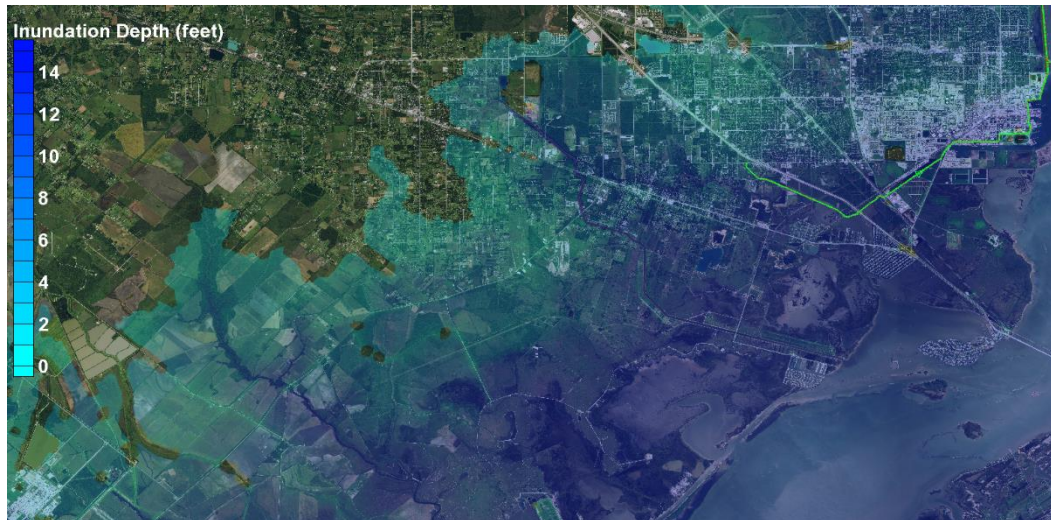


Figure 12-20. Inundation pattern for the 500-yr proxy storm simulation in the Texas City (south)/La Marque/Bayou Vista area, no-dike condition and the future sea level scenario.

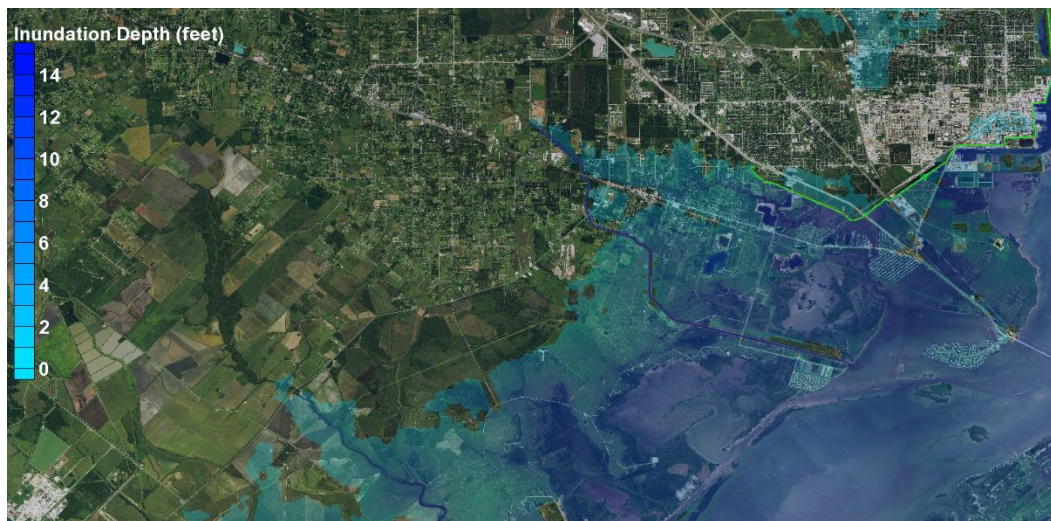


Figure 12-21. Inundation pattern for the 500-yr proxy storm simulation in the Texas City (south)/La Marque/Bayou Vista area, with-dike condition and the future sea level scenario.

For the existing condition (without the Ike Dike), for the 500-yr proxy storm simulation with the future sea level the peak surge on the east side of the Texas City levee is 20.5 ft, and on the southwest side of the levee it is 22.5 ft. Again, the extremely high surge levels on the south and southwest sides of the levee appear to be the source of the inundation inside the levee. There is extensive flanking of the levee system on the southwest side as well as steady flow over the crest of the levee. This hurricane, at

this sea level, completely fills the polder inside the levee ring with peak water levels that exceed 14 ft NAVD88.

For the same 500-yr proxy storm, but at the present-day sea level, widespread inundation inside the levee occurs as well. The depth and extent of inundation lie between those for the 100-yr and 500-yr proxy storms at the future sea level.

The 17-ft Ike Dike prevents inundation via steady overflow or flanking inside the Texas City levee for the 100-yr proxy storm and the future sea level scenario, and for all the 500-yr proxy storm simulations. These storm conditions reflect severe and rare hurricanes at elevated sea levels. In Figures 12-18 and 12-21, the few isolated areas inside the levee that do seem to indicate some inundation are actually low lying or water areas that are raised by the +2.4 ft in sea level and become deeper water areas in the model at the beginning of the simulation. These areas do not reflect increases due to flow over the levee or to flanking flow around the southwest terminus of the levee.

With the Ike Dike in place, the existing Texas City levee becomes a very substantial secondary line of defense. Together, these two risk reduction measures greatly reduce the risk of inundation within the Texas City industrial area, reducing the possibility to extremely low probabilities as evidenced by the positive results for the 500-yr proxy storm and the future sea level scenario. With the dike in place, the potential vulnerability at the southwest terminus of the Texas City levee does not lead to any inundation inside the levee for any of the storms that were simulated.

With the Ike Dike in place, peak surge levels on the eastern side of the levee are 9 and 11 ft for the 500-yr proxy storms simulations, for the present-day and future sea level scenarios, respectively. The east-facing side of the levee is where wave conditions will be greatest for these storms because of the strong winds from the east and the available wind fetch within Galveston Bay to the east of the levee. These peak surge levels are roughly equal to or less than the peak surge levels that were experienced during Hurricane Ike at this location. On the south side of the levee, where wave conditions are expected to be lower than on the east side, peak surge levels for the two with-dike, 500-yr proxy storms simulations were 11 and 13 feet for the two sea level scenarios, which are also similar to the surge levels that were experienced during Hurricane Ike. Wave

overtopping of the Texas City levee for the 500-yr proxy storm and the future sea level scenario is expected to be comparable to or less than the magnitude of wave overtopping that was experienced during Hurricane Ike in 2008.

Bayou Vista and Hitchcock areas

The Bayou Vista and Hitchcock areas are more susceptible to inundation. Bayou Vista, which is a small community in a very low-lying area, is located just to the southwest of, and adjacent to the southern tip of, the Texas City levee. Hitchcock lies to the west and southwest of the Texas City levee, and to the west of Bayou Vista. There are two other communities in very low-lying areas south of Bayou Vista, Tiki Island and Harborwalk. See Figure 12-1 for the exact locations of these communities.

With the Ike Dike in place, peak storm surge values in the Bayou Vista area, for Hurricane Ike, the two proxy storms, and for both sea level scenarios, are summarized as follows. For the Hurricane Ike simulation, with the Ike Dike in place, peak surge levels at Bayou Vista are 4 ft and 6.5 ft for the present-day and future sea levels, respectively. For the 100-yr proxy storms, the corresponding peak surges for the two sea levels are 8 ft and 10.5 ft. For the 500-yr proxy storms, the corresponding peak surges are 11 ft and 13 ft.

As seen in Figures 12-17 and 12-18 for the 100-yr proxy storm, and Figures 12-20 and 12-21 for the 500-yr proxy storms (both for the future sea level), the Ike Dike provides a considerable reduction in the extent and depth of inundation for the southeastern Hitchcock area. However, the lowest-lying areas remain inundated, even with the Ike Dike in place. The Bayou Vista area and the other low-lying communities are inundated for all the 100-yr and 500-yr proxy storm simulations.

For the Hurricane Ike simulation for present-day sea level with the Ike Dike in place, storm surge levels are sufficiently reduced to prevent inundation in the Tiki Island and Harborwalk communities, and in some parts of the Bayou Vista community. The potential for wave overtopping is not considered in this analysis. The Ike Dike is very effective in preventing inundation within the Hitchcock area for the Hurricane Ike simulation and present-day sea level.

Figure 12-22 shows inundation for Hurricane Ike, with the Ike Dike in place, for the future sea level scenario. The Ike Dike is rather effective in preventing inundation within the Hitchcock area. The lowest-lying communities remain inundated.

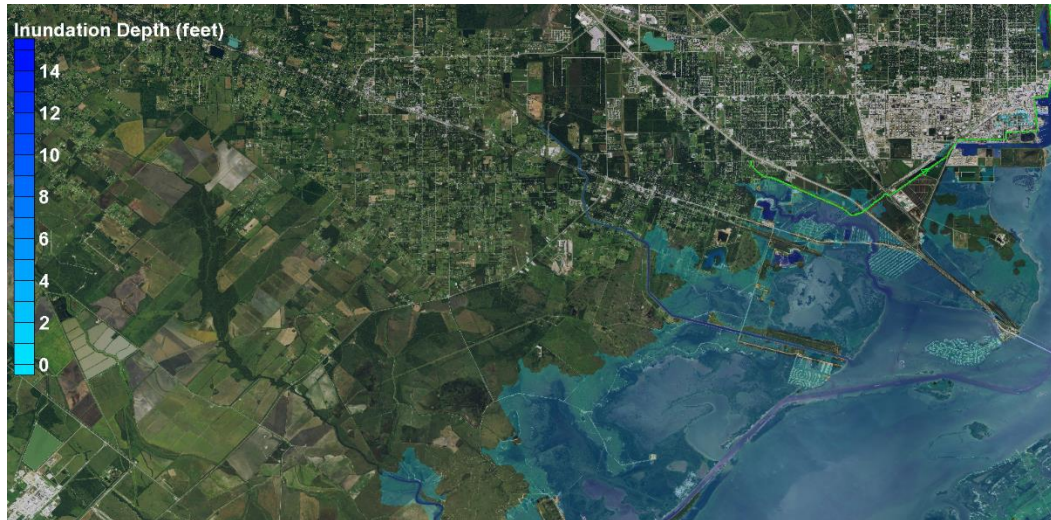


Figure 12-22. Inundation pattern for the Hurricane Ike simulation, in the Texas City (south)/La Marque/Bayou Vista area, with-dike condition and the future sea scenario.

For the low lying communities of Tiki Island and Harborwalk, the strategies mentioned previously for Galveston Island and Bolivar Peninsula appear to be the only feasible options to reduce the risk of flooding from the gulf and bay sides to a greater degree than the risk reduction the Ike Dike provides. These include raising the first floor elevations of structures, and/or construction of ring levees/dikes/walls around concentrations of structures. If ringing these communities is not acceptable to the residents, elevating the structures might be the only viable option if additional risk reduction is desired.

To achieve additional risk reduction in the Hitchcock and Bayou Vista areas, structural measures could be implemented along the possible alignments shown in Figure 12-23. Measures to further reduce the residual risk could include levees/dikes, walls or combinations of these features. The alignments shown in Figure 12-23 generally follow existing transportation infrastructure, either roads or rail lines, where possible. Different alignments would require gates in certain locations, either to allow train, vehicle or navigation access. In light of the relatively sparse density of structures in the Hitchcock area and the likely cost of these structural alternatives, it seems unlikely that such lengthy secondary lines of defense would be cost effective.

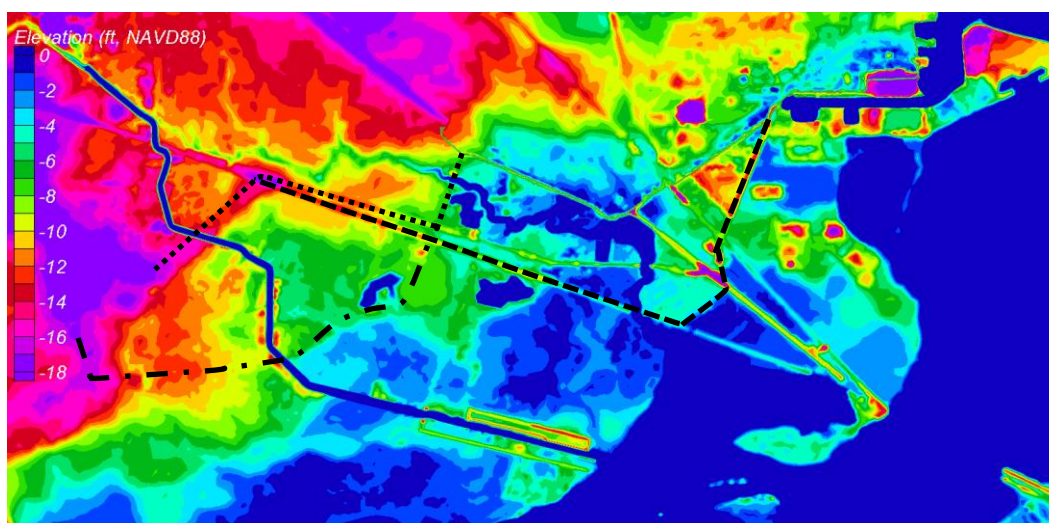


Figure 12-23. Possible alignments for a more extensive dike/levee/wall system that reduces residual flood risk for the Hitchcock and Bayou Vista areas.

Structural measures may not be acceptable to a community like Bayou Vista. Therefore, raising the first-floor elevations of structures is likely to be only feasible option to achieve any further risk reduction in this area.

The crest elevations of any additional measures that are taken would depend on the desired level of risk reduction. These levee/dike alignments could accommodate a reasonable volume of wave overtopping, so crest elevations would likely range from 11 to 16 ft to cover the range of peak surge experienced for the two proxy storms and both sea levels. The crest elevation estimates allow for 3 ft of freeboard above the with-dike peak surge elevations in order to reduce wave overtopping to manageable levels.

San Leon/Texas City (north)/Bacliff/Dickinson

Figures A.22 through A.24 in Appendix A show inundation maps for the sub-region that includes the San Leon, Texas City (north), Bacliff, and Dickinson communities. Maps are shown for the simulations of Hurricane Ike and the 100-yr and 500-yr proxy storms.

For the Hurricane Ike simulation, and for present-day sea level, the 17-ft Ike Dike eliminates inundation throughout this entire sub-region. The presence of the dike reduces the peak surge in Dickinson Bay from 11.5 ft to 3.5 ft, a surge suppression of 8 ft. For the Ike simulation and for the future sea level scenario, which is +2.4 higher than the present-day sea level, the Ike Dike reduces peak surge levels from 14 ft to 6 ft. This reduction in peak surge eliminates inundation everywhere except in a few

of the lowest-lying areas along the Dickinson Bay shoreline, including the lowest-lying parts of San Leon, and areas immediately adjacent to the Dickinson and Gum Bayous. The lowest-lying part of San Leon is subjected to flooding from the Dickinson Bay side for this storm and the future sea level scenario. See Figure 12-1 for a map showing these locations.

Without the Ike Dike, for the more severe 100-yr and 500-yr proxy storms, and for both sea level scenarios, this sub-region is subjected to widespread inundation, particularly for the future sea level scenario. With the 17-ft Ike Dike in place, because of surge suppression, there are substantial widespread reductions in the area that is inundated. However, some low-lying areas are still inundated even with the dike in place. For example, for the 100-yr proxy storm and present-day sea level, the presence of the dike reduces the peak surge in Dickinson Bay area from 14.5 ft to 8 ft. For the future sea level scenario, the dike reduces peak surge levels from 17.5 ft to 10 ft for this same storm. On average, surge suppression achieved with the Ike Dike is 7 ft in this sub-region.

For the 100-yr proxy storm and present-day sea level, the Ike Dike greatly reduces the amount of flooding in the Dickinson area. As was the case for the Hurricane Ike simulation, only the lowest-lying areas along Dickinson and Gum Bayous experience inundation for these conditions, although the extent of inundation for this hurricane is slightly greater than for Hurricane Ike. For the future sea level scenario, inundation in the Dickinson area is greatly reduced. Inundation in the low-lying areas around along Dickinson and Gum Bayous is a little more widespread for the higher sea level conditions compared to that for the present-day sea level.

Without the dike, inundation in the Bacliff area is extensive for the 100-yr proxy storm and both sea levels. With the Ike Dike, flooding in the Bacliff area is eliminated.

The most vulnerable area is the area around Dickinson Bay, including the San Leon community. Inundation occurs in San Leon for the 100-yr proxy storm and both sea levels; flooding occurs from both the Dickinson Bay and Galveston Bay sides.

For the 500-yr proxy storm, and present-day sea level, the presence of the dike reduces peak surge in the Dickinson Bay area from 17.5 ft to 10 ft. For the future sea level scenario, the Ike Dike reduces peak surge levels from 20 ft to 12 ft. On average surge suppression is 7 to 8 ft.

The Ike Dike greatly reduces the amount of flooding that is experienced in the Dickinson area for the 500-yr proxy storm and both sea level scenarios. However, even with the Ike Dike in place, several areas around Dickinson are inundated for this storm. The areas that remain inundated in Dickinson for this storm and both sea levels are the same as the areas that remain inundated for the 100-yr proxy storm and the future sea level, although they are expanded for the 500-yr proxy storm.

For the 500-yr proxy storm and both sea levels, flooding in the Bacliff area is eliminated by the Ike Dike.

The low-lying San Leon area is inundated from both the Dickinson Bay and Galveston Bay sides for the 500-yr proxy storm and both sea levels.

To graphically illustrate these some of these observations and more precisely identify the areas having the highest residual risk with the Ike Dike in place, Figure 12-24 shows the widespread inundation that occurs for the no-dike condition, for the 100-yr proxy storm and the future sea level scenario. The sub-region is completely inundated including much of the Dickinson area. Inundation for the 500-yr proxy storm and the future sea level is slightly more widespread than that shown in Figure 12-24.

Figures 12-25 and 12-26 show the inundated areas for the 100-yr and 500-yr proxy storms, respectively, with the Ike Dike in place, and for the future sea level scenario. The Ike Dike reduces the risk of flooding in the Bacliff area to a very low probability of occurrence. However, even with the dike in place, the Dickinson and San Leon communities have residual risk. These two figures indicate the size of the areas in Dickinson that have the greatest residual risk of flooding, and they show how the extent of inundation in these areas varies between the two proxy storms.

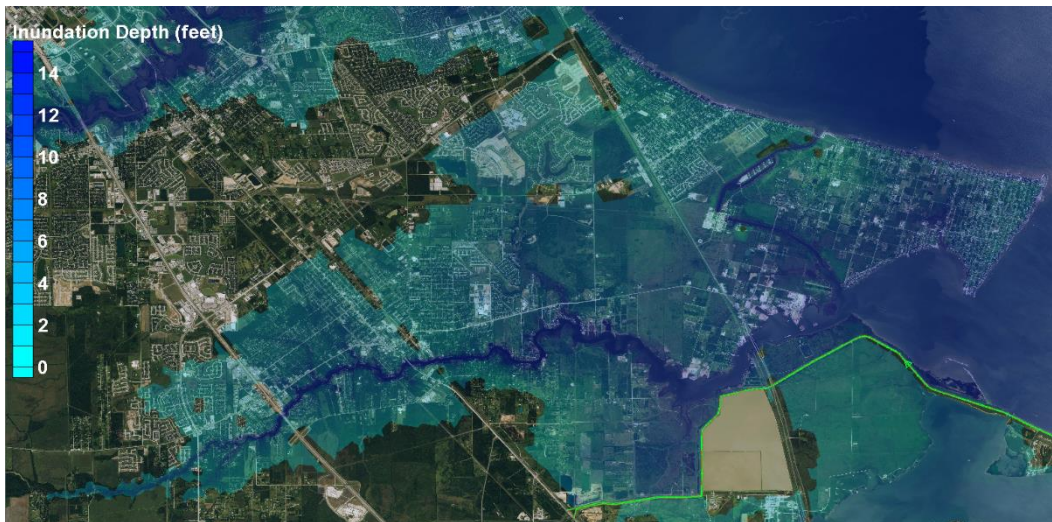


Figure 12-24. Inundation pattern for the 100-yr proxy storm simulation in the San Leon/Texas City (north)/Bacliff/Dickinson area, no-dike condition and the future sea level scenario.

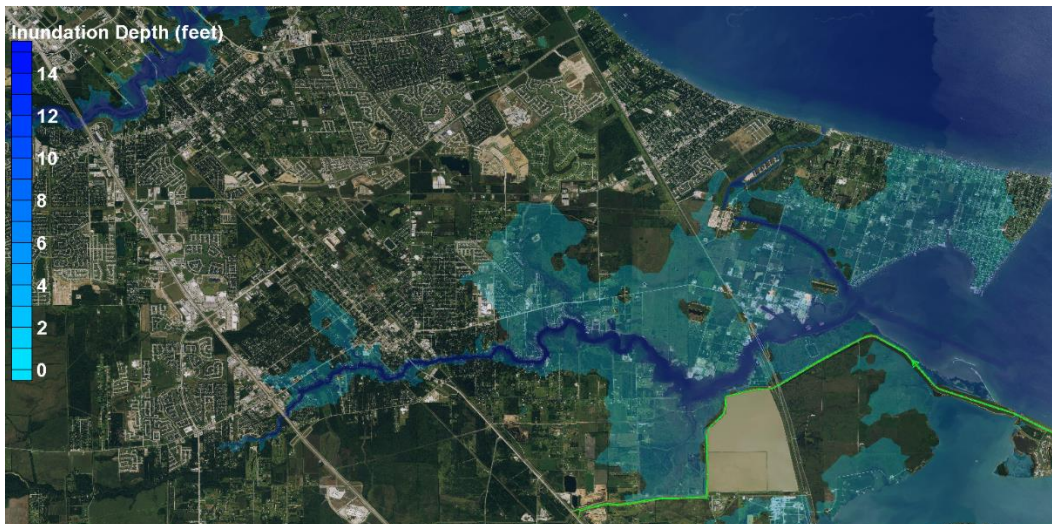


Figure 12-25. Inundation pattern for the 100-yr proxy storm simulation in the San Leon/Texas City (north)/Bacliff/Dickinson area, with-dike condition and the future sea level scenario.

The figures also indicate those areas around the Dickinson Bay shoreline, including San Leon, that have the greatest residual risk. The residual risk is much higher around Dickinson Bay because of the very low-lying terrain. Figure 12-27 shows the topographic elevations in this sub-region. Much of San Leon is situated on topography having elevations less than 8 ft NAVD88.

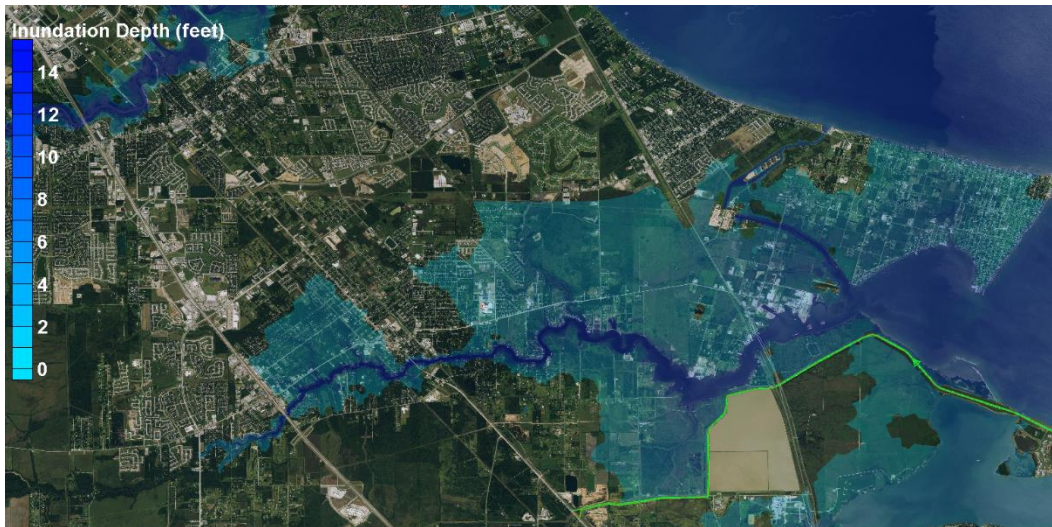


Figure 12-26. Inundation pattern for the 500-yr proxy storm simulation in the San Leon/Texas City (north)/Bacliff/Dickinson area, with-dike condition and the future sea level scenario.

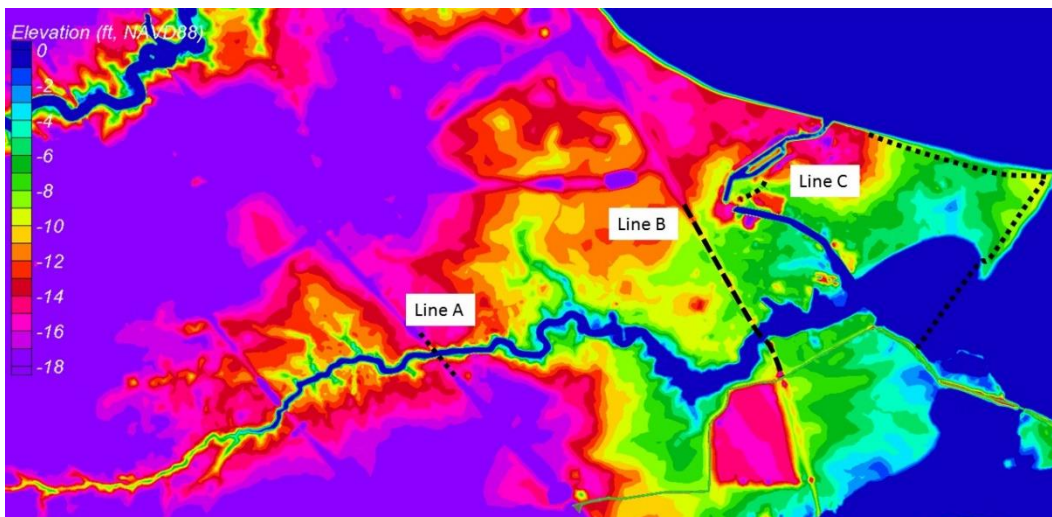


Figure 12-27. Topographic elevations in the San Leon/Texas City (north)/Bacliff/Dickinson areas, in feet relative to the NAVD88 vertical datum, and possible secondary lines of defense.

There are several possible secondary lines of defense that can lessen the residual flood risk in this sub-region. The inundation maps and elevation map can be used to assess possible secondary lines of defense that could be implemented now or in the future as sea level rises to further reduce the flood risk in these areas.

One measure that can reduce residual risk to part of the Dickinson area involves a short section of levee or wall and a small gate to enable navigation when the gate is not closed, at the location indicated as “Line 1” in Figure 12-27. This secondary line of defense is tied into an existing

elevated railroad bed where the rail line crosses the Dickinson Bayou. This site is located just to the east of where Highway 3 crosses the bayou. The rail line was selected as the site because it has an existing elevation of nearly 18 ft NAVD88. This secondary measure could reduce the residual risk to the low-lying floodplain area of Dickinson, which lies just to the east of the rail line, to a very low probability. The water that inundates this part of Dickinson enters the flood plain via the Dickinson Bayou.

A second possibility that could reduce residual risk for a much larger area, including the entire Dickinson area, is a levee/dike/wall along Highway 146. This secondary line of defense is shown as “Line B” in Figure 12-27. This alignment also would require a gate at the entrance to Clear Lake. It would be incorporated into sections of the existing highway infrastructure. The Gulf Coast Community Protection and Recovery District (2016) also considered and proposed such a measure along this highway as a primary line of defense for the western shoreline of Galveston Bay. As a secondary line of defense, the levee/dike/wall/gate system would be much lower in elevation, much shorter in length, and much less substantial in cross section than a primary line of defense.

Neither of the secondary defense lines, A nor B, reduces the residual flood risk for areas located to the east of them, including the community of San Leon. Any significant flood risk reduction for San Leon must be achieved with measures that address flooding from both the Galveston Bay and Dickinson Bay sides of the peninsula. Inspection of the San Leon area in Google Earth reveals an area that is characterized by an abundance of long private docks along the east-, south- and west-facing shorelines of the San Leon peninsula, and a small dock facility and embayment on the Dickinson Bay side.

A number of approaches to reduce residual flood risk in this area are possible. Most likely, raising the elevations of structures as part of a long-term community plan is the only feasible approach. Construction of risk reduction measures along the periphery of the peninsula, across the open water leading to Dickinson Bay, and tying into the Texas City levee can be done; however, it seems problematic for a number of reasons, including real estate and rights-of way issues, public acceptability, and cost.

Construction of a levee/dike/wall would either require removal of the docks, construction seaward of the docks, or construction landward of them, perhaps by elevating existing roads that are set back from the coast line. There is a shore-parallel road on the side of the peninsula facing Galveston Bay, but not along the south-facing shoreline. A possible alignment for such a structural approach is indicated as “Line C” in Figure 12-27, although the actual alignment would likely have to be much more irregular than this to integrate it into existing roads. The alignment shown would tie into the Texas City levee and it would require construction of a substantial navigation gate in open water.

Each of the alignments, Lines A, B or C, will differ in complexity of implementation, costs, benefits, and other pros and cons. A structure on Line C appears to be a complex and expensive alternative to implement, and the least likely. An analysis of costs, benefits, and other factors would need to be done to examine the feasibility of any of these risk reduction measures.

The crest elevations of any of these measures would depend on the desired level of risk reduction. Crest elevations would likely range from 11 to 14 feet for lines A and B, and 14 to 16 ft for Line C, for the future sea level scenario. These elevations allow for freeboard above the with-dike peak surge elevations in order to reduce any wave overtopping to manageable levels. Approximate amounts of freeboard that are included here in the elevation estimates are: 1 ft of freeboard at Line A, 2 ft at Line B and 4 ft of freeboard at Line C.

Clear Lake/Bayport/La Porte

Figures A.25 through A.27 in Appendix A show inundation maps for the sub-region that includes the Clear Lake, Bayport and La Porte areas. Maps are shown for the simulations of Hurricane Ike and the 100-yr and 500-yr proxy storms.

For the Hurricane Ike simulation, and for present-day sea level, the 17-ft Ike Dike eliminates inundation throughout this entire sub-region. The presence of the dike reduces the peak surge at the entrance to Clear Lake from 11.5 ft to 2.5 ft, a surge suppression of 9 ft; and at Morgan’s Point the peak surge is reduced from 13 ft to 2 ft, a surge suppression of 11 ft. For the Ike simulation and for the future sea level scenario, which is +2.4 higher than the present-day sea level, the Ike Dike reduces peak surge

levels from 14.5 ft to 5 ft at the entrance to Clear Lake, and from 16 ft to 5 ft at Morgan's Point. Surge suppression was 9.5 ft to 11 ft for the future sea level scenario. This considerable reduction in peak surge eliminates inundation nearly everywhere in this sub-region, except in a few of the lowest-lying areas at the entrance to Clear Lake at Seabrook and Clear Lake Shores and along Nassau Bay.

Without the Ike Dike in place, for both the 100-yr and 500-yr proxy storms, and for both sea level scenarios, this sub-region is subjected to widespread inundation, particularly for the future sea level scenario. Figure 12-28 shows the extent of inundation for the 100-yr proxy storm and the future sea level scenario, without the Ike Dike in place. The NASA facility adjacent to Nassau Bay is inundated. Bayport is inundated as are all the communities along the western shoreline of Galveston Bay, La Porte, Morgan's Point, Shoreacres, Clear Lake Shores, Seabrook and Kemah. Inundation for the 500-yr proxy storm and the future sea level is even more widespread.

Figures 12-29 and 12-30 show the inundated areas for the 100-yr and 500-yr proxy storms, respectively, and the future sea level scenario, for the with-dike condition. With the 17-ft Ike Dike in place, there are substantial widespread reductions in the area inundated. However, some low-lying areas are still inundated, and most of them that have a higher density of structures are located closer to the Galveston Bay shoreline. These lower-lying areas have the greatest residual risk of flooding with the Ike Dike in place

Flooding in the vicinity of the NASA facility, at Morgan's Point, and at LaPorte is eliminated. At Bayport flooding is nearly eliminated for the present-day sea level, but there is some inundation in the southern part of Bayport for the future sea level scenario. Also, with the dike in place, inundation remains in those areas that are close to the entrance to Clear Lake, in the Clear Lake Shores, Seabrook and Kemah areas, for both sea levels. These are areas having higher residual risk.

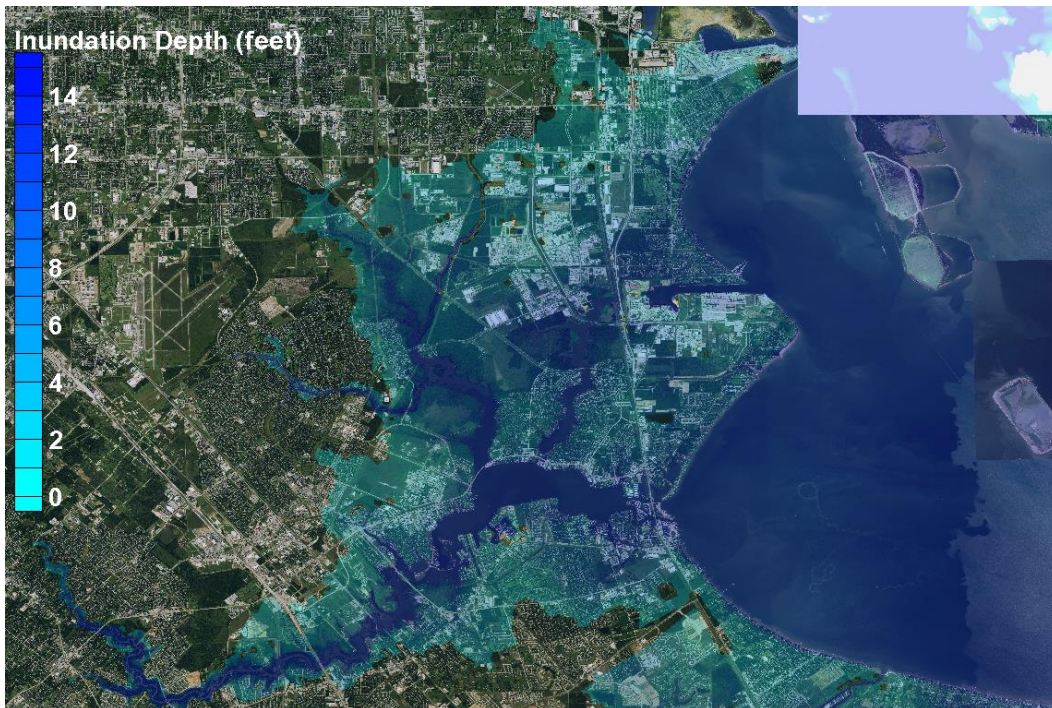


Figure 12-28. Inundation pattern for the 100-yr proxy storm simulation in Clear Lake/Bayport/La Porte areas, no-dike condition and the future sea level scenario.

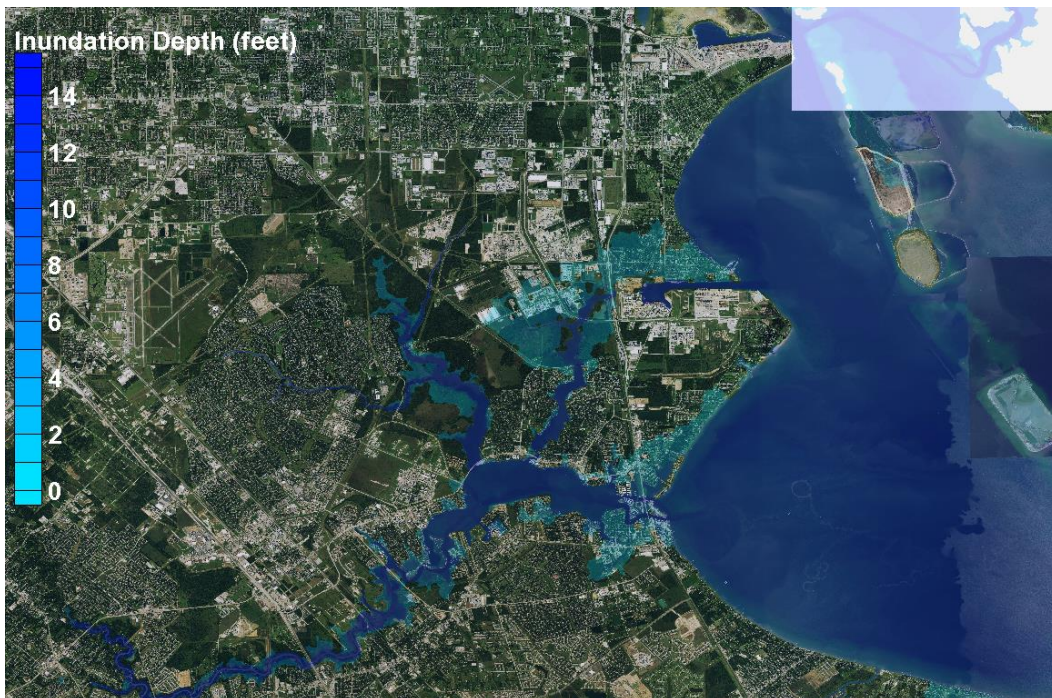


Figure 12-29. Inundation pattern for the 100-yr proxy storm simulation in Clear Lake/Bayport/La Porte areas, with-dike condition and the future sea level scenario.

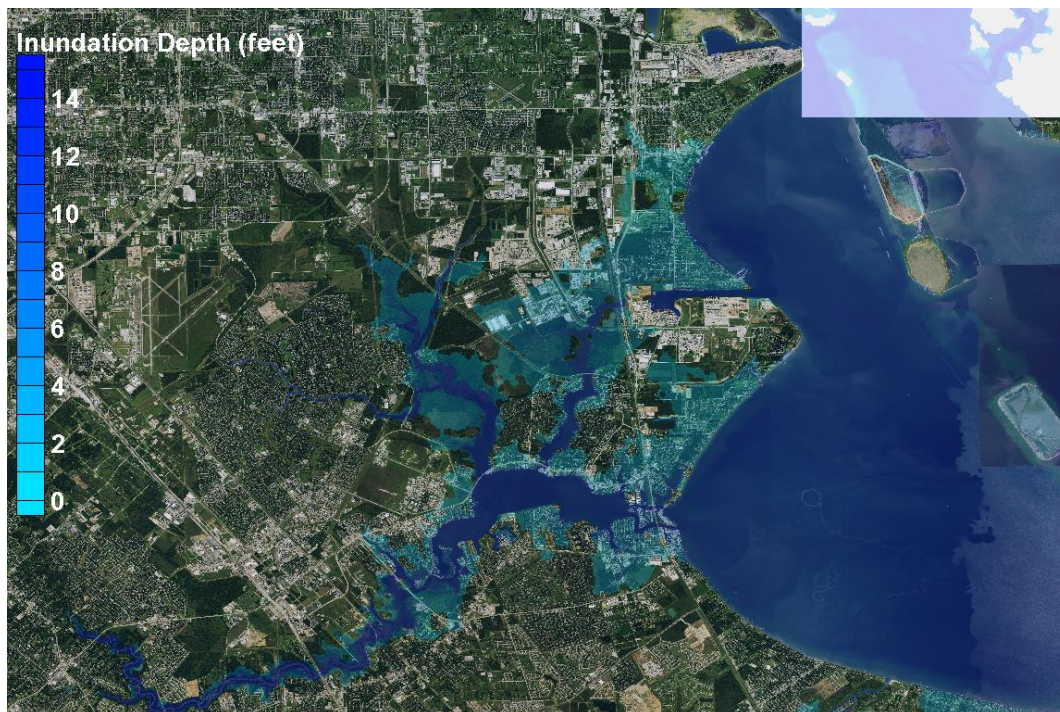


Figure 12-30. Inundation pattern for the 500-yr proxy storm simulation in Clear Lake/Bayport/La Porte areas, with-dike condition and the future sea level scenario.

For the 500-yr proxy storm and the future sea level, these same areas are inundated with the Ike Dike in place. In addition to these areas, other low-lying areas adjacent to the Clear Lake shoreline also are inundated, including areas on the periphery of the NASA facility in Nassau Bay (see Figure 12-30). The southern part of La Porte is inundated for this storm and the future sea level scenario. However, inundation at Morgan's Point is eliminated by the Ike Dike even for the 500-yr proxy storm and the future sea level.

To reduce the residual risk in this sub-region, there are several possible measures that can be taken. The alignments of possible measures are shown in Figure 12-31, which also shows the topographic elevations in the sub-region.

One possible measure involves a levee/dike/wall system that is built along Highway 146, which could be incorporated into the existing highway infrastructure. The Gulf Coast Community Protection and Recovery District (2016) also considered and proposed such a measure along this highway as a primary line of defense. As a secondary line of defense, the levee/dike/wall/gate system would be much lower in elevation, much shorter in length, and much less substantial in cross section. This option

would also require a gate to facilitate navigation at the entrance to Clear Lake. The two sections that comprise this secondary line of defense are shown as “Line A” in Figure 12-31.

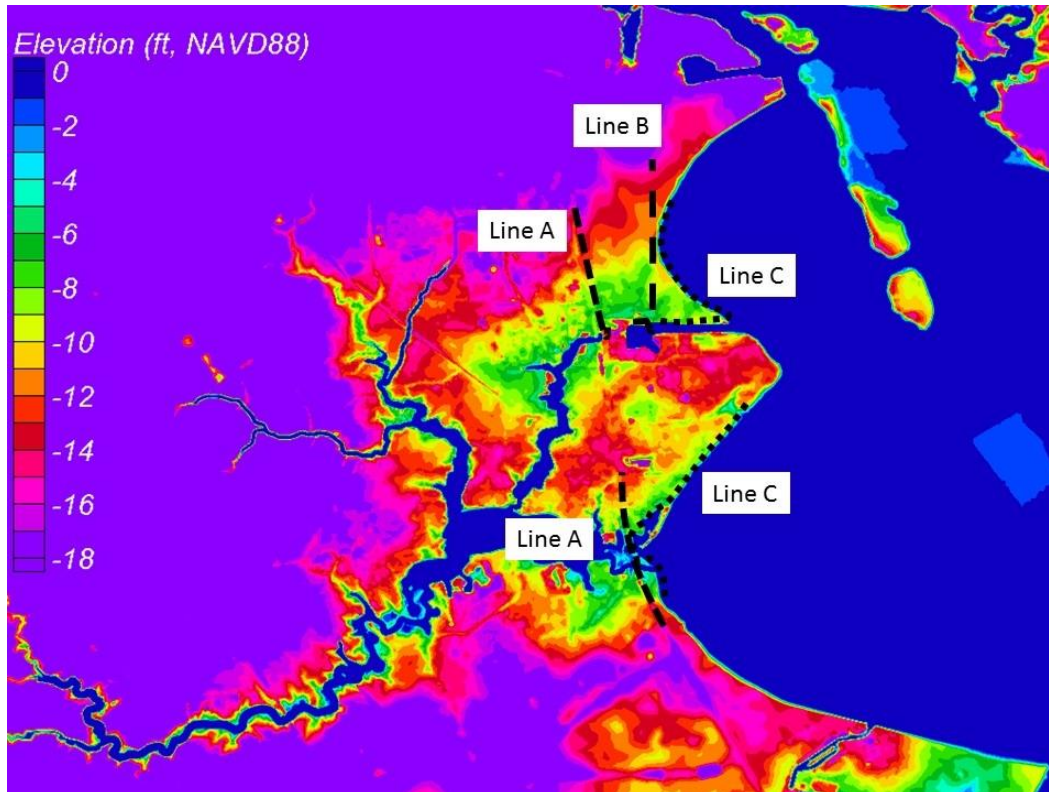


Figure 12-31. Topographic elevations in the Clear Lake/Bayport/La Porte areas, in feet relative to the NAVD88 vertical datum, and possible secondary lines of defense.

The upper section of the secondary line of defense, Line A, could be replaced by another measure along an alignment indicated as “Line B” in Figure 12-31. This potential line of defense is positioned along another smaller road, South Broadway Street, which also runs north to south through most of LaPorte. This alignment would reduce flood risk for a greater area. However, the narrowness of the available footprint and rights of way for this road, and the need for many gates or other means to provide access to side streets on either side of it, probably preclude this alignment as being a viable alternative. The larger dimensions of the Highway 146 footprint and rights of way probably make it the better alternative.

The only other apparent option which would provide the greatest risk reduction for the broadest area would be a secondary line of defense right at the Galveston Bay shoreline, taking the alignment shown in Figure 12-31

as “Line C”. However, judging from the built environment and the many docks along the bay shoreline, there might be public opposition to construction of any structural measures at the coast.

The other option is to raise the elevations of individual structures as part of a long-term strategy to do so in the most vulnerable areas.

Each of the possible alignments for a secondary line of defense will differ in ease of implementation, costs, benefits, real estate and rights of ways issues, and other pros and cons. An analysis of costs, benefits, and other factors, would need to be done to examine the feasibility of any of these levee/dike/wall/gate system alternatives.

The crest elevations of any of these measures depends on the desired level of risk reduction. Crest elevations would likely range from 13 to 16 feet for any measures taken along Line A. These elevations allow for freeboard above the with-dike peak surge elevations in order to reduce any wave overtopping to manageable levels. Approximate amounts of freeboard that are included here are 2 to 4 ft.

Houston Ship Channel

Upper Houston Ship Channel (eastern portion)

Figures A.28 through A.30 in Appendix A show inundation maps for this sub-region that includes the eastern half of the upper reaches of the Houston Ship Channel. Maps are shown for the simulations of Hurricane Ike and the 100-yr and 500-yr proxy storms.

For both of the Hurricane Ike simulations, the presence of the 17-ft Ike Dike reduces the peak surge from 13.5 ft to 2.5 ft for the present-day sea level; and, for the future sea level scenario, the peak surge is reduced from 16.5 ft to 5 ft. On average, the surge suppression for the Hurricane Ike simulations is approximately 11 ft. This substantial reduction in peak surge eliminates inundation nearly everywhere in this sub-region for all but isolated extremely low-lying areas.

For the 100-yr proxy storm, the 17-ft Ike Dike reduces peak surge from 18.5 ft to 10 ft for the present-day sea level and from 21.5 ft to 12 ft for the future sea level scenario. On average, the surge suppression for the 100-yr proxy storm is approximately 9 ft for these two sea levels.

Figures 12-32 and 12-33 show the inundated areas for the 100-yr proxy storm and the future sea level scenario, for both the no-dike and with-dike simulations respectively.

For the no-dike case (see Figure 12-32), there is significant inundation to many industrial sites. At peak surge levels of 21.5 ft for this case, extensive economic damage is expected. In addition to economic losses, inundation creates the potential for significant environmental damage. This is a heavily industrialized area, having many petro-chemical facilities.

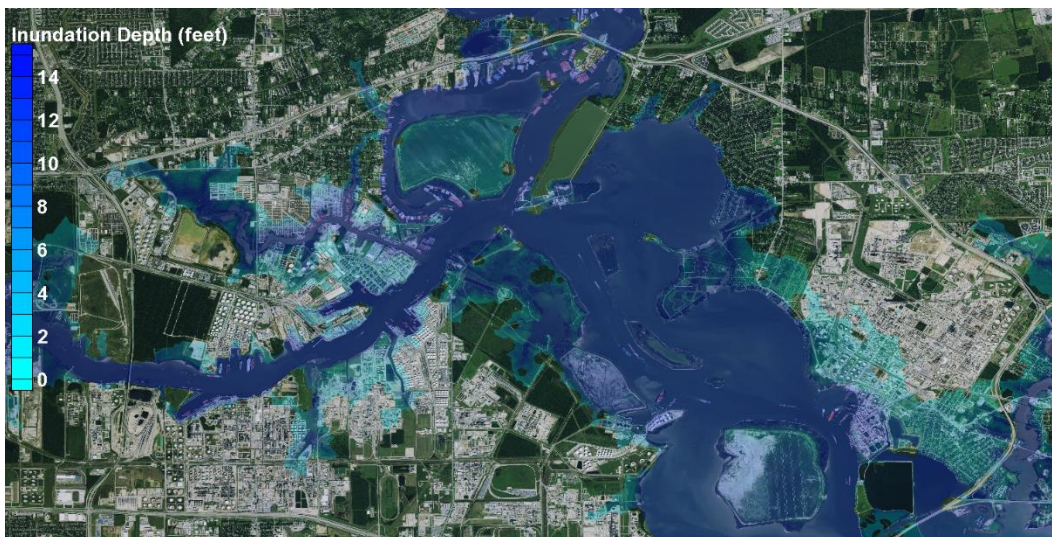


Figure 12-32. Inundation pattern for the 100-yr proxy storm simulation in the eastern portion of the upper Houston Ship Channel, no-dike condition and the future sea level scenario.

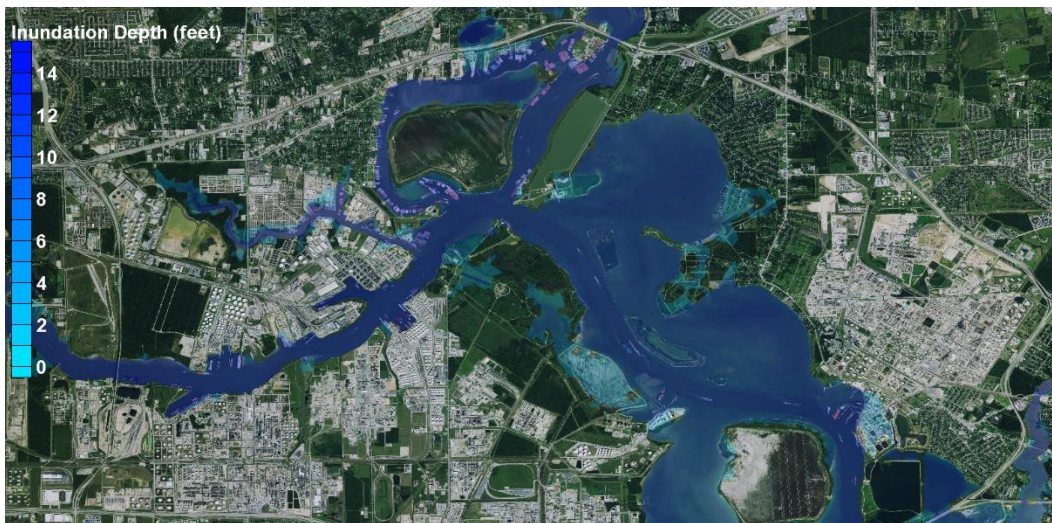


Figure 12-33. Inundation pattern for the 100-yr proxy storm simulation in the eastern portion of the upper Houston Ship Channel, with-dike condition and the future sea level scenario.

Inspection of Google Earth imagery shows that many areas of the sub-region are heavily populated with storage tanks. Ecological impacts could result from petro-chemical spills associated with storage facilities and/or tanks that are damaged as a result of inundation by the storm surge and accompanying wave energy/forces.

With the 17-ft Ike Dike in place, there are substantial reductions in the areas that are inundated (see Figure 12-33). However, inundation still occurs in a few of the lowest-lying areas, although the depth of inundation in these areas is greatly reduced by the dike. Elevations for the sub-region are shown in Figure 12-34 (note the change in elevation scale used in the figure, compared to all previous elevation figures). A few of the industrial facilities are located in low-lying areas where topographic elevations are less than 9 ft above NAVD88.

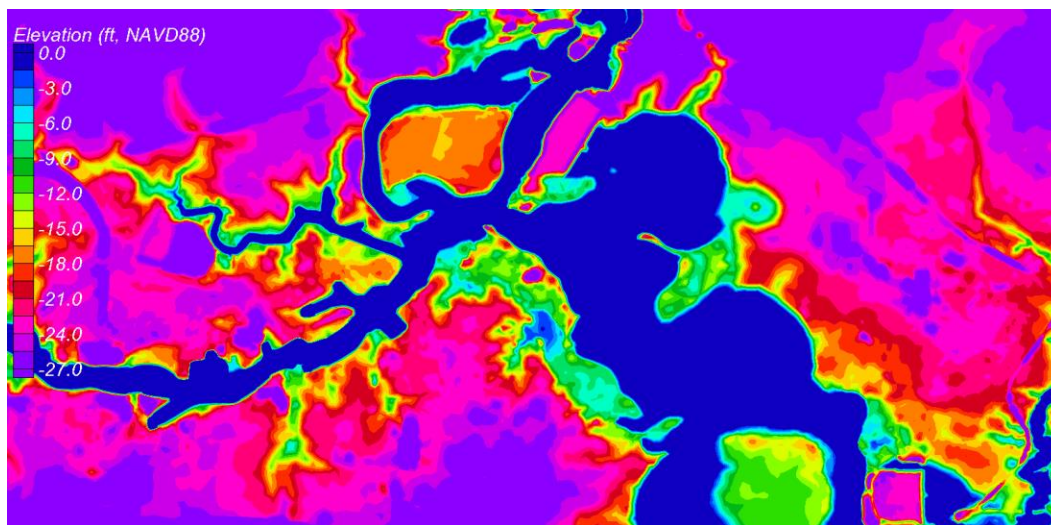


Figure 12-34. Topographic elevations in the eastern portion of the upper Houston Ship Channel, in feet relative to the NAVD88 vertical datum.

For the 500-yr proxy storm, the 17-ft Ike Dike reduces the peak surge from 22 ft to 12.5 ft for the present-day sea level and from 25 ft to 14.5 ft for the future sea level scenario. On average, the surge suppression for the 500-yr proxy storm is approximately 10 ft for these two cases.

Figures 12-35 and 12-36 show the inundated areas for the 500-yr proxy storm and the future sea level scenario, for both the no-dike and with-dike simulations respectively.

For the no-dike case (Figure 12-35), because of the 25-ft peak storm surge, there is much more widespread inundation and deeper depths of

inundation in industrial areas throughout the sub-region than for the 100-yr proxy storm and future sea level. As seen in Figure 12-36, the Ike Dike greatly reduces the extent of inundation for this event. Where inundation still occurs, depths are greatly reduced, by approximately 10 ft, which is the amount of surge suppression.

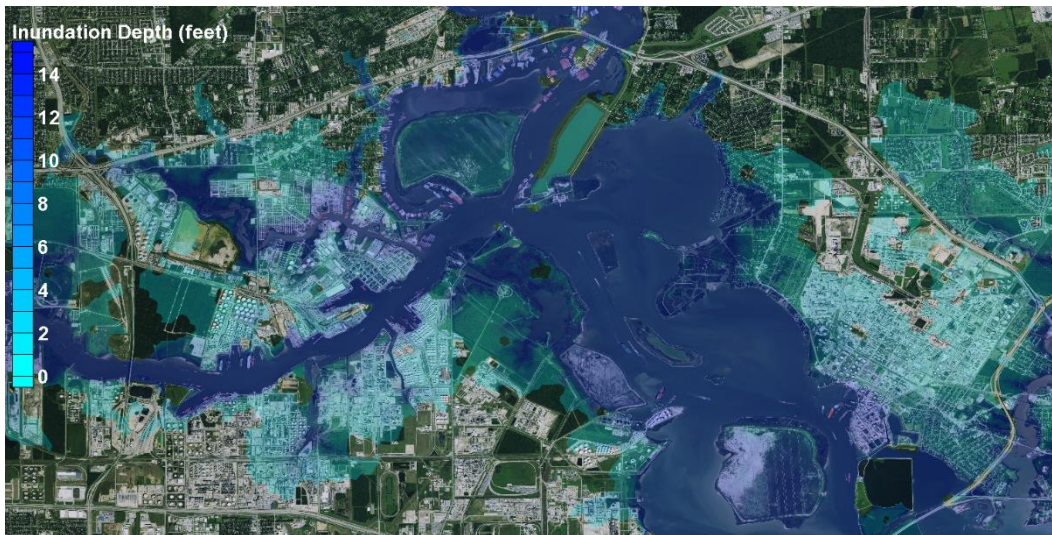


Figure 12-35. Inundation pattern for the 500-yr proxy storm simulation in the eastern portion of the upper Houston Ship Channel, no-dike condition and the future sea level scenario.

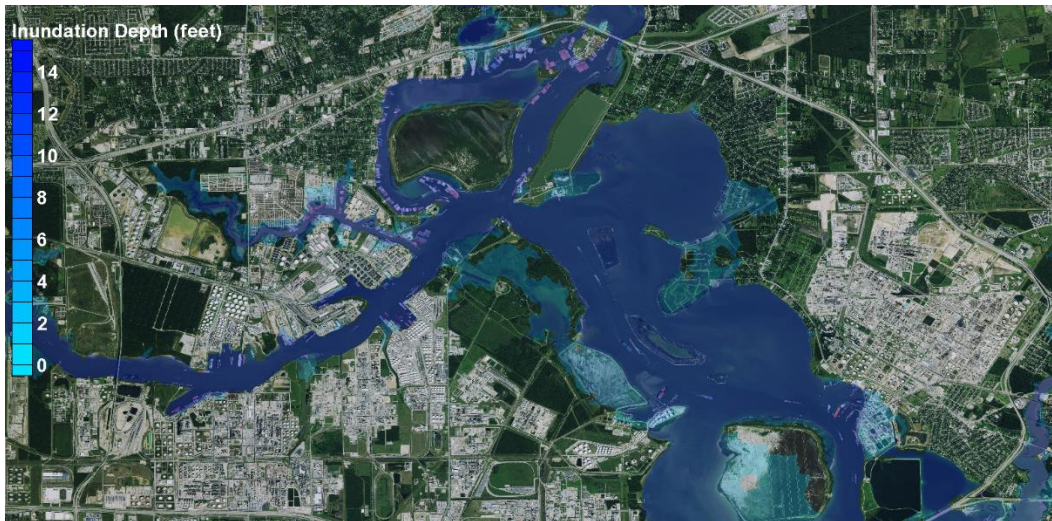


Figure 12-36. Inundation pattern for the 500-yr proxy storm simulation in the eastern portion of the upper Houston Ship Channel, with-dike condition and the future sea level scenario.

In areas having undesirable residual risk, levees/dikes/walls built to ring individual facilities can reduce it to the desired level. In light of the peak surge levels for the 100-yr and 500-yr proxy storms, and both sea level scenarios, the elevations of such features would probably need to be in the range of 11 to 16 ft, depending on the desired level of risk reduction and exposure of the site/levee to wave action.

Upper Houston Ship Channel (western portion)

Figures A.31 through A.33 in Appendix A show inundation maps for this sub-region that comprises much of the western half of the upper reaches of the Houston Ship Channel. Maps are shown for the simulations of Hurricane Ike and the 100-yr and 500-yr proxy storms.

The storm surge conditions in this part of the upper ship channel are nearly the same as those in the eastern portion of the upper ship channel, for both no-dike and with-dike conditions and for both sea level scenarios.

Figures 12-37 and 12-38 show the inundated areas for the 100-yr proxy storm and the future sea level scenario, for both the no-dike and with-dike simulations respectively. Figures 12-39 and 12-40 show the inundated areas for the 500-yr proxy storm and the future sea level scenario, for both the no-dike and with-dike simulations respectively.

Observations and conclusions regarding the extent and depths of inundation for the western portion of the upper reaches of the Houston Ship Channel are the same as those for the eastern portion. With the 17-ft Ike Dike in place, there are substantial reductions in the areas that are inundated and inundation depths are reduced by amounts roughly equal to the average surge suppression values. However, inundation still occurs in a few of the lowest-lying areas with the dike in place, although the depth of inundation in these areas is greatly reduced. Elevations for the western sub-region are shown in Figure 12-41.

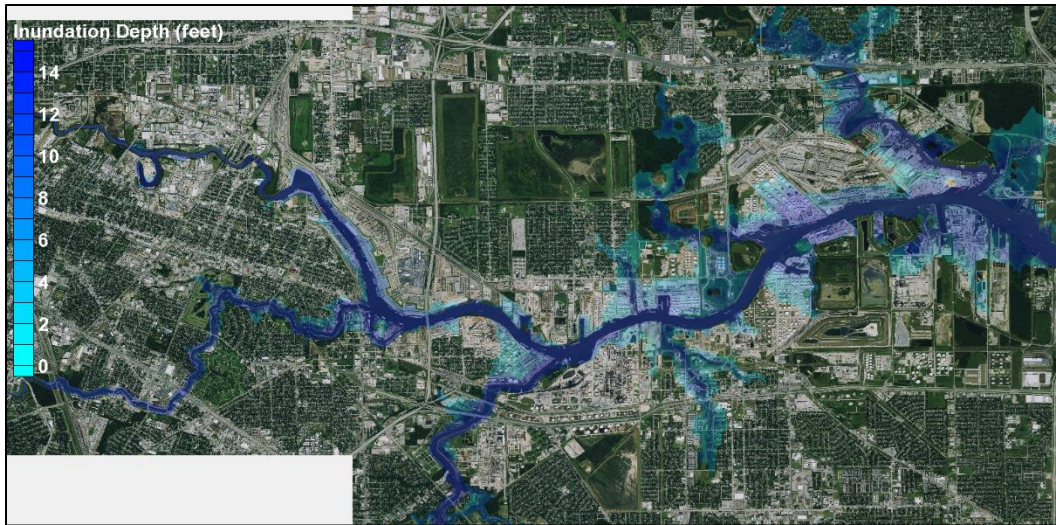


Figure 12-37. Inundation pattern for the 100-yr proxy storm simulation in the western portion of the upper Houston Ship Channel, no-dike condition and the future sea level scenario.

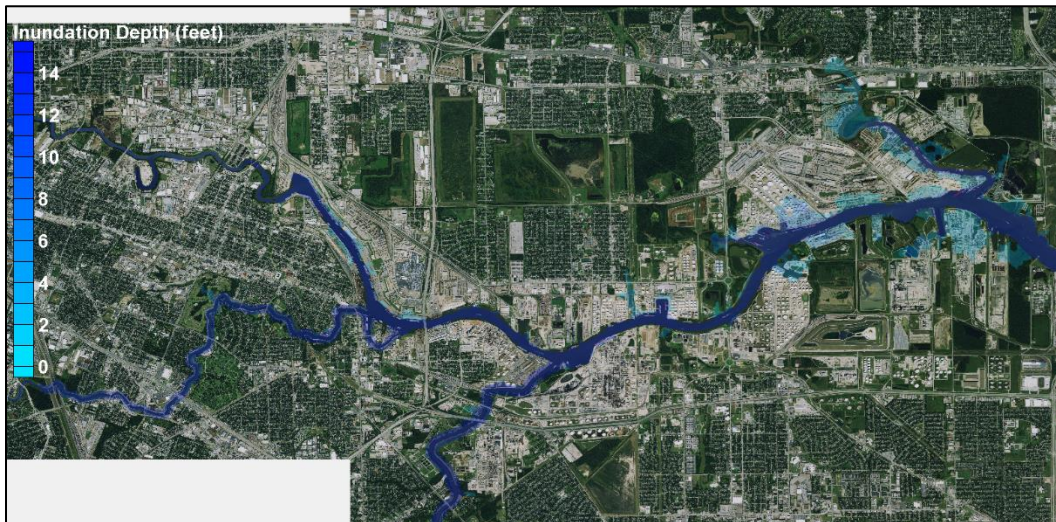


Figure 12-38. Inundation pattern for the 100-yr proxy storm simulation in the western portion of the upper Houston Ship Channel, with-dike condition and the future sea level scenario.

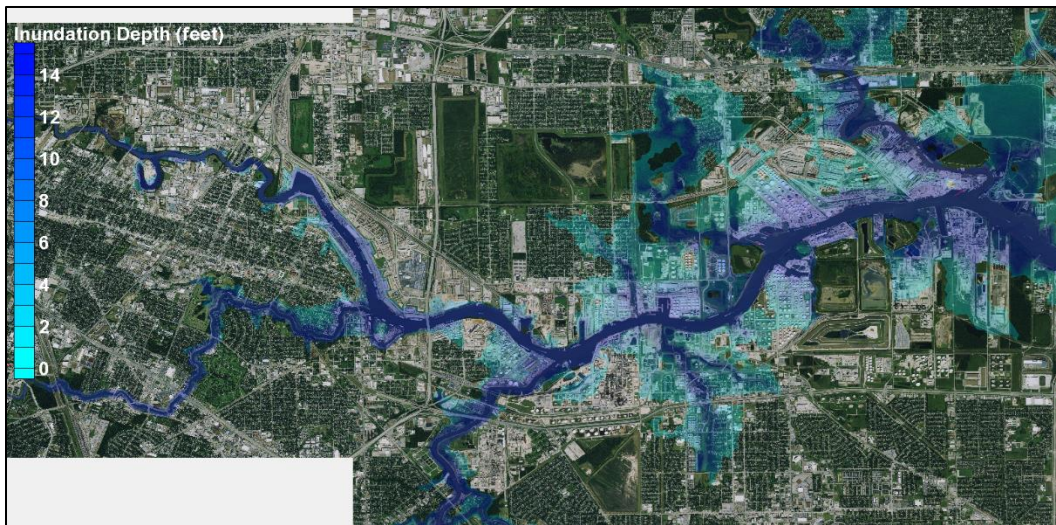


Figure 12-39. Inundation pattern for the 500-yr proxy storm simulation in the western portion of the upper Houston Ship Channel, no-dike condition and the future sea level scenario.

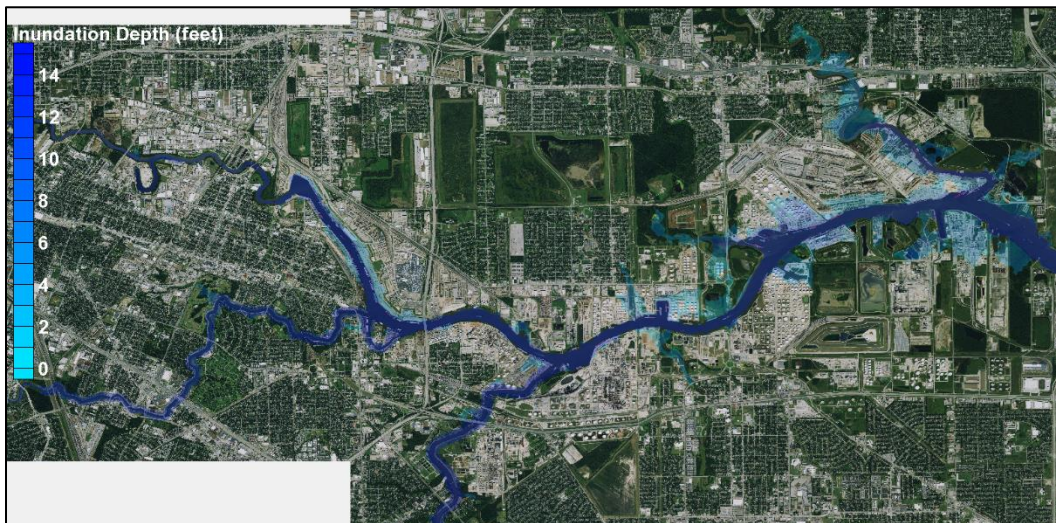


Figure 12-40. Inundation pattern for the 500-yr proxy storm simulation in the western portion of the upper Houston Ship Channel, with-dike condition and the future sea level scenario.

The 17-ft Ike Dike is extremely effective in suppressing the peak storm surge amplitude in the upper Houston Ship Channel reaches of Galveston Bay for severe hurricanes that would otherwise produce very large and damaging storm surges in this region. As is the case for the Texas City industrial area, the magnitude of the surge suppression achieved with the Ike Dike is sufficient to reduce the risk of inundation to a very low probability in most of these highly industrialized areas. This is a major advantage for this regional approach to flood risk reduction.

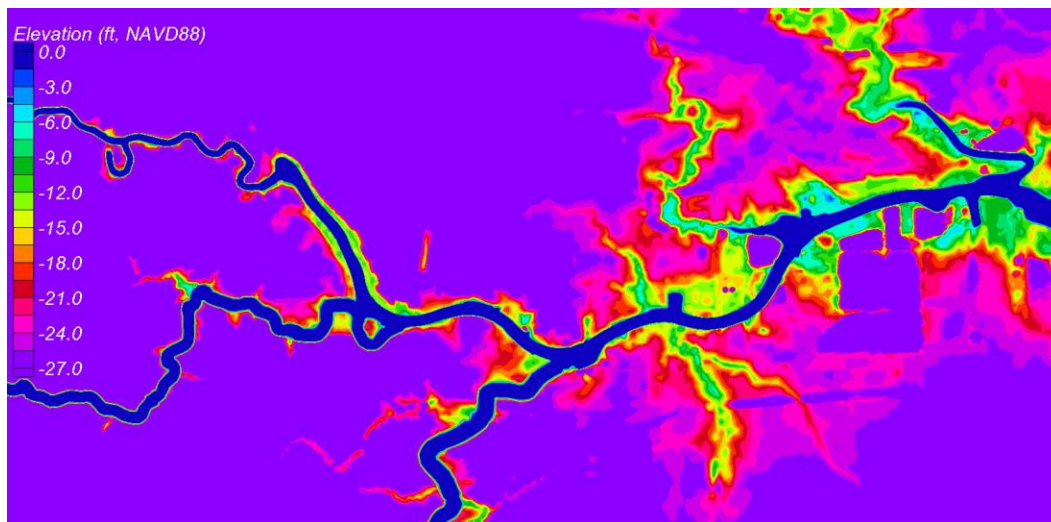


Figure 12-41. Topographic elevations in the western portion of the upper Houston Ship Channel, in feet relative to the NAVD88 vertical datum.

The “Centennial Gate” option was originally proposed by the Rice University SSPEED Center as a stand-alone surge suppression measure to prevent storm surge penetration into the upper reaches of the Houston Ship Channel. The 500-yr proxy storm, for existing conditions and the future sea level scenario, produces peak surges that reach nearly 25 ft in this area. With the coastal spine in place, peak surge levels that are generated in the upper ship channel (14 to 15 ft) would be about 1 ft higher than those experienced during Hurricane Ike. Except for very low-lying areas, the Ike Dike seems to be quite effective in suppressing surge levels in the upper ship channel area, probably precluding the need for a “Centennial Gate” as a risk reduction measure for this region. If sea level is expected to be much higher than the future sea level of +2.4 ft, or if Ike Dike gate operations enable more of the hurricane surge forerunner to penetrate into Galveston Bay prior to gate closure, perhaps adding several feet of water to the system, the need for such a gate can be revisited.

13 Examination of Alternate Ike Dike Configurations

Dike Configurations

Introduction

The original set of storm simulations that were made to examine benefits of the Ike Dike concept involved a long dike that followed the shoreline, began just south of Freeport, TX, and ended just to the east of High Island, TX. The original dike alignment followed the long continuous green line that is shown in Figure 13-1, which follows the coastline. The eastern terminus of the original dike is shown by the blue star in Figure 13-1; the location of High Island is shown by the yellow star. The dike included gate systems at both San Luis Pass and Bolivar Roads in order to provide a single continuous line of defense. Results from those initial simulations were discussed in Chapter 8; and, they suggested that flanking around the eastern terminus of the dike lead to significant increases in peak storm surge levels of several feet throughout Galveston Bay.

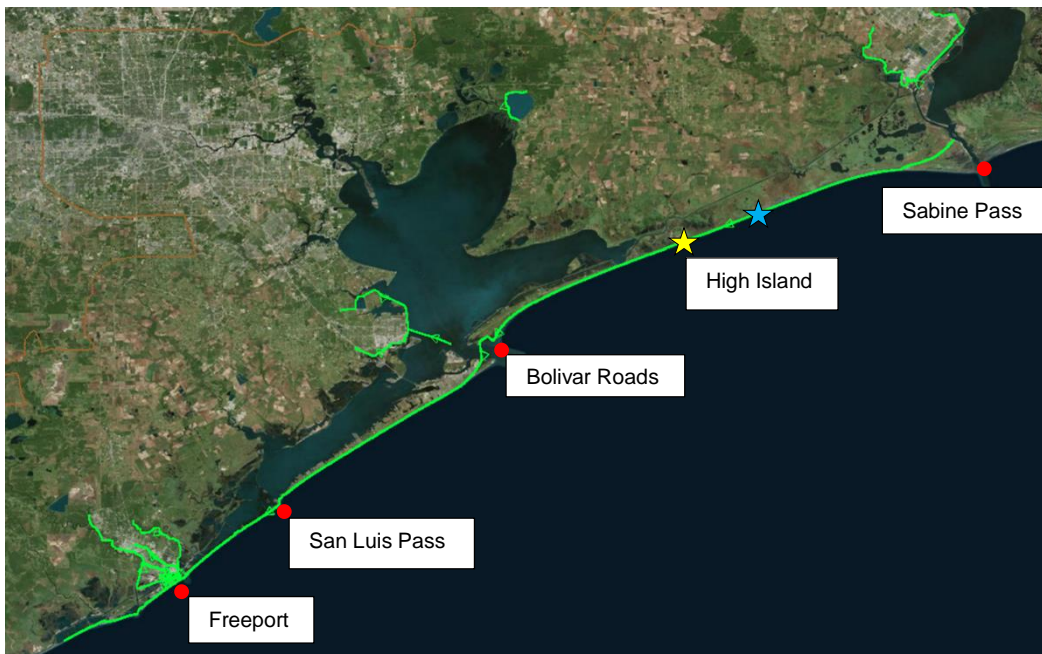


Figure 13-1. Alignment of the original and extended conceptual Ike Dikes.

To reduce the adverse effects of flanking, the original alignment was extended further to the east, all the way to Sabine Pass, TX. The extended dike alignment is shown in Figure 13-1, as the full extent of the green line that follows the shoreline. Near Sabine Pass the dike alignment veered slightly inland and followed an historic sand dune line.

An analysis of reductions in peak storm surge achieved with the extended dike was the subject of Chapters 10 through 12. This chapter presents results for several alternate Ike Dike configurations that have been identified or proposed by others.

Alignment 1a – A Modification of the Extended Ike Dike

Dutch partners in the Ike Dike investigation identified several other possible alignments for a long coastal spine. Each of them involved tying the dike into higher ground elevations at alternate locations on both its eastern and western ends (Van Berchem et al., 2016).

On the eastern end, in addition to the coastal alignment shown in Figure 13-1 that extended all the way to Sabine Pass, they identified an inland option. That option, the State Highway 124 option (referred to here as SH 124), left the coast and turned inland at High Island and then followed SH 124 north to Winnie, TX. This alignment for the eastern termination section of the dike is shown in Figure 13-2. The inland alignment is significantly shorter, and therefore potentially less costly, than the extended dike alignment; although, a gate system at the Intercoastal water waterway just north of High Island would probably be required, which increases the cost. The SH 124 alignment for the eastern section that is modeled assumes that a gate system is in place.

On the western end, van Berchem et al. (2016) identified two options. One option, the Bluewater Highway alignment, is similar to the extended dike alignment that has been previously modeled in this study. This option began at the western end of Galveston Island, crossed San Luis Pass with a gate system, followed or paralleled the Bluewater Highway south of the pass, and ended at Texas City where it tied in to the existing levees there.



Figure 13-2. Ike Dike Alignment 1a (western+middle+eastern sections).

A second option crossed San Luis Pass from the western end of Galveston Island, immediately turned inland at that point, headed toward the north-northwest and crossed both West Bay and wetlands of the Brazoria National Wildlife Refuge, and then veered northwest until it intersected County Road 227 (Hoskins Mound Road). This option would require a gate system to provide water exchange with Christmas Bay. This option might generate considerable opposition based on environmental concerns. Therefore, the coastal alignment that has been utilized to date in this study was retained for any western termination dike section in the alternate alignments, except that it is terminated on the northeast side of Freeport and ties into the existing levees there (see Figure 13-2).

Because of the possible cost savings associated with the shorter SH 124 option identified by van Berchem et al. (2016), and its beneficial effect on reducing flanking flow, it was included as the eastern section in the alternate dike alignments that were examined further. This alternate Ike Dike configuration is designated as Alignment 1a and is shown in its entirety in Figure 13-2. The alignment is comprised of three sections of dike, each having a crest elevation of 17 ft NAVD88: 1) an eastern section that follows SH 124, northward, from High Island toward Winnie and ends at Winnie where roadway elevations exceed 17 ft, 2) a middle section that

extends from High Island to the western end of Galveston Island, and includes a gate system at Bolivar Roads, and 3) a western section that extends the dike across San Luis Pass (includes a gate system there), follows the shoreline, ends at Freeport, and ties into the existing levee system there. The alignment of the western section parallels the Bluewater Highway option identified by van Berchem et al. (2016). A 17-ft NAVD88 crest elevation was used for all dike sections and the gate systems in Bolivar Roads and San Luis Passes, in Alignment 1a.

Alternate Alignment 1b – Alignment 1a with Lowered Gate Elevations

Preliminary design analyses was performed by the Dutch study partners for gate systems at both Bolivar Roads and San Luis Pass (see Jonkman et al., 2015). They designed both a navigational gate section and an environmental gate section at each pass. The navigational sections enable safe navigation, and the environmental sections allow increased water exchange between the Gulf and the interior bays when the gate systems are open. Both navigation and environmental sections are to be fully closed during a hurricane surge event.

Table 13-1 shows the lengths of, and crest elevations of, the navigation and environmental gate sections at both passes, as specified by Jonkman et al. (2015). As part of the gate system in San Luis Pass, some of the shallower portions of the pass would be permanently closed with a section of dike. This closure section extended for a length of 2624 ft (800 m), and had a crest elevation of 17 ft (5.2 m), as does the rest of the 17-ft Ike Dike.

Table 13-1. Summary of Lengths and Crest Elevations for the Navigation and Environmental Gate Sections (from Jonkman et al. (2015))

Gate Location	Navigation Section Length (meters, feet)	Navigation Section Elevation (meters, feet)	Environmental Section Length (meters, feet)	Environmental Section Elevation (meters, feet)
Bolivar Roads	200, 656	3.0, 9.8	2800, 9184	4.2, 13.8
San Luis Pass	50, 164	3.0, 9.8	150, 492	4.2, 13.8

Crest elevations for both gate sections, at both passes, were designed to allow significant wave overtopping and even steady overflow during more intense hurricane events. Lower gate crest elevations were selected in order to reduce construction costs. The volume of water that enters the bays as a result of wave overtopping only, which can occur while the still water level is below the gate crest elevation, is expected to be much less than the volume associated with steady flow over the gates. When it occurs, steady flow will only last for up to several hours before and after the time of peak surge. It was expected that the amount of steady flow over the lower gates would not lead to a significant increase in storm surge levels within the bays, because of the large water storage capacity of Galveston and West Bays relative to the volume of overtopping and overflow.

To quantify the influence of steady overflow on surge levels within the bay, particularly at the City of Galveston which is immediately adjacent to the Bolivar Roads gate system and which is vulnerable to flooding from the bay side, an alternate dike configuration was considered in the analysis. Alignment 1b was developed, in which the 17-ft crest elevation of the dike in Alignment 1a was lowered to the elevations shown in Table 13-1, at the locations of both gate systems. The lower gate elevations were represented in the grid mesh used in the storm surge modeling by changing grid node and element elevations at the approximate positions of the gates and approximately for the lengths shown in the table.

At the Bolivar Roads navigation gate, Jonkman et al. (2015) also discuss the possibility of leaving a gap between the bottom of the gate and the sea floor or scour blanket. Such an opening would allow water leakage into the bays during the entire storm duration following gate closure, including the time while the wind-driven surge forerunner is building a day or more in advance of the hurricane's arrival, as well as during the time of peak surge as the storm makes landfall. This source of leakage is not considered in the surge modeling done here for dike Alignment 1b or in any of the alternate alignments; however, its influence on surge levels within the bay should be examined if the final design calls for a gap beneath the navigation gate.

Alternate Alignment 2

The Gulf Coast Community Protection and Recovery District (2016a and 2016b), GCCPRD, recently completed its own storm surge suppression study to investigate measures for reducing hurricane flood risk for the north Texas coast. For their central region, which encompassed Chambers, Harris and Galveston counties, the GCCPRD's final recommendation included a coastal spine, or dike, along with several other localized risk reduction measures inside the bay, including a ring dike for the City of Galveston. The coastal spine recommended by the GCCPRD extended from the western end of Galveston Island, across Bolivar Pass, and ended at High Island. A gate system was included at Bolivar Roads. The GCCPRD coastal spine ended at the western end of Galveston Island, with no gate system at San Luis Pass. The recommended coastal spine was situated inland, parallel to existing highways on both Galveston Island and Bolivar Peninsula, and not at the shoreline as it is treated in the alignments considered here. The GCCPRD coastal spine had higher dike crest elevations that ranged from 18 to 21 ft.

The portion of the GCCPRD coastal spine that lies along Bolivar Peninsula and ends at High Island is shorter than the Ike Dike alignment that was originally considered as part of this feasibility study and shorter than the extended dike that was most recently considered. The limited eastward extent of the GCCPRD dike raised questions regarding the role of flanking flow on storm surge elevations in Galveston Bay, as well as the trade-offs between dike cost and flood risk that might be associated with omission of an eastern termination section, like those shown in Figures 13-1 and 13-2.

To examine these questions, an Alignment 2 for the Ike Dike concept was developed and analyzed. Alignment 2 is shown in Figure 13-3, and it involves a 17-ft NAVD88 dike that extends from the western end of Galveston Island, across Bolivar Roads, and ends at High Island just like the GCCPRD plan. Unlike the GCCPRD dike, Alignment 2 follows the shoreline. Alignment 2 is nearly identical in length/extent compared to the coastal spine recommended by the GCCPRD, although the crest elevations and details of the alignment differ. Alignment 2 represents the middle section, only, of the alignments shown in Figures 13-1 and 13-2, without any eastern or western termination sections.



Figure 13-3. Ike Dike Alignment 2 (middle section only).

The GCCPRD plan terminates at the western end of Galveston Island, and it avoids the cost of both a gate complex at San Luis Pass and a coastal spine segment that runs from San Luis Pass south to Freeport.

Consideration of an Alignment 2 also enables an analysis of the trade-offs between changes in dike length and changes in storm surge reduction that are associated with omission of both eastern and western termination sections like those shown in Figures 13-1 and 13-2.

Alternate Alignment 3

Termination of the coastal spine at the western end of Galveston Island with no gate system at San Luis Pass, as recommended by the GCCPRD, enables propagation of the hurricane surge forerunner into West Bay; and, it precludes any means for operationally controlling the forerunner's influence on surge levels within West Bay prior to gate closure or timing gate closure to coincide with low tide stage in the bays. Termination of the dike at this location also significantly increases peak storm surge levels within West Bay; it enables propagation of the peak storm surge through San Luis Pass as well as flow over the barrier island south of the pass once it becomes inundated.

Alternate Alignment 3, shown in Figure 13-4 and having a middle dike section and an eastern termination segment but with no western termination section, was developed to isolate the role of the western section on storm surge reduction. Results from simulations made with both Alignments 3 and 1a enable an assessment of how storm surge is increased in West Bay in the absence of both a western termination section and a gate system at San Luis Pass: along different parts of Galveston Island, along the north shore of West Bay, along the bay side of the City of Galveston, and near Texas City. The simulations also enable an assessment of how much, if any, the additional surge penetration influences storm surge levels beyond West Bay, into Galveston Bay, particularly along its western shoreline.



Figure 13-4. Ike Dike Alignment 3 (middle+eastern sections).

Storm Surge Simulations Made for the Alternate Dike Alignments

Four storm surge simulations were made for each of the four alternate dike alignments, Alignments 1a, 1b, 2 and 3. All simulations for alternate dike alignments were made for the future sea level scenario, which is 2.4 ft higher than present sea level (i.e., a future sea level of 3.31 ft, NAVD88). This future sea level scenario is the same SLR1 scenario that was considered previously in the extended Ike Dike analysis discussed in Chapters 10 through 12. For each dike alignment, simulations were made for the 10-yr, 100-year, and 500-yr proxy storms and for Hurricane Ike, using the same improved modeling approach that was adopted for the extended Ike Dike simulations. Peak storm surge results for each of these simulations were provided to the economics team for further analysis.

It is important to note that each of the three proxy storms makes landfall at San Luis Pass, and all three are of a size (i.e., radius to maximum winds) that produces maximum coastal surges near Bolivar Roads and along the western shoreline of Galveston Bay. Each proxy storm produces lesser peak storm surges at San Luis Pass, the location of landfall. These three storms were selected to best replicate probabilistic ARI storm surge values at the City of Galveston and along the western side of Galveston Bay, not at San Luis Pass or elsewhere, such as at High Island. These three proxy storms are probably not the storms that produce the 10-yr, 100-yr, and 500-yr ARI storm surge values at San Luis Pass. The increase in storm surge and flood risk within West Bay, which arises in the absence of the western dike section, will be understated by the sole use of these three proxy storms.

Hurricane Ike made landfall near Bolivar Roads and generated its peak surge further to the east, in the vicinity of High Island. Results for the Hurricane Ike simulations shed insight concerning how much additional flanking occurs when the maximum surge occurs in the vicinity of the eastern termination section, compared to flanking associated with the three proxy storms where the peak coastal surge near High Island is less than the maximum surge in the vicinity of Bolivar Roads.

Peak Surge Maps for Each Dike Alignment/Storm Simulation

Figures 13-5 through 13-8 show maximum water surface elevation maps (in feet, NAVD88) for the 10-yr proxy storm (Storm 535) and all four alignments, 1a, 1b, 2 and 3, respectively: 1a (western + middle + eastern

sections with 17-ft gate elevations), 1b (western + middle + eastern sections with lower gate elevations), 2 (middle section only) and 3 (middle + eastern sections), in that order. Figures 13-9 through 13-12 show maximum water surface elevation maps for the 100-yr proxy storm (Storm 033) and all four alignments. Figures 13-13 through 13-16 show maximum water surface elevation maps for the 500-yr proxy storm (Storm 036) and all four alignments. Figures 13-17 through 13-20 show maximum water surface elevation maps for Hurricane Ike and all four alignments.

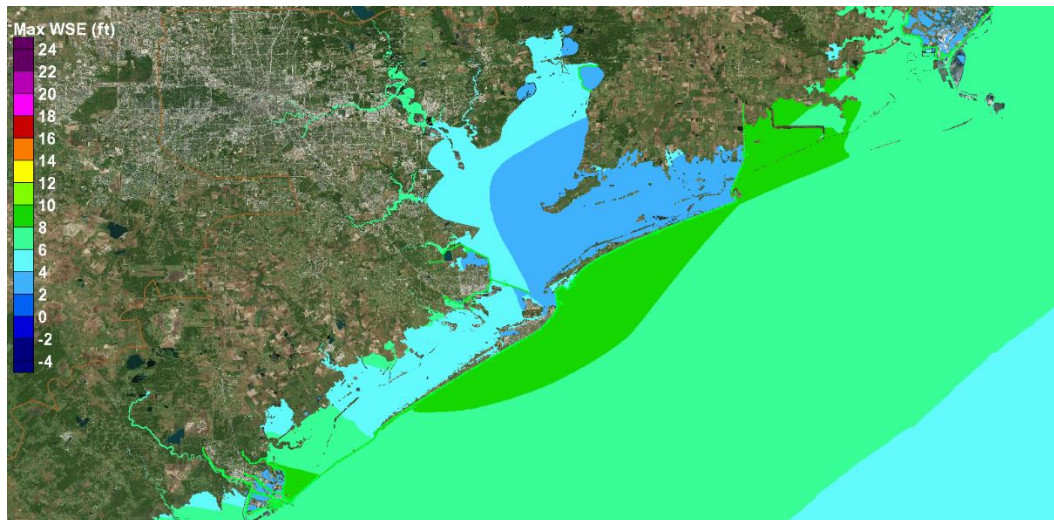


Figure 13-5. Dike alignment 1a (western+middle+eastern sections). Storm 535 (10-yr proxy). Maximum water surface elevation field (in feet, NAVD88) for the future sea level scenario (SLR1, +3.31 ft NAVD88).

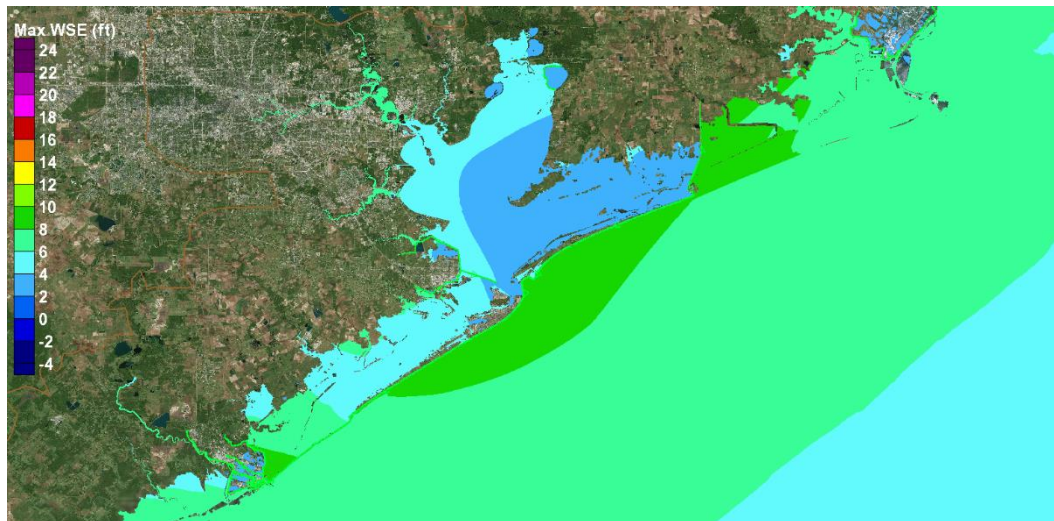


Figure 13-6. Dike alignment 1b (western+middle+eastern sections with lowered gate elevations). Storm 535 (10-yr proxy). Maximum water surface elevation field (in feet, NAVD88) for the future sea level scenario (SLR1, +3.31 ft NAVD88).

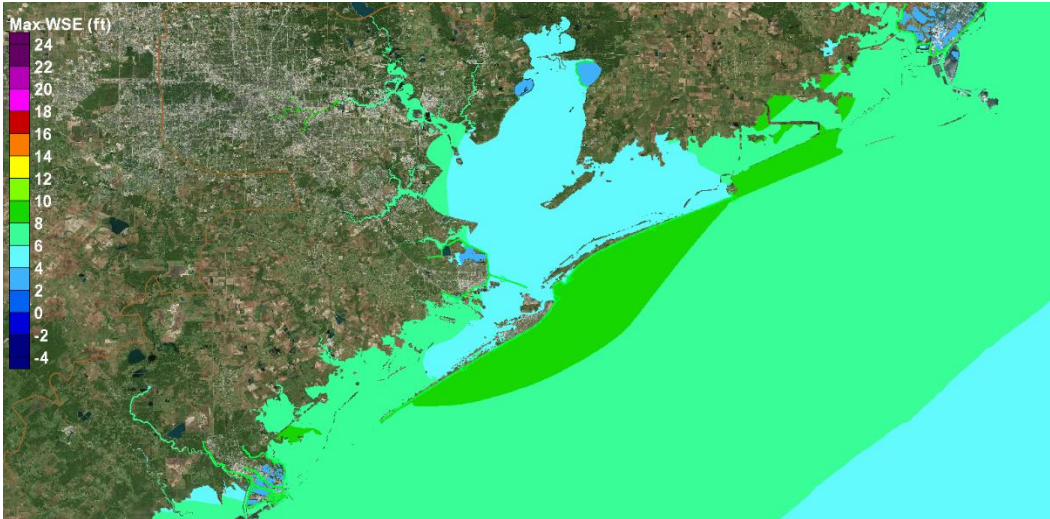


Figure 13-7. Dike alignment 2 (middle section only). Storm 535 (10-yr proxy). Maximum water surface elevation field (in feet, NAVD88) for the future sea level scenario (SLR1, +3.31 ft NAVD88).

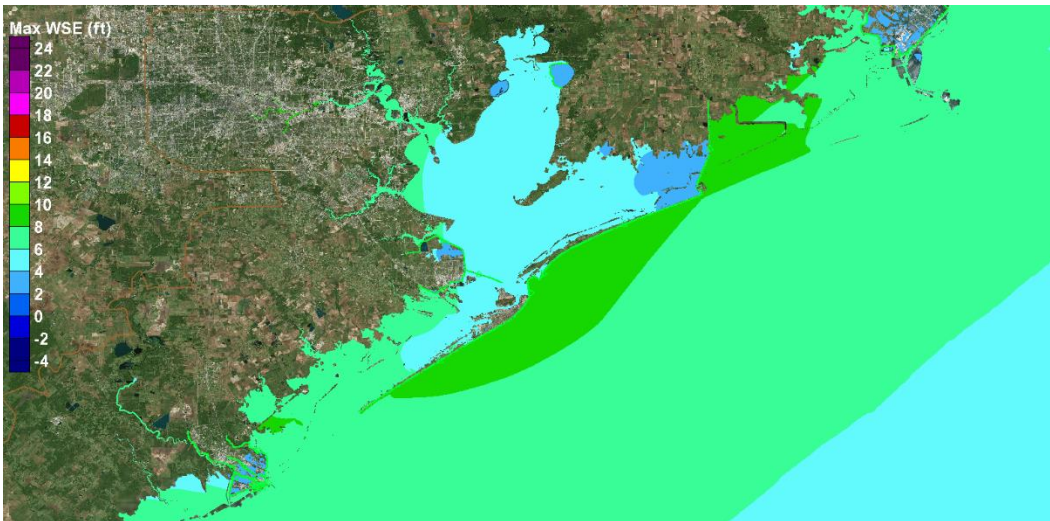


Figure 13-8. Dike alignment 3 (middle+eastern sections). Storm 535 (10-yr proxy). Maximum water surface elevation field (in feet, NAVD88) for the future sea level scenario (SLR1, +3.31 ft NAVD88).

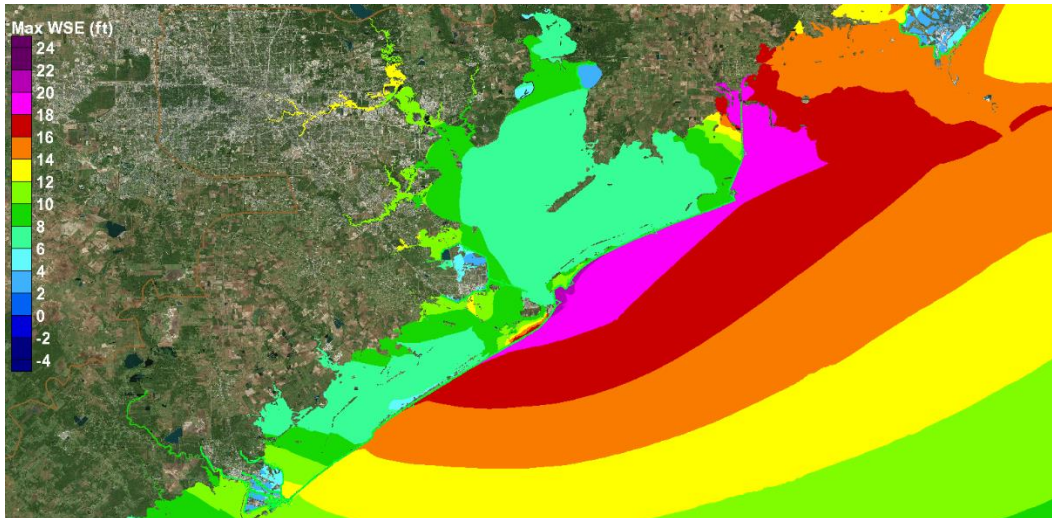


Figure 13-9. Dike alignment 1a (western+middle+eastern sections). Storm 033 (100-yr proxy). Maximum water surface elevation field (in feet, NAVD88) for the future sea level scenario (SLR1, +3.31 ft NAVD88).

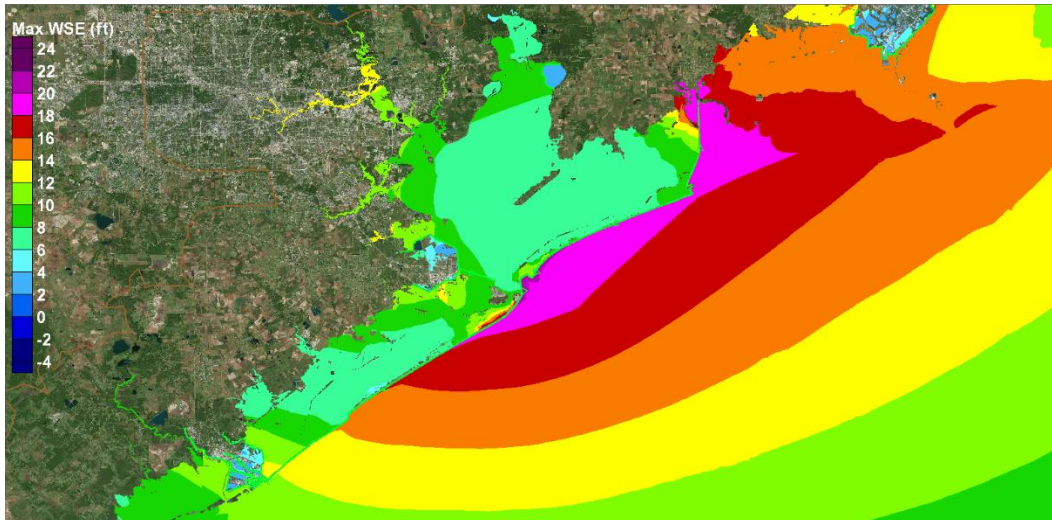


Figure 13-10. Dike alignment 1b (western+middle+eastern sections with lowered gate elevations). Storm 033 (100-yr proxy). Maximum water surface elevation field (in feet, NAVD88) for the future sea level scenario (SLR1, +3.31 ft NAVD88).

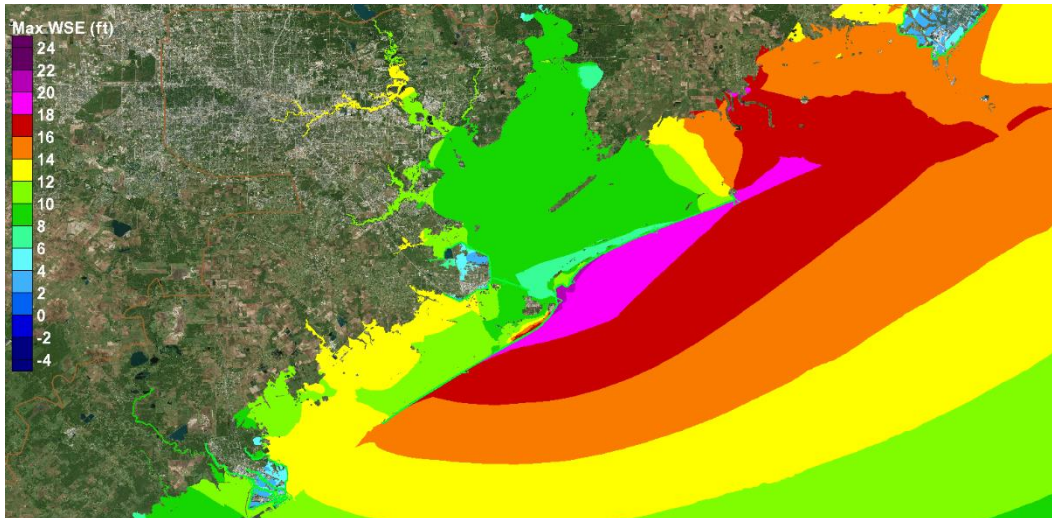


Figure 13-11. Dike alignment 2 (middle section only). Storm 033 (100-yr proxy). Maximum water surface elevation field (in feet, NAVD88) for the future sea level scenario (SLR1, +3.31 ft NAVD88).

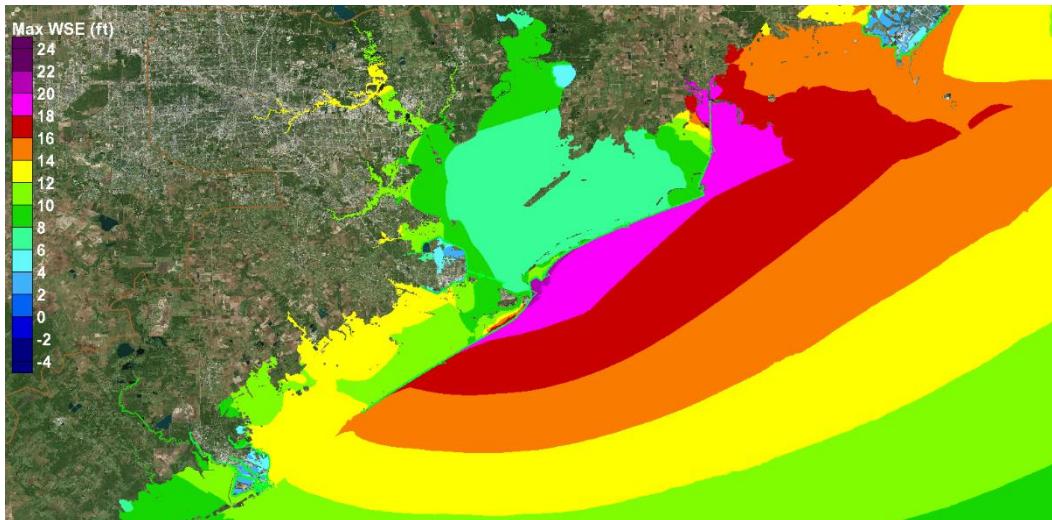


Figure 13-12. Dike alignment 3 (middle+eastern sections). Storm 033 (100-yr proxy). Maximum water surface elevation field (in feet, NAVD88) for the future sea level scenario (SLR1, +3.31 ft NAVD88).

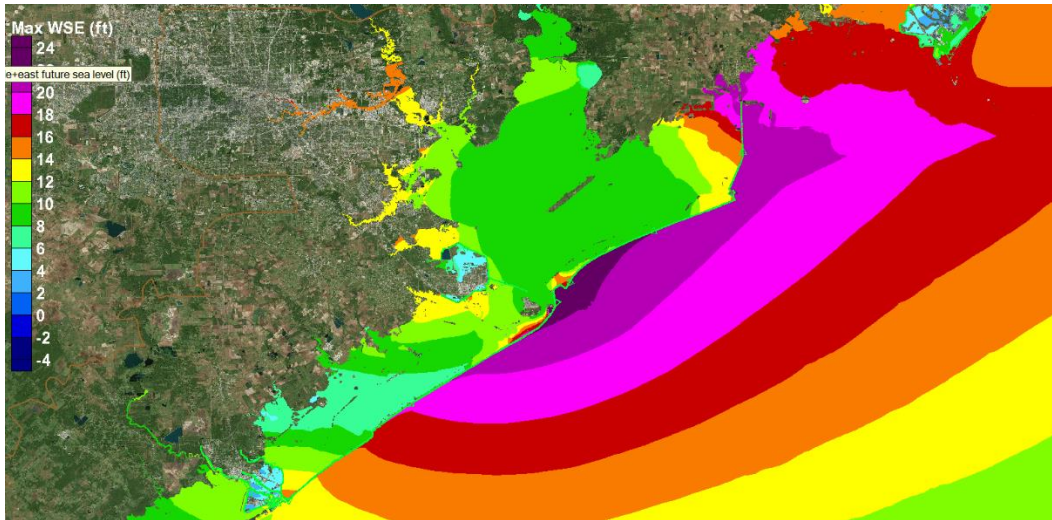


Figure 13-13. Dike alignment 1a (western+middle+eastern sections). Storm 036 (500-yr proxy). Maximum water surface elevation field (in feet, NAVD88) for the future sea level scenario (SLR1, +3.31 ft NAVD88).

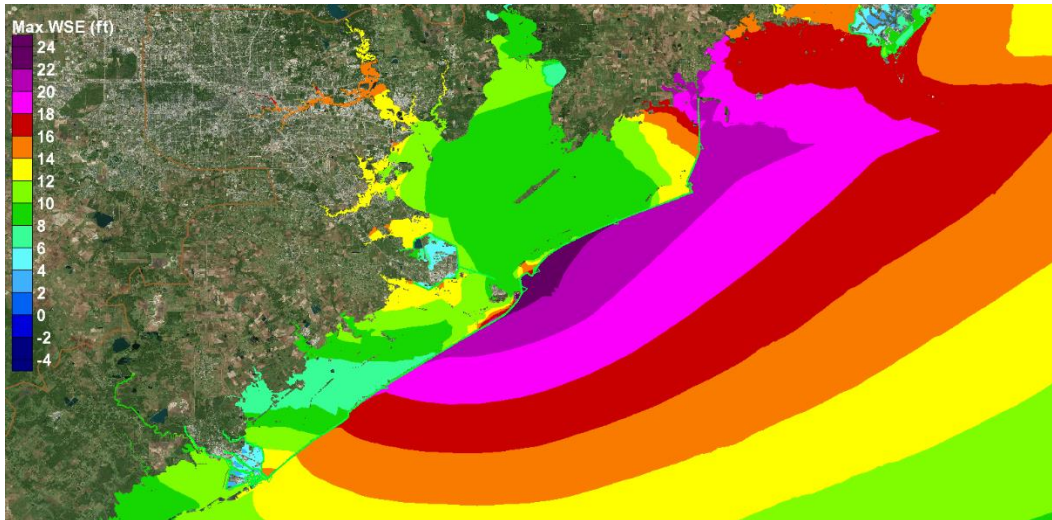


Figure 13-14. Dike alignment 1b (western+middle+eastern sections with lowered gate elevations). Storm 036 (500-yr proxy). Maximum water surface elevation field (in feet, NAVD88) for the future sea level scenario (SLR1, +3.31 ft NAVD88).

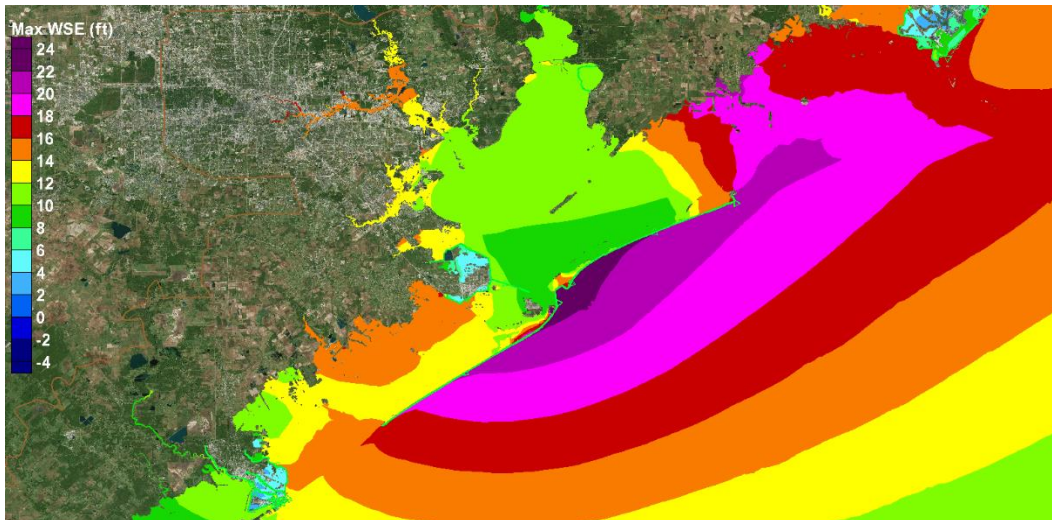


Figure 13-15. Dike alignment 2 (middle section only). Storm 036 (500-yr proxy). Maximum water surface elevation field (in feet, NAVD88) for the future sea level scenario (SLR1, +3.31 ft NAVD88).

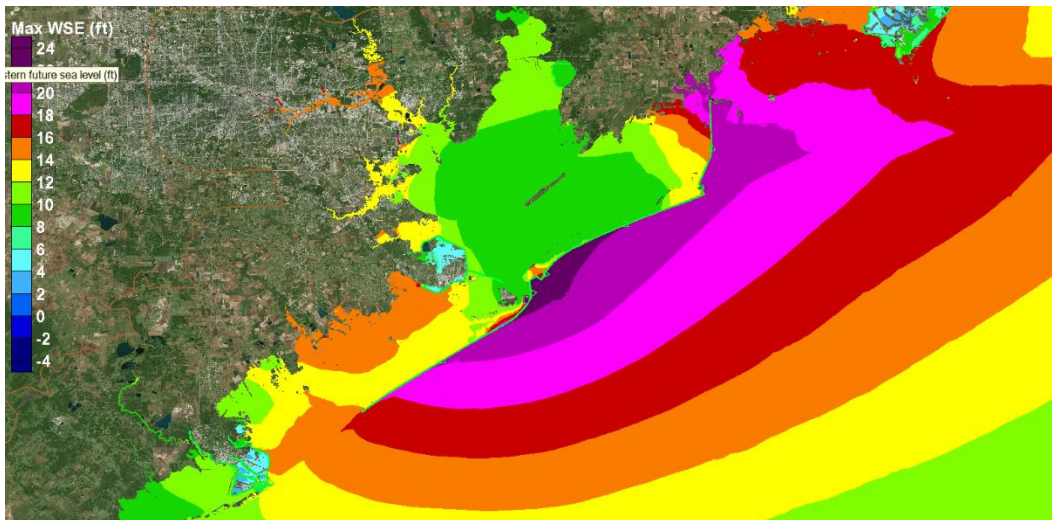


Figure 13-16. Dike alignment 3 (middle+eastern sections). Storm 036 (500-yr proxy). Maximum water surface elevation field (in feet, NAVD88) for the future sea level scenario (SLR1, +3.31 ft NAVD88).

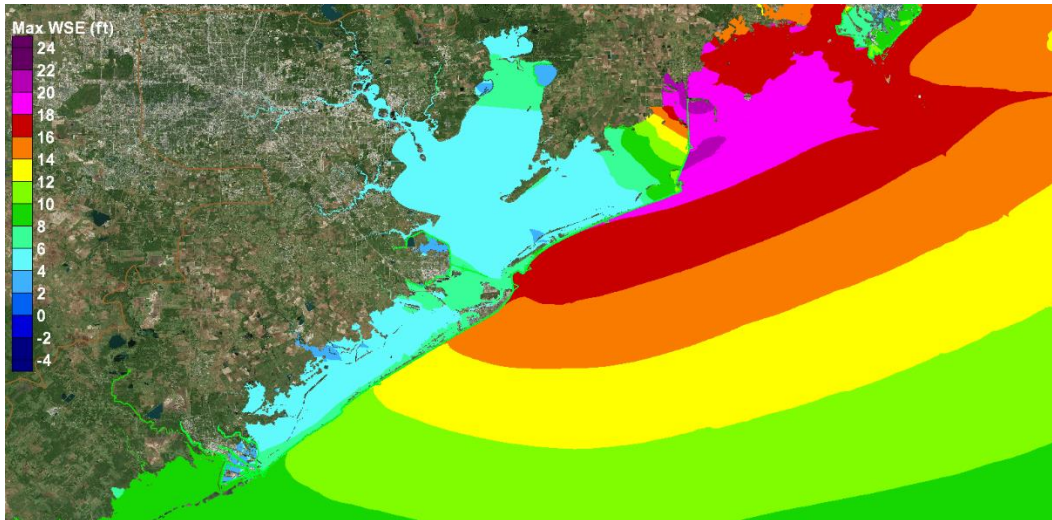


Figure 13-17. Dike alignment 1a (western+middle+eastern sections). Hurricane Ike. Maximum water surface elevation field (in feet, NAVD88) for the future sea level scenario (SLR1, +3.31 ft NAVD88).

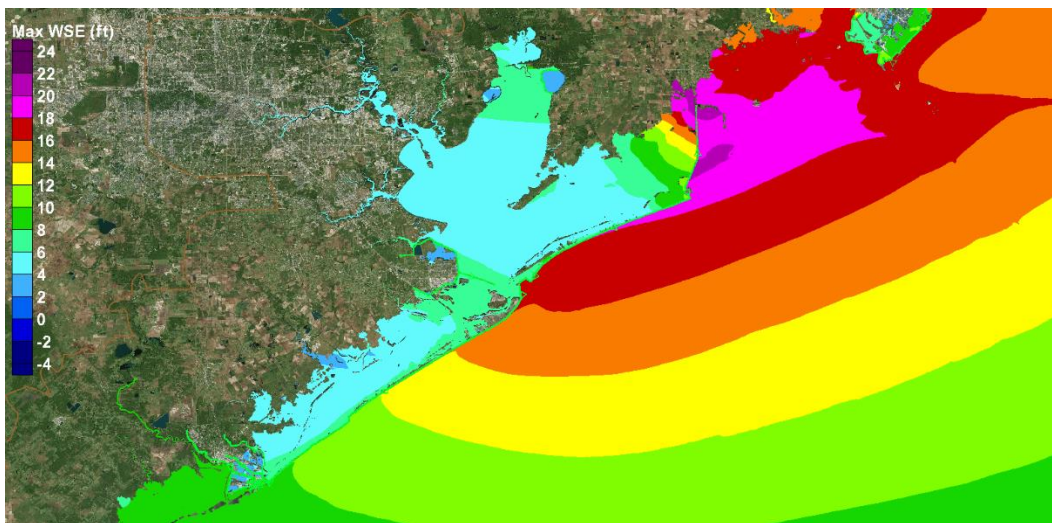


Figure 13-18. Dike alignment 1b (western+middle+eastern sections with lowered gate elevations). Hurricane Ike. Maximum water surface elevation field (in feet, NAVD88) for the future sea level scenario (SLR1, +3.31 ft NAVD88).

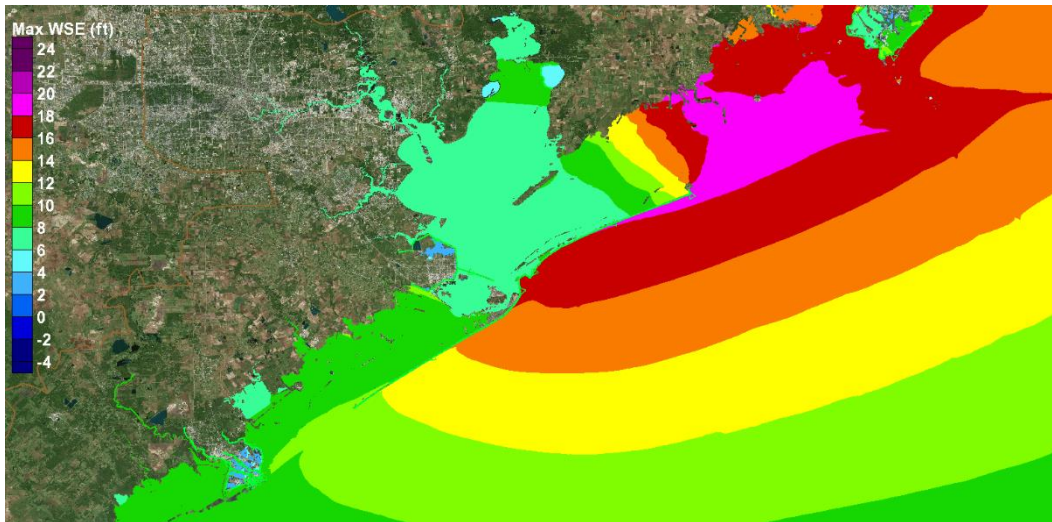


Figure 13-19. Dike alignment 2 (middle section only). Hurricane Ike. Maximum water surface elevation field (in feet, NAVD88) for the future sea level scenario (SLR1, +3.31 ft NAVD88).

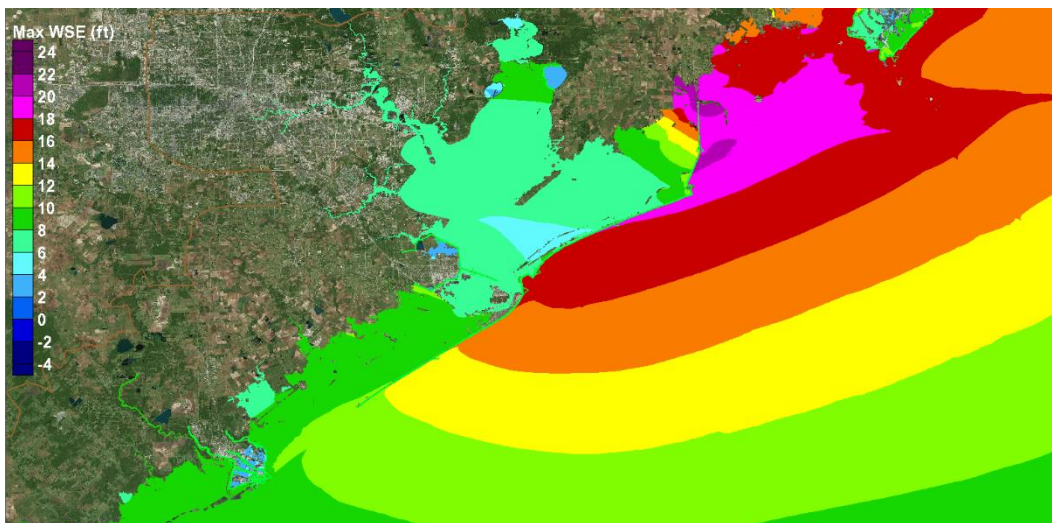


Figure 13-20. Dike alignment 3 (middle+eastern sections). Hurricane Ike. Maximum water surface elevation field (in feet, NAVD88) for the future sea level scenario (SLR1, +3.31 ft NAVD88).

Extraction of Peak Storm Surge Values for Analysis

Quantitative examination of the differences in peak surge for the various alternate dike alignments was facilitated by extracting values from each peak storm surge field that was used to create a peak surge map, at a series of points. The locations of the points are shown in Figure 13-21, and the latitude/longitude coordinates of each are listed in Appendix B. Peak surge values at each location, for each of the four alignments, and for each of the four storms, also are provided in Appendix B. All simulations reflect use of the future sea level scenario, SLR1.

Values from the peak surge maps associated with the extended dike alignment which terminates at Sabine Pass and which was extensively discussed in Chapters 10 through 12, also are given in Appendix B for the same locations, same storms, and the same future sea level scenario.



Figure 13-21. Locations for extracted peak storm surge values and water surface elevation times series.

Comparison of Two Different Alignments for an Eastern Termination Section.

The extended Ike Dike has been the focus of the study thus far; and its eastern portion followed the shoreline along Bolivar Peninsula and it followed the shoreline, or nearly so, all the way to its termination at Sabine Pass. Alignment 1a reflects a modification to the extended dike. The following changes are based on work done by van Berchem et al. (2016): 1) the dike is shortened on its eastern end, 2) reoriented at High Island to have a mostly north-south alignment that follows state highway SH 124 north of High Island, and 3) ends at Winnie, TX. Both alignments for the eastern portion, the coastal alignment in the original extended dike and Alignment 1a, were primarily designed to minimize flanking during the storm and the subsequent entry of water into Galveston Bay.

Examination of the peak storm surge maps and location-specific values extracted from the maps reveals both similarities and differences between the two alignments. Peak surge maps for the extended dike alignment were presented and discussed in Chapter 11. Comparison of the with-dike maps with maps for the no-dike condition is informative as well. The no-dike maps also were presented in Chapter 11.

For the 10-yr proxy storm, Storm 535 run at the future sea level SLR₁, a comparison of the peak surge maps for both Alignment 1a (Figure 13-5) and the extended dike (Figure 11-17) illustrates both the similarities and differences. Inside the dike, peak surge throughout most of Galveston Bay including its western shoreline, throughout West Bay and its adjacent shorelines, and along much of Bolivar Peninsula, differences in peak surge between the two different eastern alignments are very small, 0.1 ft or less. Peak surge values for Alignment 1a are consistently slightly less than those for the extended dike. Alignment 1a is slightly more effective than the extended dike in reducing flanking. Some differences are evident in the immediate vicinity of the eastern dike sections. Here, peak surge maps show that termination of the dike at Sabine Pass allows a few more feet of peak surge due to flanking, compared to Alignment 1a. Alignment 1a is tied into higher ground, is a complete barrier with no gaps, and no flow over the 17-ft dike occurs for this storm, so flanking is completely eliminated by this alignment and for this storm. The extended dike allows some flanking flow into Galveston Bay through the Intercoastal Waterway and over inundated low lying terrain if the surge is high enough at Sabine Pass to cause inundation to occur, as is the case for this storm.

Comparison of the peak surge maps for Alignment 1a (see Figure 13-5) and the no-dike condition (see Figure 11-13) shows that there is a slightly higher peak surge value, an amplification, outside the eastern section of Alignment 1a compared to the peak surge at the same location without any dike in place. This small amplification is a local effect that is constrained to the immediate vicinity just outside the dike; and it extends along the entire eastern section of Alignment 1a, from Winnie all the way to High Island. The effect of amplification does not extend very far eastward and definitely not to Port Arthur. The reason for the local amplification in peak surge is the following. The counterclockwise rotating wind field of hurricanes that approach from the southeast pushes water, which has inundated the low lying terrain, against the eastern dike section of Alignment 1a. This process causes a storm surge build-up against the eastern dike section that would not, otherwise, occur without the presence of the dike. This is the same “long-dike” effect that was discussed previously for the open coast along Galveston Island and Bolivar Peninsula, in which the storm surge right at and along the dike is increased by the presence of the long coastal dike itself.

Examination of the peak surge results for Alignment 1a suggests that a modification to the eastern section in Alignment 1a should be considered at its northern terminus, if this general alignment is adopted. The change involves realigning the dike in such a way that it departs from highway SH 124, rings the eastern side of Winnie, and ties into Highway 73. Such an alignment provides improved storm surge reduction to those parts of Winnie that lie east of SH 124, and it can best address the local influence of surge amplification on Winnie.

For the much more severe 100-yr proxy storm (Storm 033), inside the dike, peak surges for Alignment 1a (Figure 13-9) also are generally slightly less than those for the extended dike (Figure 11-25). Results in Appendix B quantify the differences. Throughout both Galveston and West Bays, peak surges for Alignment 1a are generally 0.1 or 0.2 ft less than those for the extended dike. In light of the relatively small differences between the two eastern section alignments, it is clear that both alignments are similarly effective in reducing the peak storm surge in all of the aforementioned areas inside the dike for this severe hurricane.

Compare peak surge maps in Figure 13-9 (Alignment 1a) with Figure 11-21 (existing, no-dike conditions for Storm 033). Again, surge amplification outside the eastern dike section of Alignment 1a is evident for this storm. Having the eastern termination section for Alignment 1a located inland allows a greater surge to develop along the outside of the dike due to hurricane force winds acting on very shallow water over inundated terrain. As was the case for the 10-yr proxy storm, the amplification effect is seen only in the immediate vicinity of the eastern dike section; the effect does not extend to Port Arthur.

Greater peak surges are evident inside the eastern section of Alignment 1a for the 100-yr proxy storm, compared to those for the 10-yr proxy storm. The higher open coastal surge for the 100-yr proxy storm and its amplification due to the eastern dike section result in a peak surge of approximately 18 ft along the outside of the dike. This magnitude of surge causes steady flow over the dike, and the resulting overflow substantially increases peak surge levels just inside the dike throughout the region from Winnie to High Island. In this region, peak surges for Alignment 1a (see Figure 13-9) are generally greater than they are for the extended dike alignment (see Figure 11-25).

For the 100-yr proxy storm, the extended dike alignment that ends at Sabine Pass provides substantial and widespread storm surge reduction between Winnie and Port Arthur, in the geographical area that lies east of the position of the Alignment 1a eastern section. Reductions in peak surge of 3 to 8 ft are evident from the peak surge maps. The eastern section of Alignment 1a provides no surge reduction benefits in this same region; as this region lies outside the dike.

Peak surge results for Storm 036, the 500-yr proxy storm, are similar to those seen for the 100-yr proxy, Storm 033. For Storm 036, compare Figure 13-13 (Alignment 1a) with Figure 11-33 (extended dike), and compare Figure 13-13 with Figure 11-29 (existing, no-dike conditions). Inside the dike, along most of Bolivar Peninsula, along the western shoreline of Galveston Bay, at the City of Galveston, and throughout West Bay, differences between the two eastern section alignments in these areas are quite small for this proxy storm as well, 0.1 to 0.2 ft in most places. Again, peak surges for Alignment 1a are slightly less than those for the extended dike. For this very severe and rare hurricane, both eastern section alignments are similarly effective in reducing the peak storm surge

in all of the key areas that lie inside the dike. Alignment 1a is slightly more effective.

The amplification effect east of the Alignment 1a eastern dike section from High Island to Winnie is less evident for this storm. Steady overflow of the eastern section occurs for both the 100-yr and 500-yr proxy storms. However, the peak surge for Storm 036 is several feet higher than the elevation of the dike. The long-dike effect is less pronounced once surge levels exceed the crest elevation of the dike and overflow predominates.

Results and findings for Hurricane Ike, are similar to those for the 100-yr and 500-yr proxy storms, but there are some noticeable differences as well. Compare Figure 13-17 (Alignment 1a) with Figure 11-9 (extended dike) and compare Figure 13-17 with Figure 11-5 (existing no-dike conditions for Hurricane Ike). As was seen for the proxy storms, inside the dike throughout most of Galveston and West Bays, peak surges for Alignment 1a are generally less than those for the extended dike. The magnitude of these differences in peak surge are slightly greater for Ike than they are for the 100-yr and 500-yr proxy storms. In the bays, peak storm surge levels for Alignment 1a are mostly 0.5 to 1 ft less than peak surges for the extended dike alignment. However, also note that the peak surges for Hurricane Ike within Galveston and West Bays, for either alignment of the eastern dike section, are only 4 to 7 ft, and they are not so problematic from a flooding perspective.

This greater differences seen for Ike (0.5 to 1 ft) compared to the proxy storms (less than 0.2 ft) suggest that flanking flow was a greater for Hurricane Ike than it was for the proxy storms. Results also show that Alignment 1a is more effective than the extended dike in eliminating/reducing the increased flanking flow.

The greater flanking flow is attributed to one or more of the following factors. The Hurricane Ike surge forerunner had a longer duration and higher amplitude than the forerunner for the proxy storms, which is expected to cause greater flanking flow and lead to flanking earlier in the storm for the extended dike alignment. Hurricane Ike also included the astronomical tide which may have exacerbated flanking during the forerunner development stage and possibly later. Also, the zone of peak surge for Ike was located closer to the eastern end of the extended dike than was the case for the proxy storms. The landfall location for Ike was at

Bolivar Roads; whereas, for the proxy storms, landfall occurred further south at San Luis Pass. Also, the peak surge for Ike in the vicinity of Sabine Pass to Port Arthur, which drives the flanking for the extended dike, was significantly higher for Ike compared to peak surge at the same location for the 100-yr proxy storm and slightly more than the 500-yr proxy storm.

As is the case for the 100-yr and 500-yr proxy storms, peak surge results for Hurricane Ike show that for the region just inside the eastern section of Alignment 1a, peak surges for Alignment 1a generally exceed those for the extended dike alignment. For Alignment 1a, Ike created very high surges just outside the eastern dike section, surge amplification occurred, and overflow of the eastern section occurred. The steady flow over the eastern dike section of Alignment 1a leads to the increased peak surge levels just inside the dike, throughout the region from Winnie to High Island.

For Hurricane Ike, as was the case for the proxy storms, the peak surge maps indicate that the extended dike alignment that ends at Sabine Pass provides substantial storm surge reduction between Winnie and Port Arthur. Reductions of 3 to 10 ft in peak surge values occurred in this region, increasing from west to east, compared to peak surges for Alignment 1a.

Both alignments are quite effective at preventing significant increases to peak surge levels as a result of flanking flow. A cost-benefit analysis done for the two eastern section alignments should consider not only the cost of each alignment and the resulting peak surges in the Houston-Galveston area, but also the reduction in storm surge that is achieved in the region from Bolivar Peninsula to Port Arthur, as well as any other potential benefits. For example, the longer and presumably more expensive coastal alignment of the extended Ike Dike provides greater flood risk reduction benefits to the Port Arthur area, and it can provide protection for and longer-term stability for the coastal highway in this region.

Surge Reduction in the Houston-Galveston Region with and without an Eastern Termination Section

Analysis of Peak Surge Elevations

The previous section compared two different alignments for an eastern termination section. Both alignments produced similar reductions in peak storm surge throughout the immediate Houston-Galveston region, with Alignment 1a being just slightly more effective in reducing peak surge in the key areas along the western shoreline of Galveston Bay.

In this report section, the merits of having any eastern termination section at all are evaluated in terms of the magnitude of peak storm surge reduction for the immediate Houston-Galveston region, in those areas having the greatest potential for damage/loss along the western shoreline of Galveston Bay. The analysis does not consider surge reduction benefits that are accrued east of Galveston Bay.

Neither the eastern portion of the extended Ike dike nor the eastern termination section that is included in dike Alignments 1a, 1b and 3 appears to produce the widespread significant reduction in peak surge that was initially anticipated. The initial assessment was based on an examination of results from the first bracketing set of storm surge simulations that were made in this study, which involved an Ike Dike which ended just to the east of High Island. Those initial results were discussed in Chapter 8. The perceived importance of flanking flow around the eastern end of the dike on peak surge levels along the western shoreline of Galveston Bay, and into the upper reaches of the Houston Ship Channel, was apparently overstated in that modeling. The first set of simulations utilized a global slope limiting approach to stabilizing the storm surge simulations, which tended to overestimate the peak storm surge within some parts of the bays and in some inundated areas by as much as several feet.

A comparison of peak surge results for Alignments 2 (middle section only) and 3 (middle+eastern sections), from more recent simulations made using the current, improved model set-up, provides a more reliable and definitive assessment of the storm surge reduction value of an eastern termination section. Qualitative inspection of the peak surge maps for Alignments 2 and 3 illustrates the influence of the eastern termination section on peak surge levels in key areas. Compare Figures 13-7 and 13-8

for the 10-yr proxy storm; compare Figures 13-11 and 13-12 for the 100-yr proxy storm; compare Figures 13-15 and 13-16 for the 500-yr proxy storm; and compare Figures 13-19 and 13-20 for Hurricane Ike. Also refer to tabular peak surge results provided in Appendix B for both alignments.

For the 10-yr, 100-yr, and the 500-yr proxy storms, the eastern termination section only reduces peak surges by very small amounts, 0.2 ft or less at most locations along the western shoreline of Galveston Bay, including the City of Galveston and in the upper reaches of the Houston Ship Channel. For all three proxy storms, the eastern termination section has a negligible influence on peak surge values within West Bay. The peak surge reduction benefit of the eastern termination section is greater on eastern Bolivar Peninsula, where reductions in peak surge range from 0.1 to 0.6 ft for the 10-yr proxy storm, are approximately 0.8 ft for the 100-yr proxy storm, and 0.6 ft for the 500-yr proxy storm.

Surge reduction achieved with the eastern termination section is greater for Hurricane Ike, compared to that achieved for the three proxy storms. With the eastern termination section, peak surges along the western shoreline of Galveston Bay are decreased by amounts of up to 1 ft north of San Leon and by a few tenths of a foot at locations south of Dickinson Bay. In West Bay, as was the case for the proxy storms, peak surges are effectively unaltered by the presence of the eastern dike section. Along the eastern end of Bolivar Peninsula, the eastern dike section reduces peak surges more significantly, by as much as 2.3 ft.

It is important to note that for Hurricane Ike, peak surges along the western shoreline of Galveston Bay are only approximately 7 ft with only the middle dike section in place (Alignment 2). Even this surge level, and without the 1-ft reduction due to the eastern section, is not so problematic in terms of flood damage and economic losses, for most of the Houston-Galveston region.

The cost of, and the regional and local flood risk reduction benefits associated with, constructing an eastern dike section should be examined for additional storms to confirm the findings for the proxy storms and Hurricane Ike. In light of the relatively small reductions in peak surge that accrue with the eastern termination section for the severe storms examined here, an eastern section that extends beyond High Island might not be cost-effective as a means for reducing flood risk in the Houston-

Galveston area. The coastal spine option proposed by the GCCPRD ended at High Island.

Analysis of Water Surface Elevation Time Series

An explanation follows for why the reductions in peak storm surge along the western side of Galveston Bay, which result from inclusion of an eastern termination section, are relatively small. To support this analysis graphs showing the variation in water surface elevation as a function of time were created for five locations indicated with red dots in Figure 13-21, for both the 100-yr proxy storm and Hurricane Ike. The five locations are: 1) Bayport, located along the western shoreline of Galveston Bay toward the northern part of the bay, 2) on the bay side of the City of Galveston, 3) San Luis Pass on the open gulf side of the pass, 4) Galveston Is (bay west) which is located just inside San Luis Pass along the western end of Galveston Island, and 5) Bolivar Peninsula (bay east) which is located in Galveston Bay on the eastern end of Bolivar Peninsula. This discussion only focusses on results at Bayport, City of Galveston and Bolivar Peninsula, which are most relevant to this topic.

Figure 13-22 shows water surface elevations for Storm 033, the 100-yr proxy storm, and the future sea level scenario, SLR1. There are three panels in Figure 13-22, one each for Alignment 2 which is comprised of a middle dike section only (top panel), Alignment 3 which is comprised of middle + eastern dike sections (middle panel) and Alignment 1a which is comprised of western + middle + eastern dike sections (bottom panel). The analysis here only focusses on the top and middle panels of the figure, to illustrate the effect of the eastern termination section.

For the 100-yr proxy storm, as it approaches the Texas coast from the southeast, the winds are steadily blowing from the northeast, due to the counterclockwise wind circulation around the hurricane's eye. This wind direction persists right up to the time of landfall. This prevailing wind direction acts to force a set up (an increase) in the water surface on the western side of Galveston Bay as evidenced at Bayport (red curves in Figure 13-22) and at the City of Galveston (black curves). Concurrently, the same winds are acting to set down (decrease) the water surface along the eastern side of the bay including the area adjacent to eastern Bolivar Peninsula (green curves). Water is being pushed by the wind from the east side of Galveston Bay to the west side. This pattern of developing set

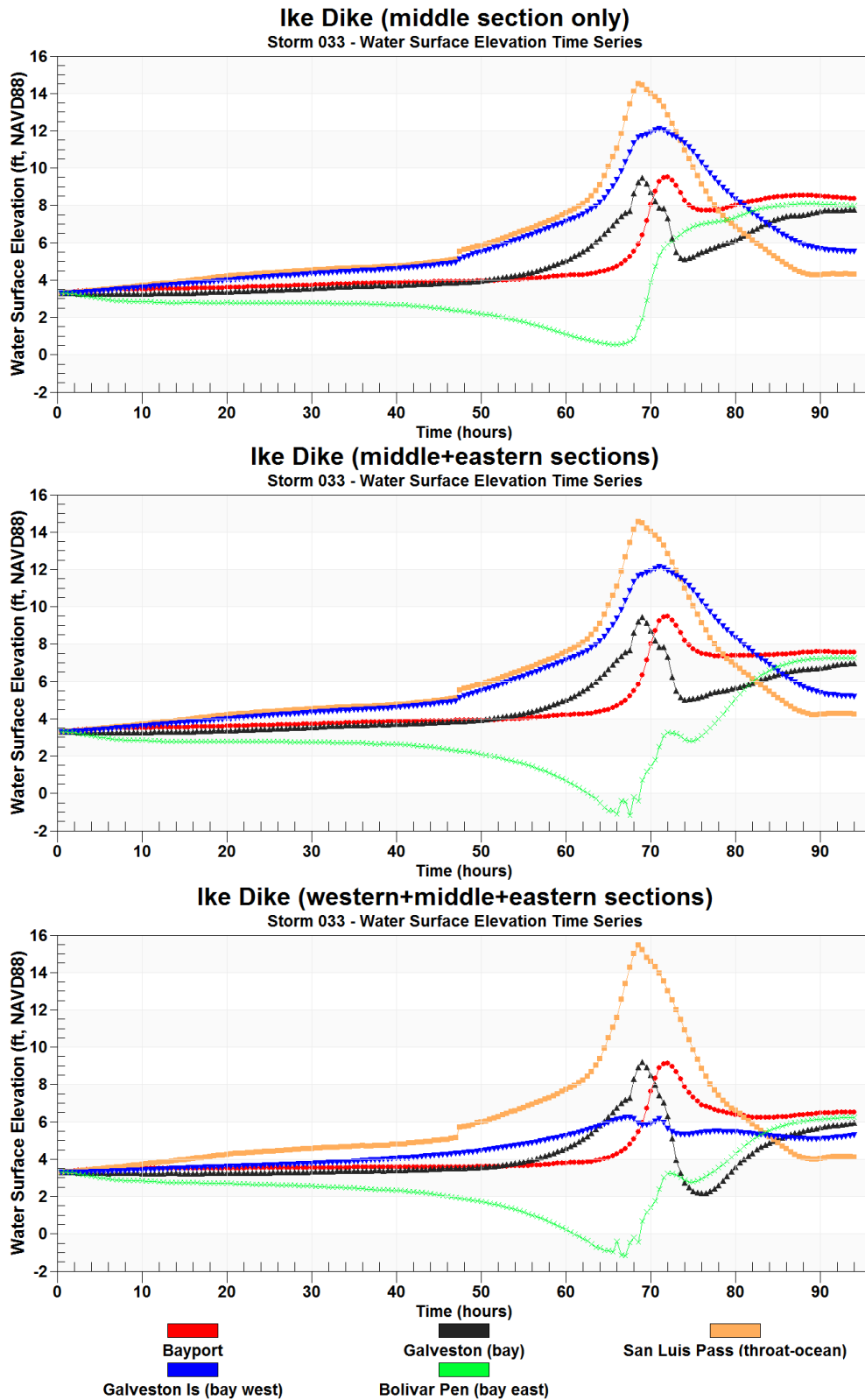


Figure 13-22. Water surface elevation times series for Storm 033, future sea level scenario SLR1, and different Ike Dike alignments. Top panel (Alignment 2). Middle panel (Alignment 3). Bottom panel (Alignment 1a).

up/set down is clearly seen prior to hour 65 in Figure 13-22. The set-up/set-down begins slowly for the first 40 hours, and then it occurs at a faster rate as the hurricane approaches landfall and winds within the bay grow stronger between hours 40 and 65. Hour 65 is just a few hours before landfall.

The peak storm surge along the western shoreline of Galveston Bay occurs around hour 70, first at the City of Galveston and then a short time later at Bayport, as shown in the red and black curves, respectively. Surge peaks around hour 70 at both locations are the result of local wind set-up that is forced by the hurricane's core winds acting directly on water within the bay. The peak surge at both locations is only slightly lower with the eastern termination section in place; compare the red and black curves in the top and middle panels of Figure 13-22 at the time of peak surge. The difference is due to flanking that occurs without the eastern section. In terms of peak surge levels, the effects of flanking are quite small at Bayport, the City of Galveston and along the rest of the western bay shoreline. Differences are 0.2 ft or less. The amount of flanking flow is neither great enough, nor does it occur early enough, to significantly raise peak surge levels along the western shoreline of the bay.

The influence of flanking is most clearly evident in water surface elevation differences at the bay side of Bolivar Roads (differences in the green curves between top and middle panels), beginning around hour 50. Flanking that occurs without the eastern section results in less set-down on the eastern side of the bay. Water entering Galveston Bay due to flanking is in part offsetting the set down of the water surface by the wind.

After the eye of the storm passes through Galveston Bay, wind speeds rapidly decrease, and the water surface elevation throughout the bay equilibrates or "levels out" in the absence of strong wind forcing. This is evident in Figure 13-22 at the end of the simulation, after hour 90. The water surface elevation curves at Bayport, the City of Galveston, and at eastern Bolivar Peninsula are all approaching a similar value, the equilibrated level. This level is established by the amount of water volume that enters the bays due to flanking and flow over the dike that occurs during the storm.

As this leveling out process occurs, the peak surge along the bay side of Bolivar Peninsula, an area that was set down by the wind for most of the

storm, is finally realized. The time of peak surge along Bolivar Peninsula occurs close to hour 90, some 20 hours later than the time of peak surge along the western shoreline of Galveston Bay which occurred at around hour 70.

For the 100-yr proxy storm the added influx of water into the bay due to flanking does not significantly contribute to the peak surge magnitude along the western side of Galveston Bay that was forced much earlier by the wind; but it does contribute to peak surges throughout much of the rest of the bay particularly in areas where the bay was set down by the peak winds. The difference in the “leveled out” water surface, with and without the eastern termination section, which is approximately 0.5 ft, is indicative of the additional volume of water that entered the bay due to the flanking which occurs without an eastern dike section.

The same general findings were observed for the even more severe, and rarer still, 500-yr proxy storm. For both of these proxy storms, which are the highest surge producing events among the four storms examined, the peak surges along the western shoreline of Galveston Bay are primarily dictated by the strong forcing associated with the peak winds that occur within the bay around the time of landfall. Peak surges are only minimally influenced by flanking so the eastern dike section, which effectively reduces flanking, has minimal influence on them.

A second similarly formatted figure, Figure 13-23, shows water surface elevation time series for Hurricane Ike and the future sea level scenario, SLR1. Ike was a storm that had its maximum surge zone near High Island, and it had a high peak surge there, approximately 18 to 20 ft. It provides an opportunity to the influence of the eastern dike section in reducing surge levels within the bay for an event having a higher potential for flanking than the 100-yr proxy storm.

The influence of flanking, and the greater amount of flanking that occurs for Ike, are evident by comparing the green curves in the top and middle panels of Figure 13-23. In the middle panel of Figure 13-23, which reflects the dike configuration with the eastern termination section in place, beginning at hour 1035 the water surface set-down in eastern Galveston Bay becomes evident as the core hurricane winds approach and then act directly on the bay. Compare the green curves in the top and middle panels of Figure 13-23 between hours 1035 and 1050. The same

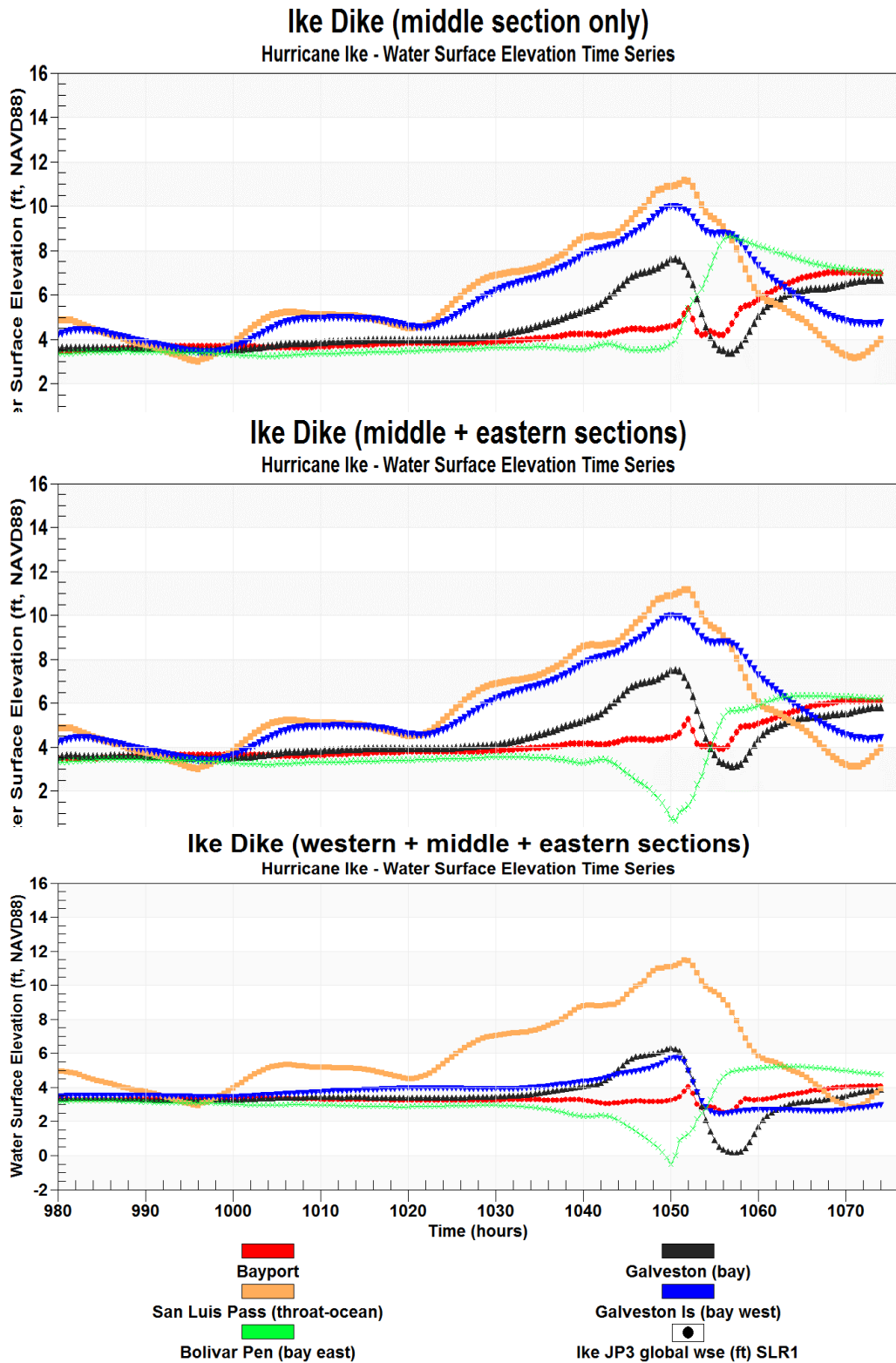


Figure 13-23. Water surface elevation times series for Hurricane Ike, future sea level scenario SLR1, and different Ike Dike alignments. Top panel (Alignment 2). Middle panel (Alignment 3). Bottom panel (Alignment 1a).

development of wind set down is not seen in the top panel, which reflects the absence of an eastern section; the amount of wind set-down on the eastern side of Galveston Bay is much less than for the case with the eastern dike section, by about 2 ft, due to the higher volume of flanking flow. The larger influx of water into Galveston bay associated with flanking mostly offsets any decrease in water surface elevation due to wind set-down.

The difference in the “leveled out” water surface elevation at the end of the water surface elevation time series graphs after hour 1070 also is indicative of the amount of flanking. The difference in equilibrated water level between Alignments 2 and 3 for Ike is approximately 1 ft, which is larger than it was for the 100-yr proxy storm. This is further evidence of an increased amount of flanking flow that occurred for Ike, which is reduced by the eastern termination section.

For Ike, the main driver of the peak storm surge experienced in different parts of Galveston Bay is somewhat different than it was for the 100-yr proxy storm. For the 100-yr proxy, peak surge at both Bayport and Galveston was driven by the strongest winds acting on the bay at landfall. For Ike, the surge values that occur at Bayport and Galveston at around hour 1050, which are forced by the locally high winds that occur with landfall are only minimally influenced by the flanking that occurs. Differences in surge level at this time are only several tenths of a foot for the two alignments. This finding is similar to that seen for the 100-yr proxy storm. The flanking that has occurred prior to hour 1050 is apparently not early enough and not great enough to significantly influence the peak surge associated with the strongest winds acting within the bay. The presence of an eastern dike section has little influence on the initial wind driven peak surges that occur at this time.

At Galveston the surge value at hour 1050 is the peak surge for the entire event; however, at Bayport, the peak surge for the entire event is associated with the leveling out of the bay in the latter stages of the storm (at around hour 1070). This occurs some 20 hours after landfall and after the storm had moved through the region. See the red curves in Figure 13-23, both upper and middle panels, where the event peak surge at Bayport occurs after hour 1065. An explanation for the different behavior follows.

For Hurricane Ike, because it made landfall at Bolivar Roads, peak winds in Galveston Bay were directed more to the south than were the peak winds for the 100-yr proxy storm. For this more southerly wind direction Bayport was not located at the downwind side of the bay as it was for Storm 033. The amount of wind set-up that occurred there at around hour 1050 was relatively small. The City of Galveston, which is located at the southwest corner of Galveston Bay, was situated at the down-wind side of the bay for Ike just as it was for the 100-yr proxy. At Galveston, the peak surge is driven by the local wind forcing, for both storms.

Also note that for the 100-yr proxy storm, local winds within the bay drove the storm surge into the upper reaches of the Houston Ship channel shortly after landfall forcing high surges there. No such process occurred for Hurricane Ike, because of the different landfall location and different wind field patterns within the bay after landfall. After the eye of the storm moved through, the bay, winds from the west were prevalent.

For Ike, without the eastern termination section, the peak surge at the eastern end of Bolivar Peninsula does not occur very late in the storm and it is not associated with the leveling out of the bay water surface after the storm has moved through. Instead, the peak surge is more strongly forced by the flanking that occurs both before and near the time of peak surge and by the prevailing winds from the west after the storm moves inland which sets up the water surface on the east side of the bay. See the green curve in the top panel of Figure 13-23, where the peak surge occurs at about hour 1055.

But even Hurricane Ike, which had high potential for flanking on the eastern side, did not produce surge levels for Alignment 2 that would cause significant loss/damage in key areas of Galveston Bay along its western shoreline and into the Upper Houston Ship Channel. Peak surges in these areas were approximately 7 ft for Alignment 2. The eastern dike section included in Alignment 3 reduced these surges by as much as a foot, but they were already at relatively low damage-causing levels.

A central question is: for Alignment 2, are there storms that produce inundation-causing surge levels in the key areas of Galveston Bay, like the 100-yr and 500-yr proxy storms, that also generate high flanking such that the presence of an eastern termination section (Alignment 3) reduces the peak surges by significant amounts, not just one or two tenths of foot? A

related question is: are there extreme storms that produce enough flanking flow with flanking early enough such that flanking has a strong influence on the magnitude of the wind-driven peak surges.

Storms that produce the most flanking flow for Alignment 2 would tend to have their maximum surge zone at High Island, and have very high peak surge levels there, like Hurricane Ike. Hurricane forward speed and the duration of high surge levels could also play a role in influencing the volume of flanking flow. Storms that have their peak surge at High Island would tend to have their maximum wind band at the same location, and not along the western shoreline of Galveston Bay, which is some 30 miles away. Also, wind directionality for severe storms that make landfall more to the east, like Ike, might not be conducive to generating high peak surges all along the western Galveston Bay shoreline and into the upper Houston Ship Channel.

It appears as though the highest surge producing storms and the most damaging storms for the western shoreline of Galveston Bay and the upper Houston Ship Channel are those having the following characteristics: 1) an approach from the southeast, 2) a landfall location that is south of Bolivar Roads, and 3) highest winds located right at Galveston and along the western bay shoreline. These conditions lead to a maximum set-up along the entire west side of the Bay and then a push of the water up into the upper Houston Ship Channel after landfall and strong winds are directed to the north. It is not surprising that the storms that best matched the extreme 100-yr and 500-yr surge levels all along the western bay shoreline and into the upper reaches of the Houston Ship Channel are storms like that had these characteristics, the selected proxy storms.

Extreme storms for which flanking might play a greater role than was seen for the 100-yr and 500-yr proxy storms, might be slower moving versions of these same severity/size of storms. Both Storms 033 and 036 have 11-kt forward speeds. Perhaps, storms with same the intensity but larger size could also produce more flanking flow. These two storms were fairly large given their intensity. The radius-to-maximum-winds for Storms 033 and 036 were 26/37 nm and 22/32 nm, respectively. The first number is the radius offshore and the second number is the radius at landfall; the latter reflects the storm filling process near landfall. Storms having a larger radius-to-maximum-winds would have to make landfall further to the south in order to have the maximum wind bands at Galveston. Storms

with very high intensities are less likely to also have large radii-to-maximum winds.

It would be informative to examine other storms that produce high surge values for the west shoreline of Galveston Bay, like the 100-yr and 500-yr statistical surge values, that also might have flanking flows that are higher than those for the 100-yr and 500-yr proxy storms, if such storms are realistic. Candidates might be other storms that were considered as possible 100-yr or 500-yr proxy storms. These would be simulated with and without the eastern dike section in place (Alignments 3 and 2), to see if they also show the same dominance of the local wind in generating the peak surge and a minimal reduction in peak surge achieved with the eastern termination section in place. The other storms examined might include slower moving storms that might lead to higher flanking volumes prior to landfall as well as larger storms that have maximum winds at Bolivar Roads and higher surges at High Island.

Storm Surge Reduction Benefits of a Western Termination Section

Without a gate system at San Luis Pass, which is an important feature of the western termination section, as long as the water level on the open coast is higher than the water level inside the pass, then the water surface gradient across the pass forces water to flow into West Bay. If the water level is higher in West Bay than it is in Galveston Bay, water will flow into Galveston Bay from West Bay. This flow in turn increases water levels inside Galveston Bay. Consequently, the hurricane forerunner surge can propagate through San Luis Pass and into West Bay, and then perhaps into Galveston Bay, a process that can begin a day or more before the hurricane makes landfall. The same process occurs during development of the peak surge, following the forerunner stage, as the open coast water level continues to rise with the arrival of the hurricane's core winds over the continental shelf. The absence of a gate system at San Luis Pass allows the peak storm surge to propagate into West Bay as well. Without the land barrier portion of the western termination section, once the open coast surge level exceeds the elevation of the barrier island along the Bluewater Highway, additional water flows into West Bay.

The prevailing wind pattern that develops within the bays for approaching hurricanes can reduce the amount of water which flows through San Luis Pass and into the bays. For hurricanes that approach from the southeast,

the most common direction, the wind-induced water surface elevation setup tends to occur along the western side of Galveston Bay, in response to winds that blow from the east or northeast. These same winds can set up the western end of West Bay, adjacent to San Luis Pass. This prevailing wind pattern occurs due to the counterclockwise rotating wind fields associated with the hurricane. Wind setup on the western end of West Bay tends to reduce the water surface elevation difference between the open coast and West Bay, thereby reducing flow into the bay. As wind setup develops on the west side of Galveston Bay, flow from West Bay into Galveston Bay is reduced.

Because West Bay is hydraulically connected to Galveston Bay, there is potential for the forerunner and peak storm surge to propagate from West Bay into Galveston Bay, a process that depends upon the wind forcing that is acting in both bays and the open coast water levels. The Texas City Dike and the man-made peninsulas on the north and south sides of West Bay, upon which the I-45 highway is built, influence the hydraulic connectivity between West and Galveston Bays. These features retard, but do not eliminate, the movement of water from one bay to the other.

A comparison of peak storm surge results for Alignments 1a and 3 enables assessment of the surge reduction benefits of the western termination section. Alignment 1a is comprised of the western + middle + eastern dike sections; whereas, Alignment 3 is comprised of the middle section plus the eastern section, but with no western section. Compare peak surge maps for Alignments 1a and 3 for the 10-yr proxy storm (compare Figures 13-5 and 13-8), the 100-yr proxy storm (compare Figures 13-9 and 13-12), the 500-yr proxy storm (compare Figures 13-13 and 13-16), and Hurricane Ike (compare Figures 13-17 and 13-20). The tabulated peak surge values that are listed in Appendix B, and the water surface elevation time series shown in Figures 13-22 and 13-23 (the middle and bottom panels), provide valuable insights as well. The middle panel in both figures shows results for Alignment 3 (no western section), and the bottom panel shows results for Alignment 1a (with the western section).

Qualitatively, for all four storms, the peak storm surge maps with and without a western termination section show that the most significant differences are in West Bay; along Galveston Island west of the City of Galveston, and along the northern shoreline of West Bay west of Texas City. For all four storms, the storm surge significantly penetrates into

West Bay without the western termination section in place. Within Galveston Bay, along its western shoreline including the City of Galveston, peak surge levels also are reduced with the western termination section in place. The peak storm surge maps suggest that the western termination section has a much greater positive influence in the Houston-Galveston region than does the eastern termination section. The western section results in greater surge reductions, over a wider geographic area, in areas having higher potential for damage and economic losses.

The tabular peak surge data that are listed in Appendix B enable a more quantitative assessment of the magnitude of storm surge reduction that is achieved with the western termination section. On Galveston Island, the benefit of the western section decreases from west to east, from San Luis Pass toward the City of Galveston. In terms of reduction in peak surge, for the 10-yr proxy storm, peak surge in West Bay is reduced by 1.9 ft, 1.2 ft, and 0.9 ft at the western, middle, and eastern ends of Galveston Island, respectively, and by 0.8 ft at the bay side of the City of Galveston near the University of Texas Medical Branch. For the 100-yr proxy storm, the reductions in peak surge at the same four locations are 5.9 ft, 4.9 ft, 0.8 ft and 0.3 ft, respectively. For the 500-yr proxy storm, the reductions at the same four locations are 6.7 ft, 5.7 ft, 1.3 ft and 0.3 ft, respectively; and for Hurricane Ike, the reductions at the same locations are 4.3 ft, 3.3 ft, 2.3 ft and 1.3 ft, respectively. Reductions in peak surge achieved with the western section are largest near San Luis Pass and smaller with increasing distance from the pass.

Peak surges also are reduced along the northern shoreline of West Bay with the western termination section. As was the case along Galveston Island, the reductions in surge lessen in magnitude from west to east. For example, near the Amoco Chemicals Reservoir (designated as the West Bay (north) location) which is north of San Luis Pass, peak surges are reduced by 1.7 ft, 5.5 ft, 6.3 ft, and 5.4 ft for the 10-yr, 100-yr, 500-yr proxy storms and Hurricane Ike, respectively. Much further to the east, near Bayou Vista which is immediately south of Texas City at the east end of West Bay (designated as the West Bay (east) location), peak surges are reduced by 1.1 ft, 2.3 ft, 2.4 ft, and 3.2 ft for the 10-yr, 100-yr and 500-yr proxy storms, and Hurricane Ike, respectively.

In general, the western termination section has a much greater benefit in reducing surge along the western and central parts of Galveston Island, in

those areas that lie to the west of the City of Galveston. This is primarily due to the presence of the I-45 highway peninsulas that reduce the movement of water, past them, to the west. Flow to the west is mostly constrained to the open water gap between the two man-made peninsulas, which retards surge penetration past this point. Surge penetration past this point is not prevented; it is just reduced.

For Hurricane Ike, the western termination section has a greater positive influence at the City of Galveston, compared to any of the 3 proxy storms, even the more intense 100-yr and 500-yr proxy storms. In the absence of the western section, the storm surge penetrates into this area more effectively for Hurricane Ike than for any of the proxy storms.

Interestingly, and perhaps counterintuitively, the absence of a western termination section leads to a larger increase in peak surge at the City of Galveston for the 10-yr proxy storm than for the more intense 100-yr and 500-yr proxy storms. In fact, while the two most intense proxy storms lead to the greatest increases in peak surges in eastern and central West Bay, the increase in peak surge at the City of Galveston is the least for these two storms, even less than the 10-yr proxy storm and Hurricane Ike. Reasons for these differences are discussed later in this section.

Within Galveston Bay, the western termination section has a beneficial effect by reducing peak surges along the western shoreline of the bay and into the upper reaches of the Houston Ship Channel. The western section reduces peak surge levels along the western Galveston Bay shoreline by amounts of 0.5 to 0.8 ft for the 10-yr proxy storm. The magnitude of the peak surge reduction is fairly uniform along this long stretch of shoreline. Peak surge is reduced by smaller amounts for the 100-yr proxy storm, 0.1 to 0.5 ft, and by even smaller amounts of 0.1 to 0.3 ft for the 500-yr proxy storm. For Hurricane Ike, the benefits of the western termination section are greater than they are for the proxy storms; reductions in peak surge range from 1.1 to 2.1 ft along the western shoreline of Galveston Bay. North of Clear Lake and into the upper reaches of the Houston Ship Channel, reductions in peak surge are approximately 2 ft; south of Clear Lake reductions are closer to 1 ft.

Analysis of Temporal Changes in Water Surface Elevation and Velocity

Results indicate that, without the western termination section, there is much greater surge penetration past the City of Galveston and into Galveston Bay for Hurricane Ike than there is for any of the three proxy

storms. Results also suggest that surge penetration into Galveston Bay is greater for the 10-yr proxy storm than it is for the more intense 100-yr and 500-yr proxy storms, which produce greater open coast surges at San Luis Pass. Examination of the water surface elevation time series graphs in Figures 13-22 (the 100-yr proxy storm) and 13-23 (Hurricane Ike) sheds additional insight on why this is the case, as does consideration of the winds and water velocities for each of these storms. In both figures, the middle panel shows the time series for Alignment 3 (no western termination section) and the bottom panel shows time series for Alignment 1a (having the western section).

In Figure 13-22 (middle panel), which is for the 100-yr proxy storm and a middle dike section only with no western termination section, the close similarity of the orange curve (outside San Luis Pass) and the blue curve (inside the pass) for the hours between 0 and 40 shows that the surge forerunner propagates through San Luis Pass with only a small amount of attenuation. During this 40-hour period of time, the water surface elevation increases by about 1 ft inside San Luis Pass. At the City of Galveston (black curve) which is located at the eastern end of West Bay, the water surface increases by only a few tenths of a foot during this same period of time.

Inspection of the water velocity fields as a function of time for the 100-yr proxy storm revealed that prior to hour 36, the forerunner surge that was developing on the open coast forced water into West Bay through San Luis Pass, and then that water moved toward the east within West Bay, past the City of Galveston primarily via the deeper channel that serves the Port of Galveston, and then into Galveston Bay. The peninsulas which are part of I-45 slowed the movement of water from West Bay to the east toward Galveston and Galveston Bay, but did not prevent it.

At around hour 37 or 38, the winds within Galveston Bay increased to a speed that was sufficient to set up the western side of Galveston Bay in such a way that water began to reverse direction and flow from Galveston Bay past the City of Galveston and into West Bay through gap between the I-45 peninsulas. At this point in time, propagation of the forerunner from West Bay into Galveston Bay ceased.

After hour 38 the surge forerunner and then, eventually, the peak surge continued to propagate through San Luis Pass and into West Bay as the

coastal surge level increased and remained above the water level inside the bay. The wind setup on the western side of Galveston Bay grew as the hurricane approached landfall and winds became stronger; and in response, flow continued from Galveston Bay into West Bay. The convergence of flow into West Bay, through San Luis Pass and from Galveston Bay, lead to increases in storm surge levels in West Bay. This pattern of surge development continued until after landfall.

Following landfall, as the storm moved inland, winds shifted to blow from the west, then the southwest and them from the south; and as the shift in wind direction occurred, and water began to be pushed from West Bay back into Galveston Bay as the south end of Galveston Bay was set down and the northern side of Galveston Bay was set up by the wind, pushing water into the upper Houston Ship Channel.

For Alignments 1a and 3, peak surge values at Galveston and Bayport, and at other locations along the western shoreline of Galveston Bay, differ by about 0.2 to 0.4 ft for this storm. Values for Alignment 3, without the western section, slightly exceed those for Alignment 1a, with the western section in place. This amount is comparable to and consistent with the magnitude of forerunner propagation that had developed at Galveston and Bayport prior to hour 36, a few tenths of a foot.

For the 10-yr proxy storm, examination of the velocity and water surface elevation fields as function of time showed that propagation of the forerunner surge into West Bay, past the City of Galveston, and into Galveston Bay lasted for 10 hours longer than it did for the 100-yr proxy storm. The longer duration occurred because it took longer for the winds in Galveston Bay to increase to the point that enough wind set-up developed on the west side of the bay such that the flow direction was reversed and propagation of the forerunner surge from West Bay into Galveston Bay ceased. By the time forerunner propagation ceased, more water had entered Galveston Bay than entered during the 100-yr proxy storm. Peak surge values at Galveston and Bayport, and at other locations along the western shoreline of Galveston Bay, differ by about 0.7 to 0.9 ft for the 10-yr proxy storm. These amounts are greater than those for the 100-yr and 500-yr proxy storms. Again, values for Alignment 3 without the western section slightly exceeded those for Alignment 1a, with the western section in place.

For Hurricane Ike (Figure 13-23), the forerunner development period was prior to hour 1040. At about hour 1040, the center of the hurricane entered the continental shelf region off Texas. The Hurricane Ike simulation was made with the astronomical tide; whereas, the proxy storm simulations were made with no astronomical tide. The effects of the tide are evident in the water surface elevation time series shown in the figure.

During this time, the top panel (Alignment 3 with no western termination section) shows that the forerunner is slightly attenuated by San Luis Pass, as was the case for the 100-yr proxy storm. The magnitude of the forerunner + tide amplitude at hour 1040 outside the pass is approximately 5.2 ft. The 3.3 ft future sea level value was subtracted from the water surface elevation to arrive at this value for the amplitude. Because the Ike simulation also includes the astronomical tide, estimates of the surge forerunner are approximate. Just inside the pass, the forerunner + tide amplitude is about 4.5 ft. The small decrease in forerunner + tide amplitude reflects the attenuation through the pass.

Analysis of the water velocity and water surface elevation fields as a function of time for Hurricane Ike indicated a strong net movement of water into West Bay, and then from West Bay into Galveston Bay. This occurred despite periodic fluctuations associated with the ebbing and flooding of the astronomical tide. Prior to hour 1040, propagation of the forerunner surge into West Bay and into Galveston Bay continued pretty much unabated; however, propagation was somewhat reduced by the I-45 peninsulas and by the Texas City Dike. During this entire time, winds in Galveston Bay had directions and magnitudes that were not sufficient to cause a cessation in propagation of the forerunner into Galveston Bay. For this reason, Hurricane Ike produced greater forerunner propagation into Galveston Bay than did the proxy storms.

Figure 13-24 shows an example of the water surface elevation and velocity fields that are associated with propagation of the surge forerunner surge into Galveston Bay. The fields are for Hurricane Ike. The figure shows a snap-shot in time at hour 1040. The following important features are labeled: a) propagation of the forerunner and building coastal surge through San Luis Pass and over the inundated barrier island south of the pass, b) propagation eastward within West Bay, c) flow through the gap between the I-45 peninsulas, d) eastward flow through the navigation

channel at the Port of Galveston, e) flow around the east end of the Texas City Dike and into Galveston Bay.

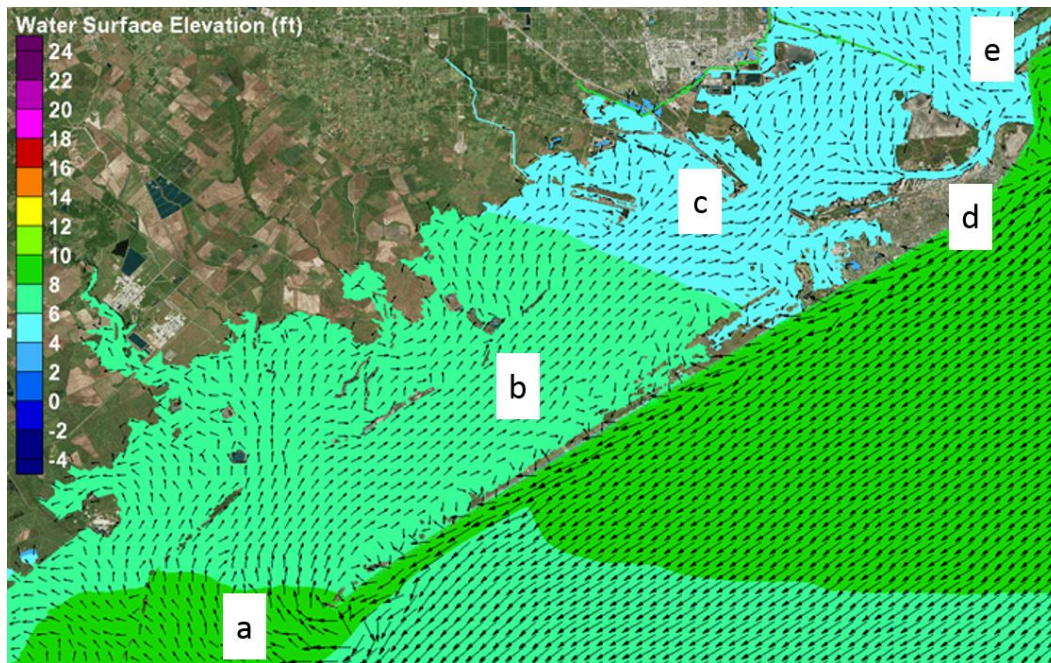


Figure 13-24. Illustration of surge forerunner propagation into West Bay, and from West Bay into Galveston Bay for Hurricane Ike, Alignment 3, and the future sea level scenario SLR1.

An estimate of the amplitude of the forerunner that has propagated into West Bay, past the I-45 peninsulas and Texas City Dike, and into Galveston Bay can be made by examining differences between the water surface elevation time series curves for Bayport (red curve) and Galveston (black curve) displayed in the middle and bottom panels in Figure 13-23. The bottom panel reflects a western termination section in place so neither tide nor forerunner can propagate into West Bay via San Luis Pass. At hour 1040 the approximate differences are 1.1 ft for Galveston and 1 ft for Bayport. At the time of peak surge for each location, the approximate differences are 1.1 ft for Galveston and 1.2 ft for Bayport. For Ike, the amount of forerunner penetration into both West Bay and Galveston Bay appears to be between 1 and 1.2 ft, which is larger than that for any of the proxy storms.

The western termination section has much greater regional surge reduction benefits than the eastern termination section, particularly along western and central Galveston Island and along the northern shoreline of West Bay west of Texas City. Without the western termination section, the hurricane surge forerunner can propagate into West Bay, with relatively

little attenuation. The peninsulas of I-45 and, to a lesser degree, the Texas City Dike retard surge propagation in a fairly significant way; however the forerunner propagation into Galveston Bay can reach 1 ft or slightly more for a substantial open coast forerunner like that which occurred during Hurricane Ike and wind conditions within Galveston Bay that are favorable for forerunner penetration into Galveston Bay (weak winds and/or wind directions that not blowing from the east or northeast).

Without the western termination section, the peak surge associated with the hurricane's core winds can also propagate rather efficiently into West Bay and lead to significant increases in peak surge throughout the bay, particularly west of the I-45 peninsulas.

An analysis should be performed to examine the cost of the western dike section, either a gate at San Luis Pass alone or in concert with a land barrier along the Blue Water Highway, and the flood risk benefits that accrue from it in both West Bay and Galveston Bay. The land barrier along the Bluewater Highway might simply involve raising the elevation of the highway to an elevation less than the 17 ft Ike Dike, and armoring it to be able to withstand overtopping.

In such an analysis though, it is important to note the following. The 100-yr proxy storm, Storm 033, was selected to best match the 100-yr ARI water levels at Galveston and along the western shoreline of Galveston Bay, not at San Luis Pass. At San Luis Pass, Storm 033 produces peak surge levels that are less than the 100-yr ARI water levels at this location. The damages prevented along Galveston Island and elsewhere in West Bay by the western termination section would be greater for a hurricane that produces the 100-yr ARI water surface elevation at San Luis Pass, compared to damages prevented by the event that produces the 100-yr ARI water level at Galveston. Analysis should consider additional storms that best replicate the 10-yr, 100-yr and 500-yr statistical surge levels at San Luis Pass.

Another factor that supports inclusion of the western termination section in the Ike Dike concept, particularly a gate at San Luis Pass, is the ability to not only prevent the forerunner and peak surge from entering West Bay, but also as a means for controlling the water level inside the bays at the time when the surge gates are closed. It might be advantageous to try and use the timing of gate closure as a means to minimize the amount of water

in the bays, in advance of an approaching hurricane. Such an operational procedure might dictate closing the gates when low astronomical tide creates a minimum water surface inside the bays. Having gates at both San Luis Pass and Bolivar Roads could achieve this operational objective fully; a gate system only at Bolivar Roads can only do this partially. A desire to control the water level inside the bays might become increasingly more important as mean sea level rises.

Influence of Lowered Gate Elevations on Interior Surge Levels

Alignment 1b has the same footprint as Alignment 1a. However, dike crest elevations in Alignment 1b are lowered from 17 ft NAVD88 to elevations that correspond to preliminary design elevations for the navigation (9.8 ft NAVD88) and environmental (13.8 ft NAVD88) gate systems at both Bolivar Roads and San Luis Passes. Both alignments 1a and 1b have western, middle and eastern dike sections.

By comparing results for Alignments 1b and 1a, it is evident that the effect of lower gate elevations on peak surge levels behind the dike is relatively small; the lower gate elevations lead to slightly higher storm surge levels. Among the three proxy storms, the greatest increases in peak surge occur for Storm 036, the 500-yr proxy storm, which produces the highest open coast storm surges and therefore produces the greatest magnitude and duration of flow over the gates. There is some spatial variability in the peak surge increases within the bays. For Storm 036, the greatest increase in peak surge is 0.5 ft immediately behind the gates at Bolivar Roads pass. With increasing distance away from the gates the amount of the increase in peak surge lessens. For example, the magnitude of the increase in the vicinity of the University of Texas Medical Branch is slightly less, 0.4 ft; and the increase is reduced further to 0.3 ft on the bay side of the western end of the City of Galveston. Elsewhere in West Bay increases range from 0.1 to 0.3 ft. Along the western shoreline of Galveston Bay and into the upper reaches of the Houston Ship Channel, increases of peak surge for Alignment 1b are no more than 0.3 ft, and less than that value in many locations.

For Storm 033, the 100-yr proxy storm, which is the only other proxy storm that produces significant flow over the gates, the greatest increase is, again, immediately behind the gates at Bolivar Roads Pass. The magnitude of the increase at this location is 0.2 ft. In the vicinity of the University of Texas Medical Branch the increase is slightly higher, 0.3 ft;

and the increase is 0.2 ft on the bay side of the western end of the City of Galveston. Elsewhere in West Bay, increases were 0.1 to 0.2 ft. Along the west shoreline of Galveston Bay and into the upper reaches of the Houston Ship Channel, increases are 0.2 ft or less.

For less intense hurricane events, like the 10-yr proxy storm which produces little or no overtopping or no steady flow over the gates, there are no significant increases to peak storm surge levels behind the dike associated with the lowered gate crest elevations.

These increases in peak surge level, which are relatively small even for the most intense hurricanes, will require a small increase in design elevation for any secondary lines of defense within the bays, such as a ring levee/wall system along the bay side of the City of Galveston.

14 Water Level Considerations for Operating the Ike Dike Storm Surge Gates

Introduction

Model simulations discussed in previous chapters showed that the Ike Dike concept significantly reduced peak storm surge levels within Galveston and West Bays for severe hurricanes. The land portions of the coastal spine reduced surge in the bays by greatly diminishing the flow of water over the low-lying barrier islands. Gate systems, at Bolivar Roads and San Luis Passes, reduced storm surge by restricting flow into the bays through the passes. Flow was reduced in both the early stages of surge build-up, i.e., during the forerunner stage of surge development when the storm was far offshore in the Gulf of Mexico, as well as during the latter stages as the storm approached the coast and made landfall during which time the core winds forced much higher surge levels.

However, even with the dike in place and the gates closed, significant storm surge can be locally generated within the bays by hurricane-force winds. This facet of surge generation arises due to the bays' large size and its shallow depth. Strong winds acting internally within the bays push water from the upwind side of the bay toward the down-wind side, stacking water against the down-wind shoreline and elevating local surge levels there. The amount of water within the bays at the time of gate closure influences the peak surge elevation. A higher antecedent water level leads to a higher peak surge.

All storm surge simulations made thus far have necessarily assumed (due to a surge model limitation) that the surge gates are closed at the outset of the simulation, and that no surge forerunner has propagated into the bays through the passes for the duration of the simulation. In reality, some degree of forerunner propagation into the bays is expected prior to the time of gate closure; and the actual time of gate closure will dictate the water level that exists inside Galveston and West Bays.

From the perspective of operating the storm surge gates in a way that minimizes peak storm surge inside the bays, it is desirable to minimize the amount of water within the bays at the time of gate closure. This chapter focusses solely on minimization of the antecedent water level within the bays at the time gates are closed, in order to minimize interior surge levels. Other factors that might influence the timing of gate closure, such as operational constraints associated with the gates themselves, navigation safety, or throughput of vessel traffic in anticipation of an approaching hurricane, are not considered here.

Processes that Influence Antecedent Water Levels

A number of physical processes contribute to longer-term changes in water surface elevation along the Texas coast, all of which can influence the antecedent water level conditions that exist inside the bays at any particular time during hurricane season. Month-to-month changes in the monthly mean sea level along the Texas coast, and in Galveston and West Bays, are caused by seasonal variation in the thermal expansion of surface waters in the Gulf of Mexico. Such changes also are influenced by the seasonally-varying prevailing winds and atmospheric pressure patterns in the Gulf, and by seasonal changes in riverine runoff amounts that enter the bays. In addition to seasonal and Gulf-scale changes in mean sea level, there are annual changes in mean sea level arising from some of the same physical phenomena occurring at global spatial scales, and at annual and decadal time scales.

Other tidal and meteorological processes vary over shorter time scales and they influence antecedent water levels in the bays as well. One such process is the astronomical tide. Astronomical tides within the Gulf of Mexico are forced by net water fluxes through the Yucatan and Florida Straits which connect the Gulf with other larger adjacent water bodies and by the gravitational pull of the moon and sun on the Gulf's waters. Other physical processes that influence the antecedent water level are the wind-driven forerunner and the volume mode forerunner, both of which are associated with the presence of a hurricane. Both types of forerunners were introduced in Chapter 5.

These different contributors to antecedent water levels are discussed further, below.

Mean Sea Level

All of the with-dike storm simulations assumed that the storm surge gates at both Bolivar Roads and San Luis Passes were closed at the beginning of the simulation. Therefore, in essence, the antecedent water level within the bays at the time of gate closure, was equal to the initial water surface elevation value that was adopted for the simulation. The antecedent water level was set to either 0.91 ft NAVD88 for present sea level or 3.31 ft NAVD88 for the future sea level scenario.

The present-day sea level includes a current estimate of long-term mean sea level at Galveston Pleasure Pier, 0.50 ft (0.152 m) NAVD88 plus an additional amount of 0.41 ft (0.125 m). This added amount represents a seasonal mean sea level adjustment that reflects the late summer portion of the hurricane season, the time when the most intense hurricanes that influenced the Texas Coast have tended to occur, historically. The long-term mean sea level value was extracted from the following NOAA web site (<https://tidesandcurrents.noaa.gov/datums.html?id=8771510>).

Figure 14-1 shows the average monthly mean sea level for the Galveston Pier 21 gage, which is located on the bay side at the Port of Galveston. The graph is based on data from the following NOAA web site, (<https://tidesandcurrents.noaa.gov/sltrends/seasonal.htm;jsessionid=86oDDo3CDCFEE25287DB39611EA5E206?stnid=8771510>).

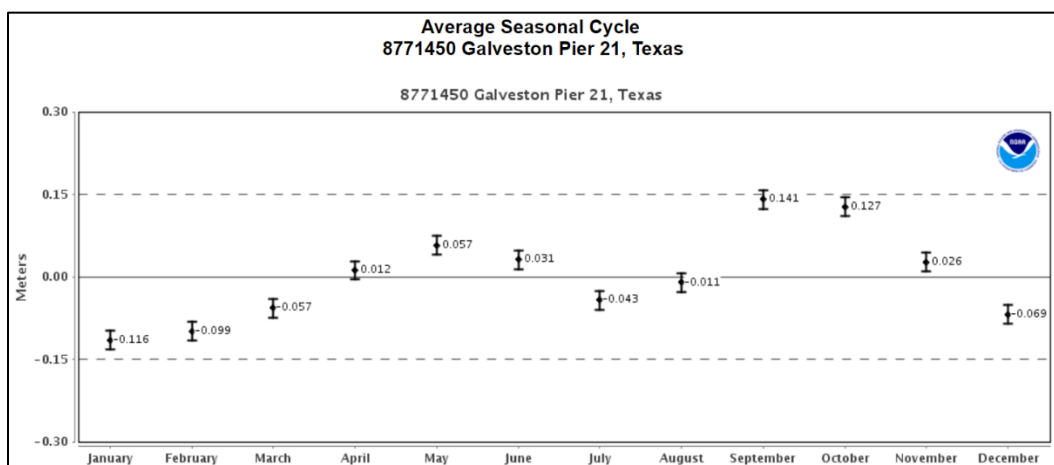


Figure 14-1. Computed average monthly mean sea level at Galveston Pier 21, Texas.

Data from the Pier 21 NOAA gage was selected for display in lieu of data from the open-coast Galveston Pleasure Pier gage because of the former's very long data record and continuous availability of data through to the present. Available overlapping data for both the Galveston Pier 21 bay site and the Galveston Pleasure Pier open coastal site show little difference in the average monthly mean sea level between the bay and the open Gulf. Note that the vertical scale in Figure 14-1 is displayed in metric units (meters), not in feet. The seasonal mean sea level adjustment value of 0.41 ft, which we have adopted, is equivalent to a metric value of 0.125 m.

There is year-to-year variability in the monthly mean sea level values. Figure 14-1 displayed the average monthly means and "error" bars that reflect its annual variability. Figure 14-2, also displayed in metric units, shows the inter-annual variability in monthly mean sea level at Galveston Pier 21, since 1990. The figure is taken from the NOAA web site, <https://tidesandcurrents.noaa.gov/sltrends/residual1980.htm?sessionid=192977B0714E944FE6463E112A1B5477?stnid=8771450>). Note, that to produce this figure, both the average seasonal cycle and a linear trend were removed. Removal of the linear trend is intended to remove the effects of long-term mean sea level change. The figure shows how the monthly mean sea level can vary from year to year, in addition to the seasonal cycle.

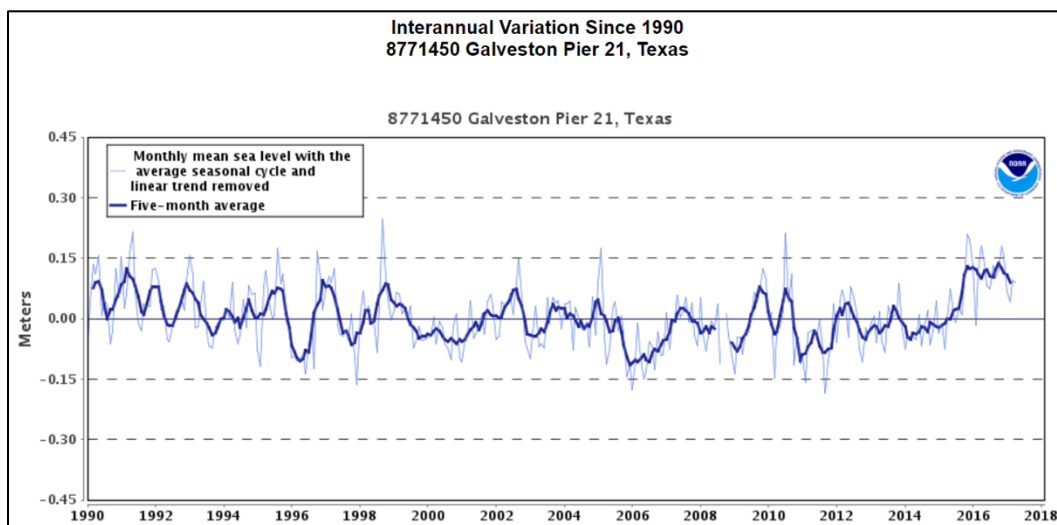


Figure 14-2. Inter-annual variability in monthly mean sea level at Galveston Pier 21, Texas.

Variability about the average monthly mean sea level can reach 0.2 m (0.66 ft) or more, which is greater than the highest average mean values in September and October shown in Figure 14-1. Also, of particular note is the unusually high and persistent variability in monthly mean sea level that was computed for 2016. Monthly, seasonal, and annual-scale changes in mean sea level strongly influence the antecedent water levels with Galveston and West Bays, at the time of hurricane occurrence. Gate operations will have no influence on these levels.

Astronomical Tide

Other processes can change antecedent water levels within the bays as well, on shorter time scales, such as periodic motions associated with the astronomical tide which oscillate with periods of approximately 12 or 24 hours.

Typical Tide Conditions at Galveston

Figures 14-3 and 14-4 are examples of the predicted astronomical tide at the Galveston Pleasure Pier, on the open coast, for two months in the middle of the peak hurricane season, August 2017 and September 2017, respectively. The figures were generated using the NOAA Tides and Currents web site (<https://tidesandcurrents.noaa.gov>). Each figure shows a 1-month record of the predicted astronomical tide, not the actual measured tide.

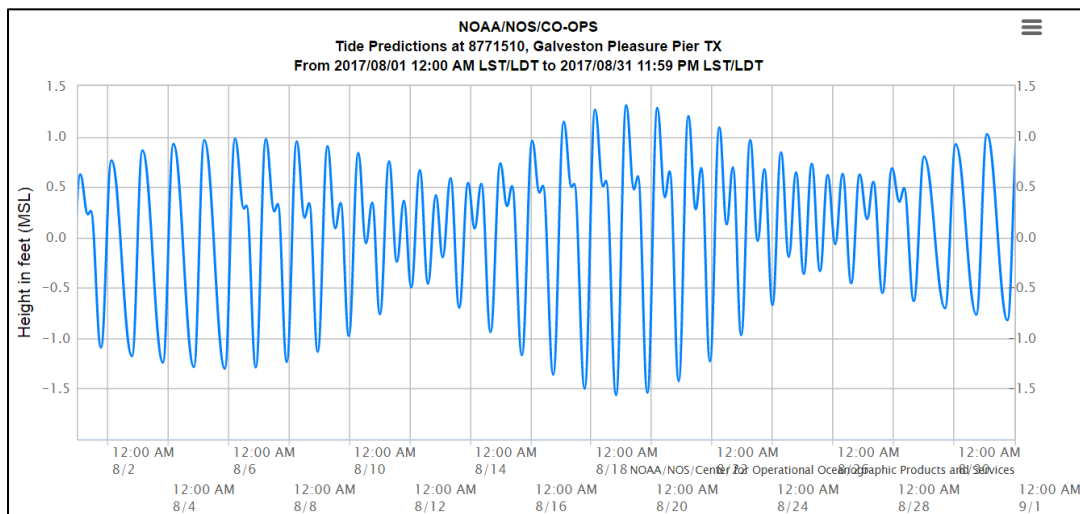


Figure 14-3. Predicted astronomical tide at Galveston Pleasure Pier, Texas, for August 2017.

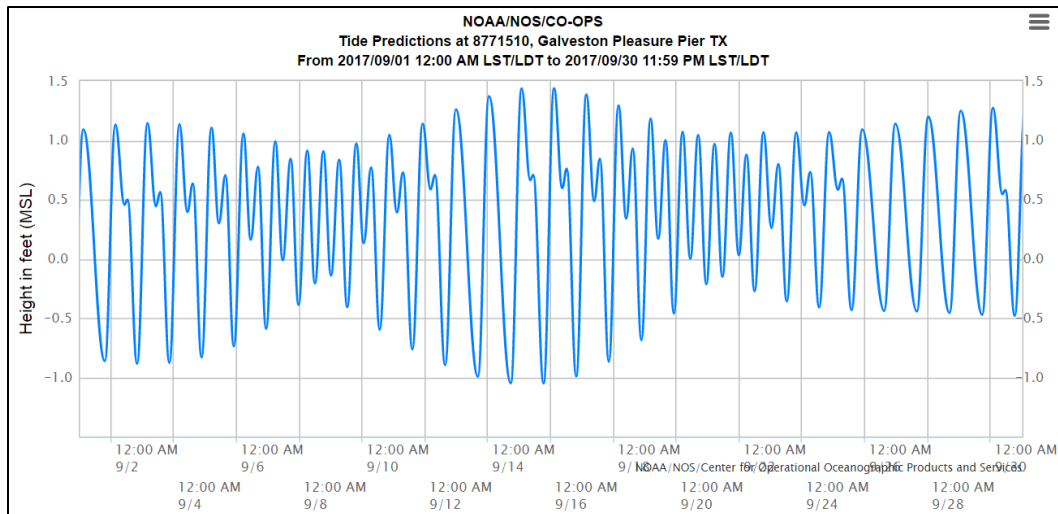


Figure 14-4. Predicted astronomical tide at Galveston Pleasure Pier, Texas, for September 2017.

The tide along the north Texas coast is considered to be a mixed tide; sometimes having one high and one low tide per day (called a diurnal tidal variation) and sometimes having two high and two low tides per day (called a semidiurnal variation). The diurnal variation is prevalent during times when the water surface elevation fluctuations from high tide to low tide (called the tide range) are greatest. The diurnal variation is prevalent for most of the month, about 75% of the time. The semi-diurnal variation is most prevalent during times when elevation fluctuations from high tide to low tide (tide range) are smallest, about 25% of the time.

Roughly, two full cycles of water surface elevation fluctuations are evident in each figure, with each cycle spanning approximately 14.5 days. Within each 14.5-day cycle, the daily highest water level values are modulated, i.e., daily maxima gradually increase from a smaller value to a greater value and then they get smaller again. The daily low water values are modulated in the same way. This general pattern repeats itself from month to month, throughout the year. The times of highest maximum elevation (and lowest minimum elevation) are called spring tide conditions; and, the times of lowest maximum elevation and highest minimum elevation are called neap tide conditions. The two 14.5-day cycles, each of which is called a spring-neap cycle, make up a lunar month, which is approximately 29 days in length. Each calendar month has about two spring-neap cycles; and that behavior is seen in Figures 14-3 and 14-4.

Tide Differences at Galveston – Open Gulf vs Galveston Bay

Bolivar Roads Pass naturally attenuates the tidal elevations, and the tide range, by about 30%. Based on NOAA data, in the open Gulf at Galveston Pleasure Pier the mean tidal range and the tidal range at spring tide is 1.46 and 2.04 ft, respectively; whereas, just inside the pass at Galveston Pier 21 the mean range and the range at spring tide is 1.02 and 1.41 ft, respectively. Tide range data were extracted from the NOAA web site: <https://tidesandcurrents.noaa.gov/stations.html?type=Datums>. The temporal characteristics of the tidal fluctuations in the bay and in the open Gulf are quite similar, except for the reduced tidal amplitude in the bay.

The surge gate structures that are built as part of the Ike Dike concept are expected to further attenuate the tide through the passes. The permanent superstructure that is built to support the retractable storm surge gates at both Bolivar Roads and San Luis Passes will permanently decrease the cross-sectional area at both passes, which will likely lead to further attenuation of the tide through the gate systems at the passes. Actual reductions of the antecedent water level within the bays that can be achieved by closing the surge gates at low tide will be determined by the natural attenuation that occurs at the passes and by additional attenuation that occurs with the surge gate systems in place. The exact amount of flood risk reduction that is achieved by closing the gates at low tide is unknown at present. The amount of flood risk reduction achieved by closing the gates at low tide can be quantified via modeling.

An Example of Measured Tide Fluctuations

A previous section described the unusually high monthly mean sea levels during 2016. Figure 14-5 shows the predicted astronomical tide (blue curve) and the actual measured water surface elevation (green curve) at Galveston Pier 21 during September 2016. The differences between measured and predicted tides clearly show the potential for higher-than-normal seasonal sea levels, relative to predicted astronomical tide values. The also show daily variations in the difference between the predicted and measured tide, due to other physical processes that are not storm related.

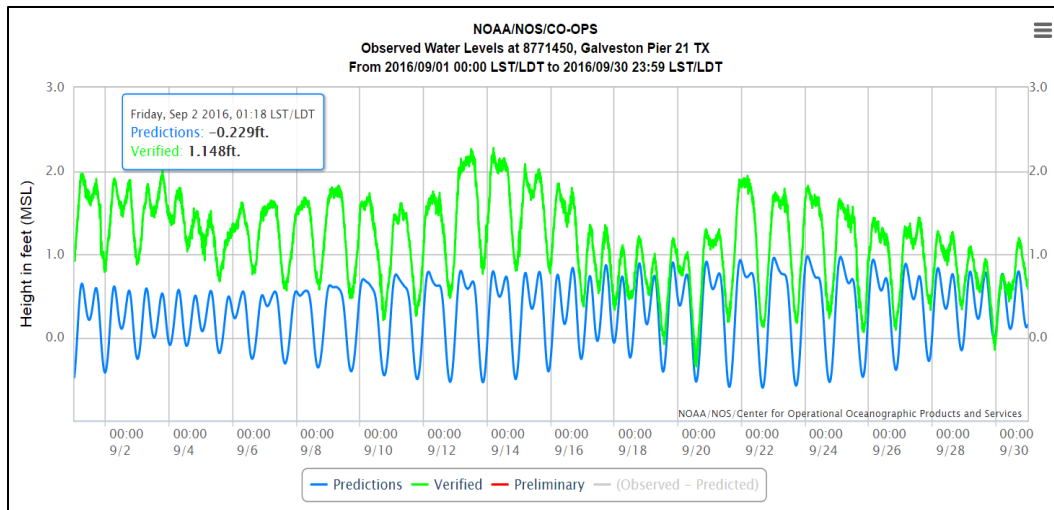


Figure 14-5. Predicted astronomical tide and measured water surface elevation at Galveston Pier 21, Texas, for September 2016.

While the mean sea level which is present during the time of hurricane occurrence cannot be controlled, the time of gate closure can be. The graph reinforces the benefit of closing the gates at low astronomical tide in order to minimize antecedent water levels within the interior bays and thereby minimize flood risk. Conversely, closing the gates at high tide increases the flood risk.

Wind-Driven Surge Forerunner

All hurricanes that traverse the Gulf of Mexico, and eventually approach the north Texas coast, will generate a significant wind-driven surge forerunner. Model results presented in Chapters 5 and 7 showed this for very intense hurricanes that approach the Houston-Galveston region from the east-southeast, southeast and south-southeast directions. The magnitude of the forerunner surge was greatest for storms having a southeast or south-southeast track and it was significantly less for an east-southeast track.

The counterclockwise circulating winds about the eye of a hurricane tend to force water movement along the continental shelf regions of the northern Gulf. An Ekman set-up, i.e the wind-driven surge forerunner, is forced at the coast; and it is created by water moving along the shelf, which is turned to the right in the northern hemisphere by the Coriolis force, and stacked against the coastline. The forerunner surge propagates westward along the Louisiana shelf and then southward along the Texas shelf. The forerunner surge seems to readily propagate into the bays via

the passes, relatively un-attenuated, as it did for Hurricane Ike. Propagation of the forerunner through the passes and into the bays is expected until the time when the surge gates are closed.

Water surface elevation changes associated with the forerunner surge generation process were discussed in Chapters 5 and 7. As described in those chapters, the wind-driven forerunner will cause the water surface elevation on the open coast and within the bays to gradually and steadily increase with time, a process which can start days before the hurricane makes landfall. As time progresses and the hurricane approaches and moves across the continental shelf off the coast of Texas, the rate of water level rise associated with the forerunner increases. Therefore, from the perspective of minimizing the antecedent water level within the bays due to the wind-driven forerunner surge, the earlier the storm surge gates are closed at both passes the better.

Recent work by Liu and Irish (2017) examined the wind-driven forerunner surge elevation along the north Texas coast for a number of synthetic land-falling hurricanes of varying intensity and size. They used a coupled wave and storm surge modeling approach that was quite similar to that applied in this study. Storm intensity was defined by the pressure deficit, i.e., the difference between far-field pressure and minimum central pressure. Storm size was characterized by the radius-to-maximum-winds. A single storm track from the southeast was considered, having a landfall location at the western limit of the City of Galveston.

Forerunner surge results were presented for a location that was positioned on the coast approximately half way between High Island and Sabine Pass. These results, shown in Figure 14-6, are considered to be generally applicable and representative of the entire Houston-Galveston region. The left hand panel of Figure 14-6 shows the forerunner surge elevation above normal, i.e., above the mean sea level, at a time 12 hours before landfall. The right hand panel shows the time of arrival for a 1-m (3.3-ft) forerunner surge level in hours before landfall. The forerunner surge elevations shown in Figure 14-6 are significant, ranging from 0.6 m (2 ft) to twice that value, 1.2 m (4 ft), for the set of storms that were considered.

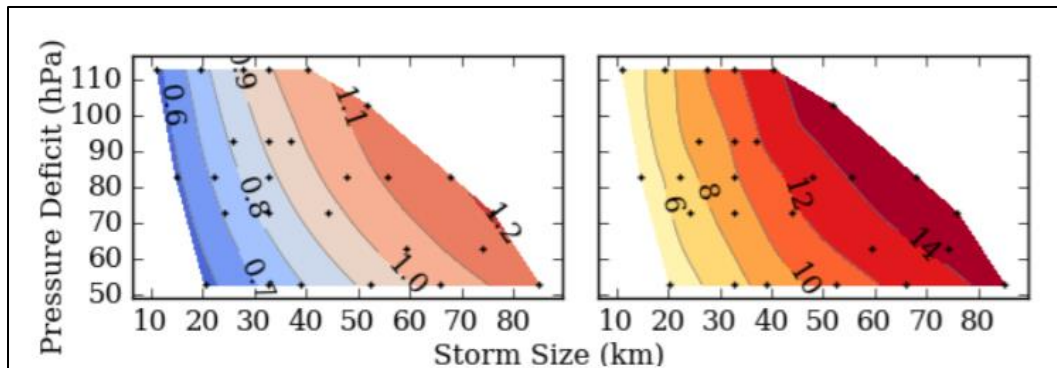


Figure 14-6. From Liu and Irish (2017). Left panel: Surge elevation above normal level (in m) 12 hours before landfall, as a function of pressure deficit and storm radius to maximum wind. Right panel: Time of arrival for a 1-m flood elevation (above normal level) in hours before storm landfall, as a function of pressure deficit and storm radius to maximum wind.

Forerunner surge is a significant contributor to flood risk in the Houston-Galveston region. Closing the gates as early as possible and practical minimizes propagation of the forerunner surge into the bays and minimizes flood risk for all areas inside the gates. Results presented in Chapters 5 and 7 suggest that closing the surge gates 24 hours prior to landfall would reduce, by an additional 50 to 60%, the forerunner surges that occur at 12 hours prior to landfall.

Surge forerunners for the 3 proxy storms and Hurricane Ike are presented and discussed in a later section of this chapter.

Volume Mode Forerunner

The volume mode oscillation that was investigated and identified by Bunpapong et al (1985), which was briefly described in Chapter 5, suggested that this phenomenon could produce oscillatory water surface fluctuations having an amplitude of up to 2 ft along the Texas coast (for major hurricanes having a pressure deficit of 120 mb), and having a period of oscillation of 28 to 30 hours. Such water level changes are comparable in magnitude to those associated with the astronomical tide and with the wind-driven forerunner; and as such, changes of this magnitude will have implications for storm surge gate operations and closure. This phenomenon has not been widely studied; and, it has been neglected in all coastal flood risk engineering studies of which the authors are aware. Therefore this phenomenon was examined more closely as part of the present study, to ascertain its importance in surge gate operations. This phenomenon is examined and discussed in much greater detail later in this chapter.

Wind-Driven Forerunner - Proxy Storms and Hurricane Ike

The wind-driven surge forerunner is one of the most important phenomena that affects surge gate operations because it persistently and steadily increases the water surface elevation with time as a hurricane moves through the Gulf and approaches the Texas coast. This phenomenon leads to a steady rise in water surface elevation within Galveston Bay, and thus it leads to a steady increase in flood risk. The potential magnitude of elevation change associated with the wind-driven forerunner is higher than that for the astronomical tide or the volume mode forerunner.

Development of the wind-driven surge forerunner for the 10-yr, 100-yr and 500-yr proxy storms, and Hurricane Ike is examined below. Results for the proxy storms shed some light on the roles of forward speed, storm intensity, and storm size on wind-driven forerunner characteristics. Results for Ike, both as it was simulated with the model and as it was measured during the actual event, are presented and discussed.

10-yr Proxy Storm

Figure 14-7 shows the temporal variation in water surface elevation at the Galveston Pleasure Pier, an open-coast location, and at three locations inside Galveston Bay: 1) Clear lake (east) which is located at the entrance to Clear Lake, 2) Alexander Island which is located at the northern end of Galveston Bay adjacent to the Houston Ship Channel, and 3) Houston Ship Channel (upper) which is located at the uppermost end of the ship channel near central Houston. The format of the graph in Figure 14-7, specifically the choice for vertical scale, is intended to focus on the development of the wind-driven surge forerunner, not the peak surge.

The 10-yr proxy storm is a relatively weak hurricane. It has a minimum central pressure of 975 mb, a maximum surface wind speed of 68 kts, which reflects Category 1 hurricane on the Saffir-Simpson wind scale, a radius-to-maximum-winds of 18 nm which increases to 22 nm as the storm approaches landfall, a typical storm size, and a rather slow constant forward speed of 6 kts.

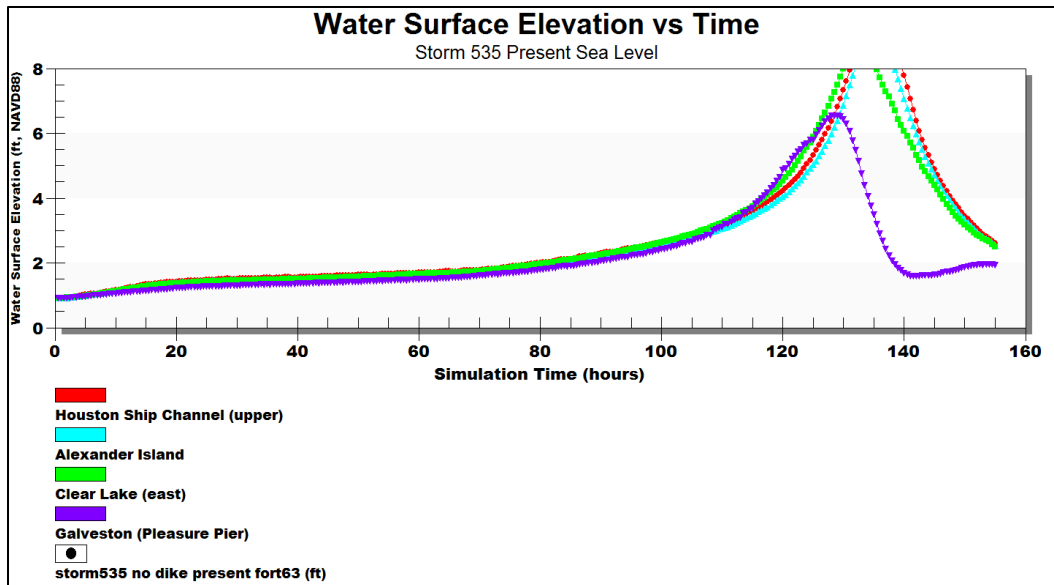


Figure 14-7. Water surface elevation changes with time associated with the wind-driven forerunner surge, both inside and outside Galveston Bay, for the 10-yr proxy storm.

Simulation time is shown on the horizontal axis in Figure 14-7, and several key times during the hurricane's transit in the Gulf are noted here. The eye of this hurricane enters the Gulf at hour 10 of the simulation. Upon entry the idealized wind fields, which are nearly circular about the eye for this synthetic storm and which blow in the counterclockwise direction about the eye, begin to generate far field east-to-west blowing winds all along the northern continental shelf regions of the Gulf. The along-shelf winds begin to force an along-shelf movement of water which, in turn, generates a small Ekman set at the shoreline, i.e. the wind-driven surge forerunner. As the storm gets closer to the Texas coast, wind speeds on the shelf increase, forcing an increase in speed of the along-shelf moving water, which in turn leads to a greater Ekman set-up.

At hour 58.5, which is 72 hours (3 days) prior to landfall, the eye of the hurricane is still positioned well beyond the edge of the continental slope off the Texas Coast. The water surface elevation at this time, at the Galveston Pleasure Pier, is 1.5 ft NAVD88, which is 0.6 ft above the approximate mean sea level value of 0.9 ft. Following entry, during the first two days of the hurricane's transit through the very deep-water parts of the central Gulf, a wind-driven forerunner surge of 0.6 ft already has been generated at the coast in the Houston-Galveston region by this slow-moving storm. During the entire time leading up to this point, the wind-driven forerunner has effectively propagated into all parts of Galveston Bay, with very little attenuation.

At hour 82.5, which is 48 hrs (2 days) prior to landfall, the water surface elevation has reached 1.9 ft. The eye crosses the outer edge of the continental slope off the Texas coast a short time later, at hour 85.5 of the simulation. During the previous 24 hours, the magnitude of wind-driven forerunner surge at Galveston increased by 0.4 ft, from 0.6 to 1.0 ft. Importantly, the rate at which the water surface elevation rises, i.e., the slope of the curve in the figure, is increasing at this time, as the storm approaches the Texas coast. As the eye approaches the continental slope off the Texas coast, the rate of water level rise associated with the forerunner begins to accelerate.

At hour 106.5, which is 24 hours before landfall, the eye has moved up the continental slope and is approaching the edge of the continental slope. The eye crosses the edge of the continental shelf, off the Texas coast, at hour 110, and it moves into the increasingly more shallow water. The rate at which the water surface elevation is rising due to the surge forerunner continues to accelerate, as evidenced by the changing slope of the curves seen in the figure. The rate of rise is increasing as stronger winds move onto the shallower shelf regions in advance of the approaching eye, enhancing alongshore movement of water and formation of the Ekman setup. During the previous 24 hours, the water surface elevation at Galveston has risen by 0.9 ft, from 1.9 ft to an elevation of 2.8 ft NAVD88. The magnitude of the forerunner surge at this time is 1.9 ft, relative to the mean sea level. Even for this relatively weak hurricane, 24 hours (1 day) before landfall, the wind driven forerunner has increased local water levels by roughly 2 ft. During this entire period of time, up to this point, the wind-driven forerunner has effectively propagated into all parts of Galveston Bay, with very little attenuation.

At hour 118.5, which is 12 hours before landfall, the water surface at the Galveston Pleasure Pier is 4.4 ft NAVD88, which is 3.5 ft above mean sea level. The water level rose by another 1.6 ft during the previous 12 hours alone, at an accelerating rate.

The simulated forerunner surge magnitude for the proxy storm can be roughly compared to the elevation suggested by the work of Liu and Irish (2017). The 10-yr proxy storm has a central pressure deficit of 38 mb (the difference between the far-field pressure of 1013 mb and the central pressure is 975 mb). For this pressure deficit and a radius-to-maximum-winds value of 18 nm (33 km) for most of its duration, results from the

work by Liu and Irish (2017), which are shown in Figure 14-6, suggest a forerunner surge value of between 0.6 and 0.7 m (2.0 and 2.3 ft) at a time that is 12 hours before landfall. The value of 3.5 ft from the present study is significantly higher than the value suggested by the work of Liu and Irish (2017).

It is possible that the slow-moving nature of the 10-yr proxy storm leads to a higher wind-driven forerunner surge at Galveston than does a faster moving storm having all other characteristics the same. There is some evidence that this might be the case, based upon results shown in the volume-mode forerunner analysis section that is presented and discussed later in this chapter. Liu and Irish (2017) did not examine the influence of forward speed on forerunner magnitude. All the storms that they considered and simulated had the same forward speed, 11 kts, which is nearly twice as fast as the speed of the 10-yr proxy storm, 6 kts. A difference in their model set-up compared to that used in the present study, such as the treatment of bottom friction, might also contribute to the difference in estimated surge forerunner magnitude.

Forerunner surge results for the 10-year proxy storm show the importance of early closure in operating the storm surge gates, which are an integral component of the Ike Dike concept. First, the wind-driven forerunner is not appreciably attenuated as it propagates through the passes and into the bays. There are only small differences between the water surface elevation at the open coast Galveston Pleasure Pier site and at locations throughout the bay, including even the upper reaches of the Houston Ship Channel. This observation is true for the entire forerunner surge development period prior to hour 118.5, which is 12 hours prior to landfall. Second, for this storm, decisions to close the storm surge gates at 72 hrs, 48 hrs, 24 hrs, and 12 hrs prior landfall, would result in forerunner surge magnitudes within Galveston Bay approximately of 0.6, 1.0, 1.9 and 3.5 ft, respectively, relative to mean sea level, at the time of gate closure. Any delay in closing the gates can lead to an increase in flood risk within the bay; so the sooner gates are closed the better. The potential increase in flood risk within the bay, that is associated with penetration of the wind-driven forerunner surge into the bay prior to gate closure, can be mitigated to a degree through an earlier gate closure and/or timing of gate closure to coincide with a time of low astronomical tide.

100-yr Proxy Storm

Figure 14-8 shows the variation in water surface elevation with time for the 100-yr proxy storm, at the same four locations that are shown in Figure 14-7. The 100-yr proxy is an intense hurricane, having a minimum central pressure of 930 mb, a maximum surface wind speed of 100 kts, which is a Category 3 hurricane on the Saffir-Simpson wind scale. The storm has a radius-to-maximum-winds of nearly 26 nm which increases to 37 nm as the storm approaches landfall, which is a rather large value; and it has a constant forward speed of 11 kts, which is an average value. Compared to the 10-yr proxy storm, the 100-yr proxy storm is more intense, larger, and it moves at nearly twice the forward speed, so it spends much less time transiting the Gulf of Mexico.

The eye of the 100-yr proxy storm was located just inside the Gulf at the beginning of the simulation, i.e., at hour zero. It began its initial spin-up from rest and began its transit, all while inside the Gulf. The start-up time, hour zero, corresponds to a time that is approximately 72 hours (3 days) prior to landfall.

At hour 22, which is 48 hours (2 days) prior to landfall, the eye of the hurricane is still in very deep water and well seaward of the edge of the continental slope off the Texas Coast. The water surface elevation at this time, at the Galveston Pleasure Pier, is 2.0 ft NAVD88, which is 1.1 ft

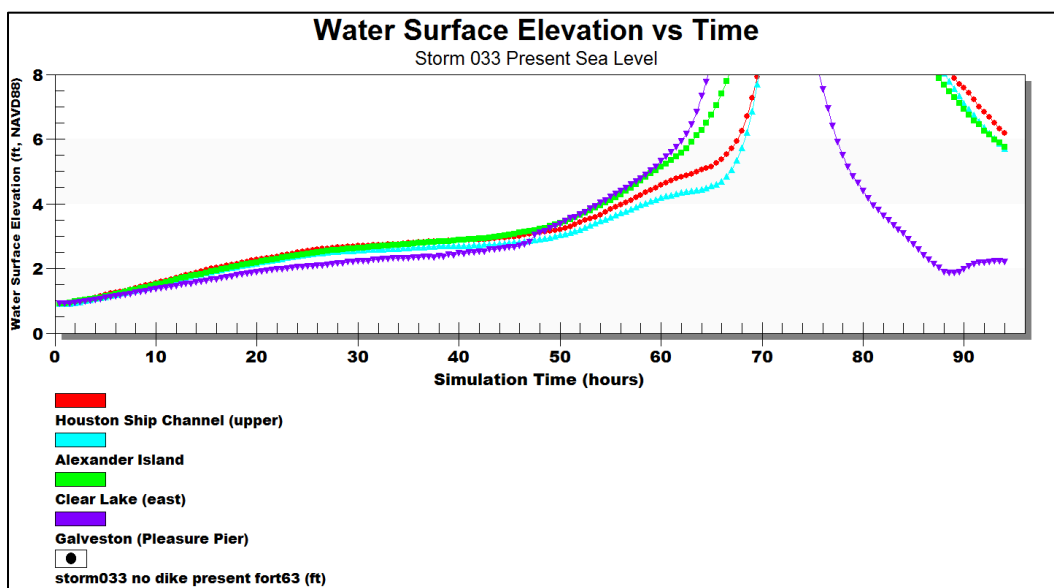


Figure 14-8. Water surface elevation changes with time associated with the wind-driven forerunner surge, both inside and outside Galveston Bay, for the 100-yr proxy storm.

above the approximate mean sea level value of 0.9 ft. Early development the wind-driven forerunner is rapid for this storm, reflected by the increase of 1.1 ft in the first 24 hours. Because the hurricane is more intense, stronger winds develop quickly over the continental shelf regions, leading to earlier formation of higher Ekman set-up at the coast.

At hour 46 of the simulation, the eye of the storm is positioned at the seaward edge of the continental slope. At this time, which is 24 hrs (1 day) prior to landfall, the water surface elevation at Galveston Pleasure Pier is 2.7 ft NAVD88, which reflects a forerunner surge magnitude of 1.8 ft relative to mean sea level. During the previous 24 hours, the wind-driven forerunner surge magnitude at Galveston increased by 0.7 ft, from 1.1 ft to 1.8 ft. The rate of water surface rise at Galveston is greater during the first 24 hours (1.1 ft) compared to the second 24 hours (0.7 ft). At first glance this seems counterintuitive. The anomaly is likely related to the storm's origin inside the Gulf and its rapid spin-up from zero intensity to full intensity over a relatively short time while it is already inside the Gulf. After hour 30, the rates of water level rise appear to be more like those seen for the 10-yr proxy storm, having a persistent acceleration in the rate of rise.

At hour 58, which is 12 hours before landfall, the eye has moved up the continental slope; and it is positioned at the edge of the continental shelf at hour 59. During the previous 12 hours, the water surface elevation at Galveston rose from 2.7 ft to 4.8 ft NAVD88, an increase of 2.1 ft in only 12 hours. The water surface elevation of 4.8 ft reflects a 3.9-ft forerunner surge magnitude, relative to mean sea level. The rate at which the water surface elevation is rising due to the surge forerunner is accelerating, as seen in the figure.

The simulated forerunner surge for the 100-yr proxy storm also can be compared to the forerunner surge magnitude that is based upon the work of Liu and Irish (2017). For the 100-yr storm, which has a central pressure deficit of 83 mb and a radius-to-maximum-winds value of 26 nm (48 km) for most of its duration, results from the work by Liu and Irish (2017), which are shown in Figure 14-6, suggest a forerunner surge magnitude of approximately 1.05 m (3.4 ft). The value of 3.9 ft from the present study is only slightly higher. Note that the forward speed of the 100-yr proxy storm, 11 kts, is the same as the speeds of all storms considered by Liu and

Irish (2017). This suggests that the larger discrepancy seen for the 10-yr proxy storm might be due, at least in part, to its slower forward speed.

Forerunner surge results for the much more intense 100-year proxy storm also show the importance of early storm surge gate closure. As was the case for the 10-yr proxy storm, during the forerunner development period prior to hour 46, there are small differences between the water surface elevation at the open coast Galveston Pleasure Pier site and all locations throughout the bays, showing propagation of the forerunner into the bay with little attenuation. Some of that difference is due to the effect of stronger prevailing winds within Galveston Bay which act to set up the western side of the bay. For the 100-yr proxy storm, decisions to close the storm surge gates at 48 hrs, 24 hrs, and 12 hrs prior landfall, would result in forerunner surge magnitudes within Galveston Bay approximately of 1.1, 1.8 and 3.9 ft, respectively, relative to mean sea level, at the time of gate closure. For an intense storm such as this one, closing the gates at least 24 hrs before landfall seems to be absolutely necessary, as does timing of closure to coincide with low astronomical tide.

500-yr Proxy Storm

Figure 14-9 shows the variation in water surface elevation with time for the very intense 500-yr proxy storm, at all four locations. The 500-yr proxy storm has a minimum central pressure of 900 mb, a maximum surface wind speed of 112 kts, which is right on the borderline between a Category 3 and 4 hurricane on the Saffir-Simpson wind scale. The storm has a radius-to-maximum-winds of nearly 22 nm which increases to 32 nm as the storm approaches landfall, a rather large value; and it has a constant forward speed of 11 kts which is an average value. Compared to the 100-yr proxy storm, the 500-yr proxy storm is more intense, not quite as large but still rather large, and it moves at the same forward speed, 11 kts.

Like the 100-yr proxy storm, the eye of the 500-yr proxy storm was located just inside the Gulf at the beginning of the simulation, i.e., at hour zero. It began its initial spin-up from rest and began its transit, all while inside the Gulf. The start-up time, hour zero, corresponds to a time that is approximately 72 hours (3 days) prior to landfall.

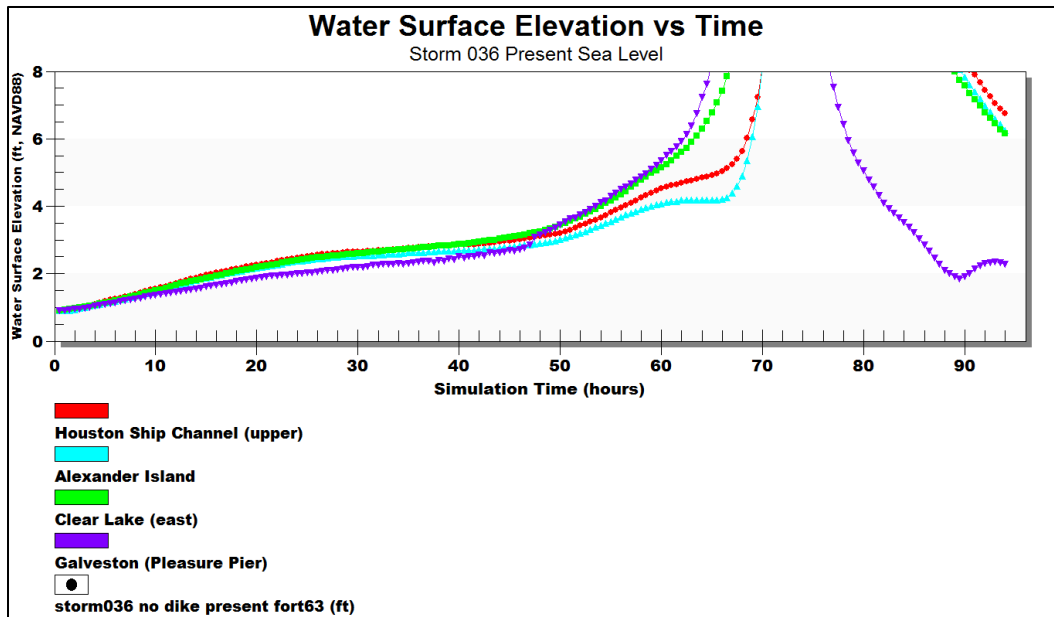


Figure 14-9. Water surface elevation changes with time associated with the wind-driven forerunner surge, both inside and outside Galveston Bay, for the 500-yr proxy storm.

For the first 46 hours of the simulation, the time which is 24 hrs (1 day) prior to landfall, the water surface elevation at Galveston Pleasure Pier is essentially the same for the 500-yr proxy storm as it was for the 100-yr proxy storm. Despite the higher intensity for the 500-yr proxy storm, its smaller size apparently offsets the intensity difference in the development of the surge forerunner. Both storms produce water surface elevations of 2.0 and 2.7 ft NAVD88 at hours 22 and 46 of the simulation, respectively, which are 48 and 24 hours prior to landfall, respectively. Forerunner surge magnitudes are 1.1 and 1.8 ft at these same two times.

At hour 58, which is 12 hours before landfall, the hurricane eye has moved up the continental slope. It is positioned right at the edge of the continental shelf at hour 59. During the previous 12 hours, the wind forerunner surge at Galveston rose from 2.7 ft to 4.9 ft NAVD88, an increase of 2.2 ft in only 12 hours. This elevation is slightly higher than the elevation for the 100-yr proxy storm, suggesting that the intensity difference is prevailing over the influence of a smaller size. This makes sense because the core winds are now moving onto the shelf. The eventual peak surge at Galveston Pleasure Pier for the 500-yr proxy storm, which is dictated by the winds on the shelf, is several feet higher for the 500-yr proxy storm than peak surge for the 100-y proxy storm. The water surface elevation of 4.9 ft for the 500-y proxy storm, 12 hours before landfall, reflects a 4.0-ft forerunner surge magnitude relative to mean sea level. As

was the case for the other proxy storms, the rate at which the water surface elevation is rising due to the surge forerunner is accelerating.

The simulated forerunner surge elevation for the 500-yr proxy storm also can be compared to the elevation suggested by the work of Liu and Irish (2017). For the 500-yr storm, which has a central pressure deficit of 113 mb and a radius-to-maximum-winds value of 22 nm (41 km) for most of its duration, results from the work by Liu and Irish (2017), which are shown in Figure 14-6, suggest a forerunner surge value of approximately 1.07 m (3.5 ft). The value of 4.0 ft from the present study is only slightly higher. The slightly higher value for the 500-yr proxy storm compared to the 100-yr proxy storm, as computed in this study, is quite consistent with the results of Lie and Irish (2017) which also show a same small difference, despite the large intensity difference.

As was the case for the 100-yr proxy storm, closure of the storm surge gates at least 24 hrs before landfall seems to be absolutely necessary, as does timing of the closure to coincide with low astronomical tide.

Simulated Hurricane Ike

Figure 14-10 shows the variation in water surface elevation with time for Hurricane Ike, as simulated by the storm surge model. Hurricane Ike had the following characteristics: 1) a minimum central pressure of between 968 and 946 mb as it transited the Gulf, having a value of about 950 mb for much of time while in the Gulf; a maximum surface wind speed that varied between 70 and 95 kts, a value of between 85 to 95 kts during most of its time in the Gulf, which corresponds to a Category 2 hurricane on the Saffir-Simpson wind scale; 2) an unusually large size, having considerable asymmetry in the wind field, with a large area of hurricane force winds on its right hand side, and having a radius-to-maximum-winds that varied from 26 nm to 72 nm; 3) a variable forward speed of 7 to 11 kts, 7 kts when it entered the Gulf and gradually increasing to 11 kts as the storm transited the shelf and approached landfall.

The hurricane's transit through the Gulf lasted 81 hours; starting at hour 971 of the simulation when it first entered the Gulf and ending at hour 1051 when it made landfall. The hurricane's eye crossed the seaward edge of the continental slope off the Texas shelf at hour 1024.5 and it crossed the seaward edge of the continental shelf at hour 1038.

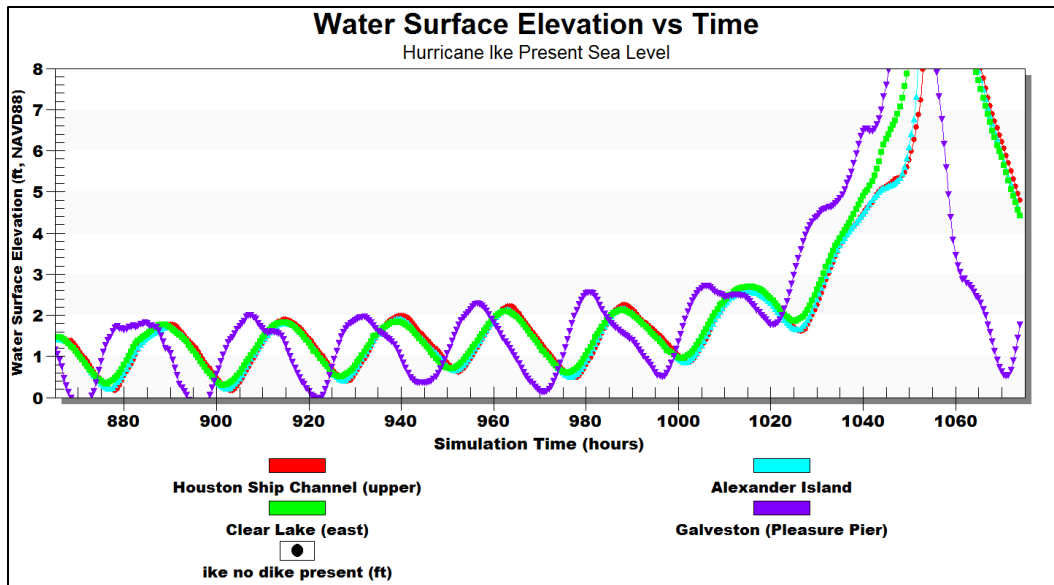


Figure 14-10. Water surface elevation changes with time associated with the wind-driven forerunner surge, both inside and outside Galveston Bay, for Hurricane Ike.

The Hurricane Ike storm surge simulation included the astronomical tide, unlike the proxy storm simulations which did not. The predominant diurnal tidal oscillations, having a period of 24 hours, are quite evident in Figure 14-10. The tide range was rather large when the hurricane occurred, a range of 2 to 2.5 ft.

Aside from the tidal fluctuations, a slow steady rise in water surface elevation is evident, which is caused by the wind-driven forerunner. As was the case for the proxy storms, the rate of water level rise due to the forerunner begins to rapidly accelerate once the eye approaches the seaward edge of the continental slope. In the case of Hurricane Ike that point in time occurs about 27 hours before landfall, at around hour 1024 of the simulation. At this point in time the water surface elevation appears to be about 2.4 ft NAVD88, about 1.5 ft above the mean sea level value of 0.9 ft NAVD88.

For the 24 hours before the eye reaches the continental slope, the acceleration in water level rise is quite evident, and it begins at around hour 1000. This time is approximately 48 hours before landfall (actual landfall is at hour 1051). The early acceleration in water level rise associated with the forerunner is attributed to the large asymmetric size of Ike, which produced higher winds on the Louisiana-Texas shelf, earlier in the storm, than would otherwise be expected for a smaller sized storm.

By the time the storm reaches the seaward edge of the continental shelf, at hour 1038, the wind-driven forerunner surge has reached a much higher elevation of approximately 5.7 ft NAVD88, 4.8 ft above mean sea level. This time corresponds approximately to a time that is 12 hours before landfall. The highest surge level associated with the forerunner is approximately 6.6 ft NAVD88, 5.7 ft above sea level, which occurs around hour 1040 or slightly later. The storm surge due to the hurricane's core winds occurs after this time, as the eye moves further onto the shelf and wind directions change from being directed alongshore to being directed onshore.

The simulated forerunner surge elevation for Hurricane Ike can be roughly compared to the elevation suggested by the work of Liu and Irish (2017). Assuming a representative central pressure deficit value of 60 mb, and a radius-to-maximum-winds value of 50 nm (92 km), a middle value based on quite variable observations of the observed radius-to-maximum winds, results from the work by Liu and Irish (2017) suggest a forerunner surge value of approximately 1.25 m (4.1 ft). The value of 4.8 ft from the present study is slightly higher, but similar.

Closure of the storm surge gates at the low astronomical tide event which occurs at hour 996 of the simulation, which is 55 hours (more than 2 days) prior to landfall, would have occurred when the water surface elevation at Galveston Pleasure Pier was 0.5 ft NAVD88, which is below the mean sea level value of 0.9 ft. Closure at around this time would minimize flood risk in Galveston Bay, by minimizing the water level inside the bay, which is about 1 ft NAVD88, nearly equal to mean sea level, at this same time. Note that at this time, the eye of Ike would have still been in the deep-water central region of the Gulf, when there would have been considerable uncertainty in its actual landfall location and time.

Closure of the gate 24 hours later, at hour 1020 of the simulation which corresponds to the next low tide event, would have occurred when the water surface elevation at Galveston Pleasure Pier was 1.8 ft NAVD88, 1.3 ft higher than the elevation at the previous low tide. The 24-hr delay in closure would lead to an increase in flood risk within the bays, by enabling the surge forerunner to grow and propagate relatively un-attenuated into the bays. This analysis does not consider the influence of the surge gate infrastructure that is built at Bolivar Roads, or at San Luis Pass, on tidal propagation into the bays. Any lag in time or change in tide characteristics

can in turn influence when gate closure achieves the desired minimum water surface elevation inside the bays. A lag in time between low tide on the open coast and low tide in Galveston Bay of approximately 5 hours is evident in Figure 14-10 without any surge gate system in place.

Observations of Forerunner Propagation into Galveston Bay during Hurricane Ike

Propagation of the wind-driven surge forerunner into Galveston Bay during Hurricane Ike was investigated using water surface elevation measurements that were made during the storm. Results from the Hurricane Ike model simulation suggested that there was little attenuation of the wind-driven forerunner through the passes and into the bays. Measured data were used to confirm the model results. The measured data also provide an opportunity to evaluate model accuracy in predicting the wind-driven forerunner for this hurricane event, which produced a very large forerunner surge.

Measured data, that were acquired and archived by NOAA, were examined for the seven locations shown in Figure 14-11. The choice of stations enables assessment of the propagation of the forerunner, and any attenuation it might undergo, as it enters Galveston Bay through Bolivar Roads, propagates within the Bay and then into the upper reaches of the Houston Ship Channel.



Figure 14-11. Stations where measured water surface elevation data were used to assess forerunner propagation into Galveston Bay during Hurricane Ike.

The series of Figures 14-12a through 14-12g show the time variation in water surface elevation at each of the seven gage sites. These graphs were generated using the NOAA Tides and Currents web site. The figures are shown in the order in which the forerunner propagates into the bay, starting with the Galveston Pleasure Pier site on the open coast, then the City of Galveston inside of Bolivar Roads, several sites along the western side of Galveston Bay from south to north, and eventually ending with the Manchester Houston site in the upper reaches of the Houston Ship Channel.

In all graphs, the predicted astronomical tide is shown as a blue curve. Measured water surface elevation data are either shown in green or red, green for verified data, red for preliminary data that have not been verified. Water surface elevation is displayed in feet, relative to mean sea level (MSL), which is the long term mean sea level for the gage site. Note, that the vertical elevation scales vary for some of the figures. In all graphs, the deviation between the measured water surface elevation (either verified or preliminary) and the predicted tide reflects some combination of the magnitude of the wind-driven forerunner as the hurricane transits the Gulf and the vertical offset between the seasonal mean sea level that was present at the time of the storm in September of 2008 and the long-term mean sea level at that gage site.

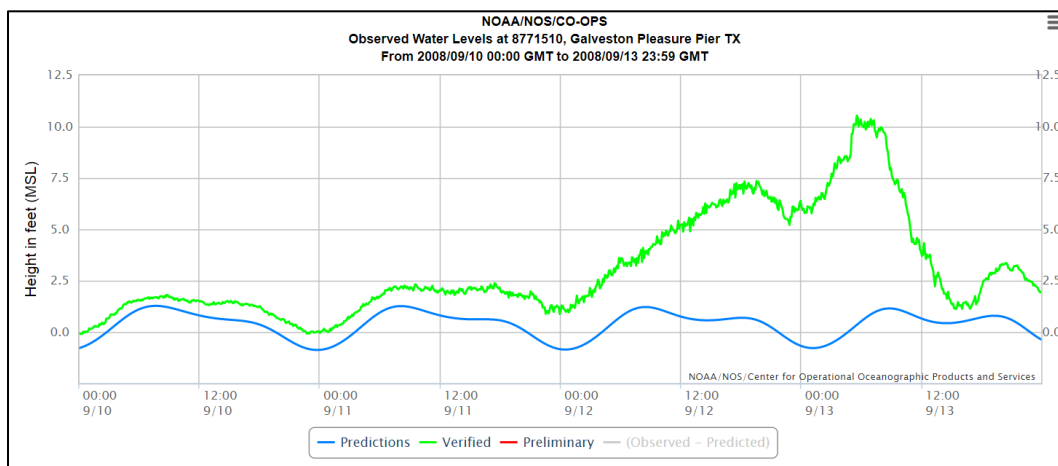


Figure 14-12a. Measured water surface elevation during Hurricane Ike, at the Galveston Pleasure Pier gaging station.

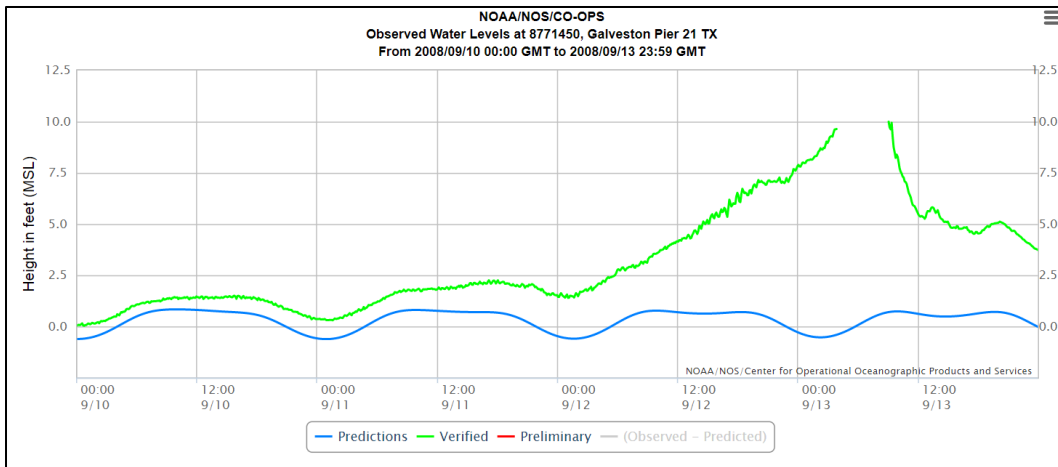


Figure 14-12b. Measured water surface elevation during Hurricane Ike, at the Galveston Pier 21 gaging station.

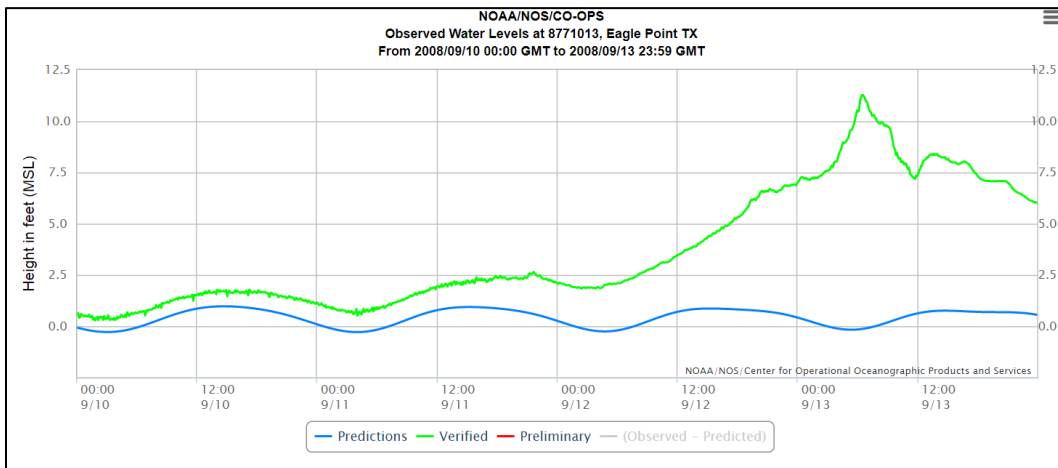


Figure 14-12c. Measured water surface elevation during Hurricane Ike, at the Eagle Point gaging station.

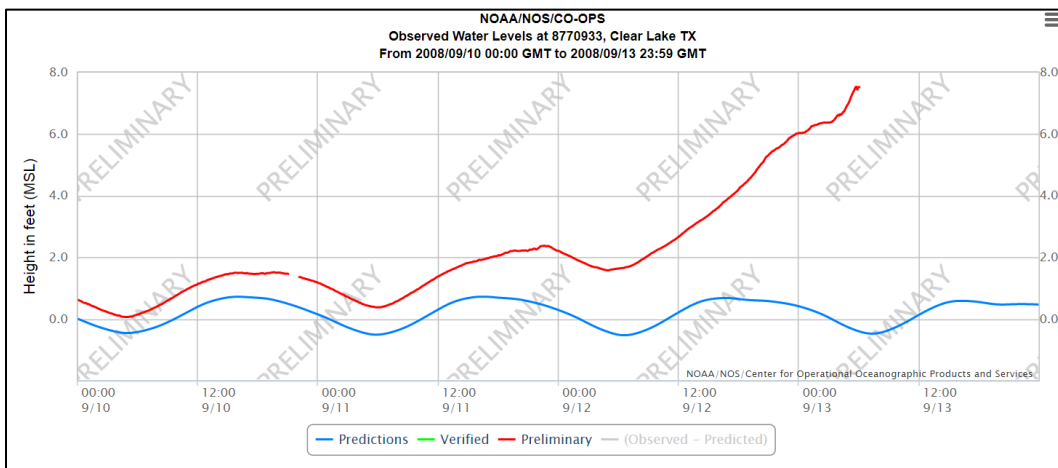


Figure 14-12d. Measured water surface elevation during Hurricane Ike, at the Clear Lake gaging station.

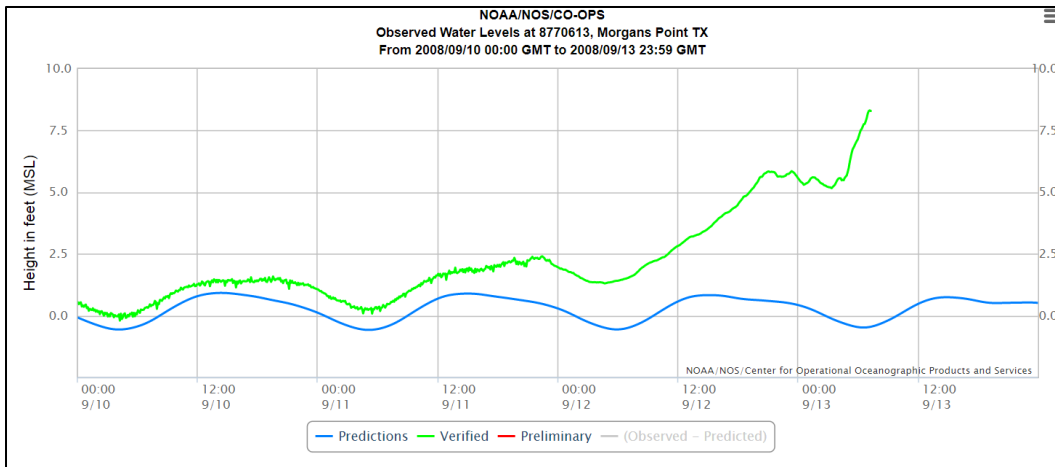


Figure 14-12e. Measured water surface elevation during Hurricane Ike, at the Morgan's Point gaging station.

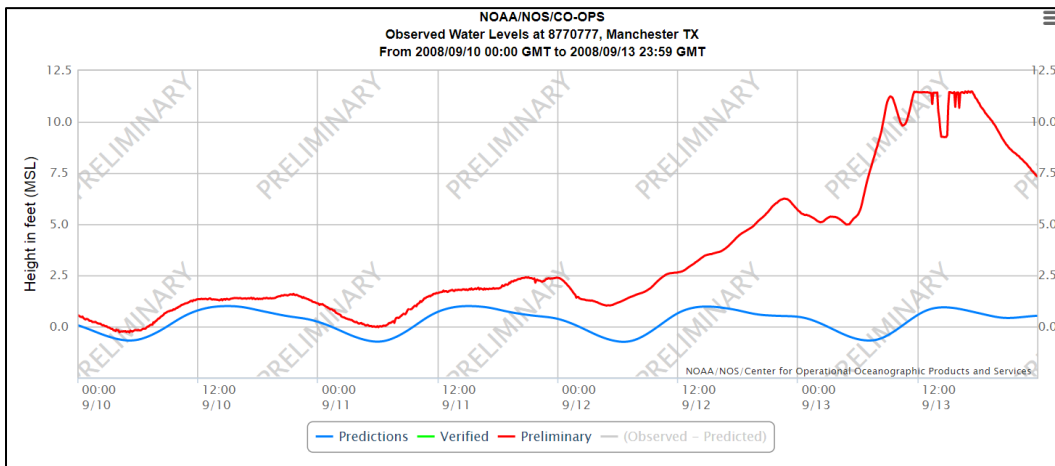


Figure 14-12f. Measured water surface elevation during Hurricane Ike, at the Manchester gaging station.

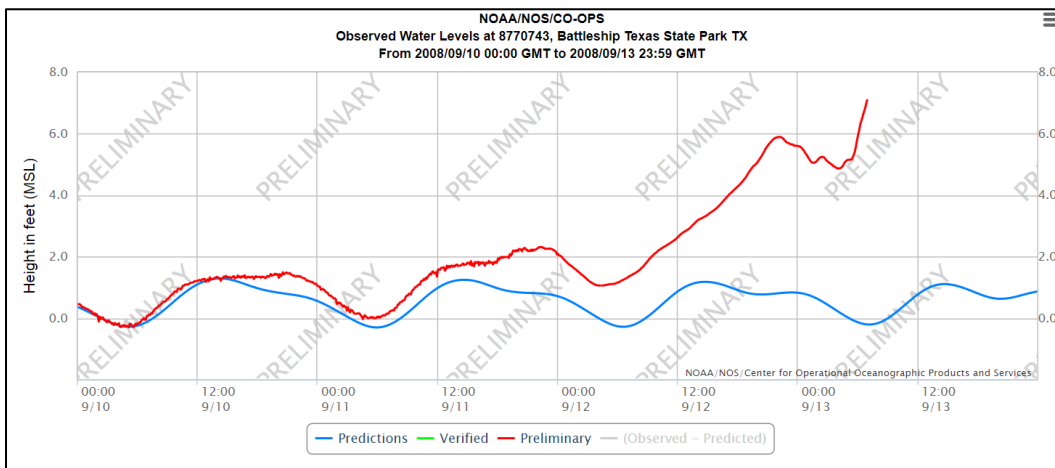


Figure 14-12g. Measured water surface elevation during Hurricane Ike, at the Battleship Texas State Park gaging station.

All graphs display the measured water surface elevation for the same period of time, September 10-13, 2008. In each graph, time is displayed on the horizontal axis relative to Greenwich Mean Time (GMT), which is ahead of Central Daylight Time, CDT, by 5 hours. For example, the eye of Hurricane Ike crossed the Texas coast at approximately 2:10 am CDT on the morning of September 13, which corresponds to 7:10 am GMT. Hurricane Ike passed over Cuba and entered the Gulf of Mexico at 4:00 pm CDT on September 9, which is 9:00 pm GMT on that same day.

The deviation in water surface elevation at hour 00 on September 10, just hours after the hurricane's eye entered the Gulf, is consistent for the first six gage locations, and it measures about 0.5 ft. The lack of a deviation at the Battleship Park gage (Figure 14-12g) is likely due to some type of a vertical datum issue. There is no physical explanation why the deviation at this gage location should differ significantly from the deviation at the other gages.

Both qualitatively and quantitatively, both the measured water surface elevation time series and the deviation between measured water surface elevation and predicted tide are quite similar at all of the gage sites. At hour 00 GMT on September 11, which is around the time of low astronomical tide and about 51 hours before landfall, the deviation is consistent for all the gages, approximately 0.6 to 0.7 ft (accounting for the datum discrepancy at the Battleship Park site). At hour 00 GMT on September 12, which is around the next time of low astronomical tide and about 27 hours before landfall, the deviation is again quite consistent for all the gages, approximately 2 ft. During the previous 24-hr period, the surge forerunner magnitude increased by 1.3 to 1.4 ft, nearly the same increase as the simulated value (1.3 ft) that was discussed in the previous report section.

The maximum water surface elevation associated with the wind driven forerunner ranges from about 6.0 to 7.2 ft MSL at all seven gage sites. The model results for Hurricane Ike indicate a maximum value of the forerunner surge to be 6.5 ft NAVD88 at the Galveston Pleasure Pier site, which after adjusting to a consistent vertical datum is about 6 ft relative to the long term mean sea level, or approximately 1 ft less than the measured maximum elevation value at the same site.

Approximate maximum elevation values associated with the wind-driven forerunner and tide, at each of the seven gage sites, are: 7.2, 7.2, 6.5, 6.0, 6.2, 6.3, 6.3 ft MSL. Values were estimated from the graphs. The consistency of peak values at all seven sites indicates that the wind-driven forerunner surge is relatively un-attenuated by the Bolivar Roads Pass or during its propagation through Galveston Bay and into the upper reaches of the Houston Ship channel. Values generally tend to decrease in the direction of forerunner propagation into and then through the bay. The peak values are also influenced to a degree by the local wind set-up that occurs in response to local winds within the bay, which likely influences some of the variability in peak values from site to site.

The measured forerunner peak at Galveston Pleasure Pier occurs at a time that is about 13 hours before landfall. The time lag between the times of maximum forerunner surge and landfall is very similar to the value of about 10 or 11 hours that is seen in the model results for Hurricane Ike. At other locations, the measured time lag ranges from 7 to 12 hours.

Volume Mode Forerunner – Modeling and Analysis Approach

Selection of the Storm Set

An initial set of model simulations was defined to first confirm the occurrence of the volume mode oscillation, or volume mode forerunner, identified by Bunpapong et al (1985), and then to examine its dependency on different hurricane characteristics. Results from the simulations were used to examine the volume mode oscillation's generation mechanism and general properties. They also were used to examine the dependency of the oscillation's characteristics, such as its period and amplitude, as a function of the hurricane's track, intensity, size and forward speed. Bunpapong et al (1985) examined the same types of dependencies and results from the present study are compared/contrasted to those from their study.

Four different tracks were developed to represent movement of a hurricane into the Gulf of Mexico, through either the Florida Straits or the Yucatan Straits, thereby triggering the volume mode oscillation. The tracks reflect paths of storms that are expected to have less dissipation in strength caused by interference with adjacent land masses, which is expected for those hurricanes that enter the Gulf in an intense state, such as Category 3, 4 and 5 storms on the Saffir-Simpson intensity scale. The four tracks considered in the present study are shown in Figure 14-13.

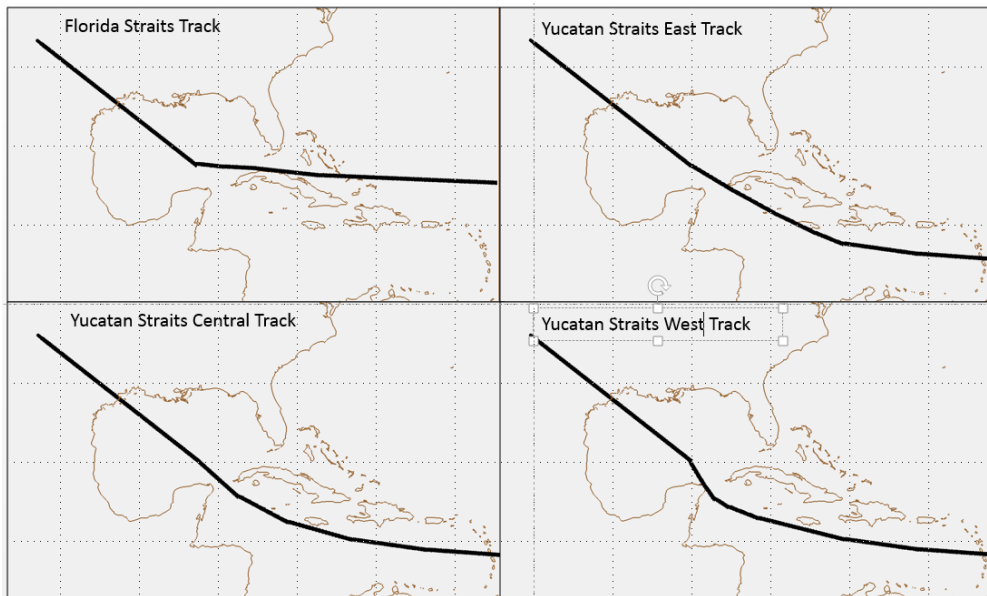


Figure 14-13. Hurricane tracks considered in the volume mode oscillation analysis.

The four tracks follow different paths leading up to entry into the Gulf and shortly after entry. However, following entry, all storms on all four tracks follow the same straight-line path as the storm moves toward the northwest through the central Gulf toward the Texas coast. All storms transit the continental slope and Texas shelf, make landfall at San Luis Pass, and continue inland toward the northwest on the identical path.

One of the tracks involved storm entry on the south side of the Florida Straits. Three tracks involved entry through the Yucatan Straits. The East and West Yucatan tracks were developed to examine the influence of hurricane winds on fluxes through the ports as a hurricane enters the Gulf, with winds on these two tracks either reinforcing or retarding water flux through the straits that is associated with what is believed to be the main driver of water flux, the atmospheric pressure gradients. Atmospheric pressure gradients in the general vicinity of the hurricane, which lead to formation of a dome of water beneath the hurricane's low pressure center which then propagates with the moving storm, are believed to be the primary driver of the water flux through the ports. Wind forcing is thought to be a lesser contributor. However wind influence was examined by having a track through the center of the Yucatan Straits, as well as paths that lie along either edge of the straits.

The full set of storms that were simulated are shown in Table 14-1. Storms are grouped by track.

Table 14-1. Storm Set Adopted for the Volume Oscillation Forerunner Analysis

Storm Track/Identifier Name	Central Pressure (mb)	Forward Speed (kts)	Radius-to-Maximum-Winds (nm)
Yucatan Straits - Central Track			
Central Yucatan Track Storm01	930	6	18
Central Yucatan Track Storm02	930	12	18
Central Yucatan Track Storm03	930	18	18
Central Yucatan Track Storm04	930	12	10
Central Yucatan Track Storm05	930	12	30
Central Yucatan Track Storm06	900	12	18
Yucatan Straits – East Track			
Eastern Yucatan Track Storm01	930	6	18
Eastern Yucatan Track Storm02	930	12	18
Eastern Yucatan Track Storm03	930	18	18
Yucatan Straits – West Track			
Western Yucatan Track Storm01	930	6	18
Western Yucatan Track Storm02	930	12	18
Western Yucatan Track Storm03	930	18	18
Florida Straits			
Florida Track Storm01	930	6	18
Florida Track Storm02	930	12	18
Florida Track Storm03	930	18	18
Florida Track Storm04	930	12	10
Florida Track Storm05	930	12	30
Florida Track Storm06	900	12	18

Six storms were simulated for the Central Yucatan track. The first three storms, 01, 02 and 03, were selected in order to examine the influence of storm forward speed on forerunner development. Forward speeds of 6, 12 and 18 kts, reflecting a typical range for Gulf of Mexico hurricanes, were adopted for this purpose; with storm intensity (reflected by the minimum central pressure) and storm size (reflected by the radius-to-maximum-winds) held constant for all three storms. Storm 02 (radius-to-maximum-winds value of 18 nm) and Storms 04 and 05 (radius to maximum winds values of 10 and 30 nm, respectively) were defined to examine the influence of storm size on volume mode forerunner development, with intensity and forward speed held constant. Size values that were considered also reflect a reasonable range for Gulf hurricanes. Storm 06 (minimum central pressure of 900 mb) was defined to compare with Storm 02 (minimum central pressure of 930 mb) to assess the influence of storm intensity on the volume oscillation characteristics. Both values reflect very intense hurricanes. The same set of six storms was simulated for the Florida Straits track to examine the same dependencies.

Only three storms were simulated for both the east and west Yucatan Straits tracks. They were defined to only examine the influence of forward speed.

For all simulations shown in Table 14-1, the peripheral surface atmospheric pressure was set to 1013 mb. Therefore, for the 930-mb storms, the maximum central pressure deficit, the difference between the minimum central pressure and the far-field pressure was 83 mb; and for the 900-mb storms, the pressure deficit was 113 mb. The storms considered by Bunpapong et al (1985) in their analysis of hypothetical hurricanes mostly had a constant pressure maximum pressure deficit of 80 mb. For all storms simulated in the present study, the Holland B parameter which controls the radial variation of pressure field was set to a constant, typical value of 1.27.

Isolation of the Volume Mode Oscillation

To isolate the volume mode forerunner from the wind-driven forerunner, the following modeling procedure was adopted. Some iteration was required to arrive at a satisfactory procedure. Once the storm entered the Gulf at full intensity either via the Yucatan or Florida Straits it was allowed to advance some distance into the Gulf, also at full intensity, in order to fully trigger the volume oscillation. Then, storm intensity was steadily

decreased by increasing the storm's central pressure until it was nearly equal to the peripheral pressure. The intensity decay occurred rather rapidly, over a duration of about 24 hours, and the intensity decay process ended while the storm center was still situated in the deep waters of the Gulf of Mexico. Concurrently, as the central pressure increased, wind speed was steadily decreased in magnitude to small values in both the storm's core and in the far field. Note that the hurricane wind model only allowed the central pressure to be raised to a value that was slightly less than the ambient far-field pressure value, but not exactly equal to it. This limitation had some bearing on the modeling approach.

The small wind speed values that resulted along the Texas and Louisiana shelves due to the small residual pressure difference in the hurricane wind model still generated a small wind-driven forerunner along the Texas coast which obfuscated the water surface elevation changes induced by the volume oscillation forerunner. To further eliminate the effect of wind and surface atmospheric pressure along the Louisiana and Texas shelves, a spatial mask was applied over these two shelf regions. Within the entire masking region, wind speeds were set to zero and atmospheric pressure was set to the far field value of 1013 mb. The wind/pressure masking was applied throughout the entire simulation duration.

Color-shaded contours in Figure 14-14 shows the maximum wind speed field for Storm 02 on the Central Yucatan track. The figure depicts maximum wind speed at each node of the storm surge model grid mesh, for the entire simulation, regardless of when the maximum wind speed occurred during the simulation. Core winds of the hurricane, having the highest wind speeds while at full intensity, are reflected by the yellow and orange colors. The yellow/orange trace reflects storm movement through the straits and into the Gulf while at full intensity. The region of intensity decay is evident in the central Gulf area where maximum wind speeds transition from yellow to orange to green to light blue in color, in the direction of storm advance along the storm track. The Florida Straits storms began their intensity decay slightly to the northwest of where the Yucatan Straits storms began their intensity decay.

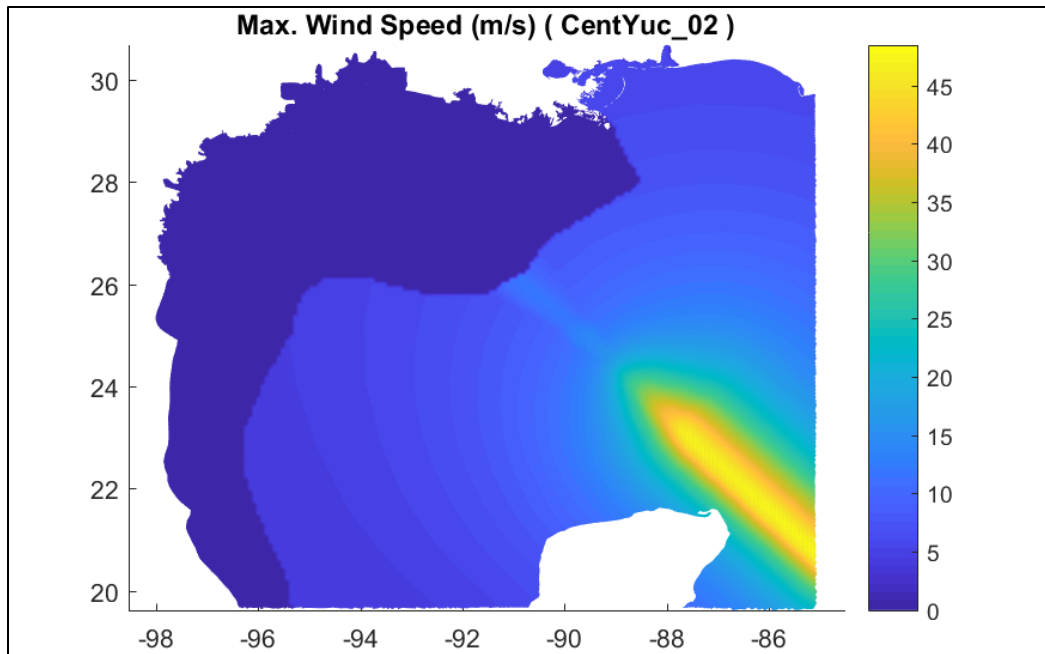


Figure 14-14. Maximum wind surface fields, including implementation of wind masking, for Central Yucatan Storm 02.

The wind/pressure masking region is shown by the darkest blue region in Figure 14-14, which lies along the Louisiana and Texas continental shelves and slopes, where wind speeds are set to zero and atmospheric pressures are set to ambient pressure throughout the entire storm simulation. The masking region begins just seaward of the outer edge of the continental slope and extends inland to the interior storm surge model boundary. The same masking region was applied for all storms.

Volume Mode Forerunner - Generation Mechanism

Water Fluxes Into/Out of the Gulf of Mexico

Analysis of Storm 01 on the Central Yucatan Track was performed to confirm the generation mechanism for the volume mode forerunner that was identified by Bunpapong et al (1985). This particular storm was similar to one of the hypothetical storms that they examined, HUR3, which had a track through the Yucatan Straits, landfall on the Texas coast, a maximum pressure deficit of 80 mb, a radius to maximum winds of 16 nm and a forward speed of 8 kt.

Bunpapong et al (1985) found that the volume oscillation, a Helmholtz-type oscillation in which the entire water surface within the entire Gulf rises and falls in unison, was triggered as a hurricane entered the Gulf. They found that the amplitude of the volume mode oscillation was closely related to the net water flux (i.e., flow rate, or water volume per unit time) that entered/exited the Gulf.

To facilitate analysis of water flux, transects were defined across both the Florida and Yucatan Straits. Transects at each of the straits are shown in Figure 14-15. Transects were defined to fully span the distance between adjacent land masses enabling accurate computation of the water flux that enters/leaves the Gulf of Mexico as a storm approaches and then enters the Gulf. Hourly values of water fluxes across both transects were computed using hourly velocity and water surface elevation fields computed by the storm surge model.

Figure 14-16 shows the variation with time of water flux through the Florida and Yucatan Straits, and the net flux, for Storm 01 on the Central Yucatan Track. The red curve shows flux through the Yucatan Straits, the green curve shows flux through the Florida Straits, and the blue curve shows the net flux. For the red curve (Yucatan Straits), positive values of flux reflect water flux into the Gulf, and negative values denote flux out of the Gulf. For the green curve (Florida Straits), positive values reflect water flux out of the Gulf, and negative values reflect flux into the Gulf.

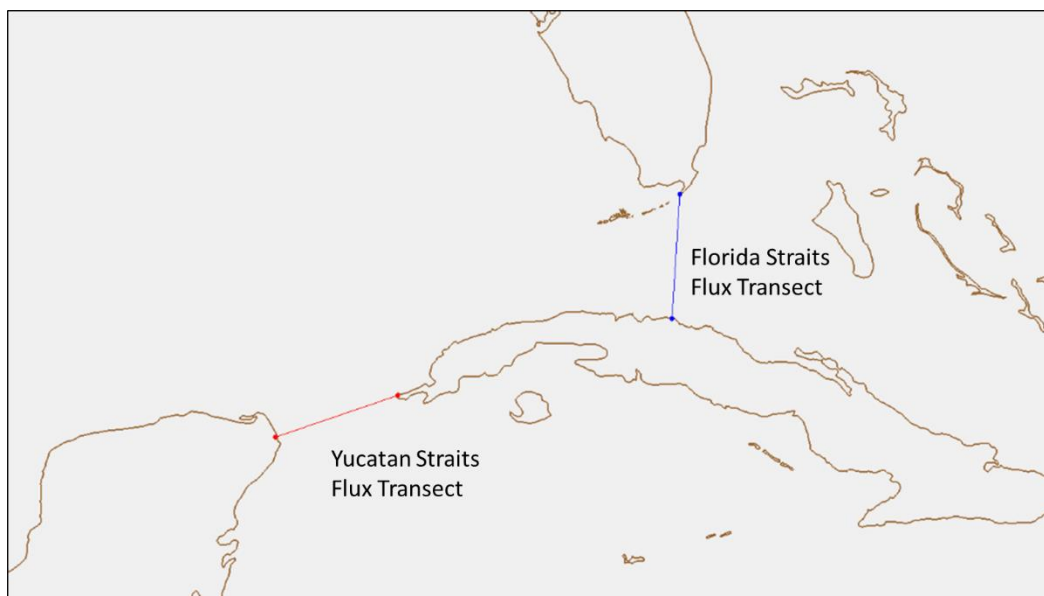


Figure 14-15. Transects for computing volume fluxes at the Florida and Yucatan Straits.

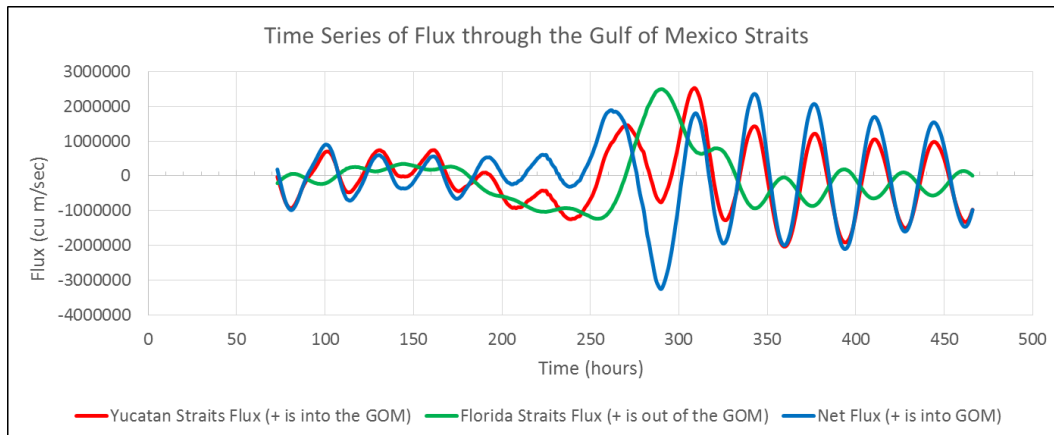


Figure 14-16. Fluxes through the Florida and Yucatan Straits, and the net flux into/out of the Gulf, for Storm 01 on the Central Yucatan track.

For the blue curve, the net water flux curve, positive values reflect net flux into the Gulf; whereas, negative values reflect net flux out of the Gulf. The horizontal axis in Figure 14-16 displays the hours of simulation time. The figure shows fluxes for most of the storm duration, excluding only the first 72 hours when the storm is situated far away from the Gulf.

The flux time series in Figure 14-16 display several notable features. One, the most obvious, is the cyclical nature of all three flux values. All three flux graphs display cyclical changes; and all three flux signals have a nearly constant period of oscillation. The eye of the hurricane passes through the Yucatan Straits, i.e., the eye crosses the flux transect and enters the Gulf, at hour 258. Prior to hour 240, all three flux graphs show regular oscillations, and for all three graphs the period of oscillation is approximately 29 to 32 hrs. After hour 300, when the hurricane is well into the Gulf, all three flux graphs again show regular oscillations, and for all three graphs the period of oscillation is approximately 33 to 35 hrs. Bunpapong et al (1985) found the period of the volume oscillation to be similar but slightly less, ranging from 28 to 30 hours, for tracks that also involved storm entry through the Yucatan Straits and landfall along the Texas coast.

A second feature that is evident in Figure 14-16 is the difference in amplitude of the flux oscillations before storm entry into the Gulf and those after storm entry. Prior to hour 258, the time of entry, the amplitude of the oscillatory variations in the flux is noticeably smaller than the amplitude of flux oscillation after entry. It appears as though the initial spin-up of the hurricane at the beginning of the model simulation excited a small volume oscillation, presumably an artifact from starting

the model at rest, initially. The flux oscillation triggered by hurricane entry into the Gulf, after hour 258, has a much greater amplitude (several times larger) than the initial oscillation.

A third feature is that both prior to and after entry the amplitude of oscillation is steadily damped, presumably due to bottom friction influence. However, in both cases damping takes place rather slowly during the six days both before and after entry. Bunpapong et al (1985) also found that the volume oscillation was damped with time.

Examination of the water fluxes leading up and during storm entry sheds light on the triggering of the volume oscillation. Beginning at around hour 180, and continuing through to the time of entry at hour 258 (a time span of approximately 3 days), water flux through the Yucatan Straits is persistently being drawn out of the Gulf toward the low pressure eye of the hurricane as the storm approaches the Gulf, but with some slight oscillation presumably due to the initial model start-up. During this same period of time, water flux through the Florida Straits begins to enter the Gulf on a persistent basis, presumably due to water in the southeastern Gulf being drawn out through the Yucatan Straits, and also with some oscillation from the initial model start-up. During this same time period, the net flux entering/leaving the Gulf is oscillating about a small positive mean value (i.e. net flux into the Gulf). Shortly before entry, at around hour 250, the water flux continues to enter the Gulf through the Florida Straits; however, flux at the Yucatan Straits begins to change direction and enter the Gulf. Right around the time of entry, hour 258, the net flux into the Gulf reaches a local (in time) maximum value.

Shortly after entry, net flux through the Florida Straits begins to persistently leave the Gulf, presumably due to water surface elevation gradients associated with arrival of the hurricane eye into the Gulf along with its underlying dome of water. A larger-amplitude oscillation in the net flux commences through the Yucatan Straits, with a smaller oscillatory flux through the Florida Straits, as the volume oscillation is triggered following storm entry.

Water Surface Elevation and Velocity Patterns Associated with the Moving Hurricane

Figures 14-17 through 14-19 shed additional light on the dynamics that cause the observed trends in water flux through the straits. Each of the three figures represents a snap-shot taken at a different time in the simulation. Each figure has two panels: the top panel shows the water surface elevation field at one snap-shot in time; and the lower panel shows the velocity field in black vectors and the flux per unit width (depth-averaged current speed multiplied by the total water depth) field at the same time. The two flux transects are shown in both panels as thin black line segments.

Figure 14-17 shows model results for hour 220, which is 38 hours before the time of storm entry into the Gulf. At hour 220, flux is persistently directed into the Gulf through the Florida Straits and directed out of the Gulf through the Yucatan Straits (also see Figure 14-16). The upper panel, which reflects the water surface elevation field displayed as color shaded contours, clearly shows the circular dome of water beneath the eye of the hurricane, with the orange color denoting the highest water surface elevations.

The dome is formed by water that has been drawn there from surrounding areas by gradients in atmospheric pressure, which is called the inverted barometer effect. Water is steadily being drawn toward the eye as the hurricane moves along its path. At this time in the simulation, water is being pulled out of the Gulf through the Yucatan Straits toward the eye in response to the atmospheric pressure gradients which tend to drive this direction of water movement. In response to the atmospheric and water surface gradients that develop inside the Gulf, water is being drawn into the Gulf through the Florida Straits. The eye of the hurricane is close enough to the straits to force this predominant flux pattern at both straits.

The flux pattern at both straits is illustrated in the lower panel of Figure 14-17. The lower panels show depth-averaged velocity vectors, indicating the direction of water movement and water flux, as black arrows. The magnitude of flux per unit width is shown as color shaded contours.

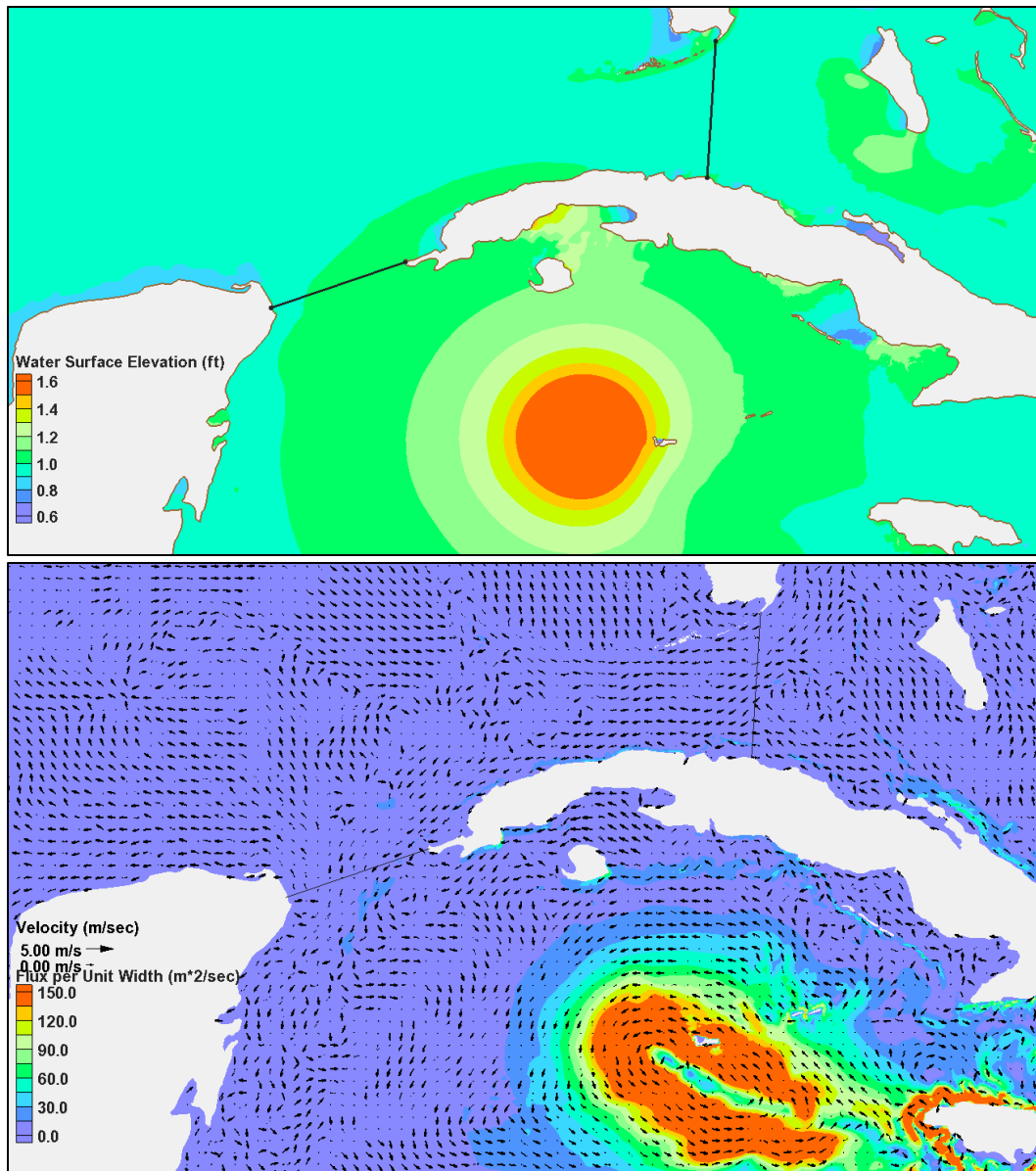


Figure 14-17. Water surface elevation field (top panel) and velocity vectors/flux per unit width field (bottom panel) for Storm 01 on the Central Yucatan track at hour 220.

Figure 14-18 shows conditions at hour 258, the time when the eye is at the Yucatan Straits and entering the Gulf. The position of the eye is reflected by the position of the dome of water beneath it, as seen in the top panel. Again, as seen in the bottom panel, water flux is being drawn into the Gulf through the Florida Straits, and it is being drawn toward the eye of the hurricane. The flux pattern at the Yucatan Straits is complex, with flux directed both into and out of the Gulf on opposite sides of the eye and on opposite sides of the flux transect. The opposing flux contributions are beginning to negate each other, and flux is transitioning from being

directed out of the Gulf to flux being directed into the Gulf, as water is being drawn toward the moving eye. A highly complex pattern of flux per unit width is seen in the wake of the hurricane, a complexity also seen by Bunpapong et al (1985).

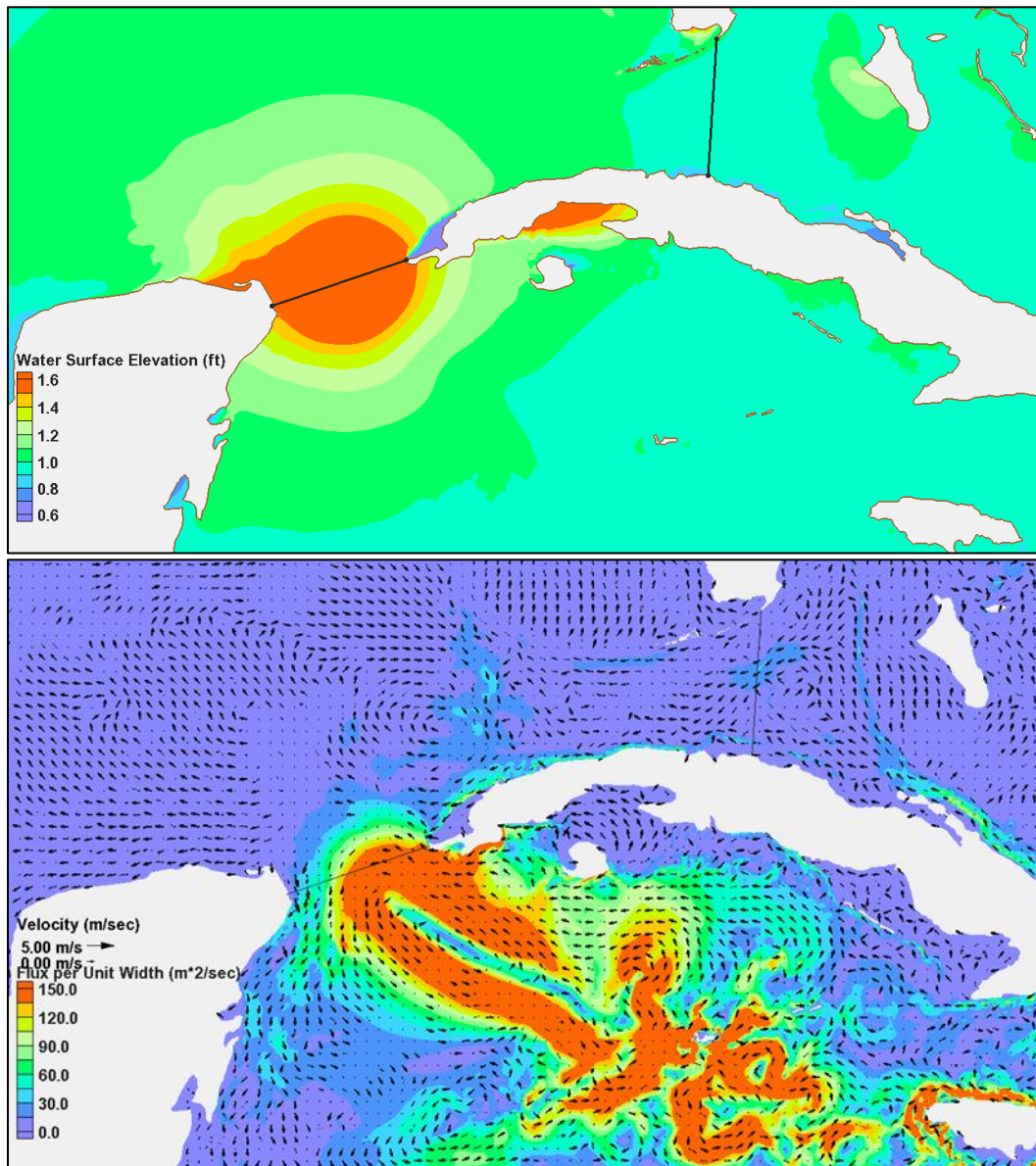


Figure 14-18. Water surface elevation field (top panel) and velocity vectors/flux per unit width field (bottom panel) for Storm 01 on the Central Yucatan track at hour 258.

Figure 14-19 shows conditions at hour 271, 13 hours after the hurricane eye entered the Gulf. Entry has triggered the volume oscillation. At this time, the net flux, which is directed into the Gulf, has already reached its greatest value and is beginning to decrease (see the blue curve in Figure 14-16).

Also at this time, flux through the Florida Straits is starting to change direction in response to the volume oscillation that has been excited and by the water surface elevation gradients that arise from the fact that the dome of water is now situated inside the Gulf.

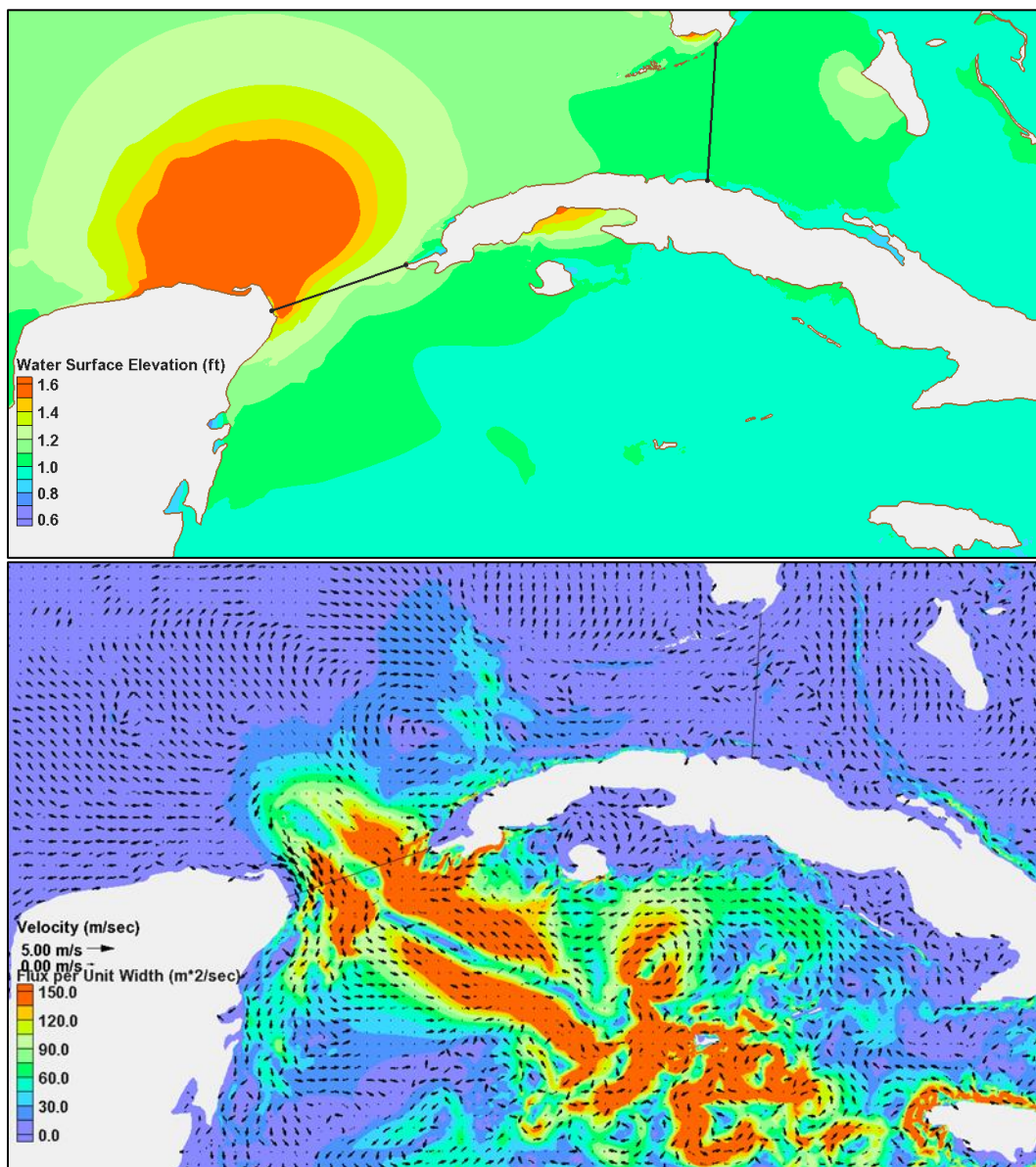


Figure 14-19. Water surface elevation field (top panel) and velocity vectors/flux per unit width field (bottom panel) for Storm 01 on the Central Yucatan track at hour 271.

Instead of water flux being drawn into the Gulf, flux is beginning to change direction and be directed out of the Gulf as part of the volume mode oscillation (see the lower panel in the figure). At the Yucatan Straits, flux is moving both into and out of the Gulf, on opposite sides of the straits. But in an average sense, at this time and from this point onward, generation of the volume oscillation begins to dominate the fluxes at both the Yucatan and Florida Straits; and fluxes at both straits become oscillatory in nature.

Water Surface Elevation Changes Induced by the Volume Oscillation

Bunpapong et al (1985) found that the entire Gulf responds very quickly to excitation of the volume mode oscillation, a Helmholtz-type oscillation in which the water surface throughout the Gulf oscillates vertically up and down in unison. This can be seen best by examining the temporal variation of water surface elevation at various locations within the Gulf. Water surface elevation results are presented below for nine model output locations, which are shown in Figure 14-20.



Figure 14-20. Locations of model output to examine water surface elevation changes associated with the volume mode oscillation.

All of the observation points shown in Figure 14-20 are located within the wind/pressure masking region that was applied to the western Gulf (see Figure 14-14). Inside the masking region there are no hurricane-related atmospheric pressure gradients, and there are no non-zero wind speeds, both of which would tend to induce changes in the water surface elevation. Therefore, selecting output locations within the masking region should help isolate the influence of the volume mode oscillation.

Volume Oscillation at Deep Water Locations

Five of the nine output points shown in Figure 14-20 are located in deep water. Four are in very deep water, with corresponding water depths of several thousand meters; and all of them they are situated either over the continental slope or near its seaward edge. The fifth deep-water point lies at the edge of the continental shelf directly off the Texas coast. Both of the deep-water points titled “Track Points” lie on that portion of the storm track that was common to all the simulated storms as they transited the continental slope and shelf and eventually made landfall at San Luis Pass.

Figure 14-15 shows the water surface elevation as a function of time for all five deep-water output locations. Results confirm the presence of the volume mode oscillation and the Helmholtz-type nature of the oscillation, in which the surface of the entire Gulf oscillates up and down in unison.

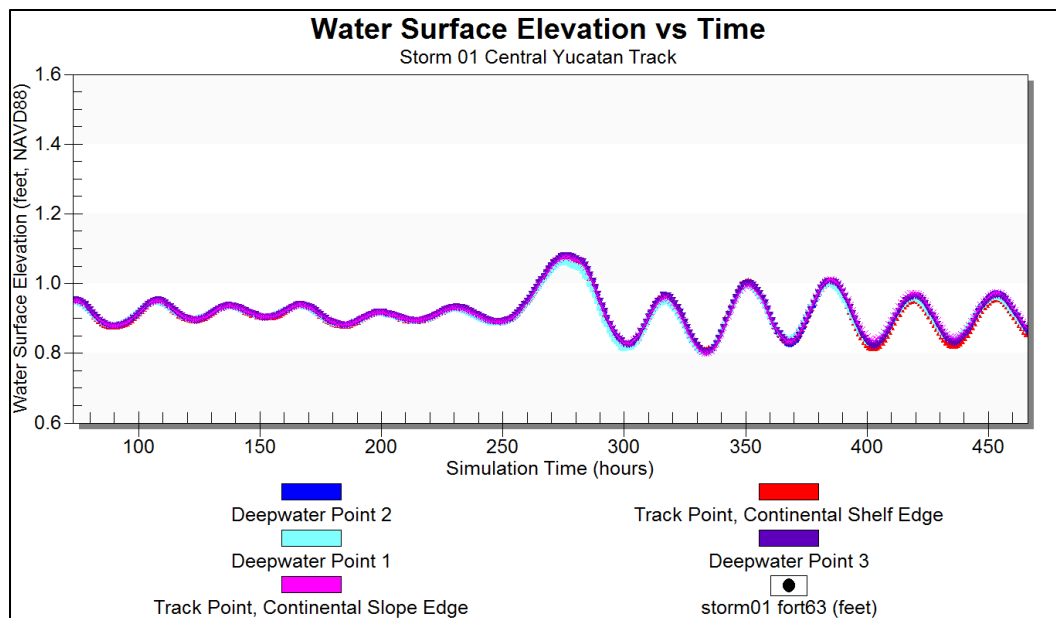


Figure 14-15. Water surface elevation as a function of time for the five deep-water output locations, for Storm 01 Central Yucatan Track.

The points, which are widely spread throughout the entire western Gulf, all show the same cyclical elevation variation, with no significant phase or amplitude difference from location to location. The Helmholtz mode oscillation throughout the Gulf is apparent before storm entry at hour 258 of the simulation, presumably caused by the initial start-up. The volume oscillation is more pronounced after entry. The average period of elevation oscillations following storm entry, is between 33 and 34 hrs, which is slightly greater than the periods found by Bunpapong et al (1985), which were 28 to 30 hr.

The first peak in the elevation oscillation following storm entry occurs at hour 280, 22 hours after the time of entry. This lag time is similar to the value of 24 hrs found by Bunpapong et al (1985) for a storm they examined, HUR3, which had a similar intensity, size and forward speed, also entered through the Yucatan Straits, and also made landfall on the Texas coast. They observed some dependence of the lag time on forward speed, based on their full set of simulations.

Storm 01 on the Central Yucatan track, with its constant forward speed and on the specified track, would make landfall approximately 114 hours after entering, i.e., landfall at hour 372. As seen in Figure 14-15, hour 372 corresponds to the time of an elevation trough following the third peak. Several elevation oscillations occur while the storm transits the Gulf. Of course, any deviations from the specified track, or changes in forward speed, after the storm enters the Gulf would influence the timing of the oscillation peaks/troughs with the time of landfall.

The elevation anomaly that is associated with the first peak following storm entry is noticeably higher than subsequent oscillation peaks. Each of the storm simulations comprising the initial storm set was made using present-day mean sea level as the initial water level in the surge model. Present-day sea level corresponds to a water surface elevation of 0.91 ft NAVD88. The elevation of the first peak, relative to this “mean” level, is approximately 0.2 ft. Subsequent peaks had smaller maximum elevation values, approximately 0.1 ft, relative to mean sea level.

Confirmation for the Volume Oscillation's Generation Mechanism

To further confirm the causation mechanism for the volume mode oscillation, a calculation was made to examine the relationship between net flux into/out of the Gulf and water surface elevation changes inside the Gulf. First, the computed change in net water flux entering/leaving the Gulf through both transects was computed at 1-hr time increments, using hourly values of computed water flux passing both transects. Second, the net water flux value at each hourly time increment was divided by the surface area of the entire Gulf of Mexico (that area which is contained inside of the transects), and then multiplied by the time increment of one hour, to calculate hourly values of the change in water surface elevation based solely upon the change in net water flux. Third, beginning with the initial water surface elevation value for the simulation, the change in water surface elevation at each hourly increment was added to the elevation at the previous time increment to compute an updated water surface elevation. This calculation was repeated for each hourly time increment, for the entire simulation duration. In other words, a time series of water surface elevation was computed based solely upon the net water flux entering/leaving the Gulf and the assumption that the water surface elevation within the Gulf rose and fell in unison in response to changes in the net water flux, i.e., simple conservation of water mass within the Gulf.

The water surface elevation time series computed based on flux through the transects was then compared to the simulated water surface elevation time series at the deep-water point on the edge of the continental shelf off the Texas coast (see its location in Figure 14-14). The comparison was done to see if the water surface elevation changes inside and throughout the Gulf (at all the deep water points shown in Figure 14-15) could be explained simply by the conservation of water mass that enters/leaves the Gulf through the Florida and Yucatan Straits. Figure 14-16 shows the results of this comparison. Note that water surface elevation is graphed in metric, not English, units.

The similarity in both sets of results shows, and confirms, that the volume mode oscillation is directly related to the net water flux that enters/leaves the Gulf. Much of the computed water surface elevation change signal can be explained simply by the net water flux through the transects, the principle of conservation of water mass within the Gulf, and the assumption that the water surface of the Gulf moves up and down in unison in response to changes in the net flux.

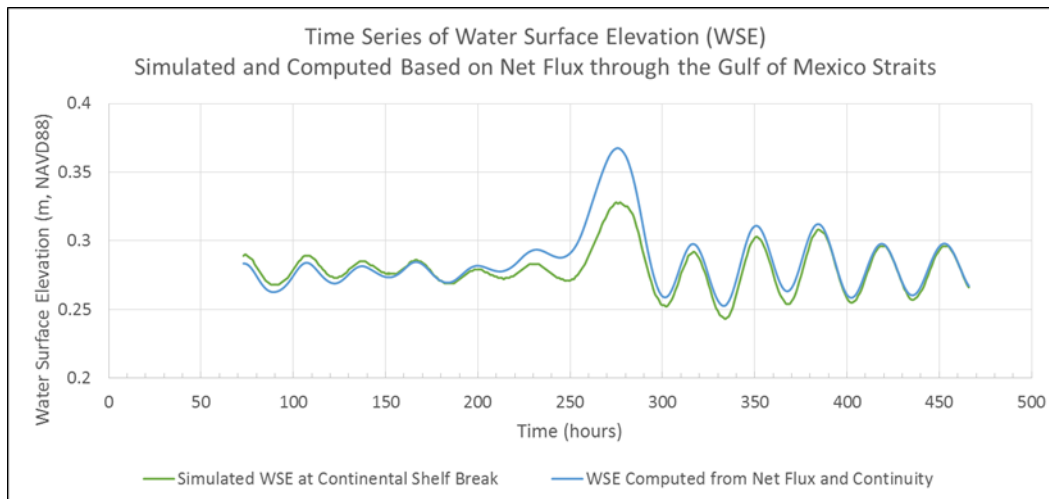


Figure 14-16. Comparison of water surface elevation response computed using net water flux and conservation of mass with the simulated free surface elevation response inside the Gulf.

The higher simulated elevation at around hour 275, seen in both Figures 14-16 and 14-15, that is associated with the first cycle of the volume oscillation is consistent with the higher elevation computed based on the net water flux entering the Gulf. The difference between the two curves at this time is attributed to the additional role of atmospheric pressure gradients that draw water from surrounding areas, through both transects, toward the eye, and the proximity of the eye near the transects at this time of the simulation (recall that storm entry into the Gulf occurred at hour 258). The agreement between simulated water surface elevation and elevation computed using only the net flux is particularly close for all prior and subsequent cycles of the volume oscillation, when the hurricane eye is further away from the transects.

Volume Oscillation at Shallow Water Locations

Four of the nine model output locations shown in Figure 14-14 are located along the north Texas coast in very shallow water, just seaward of several entrances to bays that are situated along the Texas coast. One of the output locations is the Galveston Pleasure Pier, near Bolivar Roads; and it is representative of open coast conditions in the Houston-Galveston region. Other coastal points are located either north or south of the Houston-Galveston area, Sabine Pass (north), Freeport (south), and Port O'Connor (south). Figure 14-17 shows the water surface elevation as a function of time for these four output locations. Results for the deep-water point at the edge of the Texas continental shelf (the red curve) are shown as well, for reference.

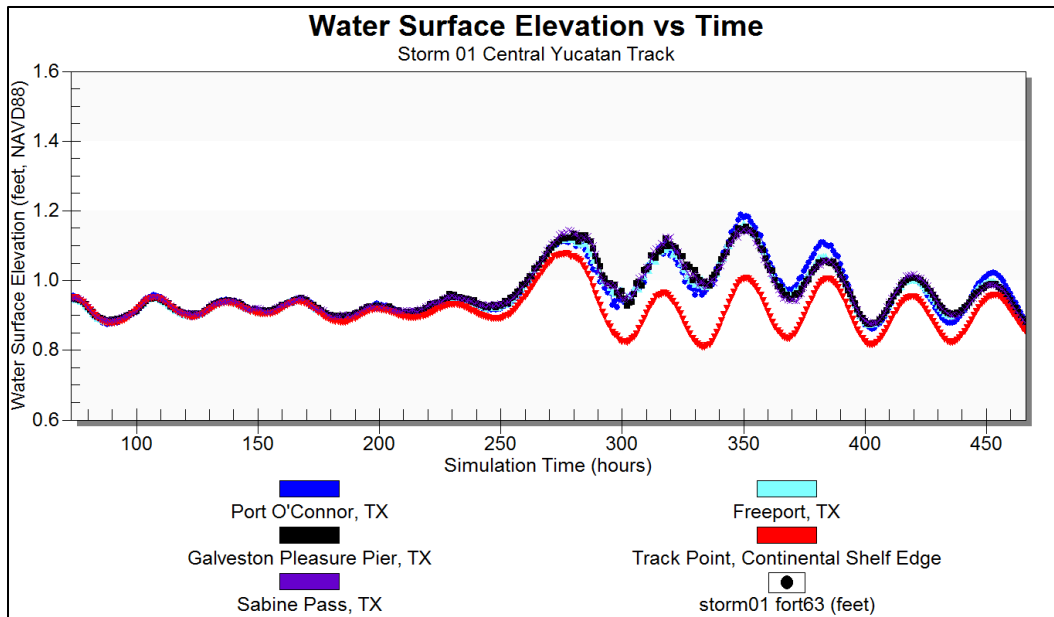


Figure 14-17. Water surface elevation as a function of time for the four shallow water output locations, for Storm 01 Central Yucatan Track.

Following entry of the hurricane into the Gulf, peak elevation values at the shallow water locations are consistently greater than values in deep water. There appears to be somewhat of an elevation offset, deviation or anomaly, between the oscillations in deep water and those in shallow water at the coastline. Deviations between shallow and deep water points are greatest for the second and third peaks, less for the first and fourth peaks and less for the fifth and sixth peaks. Recall that eye would have made landfall, aside from wind and pressure masking, at around hour 372. These results suggest that a longer-period oscillation or some other shallow water dynamic might be present, in addition to the 33 to 34-hr volume mode oscillation.

The water surface elevations corresponding to the first three peaks of the oscillation are of comparable magnitude, approximately 0.25 ft above the mean sea level. The third peak is the highest, albeit by a small amount compared to the previous two. The amplitudes of the peaks, relative to the mean sea level, appear to decay with time after hour 350. Bunpamong et al (1985) also observed a slow decay in the amplitude of the volume oscillation.

The maximum elevation anomaly at the shallow water sites, 0.25 ft, is significantly smaller than the 0.7 ft volume oscillation amplitude value in shallow water found by Bunpamong et al (1985) for the similar storm,

HUR3. A possible reason for the discrepancy in magnitude of the volume oscillation is discussed later in this chapter.

Examination of the Shallow Water Anomaly – Far-Field Influence of the Wind-Driven Forerunner

An explanation for the vertical elevation offset in shallow water, i.e., the elevation anomaly that exists along with the pure volume oscillation, was examined further. The magnitude of the elevation anomaly is small; however, an understanding of its generation is worthwhile because it is related to the same physical processes that lead to a wind-driven surge forerunner. An analysis was done utilizing a series of snap shots, in time, of the water surface elevation field for the entire Gulf of Mexico. The first few snap shots shown below reflect conditions prior to and at the time of storm entry into the Gulf. Subsequent snap-shots show water surface elevation fields at times which correspond to the water surface elevation peak and trough for each of the first four cycles of the volume oscillation.

Figure 14-18 shows the water surface elevation field that exists 48 hours prior to the time of storm entry into the Gulf. The snap-shot corresponds to hour 210 of the simulation in Figure 14-17. The figure clearly shows the dome of water beneath the eye of the hurricane, which sits southeast of the Yucatan Straits. Within the Gulf, the water surface is rather uniform in elevation, which is consistent with the small Helmholtz oscillation that existed prior to storm entry, an artifact of the initial model spin-up. There are no significant elevation anomalies evident on the continental shelf off the Texas coast or on any other continental shelf region in the Gulf.

Figure 14-19 shows the water surface elevation field 24 hours prior to the time of storm entry into the Gulf. The snap-shot corresponds to hour 234. Again, the figure shows the dome of water beneath the eye of the hurricane, which has now moved closer to the Yucatan Straits transect. Within the Gulf, the water surface field is rather uniform in elevation except for the emergence of a small elevation anomaly along the Florida, Alabama and Mississippi continental shelves. There are no significant elevation anomalies evident along the Texas shelf or any other continental shelf region in the western Gulf.

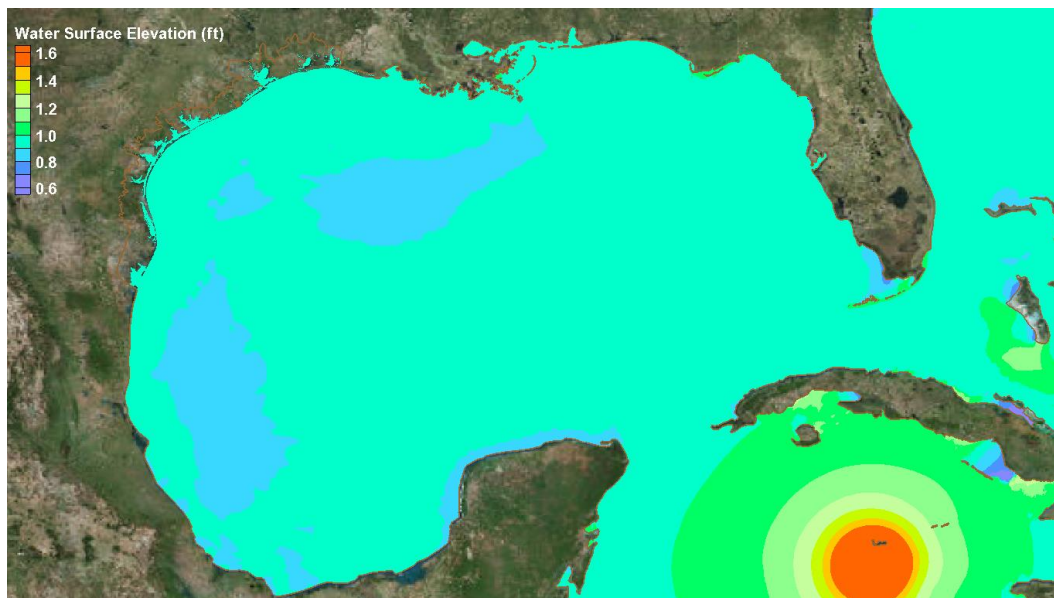


Figure 14-18. Water surface elevation field at hour 210, 48 hours before storm entry, for Storm 01 on the Central Yucatan Track.

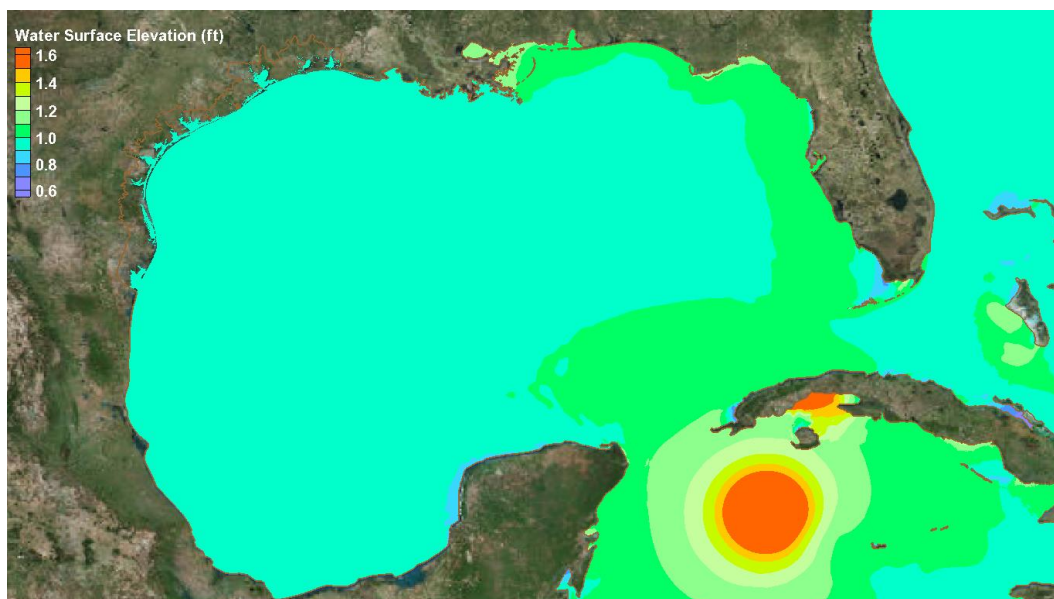


Figure 14-19. Water surface elevation field at hour 234, 24 hours before storm entry, for Storm 01 on the Central Yucatan Track.

Figure 14-20 shows the water surface elevation field at the time of storm entry into the Gulf, hour 258. Within the Gulf, the water surface elevation field is rather uniform except in the vicinity of the hurricane (which is due to atmospheric pressure gradients) and except for the further development of the elevation anomaly along the Florida, Alabama and Mississippi continental shelves.

Recall that the wind/pressure mask is not applied to atmospheric forcing in the eastern Gulf, or along the continental shelves of Florida, Alabama and Mississippi. The counterclockwise circulating winds about the eye promote along-the-shelf and alongshore water movement through these shelf regions of the eastern Gulf. The elevation anomaly has the appearance of an Ekman set-up, with higher elevations at the coastline and lower elevations at the shelf break and beyond in deep water. The Ekman set-up is produced by water moving along the shelf, which is turned to the right in the northern hemisphere by the Coriolis force, and stacked against the coastline. Because of the very wide continental shelf off the Florida Gulf coast, this region is very susceptible to formation of Ekman set-up for winds that blow along the shelf toward the north. Interestingly, the appearance of a small Ekman set-up was evident on these same areas, as seen in Figure 14-19, even before the eye enters the Gulf.

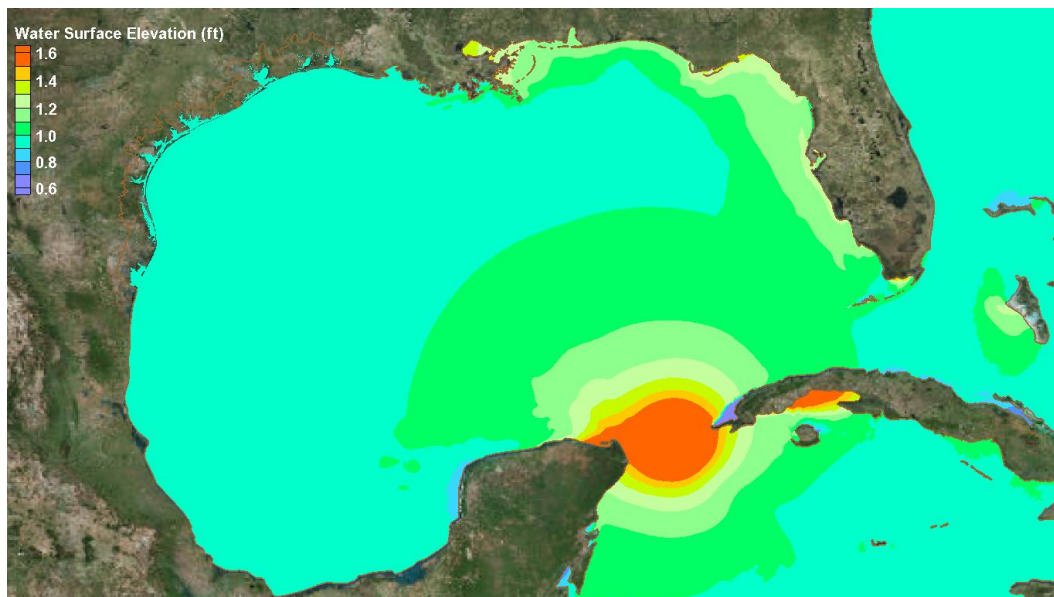


Figure 14-20. Water surface elevation field at hour 258, the time of storm entry, for Storm 01 on the Central Yucatan Track.

In addition to causing an Ekman set-up, water moving northward along the Florida shelf will stack up in Apalachee Bay, Florida, which lies east of Apalachicola. Water movement along the northern Gulf shelf adjacent to Alabama and Mississippi will stack up against the Mississippi River Bird's Foot delta, resulting in accumulation within Lake Pontchartrain. Each of these processes, and their influence on water and water surface elevation, are evident in the figure.

In Figure 14-20 there also is evidence of water movement around the Bird's Foot delta toward the west; however, there is no noticeable elevation anomaly along the Louisiana or Texas shelves at this point in time.

Figure 14-21 shows the water surface elevation field at hour 278 of the simulation, which corresponds to the peak elevation that is associated with the first volume oscillation. The intensity of the storm is still near full strength, so the dome of water beneath the low pressure center is still present as is wind forcing along the shelf regions of the eastern Gulf. Intensity decay is just beginning. Within the Gulf, further development of the elevation anomaly along the Florida, Alabama and Mississippi continental shelves is evident. The elevation anomaly continues to have the appearance of an Ekman set-up, with higher elevations at the coastline and lower elevations at the shelf break. Clear evidence persists for water

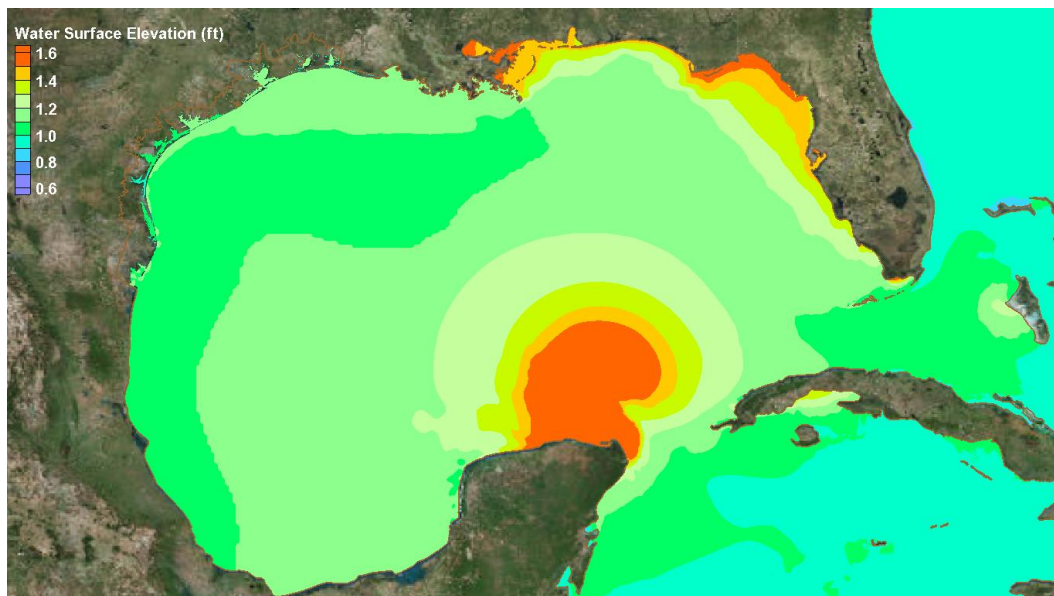


Figure 14-21. Water surface elevation field at hour 278, the time of the first elevation peak, for Storm 01 on the Central Yucatan Track.

moving northward along the Florida shelf and stacking up in Apalachee Bay, as well as water movement along the northern Gulf shelf adjacent to Alabama and Mississippi and stacking of that water against the Mississippi River Bird's Foot delta with accumulation in in Lake Pontchartrain and Lake Borgne. There is also evidence of water movement around the Bird's Foot delta toward the west, the first appearance of the elevation anomaly in shallow water on both the Louisiana and north Texas shelves.

Figure 14-22 shows the water surface elevation field at hour 301 of the simulation, the time of the elevation trough which is associated with the first volume oscillation. The intensity of the storm has diminished significantly by this time, and only remnants of the dome of water beneath the eye are evident in the center of the Gulf. Forcing of the Ekman setup along the Florida, Alabama and Mississippi continental shelves by the wind has decreased.

The elevation anomaly along the shelf regions of the northern Gulf continues to exhibit the appearance of an Ekman set-up, which is confined to the continental shelf. Wind and pressure forcing along the Louisiana and Texas shelves has been zeroed out since the beginning of the simulation. However, a shallow water elevation anomaly is evident along the Louisiana and Texas shelves. This is evidence for propagation of the

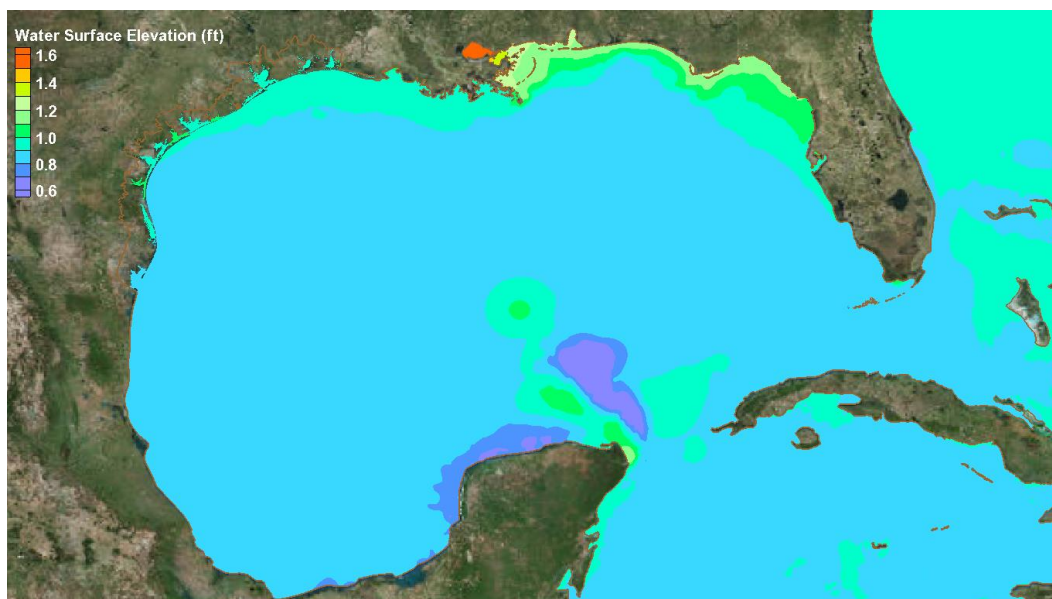


Figure 14-22. Water surface elevation field at hour 301, the time of the first elevation trough, for Storm 01 on the Central Yucatan Track.

Ekman set-up as a free wave toward the west along both the Louisiana and north Texas shelves. The Ekman set-up that was forced on the shelf regions of the eastern Gulf, propagates as a free wave from east to west, along the shelf once forcing is diminished or ceases. The magnitude of the Ekman setup is clearly decreasing in the eastern half of the Gulf due to cessation of the wind forcing. Also, there is emerging evidence of a southward movement of the Ekman set-up wave, as a free wave, along the narrower south Texas shelf, as the elevation anomaly increases in this region.

Throughout the rest of the Gulf, the water surface elevation is rather uniform as is expected for a pure Helmholtz oscillation.

Figures 14-23 and 14-24 show Gulf-wide water surface elevation fields at the times of both peak and trough, respectively, which are associated with the second volume oscillation. During both of these times there is no longer any wind forcing of the Ekman set-up; it is propagating as a free wave in the counterclockwise direction along the continental shelf regions of the northern Gulf. The elevation anomaly associated with the propagation of this free wave continues to be constrained to the continental shelf. Water surface elevations throughout the rest of the Gulf are rather uniform during both snap-shots, consistent with the Helmholtz mode of oscillation.

The magnitude of the elevation anomaly has decreased significantly along the Florida shelf as the Ekman setup wave propagates out of this region. The magnitude of the anomaly also is decreasing along the Alabama and Mississippi shelves, east of the Bird's Foot delta, for the same reason. West of the delta, the elevation anomaly persists along the Louisiana and Texas shelves. There is more evidence of southward propagation of the free wave along the southernmost Texas shelf, in the form of an increasing magnitude of the elevation anomaly there. In prior snap-shots, the elevation anomaly had not appeared this far south.

Figures 14-25 and 14-26 show the water surface elevation field at times corresponding to the elevation peak and trough, respectively, which are associated with the third volume oscillation. The trends that were observed during the second volume oscillation continue. The magnitude

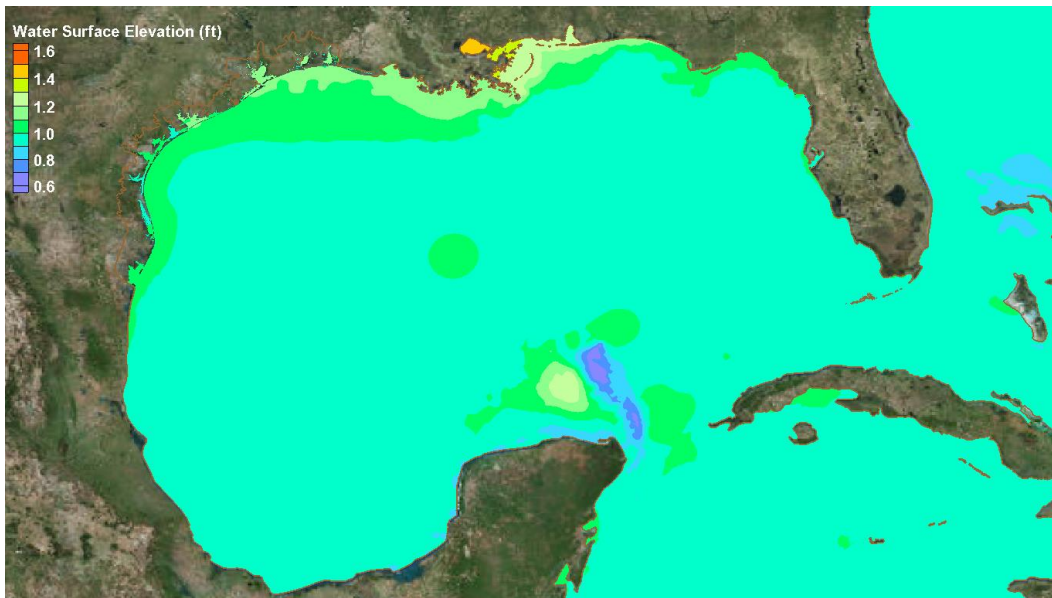


Figure 14-23. Water surface elevation field at hour 318, the time of the second elevation peak, for Storm 01 on the Central Yucatan Track.

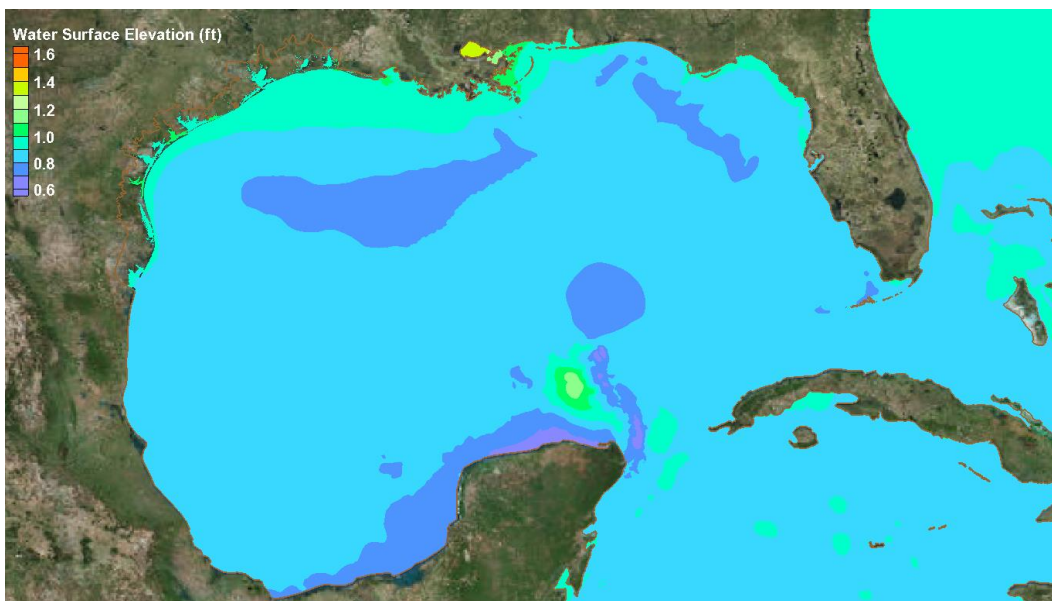


Figure 14-24. Water surface elevation field at hour 334, the time of the second elevation trough, for Storm 01 on the Central Yucatan Track.

of the elevation anomaly continues to decrease everywhere along the eastern and northern Gulf shelves east of the Bird's Foot delta. The anomaly persists along the Louisiana and Texas shelves; and the southward propagation of the free wave along the southern Texas shelf continues as evidenced by an increasing magnitude and southern extent of the elevation anomaly there.

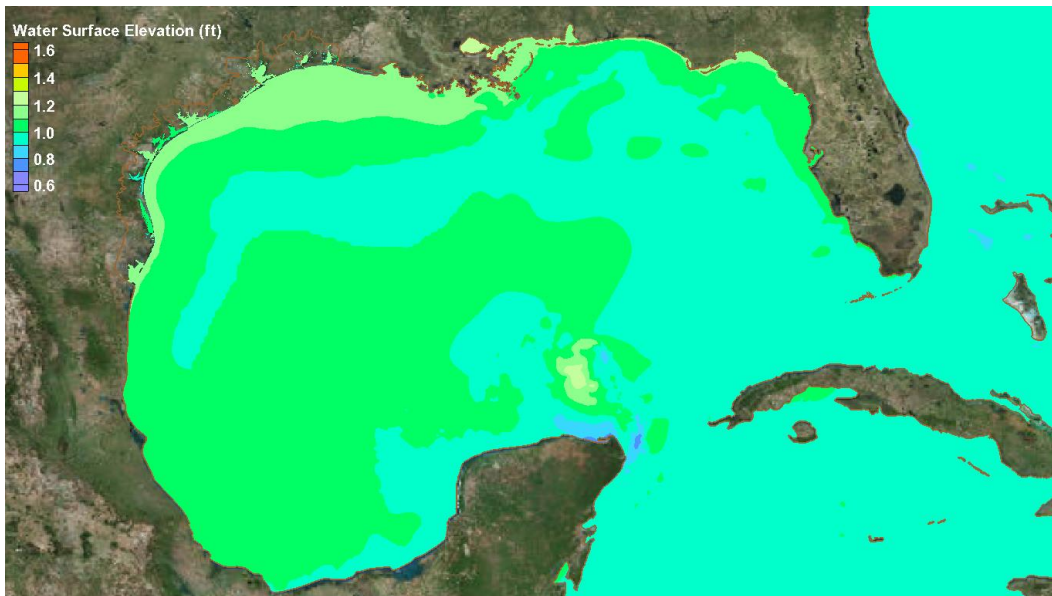


Figure 14-25. Water surface elevation field at hour 351, the time of the third elevation peak, for Storm 01 on the Central Yucatan Track.



Figure 14-26. Water surface elevation field at hour 368, the time of the third elevation trough, for Storm 01 on the Central Yucatan Track.

Figures 14-27 and 14-28 show the water surface elevation field at the times of the peak and trough, respectively, which are associated with the fourth volume oscillation. The trends that were observed during the third volume oscillation continue. At both of these times, the magnitude of the elevation anomaly continues to decrease everywhere in the Gulf. The uniform rising and falling water surface elevation throughout much of the Gulf is consistent with the Helmholtz oscillation.

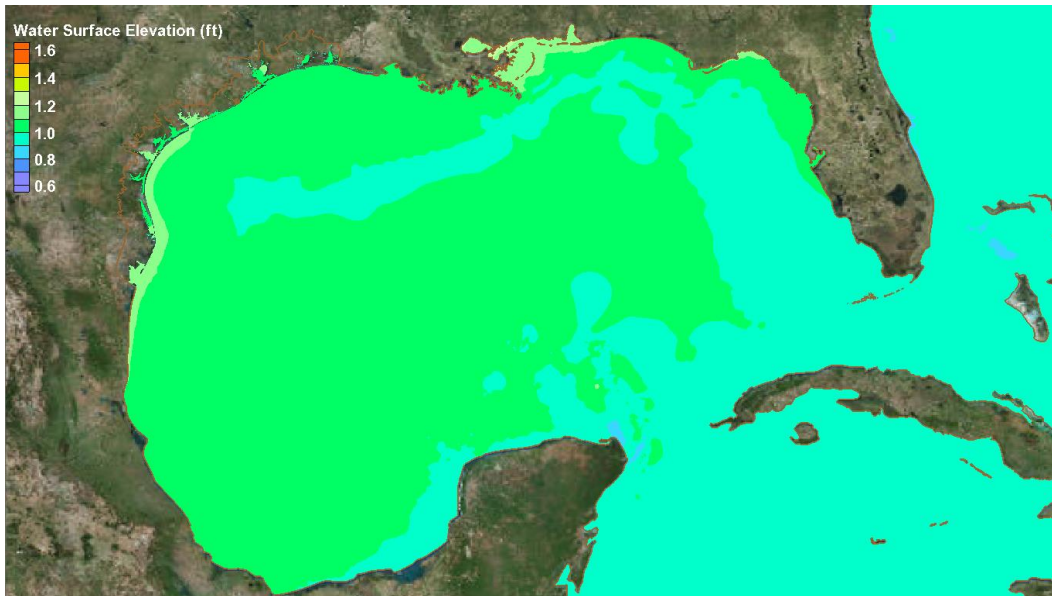


Figure 14-27. Water surface elevation field at hour 385, the time of the fourth elevation peak, for Storm 01 on the Central Yucatan Track.

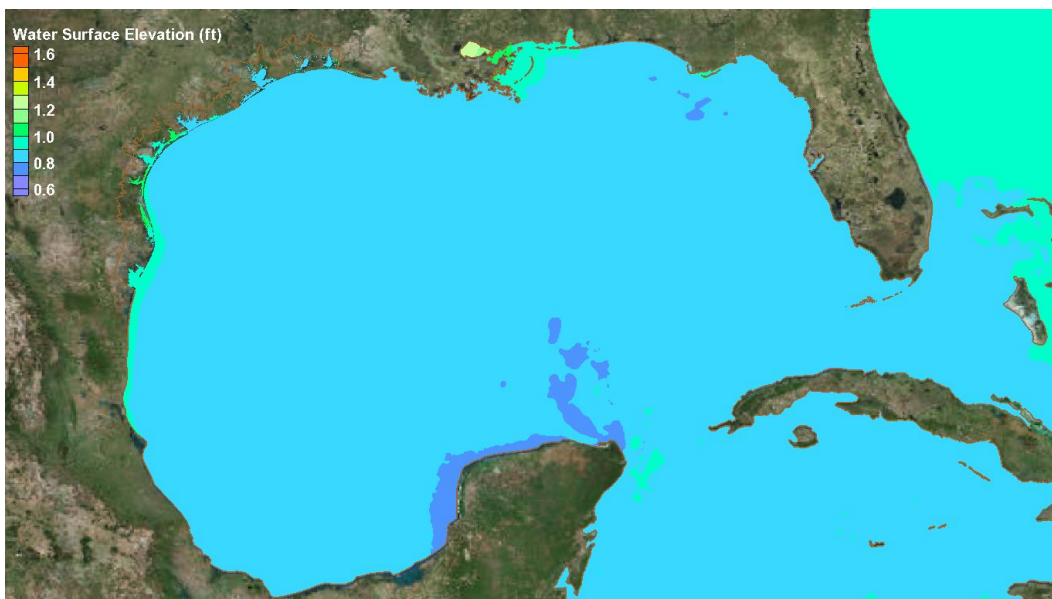


Figure 14-28. Water surface elevation field at hour 403, the time of the fourth elevation trough, for Storm 01 on the Central Yucatan Track.

The time series graph in Figure 14-17 also shows the decreasing amplitude of the elevation anomaly later in the simulation and the persistence of the volume oscillation, i.e., uniformity in water surface elevation through the Gulf, in the latter stages of the simulation.

It is very important to remember that the residual elevation anomaly which is evident at the shallow water output locations shown in Figure 14-17 is an artifact of the inability of the current modeling approach to fully

isolate the volume oscillation in shallow water throughout the entire Gulf. Steps were taken to eliminate the effects of wind-driven Ekman set-up along the Texas and Louisiana shelves, with partial success.

It is also important to recognize that the residual elevation anomaly does not in any way reflect the full contribution of the wind-driven Ekman set-up that would be expected along the Louisiana and Texas shelves had the storm intensity not been decayed or had the wind and pressure forcing not been zeroed out in the western Gulf of Mexico. The analysis above shows the importance of the Ekman set-up throughout the northern Gulf, first as a forced wave, and then its potential to propagate as a free wave along the northern Gulf shelf, around the Bird's Foot Delta and into the Louisiana and Texas shelf regions. As discussed previously, this dynamic appears to be a potential contributor to the wind-driven forerunner surge that is experienced at the Texas coast for slow-moving hurricanes.

Propagation of the Volume Mode Forerunner into Galveston Bay

Figure 14-29 shows time series of water surface elevation at three locations within Galveston Bay, along with the time series at the open-coast Galveston Pleasure Pier location. The three in-bay locations are: 1) the City of Galveston; 2) Morgan's Point which lies at the northern edge of Galveston Bay, along the Houston Ship Channel; and, 3) the Houston Ship Channel (upper) location which is situated at the uppermost end of the

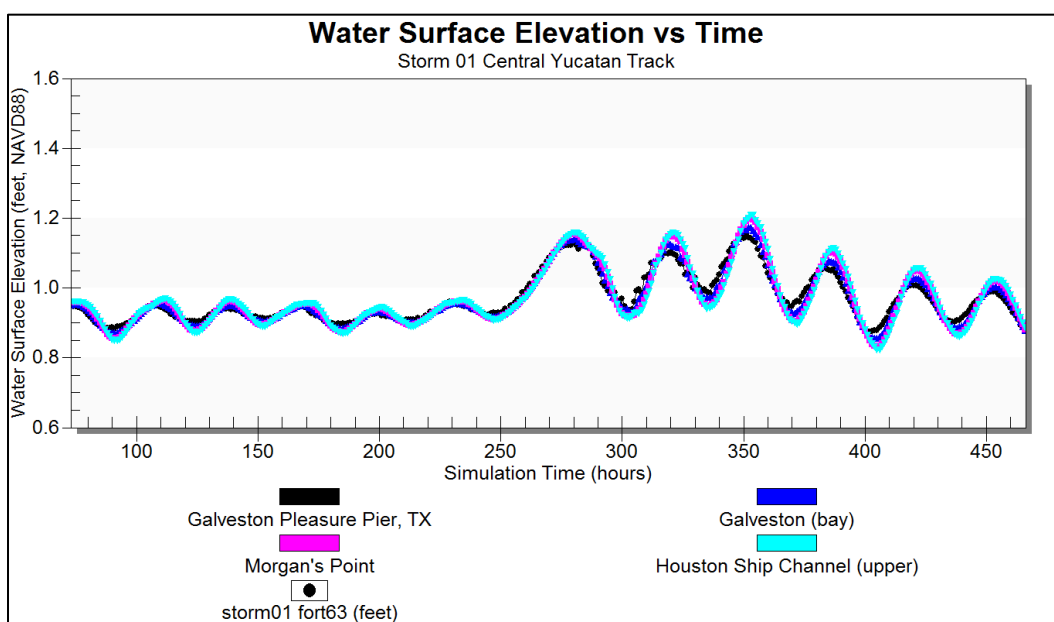


Figure 14-29. Water surface elevation as a function of time for three locations in Galveston Bay and the Galveston Pleasure Pier on the open Gulf, for Storm 01 Central Yucatan Track.

ship channel. Considered together, the results illustrate how the volume mode forerunner readily penetrates into the bay from the open Gulf, through Bolivar Roads pass. This behavior is quite similar to that seen for the wind-driven forerunner.

For the volume mode oscillation, the water surface elevation variation with time inside the bay is quite similar to that seen at the open coast. The volume oscillation is not attenuated as it propagates through the Bolivar Roads Pass and into Galveston Bay. In fact, for the volume mode oscillation, the amplitude increases slightly as the oscillation propagates up the ship channel, as evident in the higher elevation highs and lower elevation lows at all three locations. Amplitude is greatest in the upper ship channel, albeit by a small amount.

Close inspection of Figure 14-29 also shows that there is a small phase lag between the oscillation at the open coast and inside the bay. The phase lag increases slightly as the oscillation propagates into the bay and then up the Houston Ship Channel. The greatest phase lag between the open coast and locations inside they bay occurs at the upper end of the ship channel, a lag time of a few hours. The phase lag is similar to that seen for the Hurricane Ike wind-driven forerunner surge. Both phenomena seem to propagate into the bay and up the ship channel as long shallow-water wave, whose propagation speed is related to the local water depth and its propagation path.

Volume Mode Forerunner – Dependence upon Hurricane Characteristics

Influence of Storm Track and Forward Speed

To further examine the general behavior of the volume mode oscillation, its characteristics, and its dependence on hurricane characteristics, the dependence on storm track and forward speed was investigated first. Behavior of the volume oscillation is examined primarily in terms of the changes in water surface elevation with time.

Storms Having the Slowest Forward Speed

Figure 14-30 shows the computed change in water surface elevation, with time, at the Galveston Pleasure Pier location in shallow water. Results in the figure are shown for four storms, each of which has the same intensity, size and forward speed; each has a minimum central pressure of 930 mb, a radius-to-maximum-winds of 18 nm (the middle of the three values that were considered), and a forward speed of 6 kt (the slowest of the three forward speeds that were considered). Each storm takes one of the four different tracks that were considered, three that enter through the Yucatan Straits (Eastern Yucatan Storm 01, Central Yucatan Storm 01, and Western Yucatan Storm 01) and one that enters through the Florida Straits (Florida Storm 01). Results for the three Yucatan storms are discussed here, results for the Florida storm in the next section.

For the three storms that enter the Gulf through the Yucatan Straits, the water surface elevation time series are similar. Following entry into the Gulf at around hour 255 to 260, volume oscillations are prevalent for all three storms; and for each storm, the volume oscillations have similar periods of approximately 30 to 35 hours.

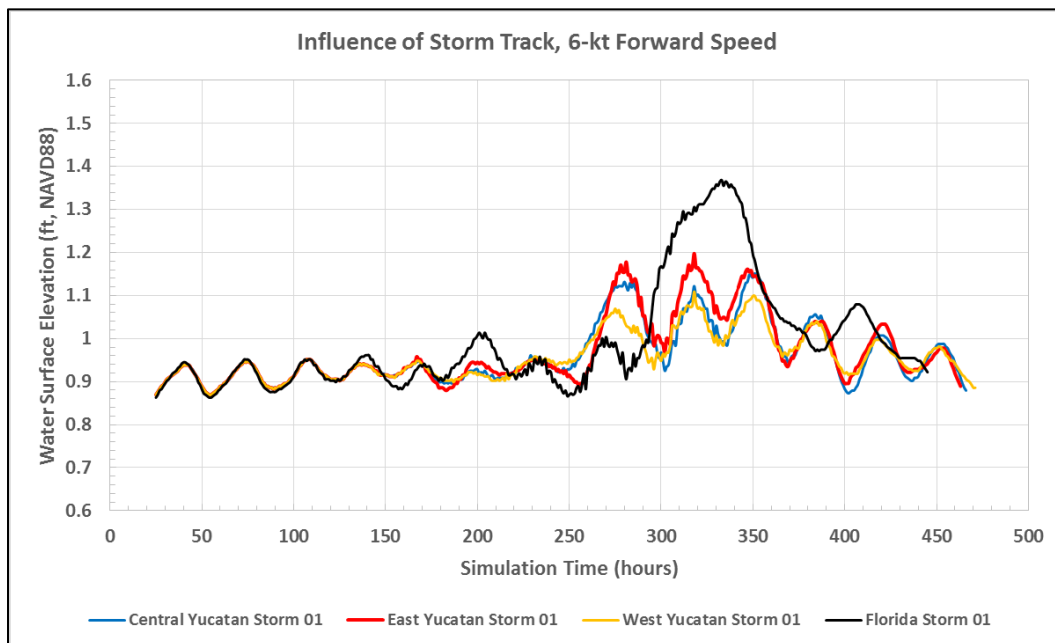


Figure 14-30. Dependence of the volume mode oscillation on storm track for the slowest moving storms (6-kt forward speed).

The initial volume oscillation that occurs at around hour 275 is most pronounced for the Eastern Yucatan track storm, slightly less so for the central Yucatan track storm, and least pronounced for the Western Yucatan track storm. This is probably due to the fact that as the hurricane approaches and enters the Gulf on the east side of the Yucatan Straits, the counterclockwise circulating hurricane winds tend to push water out of the Gulf, in the same direction as the water which is drawn out of the Gulf toward the low pressure center, reinforcing each other. The opposite would be true for the western Yucatan track, with winds tending to push water into the Gulf as the storm enters, in opposition to water being drawn out of the Gulf toward the eye. For the Central Yucatan track, winds on one side of the eye are pushing water into the Gulf, and on the opposite side they act to push water out of the Gulf, partially offsetting each other.

Subsequent volume oscillations for the storms on all three Yucatan tracks have more similar amplitudes. During subsequent oscillations, the eye is positioned well inside the Gulf and moving away from the Yucatan Straits. As the three simulations progress in time, the eye is located in a similar or the same position for all three tracks. This reinforces the notion that the large differences in the first peak are primarily due to the differences in position of the eye at the time of storm entry into the Gulf. It is unlikely that a gate system at Bolivar Roads would close during the first volume oscillation when differences are greatest. Closure is more likely during later oscillations when differences are much smaller.

For all three Yucatan tracks, the volume oscillations appear to be superimposed on another, longer-period elevation oscillation such that the first three oscillation cycles between hours 260 and 370 are generally offset by higher positive elevation values. As shown and discussed in the previous section on Central Yucatan Track Storm 01, this residual elevation anomaly is due to the Ekman set-up, first manifested as a forced wave along the Florida, Alabama, Mississippi shelves, then as a free wave that eventually propagates along the Louisiana and Texas shelves.

The maximum magnitude of this elevation anomaly is greatest for the east Yucatan track, which makes sense. The hurricane eye on the eastern Yucatan track is closer to the Florida Shelf than the eye on the other two tracks, which leads to slightly higher winds on the Florida shelf and a slightly higher magnitude of Ekman set-up. The eye is farthest from the

Florida shelf for the western Yucatan track, leading to a slightly smaller elevation anomaly for this track.

The amplitudes of the volume oscillation for all three storms are quite small, about 0.1 ft or less. The maximum magnitude of the elevation anomaly that is present, in addition to the volume oscillation, is of comparable or greater magnitude, 0.1 to 0.2 ft above mean sea level.

Water Surface Elevation Anomaly in Shallow Water for Florida Storm 01

The elevation time series for the storm that enters the Gulf through the Florida Straits (Florida Track Storm 01 shown as the black curve in Figure 14-30) exhibits a very different behavior compared to that for the three storms that enter through the Yucatan Straits. The Florida Storm 01 enters the Gulf through the Florida Straits at hour 196, and there are several small oscillations that appear following entry between hours 200 and 275 of the simulation. These appear to be volume mode oscillations; they also have periods of approximately 30 to 35 hours. However, beginning at around hour 275, the appearance of periodic oscillations is obscured by a much more pronounced and larger water surface elevation anomaly. The water surface elevation reaches a much higher maximum value, approximately 1.35 ft at around hour 335, which is nearly 0.5 ft above the mean sea level value. This maximum elevation value is significantly higher than the local maximum elevation values that are associated with individual 30- to 35-hour volume oscillation cycles for storms that entered through the Yucatan Straits. In the Florida Track Storm 01 time series there is some evidence of an oscillatory signal after the very pronounced rise/fall in elevation.

It appears that the elevation time series for Florida Track Storm 01 is much more dominated by the residual Ekman set-up than the time series for those hurricanes that enter through the Yucatan Straits. As pointed out previously, this elevation anomaly does not in any way reflect the full magnitude of Ekman set-up that would be expected at Galveston for any of these storms. However, examination of how the residual anomaly develops and how it varies with different storm tracks sheds additional insights into the generation and propagation of the Ekman set-up as a forced and free wave.

The development of Ekman setup along the Florida, Alabama and Mississippi continental shelves is expected to be larger for Florida Storm 01 because of its closer proximity to these shelf regions than storm which enter through the Yucatan Straits. Prior analysis of the far-field influence of the Ekman setup for Central Yucatan Storm 01 utilized snap-shots of the water surface elevation fields in the entire Gulf. To examine the Ekman set-up generation process in the eastern Gulf and its propagation along the northern Gulf continental shelves for Florida Storm 01, time series of water surface elevation at a number of shallow-water coastal locations around the Gulf of Mexico periphery were graphed and examined. These locations are shown in Figure 14-31.



Figure 14-31. Locations for analyzing water surface elevation time series around the Gulf of Mexico periphery for Florida storm 01.

Figure 14-32 shows the water surface elevation time series at each of these shallow-water coastal locations for the Florida Storm 01. Along the western Florida coast, as the hurricane approaches and then enters the Gulf through the Florida Straits, winds along the west Florida shelf are directed offshore, such that the water surface elevation at the coast is set down, i.e., lowered, by the wind. This behavior is evident by the steady decrease in water surface elevation at the three Florida sites between the hours of 150 and 225. Entry of the storm into the Gulf occurred at hour 196. The greatest magnitude of water surface elevation set-down is at Naples which is closest to the eye of the hurricane and nearest the stronger wind speeds. The smallest set-down occurs at Apalachicola which is

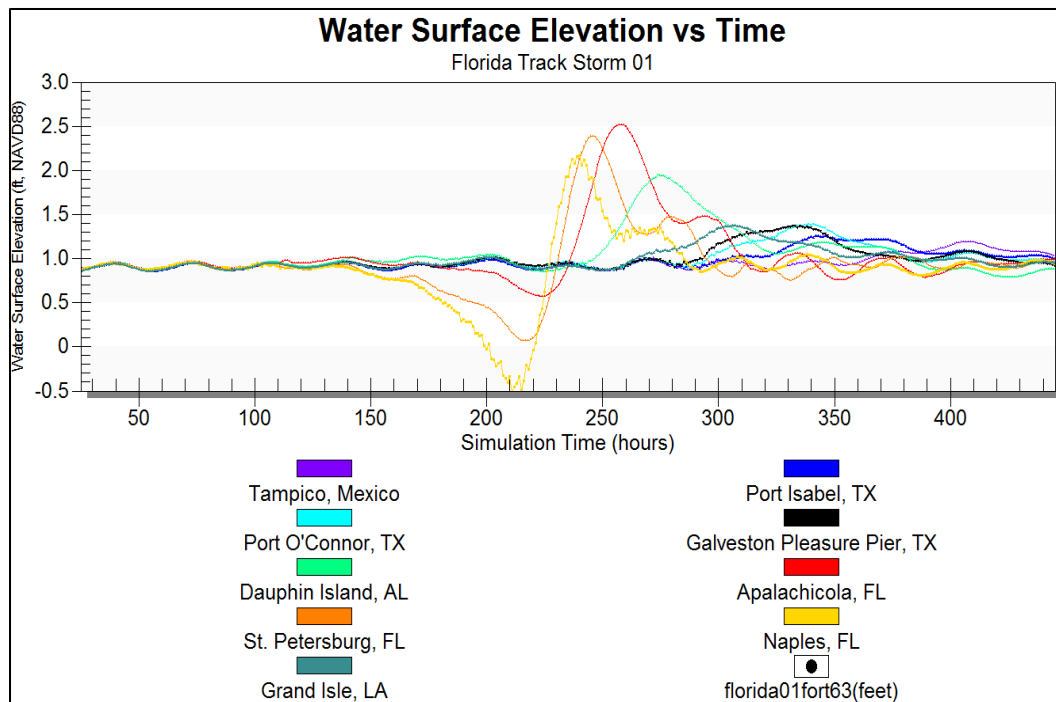


Figure 14-32. Water surface elevation time series for Florida Track Storm 01 at locations around the periphery of the Gulf of Mexico.

farthest from the eye of the hurricane and where winds are relatively weaker.

Once the hurricane has entered and has moved toward the interior of the Gulf, some 30 hours later, winds along the west Florida shelf begin to have more of an alongshore wind component, blowing from south to north. These winds push water northward along the Florida shelf, and that moving water is turned toward the right by the Coriolis force, stacking it up against the western coastline of Florida, i.e., formation of the Ekman set-up.

Figure 14-32 shows that the Ekman set-up moves as a forced wave northward along the Florida shelf, as evidenced by the lagged (in time) water surface elevation peaks which occur first at Naples (hour 235), then at St. Petersburg (hour 245), then at Apalachicola (hour 260). The maximum value of the elevation anomaly that is associated with the Ekman setup increases from south to north; and the greatest elevation associated with the forced wave that moves along the Florida continental shelf occurs at Apalachicola, which is the most removed from the location of the hurricane eye. The peak elevation at Apalachicola reaches a value of about 1.6 ft above mean sea level.

The forced shelf wave then continues to move eastward along the northern Gulf shelf as a forced wave, then as a free wave as the storm intensity is decreased significantly. This movement is clearly evidenced by the lagged elevation peak at Dauphin Island, AL, which occurs at around hour 275, and then the occurrences of the elevation peak at Grand Isle, LA, which is located west of the Mississippi River Bird's Foot at hour 305.

Propagation of the Ekman set-up as a free wave along the Louisiana shelf and then down the Texas shelf is seen in the arrival of the peak elevation at Galveston Pleasure Pier at hour 335. Peaks in the water surface elevation time series at Port O'Connor (hour 340) and Port Isabel (sometime between hours 350 and 370), TX, and Tampico, Mexico (hour 410), also show that the shelf wave continues to propagate as a free wave along the entire relatively narrow southern Texas and Mexico continental shelves despite no local wind or pressure forcing. This same propagation path was shown for the Central Yucatan storm 01 in a previous section.

The increasingly smaller amplitude of the lagged peaks at these locations as the Ekman set-up wave advances can be seen in the water surface elevation signals, reflecting dissipation of the wave. As the amplitude of the wind-driven Ekman setup wave decreases, the influence of the volume oscillations become more noticeable in the elevation time series, as seen at all the Texas locations.

For this slow moving storm, having a constant forward speed of 6 kt, the arrival time of the residual elevation anomaly at Galveston indicates that the Ekman setup wave propagates at a speed that is fast enough to arrive at Galveston prior to the time of hurricane landfall at San Luis Pass. Florida Storm 01 entered the Gulf, crossing the Florida Straits transect, at hour 196 of the simulation. At its constant forward speed, a hurricane on this track would have made landfall at San Luis Pass at hour 347. The peak water surface elevation at Naples, FL, occurs at around hour 235 of the simulation; and at Galveston it occurred at around hour 335, 100 hours (roughly 4 days) later. Assuming an approximate travel distance from Naples to Galveston of 900 nm along a path near the coastline, or 750 nm along a path that is parallel to the coastline but positioned roughly midway between the outer continental shelf edge and the coastline, a propagation speed for this shelf wave between these two locations can be estimated, 7.5 to 9 kt (3.8 to 4.6 m/sec). Using the 105-hr time lag between the water surface elevation anomaly peaks at Grand Isle, LA and

Tampico, Mexico, and using the same methodology for computing path length (750 and 720 nm), propagation speeds of 6.9 to 7.1 kt (3.5 to 3.7 m/sec) are estimated for the speed of the shelf wave between these two locations. Kennedy et al (2011) found that the Hurricane Ike wind-driven forerunner, which was forced by the same type of mechanism, propagated along the Texas coast as a dissipative free wave with a propagation speed of 5 to 6 m/sec.

Storms Having Faster Forward Speeds

Figure 14-30 compared volume oscillations at Galveston Pleasure Pier for storms having the same size and intensity characteristic on each of the four tracks, all of them having the slowest forward speed of 6 kt. Figures 14-33 and 14-34 show the volume oscillations for the same storms on the four tracks, all having a forward speed of 12 kt (Figure 14-33) and 18 kt (Figure 14-34), respectively. Results are shown at Galveston Pleasure Pier.

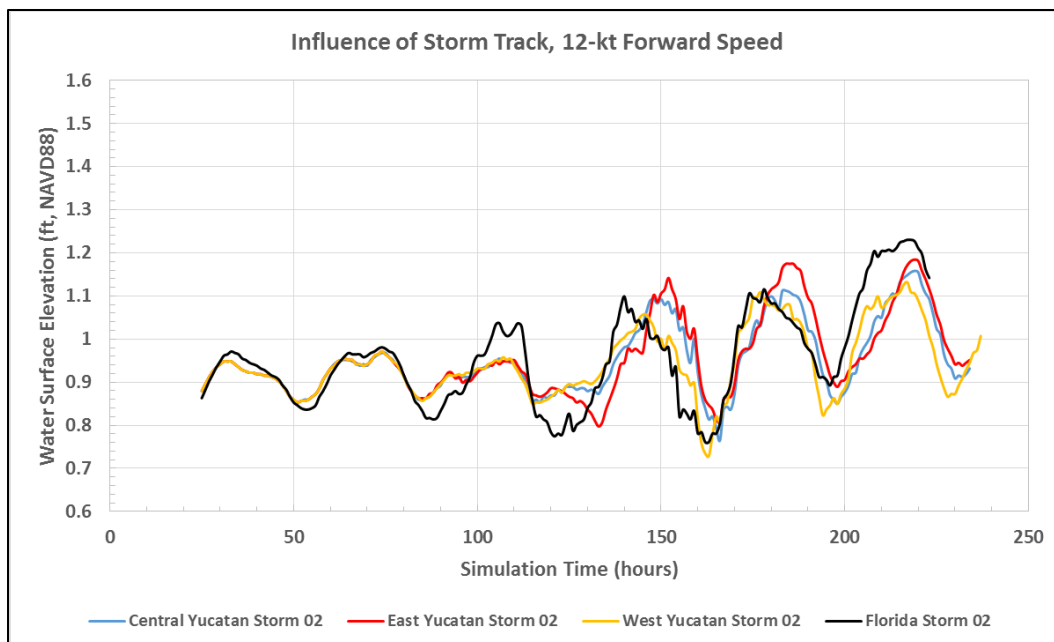


Figure 14-33. Dependence of the volume mode oscillation on storm track for storms having a 12-kt forward speed, on all four tracks.

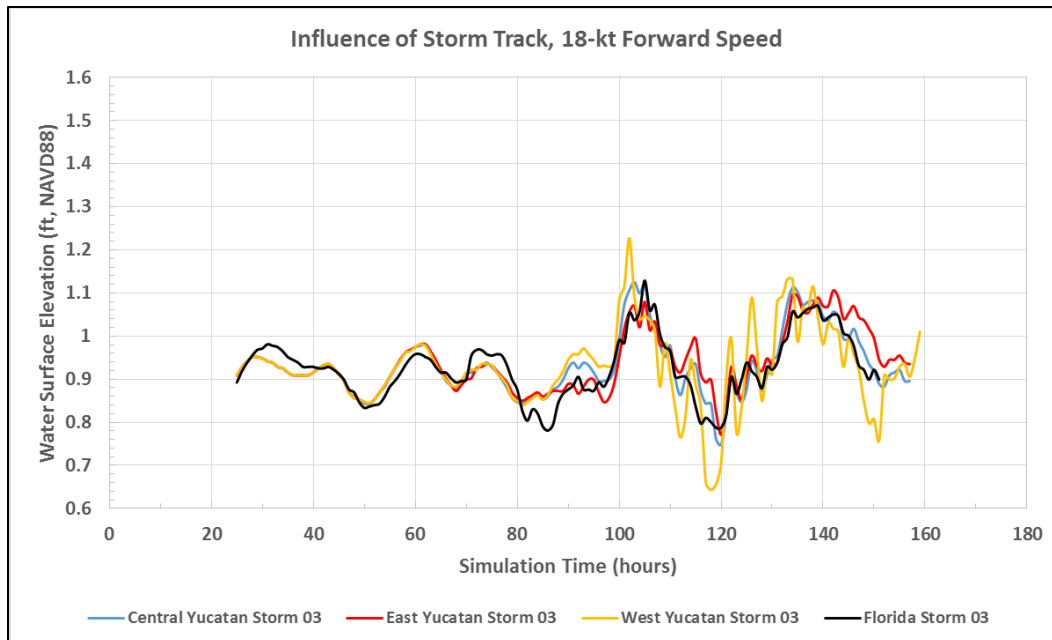


Figure 14-34. Dependence of the volume mode oscillation on storm track for storms having an 18-kt forward speed, on all four tracks.

The period of the volume oscillation appears to be the same for the elevation signals shown in both figures, in the range of 30 to 35 hours, irrespective of track; and it appears to be the same as the period for the slowest moving storms. The period of the volume oscillation does not appear to vary significantly with track or forward speed. This finding is consistent with the same observation made by Bunpapong et al (1985), although they found periods to be slightly shorter, in the range of 27 to 30 hours.

Both Figures 14-34 and 14-35 show that the amplitude of the volume oscillations is quite similar for all of the storms, on all tracks, roughly 0.15 ft. There seems to be little change in amplitude depending upon whether the storm enters through the Yucatan or Florida Straits. The amplitude seems to be rather independent of forward speed for the faster speeds, 12 kt or 18 kt; although the amplitude of the volume oscillation for the faster moving storms seems to be slightly larger than that for the slowest-moving storm (6 kt), which was closer to 0.1 ft. Amplitudes for all these storms are significantly smaller than the amplitudes found by Bunpapong et al (1985).

The influence of the residual elevation anomaly associated with the Ekman set-up wave is similar for storms on all four tracks, for the 12-kt forward speed. For the 18-kt forward speed, the same observation is made. However, it appears as though the residual anomaly that is generated in the eastern Gulf shelves is a function of forward speed, with less anomaly occurring at Galveston for faster storms. A faster moving storm is apparently less effective in generating Ekman set on the eastern Gulf shelf regions and/or the storms having forward speeds of 12 and 18 kt “outpace” the speed at which the residual Ekman set-up wave propagates along the shelf.

Quantitative Analysis of Volume Oscillation Characteristics

In addition to a qualitative analysis of volume oscillation characteristics, which was based primarily upon graphs of water surface elevation time series, a quantitative analysis of the time series at the Galveston Pleasure Pier also was undertaken. The analysis involved calculation of various volume oscillation parameters using model-generated time series data. The results of that analysis, which was performed for each storm, are presented in Table 14-2. All results are shown for the Galveston pleasure Pier model output location.

The first column in Table 14-2 lists the different hurricanes that were simulated, grouped by track. Table 14-1 listed the forward speed, intensity, and radius-to-maximum-winds for each storm. The second column in Table 14-2 lists only the storm’s forward speed. The third column lists the “lag time to first peak,” which is defined as the difference between the time when the storm enters the Gulf and the time of occurrence of the water surface elevation peak that is associated with the first volume oscillation following entry into the Gulf. The fourth column lists the “lag time to first trough,” which is defined in a similar way to the previous quantity, but involving the time of occurrence of the first trough. The fifth column is the average period of the volume oscillation for that storm. Average period was computed based upon the time differences between successive peaks and between successive troughs, for as many full volume oscillation cycles as were available. All the individual period values were then used to compute an arithmetic mean value. The average amplitude value listed in column six was computed in a similar way as the previous quantity. Differences in elevation between successive peaks and troughs were used to compute amplitude values for each of the full volume oscillations. All the individual amplitude values were then used to

Table 14-2. Quantitative Characteristics of the Volume Mode Oscillation for the Full Storm Set at Galveston Pleasure Pier

Storm	Forward Speed (kt)	Lag Time to First Peak (hr)	Lag Time to First Trough (hr)	Average Period (hr)	Average Amplitude (ft)	Average Peak Elevation (ft)	Average Trough Elevation (ft)	Maximum Elevation (ft)
						Elevation Relative to Sea Level, 0.91 ft NAVD88		
Yucatan Straits - Central Track								
CentralYucatanTrackStorm01	6	21	43	34	0.09	0.21	0.03	0.24
CentralYucatanTrackStorm02	12	17	35	32	0.13	0.20	-0.07	0.21
CentralYucatanTrackStorm03	18	14	31	32	0.15	0.21	-0.09	0.21
CentralYucatanTrackStorm04	12	19	35	34	0.06	0.12	0.00	0.14
CentralYucatanTrackStorm05	12	17	35	34	0.26	0.37	-0.16	0.40
CentralYucatanTrackStorm06	12	17	35	34	0.21	0.30	-0.11	0.34
Yucatan Straits – East Track								
EasternYucatanTrackStorm01	6	29	50	34	0.09	0.24	0.06	0.30
EasternYucatanTrackStorm02	12	24	38	33	0.14	0.26	-0.02	0.27
EasternYucatanTrackStorm03	18	16	33	36	0.12	0.19	-0.06	0.21
Yucatan Straits – West Track								
WesternYucatanTrackStorm01	6	9	30	35	0.07	0.18	0.03	0.21
WesternYucatanTrackStorm02	12	10	28	35	0.15	0.20	-0.11	0.24
WesternYucatanTrackStorm03	18	10	26	32	0.24	0.27	-0.20	0.30
Florida Straits								
FloridaTrackStorm01	6	4	26	32	?	?	?	0.47
FloridaTrackStorm02	12	6	21	37	0.14	0.17	-0.10	0.21
FloridaTrackStorm03	18	4	18	33	0.13	0.14	-0.12	0.21
FloridaTrackStorm04	12	11	21	36	0.07	0.11	-0.03	0.11
FloridaTrackStorm05	12	5	21	36	0.26	0.30	-0.22	0.37
FloridaTrackStorm06	12	11	26	35	0.20	0.24	-0.16	0.27

compute an arithmetic mean. The difference between successive peaks and troughs was used to minimize the influence of the residual elevation anomaly on computed amplitude values. Columns seven and eight list the average peak elevation and average trough elevation values for successive volume oscillations. These values were computed as arithmetic means of discrete peak/trough elevation values for each of the full oscillations; and then the present-day mean sea level value of 0.91 ft NAVD88 was subtracted from the average values to reference them to mean sea level. The raw average peak/trough values include any effects of the residual elevation anomaly. However, the difference between the average peak and average elevation values is approximately equal to the average amplitude values. The last column lists the maximum peak elevation value, relative to mean sea level.

The average period is quite consistent across all simulations, ranging from 32 to 37 hours, with a mode value of 34 hrs. These values are similar to, but slightly higher than, the 28 to 30 hours reported by Bunpapong et al (1985).

For all storms, the average amplitude values are less than 0.3 ft, which is quite small, and the amplitudes are significantly less than values reported by Bunpapong et al (1985) for similar storms. Possible reasons for this discrepancy are discussed below in the next section. The average amplitudes values are rather independent of storm track. Storms 01, 02 and 03 in each track category reflect increasing forward speed from 6 kt to 12 kt to 18 kt. In general, the average amplitude increases with increasing forward speed for storms entering through the Yucatan Straits. The same trend is not apparent for storms entering the Florida Straits.

The lag times to first peaks and trough do appear to generally decrease with increasing forward for storms entering through the Yucatan Straits. However, there is variability in the values and in the amount of the decrease among the different tracks.

Discrepancy with the Volume Oscillation Amplitudes Found by Bunpapong et al (1985)

Reasons for the aforementioned discrepancy in amplitude values for the volume oscillation between the present study and the work of Bunpapong et al (1985) are uncertain. However, one contributing factor is probably the close proximity of the open water model boundaries to the Gulf of Mexico, in the modeling done by Bunpapong et al. (1985). One of their open-water model boundaries was located right where the Florida Straits transect is located in the present study. Another open-water boundary condition was located not too far from the Yucatan Straits near the Cayman Islands in the Caribbean Sea. Model boundary conditions are, by their very nature, approximations to the full set of equations conservation of water mass and momentum. There are inherent errors in any and all approximations. Error in the open-water boundary conditions might have translated into error in the computed water flux through the Florida Straits, and perhaps to a lesser degree the Yucatan Straits, which in turn might have contributed to error in the net flux that enters/leaves the Gulf, and subsequently resulted in error in the computed volume oscillation. The amplitude of the volume oscillation is critically dependent upon accurate calculation of the fluxes through both straits. A boundary located right at the Florida Straits is not ideal.

The storm surge model used in the present study has its eastern open water boundary located very far away from the Gulf of Mexico; it is located in the middle of the Atlantic Ocean. The model has been shown to predict well the astronomical tides, storm surge, and the combination of the two, in the Gulf of Mexico. Accurate simulation of the tides in the Gulf of Mexico requires accurate simulation of the water flux through both straits that lead to/from the Gulf. It is believed that the present modeling is much more accurate in computing fluxes through the straits in part because of its open-water boundary location. The modeling done by Bunpapong et al (1985) was not verified for astronomical tides in their report.

The choice of boundary locations made by Bunpapong et al (1985) seems reasonable for a study done at that time. Substantially more computational resources would have been required to extend the model boundaries to a location far-removed from the Gulf using the rectangular structured grid mesh modeling approach which was applied. Such an

option was probably not an option for them, and they most likely made the only choice that was feasible for them at the time.

Influence of Storm Intensity

Storms having different minimum central pressures of 930 and 900 mb, but having all other characteristics the same, were run for both the Central Yucatan and Florida tracks. Dependence of the volume oscillation on storm intensity was examined using results from these pairs of simulations. Figures 14-35 and 14-36 show differences in the volume oscillation for both tracks, the Central Yucatan and the Florida tracks, respectively. Both sets of results show a clear dependence of the amplitude of the oscillation on storm intensity. The same observation was made by Bunpapong et al (1985). The increases in amplitude with increasing intensity (i.e. decreasing minimum central pressure) are quantified in Table 14-2, comparing Storms 02 and 06 for these two tracks. Even the average amplitudes for the most severe 900-mb storms, 0.2 ft, are quite small.

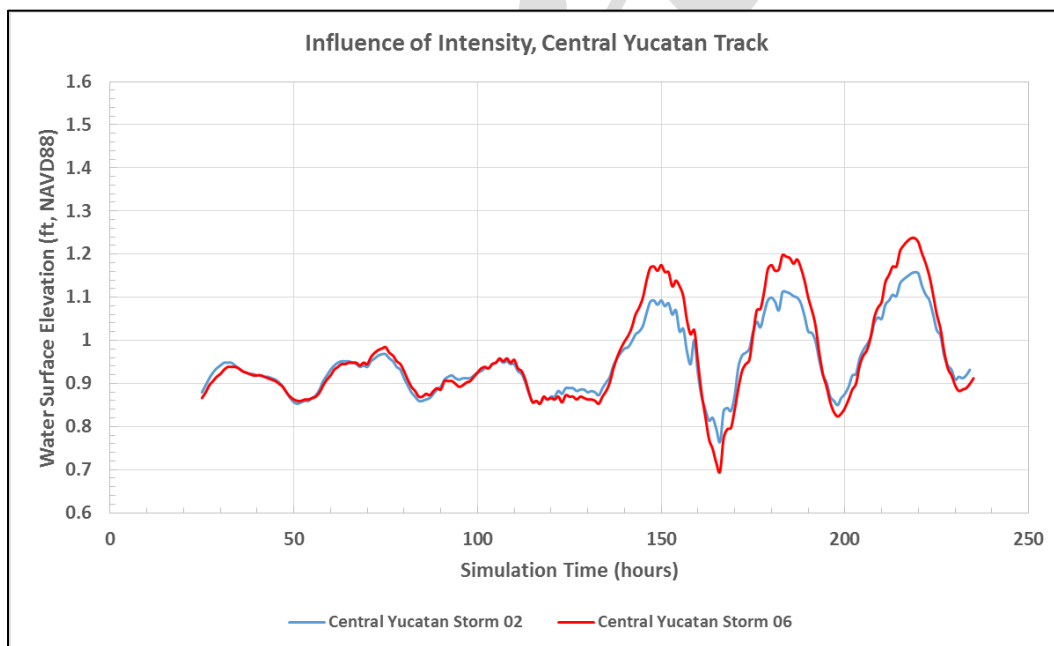


Figure 14-35. Dependence of the volume mode oscillation on storm intensity for storms on the Central Yucatan track.

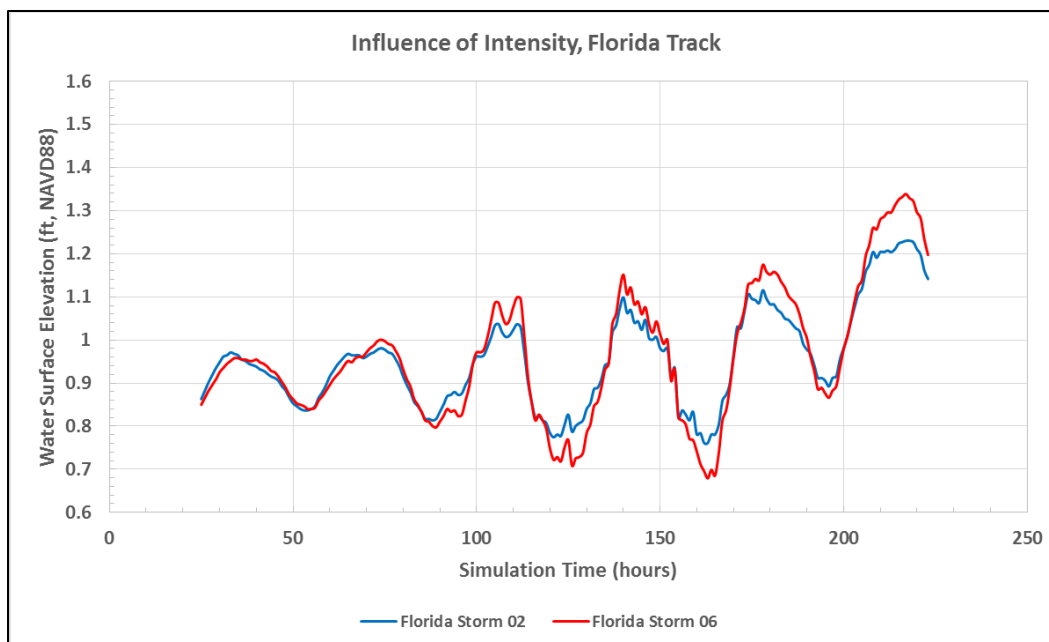


Figure 14-36. Dependence of the volume mode oscillation on storm intensity for storms on the Florida track.

Influence of Storm Size

Storms having different sizes, defined by different radius-to-maximum-winds values of 10 nm (the “04” storms), 18 nm (the “02” storms) and 30 nm (the “05” storms), but having all other characteristics the same, also were run for both the Central Yucatan and Florida tracks. The dependence of volume oscillation on storm size was examined using results from these simulations.

Figures 14-37 and 14-38 show differences in the volume oscillation for both tracks, the Central Yucatan and the Florida tracks, respectively, for all three storm sizes. Both sets of results show a clear dependence of the amplitude of the volume oscillation on storm size. Comparing this set of two figures with the previous set of two, the influence of storm size is seen to be greater than the influence of storm intensity. These same observations were made by Bunpapong et al (1985). The increases in amplitude with increasing storm size are quantified in Table 14-2, comparing Storms 02, 04, and 05 for each of these two tracks. The average amplitude values, 0.26 ft for both of the large 30-nm storms, which also are intense and have 930-mb central pressures, are quite small relative to other potential contributions to the water level that is experienced during a hurricane, such as the tide and wind-driven forerunner.

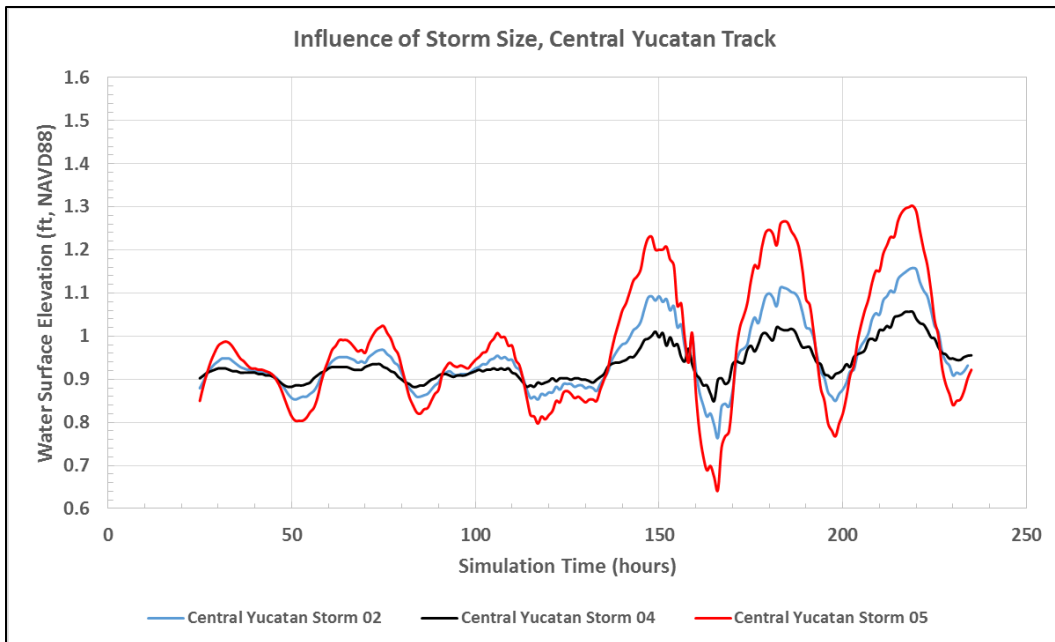


Figure 14-37. Dependence of the volume mode oscillation on storm size for storms on the Central Yucatan track.

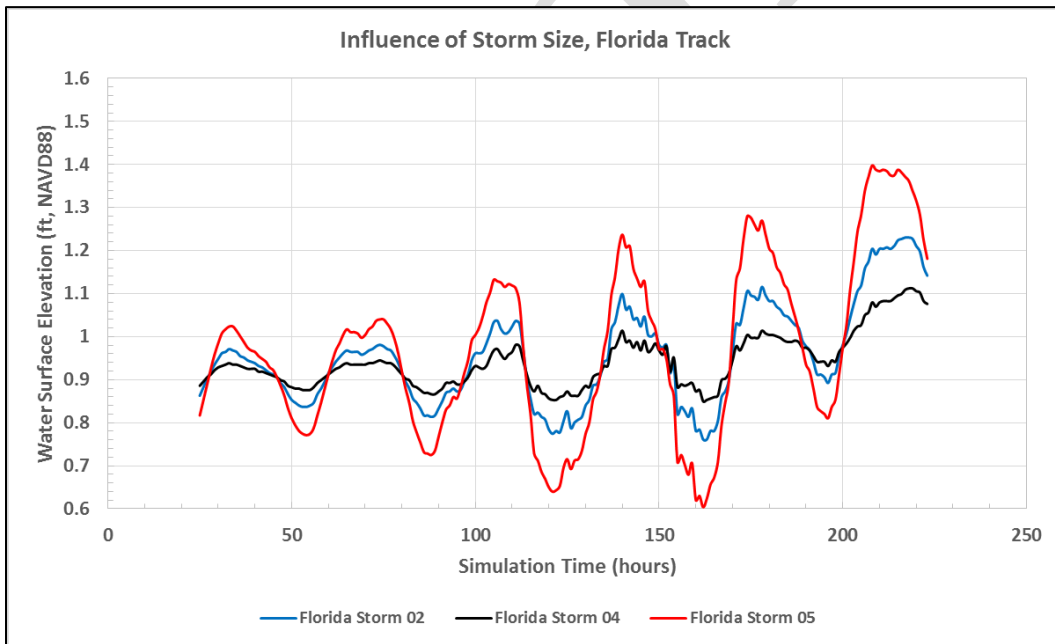


Figure 14-38. Dependence of the volume mode oscillation on storm size for storms on the Florida track.

Influence of Forward Speed on the Wind-Driven Forerunner and Peak Surge Development

Selection of a Storm Set for Analysis

Results from analyses of the volume mode forerunner suggested that the amplitude of the wind-driven forerunner might be sensitive to a hurricane's forward speed. Liu and Irish (2017) did not investigate the dependency of wind-driven forerunner amplitude on forward speed, only dependencies on size and intensity. In light of the importance of the wind-driven forerunner on antecedent water level inside Galveston and West Bays, and consequently the importance to Ike Dike storm surge gate operations, the dependence of forerunner and peak surge development on forward speed was investigated further.

Storms 01, 02 and 03 (see Table 14-1) on the Central Yucatan track (see Figure 14-13), which were considered in the volume mode forerunner analysis, were re-simulated to focus on wind-driven forerunner surge and peak surge development, and the interaction between the two. Unlike the simulations that were made to try and isolate the volume mode forerunner, the new simulations were made with no intensity decay after the hurricane entered the Gulf and with no application of the wind/pressure mask that zeroed out the wind speeds over the western Gulf shelf. The peak intensity for each hurricane was maintained during the entire transit through the Gulf, before, during and after landfall. All three storms followed the same track, which had landfall occurring near San Luis Pass. All three had the same intensity and size, a minimum central pressure of 930 mb and a radius-to-maximum winds of 18 nm. The three storms differed only in their forward speed; speeds of 6, 12 and 18 kts for Central Yucatan Storms 01, 02 and 03, respectively. All three storms were simulated with a seasonal/long-term mean sea level value of 0.9 ft NAVD88.

The Analysis Approach

The temporal variation of water surface elevation was examined first, at the five locations shown in Figure 14-39, to identify differences attributable to varying forward speed. The observation point at Galveston Pleasure Pier was selected to characterize the forerunner and peak surge on the open coast. The location at the City of Galveston, on the bay side, was selected to examine propagation of the forerunner and peak surge



Figure 14-39. Locations for examining variation of water surface elevation with time, to assess influence of hurricane forward speed.

through Bolivar Roads pass and into Galveston Bay, and any attenuation in forerunner amplitude that might occur through the pass. The other three in-bay locations, entrance to Clear Lake, close proximity to Alexander Island and the upper Houston Ship Channel, were selected to examine forerunner and peak surge propagation into the rest of Galveston Bay, into areas with potential for high economic losses due to flooding.

Some of the figures in these sections show the temporal variation of the water surface elevation for Central Yucatan Storms 01, 02 and 03, respectively. In these figures, water surface elevation is graphed on the vertical axis, and simulation time (in terms of elapsed real time) is graphed on the horizontal axis. Each figure displays results for all five locations. In each figure, water level results are displayed for a 60-hour window of time, beginning approximately 48 hours prior to landfall and ending roughly 12 hours after landfall.

The spatial characteristics of the water surface elevation field, and its dependency on forward speed, were examined as well. Figures showing snap shots of the water surface elevation field throughout the region at the time of landfall were used to assess storm surge levels along the inner shelf on the open coast, and within the bay. Other figures show water surface elevation profiles, which depict the spatial variation of water surface elevation at a snap-shot in time, along two transects. The two transects

considered here are shown in Figure 14-40. One is located inside Galveston Bay. It is oriented to be roughly parallel to the wind direction within the bay around the time of landfall, when winds set up the western side of Galveston Bay and set down the eastern side of the bay. The other transect is located on the open coast, in the inner shelf region. It is oriented to lie in the cross-shelf direction, parallel to the track heading, which is also shown in the figure. In these figures, water surface elevation is graphed on the vertical axis and distance measured along a transect is graphed on the horizontal axis. Distance is measured starting at the easternmost end of the in-bay transect, and from the offshoremost end of the open coast transect. Both the elevation snapshots and profile graphs were used to assess the degree of bay infilling due in large part to forerunner propagation into the bay, and how the amount of bay infilling varied with forward speed.

Other figures show maps of water surface elevation maxima, like those shown often in previous chapters. Maximum water surface elevation, throughout the region are shown, regardless of when the maxima occurred during the storm simulation.

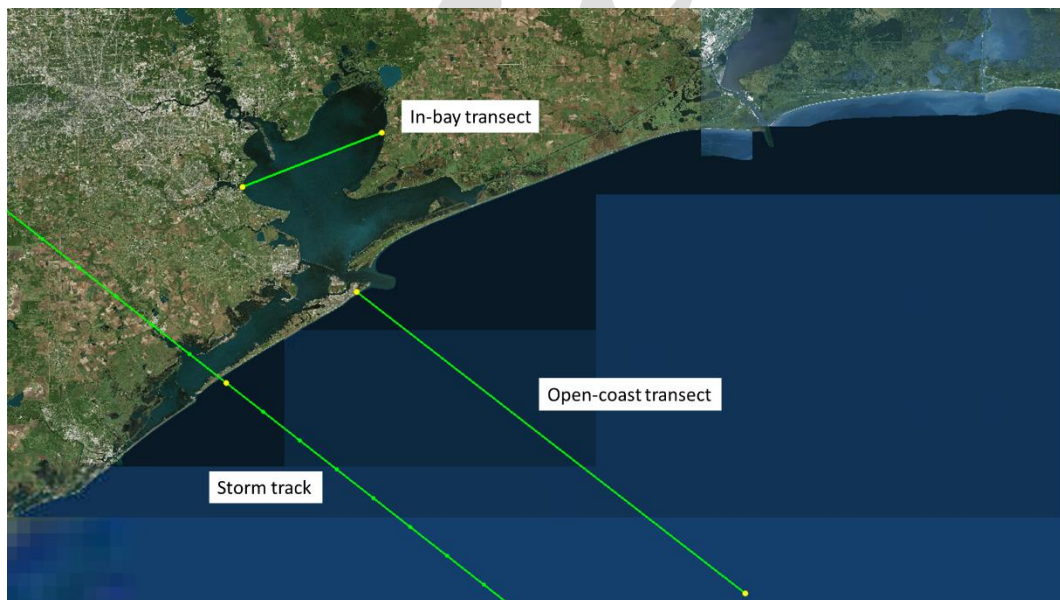


Figure 14-40. Locations for profiles for examining spatial variation of water surface elevation at a snapshot in time, to assess influence of hurricane forward speed.

Results for each storm are discussed in separate sections below. However, a summary of observations is presented here, which are generally to be expected for severe hurricanes that approach from the southeast and make landfall in the vicinity of Freeport to Galveston Island. Results show that forward speed has a significant influence on the following aspects of storm surge: 1) development and amplitude of the wind-driven forerunner surge along the open coast and inside Galveston Bay, 2) the magnitude of the peak surge experienced inside Galveston Bay, 3) the duration of high surge conditions both at the open coast and inside the bay, and 4) the difference between the open coast peak surge and peak surge experienced within the bay. On the other hand, results show that forward speed has less of an influence on peak surge at the open coast, even though it has great influence on peak surge inside the bay. The causative surge dynamics that lead to these observations are discussed in subsequent sections.

Central Yucatan Storm 01 (6-kt Forward Speed)

Figure 14-41 shows graphs of time series of water surface elevation for Central Yucatan Storm 01 which is the slowest moving storm of the three. Development of a substantial wind-driven forerunner is evident prior to landfall. This storm makes landfall at hour 372 of the simulation.

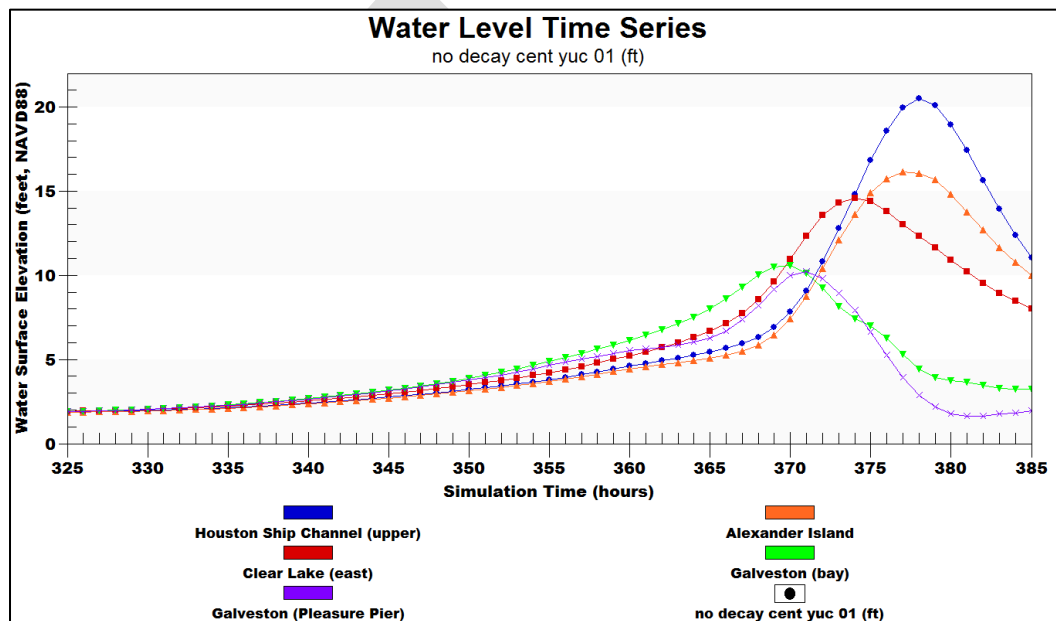


Figure 14-41. Temporal variation of water surface elevation for Central Yucatan Storm 01 (6-kt forward speed).

Several days before landfall, the amplitude of the forerunner begins to steadily grow, with a slowly accelerating rate of rise in elevation. The eye of this hurricane reached the outer edge of the continental slope off the Texas coast at hour 326, 48 hours before landfall. At this time the water surface elevation at the open-coast Galveston Pleasure Pier location was 1.9 ft NAVD88, which corresponds to a wind-driven forerunner surge amplitude of 1.0 ft relative to the mean sea level adopted for the simulations. The water surface elevation is the same at all four locations inside the bay; and the in-bay elevation is equal to the open-coast elevation. The forerunner effectively propagates into Galveston Bay, relatively un-attenuated, for this slow-moving storm.

As the eye reaches the outer edge of the continental shelf, 22 hours later at hour 348 of the simulation, the water surface elevation at the open coast has increased to 3.6 ft NAVD88 (a forerunner amplitude increase from 1.0 ft to 2.7 ft). Likewise, the water surface elevation has increased throughout the bay, with values at the four in-bay locations being nearly the same as that on the open coast or slightly less, i.e., values ranging from 3.0 to 3.6 ft NAVD88. The variability in water surface elevation inside the bay is greater at this particular time due to the increasing influence of local wind. Winds are acting on the water inside the very shallow Galveston Bay to set up or set down different parts of the bay, depending on wind direction. Wind speeds are increasing as the storm moves closer to shore, and the degree of variability in water surface elevation inside the bay increases accordingly.

At hour 360 of the simulation, the eye is midway across the Texas shelf, 12 hours before landfall. At this time, the water surface elevation at the coast is 6.1 ft NAVD88, which corresponds to a forerunner amplitude elevation of 5.2 ft. At other locations inside the bay, elevations range from 4.4 to 6.1 ft. Variability inside the bay increases as the wind speed increases.

Figure 14-42 shows the water surface elevation field at landfall for Storm 01, which occurs at hour 372 of the simulation. The location of the in-bay and open-coast transects also are shown in the figure. The surge elevation at the open coast Galveston Pleasure Pier site is 9.2 ft NAVD88. Surge elevations inside the bay are equal to or greater than this value: 9.2 ft at Galveston (bay side), 13.6 ft at Clear Lake, 10.4 ft in the vicinity of Alexander Island, and 10.8 ft in the upper Houston Ship Channel.

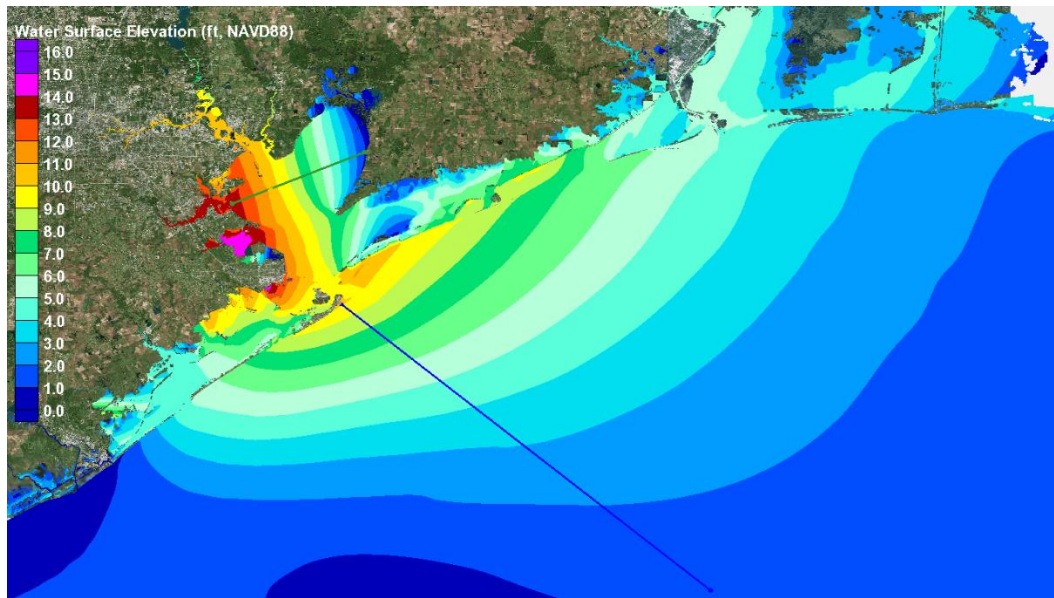


Figure 14-42. Snap shot of water surface elevation at landfall for Central Yucatan Storm 01 (6-kt forward speed).

The maximum water surface elevation on the open coast is almost 11 ft NAVD88; this value occurs just north of the north jetty at Bolivar Roads.

Inside Galveston Bay, the large gradient in water surface elevation forced by the strong winds acting on shallow water is quite evident. The maximum surge elevation at this snap shot in time occurs near Dickinson, located on the western side of the bay, where water surface elevations are between 14 and 15 ft NAVD88. On the eastern side of the bay, water surface elevations are much smaller, 1 ft NAVD88 or less, a difference in water elevation of nearly 15 ft from one side of the bay to the other. The positive elevation value on the eastern/up-wind side, and the much larger value on the down-wind/western side indicate a large amount of water already has been introduced into the bay by the time landfall occurs.

Figure 14-43 shows the spatial variation of water surface elevation along the two transects, at this same time, at landfall. On the open coast (blue curve in the figure), the elevation profile has a distinct concave-up shape, where the water surface slope increases with decreasing water depth. This profile shape is characteristic of a gently sloping inner shelf and a momentum balance that primarily involves a balance between the onshore component of the effective wind stress and the cross-shelf water surface slope. The term effective wind stress means wind stress divided by the water depth, which is how the term appears in the momentum balance.

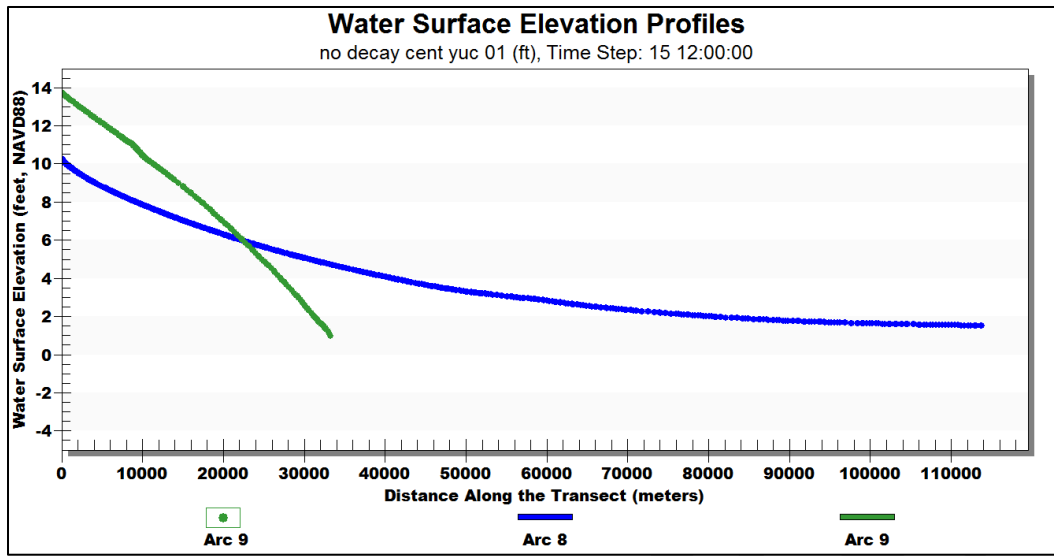


Figure 14-43. Water surface elevation profiles at landfall for the in-bay and open-coast transects, for Central Yucatan Storm 01 (6-kt forward speed).

The water surface elevation at the seaward terminus of the open-coast transect is approximately 1.5 ft NAVD88, a value that is influenced by both the wind conditions and the amount of water on the inner shelf. The latter is influenced by the forerunner surge. Water surface elevation at the coastline is about 10 ft NAVD88. The difference between elevations at the inshore and offshore ends of the open-coast transect is approximately 8.5 ft.

The shape of the water surface elevation profile inside the bay (green curve) is quite different from that on the open coast, having a nearly linear variation with distance but with a slightly concave-down shape. This shape is expected in light of the rather uniform bottom surface elevation of the bay and the predominant momentum balance between the across-bay directed effective wind stress and the water surface slope in the same direction. The slight downward concavity in shape is due to the large degree of tilt in the water surface (set up on the western side and set down on the eastern side), which leads to a greater water depth on the western side. The greater water depth leads to a reduction in effective wind stress on the western side of the bay, which in turn leads to a smaller water surface slope. This is in contrast to the eastern side where the water depth is less, so the effective wind stress is greater, and therefore the water surface slope is greater.

Figures 14-42 and 14-43 indicate that for this slow moving storm, at the time of landfall, roughly 7 additional feet of water has been added throughout Galveston Bay. The additional water is mostly due to early wind-driven forerunner surge propagation through the passes, augmented and in part by more recent flow over the barrier islands as the open coast surge elevation exceeds the land elevation on the barrier islands.

Figure 14-44 shows the peak water surface elevation map for Storm 01. Note the elevation scale is different from the scale used in Figure 14-42, in order to cover the maximum values encountered during the entire event, which exceed 21 ft NAVD88 near Houston. At all five locations, peak elevations experienced during the storm are higher than the elevations that were present at the time of landfall. Peak elevations on the open coast at the Pleasure Pier location (10.6 ft NAVD88) and at the bayside of Galveston (10.6 ft NAVD88) each occurred two hours before landfall. After landfall, winds shift rapidly and begin to push all the water that resides in Galveston Bay toward the north, and up the Houston Ship Channel where the maximum surge elevations occur. This changing wind pattern leads to even higher peak surge values at Clear Lake (14.6 ft NAVD88, 2 hours after landfall, an increase of 1.0 ft from the value here at landfall), at Alexander Island (16.1 ft NAVD88, 5 hours after landfall, an increase of 5.7 ft from the value here at landfall), and in the Upper

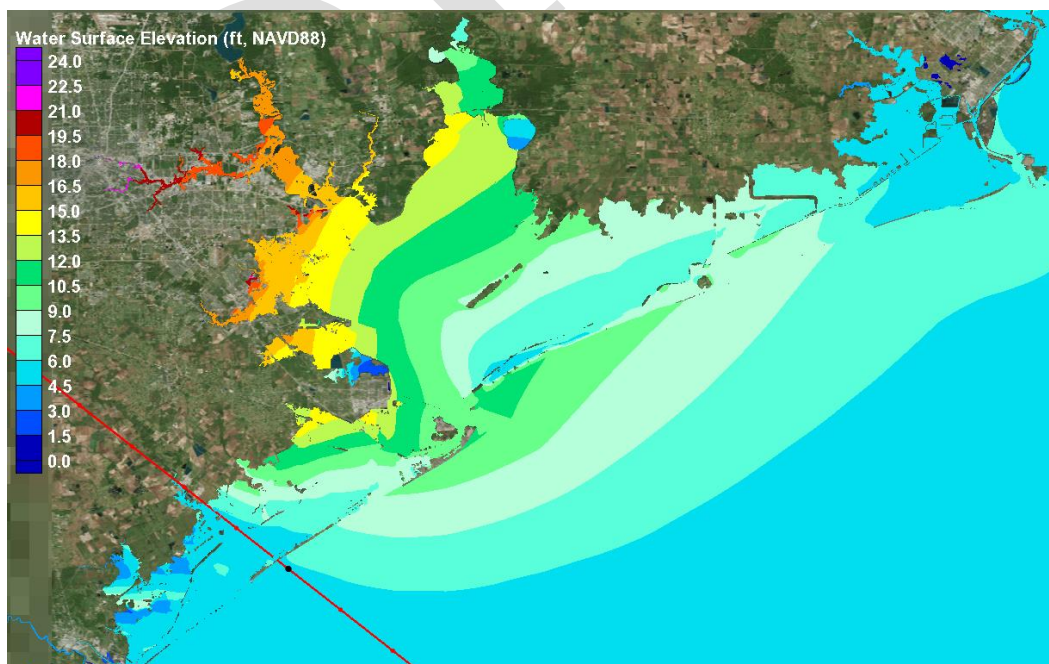


Figure 14-44. Peak water surface elevation field for Central Yucatan Storm 01 (6-kt forward speed).

Houston Ship Channel (20.5 ft NAVD88, 6 hours after landfall, an increase of 9.7 ft from the value here at landfall).

The maximum surge at the Upper Houston Ship Channel location (20.5 ft) is nearly 10 ft higher than the maximum surge elevation at the open coast. This very large elevation difference is due to the large amount of water that accumulated inside the bay before landfall, and the effectiveness of hurricane force winds in moving that water around within the bay, tilting the water surface, by setting up the water surface along the downwind side of the bay and setting it down on the upwind side of the bay. The central benefit of the Ike Dike is to substantially reduce the amount of water that enters the bay, which can then be moved about by strong winds.

Central Yucatan Storm 02 (12-kt Forward Speed)

Figure 14-45 shows results for Central Yucatan Storm 02 which has a forward speed of 12 kt, twice as fast as the speed of Storm 01. Storm 02 makes landfall at hour 188 of the simulation. As was the case with Storm 01, several days before landfall the amplitude of the forerunner begins to grow. However, the faster-moving storm leads to a forerunner growth rate that is slower than the rate for Storm 01; and therefore, the amplitude of the wind-driven forerunner surge along the Texas coast is less for the faster moving storm.

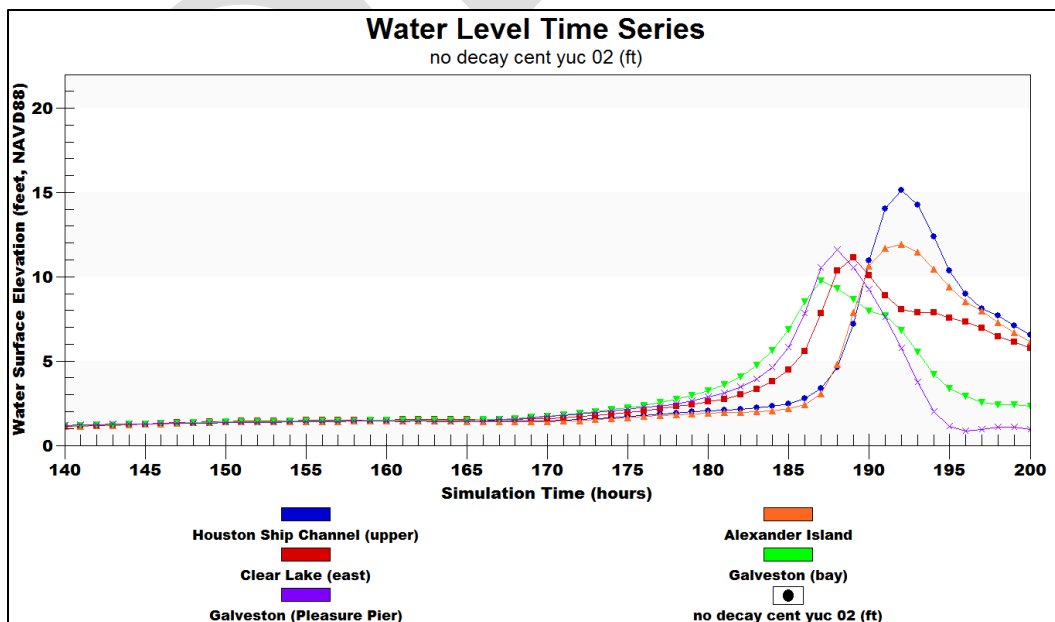


Figure 14-45. Temporal variation of water surface elevation for Central Yucatan Storm 02 (12-kt forward speed).

The eye of Storm 02 reaches the outer edge of the continental slope at hour 165, 23 hours before landfall. At this time the water surface elevation at the Galveston Pleasure Pier location is 1.4 ft NAVD88, which corresponds to a forerunner amplitude of 0.5 ft. Results for this storm also show that the forerunner effectively propagates into Galveston Bay, un-attenuated. The in-bay water surface elevations are nearly the same at all four locations, 1.4 to 1.5 ft NAVD88, and all are roughly equal to the elevation on the open coast.

As the eye reaches the outer edge of the continental shelf 11 hours later (at simulation hour 176), the water surface elevation at the open coast increases to 2.3 ft NAVD88 (corresponds to a forerunner amplitude of 1.4 ft). Likewise, elevations increase throughout the bay, with values ranging from 0.9 to 1.5 ft NAVD88 at the four in-bay locations. The elevations for Storm 02 are significantly less than elevations for the slower moving Storm 01, when the eye of both storms is at this same position. Differences in water surface elevation between the two storms are 1.2 to 1.3 ft both at the open coast location and all four locations within the bay.

At hour 182 of the simulation, the eye is midway across the Texas shelf; and the time is 6 hours before landfall. At this time, the water surface elevation at the open coast is 3.4 ft NAVD88 (corresponding to a forerunner amplitude of 2.5 ft). At locations inside the bay, water surface elevations are variable and range from 2.0 to 4.1 ft NAVD88. The increasing variability in these elevations reflects the influence of increasingly stronger local winds acting inside the bay. At all five locations, the elevations for Storm 02 are significantly less than elevations for the slower moving Storm 01, when the eye of both storms is at this same mid-shelf position. Differences between storms are 2.7 ft at the open coast and 2.0 to 2.5 ft within the bay; and, the magnitude of the differences is growing. The open coast forerunner amplitude is about half of what it was for the slowest moving Storm 01, when its eye also was situated at the mid-shelf position (2.5 ft versus 5.2 ft).

Figure 14-46 shows the water surface elevation field at landfall for Storm 02, at hour 188 of the simulation, along with the in-bay and open-coast transects. The surge elevation at the open coast Galveston Pleasure Pier site is 11.6 ft NAVD88. The surge elevation at each location inside the bay is less than this value: 9.3 ft at Galveston (bay), 10.4 ft at Clear Lake, only 4.8 ft at Alexander Island and 4.6 ft in the upper reaches of the Houston

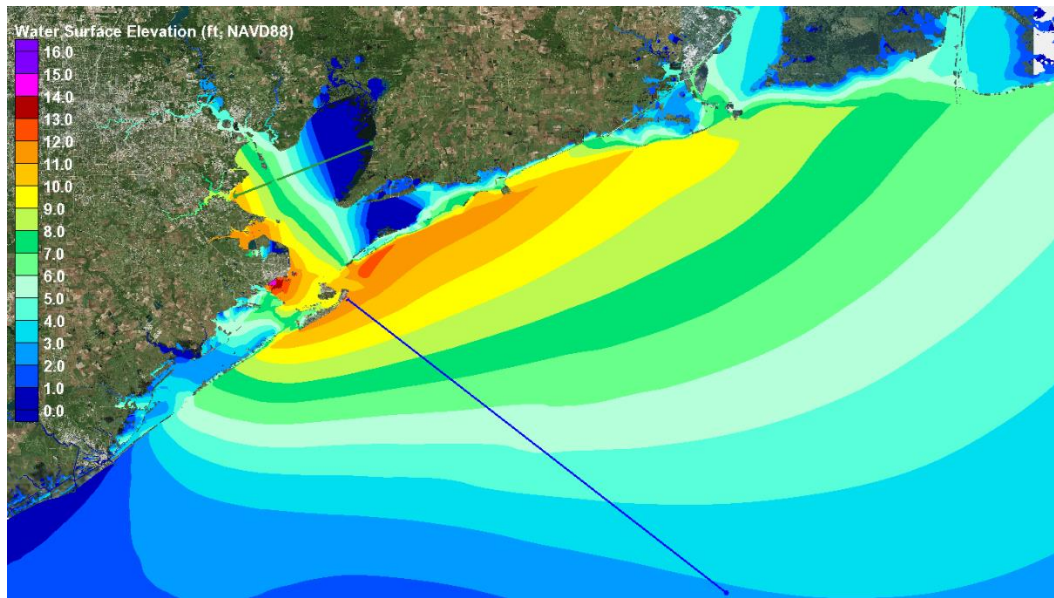


Figure 14-46. Snap shot of water surface elevation at landfall for Central Yucatan Storm 02 (12-kt forward speed).

Ship Channel. The maximum water surface elevation on the open coast is slightly greater than 12 ft NAVD88; again this value occurs just north of the north jetty at Bolivar Roads. Inside Galveston Bay, the large east-to-west gradient in the water surface elevation is evident in the figure.

Within the bay, at landfall for Storm 02, the surge elevation near Dickinson exceeds 11 ft NAVD88. Recall that, for Storm 01, the elevation at Dickinson was 14 to 15 ft. On the eastern side of the bay, water surface elevations are much smaller, compared to Storm 01, zero or negative values relative to NAVD88. This reflects a difference of nearly 11 or 12 ft from one side of the bay to the other. The lesser elevation values on both the eastern and western sides of the bay, compared to those for Storm 01, suggest that a smaller volume of water has been introduced into the bay for Storm 02, prior to landfall. This result is consistent with the lower amplitude of the wind-driven forerunner for Storm 02 seen in Figure 14-45.

Figure 14-47 shows the spatial variation of water surface elevation along the two transects, at landfall, for Storm 02. Along the open-coast transect (blue curve), the elevation profile again has a concave-up shape. This profile shape is very similar to the shape for Storm 01; both are characteristic of a gently sloping inner shelf and a momentum balance that is primarily between the onshore component of the effective wind stress and the cross-shelf water surface slope.

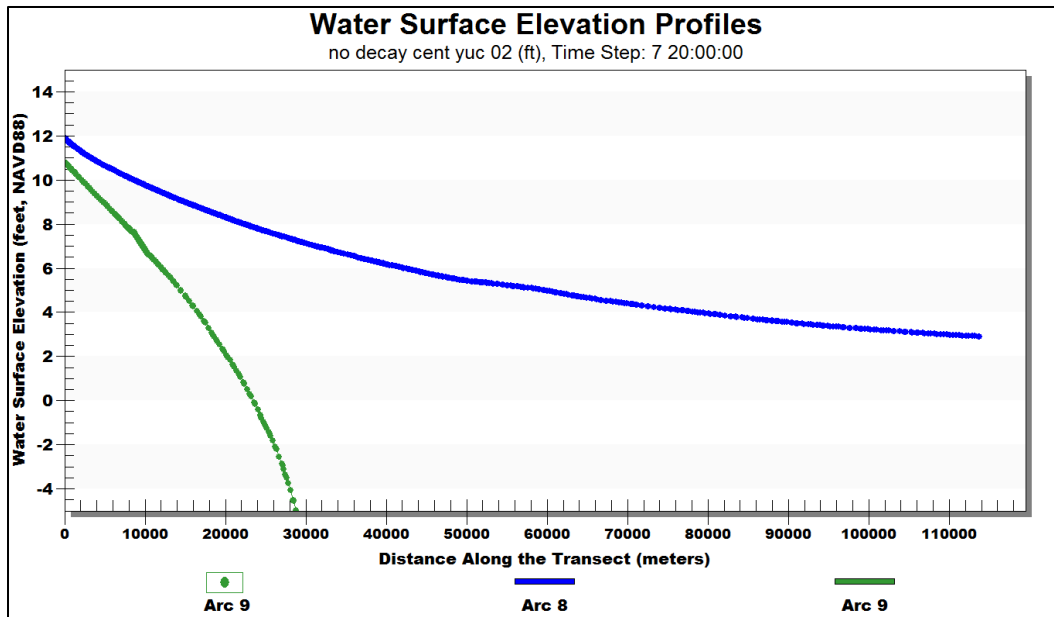


Figure 14-47. Water surface elevation profiles at landfall for the in-bay and open-coast transects, for Central Yucatan Storm 02 (12-kt forward speed).

The water surface elevation at the seaward terminus of the open-coast transect is approximately 3 ft NAVD88. This value is larger than the comparable value for Storm 01, indicating that there is more water on the inner shelf for Storm 02 than there was for Storm 01. A comparison of Figure 14-46 with 14-42, in the offshore area shown in both figures, confirms that this is the case.

The amount of water on the inner shelf is influenced by the wind-driven forerunner. The forerunner surge amplitude at the coast was less for Storm 02 than for Storm 01; however, offshore, the amplitude of the forerunner surge is greater for Storm 02 than for Storm 01. Therefore it seems that the forerunner evolution with time and the timing between forerunner development and landfall of the eye must influence the amount of water on the shelf in some way. This dynamic is examined and discussed later. The water surface elevation at the inshore end of the open-coast transect is about 12 ft NAVD88 for Storm 02; and the difference between elevations at the inshore and offshore ends of the open-coast transect is approximately 9 ft, nearly the same as it was for Storm 01.

The similarity for Storms 01 and 02, both in terms of profile shape and in elevation difference between the offshore and inshore ends of the open-coast transect, can be explained. The wind field over the shelf at this eye position is the same for both storms. The total water depths across the inner shelf are essentially the same for both storms, because small differences in water surface elevation between storms have little influence on total water depth along the transect (the total water depth influences the effective wind stress). Assuming steady state conditions on a long straight coastline/shelf, the cross-shelf shape of the water surface elevation profile is strongly influenced by a momentum balance between the effective onshore directed effective wind stress and the water surface slope. Since the effective wind stress along the transect is the essentially the same for both storms, the water surface slope along the transect also should be the same. This is why their shapes are quite similar. Deviations from a long straight coastline/shelf assumption and the unsteadiness in a moving hurricane cause small differences in the shapes of the elevation profiles. Even though the profile slopes are quite similar same, the profile for Storm 02 is shifted vertically upward compared to Storm 01 due to the presence of the additional water on the inner shelf for Storm 02.

Again, for Storm 02, the shape of the water surface elevation profile inside the bay (green curve) is quite different from the shape along the open-coast transect; and its shape is a bit different than the in-bay profile shape for Storm 01. For Storm 02, along the western side of the bay, there is a nearly linear variation in water surface elevation with distance along the transect. In contrast, the slope of the profile is much greater on the eastern side, and concave downward. This occurs because of the very shallow water on the eastern side which leads to a much greater effective wind stress and a much greater water surface slope.

Figures 14-46 and 14-47 indicate that for this faster moving storm, at the time of landfall, roughly 4 additional feet of water had been added throughout Galveston Bay. The additional water is primarily due to early wind-driven forerunner surge propagation through the passes. Because of the lower forerunner surge amplitude in general for Storm 02, the onset of flow over the barrier island would have commenced later than it did for Storm 01, lessening the contribution of barrier island overflow to the accumulation of water inside the bay.

Figure 14-48 shows the peak water surface elevation surge map for Storm 02. The peak elevation on the open coast is greater for Storm 02 than Storm 01; however, in the bay the peak elevations at all four locations are significantly less than those for Storm 01. Peak elevations on the open coast at the Pleasure Pier location (11.6 ft NAVD88) occurred at the time of landfall. At the bay side of Galveston the maximum (9.8 ft NAVD88) occurred one hour before landfall. As was the case for Storm 01, after landfall, winds shift rapidly and begin to push all the water that resides in Galveston Bay toward the north, and up the Houston Ship Channel where the maximum surge elevations occur. This changing wind pattern leads to the following peak surge values at Clear Lake (11.1 ft NAVD88, 1 hour after landfall), an increase of 0.7 ft from the value here at landfall), at Alexander Island (11.9 ft NAVD88, 4 hours after landfall, an increase of 7.1 ft from the value here at landfall), and in the Upper Houston Ship Channel (15.1 ft NAVD88, 4 hours after landfall, an increase of 10.5 ft from the value here at landfall). The maximum surge at the Upper Houston Ship Channel location (15.1 ft) is 3.5 ft higher than the maximum surge elevation at the open coast. This difference is much less than the difference for Storm 01, and the smaller difference is due to the smaller amount of water that had entered the bay prior to landfall; which was subsequently push to the north as winds shifted after landfall.

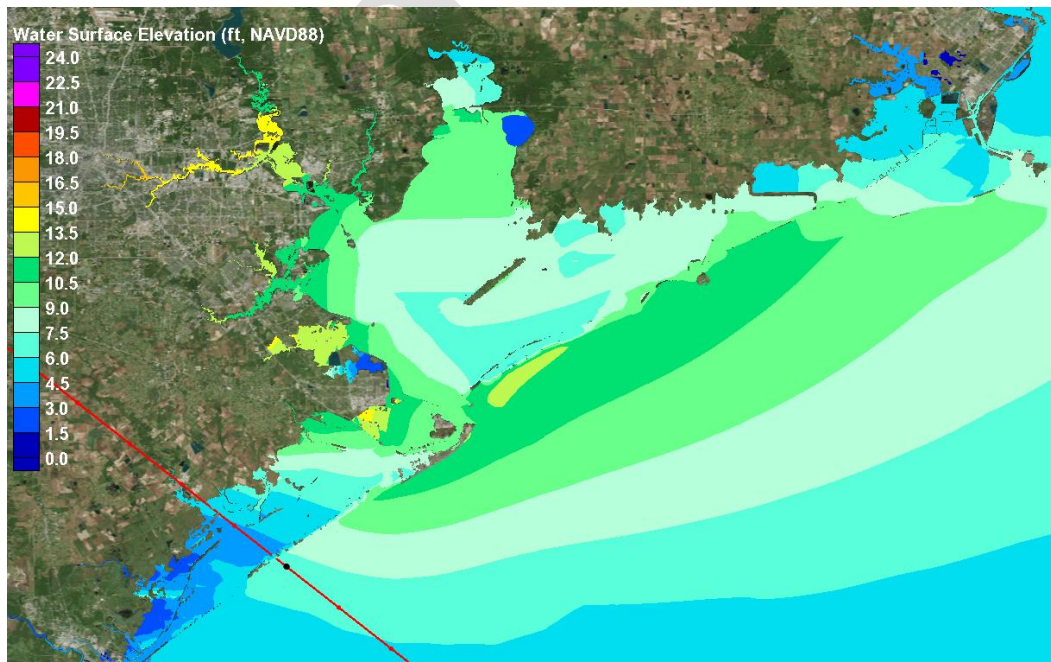


Figure 14-48. Peak water surface elevation field for Central Yucatan Storm 02 (12-kt forward speed).

Central Yucatan Storm 03 (18-kt Forward Speed)

Figure 14-49 shows the water surface elevation time series for Central Yucatan Storm 03, which moves 50% faster than Storm 02 and three times as fast as Storm 01. Storm 03 has a forward speed of 18 kt. This storm makes landfall at hour 126 of the simulation. While the storm is transiting through the Gulf, but prior to reaching the outer edge of the continental slope, the amplitude of the wind forerunner for this storm is less than the amplitude for the slowest moving Storm 01; however, the amplitude is about the same as the amplitude for the slower moving Storm 02.

The eye of Storm 03 reached the outer edge of the continental slope at hour 111, 15 hours before landfall. At this time the water surface elevation at the Galveston Pleasure Pier location was 1.4 ft NAVD88, which corresponds to a wind forerunner amplitude of 0.5 ft, the same value seen for Storm 02 for the same position of the hurricane eye. Results again show that the forerunner effectively propagates into Galveston Bay, un-attenuated; water surface elevations are nearly the same at all four in-bay locations, and all are nearly equal to the elevation value at the open coast, 1.4 ft NAVD88.

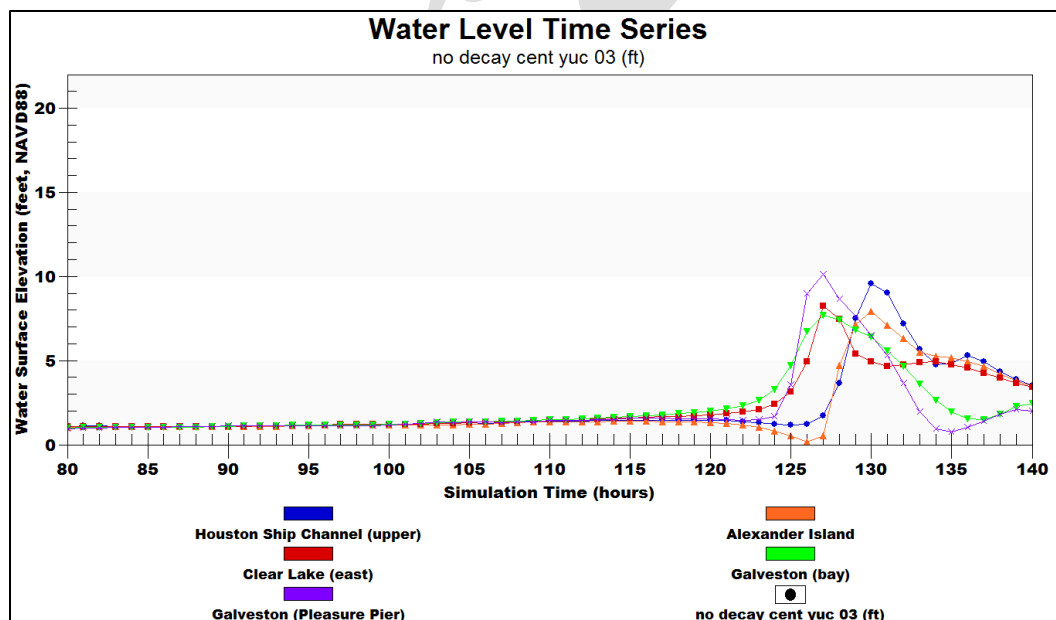


Figure 14-49. Temporal variation of water surface elevation for Central Yucatan Storm 03 (18-kt forward speed).

As the eye reaches the outer edge of the continental shelf eight hours later (at simulation hour 119), the water surface elevation value at the open coast has increased only slightly, from 1.4 to 1.5 ft NAVD88 (corresponding to a forerunner amplitude increase from 0.5 to 0.6 ft). Likewise, the forerunner amplitude has increased throughout the Bay, but only slightly, with water surface elevations values ranging from 1.3 to 1.9 ft NAVD88 at the four in-bay locations. The rate at which the forerunner amplitude is increasing is quite small, less than the rate for Storm 02 and much less than the rate for Storm 01.

This hurricane is moving very quickly across the shelf, and at hour 122 of the simulation, the eye is midway across the Texas shelf. At hour 122, just 4 hours away from landfall, the water surface elevation at the open coast, the Galveston Pleasure Pier site, is still nearly the same as it was 11 hours earlier crossing the edge of the continental slope. For this eye position, the water surface elevation at the Pleasure Pier is 2.0 ft less than it was for the slower moving Storm 02, and 4.7 ft less than it was for the slowest moving storm, Storm 01. For locations inside the bay, water surface elevations are generally higher than they are at the open coast site, ranging from 1.2 to 2.3 ft NAVD88. The variability in these elevations reflects the influence of local winds.

Figure 14-50 shows the water surface elevation field for Storm 03, at the time of landfall, which occurs at hour 126 of the simulation. At this time, the surge elevation at the open coast Galveston Pleasure Pier site is 9.0 ft NAVD88. The surge elevation at each location inside the bay at landfall is less than the open coast value, as was the case for Storm 02: 6.7 ft at Galveston (bay), 4.9 ft at Clear Lake, only 0.2 ft at Alexander Island, and only 1.2 ft in the upper reaches of the Houston Ship Channel. The maximum water surface elevation on the open coast is slightly greater than 9 ft NAVD88. As was the case for the other two storms, the maximum value occurs just north of the north jetty at Bolivar Roads.

Inside Galveston Bay, the large east-to-west gradient in the water surface elevation is evident. However, for Storm 093, the surge elevation near Dickinson is only between 6 and 7 ft NAVD88. This elevation value is much less than the 14 to 15 ft value for the 6-kt Storm 01 and 11 to 12 ft for the 12-kt Storm 02. On the eastern side of the bay, water surface elevations have negative values. The easternmost parts of the bay are

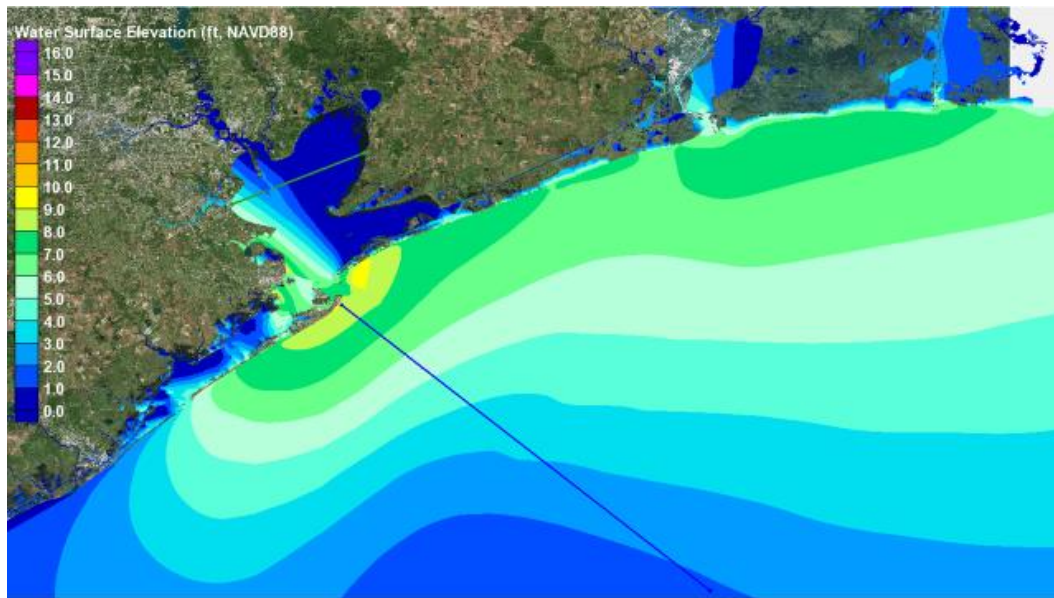


Figure 14-50. Snap shot of water surface elevation at landfall for Central Yucatan Storm 03 (18-kt forward speed).

blown dry by the strong winds. The lower elevation values on the western side of the bay, compared to those for Storms 01 and 02, even though the winds are the same at landfall, suggest that there is much less water inside Galveston Bay for storm 03 that can be moved about by the wind, just 4 hours before landfall. This result is consistent with the observed lower amplitude of the wind-driven forerunner for Storm 03, compared to the slower-moving storms, and the storm moved across the Texas shelf.

Figure 14-51 shows the spatial variation of water surface elevation along both the open-coast and in-bay transects, at landfall, for Storm 03. Along the open-coast transect (blue curve), the elevation profile again has the same concave-up shape as seen for Storms 01 and 02, where the water surface slope increases with decreasing water depth. The profile shape is very similar to the shapes for Storms 01 and 02.

Water surface elevation at the seaward terminus of the open-coast transect is approximately 2 ft NAVD88. This value is approximately 0.5 ft larger than the value for Storm 01, and 1 ft smaller than the comparable value for Storm 03, indicating that there is more/less water on the inner shelf for this storm than for Storms 01 and 02, respectively. A comparison of Figure 14-50 with Figures 14-42 and 14-46, in the offshore area, confirms that this is the case. Again, it seems that the forerunner evolution with time and the timing between forerunner development and the core wind

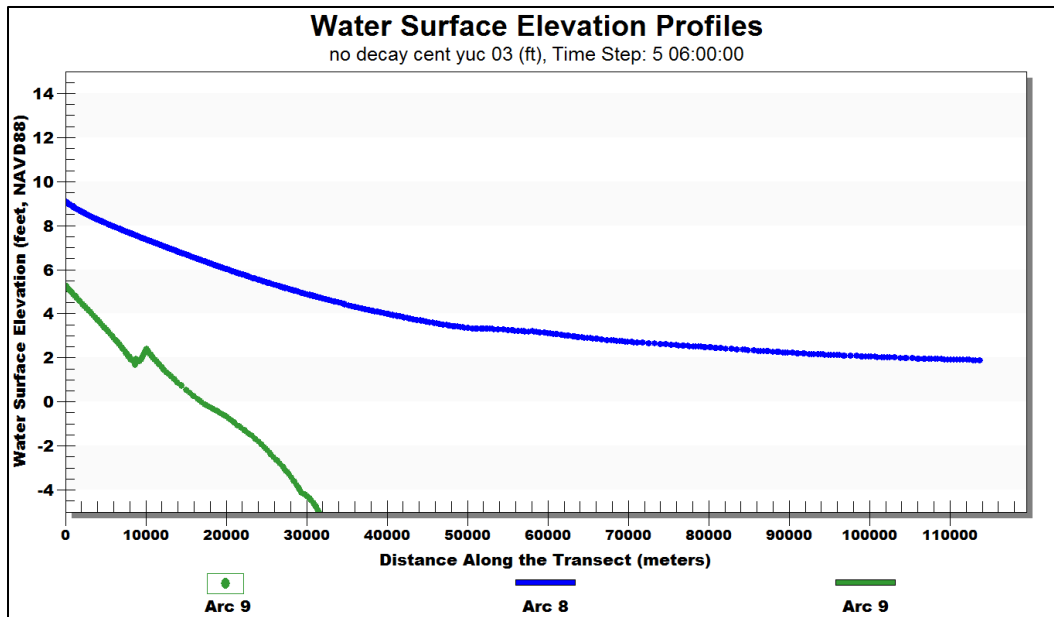


Figure 14-51. Water surface elevation profiles at landfall for the in-bay and open-coast transects, for Central Yucatan Storm 03 (18-kt forward speed).

field at landfall must influence the amount of water that is resident on the shelf at the time of landfall.

The water surface elevation at the inshore end of the open-coast transect is about 9 ft NAVD88 for Storm 03; and the difference between elevations at the inshore and offshore ends of the open-coast transect is approximately 7 ft, somewhat less than it was for Storms 01 and 02. The very fast forward speed of Storm 03 appears to influence the temporal development of the open coast storm surge on the inner shelf, seemingly reducing the peak surge at the coast. It is possible that the water on the inner shelf does not respond as quickly or fully to the imposed wind stress field for this very fast-moving storm, i.e. steady state is least achieved for Storm 03.

Again, for Storm 03, the shape of the water surface elevation profile inside the bay (green curve in figure 14-51) is quite different from the shape along the open-coast transect. The in-bay profile shape for Storm 03 is similar to the in-bay profile shape for Storm 02. For Storm 03, along the western side of the bay, there is a nearly linear variation in water surface elevation with distance along the transect. In contrast, the slope of the profile is greater on the easternmost side, and concave downward. This is the same behavior that was seen for Storm 02, and it occurs because of the very shallow water on the eastern side which leads to a much greater effective wind stress, and therefore a greater water surface slope. The small “glitch”

in the water surface elevation graph for the in-bay transect arises from wind-induced set-up/set-down on opposite sides of a dredged material placement island that is situated along the Houston Ship Channel in this area. There is much less water inside the bay at landfall for Storm 03. Water surface elevations are so small that the dredged material island is not inundated by this storm at this time in the simulation.

Figures 14-49, 14-50 and 14-51 indicate that for this very fast-moving storm, only approximately 1.5 additional feet of water had been added throughout Galveston Bay at the time of landfall. The additional water is due to early wind-driven forerunner propagation through the passes, albeit for a very small forerunner surge. Because of the very small forerunner amplitude for Storm 03, the onset of flow over the barrier island would have commenced later than it did even for Storm 02, minimizing any contribution of barrier island overflow to the accumulation of water inside the bay before the open coast surge levels quickly rose to their peak values. This occurred very rapidly because there was no gradual water surface elevation build-up because the forerunner was so small.

Figure 14-52 shows the peak water surface elevation map for Storm 03. The peak elevation on the open coast is less for Storm 03 than for Storms 02 and 01. The same is true for peak surge elevations throughout Galveston Bay. Peak elevation on the open coast at the Pleasure Pier location (10.1 ft NAVD88) occurred one hour after the time of landfall supporting the notion that the water on the inner shelf responds more slowly to the faster moving storm. At the bay side of Galveston the maximum (7.7 ft NAVD88) also occurred one hour after landfall. As was the case for Storms 01 and 02, after landfall, winds shift rapidly and begin to push all the water that resides in Galveston Bay toward the north, and up the Houston Ship Channel. This changing wind pattern leads to the following peak surge values at Clear Lake (8.3 ft NAVD88, 1 hour after landfall, an increase of 3.4 ft from the value here at landfall), at Alexander Island (7.9 ft NAVD88, 4 hours after landfall, an increase of 7.7 ft from the value here at landfall), and in the Upper Houston Ship Channel (9.6 ft NAVD88, 4 hours after landfall, an increase of 8.4 ft from the value here at landfall).

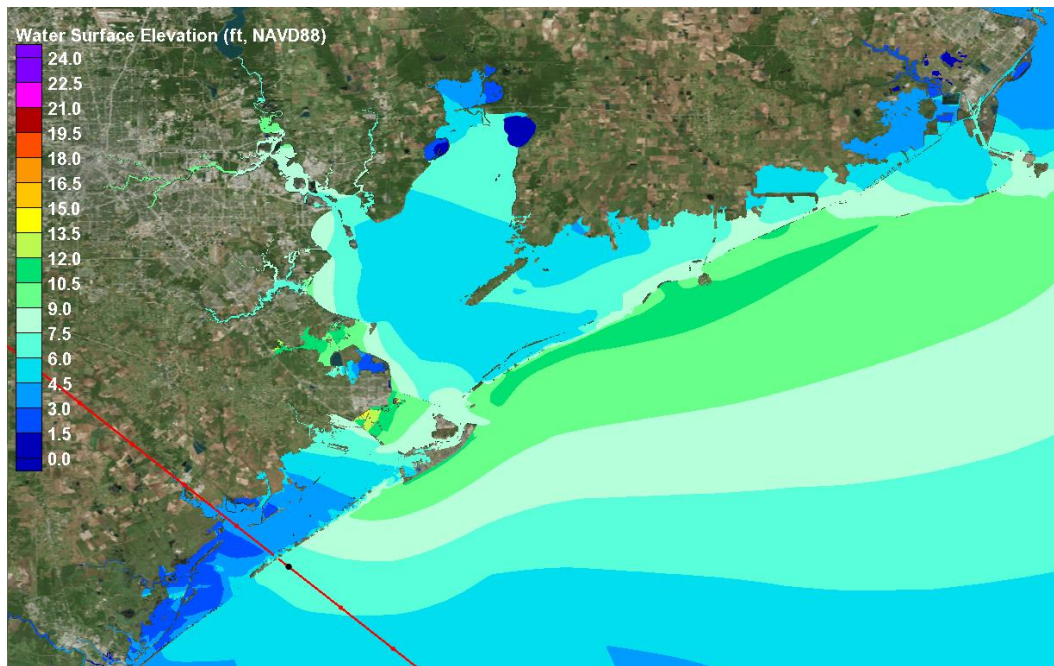


Figure 14-52. Peak water surface elevation field for Central Yucatan Storm 03 (18-kt forward speed).

The maximum surge value on the open coast at the Galveston Pleasure pier location was the least for Storm 03 (10.1 ft BAVD88) among the three storms (maximums for Storms 01 and 02 were 10.6 and 11.1 ft, respectively). At the open coast peak surge appears to have only a small sensitivity to forward speed. No clear trend in the open coast maxima was evident in terms of dependency on forward speed. The greatest open coast surge occurred for the 12-kt forward speed, with lesser values for the 6- and 18-kt storms. Reasons for the observed dependency of maximum surge level on forward speed is examined in the following section.

Peak surge values inside Galveston bay for the 18-kt Storm 03 are considerably less than those inside the Bay for the slower moving 12- and 6-kt storms. Even though the peak surge elevations at the open coast were quite similar for the three storms, peak surge values in the upper Houston Ship Channel were quite dissimilar, 20.5 ft, 15.1 ft and 9.6 ft NAVD88 for the same three storms, Storms 01, 02 and 03, respectively. The same trend is seen for all the in-bay locations: Alexander Island (16.1, 11.9, 7.9 ft for Storms 01, 02 and 03), Clear Lake (14.6, 11.1, 8.3 ft for Storms 01, 02 and 03) and the bay side of Galveston (10.6 ft, 9.8 ft, 7.7 ft for Storms 01, 02 and 03). This is a direct result of the much lower forerunner surge amplitudes that occur for the faster moving storms, which leads to much

less accumulation of water inside Galveston Bay prior to landfall, and less water to be moved around by local winds.

Clearly, the more water that enters the bay during forerunner build-up, the more is available to be forced by the local winds, which leads to increased wind setup on the downwind sides of the bay. The development of the forerunner surge amplitude on the open coast and inside the bays is highly sensitive to forward speed. In general, the faster the forward speed the less the forerunner amplitude, and the less accumulation of water inside the bays at the time of landfall due to propagation of the forerunner into the bays. Little attenuation of the forerunner occurs through the passes, for the range of forward speeds that were examined. A critical aspect of the Ike Dike surge barrier operations will be minimization of the surge forerunner within the Bay through early gate closure. Early gate closure will be crucial for slow-moving storms.

Evolution of the Wind-Driven Forerunner and Interaction with the Hurricane's Core Winds

The dynamics of forerunner development for the three storms was examined further to better understand the cause for some of the observations made concerning dependencies of forerunner surge and peak surge on forward speed. The analysis focused on the dynamics that lead to a decreasing forerunner amplitude with increasing forward speed. Also, the interaction of the forerunner with formation of the peak surge associated with the hurricane's core winds was examined, to better understand the reason(s) for why the maximum open coast peak surge occurred for the hurricane having the 12-kt forward speed, the middle value of the three speeds that were considered.

The first series of four figures, Figures 14-53 through 14-57, show snapshots in time of the water surface elevation field for Central Yucatan Storm 01, which had the slowest forward speed, 6 kt. Subsequent series of four figures each will show results for the other two storms. The color scale adopted for each of these figures, having a maximum elevation value of only 8 ft, was selected to enhance elevation resolution of the wind-driven forerunner surge. In each of these figures, the red line shows the storm track and the three darker dots which are evident on the track denote key positions of the storm, the outer edge of the continental slope, the outer edge of the continental shelf, and the location at landfall.

The first snap shot, Figure 14-53, shows Storm 01, the slowest moving storm of the three, when its eye is positioned at the outer edge of the continental slope. This position is denoted by the most offshore dark dot that is identifiable on the storm track. The location of the hurricane eye is readily identified by the circular dome of water, the region of raised water surface elevation, which is located directly beneath the eye and centered on the most offshore dot. The dome of water under the eye is due to atmospheric pressure gradients that force water from the periphery of the storm (regions of higher atmospheric pressure) toward the center (the region of lowest atmospheric pressure).

The wind-driven forerunner along the Louisiana and north Texas shelves is quite evident by the lighter blue color contour in this region. Water surface elevations are between 1.5 and 2.0 ft NAVD88 in this region. Even along the south Texas shelf there is evidence of the wind-driven forerunner, i.e., the region having water surface elevations between 1 and 1.5 ft that follows the shelf. The presence of the wind-driven forerunner surge this far south along the Texas coast is consistent with results from the volume mode forerunner analysis for this same slow-moving storm, that were presented earlier in this chapter. Slow moving severe hurricanes that approach from the southeast appear to be quite effective in generating a significant wind-driven forerunner along the entire Texas coast.

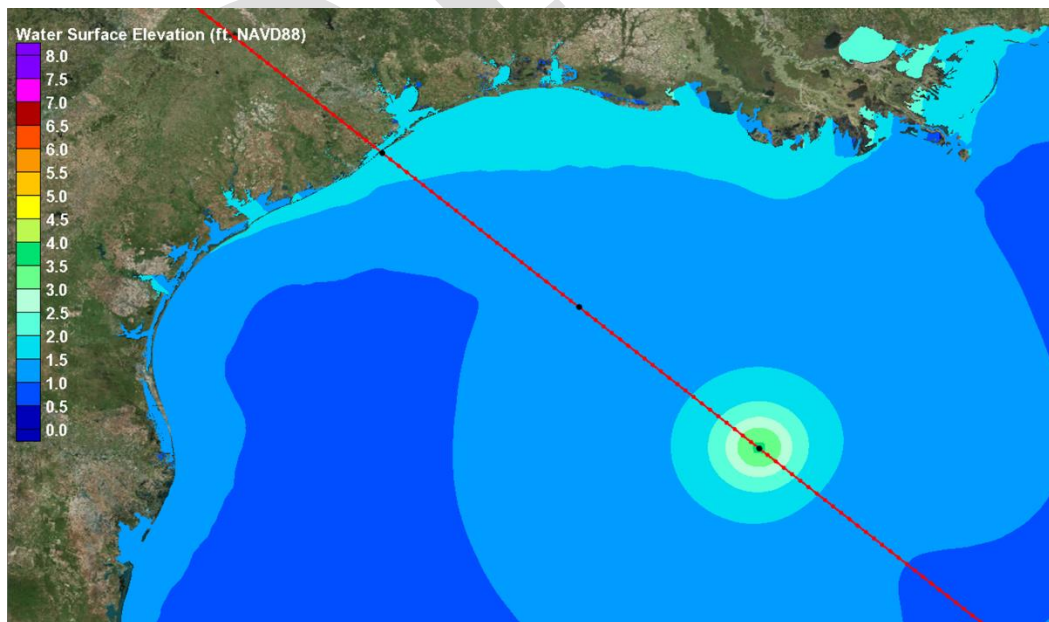


Figure 14-53. Water surface elevation map to depict the wind-driven forerunner surge on the Louisiana-Texas shelf for Central Yucatan Storm 01, when the hurricane eye is positioned at the outer edge of the continental slope.

Figure 14-54 shows a snap shot taken 22 hours later, when the eye has moved to the outer edge of the continental shelf. Considerable growth in the wind forerunner has occurred along the entire Louisiana-north Texas shelf, with water surface elevations of approximately 3.5 ft NAVD88 Galveston. The zone of maximum forerunner surge elevation, having elevations that exceed 3.5 ft, is occurring near Sabine Pass. The wind-driven forerunner south of the storm track is growing in extent and amplitude, indicating movement of a considerable volume of water southwestward along the Texas shelf driven by winds blowing along the coast, from Louisiana toward south Texas, in advance of the approaching eye.

Figure 14-55 shows a snap shot taken 12 hours later, when the eye has moved midway across the continental shelf. Considerable growth in the wind forerunner continues, with water surface elevations of approximately 6.0 ft NAVD88 at Galveston. Note that, compared to conditions 12 hours earlier, the region of highest forerunner surge along the north Texas coast is migrating toward the west, toward Galveston. The maximum forerunner surge elevations of 6.5 ft NAVD88 are occurring at Sabine Pass and Bolivar Roads. Again, considerable water is moving along the shelf toward south Texas, moving south of the track, in advance of the approaching eye. In response, the amplitude and extent of the forerunner along the south Texas shelf continues to grow.

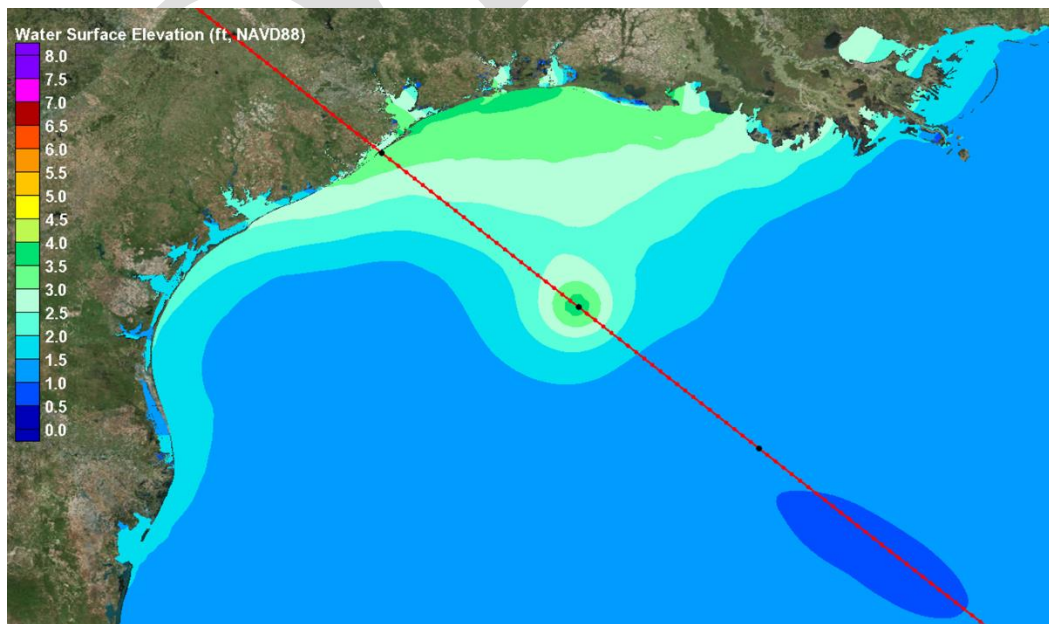


Figure 14-54. Water surface elevation map to depict the wind-driven forerunner surge on the Louisiana-Texas shelf for Central Yucatan Storm 01, when the hurricane eye is positioned at the outer edge of the continental shelf.

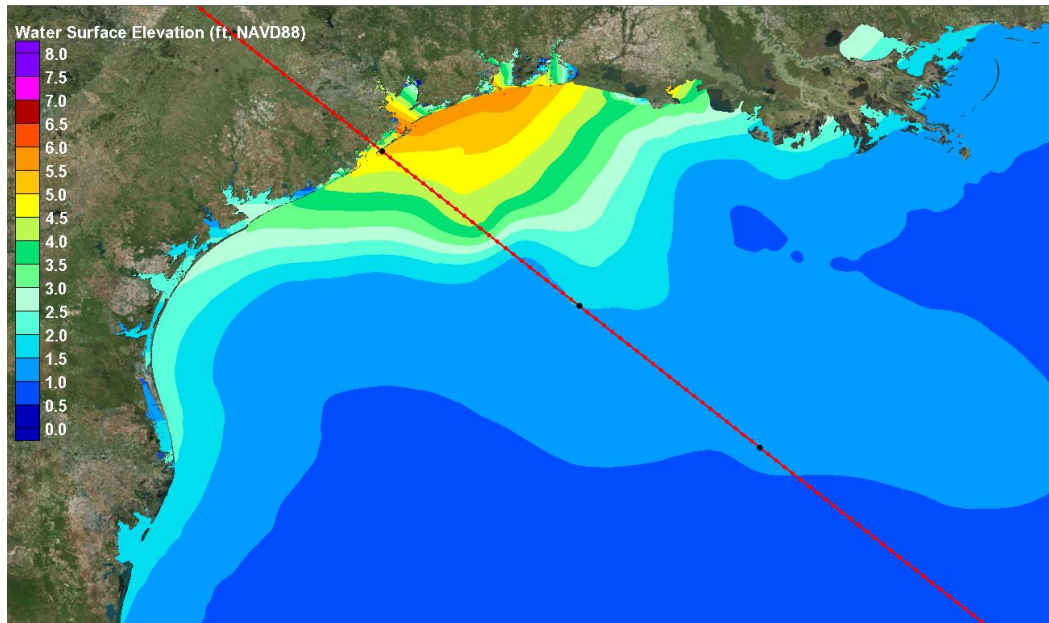


Figure 14-55. Water surface elevation map to depict the wind-driven forerunner surge on the Louisiana-Texas shelf for Central Yucatan Storm 01, when the hurricane eye is positioned in the middle of the continental shelf, just before landfall.

Figure 14-56 shows a snap shot taken 12 hours later, when the hurricane has just made land fall and the eye is positioned right at the coastline near San Luis Pass. Note that, compared to conditions 12 hours earlier, the region of highest surge has migrated further toward the west, and is situated along Bolivar Roads and Bolivar Peninsula. Again, evidence persists of considerable water movement along the Texas shelf and the presence of a significant forerunner surge in south Texas, well south of the track, although the amplitude is decreasing. The progression of snapshots clearly shows that a substantial amount of water moved to the southwest, from the Louisiana shelf to the Texas shelf, and to south of the landfall location, as the slowest moving Storm 01 moved across the shelf and approached landfall.

The next series of four figures, Figures 14-57 through 14-60, are for Central Yucatan Storm 02, which has a 12-kt forward speed. The four figures correspond to the same four eye positions along the storm track, albeit the storm is moving twice as fast as Storm 01 along the same track. The first snap shot in the series, Figure 14-57, shows Storm 02 when its eye is positioned at the outer edge of the continental slope. There is evidence of a small wind-driven forerunner surge along the entire Louisiana shelf and the entire Texas shelf. The amplitude of the forerunner is less than the amplitude for the slower moving Storm 01 throughout this entire region (compare this figure to Figure 14-53).

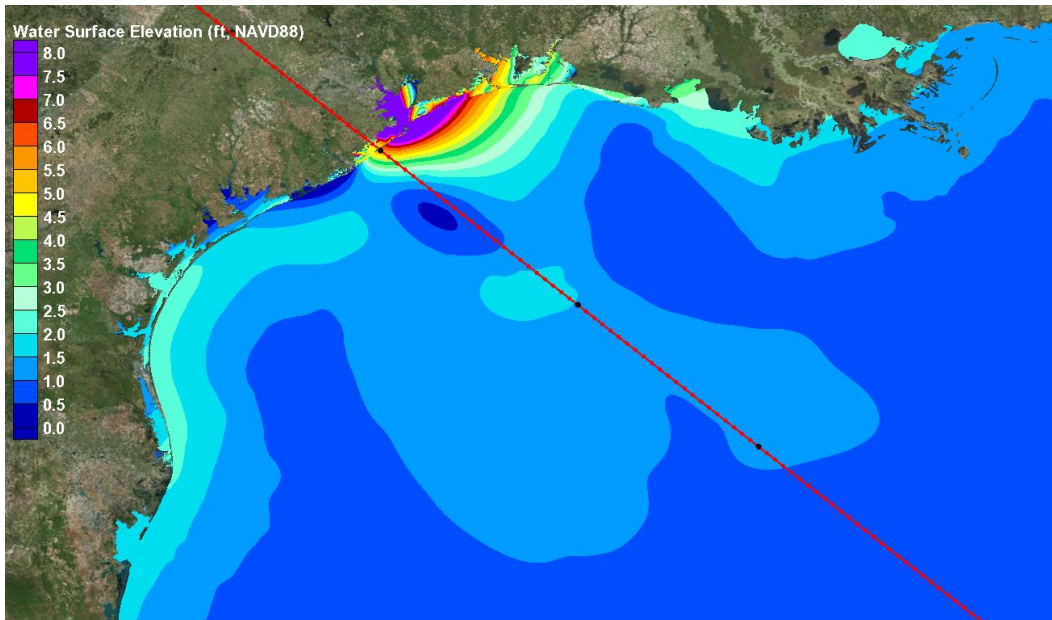


Figure 14-56. Water surface elevation map to depict the wind-driven forerunner surge on the Louisiana-Texas shelf for Central Yucatan Storm 01, when the center of the hurricane eye crosses the shoreline.

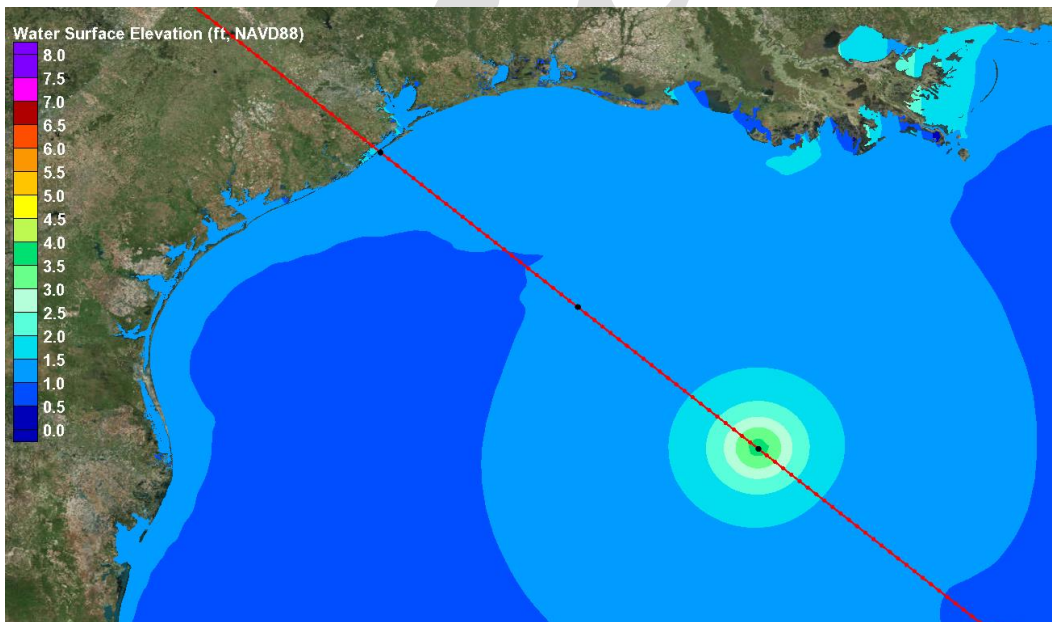


Figure 14-57. Water surface elevation map to depict the wind-driven forerunner surge on the Louisiana-Texas shelf for Central Yucatan Storm 02, when the hurricane eye is positioned at the outer edge of the continental slope.

The maximum water surface elevation associated with the wind-driven forerunner along the north Texas coastline is less than 1.5 ft NAVD88, which corresponds to a forerunner amplitude of less than 0.6 ft.

Figure 14-58 shows a snap shot taken 11 hours later, when the eye has moved to the outer edge of the continental shelf. As was the case for Storm 01, growth in the wind forerunner has occurred along the entire Louisiana-north Texas shelf during this time, with maximum water surface elevations being slightly above 2.5 ft NAVD88 just seaward of the Atchafalaya Bay in Louisiana. This maximum elevation value is less than the 3.5 ft maximum for Storm 01 for this same storm position. For Storm 02, the maximum forerunner surge elevation at Galveston is less than 2.5 ft NAVD88, compared to 3.5 ft for Storm 01. Also, note that for the faster moving storm, Storm 02, the region of maximum water surface elevation associated with the forerunner is located well to the east of where the zone of maximum forerunner surge was located for Storm 01 at this same eye position. The slower speed of Storm 01 allowed the wind-driven forerunner to develop sooner and more fully, enabling the zone of maximum forerunner surge to migrate further westward by the time the storm reached this position.

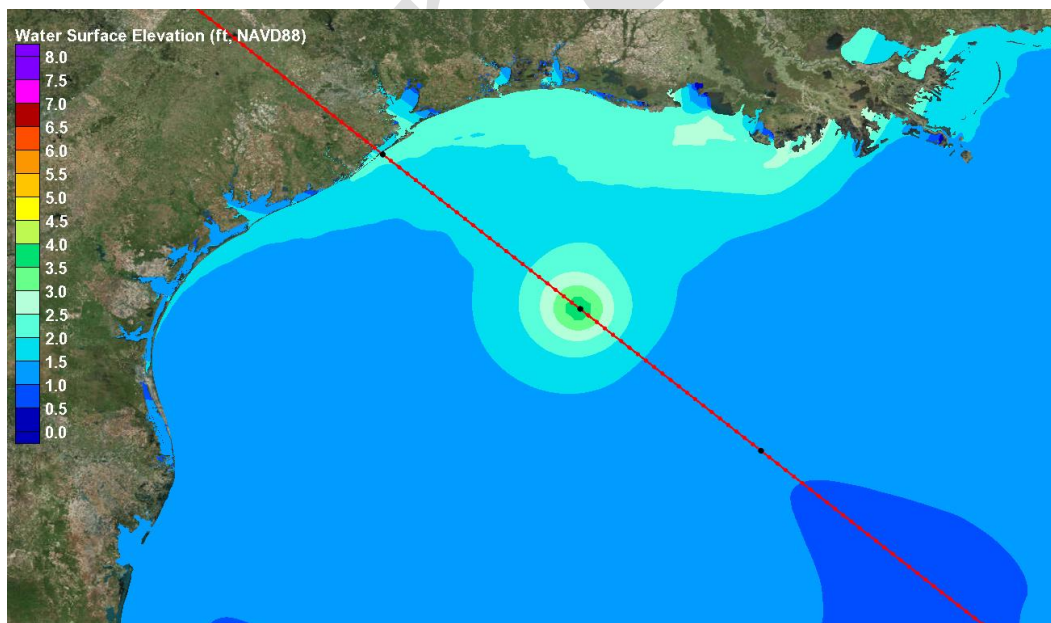


Figure 14-58. Water surface elevation map to depict the wind-driven forerunner surge on the Louisiana-Texas shelf for Central Yucatan Storm 02, when the hurricane eye is positioned at the outer edge of the continental shelf.

For Storm 02, the presence of the wind-driven forerunner south of the storm track is also evident. However, the amount of water that has moved to the southwest, past Galveston and south of the track, and the amplitude of the wind forerunner south of Galveston, is much less for the faster Storm 02 than it was for the slower moving Storm 01 (compare Figure 14-58 with Figure 14-54) south of the storm track. Much more of the water put in motion by the wind along the Louisiana and north Texas shelves resides north of the storm track line for Storm 02, when the eye of the storm is at this location.

Figure 14-59 shows a snap shot taken 6 hours later, when the eye of Storm 02 has moved midway across the continental shelf. Considerable growth in the wind forerunner is evident north of the track line, with water surface elevations of approximately 3.5 ft NAVD88 at Galveston (compared to 5.5 ft for Storm 01) and a maximum forerunner surge elevation of 5.0 ft NAVD88 just south of Lake Calcasieu, Louisiana. Note that, compared to conditions 6 hours earlier, the region of highest forerunner surge along the north Texas coast is migrating toward the west, toward Galveston. Water is moving along the shelf toward south Texas, moving south of the track line, in advance of the approaching eye. In response, the amplitude and extent of the forerunner along the south Texas shelf continues to grow. However the size and amplitude of the wind-driven forerunner is less that is was for the slower moving Storm 01.

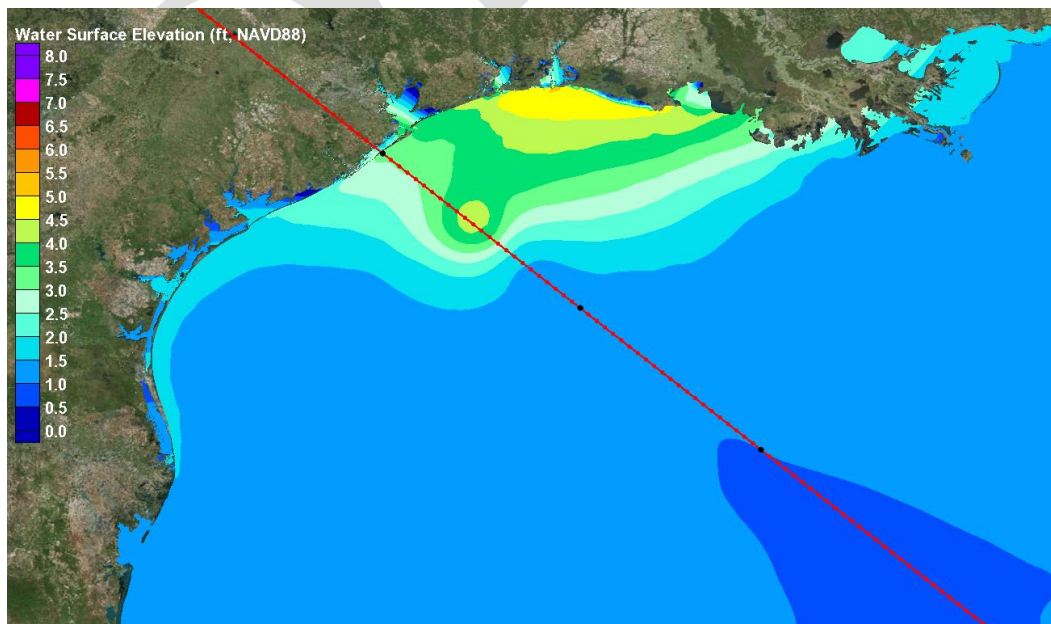


Figure 14-59. Water surface elevation map to depict the wind-driven forerunner surge on the Louisiana-Texas shelf for Central Yucatan Storm 02, when the hurricane eye is positioned in the middle of the continental shelf, just before landfall.

Figure 14-60 shows a snap shot taken 6 hours later, the time of landfall. Compared to conditions 6 hours earlier, the region of highest surge has translated further toward the west, and is situated along the Bolivar Roads and Bolivar Peninsula area. Again, evidence persists of water movement in the southwest direction along the Texas shelf and the presence of a forerunner surge along the south Texas shelf, although the amplitude is decreasing. The progression of snap-shots shows some movement of water to the southwest, moving from the Louisiana shelf to the Texas shelf and to south of the track line, as was seen for the slower Storm 01; however much less southwesterly movement occurred for Storm 02. Interestingly, for Storm 02, even though the forerunner surge amplitude was generally smaller than for Storm 01, along the open coast the surge elevation is higher in the maximum surge zone north of the track line, and the extent of the highest surge zone is greater for Storm 02, compared to Storm 01 (compare Figures 14-56 and 14-60). Apparently, the timing of the westward alongshore migration of the maximum surge forerunner zone and the arrival of the hurricane eye and its core winds is somewhat synchronous for the faster 12-kt Storm 02, producing slightly larger open coast surge elevations at the time of landfall (11.6 ft NAVD88) compared to those for Storm 01 (9.2 ft NAVD88). For the slower moving Storm 01, a substantial forerunner surge propagated westward and then to the southwest, past the Galveston Bay region, and well in advance of the

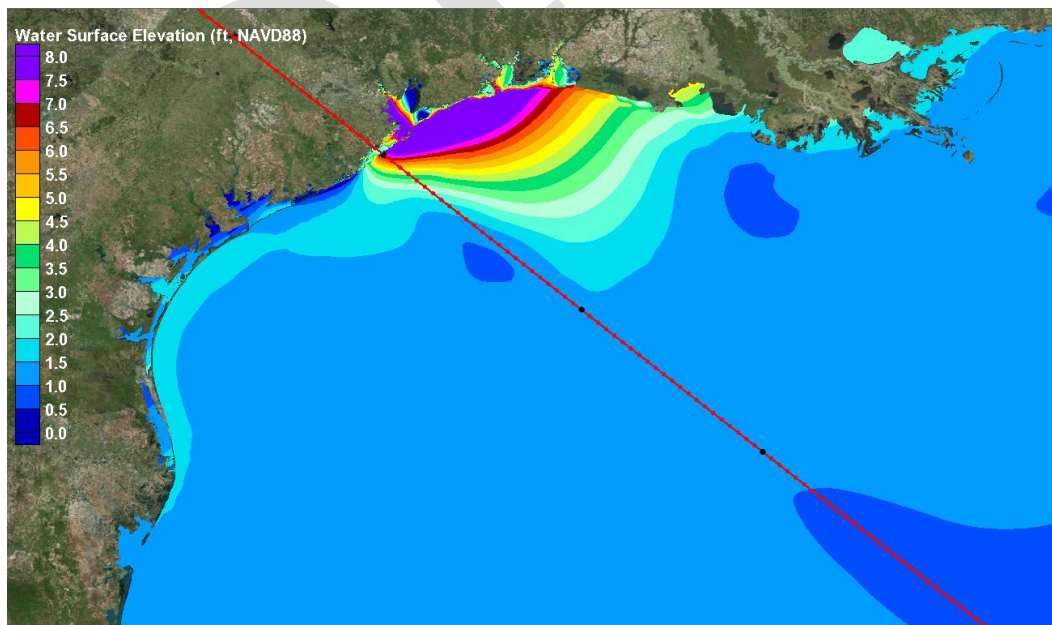


Figure 14-60. Water surface elevation map to depict the wind-driven forerunner surge on the Louisiana-Texas shelf for Central Yucatan Storm 02, when the center of the hurricane eye crosses the shoreline.

arriving hurricane core winds, apparently slightly lessening the peak surge elevation that occurred at the time of landfall for Storm 01.

The last series of four figures, Figures 14-61 through 14-64, are for Central Yucatan Storm 03, the fastest moving of the three storms, which has an 18-kt forward speed. The four figures correspond to the same four eye positions along the storm track. Note that Storm 03 moves three times as fast as Storm 01, and 50% faster than Storm 02, along the same track.

The first snap shot, Figure 14-61, shows Storm 03 when its eye is positioned at the outer edge of the continental slope. The water surface elevations in the Houston-Galveston region for this storm are quite similar to those observed for Storm 02. The maximum water surface elevation associated with the wind-driven forerunner along the north Texas coastline is less than 1.5 ft NAVD88. At Galveston Pleasure Pier, the water surface elevation is 1.4 ft NAVD88, which corresponds to a forerunner amplitude of 0.5 ft.

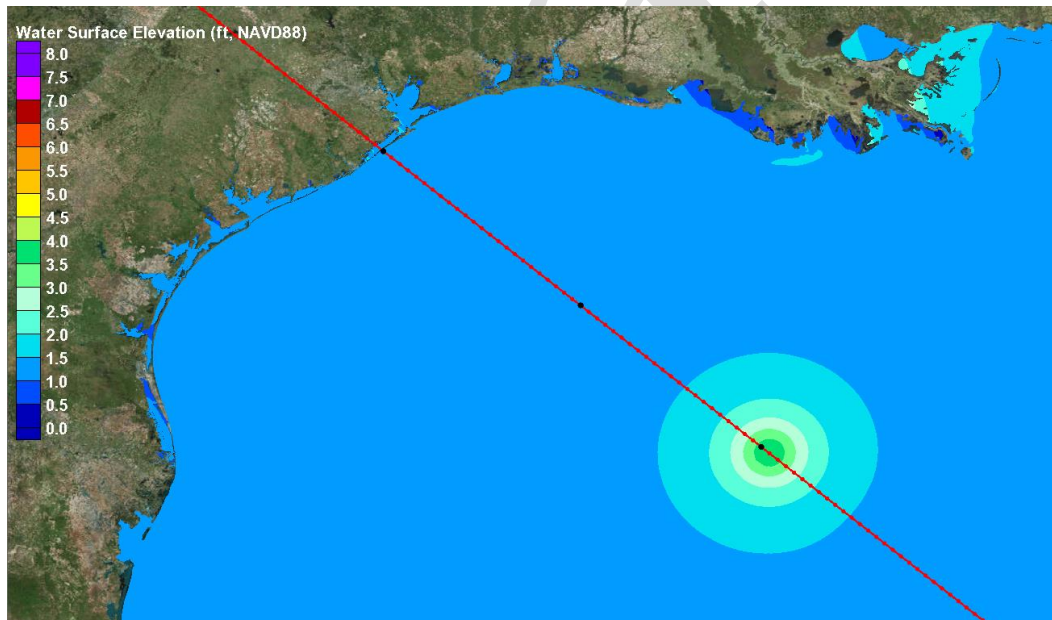


Figure 14-61. Water surface elevation map to depict the wind-driven forerunner surge on the Louisiana-Texas shelf for Central Yucatan Storm 03, when the hurricane eye is positioned at the outer edge of the continental slope.

Figure 14-62 shows a snap shot taken 8 hours later, when the hurricane's eye has moved to the outer edge of the continental shelf. Unlike the other two slower-moving storms, no significant forerunner is evident along the westernmost Louisiana coast. The highest forerunner surge, where water surface elevations are 2.5 ft NAVD88, is developing along the Louisiana coast but much further to the east, east of the Atchafalaya Bay in the vicinity of the Mississippi River Bird's Foot delta. Also there is some evidence of a slowly growing, but still a very small, forerunner surge along the Texas coast near Galveston Island. At Galveston Pleasure Pier, the water surface elevation is 1.5 ft NAVD88, slightly higher than 8 hours earlier, and much less than forerunner surge at the same location for Storms 01 and 02, 3.6 ft and 2.3 ft, respectively, for the same eye position. Compared to Storms 01 and 02, the development of the forerunner surge for this fast-moving storm is occurring much later and it is much less developed in terms of its amplitude.

Figure 14-63 shows a snap shot taken 3 hours later, when the eye of Storm 03 has moved midway across the continental shelf. Growth in the wind-driven forerunner surge is evident further to the east along the Louisiana coast, with water surface elevations reaching between 3 and 3.5 ft NAVD88. There is still no appreciable forerunner surge at Galveston Pleasure Pier, where the water surface elevation remains nearly constant

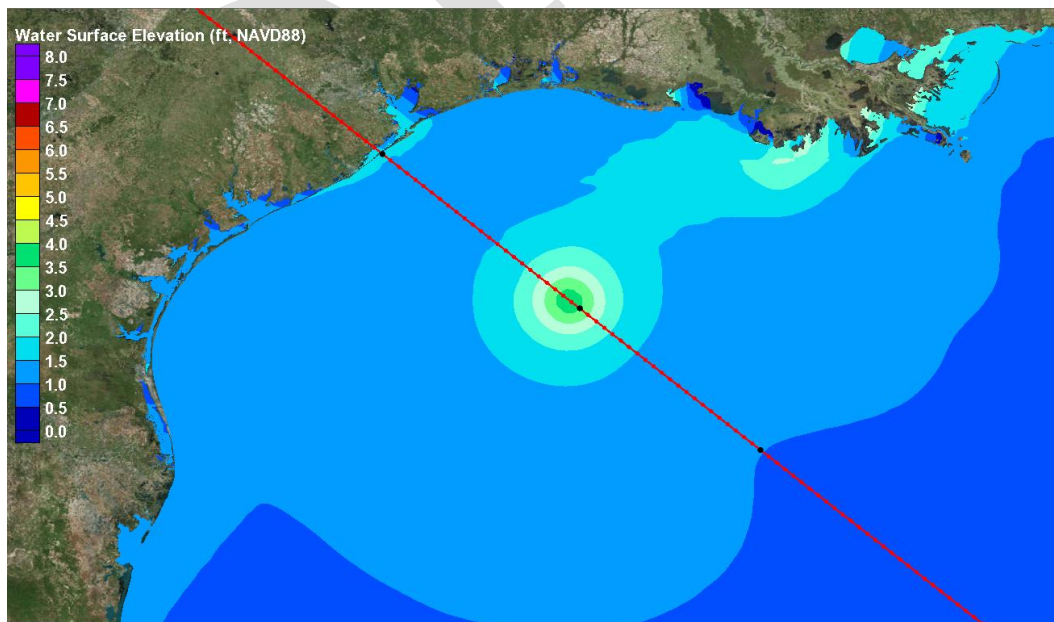


Figure 14-62. Water surface elevation map to depict the wind-driven forerunner surge on the Louisiana-Texas shelf for Central Yucatan Storm 03, when the hurricane eye is positioned at the outer edge of the continental shelf.

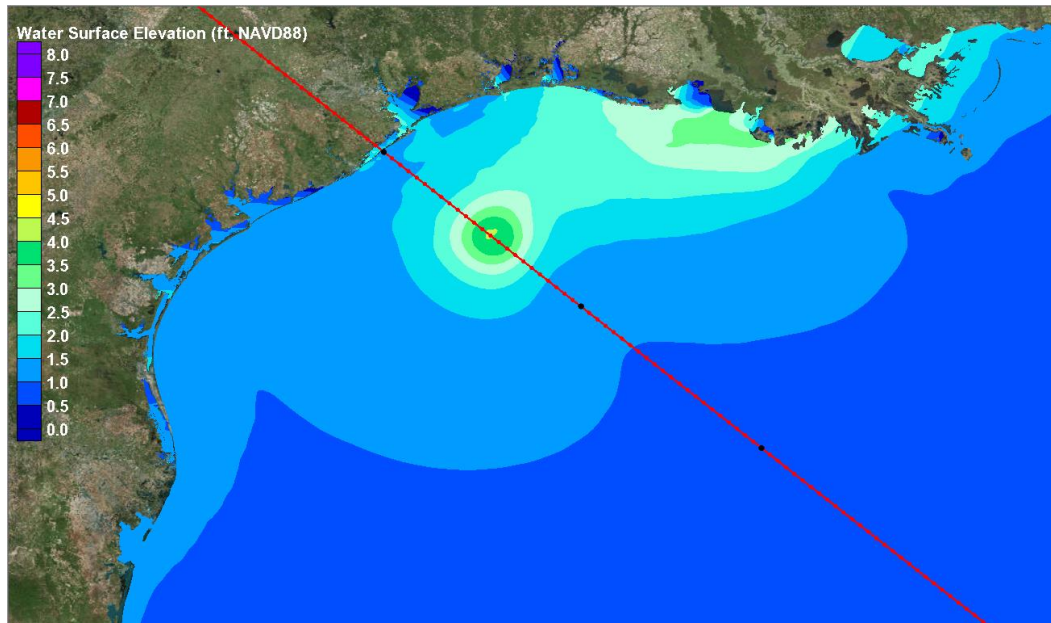


Figure 14-63. Water surface elevation map to depict the wind-driven forerunner surge on the Louisiana-Texas shelf for Central Yucatan Storm 02, when the hurricane eye is positioned in the middle of the continental shelf, just before landfall.

with a value of 1.4 ft NAVD88. Compare this small value with values of 6.1 and 3.4 ft NAVD88, for Storms 01 and 02, at the same eye position. The western edge of the forerunner surge seems to be located at Sabine Pass.

Figure 14-64 shows a snap shot taken 4 hours later, the time of landfall. Compared to conditions 4 hours earlier, the region of highest forerunner surge has migrated further toward the west, and is situated at Sabine Pass. There are two separate areas of local surge maxima seen in the figure: the forerunner surge peak that is located just east of Sabine Pass, and a core winds-associated peak located at Bolivar Roads and Bolivar Peninsula. Compared to Storm 02, in which the westward alongshore movement of the maximum surge forerunner zone and the arrival of the hurricane eye and its core winds were somewhat synchronized and produced slightly larger open coast surge elevations at Galveston Pleasure Pier at the time of landfall (11.6 ft NAVD88), the lag in arrival of the maximum forerunner surge leads to a lower peak elevation at the Pleasure Pier location, 9.0 ft NAVD88. This value is slightly less than the value for the slowest-moving Storm 01, 9.2 ft NAVD88.

The faster the forward speed, the later the development of the forerunner surge occurs on the Louisiana and north Texas shelves. The later forerunner development means later westward migration, which leads to a smaller amplitude of forerunner surge along the Texas coast.

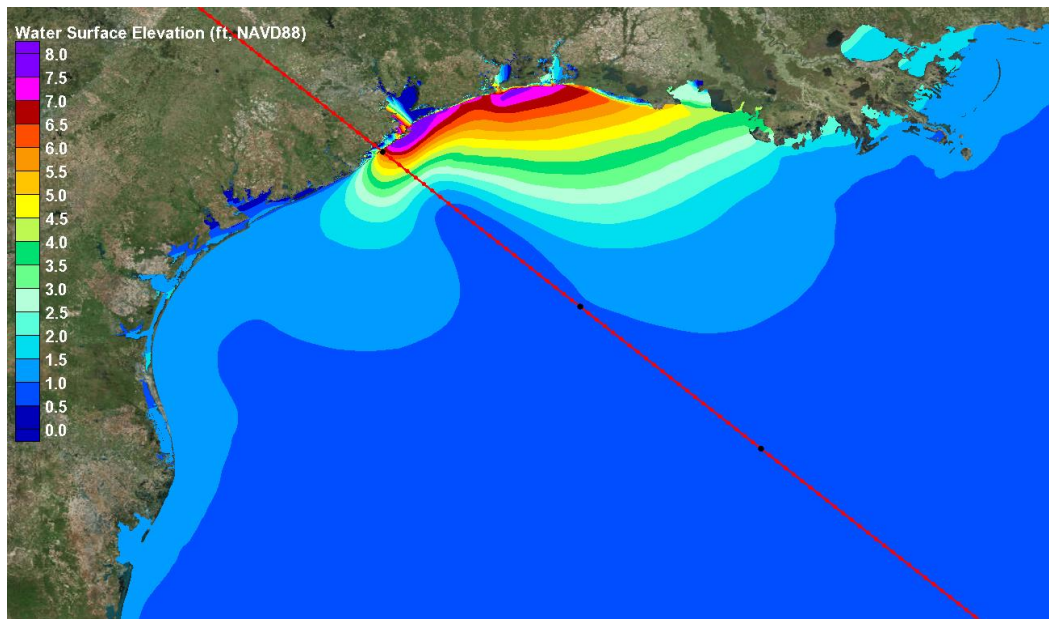


Figure 14-64. Water surface elevation map to depict the wind-driven forerunner surge on the Louisiana-Texas shelf for Central Yucatan Storm 03, when the center of the hurricane eye crosses the shoreline.

The forward speed of 12 knots (Storm 02) seems to enhance the storm surge at Galveston, due to apparent convergence of the development and westward migration of the wind-driven forerunner along the Louisiana and north Texas shelves and the arrival of high surge zone that is associated with the arrival of the hurricane's core winds on the inner shelf. This convergence leads to much more water on the inner shelf and higher peak surge levels at the shoreline. For the slowest moving storm (6-kt forward speed, Storm 01), the development of the forerunner surge and its westward migration occurred much sooner and much of the forerunner surge propagated south of the Houston-Galveston region before the core winds arrived at the inner shelf, slightly lessening the peak surge at Galveston. For the fastest moving storm (18-kt forward speed, Storm 03), the surge forerunner was latest in development and westward migration, and the peak forerunner surge arrived later than the high surge zone associated with the core winds. This lag in time between the two surge features also lessened the peak surge at Galveston, compared to the 12-kt storm, Storm 02.

Summary

Early closure of the storm surge gates at both San Luis and Bolivar Roads Passes is a critical operational feature of the Ike Dike concept. The amount of water within Galveston and West Bays at the time of gate closure

influences the peak surge elevation that will be generated by local hurricane force winds that still act on the bays after the gates are closed. A higher antecedent water level in the bays leads to a higher peak surge within the bays, and thus a greater residual flood risk. The following contributors influence the antecedent water level: long-term and seasonal and long-term mean sea level, astronomical tide, wind-driven surge forerunner, and volume mode forerunner.

The long-term relative mean sea level has been slowly rising in the Houston-Galveston region. There are seasonal changes in mean sea level that occur in the Gulf of Mexico. Late summer hurricanes (in September and October) are expected to be accompanied by seasonal mean sea levels that are 0.4 to 0.5 ft higher, on average, than the long-term mean sea level. The actual sea level at the time a hurricane occurs can be even higher than the monthly mean values. Such was the case in September 2016 when seasonal sea levels were unusually high, approximately 1 ft above the long-term mean sea level. Hurricanes that occur earlier the season (June, July and August) will most likely be accompanied by a seasonal mean sea level is not significantly different from long-term mean. The seasonal sea level will be the same inside the bay as outside, unless local precipitation raises levels significantly inside the bays.

The astronomical tide, which produces oscillatory changes in water level, can lessen the impacts of higher antecedent water levels caused by the seasonal mean sea level and the wind-driven forerunner. This can be achieved by closing the surge gates at a time of low tide. The time of occurrence of the hurricane within the 14-day spring-neap tidal cycle, and the tide range at that time, influences the potential benefits of closing the gates at low tide. At spring tide conditions, when the tide range is greatest (2.5 to 3 ft), unusually low tides that occur every 24 hours provide an opportunity to significantly lessen the residual flood risk inside the bays. At neap tide, when the tide range is smallest (0.5 to 1.5 ft), low tides are not as low and there is less opportunity to offset the elevated water levels associated with mean sea level and the wind-driven forerunner. During neap tide conditions, lows are experienced every 12 hours, which might be a small benefit in deciding when to close gates.

Generation of the wind-driven forerunner can begin once the eye of a hurricane enters the Gulf. The forerunner is forced by winds that blow along the continental shelf regions of the northern Gulf, pushing water

along the shelf, which is then turned to the “right” and stacked against the shoreline by the Coriolis force, an Ekman set-up. The wind-driven forerunner is manifested as a persistent steady rise in water level at the coast; and, the rate of rise accelerates as the hurricane gets closer to the continental slope and shelf off the Texas coast. The magnitude of the wind forerunner is dependent upon the storm’s size, intensity and forward speed. The more intense and larger the hurricane, the greater the rate of water level rise during the forerunner build-up. Slower moving storms have the potential to produce a greater forerunner surge than faster moving storms.

The wind-driven forerunner can cause an increase in water level at Galveston of as much as several feet, one or two days before landfall. Importantly, the wind-driven forerunner that is generated at the coast readily propagates through the passes and open storm surge gates into the bays, with little or no attenuation. Therefore, wind-driven forerunner surge directly increases residual flood risk inside the bays.

The development of the wind-driven forerunner amplitude both on the open coast and inside the bays is highly sensitive to forward speed for hurricanes that approach from the southeast. In general, the slower the forward speed the greater the wind-driven forerunner amplitude at Galveston and the greater accumulation of water inside the bays at the time of landfall. Because little to no attenuation of the forerunner amplitude occurs as it propagates from the open coast through the passes and into the bays, propagation of the forerunner into the bays exerts a major influence on peak surge levels inside the bay caused by high in-bay winds moving the water around within the bay. For example, for a severe 930-mb hurricane, without any surge gates in place, a threefold decrease in forward speed, from 18 kt to 6 kt, led to a two fold increase in peak surge in the upper reaches of the Houston Ship Channel (from 10 to 20 ft). A critical aspect of the Ike Dike surge barrier operation will be minimization of the surge forerunner within the Bay through early gate closure. Early gate closure will be particularly crucial for slow-moving storms. Peak surge at the open coast is much less sensitive to forward speed.

The wind-driven forerunner is much more important than the volume mode forerunner, which can be excited when a severe hurricane enters the Gulf. The amplitude of the volume mode forerunner is only a few tenths of a foot for even the largest and most intense hurricanes.

The volume mode forerunner is oscillatory by nature, with a rather predictable period of 32 to 36 hours. As with the astronomical tide, the predictability of its period provides some potential for exploitation in terms of timing gate closure. The amplitude of the volume-mode forerunner is relatively small, so the benefits of exploiting this mode of forerunner are limited.

Hurricane Ike serves as a useful example for examining these different physical processes that influence the antecedent water level, and how they might influence timing of gate closure. The figure below is a reproduction of Figure 14-12b, which was presented earlier in the chapter. The figure shows the measured water surface elevation during Ike at Galveston Pier 21 (in green), which lies inside the bay at the Port of Galveston, along with the predicted astronomical tide (in blue). Water surface elevation is displayed in feet, relative to mean sea level (MSL), which is the long term mean sea level for the gage site. Ike's landfall occurred at around hour 0700 GMT on September 13, shown by the red vertical line in the figure. The initial offset in elevation between the green and blue curves at hour 00:00 on September 10, more than 3 days before landfall, reflects about 0.5 ft of seasonal mean sea level increase above the long-term mean sea level and possibly a small contribution due to the wind-driven forerunner

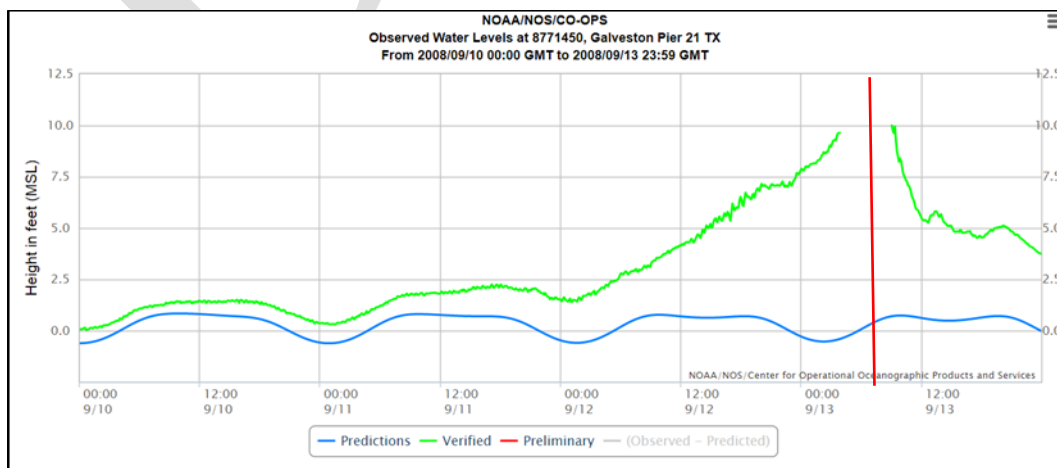


Figure 14-12b. Measured water surface elevation during Hurricane Ike, at the Galveston Pier 21 gaging station.

surge while the hurricane was beginning to transit the Gulf. Ike entered the Gulf a few hours before 00:00 on September 10. During the subsequent two days, September 10 and 11, an overall trend for increasing water level due to the wind-driven forerunner is evident, at an accelerating rate of rise, as are oscillations due to the astronomical tide.

Assuming a time of gate closure that is 12 hours before landfall, i.e., at hour 19:00 on September 12, an antecedent water level of between 6 and 7 ft would likely be present inside Galveston Bay at the time of closure. This very high antecedent level would considerably increase flood risk inside the bay, by unacceptable levels, even with the Ike Dike in place. Closing the gates at the time of low tide which occurred at around hour 03:00 on September 12 (28 hours before landfall) would have resulted in a much lower antecedent water level in the bay, approximately 1.0 to 1.5 ft, which would reduce the residual flood risk inside the bays, compared to the later closure time. Closing the gates even earlier, at the preceding low tide, which occurred at around hour 02:00 on September 11 (53 hours before landfall), while the hurricane was in the Gulf but well seaward of the Texas coast, the antecedent water level inside the bays would have been lower still, approximately equal to the long-term mean sea level value with little to no effect of the seasonal mean and wind-driven forerunner.

Very early closure of the surge gates prevents any precipitation run-off into the bays from leaving the bays, so this might also be an operational issue that needs to be considered as well.

A reliable hurricane surge forecasting model that accurately does the following: simulates the tide and forerunner surge, treats the influence of the surge gate infrastructure on long wave propagation into the bays while the gates are in the open position, treats closure of the gates during the storm's approach, and treats flow of water over closed gates, would be a very useful predictive tool. The tool could be applied to provide guidance for decision-making concerning the optimal time for closure of the surge gates. Inclusion of rainfall during the approaching storm into the model simulation, and subsequent simulation of water run-off into the bays could improve such a forecast capability.

15 Nearshore Wave and Water Level Conditions to Consider in Design of the Ike Dike

Introduction

Design of the land barrier and navigational/environmental sections of the gate systems, both of which will be constructed as part of the Ike Dike concept, will require nearshore wave information. Components of the dike might include some of the following: I-walls, T-walls, dike/levee sections, sand dunes and/or beach nourishment, overtopping and scour protection, a retractable gate at the passes, and perhaps another type of structural barrier to serve as the “environmental section” of the gate system at each of the passes. Wave forces on structures, and wave run-up, overtopping, and overflow, are all dictated by the local wave height, period and water depth conditions, among other parameters.

All components will need to be resilient to overflow and overtopping, which means they will experience minimal damage and no loss of functionality in the event the hydraulic design conditions are exceeded and the Ike Dike is overtopped. There is always some risk of this happening.

Therefore, it is informative to examine the characteristics of extreme nearshore waves and water levels that the Ike Dike might be subjected to. In this chapter, significant wave height, peak and mean wave period, and water surface elevation from the simulation of Storm 036, the 500-yr proxy storm, are presented with the extended dike in place.

Wave and water level conditions are presented for the four locations shown in Figure 15-1. The geographical location and the sea bed elevation at each location (from the model grid mesh) are shown in Table 15-1. Conditions at these four locations are believed to be reasonably representative of conditions that would be experienced along the length of the proposed Ike Dike for a very intense hurricane like Storm 036. Three of the locations, central Galveston Island, Galveston Pleasure Pier and central Bolivar Peninsula, reflect open-coast, shallow-water locations. The fourth location, Bolivar Roads, was selected to illustrate the wave conditions at the approximate location of the proposed gate system at this

pass. The Bolivar Roads location is situated within the inlet throat and is more sheltered than the three open coast sites.

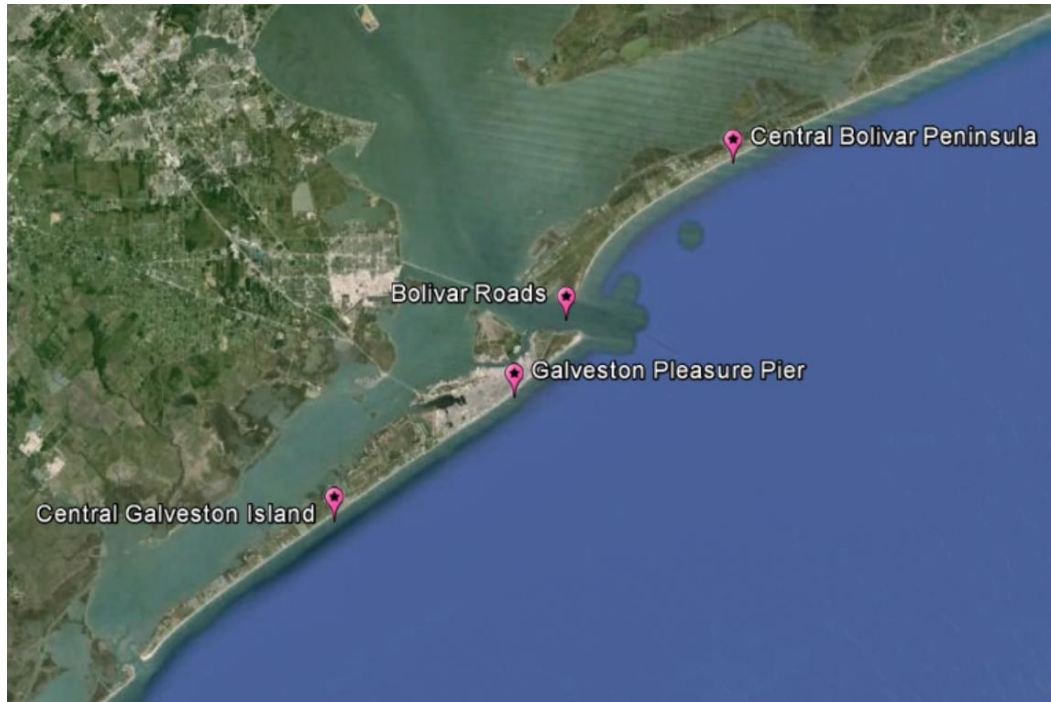


Figure 15-1. Water level and wave model output locations for Storm 036, the 500-yr proxy storm.

Table 15-1. Water level and wave condition output locations for Storm 036, the 500-yr proxy storm.

	Latitude (deg N)	Longitude (deg W)	Bottom Elevation (ft, NAVD88)
Bolivar Roads	29.34424	94.74177	-47.9
Galveston Pleasure Pier	29.2853	94.7878	-8.5
Central Bolivar Peninsula	29.4646	94.5936	-8.5
Central Galveston Island	29.1906	94.947	-8.5

Incident hurricane waves that are generated in deeper water undergo a series of complex transformations before reaching the site of the proposed retractable gate at Bolivar Roads. To reach this location, waves must first propagate over and be refracted by the irregular bathymetry of the ebb tidal shoals at the Bolivar Roads entrance. Then the waves must propagate over the pair of long jetties that stabilize the entrance channel. Both jetties will be submerged for most of the storm duration. Incoming waves will be “tripped” by the jetties and break due to the shallow water depth over the jetty crests, thereby limiting the amount of energy

contained in the waves as they penetrate into the throat. Then the incoming waves will be refracted, diffracted and broken by the complex bathymetry within the throat of the pass. Generally, waves at the location of the Bolivar Roads gate will be less energetic than the waves offshore.

The following hydraulic design parameters are shown below in a series of four figures, one figure for each parameter: a) water surface elevation relative to the NAVD88 vertical datum (the same datum listed for the bottom elevations in Table 15-1, which can be used together to compute the total water depth); b) energy-based significant wave height, c) peak spectral wave period, and d) mean spectral wave period. Figure 15-2 shows the water surface elevation as a function of time throughout the peak of the storm. Results are shown for times beginning 23 hours prior to landfall and ending 23 hours after landfall. Figures 15-3, 15-4, and 15-5 show the significant wave height, peak wave period, and mean wave period, each as a function of time for the same period of time. Each figure shows results at all four of the locations listed in Table 13-1.

Water Surface Elevation

Twenty-three hours prior to landfall, the eye of the hurricane is still in the deep water portions of the Gulf of Mexico, well seaward of the edge of the continental shelf. At this point in time, the water surface elevation at all four locations is nearly the same, slightly less than 3 ft NAVD88. This water level reflects an increase of about 2 ft compared to the ambient sea level of 0.9 ft that was adopted for the storm simulations. This 2-ft increase is due to the wind-driven hurricane surge forerunner that develops on the continental shelf, the dynamics of which were discussed in Chapters 5 and 6. The rise in water surface associated with forerunner development is increasing at a rate of about 0.16 ft/hr, before the eye of the hurricane reaches the edge of the continental shelf.

The eye of the hurricane crosses the edge of the shelf 10 hrs before landfall. At this time the forerunner amplitude reaches an elevation slightly greater than 5 ft. Once the eye crosses the edge of the continental shelf and hurricane-strength winds begin to blow over the shallow shelf, the rate of water level rise begins to accelerate until the time of landfall, reaching several feet of rise per hour.

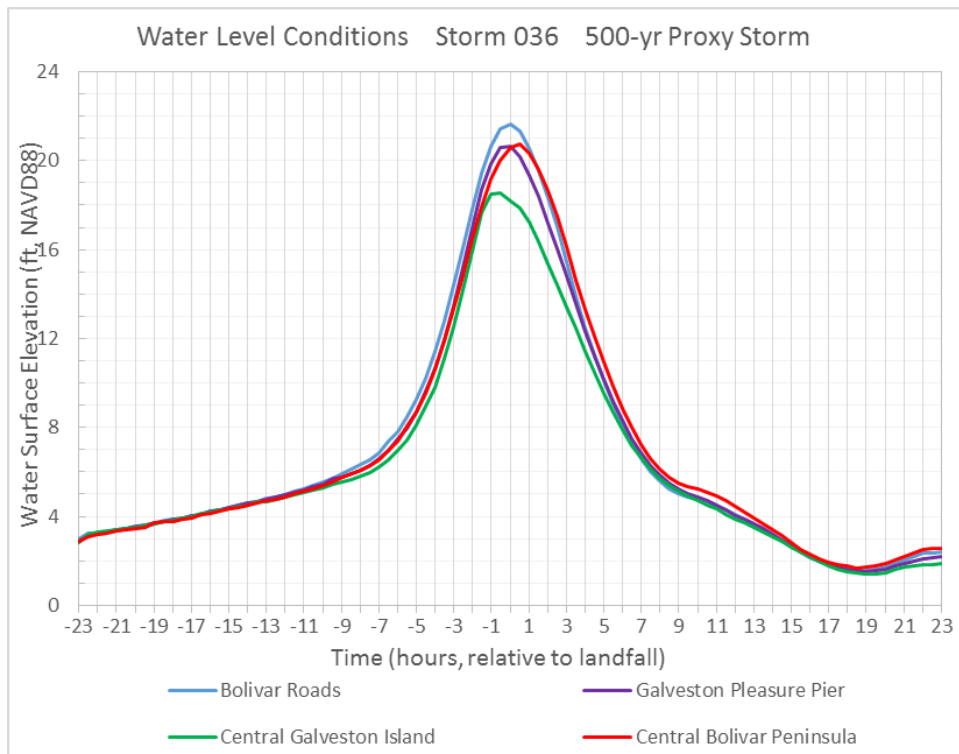


Figure 15-2. Temporal variation of water surface elevation for Storm 036, the 500-yr proxy storm.

At landfall, the storm surge at Bolivar Roads, Galveston Pleasure Pier, and the center of Bolivar Peninsula reaches its peak value of between 20 and 22 ft NAVD88. The peak surge at the center of Galveston Island is a little less, 18.5 ft, and it occurs about 1 hour prior to landfall. The onshore-directed winds at landfall are slightly stronger at the three locations with the higher peak surge. At the time of peak storm surge, the water depth at the three open coast locations is about 27 to 30 ft. After landfall as the eye moves inland, the water level falls rather rapidly at all four locations. The rate of water level decrease is quite similar to the rate at which water levels increased prior to landfall.

Significant Wave Height

The temporal evolution of the energy-based significant wave height, shown in Figure 15-3, is quite similar to that of the water surface elevation: a slow rate of increase initially, until the eye crosses the edge of the shelf, then a much faster rate of increase as the eye moves across the shelf and makes landfall. Both the growth of waves and the increase in storm surge levels are dominantly forced by the wind. The rate of decrease in wave height following landfall also is similar to the rate of rise prior to landfall, as is the case for the water level.

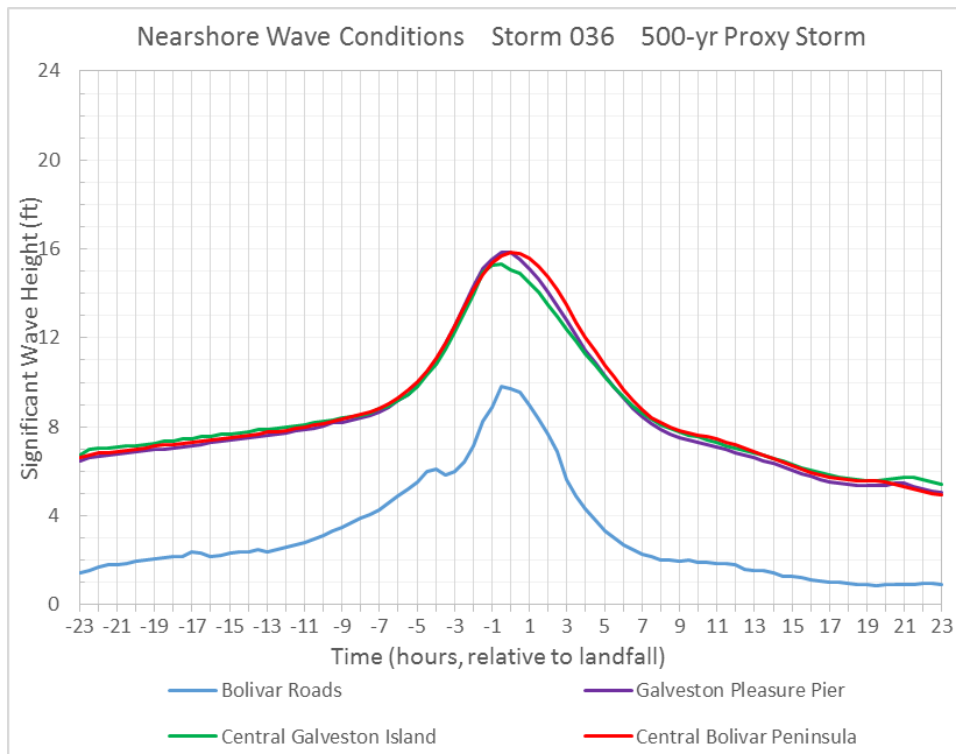


Figure 15-3. Temporal variation of significant wave height for Storm 036, the 500-yr proxy storm.

For the three open coast locations, the maximum energy-based significant wave height is approximately 16 ft at Galveston Pleasure Pier and Central Bolivar Peninsula, and 15 ft at Central Galveston Island. The maximum wave height value is approximately 55% (roughly half) of the water depth at the time of peak surge (29 ft for Galveston Pleasure Pier and Central Bolivar Peninsula, and 27 ft at Central Galveston Island) at all three open-coast sites, suggesting that the energy level contained in the waves is saturated due to wave breaking; i.e., wave height is limited by wave breaking to be a percentage of the local water depth.

The maximum significant wave height in the throat of Bolivar Roads, slightly less than 10 ft, is less than the wave height at the open coast locations, 15 to 16 ft. This lower maximum wave height is consistent with the wave transformation dynamics described earlier. It also suggests that significant wave height at this location might be strongly controlled by the depth of water over the jetties and not the local water depth (which is approximately 70 ft at the time of peak surge). Assuming an elevation of 4 ft NAVD88 for the crest of the jetties, and a maximum water surface elevation of 21.5 ft NAVD88, the water depth over the jetties is about 17.5 ft. Therefore, a 10-ft maximum wave height reflects 57% of the water

depth. This percentage also suggests a depth-limited, saturated wave-energy condition in the throat of Bolivar Roads, limited by the water depth over the submerged jetties at the peak of the storm.

Looking at two other times near the peak of the storm, one that is 2 hours before landfall (wave height of 7 ft and water depth over the jetties of 13.5 ft) and another 2 hours after landfall (wave height of 7.5 ft and water depth over the jetties of 14 ft), the ratios of significant wave height to water depth at these two times are 0.52 and 0.54, respectively (percentages of 52% and 54%). The ratios of wave height to water depth over the jetties for these two other times near landfall also suggest a controlling influence of the submerged jetties on wave conditions at the site of the proposed gate in Bolivar Roads, near the peak of the storm.

Peak Wave Period

The temporal evolution of the peak wave period is shown in Figure 15-4. Peak wave period is the period (inverse of the frequency) associated with the most energetic band in the calculated two-dimensional (frequency-direction) energy spectrum.

Prior to the hurricane eye reaching the edge of the continental shelf at hour 10 before landfall, wave conditions at the three open-coast sites are dominated by long-period (16-sec) 6- to 8-ft swell waves that were generated offshore and arrive well before the hurricane's core winds. The peak wave period at the more sheltered Bolivar Roads site is dominated by locally-generated short-period (4 to 5 sec) 1 to 3-ft wind seas. The energy associated with the longer-period swell waves that are generated well offshore is much less effective in penetrating past the complex ebb shoal bathymetry and jetty systems compared to the shorter period wind seas, which are primarily locally generated.

As the hurricane eye crosses the edge of the continental shelf and locally generated waves associated with the core winds begin to dominate, the peak period at the open-coast sites begins to down-shift. At landfall, peak periods are approximately 12 sec at the three open-coast sites. The peak period at Bolivar Roads increases to 12 sec, as the elevated storm surge levels allow longer-period waves generated on the shelf to penetrate into the inlet throat. Peak wave periods at storm landfall are between 12 and 13 sec.

Following landfall the peak periods continue to downshift to periods approaching 8 sec at the open-coast sites 3 to 6 sec in the inlet throat once surge levels have subsided.

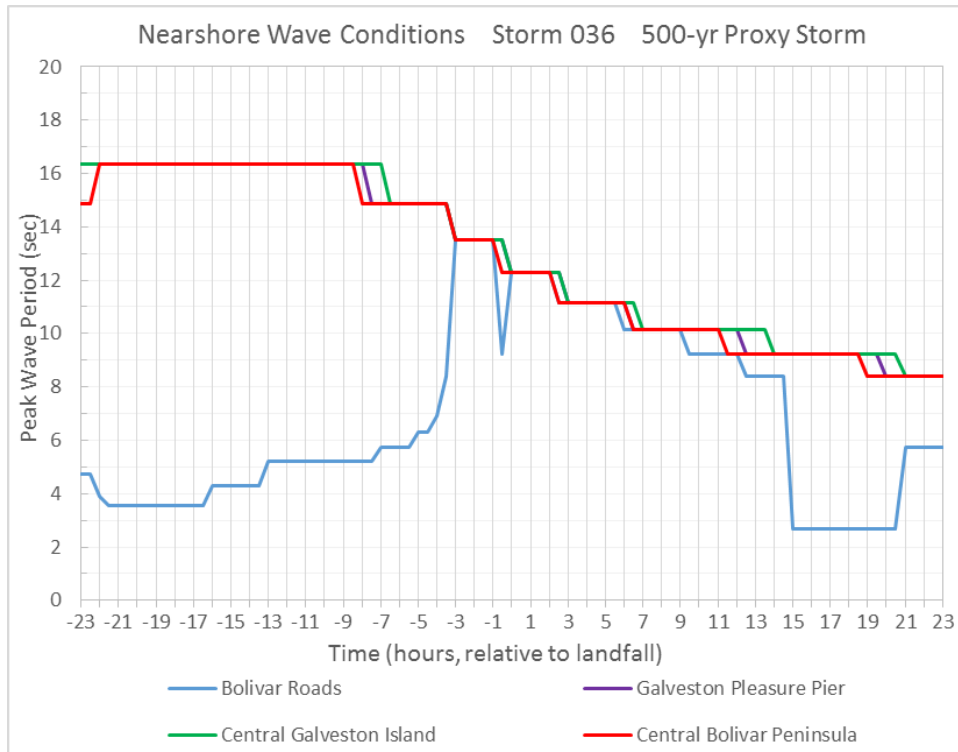


Figure 15-4. Temporal variation of peak wave period for Storm 036, the 500-yr proxy storm.

Mean Wave Period

The temporal evolution of the mean wave period is shown in Figure 15-5. Mean wave period is computed as an energy-weighted average for the entire two-dimensional energy spectrum. Generally, mean wave periods are smaller than peak wave periods.

The general pattern of temporal variation for the mean period is similar to that for the peak period. While the hurricane eye is offshore, well beyond the shelf, open-coast mean wave periods are 14 to 15 sec. Mean wave periods within the throat are 4.5 to 6 secs during this same period of time.

As the eye crosses the continental shelf break and continues toward landfall, mean wave period also downshifts from 14 to 15 sec to values of 10 to 11 sec at landfall for the open coast sites. However, as was the case for peak period, mean wave periods at the Bolivar Roads site increase from 5 sec to 8 to 9 sec during the same time span.

Following landfall, mean wave periods at the open-coast sites continue to steadily downshift from 10 to 11 sec to periods of approximately 7 sec. Mean periods at the Bolívar Roads site steadily decrease from 9 sec to 5 sec as the surge levels subside. This pattern of decreasing mean wave period after landfall is quite similar to the pattern seen for the peak period.

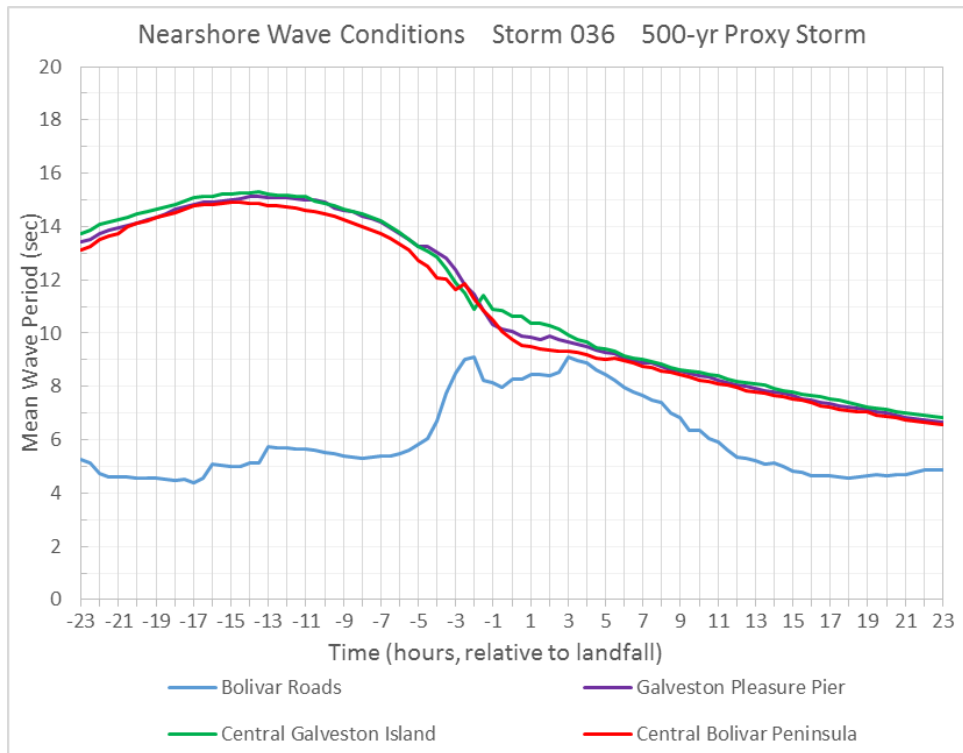


Figure 15-5. Temporal variation of mean wave period for Storm 036, the 500-yr proxy storm.

16 Summary of Key Results, Findings, and Recommendations

Regional Storm Surge Dynamics

Generation of the Open Coast Storm Surge

Hurricane storm surge along the north Texas coast is primarily influenced by two contributors. One is the development of a wind-driven surge forerunner, an Ekman wave, which is forced on the Louisiana-Texas continental shelf. The forerunner is created by water moving along the shelf that is forced by the hurricane's peripheral winds. This alongshore moving water is then directed onshore by the Coriolis force that is associated with the earth's rotation. The counterclockwise rotating wind circulation about the hurricane's eye creates winds directed to the west along the Louisiana shelf and to the southwest along the Texas shelf as a hurricane approaches the Houston-Galveston region from the southeast and south-southeast, which are the most prevalent directions of approach. The curvature of the counterclockwise circulating wind fields for these storms matches well the curvature of the Louisiana/Texas continental shelf, which enhances forerunner development for storms that take these types of tracks.

Forerunner development begins while the storm is well offshore in the deep waters of the Gulf. The forerunner is manifested as a slowly rising water surface elevation at the coast which can propagate into West bay and Galveston Bay through the passes. The increase in water surface elevation associated with the forerunner can reach 6 ft, as was observed by Kennedy et al (2011) during Hurricane Ike (2008).

The second contributor to the storm surge is the direct effect of the highest winds in the core of the hurricane as it crosses the continental shelf. These strong winds push the water that has accumulated on the shelf toward the coast. The largest open coast surge computed for the 22 major hurricanes simulated thus far (those having a very low central pressure of 900 mb) was 18 to 19 ft at Galveston Pleasure Pier.

Surge Generation within Galveston Bay

Within Galveston Bay, storm surge is highly dependent upon filling that occurs from several sources. The most significant source is surge

propagation over Galveston Island and Bolivar Peninsula as these barrier islands become inundated by the coastal surge. A second source is surge propagation through Bolivar Roads and San Luis Pass, tidal passes which connect the Gulf to the Bays. A third contributor is the local wind-set up due to strong winds within the Bays themselves, which create a gradient or tilt to the water surface inside the bay. The tilting action is in the direction of the wind, i.e., higher water surface elevation on the downwind side, lower water surface on the upwind side.

Within Galveston Bay the largest surge computed for the major hurricanes simulated thus far was 18 to 20 ft on the bay side of Galveston, 18 to 20 ft in the Texas City area, 19 ft in the Clear Lake area, 21 ft in the Bayport area and 24 to 25 feet in the upper reaches of the Houston Ship Channel.

Influence of Storm Track on Surge Development

Three storms were selected to examine the influence of track on development of the storm surge. Each storm had a different track and landfall location, but they all had the same minimum central pressure, forward speed and size (radius-to-maximum-winds). Tracks from the south, south-southeast, and southeast were considered.

Far-field winds for the hurricane that approached from the south were directed onshore during the forerunner development period. These onshore winds were the primary contributor to formation of a significant open-coast surge forerunner. Because the winds were directed onshore, they were very effective in generating the forerunner surge. Movement of water along both the wide Louisiana continental shelf and the narrower north Texas shelf was a lesser contributor to the forerunner development for this storm track.

For the storm that approached from the south-southeast, the alongshore movement of water along the Louisiana and north Texas shelves was much stronger. This movement of water is then turned to the right or toward shore by the Coriolis force to raise the water level at the coast. This process was the primary contributor to the significant forerunner that also developed for this storm track.

For the storm that approached from the southeast, the alongshore movement of water was the primary contributor to forerunner development as well. However, as the storm approached the edge of the shelf, the core winds were directed more offshore along the Louisiana

coast. These offshore winds reduced the alongshore movement of water from the Louisiana shelf toward the north Texas shelf, thereby reducing the forerunner amplitude.

These same three storms were used to examine the influence of storm track on surge development by the hurricane's core winds. Core winds are those nearest the eye, particularly on the right hand side of the storm where the wind speeds are typically highest. Whereas the storm's far field winds dominate the forerunner development process, the storm's core winds begin to dominate surge development once the storm moves onto the continental shelf. Each of the three storms had the same minimum central pressure and radius-to-maximum-winds, but their tracks differed. The storm from the south had a higher forward speed than the other two. All three storms made landfall at a different location along Galveston Island.

With storm parameters being the same, or nearly so, and for these particular landfall locations for each storm, the hurricane that approached from the south generated a maximum storm surge zone that first developed at the City of Galveston. The zone then migrated northeast to Bolivar Peninsula as the storm approached and made landfall. For the other two storms which approached from the south-southeast and southeast directions, storm surge built up from the east and northeast. For both storms, maximum surge zones developed along Bolivar Peninsula and persisted at that location through the time of landfall.

Peak surge along the open coast was greatest for the storm which approached from the south-southeast. This storm developed a significant forerunner as a result of considerable movement of water from the Louisiana shelf to the north Texas shelf. This large accumulated volume of water was then driven ashore by the core winds. Peak surge for the storm from the south was less, since this storm did not have the same volume of water moving along the Louisiana shelf and onto the north Texas shelf. The storm from the southeast produced the least amount of open coast surge. This occurred primarily because of the offshore directed winds along the Louisiana coast as the storm moved onto the shelf, which reduced the forerunner and drew down the surge before it increased with arrival of the core winds at landfall. The significant role of offshore winds did not occur for storms on either the south or south-southeast tracks.

Within Galveston Bay, at landfall, all three storms produced maximum surges at the southwest corner of the Bay, on the bay side of the City of Galveston. This high surge at the southwest corner forced water from Galveston Bay into West Bay, and prevailing winds set up the western side of West Bay.

For all three storms wind directions shifted rapidly for the few hours after landfall, first pushing water toward the western shoreline of Galveston Bay and then toward the northern shoreline. After landfall, the storm from the south transited through the center of Galveston Bay. This movement created times of relatively lower wind speeds within the Bay, as the hurricane's eye was positioned over the Bay. Wind directions near the eye changed very rapidly with passage of the eye. Coupled with the lower wind speeds, the lack of a persistent wind direction resulted in no formation of a substantial water surface elevation gradient within the bay as the storm center moved through, which might have augmented filling of the Bay. For all three storms, significant filling of Galveston and West Bays occurred due to forerunner penetration through the passes and by flow over the barrier islands. When the storm from the south did move away from the Bay, winds from the west persisted and set up the east side of Galveston and West Bays.

The eye of the storm that approached from the south-southeast direction transited along the western side of Galveston Bay; and the eye for the storm from the southeast passed well to the west of the Bay. For both storms, once the eye moved away from the Bay, persistent winds from the south formed a substantial water surface gradient within the Bay, which was superimposed on the significant filling of the Bay. This substantial south-to-north gradient was established by persistent winds from the south, which pushed water into the northern parts of the system.

Dependence of Peak Surge on Hurricane Intensity

A "direct-hit" set of four storms was simulated, each having a different central pressure (900 mb, 930 mb, 960 mb and 975 mb), but all followed the same track. Each of them approached from the south-southeast, made landfall at the City of Galveston, and subsequently moved inland along the western shoreline of Galveston Bay. The range of open coast surge levels in the maximum surge zone at Galveston, listed by storm having the greatest to least intensity, were 13.5 to 16.5 ft, 11 ft to 15 ft, 7.5 to 10.5 ft, and 7 to 8.5 ft, respectively. In the Texas City area, peak surges for the

four storms were 11 to 15 ft, 11.5 to 12.5 ft, 8.5 to 11 ft, and 8 to 8.5 ft, respectively. In the Clear Lake and Bayport areas, peak surges were 15 to 16.5 ft, 13 to 13.5 ft, 10 to 10.5 ft, and 8 to 8.5 ft, respectively, for the four storms. In the upper reaches of the Houston Ship Channel, peak surges were 19 to 20 ft, 15 ft, 12 to 12.5 ft, and 9 to 10 ft, respectively.

Results confirm that peak surge is strongly influenced by storm intensity; i.e., the greater the intensity (i.e., the lower the central pressure) the greater the peak surge. Central pressure is positively correlated with maximum wind speed, wind speed is nonlinearly related to surface wind stress, and wind stress is linearly related to water surface slope and storm surge.

Within Galveston Bay, along the western shoreline, peak surges tended to increase from the south to north, and then into the Houston Ship Channel where surge levels tended to be the highest for each storm. The counterclockwise wind circulation tended to force water into the upper reaches of the Houston Ship Channel.

Dependence of Peak Surge on Storm Track

The 21 major hurricanes (those having a 900-mb central pressure) that were originally simulated as part of the bracketing set of storms, approached the Houston-Galveston region from one of three general directions: from the south, the south-southeast and the southeast. All of the storms in each directional grouping had a unique track and a different landfall location; the tracks within each grouping were parallel with one other. Tracks for each of the storms in the group, and thus landfall locations, were separated by about 20 miles. For each of the three different groupings, results suggest that hurricanes which make landfall in the zone that extends from San Luis Pass to a location 20 miles west of the pass will produce the greatest peak surges in the Houston-Galveston region, assuming all other hurricane parameters are the same and they only differ by track. Storms that made landfall at Bolivar Roads or to the east of Bolivar Roads tended not to generate nearly as high peak surges within the Bay. For these hurricanes, the farther the landfall position was from Bolivar Roads, the more peak surges in the Bay decreased significantly.

Putting Storm Surge in the Context of Probability

Prior to the eventual simulation of a much larger set of hypothetical hurricanes, a small set of hurricanes was identified and selected to support analysis of the Ike Dike concept (three proxy storms, which are described below, and Hurricane Ike). To provide a basis for proxy storm selection and to fully and accurately characterize the probability of extreme water surface elevations for existing conditions, a full joint probability analysis was conducted by the U.S. Army Engineer Research and Development Center (ERDC) using joint probability methods. The analysis produced water surface elevation statistics for a set of locations in the Houston-Galveston region throughout the key corridor for potential economic damage and losses that lies along the western side of Galveston Bay. The approach used by the ERDC differs slightly, in some aspects, from the approach used in the FEMA Region VI Risk MAP study of the Texas coast (FEMA 2011). However, the FEMA (2011) storm surge archive was used as the underlying peak storm surge data source for the statistical analysis.

Based on the ERDC analysis, Table 15-1 summarizes several extreme water level statistics for the following key locations: the upper reaches of the Houston Ship Channel, Morgan's Point, the entrance to Clear Lake, the east side of Texas City, bay side of the City of Galveston, and the Gulf side of the City of Galveston. For each location, the mean, or expected value, of water surface elevations corresponding to the 100-yr and 500-yr ARIs (Average Recurrence Intervals) are shown. These ARI values correspond to water levels having a 1% and 0.2% chance of occurring each and every year, respectively. The water surface elevations listed in Table 16-1 account for the astronomical tide, wave contributions to the still water level, and a number of sources of uncertainty arising from various sources.

Table 16-1. Water Surface Elevation Statistics for Select Key Locations

Location	Extreme Water Surface Elevations (ft, NAVD88)					
	100-yr ARI mean	100-yr ARI 90%CL	100-yr ARI 95%CL	500-yr ARI mean	500-yr ARI 90%CL	500-yr ARI 95%CL
Houston Ship Chan (upper)	15.2	18.0	18.8	19.8	22.6	23.4
Morgan's Point	12.3	15.1	15.9	15.8	18.7	19.5
Clear Lake Entrance	11.9	14.7	15.5	15.7	18.5	19.3
Texas City (east side)	10.5	13.3	14.1	13.8	16.6	17.4
Galveston (bay side)	10.5	13.3	14.1	14.0	16.8	17.6
Galveston (Gulf side)	10.6	13.5	14.3	14.1	17.0	17.8

In addition to expected values, water levels for the 100-yr and 500-yr ARIs also shown for two different confidence levels, 90% and 95% (the 90%CL and 95%CL values, respectively). We recommend that the 90%CL ARI values be adopted for use in the feasibility assessment of the Ike Dike concept, since they provide a much higher level of confidence than use of the mean, or expected values. Values in the table show that, at all locations for both the 100-yr and 500-yr ARIs, the 90%CL values are about 3 ft higher than the expected values; and the 95%CL values are about 3.5 ft higher than the expected values.

For comparison purposes, Hurricane Ike produced maximum water surface elevations of 10.5 to 12 ft NAVD88 for much of the main portion of Galveston Bay and at the City of Galveston. In the upper reaches of the Houston Ship Channel Ike produced maximum water surface elevations of 13 to 15 ft NAVD88.

A crest elevation of 17 ft NAVD88 for the conceptual Ike Dike, which is approximately equal to the present crest elevation of the Galveston Seawall, corresponds to a 500-yr ARI water surface elevation at a 90% confidence level at the Galveston Pleasure Pier.

Strong similarity was observed between the ARI water surface elevation pattern within Galveston Bay and the maximum water surface elevation pattern in the Bay for individual severe storms that made landfall near San Luis Pass, or just to the south of the pass. Because of this similarity, it was thought that “proxy” storms could be identified from among the 223-storm FEMA (2011) set, such that one of the synthetic hypothetical hurricanes simulated in the FEMA study (2011) would produce a water surface elevation field that was quite similar to the field corresponding to a particular ARI water surface elevation field throughout the key economic corridor within the Bay. Based on this preliminary analysis using the FEMA (2011) results, the proxy storm concept seemed to have merit as a first step to placing water surface elevations and economic damages/losses in a probabilistic context. Proxy storms were identified for 10-yr, 100-yr, and 500-yr ARI water surface elevations. The proxy storms enable reductions in inundation, attributable to the Ike Dike, to be placed in a probabilistic context prior to simulating a large set of hurricanes and performing a more rigorous statistical analysis on that much larger set of results.

Storm Surge Reduction Achieved with the Ike Dike Concept: Results from Original Bracketing Set of Storms and Initial Modeling Approach

The primary benefit of the 17-ft Ike Dike concept is to greatly reduce, or eliminate in some case, the sources of bay filling, with the greatest source being flow over the barrier islands. The dike eliminates, or nearly so, a major contributor to the storm surge and subsequent flooding within Galveston Bay. Reduction of storm surge in the bay also can lead to a reduction in the amount of wave energy generated within the bay by reducing the water depth.

The dike also acts to eliminate or reduce storm surge and wave attack along the coastal barrier islands, preventing surge and waves from damaging buildings and infrastructure that lie behind the dike. Damages are reduced or prevented as long as the dike is not overtopped or subjected to steady overflow. If overtopping and overflow occurs, damages and losses behind the dike can accrue on the barrier islands. Barrier islands also can flood from the backside, the bay side. By reducing surge levels in Galveston Bay, the Ike Dike can reduce flooding of the barrier islands from the bay side.

Based on an analysis of modeled water surface elevations for the original bracketing set of storms (25 storm simulations made for both without- and with-dike conditions), which were run with the initial surge and wave model set up and modeling approach, significant flood reduction benefits accrue throughout the region because of the Ike Dike. For the direct-hit set of four storms, having central pressures of 900, 930, 960 and 975 mb, the Ike Dike concept reduced storm surge within Galveston Bay by these approximate amounts: 4.5 to 7 ft, 7 to 10 ft, 6 to 9 ft, 5 to 7 ft, respectively. The dike limited storm surge levels within the Bay to 4 to 7 ft for the 930-mb storm, 2 to 4 ft for the 960-mb storms, and 2 to 4 ft for the 975-mb storm. This indicates that the Ike Dike concept will have considerable storm surge and flooding reduction benefits for all storms, particularly for the most frequently occurring, less intense, hurricanes.

The dike significantly reduced storm surge in Galveston Bay for the rare but possible 900-mb storm, by 4.5 to 7 ft, and the 930-mb storm by 7 to 10 ft, so considerable flood reduction benefits will accrue for many locations within the region even for major storms. However, the 900- and 930-mb direct-hit storms did produce flow over the dike in some areas, extensively

in places, which would result in flood damage along the barrier islands in these areas. Overtopping and overflow occurred for some of the other 900-mb storms that produced substantial open coast storm surge which exceeded the crest height of the dike. As long as the dike is resilient and maintains its integrity while being overtopping (without or with overflow), it would reduce damages even in these overtopping and overflow situations, compared to the existing condition.

For all the 900-mb storms, the Ike Dike significantly reduces storm surge throughout Galveston Bay and the Houston Ship Channel, by amounts of up to 14 ft, depending on storm track. Reductions achieved with the dike were most often in the 6 ft to 12 ft range, which are significant reductions that will lead to significantly less damage/losses.

Storm Surge Reduction Achieved with the Ike Dike Concept: Results from the Refined Modeling Approach with the Extended Ike Dike

Reduction in Peak Storm Surge Values

Hurricane Ike and the 10-yr, 100-yr, and 500-yr proxy storms were simulated for existing conditions and with- extended Ike Dike conditions. The extended dike ends at Sabine Pass, whereas the original dike in the bracketing set simulations ended in the vicinity of the northeast end of Bolivar Peninsula, just to the east of High Island, TX. For the extended dike, a crest elevation of 17-ft NAVD88 was used except for the Galveston seawall, where actual elevations were used. Simulations used an improved model setup. Model validation for Hurricane Ike, using the revised modeling approach, is presented in Chapter 2.

Simulations were made for present-day sea level and a future sea level scenario, which is called SLR1. The SLR1 sea level is +2.4 higher than present-day sea level. Based on a comparison of the current modeling approach with past Hurricane Ike modeling done by ARCADIS (2011) in support of the Nature Conservancy, the current modeling approach captures the dominant influences of sea level change on those storm surge processes that most dictate peak storm surge values along the western shoreline of Galveston Bay. The effects of sea level change on landscape vegetation are less important than the change sea level has on water depths in the shallow coastal and bay areas.

Detailed results and discussion for results from this set of simulations, for the four-storm set, present and future sea level, are presented in Chapters 11 and 12. Results were provided to the economics team. The following four tables summarize peak storm surge results from these simulations.

Table 16-2. Peak storm surge values for Hurricane Ike (feet, NAVD88), for the present-day and SLR1 (+2.4 ft) sea level scenarios

Location	No-dike conditions		With-dike conditions	
	Present	SLR1	Present	SLR1
City of Galveston (Gulf side)	13	15	14	16
City of Galveston (bay side)	13	15	4.5	7
Galveston Island (mid-way)	10.5	13	4	6.5
Bolivar Peninsula (mid-way)	14	17.5	2	5.5
Texas City (south)	12	14	4	6.5
Texas City (east)	12	14.5	4	6.5
Dickinson Bay entrance	11.5	14	3.5	6
Clear Lake entrance	11.5	14.5	2.5	5
Morgan's Point	13	16	2	5
Upper Houston Ship Channel	13.5	16.5	2.5	5

Table 16-3. Peak storm surge values for Storm 535, the 10-yr proxy storm, (feet, NAVD88), for present-day and SLR1 (+2.4 ft) sea level scenarios.

Location	No-dike conditions		With-dike conditions	
	Present	SLR1	Present	SLR1
City of Galveston (Gulf side)	6.5	9	6.5	9
City of Galveston (bay side)	6.5	9	2	4.5
Galveston Island (mid-way)	5	7.5	2	5
Bolivar Peninsula (mid-way)	5	7.5	1	3.5
Texas City (south)	8	10	3.5	6
Texas City (east)	7	9.5	3.5	5.5
Dickinson Bay entrance	8	10.5	4	6
Clear Lake entrance	8.5	11	4	6
Morgan's Point	8.5	11	4	6
Upper Houston Ship Channel	10	13	5	7

Table 16-4. Peak storm surge values for Storm 033, the 100-yr proxy storm, (feet, NAVD88), for present-day and SLR1 (+2.4 ft) sea level scenarios

Location	No-dike conditions		With-dike conditions	
	Present	SLR1	Present	SLR1
City of Galveston (Gulf side)	16	18	18	20
City of Galveston (bay side)	14	18	6.5	10
Galveston Island (mid-way)	13	15	4	7
Bolivar Peninsula (mid-way)	16	18.5	10	10
Texas City (south)	16.5	19	8	10.5
Texas City (east)	15	17.5	7	9.5
Dickinson Bay entrance	14.5	17.5	8	10
Clear Lake entrance	15	18.5	8	10
Morgan's Point	17	20	7.5	10
Upper Houston Ship Channel	18.5	21.5	10	12.5

Table 16-5. Peak storm surge values for Storm 036, the 500-yr proxy storm, (feet, NAVD88), for present-day and SLR1 (+2.4 ft) sea level scenarios

Location	No-dike conditions		With-dike conditions	
	Present	SLR1	Present	SLR1
City of Galveston (Gulf side)	20	22	21	22.5
City of Galveston (bay side)	18	21	12	13
Galveston Island (mid-way)	16	18.5	10	13
Bolivar Peninsula (mid-way)	19	21.5	10	10
Texas City (south)	20.5	22.5	11	13
Texas City (east)	18	20.5	9	11
Dickinson Bay entrance	17.5	20	10	12
Clear Lake entrance	18	21	10	12
Morgan's Point	20	23	10	12
Upper Houston Ship Channel	22	25	12.5	14.5

Using only the approximate peak surge values that are listed in these tables, which were visually estimated from peak surge maps presented in Chapter 11, the following average values of surge reduction are achieved with the 17-ft Ike Dike: 10-yr proxy storm (4 ft), Hurricane Ike (9 ft), 100-yr proxy storm (8 ft), 500-yr proxy storm (9 ft). Surge reduction tends to be a little higher in the upper reaches of the Houston Ship Channel. Average surge reduction values for both sea levels are quite similar, so they are averaged to arrive at the reduction values cited above for each hurricane.

The primary strength of the Ike Dike concept is the regional scope of flood risk reduction benefits that the coastal spine provides to all areas that lie behind it. The 17-ft Ike Dike reduces the peak storm surge within Galveston Bay, for major surge-producing storm events, by 8 to 9 ft, on average. The areas of focus in this study are Galveston Island, Bolivar Peninsula, the western shoreline of Galveston Bay, and the upper reaches of the Houston Ship Channel. All of these key areas in the Houston-Galveston region, which presently are at risk of experiencing substantial flood-induced damages/losses, would receive significant risk reduction benefits. No areas are omitted from receiving benefits. This is true regardless of whether the area is primarily residential or primarily industrial, this is true without regard for the economic value of individual properties, structures or residences that receive the risk reduction benefits.

For the Hurricane Ike simulation, for present-day sea level, the Ike Dike eliminates flooding and inundation of residential and industrial areas nearly everywhere in the Houston Galveston region, except in some of the lowest-lying areas. Those areas that are inundated for the Ike simulation with the dike in place include some locations on central and western Galveston Island that are closest to the bay shoreline, as well as areas in and around Bayou Vista which is located just to the south of the Texas City levee. For hurricanes that produce less storm surge than Hurricane Ike, including the 10-yr proxy storm and less intense hurricanes like it, the possibility of inundation will be greatly reduced or even eliminated even in these most vulnerable areas. The value of the Ike Dike in eliminating flooding during most hurricanes, for present-day sea level, should not be understated.

Flooding in the lowest-lying areas is particularly sensitive to the antecedent water level in Galveston and West Bays, so it will be sensitive to the amount of water that enters Galveston Bay prior to closure of the flood gates at Bolivar Roads and San Luis Pass, and it will be sensitive to sea level. Rising sea level increases flood risk throughout the Houston-Galveston region.

For the Hurricane Ike simulation, for the future sea level scenario, which is +2.4 ft above present-day sea level, the Ike Dike provided widespread surge reduction and great reductions in the depth and extent of inundation throughout the region, particularly along the western shoreline of Galveston Bay.

In light of the sensitivity of flooding to sea level in lower-lying areas, quite a few more areas were inundated for Hurricane Ike at the higher future sea level, even with the Ike Dike in place. The communities along the western shoreline of Galveston Bay that experienced inundation for this hurricane event/sea level scenario included the following: most areas on central and western Galveston Island except those located on the highest topography, Bayou Vista and the surrounding area, the Tiki Island and Harborwalk communities, the lowest-lying parts of San Leon, Seabrook and Clear Lake Shores near the entrance to Clear Lake, and isolated low-lying areas along the Nassau Bay shoreline. See Figure 12-1 for a map that shows these locations. A few of the lowest-lying industrialized areas in the upper reaches of the Houston Ship Channel also experienced inundation for this storm/sea level. All along Bolivar Peninsula, the peak surge flowed over the Ike Dike for the Hurricane Ike simulation and the future sea level, subjecting areas immediately behind the dike to inundation. Parts of the City of Galveston are inundated for the Ike simulation with the future sea level. At present, and even with the Ike Dike in place, the City of Galveston is vulnerable to flooding from the bay side, although the risk of flooding from the bay side is far less than it is for existing no-dike conditions.

The inundation analysis revealed what might be a vulnerability along the Galveston seawall, near its northern end. There is a relatively small area (see Figure 12-3) where, according to the model topography, the maximum elevation along the seawall is 14 to 15 ft, NAVD88, which is 2 to 3 ft lower than the 17 ft NAVD88 elevation that exists along the rest of the seawall. In addition to flooding from the bay side, this apparent low spot is a source of inundation within the City of Galveston for the Hurricane Ike

simulation at the higher future sea level. If this area is, in fact, lower by this amount, the vulnerability should be addressed. Because of the much greater risk to the City of Galveston from flooding along the bay side for existing conditions, this vulnerability is less important than it would be with the Ike Dike in place. The vulnerability should be addressed and eliminated as part of Ike Dike implementation.

For the no-dike conditions, and for the 100-yr and 500-yr proxy storms, peak surges generated by these two severe hurricanes cause widespread inundation, and undoubtedly great damages and losses, throughout the entire region for both sea-level scenarios. In light of its high surge reduction value, the Ike Dike greatly reduces the extent and depth of inundation in the heavily residential areas along the western shoreline of Galveston Bay and in all of the heavily industrialized areas, except for a few areas, for both proxy storms and for both present and future sea-level scenarios.

The inundation analysis also revealed a possible flooding vulnerability at the southwestern terminus of the Texas City levee (see Figure 12-18). The minimum elevation of the Texas City levee is 19 ft. At the southwest terminus of the levee, the surge model elevations at the end of the levee are between 13 and 14 ft NAVD88, which is 5 to 6 feet lower than the minimum levee elevation. There is a considerable distance between the end of the levee and the nearest location on an adjacent elevated highway embankment that is at an elevation of 19 ft NAVD88. Examination of this area in Google Earth also suggests that the levee ends well short of the elevated highway. Flooding through this low spot contributes to inundation inside the Texas City levee for some of the simulations, raising the flood risk to La Marque and Texas City. With the Ike Dike in place, because of the substantial surge reduction it provides, no flow occurred through this low spot in any of the simulations. However if this area is, in fact, lower by this amount, the vulnerability should be addressed. Any weak links in the risk reduction system can compromise its effectiveness.

The 17-ft Ike Dike is extremely effective in reducing the peak storm surge around the entire perimeter of the Texas City levee and in the upper reaches of the Houston Ship Channel, for the 100-yr and 500-yr proxy storms. Without the Ike Dike these hurricanes produce extremely large storm surges and widespread inundation in these areas (as much as 22.5 ft at the Texas City levee and 25 ft in the upper Houston Ship Channel). For

the many areas in the upper ship channel that are home to petro-chemical facilities, as well as the Texas City industrial area, the magnitude of the surge suppression achieved with the Ike Dike is sufficient to reduce the risk of inundation in nearly all of the highly industrialized areas to a very low probability of occurrence. This is a major benefit of the 17-ft Ike Dike; i.e., just how well it protects the vast majority of the highly industrialized areas from inundation for even very rare hurricane events, like the 500-yr proxy storm, including those with the future sea level scenario.

Even with the Dike in place and despite the high degree of surge reduction it provides, for the higher surge levels generated by the 100-yr and 500-yr proxy storms inundation still occurs in the lower-lying residential areas, particularly for the higher sea level.

With the extended Ike Dike in place, for the 100-yr proxy storm and the higher future sea level, peak surges along the western shoreline of Galveston Bay range from 7 to 8 ft for present-day sea level, and from 9.5 to 10.5 ft for the future sea level scenario. Peak surge values for both sea level scenarios are less than peak surge levels that were observed during Hurricane Ike in 2008; so the extent and depth of flooding and inundation for the 100-yr proxy storm and either sea level would be significantly less than what was experienced during Ike.

With the extended Ike Dike in place, even for the very rare 500-yr proxy storm at the higher sea level, peak surges along the western shoreline of Galveston Bay range from 9 to 11 ft, for present-day sea level, to 11 to 13 ft for the future sea level. These values are comparable to or less than the peak surge levels during Hurricane Ike in 2008, so inundation is expected to be comparable to or less than what occurred during Ike.

Residual Risk with the Ike Dike in Place

The following discussion provides some idea of the level of residual risk to residential and industrial areas along the western shoreline of Galveston Bay with the 17-ft Ike Dike. The assessment of residual risk considers peak surge conditions for the severe 100-yr and 500-yr proxy storms, with the Ike Dike concept in place.

For Present Sea Level Conditions

With the extended Ike Dike in place, the following communities along the western shoreline of Galveston Bay still experience inundation for the 100-yr proxy storm and the present sea level scenario: all the communities just south of the Texas City levee in the vicinity of and including Bayou Vista and the southeast fringes of Hitchcock, most of San Leon, the lowest-lying areas along the Dickinson Bayou and isolated areas in eastern Dickinson adjacent to Gum Bayou, isolated areas in southern Bayport, the lower-lying areas in communities at the entrance to Clear Lake (Seabrook, Kemah, Clear Lake Shores), a few isolated areas around the periphery of Nassau Bay, and isolated industrial facilities in the upper reaches of the Houston Ship Channel.

With the Ike Dike, for the 500-yr proxy storm and present-day sea level, the following areas experience inundation that did not experience inundation for the 100-yr proxy storm for either sea level: a few more areas in southeast Hitchcock a few more areas in central and eastern Dickinson a few more areas in the communities around the entrance to Clear Lake a few more areas around Shoreacres and in southern Bayport, and more areas around the periphery of Nassau Bay.

For Future Sea Level Conditions

With the Ike Dike, the following communities along the western shoreline of Galveston Bay experience inundation for the 100-yr proxy storm and the future sea level scenario: all the communities just south of the Texas City levee in the vicinity of and including Bayou Vista and the southeast fringes of Hitchcock, nearly all of San Leon, lower-lying areas along the Dickinson Bayou, including more areas in western Dickinson (adjacent to Gum Bayou) and in central Dickinson (between I-45 and Highway 3), southern Bayport, southern Shoreacres and sections of Highway 146 near Shoreacres, communities near the entrance to Clear Lake (southern Seabrook including the coastal areas along the Galveston Bay shoreline, Kemah, Clear Lake Shores), more areas around the periphery of Nassau Bay, and a few more isolated facilities in the upper reaches of the Houston Ship Channel.

With the Ike Dike, for the 500-yr proxy storm and the future sea level scenario, the following areas experience inundation that did not experience it for the 100-yr proxy storm, for either sea level: a few more areas in southeast Hitchcock, a few more areas in central and eastern Dickinson, much of the Seabrook, Kemah, Clear Lake Shores areas, much of the coastal region northeast of Seabrook, a few more areas in southern Bayport, all of Shoreacres, new areas southern La Porte, and nearly all areas that lie along the Clear Lake and Taylor Lake shorelines, including the El Lago area and areas immediately adjacent to the NASA facility.

To place this residual risk information in a probabilistic context, the encounter probability for a 100-yr water level is approximately 25% over the next 30 years. This means that there is 25% chance that the 100-yr water level (or something greater) will be encountered during the next 30 years. The encounter probability for a 100-yr water level sometime during the next 50 years is approximately 40%. For the 500-yr water level, the encounter probability is approximately 6% over the next 30 years and approximately 10% over the next 50 years.

Consideration of Secondary Lines of Defense and Recommendations

An analysis of exposure to inundation, residual flood risk, and possibilities for secondary lines of defense are discussed in greater detail in Chapter 12. The results of this analysis are summarized here. The intent of these additional risk-reduction measures is to reduce the residual flood risk that exists in each of these areas, even with the 17-ft Ike Dike in place.

City of Galveston

The City of Galveston is at risk of flooding from both the Gulf and bay sides. Certain hurricanes, Hurricane Ike was an example, can generate a peak surge on the Gulf side that is significantly lower than the elevation of the Galveston Seawall, but still produce significant flooding in the city due to high peak storm surge along the bay side. Surge simulations done to date suggest that, in a relative sense and at the present time, Galveston is more vulnerable to flooding from the bay side than it is from the Gulf side.

Since construction of the Galveston Seawall in the early 1900's, there has been an increase in relative mean sea level in the Galveston area. The

increase in sea level has increased the risk of flooding along both the bay and Gulf sides of the city.

Further reduction in the risk of flooding is recommended for the City of Galveston. It can be achieved by raising the Galveston Seawall and by building a ring dike/wall system around the bay side of the city, with a proper transition from the much higher elevation at the Galveston Seawall to a lower dike/wall elevation on the bay side. Elevations for the Seawall and the ring dike/wall should be designed to create a consistent level of flood risk around the periphery of the City.

Ring Dike

The Ike Dike concept will greatly reduce the risk of bay-side flooding, but a significant residual risk remains for parts of the City because of the low land elevations along the bay shoreline, which are less than 6 ft NAVD88 in places. Raising elevations, where necessary, to a minimum of 8 or 9 ft in the lowest-lying areas, should be considered as a secondary line of defense measure to implement as a facet of the Ike Dike concept. Building a ring dike/wall in these areas, to a crest elevation of approximately 8 or 9 ft, helps create a more consistent level of risk associated with flooding due to storm surge from the Gulf side and from the bay side, for the present sea level.

If the Galveston Seawall also is raised to reduce the risk of flooding from the Gulf side, a measure that is discussed in the next section, then to achieve a consistent degree of flood risk on both the Gulf and bay sides, measures also would need to include construction of a more extensive and higher bay-side ring dike/wall. For a Seawall crest elevation of 22 or 23 ft, the design elevation for a ring dike/wall on the bay side would probably need to be approximately 11 ft, and perhaps more, depending on the magnitude of wave overtopping that is allowable.

If a ring dike is built to keep the water out of the City, pumping stations or other measures will probably be required to evacuate any water that does accumulate in the lower areas due to steady overflow and/or wave overtopping of the Seawall and/or the ring dike/wall on the bay side.

Raising the Galveston Seawall

Raising the Galveston Seawall is recommended for the following reasons. First, in light of the nearly two feet of relative sea level rise that has apparently occurred since the original Galveston Seawall was constructed, the current seawall elevation of 17 ft does not provide the same level of risk reduction that the seawall provided when it was originally constructed. A 2-ft increase in seawall elevation would compensate for the increase in sea level that has already occurred. With any additional future sea level rise, the existing seawall will provide even less risk reduction. The future sea level scenario of +2.4 ft suggests that the increase in seawall elevation should be 4.4 ft to maintain the level of risk reduction that was reflected in the original sea wall design (i.e., to an elevation of approximately 21.5 ft NAVD88). The present-day 100-yr, 200-yr and 500-yr 90% CL Average Recurrence Interval (ARI) water surface elevations at the Galveston Pleasure Pier have been computed to be 13.5, 14.9 and 17.0 ft NAVD88, respectively, as part of this study. Linearly adding 2.4 ft of future sea level rise to each ARI elevation, these same three statistical water level values become 15.9 ft, 17.3, and 19.4 ft, respectively. Second, the long-dike effect that will occur with construction of the Ike Dike will act to raise the ARI water levels, perhaps by a foot or so for these extreme values (i.e., further increases in ARI elevations to values of roughly 17, 18.5, and 19.5 ft, respectively, are expected). A value of 17 ft, the current seawall elevation, lies somewhere closer to the expected 100-yr ARI value for the SLR1 future sea level scenario, with the Ike Dike in place. The City of Galveston should have a lower risk of flooding than is provided by a seawall that has a crest elevation that corresponds to the 100-yr ARI value. Third, note that these ARI water surface elevation values are “still water” levels, which do not account for any short wave overtopping. Considerable wave overtopping would be expected for peak storm surges of these magnitudes. Adding 3 to 4 ft of freeboard to reduce the effects of wave overtopping, raises the desired seawall elevations to something in the range of 22 to 23 feet for the 200-yr and 500-yr ARI water levels. It is estimated that during Hurricane Ike, there was about 4 ft of freeboard on the Gulf side of the Galveston Seawall, in the light of the 13 ft peak surge that was simulated for this hurricane. The volume of wave overtopping at the Seawall which occurred during Hurricane Ike provides some indication of the volume that can be expected for this amount of freeboard above the peak surge level. The elevation of the Galveston Seawall should be raised to 22 or 23 ft or to the maximum value that is supported by the City of Galveston.

Galveston Island and Bolivar Peninsula

One measure that can be taken is raising the first floor elevation of individual structures. Elevating structures to a first floor elevation of 10 to 12 ft NAVD88 would significantly reduce the risk of flooding on the bay side of the 17-ft Ike Dike, even for the future sea level scenario. This is undoubtedly much lower than what would be required to comply with the FEMA risk maps for existing conditions.

Another measure that can be implemented is construction of a ring dike or levee around concentrations of structures, perhaps integrated with an access road on top of the levee. A ring levee with crest elevation of 10 to 12 ft NAVD88 would significantly reduce the risk of flooding. A pump station(s) might be required to evacuate any accumulating water inside the ring levee. A gate or gates might also be required to provide vehicular access. Residents are often opposed to such structural measures, because they block the view.

Bayou Vista and Hitchcock areas

In the Hitchcock and Bayou Vista areas, a levee/wall system could be constructed along one of several possible alignments shown in Figure 12-23. The crest elevations of this secondary line of defense would likely range from 11 to 16 ft to cover the range of peak surge experienced for the two most severe proxy storms and both sea levels. However, in light of the relatively sparse density of structures in the Hitchcock area, and the probable cost of these structural alternatives, it seems unlikely that such lengthy secondary lines of defense would be cost effective. Ringing the Bayou Vista area with a levee system may not be acceptable to the community.

For the low lying communities of Tiki Island, and Harborwalk, the only feasible option is likely raising the first floor elevations of structures. Ringing these communities with a levee system might not be acceptable to the communities.

San Leon, Texas City (north), Bacliff and Dickinson areas

There are several possible secondary lines of defense that can lessen the residual flood risk to a varying number of areas. Alignments of possible measures are shown in Figure 12-27.

One measure that can reduce residual risk to part of central Dickinson, the area between I-45 and Highway 3, involves a short section of levee or wall and a small gate to enable navigation on Dickinson Bayou. The measure could be constructed at a location just to the east of where Highway 3 crosses the bayou. It would have a crest elevation of about 11 to 14 ft, and would be tied into the existing rail line embankment.

A second possible measure that reduces residual risk for a much larger area, including the entire Dickinson area, is a levee/dike/wall constructed along Highway 146. It could be incorporated into sections of the existing highway infrastructure. Its crest elevation would also be 11 to 14 ft. This measure would require a gate at the entrance to Clear Lake to enable navigation.

Neither of the first two measures provides additional risk reduction to San Leon. Most likely, raising the elevations of structures as part of a long-term community plan is the only feasible approach for reducing residual risk at San Leon. Construction of risk reduction measures along the coastal periphery of the San Leon peninsula, across the open water leading to Dickinson Bay, and tying in to the Texas City Levee can be done, but it seems problematic for a number of reasons and would probably be prohibitively costly.

Clear Lake, Bayport and La Porte areas

Only one of several possible measures appears viable to reduce the residual risk in these areas. Alignments of this and other possible measures are shown in Figure 12-31.

The most viable measure involves a levee or wall system built along Highway 146, in two sections, which could be incorporated into the existing highway infrastructure. This option would also require a gate to facilitate navigation at the entrance to Clear Lake. The crest elevation of this measure would likely range from 13 to 16 feet. It is recommended that these two sections of a secondary line of defense be examined to assess their cost/benefits, and their potential for inclusion as a component of the Ike Dike implementation.

The only other option would be a secondary line of defense right at the Galveston Bay shoreline. However, judging from the built environment and the many docks along the bay shoreline, there would likely be

considerable opposition to construction of any structural measures at the coast.

Another option is to raise the elevations of individual structures as part of a long-term strategy to do so in the most vulnerable areas.

Upper Houston Ship Channel

In areas having undesirable residual risk, levees or walls built to ring individual facilities, or groups of facilities, can reduce the risk of flooding to the desired level. In light of the peak surge levels for the 100-yr and 500-yr proxy storms, and both sea level scenarios, the elevations of such features would probably need to be in the range of 11 to 16 ft, depending on the desired level of risk reduction and exposure of the site/levee to wave action.

The “Centennial Gate” was originally proposed by the Rice University SSPEED Center as a stand-alone surge suppression measure to prevent storm surge penetration into the upper reaches of the Houston Ship Channel. The 500-yr proxy storm, for existing no-dike conditions, and for the future sea level scenario, produces peak surges that reach nearly 25 ft in this area. With the Ike Dike in place, peak surge levels that are generated in the upper ship channel (14 to 15 ft) would be about 1 ft higher than those experienced during Hurricane Ike. Except for very low-lying areas, the Ike Dike seems to be quite effective in suppressing surge levels in the upper ship channel area, probably precluding the need for a “Centennial Gate” as a risk reduction measure for this region, at least for the present time.

If future sea level looks like it might exceed the 2.4 ft value that is considered in scenario SLR1, it would be worthwhile to re-examine the need for a gate at this location as a means for reducing flood risk in the upper reaches of the Houston Ship Channel to acceptable levels.

Examination of Alternate Ike Dike Configurations

Chapters 10 through 12 examined the storm surge reduction benefits of the extended Ike Dike, which started at Freeport, ended at Sabine Pass, and which followed the coastline. Chapter 13 examines a number of other possible alternate configurations for the Ike Dike, including shorter versions that provide less surge reduction. One of the other alignments

examined, Alignment 2, is quite similar to the coastal spine recommended by the GCCPRD that extends from the western end of Galveston Island to High Island. The merits of adding eastern and western termination dike sections to the alignment recommended by the GCCPRD are examined in Chapter 13, as is the influence of adopting lower crest elevations for storm surge gates at Bolivar Roads and San Luis Pass.

The Different Configurations

The original set of storm surge simulations that were made to examine benefits of the Ike Dike concept involved a long dike that followed the shoreline, began just south of Freeport, TX, and ended just to the east of High Island, TX. Those results suggested that undesirable flanking occurred around the eastern end of the dike. To reduce the adverse effects of flanking, the original alignment was extended further to the east, all the way to Sabine Pass, TX. This alignment is referred to as the extended Ike Dike, and it is shown in Figure 13-1. The extended Ike Dike alignment is the subject of Chapters 10 through 12.

A variation of the extended Ike Dike was also examined. Dutch partners in the Ike Dike investigation identified several other possible alignments for a long coastal spine. Each alignment involved tying the dike into higher ground elevations at different locations on both its eastern and western ends (Van Berchem et al., 2016).

On the eastern end, one alternate alignment, the State Highway 124 option, or SH124, left the coast and turned inland at High Island and then followed SH124 north to Winnie, TX, instead of following the coast to Sabine Pass (see Figure 13-2). This alignment was adopted for further study in light of the fact that it is shorter and potentially less costly than a coastal alignment that extended to Sabine Pass.

On the western end, van Berchem et al. (2016) identified two options. One option, the Bluewater Highway alignment, is similar to the extended dike alignment that has been previously modeled in this study. A second option crossed San Luis Pass from the western end of Galveston Island, immediately turned inland at that point, headed toward the north-northwest and crossed both West Bay and wetlands of the Brazoria National Wildlife Refuge, and then veered northwest until it intersected County Road 227 (Hoskins Mound Road). This inland alignment might generate considerable opposition based on environmental concerns.

Therefore, the coastal alignment that has been utilized to date in the extended Ike Dike was retained, except that the western dike section is now terminated on the northeast side of Freeport and ties into the existing levees there. An Alignment 1a was developed that included a middle dike section that extended from San Luis Pass to High Island, along with the SH124 eastern section alignment and the coastal western section that ends at Freeport. Alignment 1a is shown in Figure 13-2. This alignment represents a slightly different version of the extended Ike Dike shown in Figure 13-1.

Preliminary design analyses were performed by the Dutch study partners for gate systems at both Bolivar Roads and San Luis Pass (see Jonkman et al., 2015). They designed both a navigational gate section and an environmental gate section at each pass. Lower gate crest elevations were selected in order to reduce construction costs. To quantify the influence of steady overflow on surge levels within the bay, particularly at the City of Galveston which is immediately adjacent to the Bolivar Roads gate system and which is vulnerable to flooding from the bay side, an alternate dike configuration was considered in the analysis. Alignment 1b was developed, in which the 17-ft crest elevation of the dike in Alignment 1a was lowered to the elevations shown in Table 13-1, at the locations of both gate systems.

The Gulf Coast Community Protection and Recovery District (2016a and 2016b), GCCPRD, recently completed its own storm surge suppression study to investigate measures for reducing hurricane flood risk for the north Texas coast. The coastal spine recommended by the GCCPRD extended from the western end of Galveston Island, across Bolivar Pass, and ended at High Island. An Alignment 2 was developed that closely resembles the coastal spine alignment recommended by the GCCPRD; it extended from the western end of Galveston Island, across Bolivar Pass, and ended at High Island. A gate system was included at Bolivar Roads. Alignment 2, shown in Figure 13-3, represents the middle section, only, of the alignments shown in Figures 13-1 and 13-2, without any eastern or western termination sections.

An Alignment 3 was developed that was comprised of Alignment 2 plus the SH124 eastern termination section. This alignment had no western termination section. Alternate Alignment 3, shown in Figure 13-4, was developed to isolate the role of the western section on storm surge

reduction and it was intended to facilitate examination of the merits/consequences of having/not having a western termination section.

Storms That Were Simulated

Four storm surge simulations were made for each of the four alternate dike alignments, Alignments 1a, 1b, 2 and 3. All simulations were made for the future sea level scenario, which is 2.4 ft higher than present sea level (i.e., a future sea level of 3.31 ft, NAVD88). This future sea level scenario is the same SLR1 scenario that was considered previously in the extended Ike Dike analysis discussed in Chapters 10 through 12. For each dike alignment, simulations were made for the 10-yr, 100-year, and 500-yr proxy storms and for Hurricane Ike, using the same improved modeling approach that was adopted for the extended Ike Dike simulations. Peak storm surge results for each of these simulations were provided to the economics team for further analysis. Results from these simulations are discussed in Chapter 13. Results are presented graphically within the report text and in tabular form in Appendix B.

Merits of an Eastern Termination Section

Results suggest that an eastern termination section might not be cost effective in terms of flood risk reduction benefits to the Houston/Galveston region. This is the case for both of the two eastern section alignments, the SH 124 inland alignment and the coastal alignment that extends to Sabine Pass. In the Houston/Galveston region, the eastern termination section primarily benefits Bolivar Peninsula, where the potential for flood risk reduction benefits is much lower. An eastern termination section is of relatively little benefit in reducing peak surge at the City of Galveston, along the western shoreline of Galveston Bay and the upper reaches of the Houston Ship Channel in the Houston-Galveston region, areas that have a much greater potential for damage/loss. The storm surge dynamics that lead to this result are discussed in Chapter 13.

Having no eastern termination section probably means tying the Ike Dike into higher elevation on the south side of High Island. This is the termination location in the coastal spine plan recommended by the GCCPRD.

If an eastern section is adopted, costs and benefits should be considered both within and outside the Houston/Galveston region. For example, a coastal alignment for an eastern section which extends all the way to Sabine Pass provides flood risk reduction benefits to the Winnie-to-Port Arthur area which have not been considered heretofore. It can also provide protection to and stability to a coastal highway in the area. However those benefits should be accounted for in a complete cost/benefit analysis of an extended Ike Dike alignment. Additionally there are some negative consequences associated with the inland SH124 alignment, which causes local increases in peak surge just outside the dike, due to the “long dike effect.”

The original modeling approach and the initial Ike Dike simulations made with it suggested that flanking around the eastern end of the Ike Dike, which ended just east of High Island was problematic and that the dike should be extended further to the east. Subsequent simulations made with the improved modeling approach for the alternate Ike Dike configurations, showed that the original results were misleading and that flanking around the east side of the dike was not as great as first thought. Results indicate that termination of the Ike Dike at High Island, as recommended by the GCCPRD, does not significantly affect peak surge levels throughout Galveston and West Bays, except along Bolivar Peninsula.

Merits of a Western Termination Section

Termination of the coastal spine at the western end of Galveston Island with no gate system at San Luis Pass, as recommended by the GCCPRD, enables propagation of the hurricane surge forerunner into West Bay. Without a western termination section the hurricane forerunner surge can propagate through San Luis Pass and into West Bay, and then into Galveston Bay under certain wind and water level conditions, a process that can begin a day or more before the hurricane makes landfall.

The absence of a western termination section, which includes a gate system at San Luis Pass, allows the peak storm surge associated with a hurricane’s core winds to propagate into West Bay as well. Therefore termination of the coastal spine at the western end of Galveston Island significantly increases peak storm surge levels within West Bay because it enables propagation of the peak storm surge through San Luis Pass as well as flow over the barrier island south of the pass once it becomes inundated.

The peak storm surge results suggest that the western termination section has a much greater positive influence in the Houston-Galveston region than does an eastern termination section, particularly along western and central parts of Galveston Island and along the northern shoreline of West Bay west of Texas City. The western dike section results in greater surge reductions, over a wider geographic area, in areas having higher potential for damage and economic losses than does an eastern termination section.

Another factor that might support inclusion of the western termination section in the Ike Dike concept is the ability to not only prevent the forerunner and peak surge from entering West Bay, but also as a means for controlling the water level inside the bays at the time when the surge gates are closed. It might be advantageous to use the timing of gate closure as a means to minimize the amount of water in the bays, in advance of an approaching hurricane. Such an operational procedure might dictate closing the gates when low astronomical tide creates a minimum water surface inside the bays. Having gates at both San Luis Pass and Bolivar Roads could achieve this operational objective fully; a gate system only at Bolivar Roads can only do this partially. A desire to operationally control the water level inside the bays at the time of gate closure might become increasingly more important as mean sea level rises.

Also, with rising sea level, salinity within West and Galveston Bays is expected to gradually increase, due to the added volume of salt water from the open Gulf that is introduced into the bays. The added volume will be significant in light of the shallowness of the bays. Gate systems at both Bolivar Roads and San Luis Pass might provide an opportunity for managing the salinity within the bays in a beneficial way in an era of rising sea level, by reducing tidal exchange and increasing the residence time for freshwater that is introduced into the bays by the rivers. Operation of the gate systems might provide an opportunity to mitigate, to some degree, negative consequences of a more saline bay system. If there are environmental benefits for having a gate system at San Luis Pass, this would also support inclusion of a western termination section in the Ike Dike concept. Any potential for environmental benefits associated with gate systems at both passes should be explored further.

Influence of Lowered Gates at the Passes

By comparing results for Alignments 1b and 1a, it is evident that the effect of lower gate elevations on peak surge levels behind the dike is relatively

small even for the more severe hurricanes. Lower gate elevations lead to slightly higher storm surge levels for the severe hurricanes that were simulated. For less intense hurricane events like the 10-yr proxy storm, which produces little or no overtopping or steady flow over the gates, there are no significant increases to peak storm surge levels behind the dike associated with the lowered gate crest elevations.

These increases in peak surge level, which are relatively small even for the most intense hurricanes, will require a small increase in design elevation for any secondary lines of defense within the bays, such as a ring levee/wall system along the bay side of the City of Galveston.

Water Level Considerations for Operating the Ike Dike Storm Surge Gates

Early closure of the storm surge gates at both San Luis and Bolivar Roads Passes is a critical operational feature of the Ike Dike concept. The amount of water within Galveston and West Bays at the time of gate closure influences the peak surge elevation that will be generated by local hurricane force winds that still act on the bays after the gates are closed. A higher antecedent water level in the bays leads to a higher peak surge within the bays, and thus a greater residual flood risk. The following contributors influence the antecedent water level: long-term and seasonal and long-term mean sea level, astronomical tide, wind-driven surge forerunner, and volume mode forerunner.

The long-term relative mean sea level has been slowly rising in the Houston-Galveston region. There are seasonal changes in mean sea level that occur in the Gulf of Mexico. Late summer hurricanes (in September and October) are expected to be accompanied by seasonal mean sea levels that are 0.4 to 0.5 ft higher, on average, than the long-term mean sea level. The actual sea level at the time a hurricane occurs can be even higher than the monthly mean values. Such was the case in September 2016 when seasonal sea levels were unusually high, approximately 1 ft above the long-term mean sea level. Hurricanes that occur earlier the season (June, July and August) will most likely be accompanied by a seasonal mean sea level is not significantly different from long-term mean. The seasonal sea level will be the same inside the bay as outside, unless local precipitation raises levels significantly inside the bays.

The astronomical tide, which produces oscillatory changes in water level, can lessen the impacts of higher antecedent water levels caused by the seasonal mean sea level and the wind-driven forerunner. This can be achieved by closing the surge gates at a time of low tide. The time of occurrence of the hurricane within the 14-day spring-neap tidal cycle, and the tide range at that time, influences the potential benefits of closing the gates at low tide. At spring tide conditions, when the tide range is greatest (2.5 to 3 ft), unusually low tides that occur every 24 hours provide an opportunity to significantly lessen the residual flood risk inside the bays. At neap tide, when the tide range is smallest (0.5 to 1.5 ft), low tides are not as low and there is less opportunity to offset the elevated water levels associated with mean sea level and the wind-driven forerunner. During neap tide conditions, lows are experienced every 12 hours, which might be a small benefit in deciding when to close gates.

Generation of the wind-driven forerunner can begin once the eye of a hurricane enters the Gulf. The forerunner is forced by winds that blow along the continental shelf regions of the northern Gulf, pushing water along the shelf, which is then turned to the “right” and stacked against the shoreline by the Coriolis force, an Ekman set-up. The wind-driven forerunner is manifested as a persistent steady rise in water level at the coast; and, the rate of rise accelerates as the hurricane gets closer to the continental slope and shelf off the Texas coast. The magnitude of the wind forerunner is dependent upon the storm’s size, intensity and forward speed. The more intense and larger the hurricane, the greater the rate of water level rise during the forerunner build-up. Slower moving storms have the potential to produce a greater forerunner surge than faster moving storms.

The wind-driven forerunner can cause an increase in water level at Galveston of as much as several feet, one or two days before landfall. Importantly, the wind-driven forerunner that is generated at the coast readily propagates through the passes and open storm surge gates into the bays, with little or no attenuation. Therefore, wind-driven forerunner surge directly increases residual flood risk inside the bays.

The development of the wind-driven forerunner amplitude both on the open coast and inside the bays is highly sensitive to forward speed for hurricanes that approach from the southeast. In general, the slower the forward speed the greater the wind-driven forerunner amplitude at

Galveston and the greater accumulation of water inside the bays at the time of landfall. Because little to no attenuation of the forerunner amplitude occurs as it propagates from the open coast through the passes and into the bays, propagation of the forerunner into the bays exerts a major influence on peak surge levels inside the bay caused by high in-bay winds moving the water around within the bay. For example, for a severe 930-mb hurricane, without any surge gates in place, a threefold decrease in forward speed, from 18 kt to 6 kt, led to a two fold increase in peak surge in the upper reaches of the Houston Ship Channel (from 10 to 20 ft). A critical aspect of the Ike Dike surge barrier operation will be minimization of the surge forerunner within the Bay through early gate closure. Early gate closure will be particularly crucial for slow-moving storms. Peak surge at the open coast is much less sensitive to forward speed.

The wind-driven forerunner is much more important than the volume mode forerunner, which can be excited when a severe hurricane enters the Gulf. The amplitude of the volume mode forerunner is only a few tenths of a foot for even the largest and most intense hurricanes.

The volume mode forerunner is oscillatory by nature, with a rather predictable period of 32 to 36 hours. As with the astronomical tide, the predictability of its period provides some potential for exploitation in terms of timing gate closure. The amplitude of the volume-mode forerunner is relatively small, so the benefits of exploiting this mode of forerunner are limited.

Hurricane Ike serves as a useful example for examining these different physical processes that influence the antecedent water level, and how they might influence timing of gate closure. The figure below is a reproduction of Figure 14-12b, which was presented earlier in the chapter. The figure shows the measured water surface elevation during Ike at Galveston Pier 21 (in green), which lies inside the bay at the Port of Galveston, along with the predicted astronomical tide (in blue). Water surface elevation is displayed in feet, relative to mean sea level (MSL), which is the long term mean sea level for the gage site. Ike's landfall occurred at around hour 0700 GMT on September 13, shown by the red vertical line in the figure.

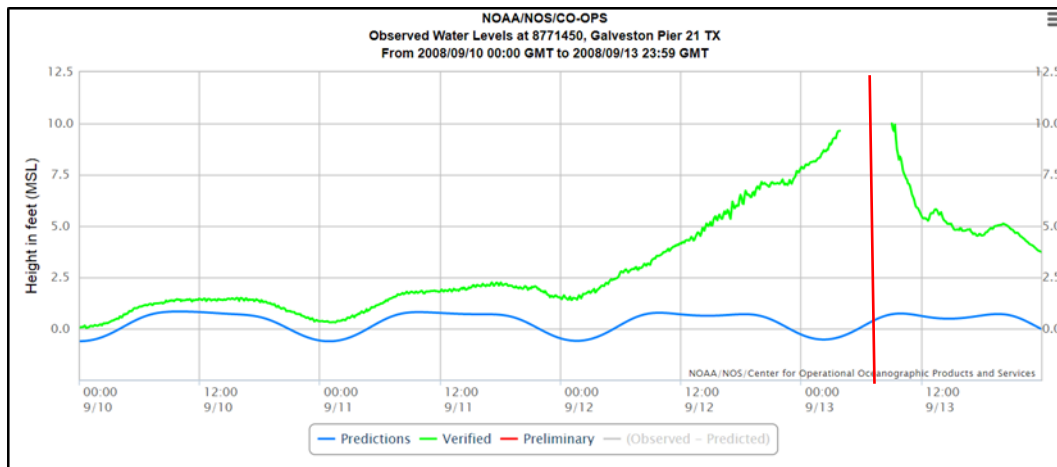


Figure 14-12b. Measured water surface elevation during Hurricane Ike, at the Galveston Pier 21 gaging station.

The initial offset in elevation between the green and blue curves at hour 00:00 on September 10, more than 3 days before landfall, reflects about 0.5 ft of seasonal mean sea level increase above the long-term mean sea level and possibly a small contribution due to the wind-driven forerunner surge while the hurricane was beginning to transit the Gulf. Ike entered the Gulf a few hours before 00:00 on September 10. During the subsequent two days, September 10 and 11, an overall trend for increasing water level due to the wind-driven forerunner is evident, at an accelerating rate of rise, as are oscillations due to the astronomical tide.

Assuming a time of gate closure that is 12 hours before landfall, i.e., at hour 19:00 on September 12, an antecedent water level of between 6 and 7 ft would likely be present inside Galveston Bay at the time of closure. This very high antecedent level would considerably increase flood risk inside the bay, by unacceptable levels, even with the Ike Dike in place. Closing the gates at the time of low tide which occurred at around hour 03:00 on September 12 (28 hours before landfall) would have resulted in a much lower antecedent water level in the bay, approximately 1.0 to 1.5 ft, which would reduce the residual flood risk inside the bays, compared to the later closure time. Closing the gates even earlier, at the preceding low tide, which occurred at around hour 02:00 on September 11 (53 hours before landfall), while the hurricane was in the Gulf but well seaward of the Texas coast, the antecedent water level inside the bays would have been lower still, approximately equal to the long-term mean sea level value with little to no effect of the seasonal mean and wind-driven forerunner.

Very early closure of the surge gates prevents any precipitation run-off into the bays from leaving the bays, so this might also be an operational issue that needs to be considered as well.

A reliable hurricane surge forecasting model that accurately does the following: simulates the tide and forerunner surge, treats the influence of the surge gate infrastructure on long wave propagation into the bays while the gates are in the open position, treats closure of the gates during the storm's approach, and treats flow of water over closed gates, would be a very useful predictive tool. The tool could be applied to provide guidance for decision-making concerning the optimal time for closure of the surge gates. Inclusion of rainfall during the approaching storm into the model simulation, and subsequent simulation of water run-off into the bays could improve such a forecast capability.

Wave Conditions to Consider in Designing the Ike Dike

Design of the land barrier and navigational/environmental sections of the gate systems, both of which will be constructed as part of the Ike Dike concept, will require nearshore wave information. All components will need to be resilient to overflow and overtopping, which means they will experience minimal damage and no loss of functionality in the event the hydraulic design conditions are exceeded and the Ike Dike is overtopped, even with overflow. There is always some risk of this happening.

Wave model results for the 500-yr proxy storm provide a reasonable estimate of the nearshore wave conditions that the Ike Dike will need to withstand, even though overtopped. Undoubtedly, armoring of the Ike Dike will be required to provide the necessary level of resilience.

Wave and water level conditions at the Galveston Pleasure Pier location are representative of open-Gulf, nearshore wave conditions, which the land barrier sections of the Ike Dike will have to withstand. Conditions for a location in the throat of Bolivar Roads Pass are more representative of those which the gate systems will have to withstand. The throat is more "sheltered" than the open gulf area by the entrance jetties, even when they are submerged, so wave conditions are expected to be lower there.

For the 500-yr proxy storm and present-day sea level, the following wave and water level conditions were calculated:

Pleasure Pier: significant wave height of 16 ft in a water depth of 29 ft, which includes a storm surge elevation of 20.5 ft NAVD88. The peak and mean wave periods at the time of landfall were 13 sec and 10 sec, respectively.

Bolivar Roads Pass: significant wave height of 10 ft in a water depth of 70 ft, which includes a storm surge elevation of 21.5 ft NAVD88. The peak and mean wave periods at the time of landfall were 12 sec and 8.5 sec, respectively.

The time of landfall corresponds well to the times of peak storm surge and the time of maximum wave conditions at both of these locations.

17 References

ARCADIS, 2011, "ADCIRC Based Storm Surge Analysis of Sea Level Rise in the Galveston Bay and Jefferson County Area in Texas," November 28, 2011, prepared for The Nature Conservancy, 49 pp.

Blain, C.A., J.J. Westerink, R.A. Luetlich, Jr. and N.W. Scheffner, 1994, ADCIRC: an advanced three-dimensional circulation model for shelves coasts and estuaries, report 4: hurricane storm surge modeling using large domains, Dredging Research Program Technical Report, DRP-92-6, U. S. Army Engineers Waterways Experiment Station.

Bunpapong, M., Reid, R.O., and Whitaker, R.E., "An Investigation of Hurricane-Induced Forerunner Surge in the Gulf of Mexico," Technical Report CERC-85-5, Coastal Engineering Research Center, U.S. Army Corps of Engineers, September 1985.

Bunpapong, M., Reid, R.O., and Whitaker, R.E., "An Investigation of Hurricane-Induced Forerunner Surge in the Gulf of Mexico," Technical Report CERC-85-5, Coastal Engineering Research Center, U.S. Army Corps of Engineers, September 1985.

Cardone, V. J., C.V. Greenwood, and J. A. Greenwood. 1992. Unified program for the specification of tropical cyclone boundary layer winds over surfaces of specified roughness. Contract Rep. CERC 92-1. Vicksburg, MS: U.S. Army Corps of Engineers Waterways Experiment Station.

Cardone, V.J., A.T. Cox, J.A. Greenwood, and E.F. Thompson. 1994. Upgrade of tropical cyclone surface wind field model. Misc. Paper CERC-94-14, Vicksburg, MS: U.S. Army Corps of Engineers Waterways Experiment Station.

Cardone, V.J. and A.T. Cox. 2009. Tropical cyclone wind field forcing for surge models: critical issues and sensitivities. *Nat Hazards* 51: 29–47.

Chouinard, L.M. and C. Liu. 1997. Model for Recurrence Rate of Hurricanes in Gulf of Mexico. *Journal of Waterway, Port, Coastal and Ocean Engineering* 123(3): 113-119.

Coastal Protection and Restoration Authority (CPRA). 2013. Greater New Orleans Flood Protection System Notice of Completion – Design Assessment by Non-Federal Sponsor. Bell City, LA: Lonnie G. Harper & Associates.

Diaconis, P. (1988). Bayesian numerical analysis. *Statistical Decision Theory and Related Topics IV*.

Dietrich, J.C., S. Bunya, J.J. Westerink, B.A. Ebersole, J.M. Smith, J.H. Atkinson, R. Jensen, D.T. Resio, R.A. Luettich, C. Dawson, V.J. Cardone, A.T. Cox, M.D. Powell, H.J. Westerink, H.J. Roberts. 2010a. A High-Resolution Coupled Riverine Flow, Tide, Wind, Wind Wave and Storm Surge Model for Southern Louisiana and Mississippi: Part II – Synoptic Description and Analysis of Hurricanes Katrina and Rita. *Monthly Weather Review*, Volume 138, 378-404.

Dietrich, J.C., S. Bunya, J.J. Westerink, B.A. Ebersole, J.M. Smith, J.H. Atkinson, R. Jensen, D.T. Resio, R.A. Luettich, C. Dawson, V.J. Cardone, A.T. Cox, M.D. Powell, H.J. Westerink, H.J. Roberts. 2010b. A High-Resolution Coupled Riverine Flow, Tide, Wind, Wind Wave and Storm Surge Model for Southern Louisiana and Mississippi: Part II – Synoptic Description and Analysis of Hurricanes Katrina and Rita. *Monthly Weather Review*, Volume 138, 378-404.

East, J.W., Turco, M.J., and Mason, Jr., R.R., “Monitoring Inland Storm Surge and Flooding from Hurricane Ike in Texas and Louisiana,” *Open File Report 2008-1365*, March 2009.

Federal Emergency Management Agency (FEMA). 2008a. Mississippi coastal analysis project. Final Report: HMTAP Task Order 18, prepared for the Federal Emergency Management Agency, Department of Homeland Security. Gaithersburg, MD: URS Group, Inc.

Federal Emergency Management Agency (FEMA). 2008b. Hurricane Ike in Texas and Louisiana, High Water Marks, FEMA Mitigation Assessment Team Report (October 2008).

Federal Emergency Management Agency (FEMA). 2011. *Flood Insurance Study: Coastal Counties, Texas: Scoping and Data Review*. Denton, TX: Federal Emergency Management Agency, Region 6 (draft, in review).

Federal Emergency Management Agency (FEMA). 2012. Operating Guidance No. 8-12 for use by FEMA staff and Flood Mapping Partners: Joint probability – optimal sampling method for tropical storm surge. Washington, DC: Federal Emergency Management Agency, Department of Homeland Security.

Federal Emergency Management Agency (FEMA). 2014. Redefinition of the Coastal Flood Hazard Zones in FEMA Region II: Analysis of the Coastal Storm Surge Flood Frequencies. Final Report prepared for the Federal Emergency Management Agency, Department of Homeland Security. Fairfax, VA: Risk Assessment, Mapping, and Planning Partners.

Gulf Coast Community Protection and Recovery District. 2016a. Storm Surge Suppression Study, Phase 2 Report, Texas General Land Office, February 2016, 73 pp.

Gulf Coast Community Protection and Recovery District. 2016b. Storm Surge Suppression Study, Phase 3 Report, Recommended Actions, Texas General Land Office, June 2016, 32 pp.

Günther, H. 2005. WAM cycle 4.5 version 2.0. Institute for Coastal Research, GKSS Research Centre, Geesthacht, Germany, 38 pp.

Interagency Performance Evaluation Task Force (IPET). 2009. Performance evaluation of the New Orleans and Southeast Louisiana Hurricane Protection System. Final Report of the Interagency Performance Evaluation Task Force. Washington, DC: U.S. Army Corps of Engineers, Department of the Army.

Jarvinen, B.R., C.J. Neumann, and M.A.S. Davis. 1984. A tropical cyclone data tape for the North Atlantic Basin, 1886–1983: contents, limitations, and uses. NOAA Tech. Memo 22. Miami, Florida: National Hurricane Center, National Weather Service.

Jonkman, S.N., Lendering, K.T., van Berchum, E. C., Nillesen, A., Mooyaart, L., De Vries, P., van Ledden, M., Willems, A., Nooij, R., Coastal spine system – interim design report, Version 0.6 (Final Draft), June 2015, 82 pp.

Kennedy, A.B., Gravois, U., Zachry, B., Luettich, R., Whipple, T. Weaver, R., Reynolds, Fleming, J. Chen, Q., and Avissar, R. (2010). "Rapidly installed temporary gauging for waves and surge, and application to Hurricane Gustav", *Continental Shelf Research* 30, 1743-1752.

Kennedy, A.B., Gravois, U., Zachry, B.C., Westerink, J.J., Hope, M.E., Dietrich, J.C., Powell, M.D., Cox, A.T., Luettich, R.L., and Dean, R.G. (2011). "Origin of the Hurricane Ike forerunner surge", *Geophys. Res. Lett.*, L08805, doi:10.1029/2011GL047090.

Komen, G. J., L. Cavaleri, M. Donelan, K. Hasselmann, S. Hasselmann, and P.A.E.M. Janssen. 1994. *Dynamics and modelling of ocean waves*. Cambridge, UK: Cambridge University Press, 560 pages.

Landsea, C.W., G.A. Vecchi, L. Bengtsson, and T.R. Knutson. 2010. Impact of Duration Thresholds on Atlantic Tropical Cyclone Counts. *Journal of Climate* 23 (10): 2508–19.

Landsea, C.W. and J.L. Franklin. 2013. Atlantic hurricane database uncertainty and presentation of a new database format. *Monthly Weather Review* 141(10): 3576–3592.

Liu, Y. and Irish, J.L. 2017. Predicting tropical cyclone forerunner surge. *Proceedings of Coastal Dynamics 2017*. Pg 47-51.

Luettich, R.A., Jr., J.J. Westerink, and N.W. Scheffner, 1992, ADCIRC: an advanced three-dimensional circulation model for shelves coasts and estuaries, report 1: theory and methodology of ADCIRC-2DDI and ADCIRC-3DL, Dredging Research Program Technical Report DRP-92-6, U.S. Army Engineers Waterways Experiment Station.

Mann, M.E., T.A. Sabbatelli, and U. Neu. 2007. Evidence for a Modest Undercount Bias in Early Historical Atlantic Tropical Cyclone Counts. *Geophysical Research Letters* 34(22): L22707.

Massey, T.C., Anderson, M.E., Smith, J.M., Gomez, J., and Jones, R., 2011. *STWAVE: Steady-State Spectral Wave Model User's Manual for STWAVE. Version 6.0. ERDC/CHL SR-11-1, U.S. Army Engineer Research and Development Center.*

Minka, T. P. (2000) Deriving quadrature rules from Gaussian processes. Technical Report, Statistics Department, Carnegie Mellon University.

Nadal-Caraballo, N.C., Melby, J.A., Gonzalez, V.M., and Cox, A.T., 2015. North Atlantic Coast Comprehensive Study (NACCS), Coastal Storm Hazards from Virginia to Maine, ERDC/CHL TR-15-5, U.S. Army Engineer Research and Development Center. (draft, under review)

National Oceanic and Atmospheric Administration (NOAA), Tides and Currents web site,
<http://tidesandcurrents.noaa.gov/stations.html?type=Water+Levels>

Neumann, C.J., G.W. Cry, E.L. Caso, and B.R. Jarvinen. 1985. Tropical Cyclones of the North Atlantic Ocean, 1871-1980. Asheville, NC: National Climatic Center.

O'Hagan, A. (1991). Bayes-Hermite quadrature. *Journal of Statistical Planning and Inference*, No. 29.

Resio, D.T., S.J. Boc, L. Borgman, V. Cardone, A.T. Cox, W.R. Dally, R.G. Dean, D. Divoky, E. Hirsh, J.L. Irish, D. Levinson, A. Niedoroda, M.D. Powell, J.J. Ratcliff, V. Stutts, J. Suhada, G.R. Toro, and P.J. Vickery. 2007. White Paper on estimating hurricane inundation probabilities. Consulting Report prepared by USACE for FEMA. Vicksburg, MS: U.S. Army Engineer Research and Development Center.

Smith, J. M., A. R. Sherlock, and D. T. Resio. 2001. STWAVE: Steady-state spectral wave model user's manual for STWAVE, Version 3.0. ERDC/CHL SR-01-1. Vicksburg, MS. U.S. Army Engineer Research and Development Center.

Smith, J.M. 2007. Full-plane STWAVE with bottom friction: II. Model overview. CHETN-I-75. U.S. Army Engineer Research and Development Center.

Smith, J.M., Jensen, R.E., Kennedy, A.B., Dietrich, J.C., and Westerink, J.J. Waves in Wetlands: Hurricane Gustav. Proceedings of the 32nd Conference on Coastal Engineering. 2010.

Texas Coastal Ocean Observation Network (TCOON) web site,
<http://www.cbi.tamucc.edu/TCOON/>

Thompson, E. F., and V. J. Cardone. 1996. Practical modeling of hurricane surface wind fields. *ASCE J. of Waterway, Port, Coastal and Ocean Engineering*, **122**(4): 195-205.

Toro, G.R. 2008. Joint probability analysis of hurricane flood hazards for Mississippi – Final URS Group Report in support of the FEMA-HMTAP flood study of the State of Mississippi. Boulder CO: Risk Engineering.

Toro, G.R., D.T. Resio, D.D., A.W. Niedoroda, and C. Reed. 2010. Efficient joint-probability methods for hurricane surge frequency analysis. *Ocean Engineering* 37(1): 125–34.

U.S. Army Corps of Engineers (USACE). 2009a. *Louisiana Coastal Protection and Restoration (LACPR)*. Final Technical Report. New Orleans, LA: New Orleans District, Mississippi Valley Division, USACE.

U.S. Army Corps of Engineers (USACE). 2009b. *Mississippi Coastal Improvements Program (MSCIP), Hancock, Harrison, and Jackson Counties, Mississippi*. Mobile, AL: Mobile District, South Atlantic Division, USACE.

U.S. Weather Bureau. Monthly Weather Review, September 1900, Vol. XXXVIII, No. 9.

Van Berchem, E.C., de Vries, P.A.L., de Kort, R.P.J. Galveston Bay Area land Barrier preliminary design, Draft version 0.9, February 2016. 66 pp.

Vecchi, G.A. and T.R. Knutson. 2011. Estimating Annual Numbers of Atlantic Hurricanes Missing from the HURDAT Database (1878–1965) Using Ship Track Density. *Journal of Climate* 24(6): 1736–1746.

Vickery, P.J., and B.O. Blanton. 2008. *North Carolina coastal flood analysis system hurricane parameter development*. Technical Report TR-08-06. Chapel Hill, NC: RENCI Renaissance Computing Institute.

WAMDI Group, 1988. The WAM Model - A Third Generation Ocean Wave Prediction Model. *Journal of Physical Oceanography*, 18, 1775-1810

Westerink, J.J., R.A. Luettich, A.M. Baptista, N.W. Scheffner and P. Farrar, 1992, Tide and storm surge predictions using finite element model, *ASCE Journal of Hydraulic Engineering*, 118(10):1373-1390.

Worley, S.J., S.D. Woodruff, R.W. Reynolds, S.J. Lubker, and N. Lott. 2005. ICOADS Release 2.1 Data and Products. *Journal of Climatology* 25:823-842.

Draft

Appendix A: Inundation Maps for the Simulated Hurricane Ike and the 100-yr and 500-yr Proxy Storms

Draft

A.1 Galveston Island (City of Galveston)

Simulated Hurricane Ike

Inundation Map – Hurricane Ike, no Ike Dike, present day sea level



Inundation Map – Hurricane Ike, no Ike Dike, SLR1 (+2.4 ft)



Inundation Map – Hurricane Ike, with Ike Dike, present day sea level



Inundation Map – Hurricane Ike, with Ike Dike, SLR1 (+2.4 ft)



A.2 Galveston Island (City of Galveston)

100-yr Proxy Storm

Inundation Map - Storm 033 (100-yr proxy), no Ike Dike, present day sea level



Inundation Map - Storm 033 (100-yr proxy), no Ike Dike, SLR1 (+2.4 ft)



Inundation Map - Storm 033 (100-yr proxy), with Ike Dike, present day sea level



Inundation Map - Storm 033 (100-yr proxy), with Ike Dike, SLR1 (+2.4 ft)



A.3 Galveston Island (City of Galveston)

500-yr Proxy Storm

Inundation Map - Storm 036 (500-yr proxy), no Ike Dike, present day sea level



Inundation Map - Storm 036 (500-yr proxy), no Ike Dike, SLR1 (+2.4 ft)



Inundation Map - Storm 036 (500-yr proxy), with Ike Dike, present day sea level



Inundation Map - Storm 036 (500-yr proxy), with Ike Dike, SLR1 (+2.4 ft)



A.4 Galveston Island (central portion)

Simulated Hurricane Ike

Inundation Map – Hurricane Ike, no Ike Dike, present day sea level



Inundation Map – Hurricane Ike, no Ike Dike, SLR1 (+2.4 ft)



Inundation Map – Hurricane Ike, with Ike Dike, present day sea level



Inundation Map – Hurricane Ike (100-yr proxy), with Ike Dike, SLR1 (+2.4 ft)



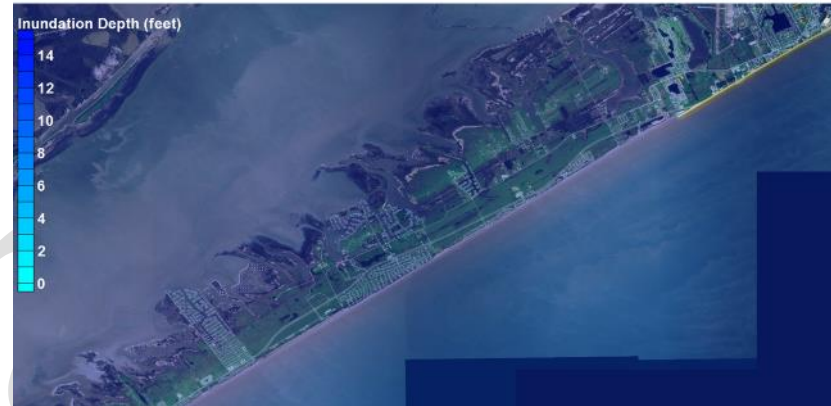
A.5 Galveston Island (central portion)

100-yr Proxy Storm

Inundation Map - Storm 033 (100-yr proxy), no Ike Dike, present day sea level



Inundation Map - Storm 033 (100-yr proxy), no Ike Dike, SLR1 (+2.4 ft)



Inundation Map - Storm 033 (100-yr proxy), with Ike Dike, present day sea level



Inundation Map - Storm 033 (100-yr proxy), with Ike Dike, SLR1 (+2.4 ft)



A.6 Galveston Island (central portion)

500-yr Proxy Storm

Inundation Map - Storm 036 (500-yr proxy), no Ike Dike, present day sea level



Inundation Map - Storm 036 (500-yr proxy), no Ike Dike, SLR1 (+2.4 ft)



Inundation Map - Storm 036 (500-yr proxy), with Ike Dike, present day sea level



Inundation Map - Storm 036 (500-yr proxy), with Ike Dike, SLR1 (+2.4 ft)



A.7 Galveston Island (western end)

Simulated Hurricane Ike

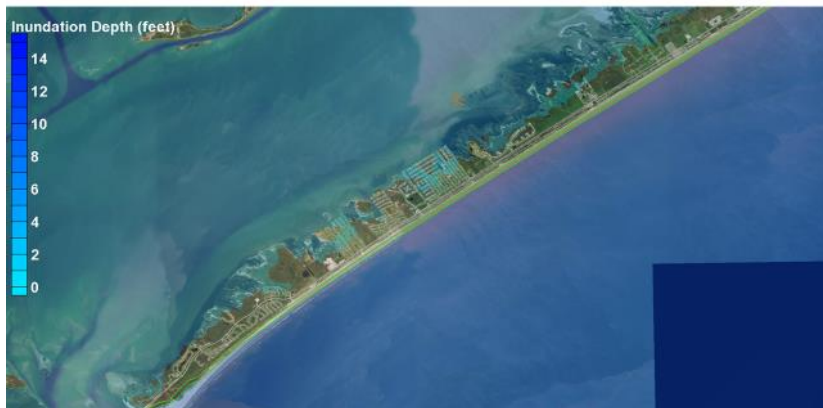
Inundation Map – Hurricane Ike, no Ike Dike, present day sea level



Inundation Map – Hurricane Ike, no Ike Dike, SLR1 (+2.4 ft)



Inundation Map – Hurricane Ike, with Ike Dike, present day sea level



Inundation Map – Hurricane Ike, with Ike Dike, SLR1 (+2.4 ft)



A.8 Galveston Island (western end)

100-yr Proxy Storm

Inundation Map - Storm 033 (100-yr proxy), no Ike Dike, present day sea level



Inundation Map - Storm 033 (100-yr proxy), no Ike Dike, SLR1 (+2.4 ft)



Inundation Map - Storm 033 (100-yr proxy), with Ike Dike, present day sea level



Inundation Map - Storm 033 (100-yr proxy), with Ike Dike, SLR1 (+2.4 ft)



A.9 Galveston Island (western end)

500-yr Proxy Storm

Inundation Map - Storm 036 (500-yr proxy), no Ike Dike, present day sea level



Inundation Map - Storm 036 (500-yr proxy), no Ike Dike, SLR1 (+2.4 ft)



Inundation Map - Storm 036 (500-yr proxy), with Ike Dike, present day sea level



Inundation Map - Storm 036 (500-yr proxy), with Ike Dike, SLR1 (+2.4 ft)



A.10 Bolivar Peninsula (western end)

Simulated Hurricane Ike

Inundation Map – Hurricane Ike, no Ike Dike, present day sea level



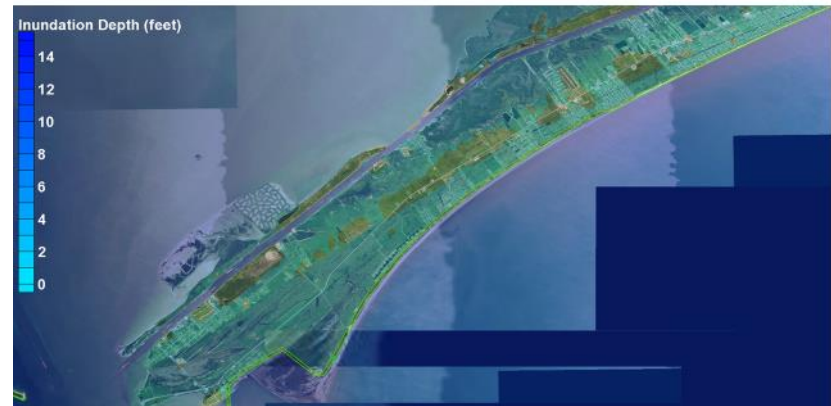
Inundation Map – Hurricane Ike, no Ike Dike, SLR1 (+2.4 ft)



Inundation Map – Hurricane Ike, with Ike Dike, present day sea level



Inundation Map – Hurricane Ike, with Ike Dike, SLR1 (+2.4 ft)



A.11 Bolivar Peninsula (western end)

100-yr Proxy Storm

Inundation Map - Storm 033 (100-yr proxy), no Ike Dike, present day sea level



Inundation Map - Storm 033 (100-yr proxy), no Ike Dike, SLR1 (+2.4 ft)



Inundation Map - Storm 033 (100-yr proxy), with Ike Dike, present day sea level



Inundation Map - Storm 033 (100-yr proxy), with Ike Dike, SLR1 (+2.4 ft)



A.12 Bolivar Peninsula (western end)

500-yr Proxy Storm

Inundation Map - Storm 036 (500-yr proxy), no Ike Dike, present day sea level



Inundation Map - Storm 036 (500-yr proxy), no Ike Dike, SLR1 (+2.4 ft)



Inundation Map - Storm 036 (500-yr proxy), with Ike Dike, present day sea level



Inundation Map - Storm 036 (500-yr proxy), with Ike Dike, SLR1 (+2.4 ft)



A.13 Bolivar Peninsula (central portion)

Simulated Hurricane Ike

Inundation Map – Hurricane Ike, no Ike Dike, present day sea level



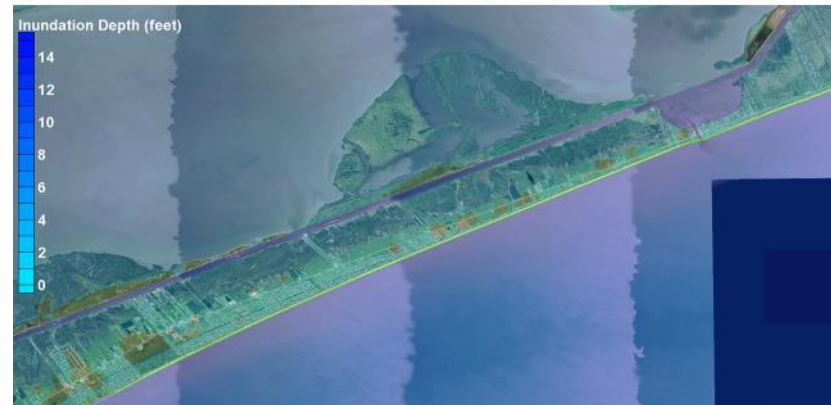
Inundation Map – Hurricane Ike, no Ike Dike, SLR1 (+2.4 ft)



Inundation Map – Hurricane Ike, with Ike Dike, present day sea level



Inundation Map – Hurricane Ike, with Ike Dike, SLR1 (+2.4 ft)



A.14 Bolivar Peninsula (central portion)

100-yr Proxy Storm

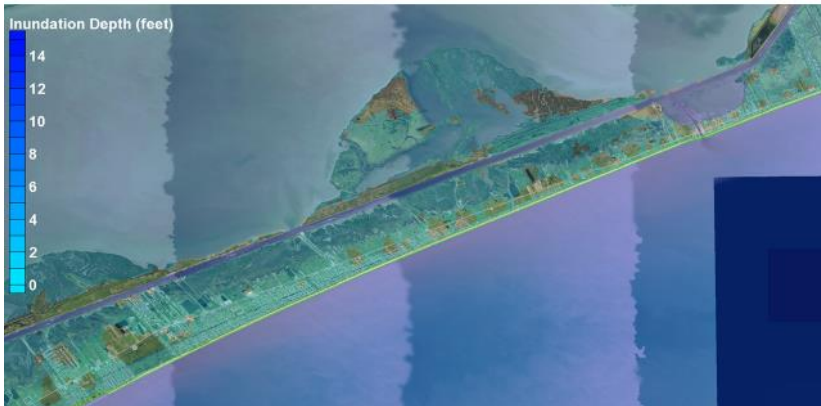
Inundation Map - Storm 033 (100-yr proxy), no Ike Dike, present day sea level



Inundation Map - Storm 033 (100-yr proxy), no Ike Dike, SLR1 (+2.4 ft)



Inundation Map - Storm 033 (100-yr proxy), with Ike Dike, present day sea level



Inundation Map - Storm 033 (100-yr proxy), with Ike Dike, SLR1 (+2.4 ft)



A.15 Bolivar Peninsula (central portion)

500-yr Proxy Storm

Inundation Map - Storm 036 (500-yr proxy), no Ike Dike, present day sea level



Inundation Map - Storm 036 (500-yr proxy), no Ike Dike, SLR1 (+2.4 ft)



Inundation Map - Storm 036 (500-yr proxy), with Ike Dike, present day sea level



Inundation Map - Storm 036 (500-yr proxy), with Ike Dike, SLR1 (+2.4 ft)



A.16 Bolivar Peninsula (eastern end)

Simulated Hurricane Ike

Inundation Map – Hurricane Ike, no Ike Dike, present day sea level



Inundation Map – Hurricane Ike, no Ike Dike, SLR1 (+2.4 ft)



Inundation Map – Hurricane Ike, with Ike Dike, present day sea level



Inundation Map – Hurricane Ike, with Ike Dike, SLR1 (+2.4 ft)



A.17 Bolivar Peninsula (eastern end)

100-yr Proxy Storm

Inundation Map - Storm 033 (100-yr proxy), no Ike Dike, present day sea level



Inundation Map - Storm 033 (100-yr proxy), no Ike Dike, SLR1 (+2.4 ft)



Inundation Map - Storm 033 (100-yr proxy), with Ike Dike, present day sea level



Inundation Map - Storm 033 (100-yr proxy), with Ike Dike, SLR1 (+2.4 ft)



A.18 Bolivar Peninsula (eastern end)

500-yr Proxy Storm

Inundation Map - Storm 036 (500-yr proxy), no Ike Dike, present day sea level



Inundation Map - Storm 036 (500-yr proxy), no Ike Dike, SLR1 (+2.4 ft)



Inundation Map - Storm 036 (500-yr proxy), with Ike Dike, present day sea level



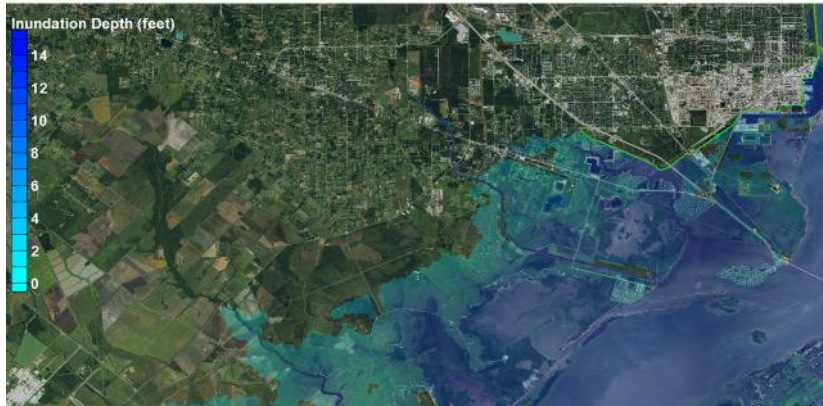
Inundation Map - Storm 036 (500-yr proxy), with Ike Dike, SLR1 (+2.4 ft)



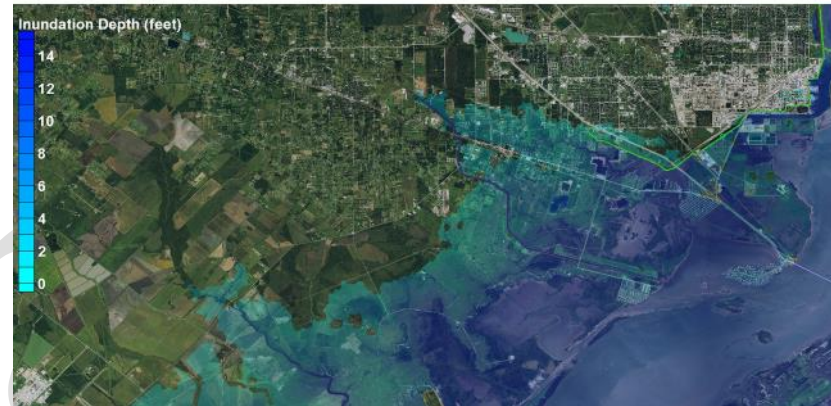
A.19 Texas City (south), La Marque, Bayou Vista

Simulated Hurricane Ike

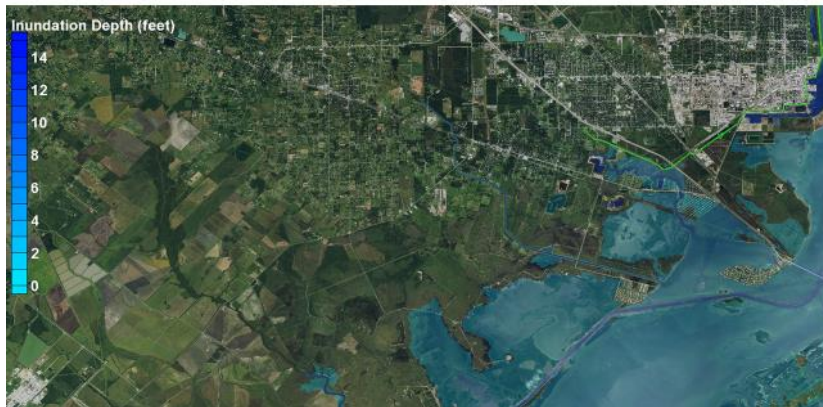
Inundation Map – Hurricane Ike, no Ike Dike, present day sea level



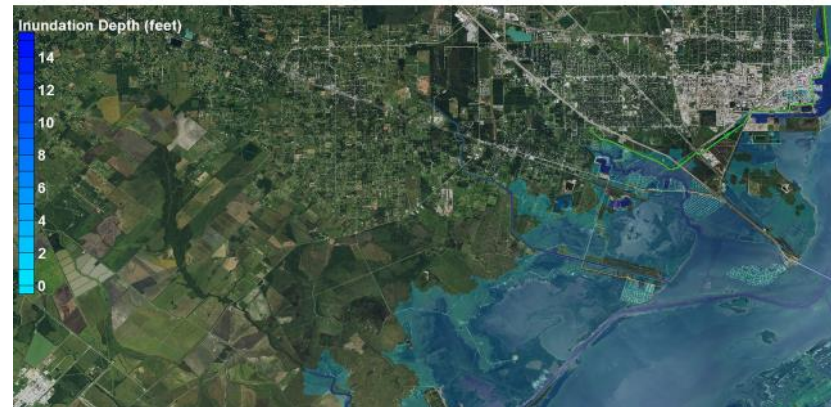
Inundation Map – Hurricane Ike, no Ike Dike, SLR1 (+2.4 ft)



Inundation Map – Hurricane Ike, with Ike Dike, present day sea level



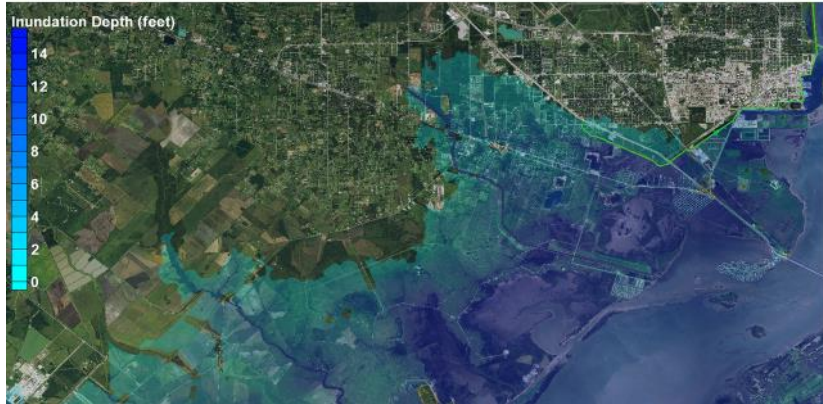
Inundation Map – Hurricane Ike, with Ike Dike, SLR1 (+2.4 ft)



A.20 Texas City (south), La Marque, Bayou Vista

100-yr Proxy Storm

Inundation Map - Storm 033 (100-yr proxy), no Ike Dike, present day sea level



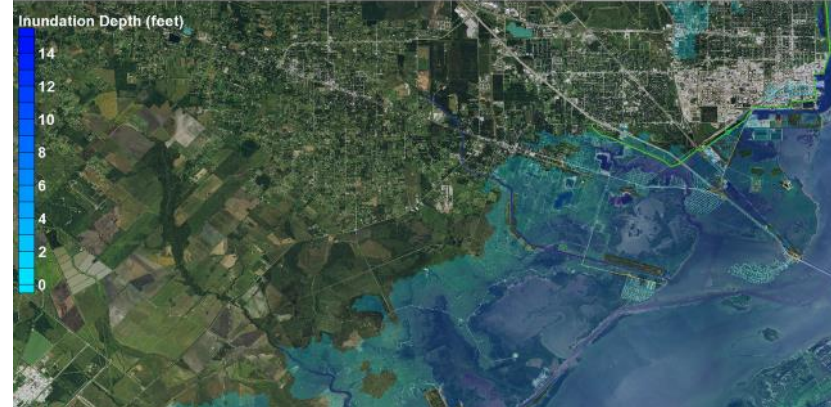
Inundation Map - Storm 033 (100-yr proxy), no Ike Dike, SLR1 (+2.4 ft)



Inundation Map - Storm 033 (100-yr proxy), with Ike Dike, present day sea level



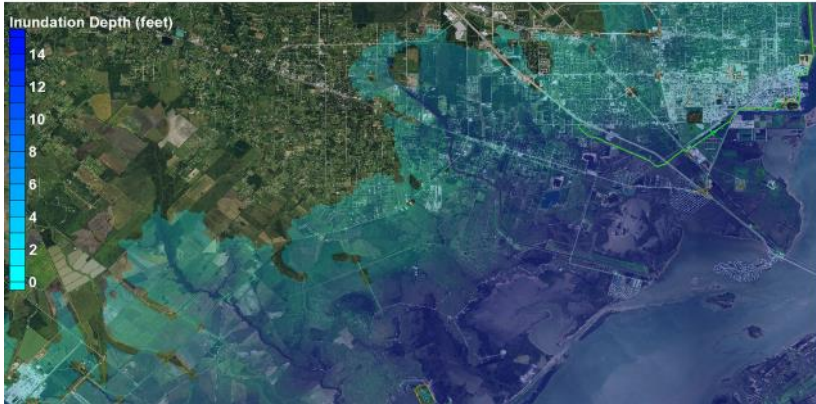
Inundation Map - Storm 033 (100-yr proxy), with Ike Dike, SLR1 (+2.4 ft)



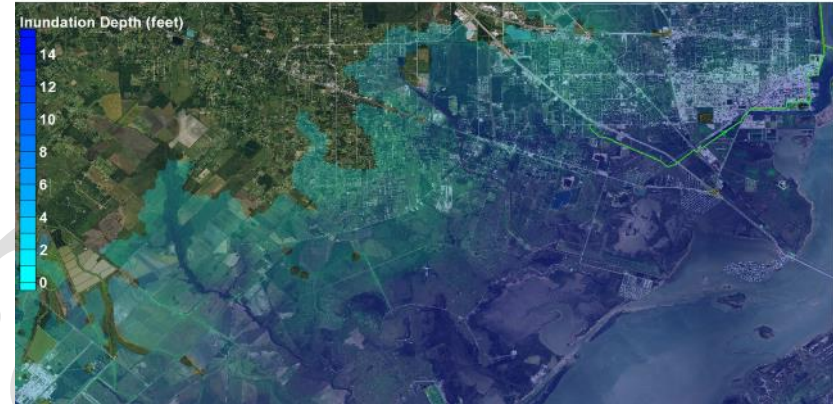
A21. Texas City (south), La Marque, Bayou Vista

500-yr Proxy Storm

Inundation Map - Storm 036 (500-yr proxy), no Ike Dike, present day sea level



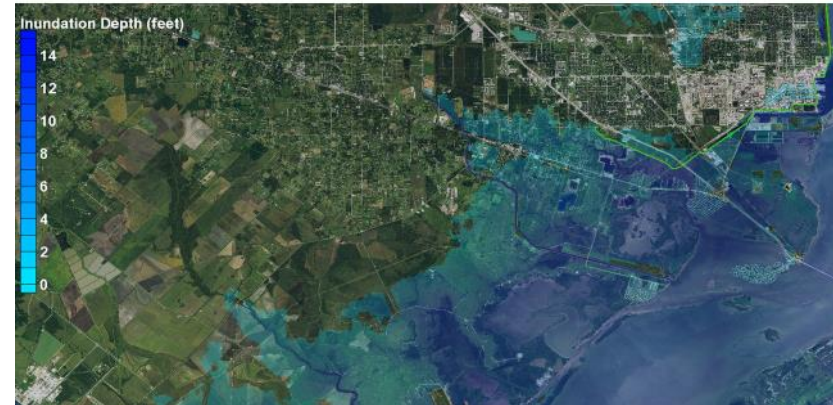
Inundation Map - Storm 036 (500-yr proxy), no Ike Dike, SLR1 (+2.4 ft)



Inundation Map - Storm 036 (500-yr proxy), with Ike Dike, present day sea level



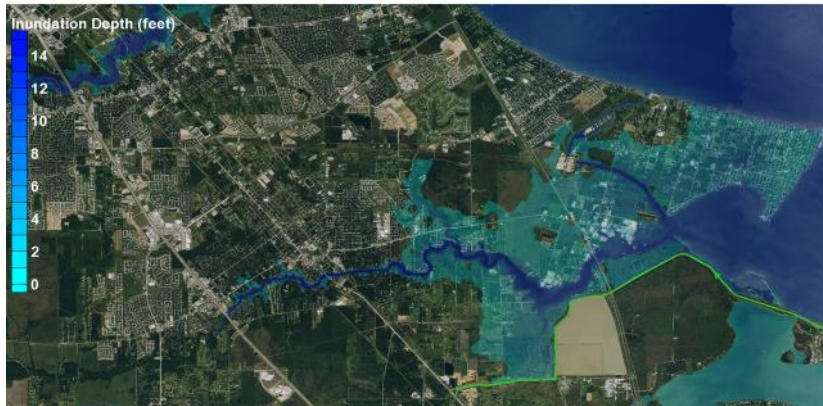
Inundation Map - Storm 036 (500-yr proxy), with Ike Dike, SLR1 (+2.4 ft)



A.22 San Leon, Texas City (north), Bacliff, Dickinson

Simulated Hurricane Ike

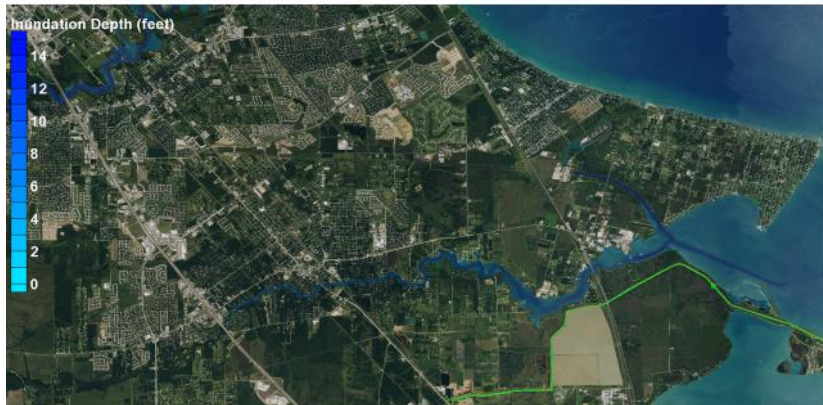
Inundation Map – Hurricane Ike, no Ike Dike, present day sea level



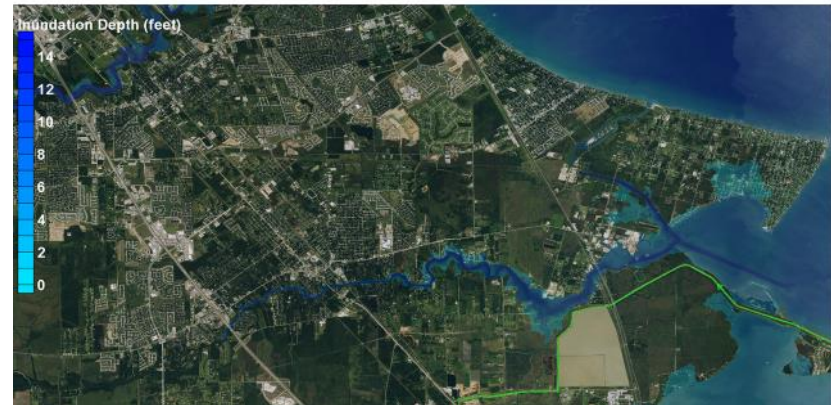
Inundation Map – Hurricane Ike, no Ike Dike, SLR1 (+2.4 ft)



Inundation Map – Hurricane Ike, with Ike Dike, present day sea level



Inundation Map – Hurricane Ike, with Ike Dike, SLR1 (+2.4 ft)



A.23 San Leon, Texas City (north), Bacliff, Dickinson

100-yr Proxy Storm

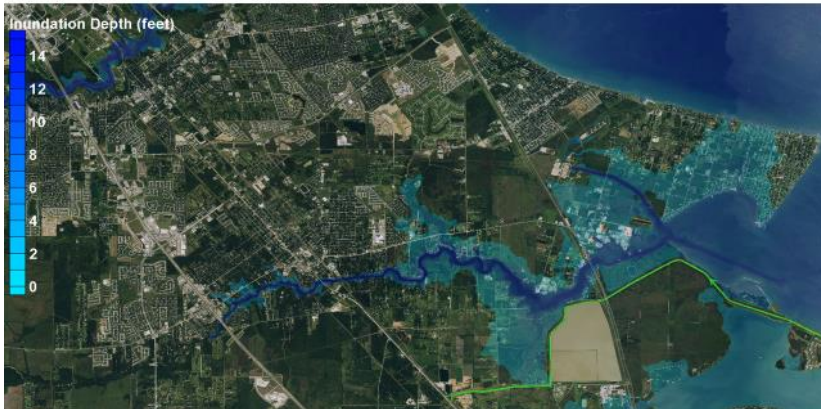
Inundation Map - Storm 033 (100-yr proxy), no Ike Dike, present day sea level



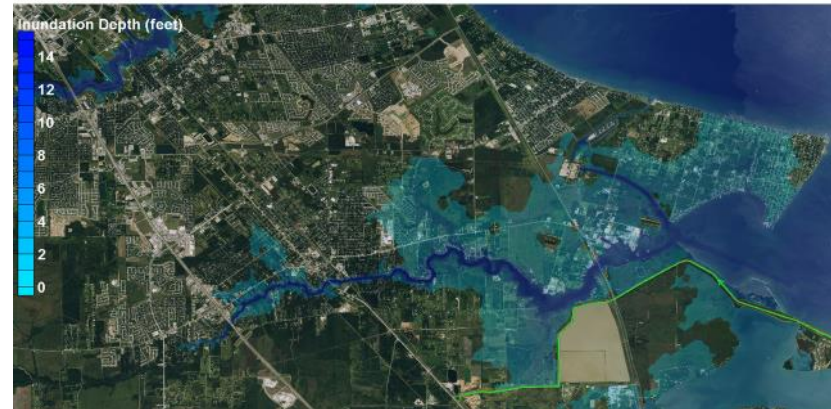
Inundation Map - Storm 033 (100-yr proxy), no Ike Dike, SLR1 (+2.4 ft)



Inundation Map - Storm 033 (100-yr proxy), with Ike Dike, present day sea level



Inundation Map - Storm 033 (100-yr proxy), with Ike Dike, SLR1 (+2.4 ft)



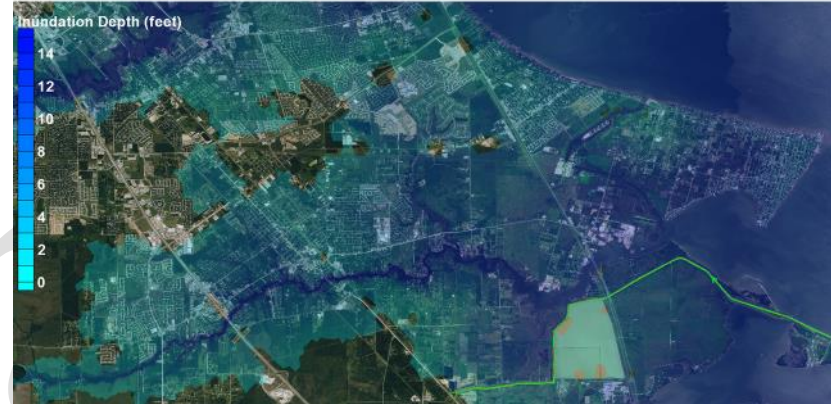
A.24 San Leon, Texas City (north), Bacliff, Dickinson

500-yr Proxy Storm

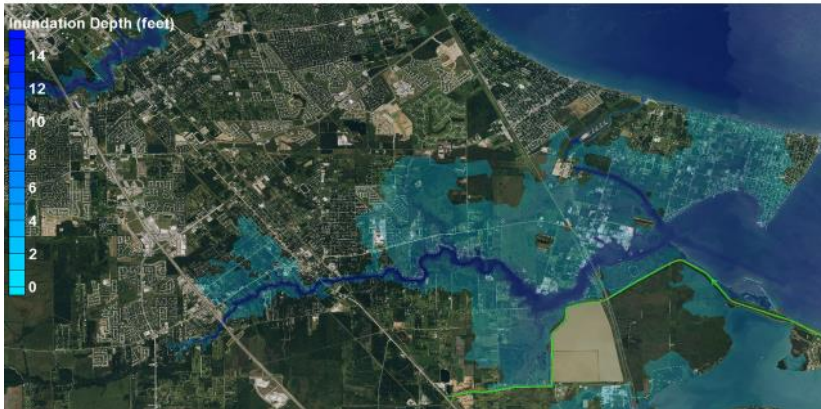
Inundation Map - Storm 036 (500-yr proxy), no Ike Dike, present day sea level



Inundation Map - Storm 036 (500-yr proxy), no Ike Dike, SLR1 (+2.4 ft)



Inundation Map - Storm 036 (500-yr proxy), with Ike Dike, present day sea level



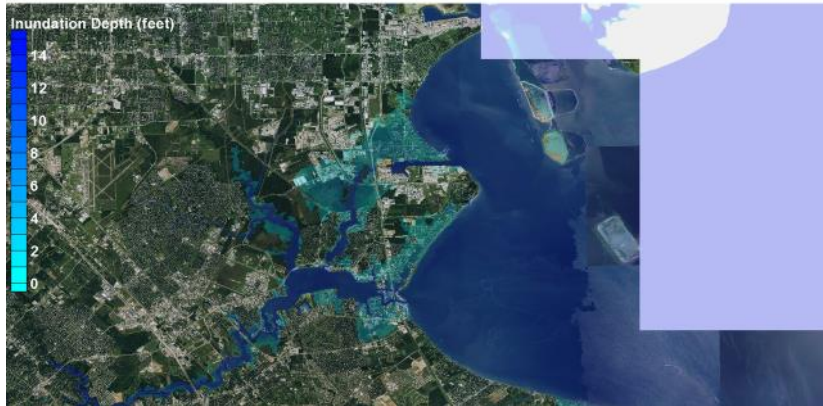
Inundation Map - Storm 036 (500-yr proxy), with Ike Dike, SLR1 (+2.4 ft)



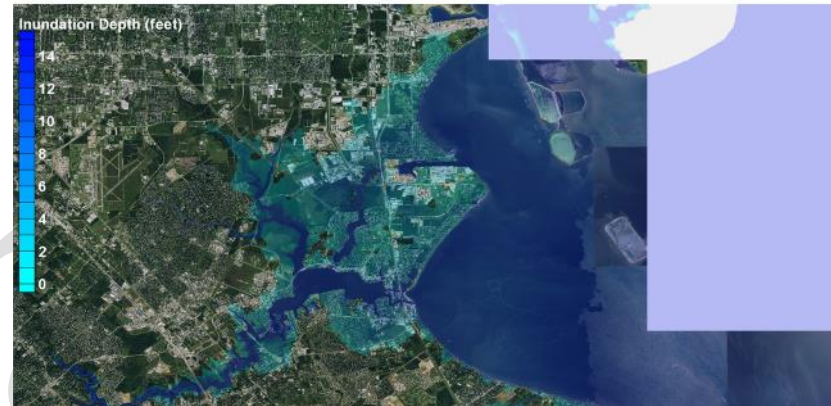
A.25 Clear Lake area, Bayport area, La Porte

Simulated Hurricane Ike

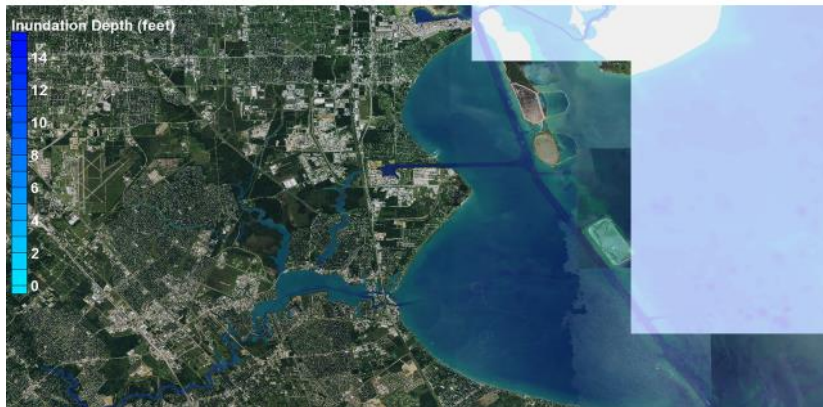
Inundation Map – Hurricane Ike, no Ike Dike, present day sea level



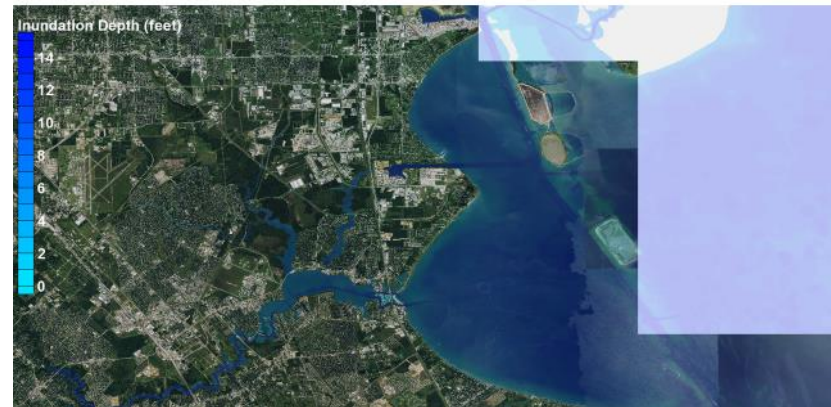
Inundation Map – Hurricane Ike, no Ike Dike, SLR1 (+2.4 ft)



Inundation Map – Hurricane Ike, with Ike Dike, present day sea level



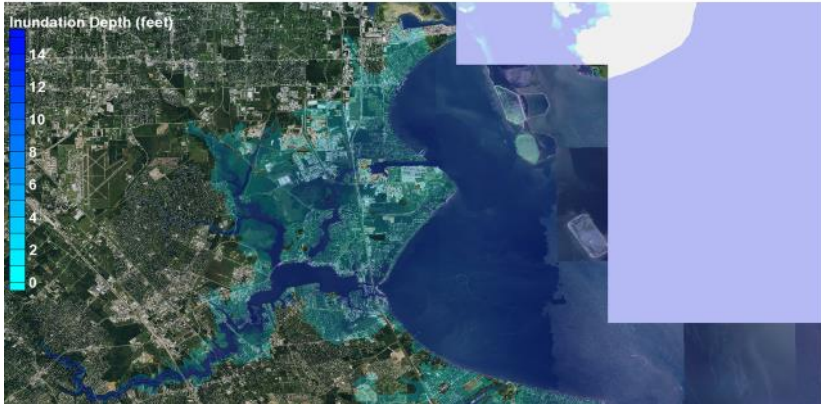
Inundation Map – Hurricane Ike, with Ike Dike, SLR1 (+2.4 ft)



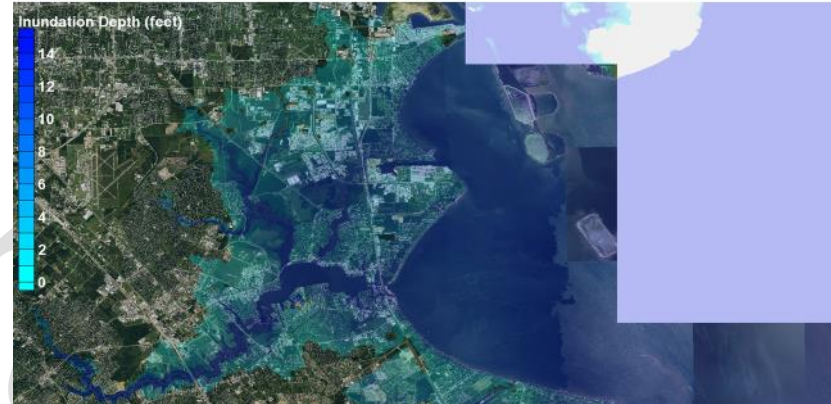
A.26 Clear Lake area, Bayport area, La Porte

100-yr Proxy Storm

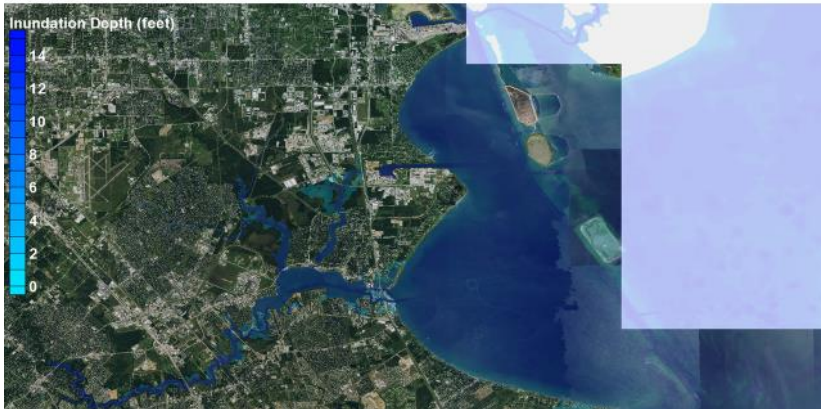
Inundation Map - Storm 033 (100-yr proxy), no Ike Dike, present day sea level



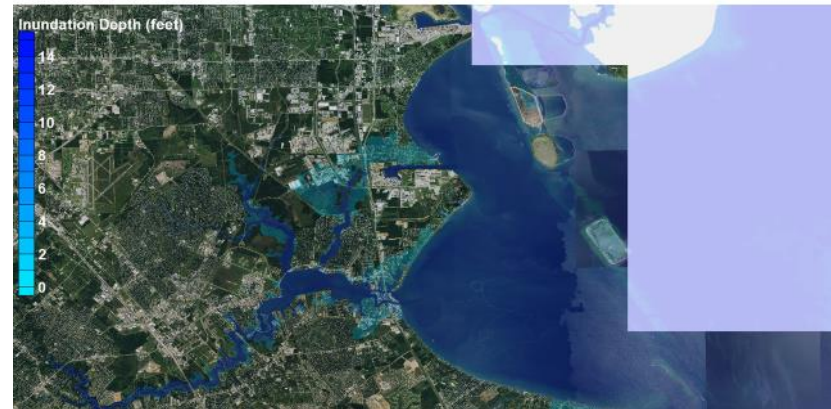
Inundation Map - Storm 033 (100-yr proxy), no Ike Dike, SLR1 (+2.4 ft)



Inundation Map - Storm 033 (100-yr proxy), with Ike Dike, present day sea level



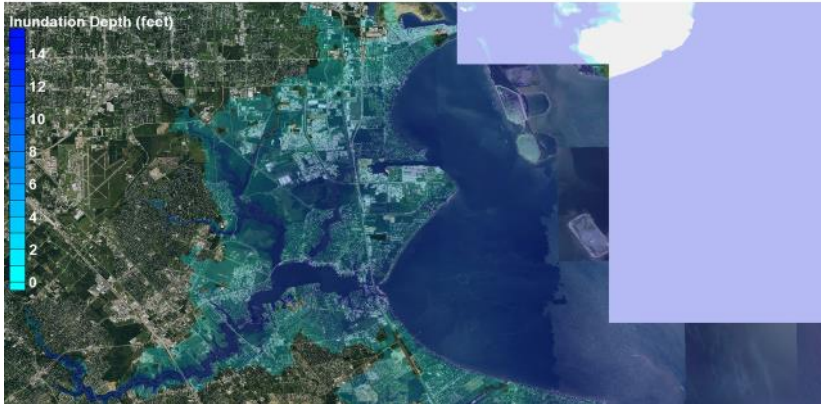
Inundation Map - Storm 033 (100-yr proxy), with Ike Dike, SLR1 (+2.4 ft)



A.27 Clear Lake area, Bayport area, La Porte

500-yr Proxy Storm

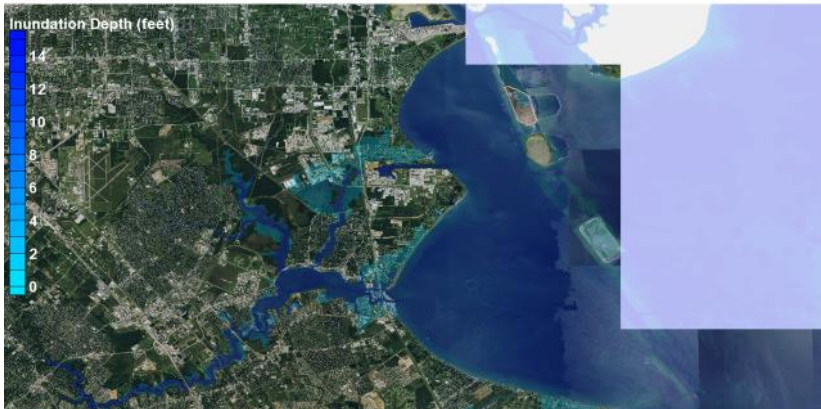
Inundation Map - Storm 036 (500-yr proxy), no Ike Dike, present day sea level



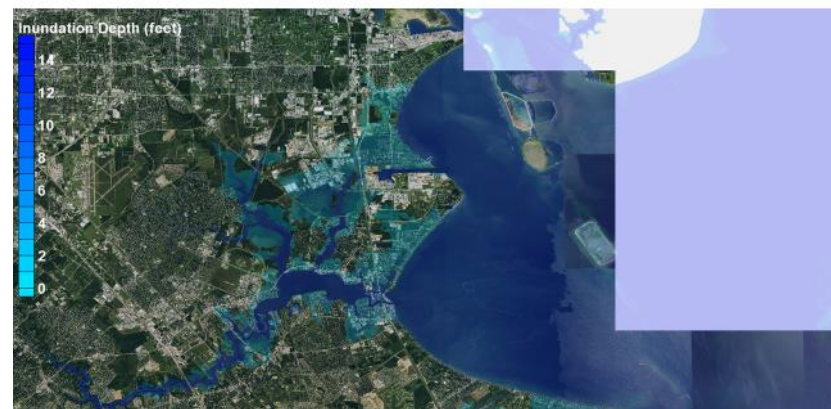
Inundation Map - Storm 036 (500-yr proxy), no Ike Dike, SLR1 (+2.4 ft)



Inundation Map - Storm 036 (500-yr proxy), with Ike Dike, present day sea level



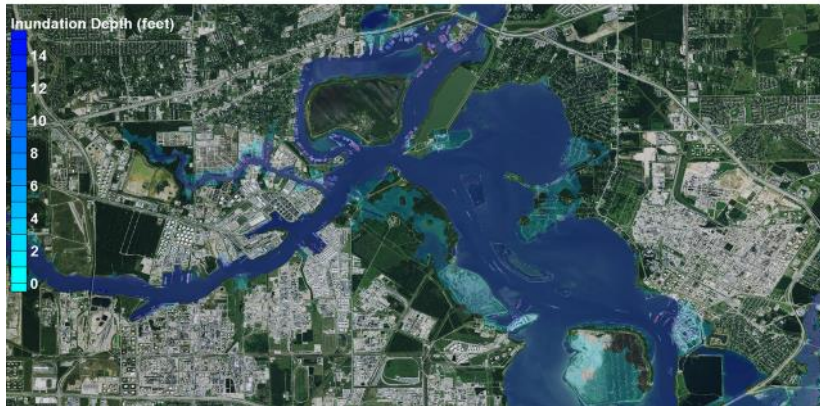
Inundation Map - Storm 036 (500-yr proxy), with Ike Dike, SLR1 (+2.4 ft)



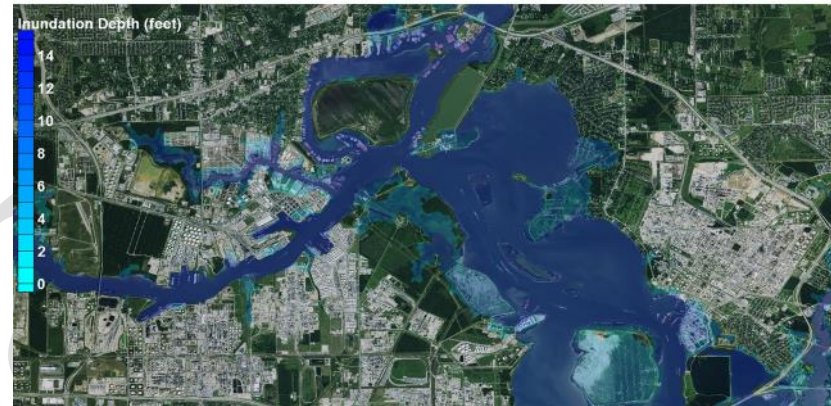
A.28 Upper Houston Ship Channel (eastern portion)

Simulated Hurricane Ike

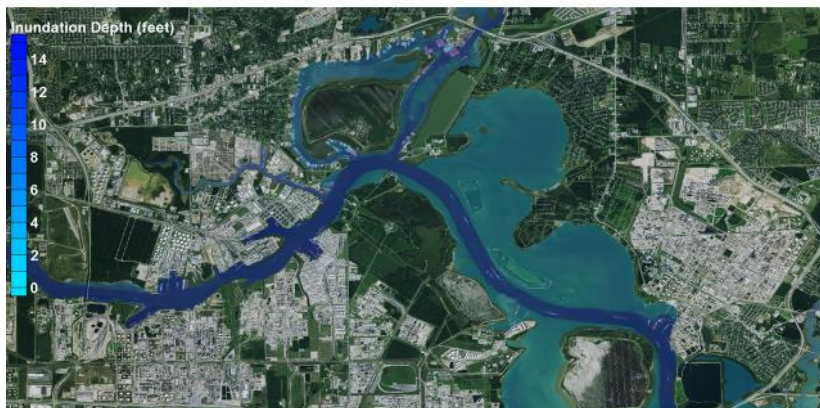
Inundation Map – Hurricane Ike, no Ike Dike, present day sea level



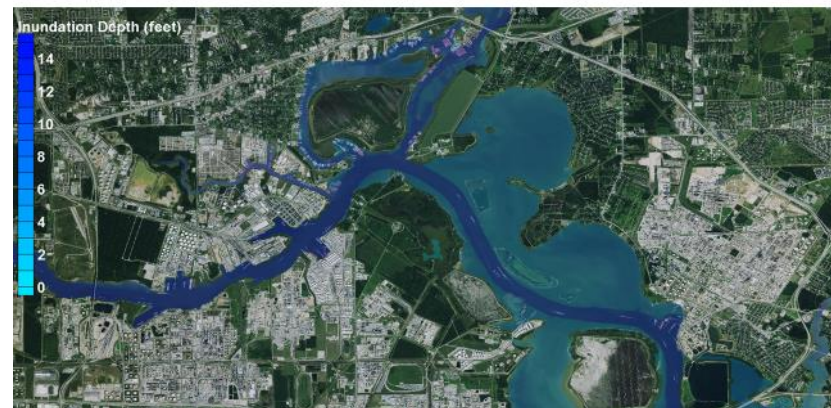
Inundation Map – Hurricane Ike, no Ike Dike, SLR1 (+2.4 ft)



Inundation Map – Hurricane Ike, with Ike Dike, present day sea level



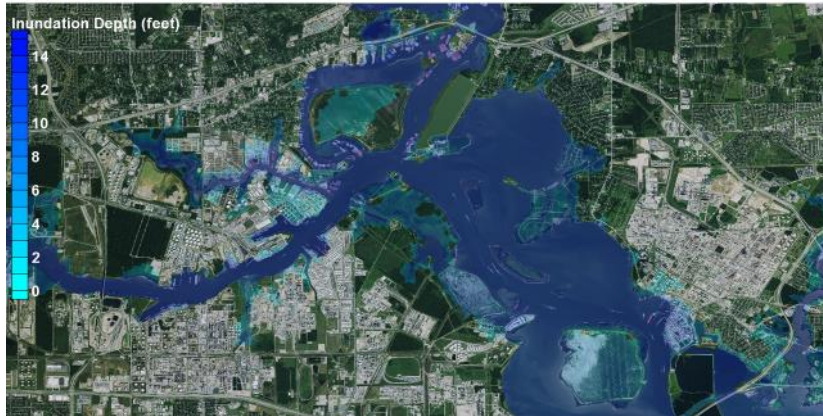
Inundation Map – Hurricane Ike, with Ike Dike, SLR1 (+2.4 ft)



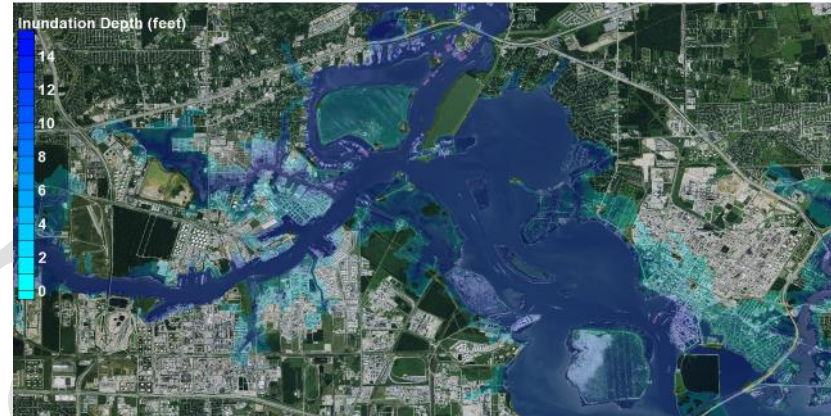
A.29 Upper Houston Ship Channel (eastern portion)

100-yr Proxy Storm

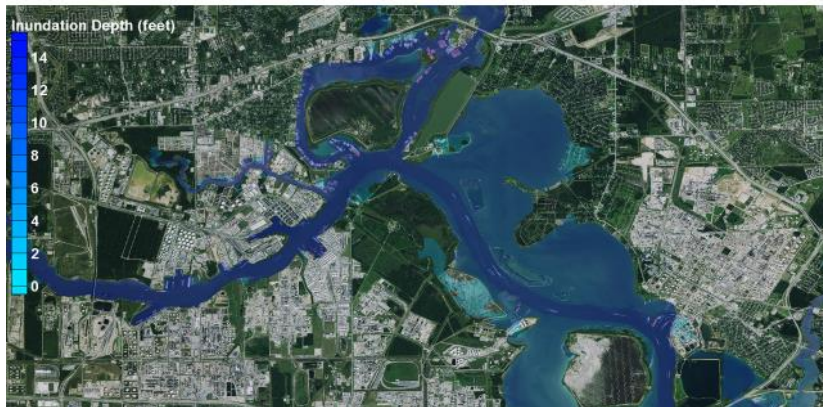
Inundation Map - Storm 033 (100-yr proxy), no Ike Dike, present day sea level



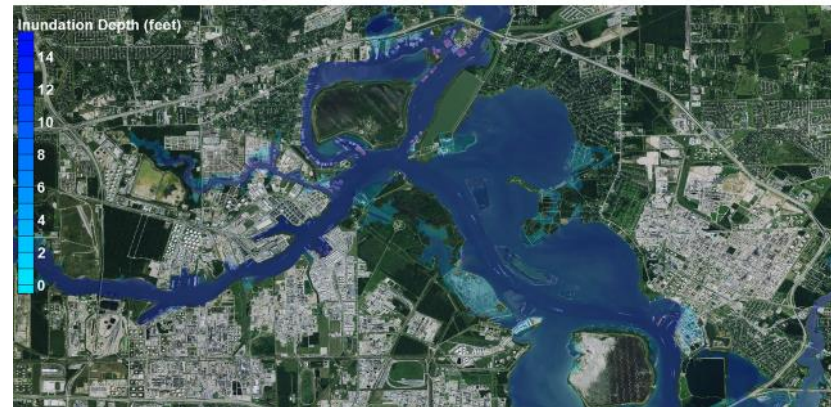
Inundation Map - Storm 033 (100-yr proxy), no Ike Dike, SLR1 (+2.4 ft)



Inundation Map - Storm 033 (100-yr proxy), with Ike Dike, present day sea level



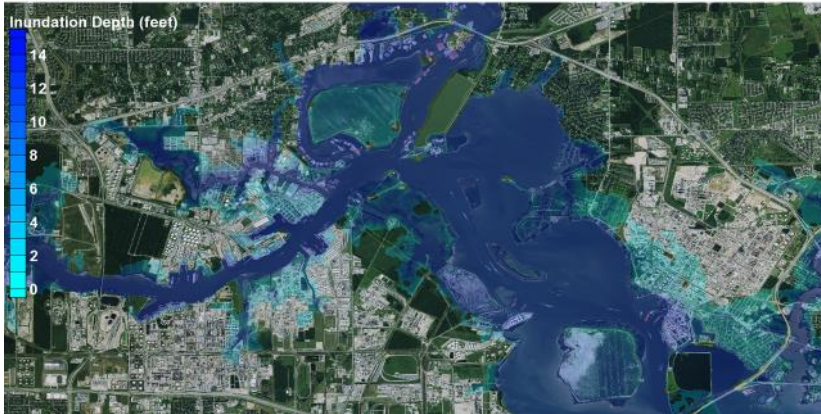
Inundation Map - Storm 033 (100-yr proxy), with Ike Dike, SLR1 (+2.4 ft)



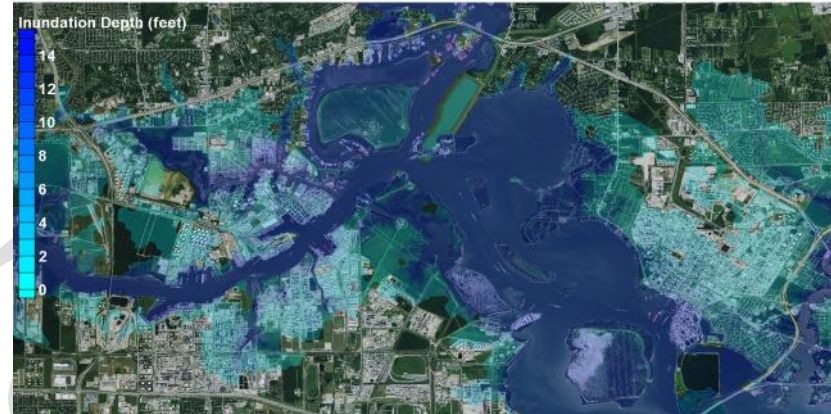
A.30 Upper Houston Ship Channel (eastern portion)

500-yr Proxy Storm

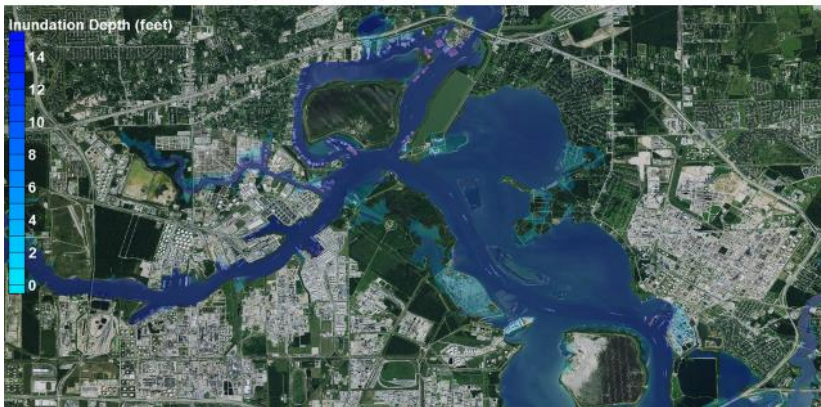
Inundation Map - Storm 036 (500-yr proxy), no Ike Dike, present day sea level



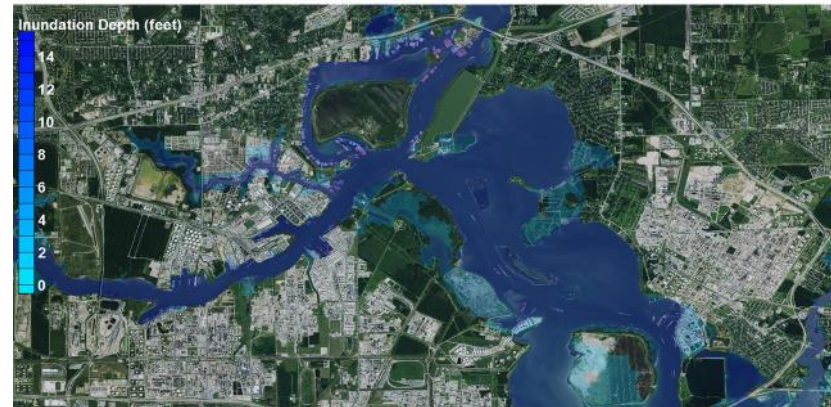
Inundation Map - Storm 036 (500-yr proxy), no Ike Dike, SLR1 (+2.4 ft)



Inundation Map - Storm 036 (500-yr proxy), with Ike Dike, present day sea level



Inundation Map - Storm 036 (500-yr proxy), with Ike Dike, SLR1 (+2.4 ft)



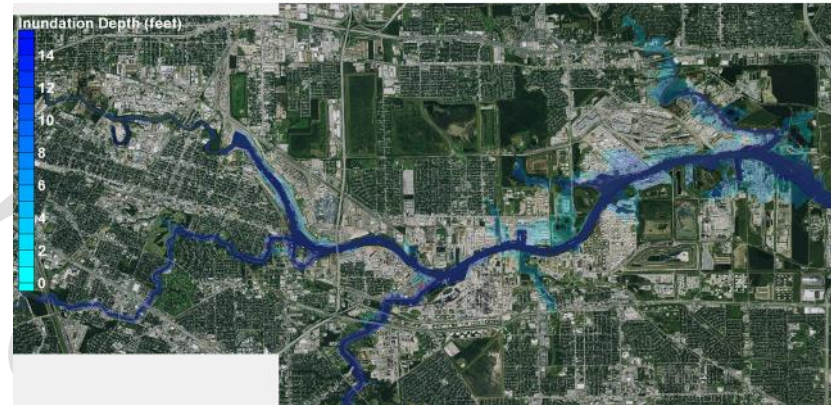
A.31 Upper Houston Ship Channel (western portion)

Simulated Hurricane Ike

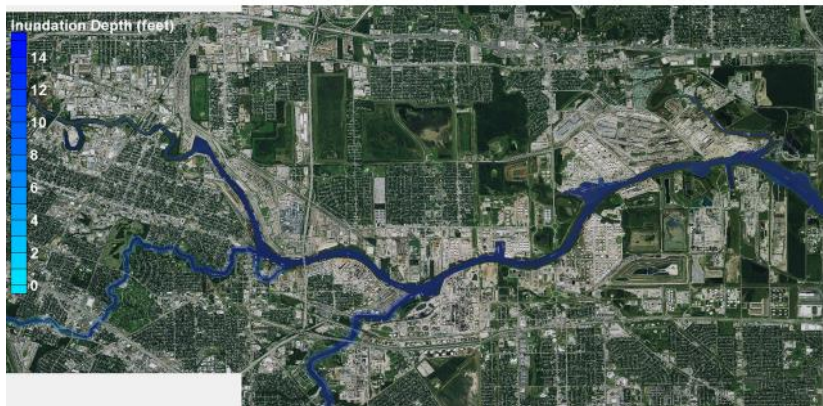
Inundation Map – Hurricane Ike, no Ike Dike, present day sea level



Inundation Map – Hurricane Ike, no Ike Dike, SLR1 (+2.4 ft)



Inundation Map – Hurricane Ike, with Ike Dike, present day sea level



Inundation Map – Hurricane Ike, with Ike Dike, SLR1 (+2.4 ft)



A.32 Upper Houston Ship Channel (western portion)

100-yr Proxy Storm

Inundation Map - Storm 033 (100-yr proxy), no Ike Dike, present day sea level



Inundation Map - Storm 033 (100-yr proxy), no Ike Dike, SLR1 (+2.4 ft)



Inundation Map - Storm 033 (100-yr proxy), with Ike Dike, present day sea level



Inundation Map - Storm 033 (100-yr proxy), with Ike Dike, SLR1 (+2.4 ft)



A.33 Upper Houston Ship Channel (western portion)

500-yr Proxy Storm

Inundation Map - Storm 036 (500-yr proxy), no Ike Dike, present day sea level



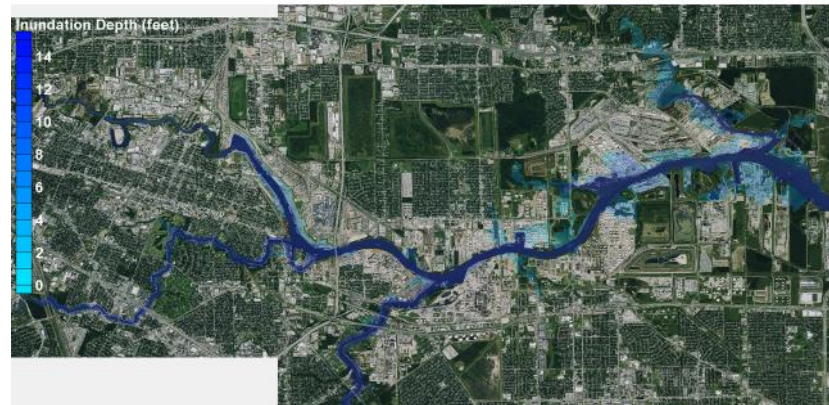
Inundation Map - Storm 036 (500-yr proxy), no Ike Dike, SLR1 (+2.4 ft)



Inundation Map - Storm 036 (500-yr proxy), with Ike Dike, present day sea level



Inundation Map - Storm 036 (500-yr proxy), with Ike Dike, SLR1 (+2.4 ft)



Appendix B: Water Surface Elevations at Selected Locations for Different Ike Dike Alignments

The tables in Appendix B show maximum water surface elevations, in feet NAVD88, for five different configurations of the Ike Dike concept at a series of locations in the Houston/Galveston region. Results reflect simulations made for the three proxy storms and Hurricane Ike. Each simulation was made for the future sea level scenario, SLR1, which is 2.4 ft above present-day sea level.

Each column in the tables shows water surface elevation values for a particular dike configuration. The different configurations are identified using the following labels:

middle only – Alignment 2 (middle section only, dike that extends from the western end of Galveston Island to High Island)

middle + east – Alignment 3 (middle + eastern sections, dike that extends from the western end of Galveston Island to High Island, then continues northward to Winnie)

extended – extended Ike Dike (middle + eastern + western sections, dike that extends from Freeport to Sabine Pass)

west+mid+east – Alignment 1a (middle + eastern + western sections, dike that extends from Freeport to High Island, then continues northward to Winnie)

lowered gates – Alignment 1b (same as Alignment 1a except gate crest elevations are lowered for the navigation gate sections at Bolivar Roads and San Luis Pass)

The crest elevation of all dike sections is 17 ft NAVD88 unless noted in Chapter 13 for Alignment 1b.

Location	Degrees W Longitude	Degrees N Latitude	Maximum Water Surface Elevation (ft, NAVD88)									
			Storm 535 (10-yr proxy storm)					Storm 033 (100-yr proxy storm)				
			middle only	middle+east	extended	west+mid+east	lowered gates	middle only	middle+east	extended	west+mid+east	lowered gates
Houston Ship Channel (upper)	95.275000	29.727500	8.3	8.3	7.6	7.6	7.5	13.5	13.5	13.3	13.1	13.3
Houston Ship Channel (mid)	95.168800	29.746900	7.9	7.8	7.2	7.1	7.1	12.9	12.8	12.7	12.5	12.7
Houston Ship Channel (lower)	95.080100	29.763500	7.4	7.4	6.7	6.7	6.7	12.2	12.2	12.0	11.9	12.1
Alexander Island	95.022800	29.726100	6.9	6.8	6.2	6.1	6.1	11.0	10.9	10.7	10.6	10.8
LaPorte	95.006316	29.646740	6.6	6.5	5.9	5.9	5.9	10.3	10.2	10.0	9.9	10.1
Bayport	94.992500	29.613700	6.3	6.2	5.6	5.5	5.5	9.6	9.5	9.3	9.2	9.4
Clear Lake (east)	95.023300	29.549400	6.7	6.6	6.0	5.9	5.9	10.3	10.2	10.0	9.9	10.1
Clear Lake (north)	95.090444	29.599394	7.6	7.5	6.9	6.8	6.8	11.9	11.9	11.7	11.5	11.7
Clear Lake (west)	95.178800	29.517700	7.7	7.7	7.0	6.9	6.9	11.7	11.7	11.4	11.2	11.4
Clear Lake (northwest)	95.122969	29.586246	7.7	7.7	7.0	6.9	6.9	12.1	12.1	11.9	11.8	11.9
San Leon	94.958400	29.509100	5.9	5.8	5.2	5.1	5.1	8.8	8.7	8.5	8.4	8.5
Dickinson	95.070417	29.450545	8.1	8.0	7.6	7.5	7.5	12.1	12.1	12.1	12.0	12.1
Dickinson Bay entrance	94.951000	29.469200	6.4	6.4	5.8	5.8	5.8	10.5	10.5	10.4	10.3	10.4
Texas City (north)	94.913100	29.445600	5.7	5.7	5.0	5.0	5.0	9.2	9.2	9.0	8.9	9.1
Texas City (east)	94.867900	29.417800	5.2	5.2	4.5	4.4	4.4	8.5	8.4	8.3	8.1	8.4
Texas City (south)	94.948600	29.338600	7.3	7.3	6.2	6.2	6.2	12.8	12.8	10.6	10.5	10.6
Galveston (bay)	94.845800	29.300400	5.2	5.2	4.5	4.4	4.4	9.5	9.5	9.4	9.3	9.5
Morgan's Point	94.978970	29.676030	6.4	6.3	5.7	5.6	5.6	9.9	9.9	9.7	9.6	9.8
West Bay (east)	94.890800	29.289400	5.2	5.2	4.5	4.4	4.4	9.5	9.5	9.4	9.2	9.4
West Bay (north)	95.218056	29.235988	7.2	7.2	5.5	5.5	5.5	12.9	12.9	7.2	7.4	7.5
San Luis Pass (throat-bay)	95.124650	29.082360	7.9	7.9	5.8	5.8	5.8	14.1	14.2	7.1	7.2	7.3
San Luis Pass (throat-ocean)	95.115080	29.082840	7.9	7.9	8.0	8.0	8.0	14.5	14.5	15.5	15.4	15.4
Bolivar Roads (throat-bay)	94.758460	29.342130	4.6	4.6	3.9	3.8	3.8	8.1	8.1	7.6	7.8	8.0
Bolivar Roads (throat-ocean)	94.741770	29.344240	9.2	9.2	9.2	9.2	9.2	20.1	20.1	20.3	20.1	20.1
Galveston Is (bay west)	95.112100	29.109200	7.3	7.3	5.4	5.4	5.4	12.1	12.1	6.1	6.2	6.3
Galveston Is (bay mid)	94.996300	29.191100	5.8	5.8	4.6	4.6	4.6	11.4	11.4	6.2	6.5	6.6
Galveston Is (bay east)	94.884300	29.276300	5.1	5.1	4.2	4.2	4.2	9.8	9.8	9.2	9.0	9.1
Bolivar Pen (bay west)	94.776100	29.386300	4.5	4.4	3.7	3.7	3.7	7.9	7.1	6.6	6.4	6.8
Bolivar Pen (bay mid)	94.635500	29.478500	4.5	4.1	3.7	3.5	3.4	8.0	7.2	6.4	6.1	6.4
Bolivar Pen (bay east)	94.510000	29.524600	4.6	4.0	3.8	3.4	3.4	8.1	7.3	6.6	6.2	6.4
Galveston Is (nearshore west)	95.081400	29.106000	8.0	8.0	8.0	8.0	8.0	15.6	15.6	15.7	15.6	15.6
Galveston Is (nearshore mid)	94.947000	29.190600	8.5	8.5	8.5	8.5	8.5	17.4	17.4	17.5	17.4	17.4
Galveston (Pleasure Pier)	94.787800	29.285300	8.9	8.9	8.9	8.8	8.8	19.1	19.1	19.2	19.2	19.1
Bolivar Pen (nearshore west)	94.673700	29.423600	9.0	9.0	9.0	9.0	9.0	20.0	20.0	20.1	20.0	20.0
Bolivar Pen (nearshore mid)	94.593600	29.464600	8.6	8.6	8.6	8.6	8.6	19.4	19.4	19.6	19.4	19.4
Bolivar Pen (nearshore east)	94.506000	29.499400	8.4	8.4	8.4	8.4	8.4	18.9	18.9	19.0	18.9	18.9
Univ Texas Medical Branch	94.779962	29.317565	4.8	4.8	4.1	4.0	4.0	9.0	8.9	8.7	8.6	8.9

Location	Degrees W Longitude	Degrees N Latitude	Maximum Water Surface Elevation (ft, NAVD88)									
			Storm 036 (500-yr proxy storm)					Hurricane Ike				
			middle only	middle+east	extended	west+mid+east	lowered gates	middle only	middle+east	extended	west+mid+east	lowered gates
Houston Ship Channel (upper)	95.275000	29.727500	15.9	15.9	15.8	15.6	15.8	7.2	6.3	5	4.2	4.6
Houston Ship Channel (mid)	95.168800	29.746900	15.3	15.2	15.1	14.9	15.2	7.2	6.3	5	4.2	4.4
Houston Ship Channel (lower)	95.080100	29.763500	14.5	14.4	14.3	14.1	14.4	7.2	6.3	5	4.3	4.6
Alexander Island	95.022800	29.726100	13.0	12.9	12.8	12.6	12.9	7.2	6.2	5	4.2	4.5
LaPorte	95.006316	29.646740	12.2	12.1	12.0	11.9	12.1	7.1	6.1	4.9	4.1	4.3
Bayport	94.992500	29.613700	11.3	11.2	11.1	10.9	11.2	7.0	6.1	4.9	4.1	4.3
Clear Lake (east)	95.023300	29.549400	12.1	12.1	11.9	11.8	11.9	7.0	6	5.1	4.6	4.8
Clear Lake (north)	95.090444	29.599394	13.9	13.9	13.7	13.6	13.7	7.0	6.1	4.8	4.2	4.3
Clear Lake (west)	95.178800	29.517700	13.8	13.7	13.5	13.4	13.5	7.0	6	5.1	4.7	4.8
Clear Lake (northwest)	95.122969	29.586246	14.2	14.1	14.0	13.9	14.0	7.0	6.1	4.8	4.3	4.4
San Leon	94.958400	29.509100	10.3	10.2	10.0	9.9	10.1	6.9	6.2	5.5	5.1	5.3
Dickinson	95.070417	29.450545	13.4	13.4	13.3	13.3	13.3	7.0	6.9	6.4	5.8	6.1
Dickinson Bay entrance	94.951000	29.469200	12.4	12.3	12.3	12.1	12.3	6.9	6.7	6.3	5.6	5.9
Texas City (north)	94.913100	29.445600	10.8	10.7	10.6	10.5	10.7	7.0	6.9	6.3	5.8	6
Texas City (east)	94.867900	29.417800	9.9	9.9	9.9	9.7	10.0	7.0	6.9	6.5	5.8	6.1
Texas City (south)	94.948600	29.338600	15.4	15.4	13.1	13.0	13.2	10.3	10.2	7.8	7	7.2
Galveston (bay)	94.845800	29.300400	11.0	11.0	11.0	10.8	11.1	7.7	7.5	7	6.3	6.7
Morgan's Point	94.978970	29.676030	11.8	11.7	11.6	11.5	11.7	7.1	6.2	4.9	4.1	4.4
West Bay (east)	94.890800	29.289400	12.1	12.0	11.1	10.9	11.2	7.9	7.8	6.5	5.9	6.2
West Bay (north)	95.218056	29.235988	14.7	14.7	8.2	8.4	8.6	9.3	9.3	4.5	3.9	3.9
San Luis Pass (throat-bay)	95.124650	29.082360	16.0	16.0	7.6	7.8	8.0	10.9	11	7.1	6.3	6.3
San Luis Pass (throat-ocean)	95.115080	29.082840	16.5	16.5	17.7	17.6	17.5	11.2	11.2	11.6	11.5	11.5
Bolivar Roads (throat-bay)	94.758460	29.342130	9.7	9.1	8.8	8.5	9.0	7.2	7.5	7.1	6.3	6.3
Bolivar Roads (throat-ocean)	94.741770	29.344240	23.1	23.2	23.3	23.2	23.1	17.0	17	17.1	17	17
Galveston Is (bay west)	95.112100	29.109200	13.6	13.6	7.2	6.9	7.1	10.0	10	6.3	5.7	5.7
Galveston Is (bay mid)	94.996300	29.191100	13.4	13.4	7.6	7.7	8.0	9.2	9.2	6.4	5.9	5.9
Galveston Is (bay east)	94.884300	29.276300	12.1	12.1	10.9	10.8	10.9	8.3	8.2	6.5	5.9	6.1
Bolivar Pen (bay west)	94.776100	29.386300	9.7	9.1	8.1	8.1	8.3	6.8	6.7	6.3	5.6	5.9
Bolivar Pen (bay mid)	94.635500	29.478500	9.8	9.2	8.2	8.2	8.4	6.9	6	4.9	4.1	4.3
Bolivar Pen (bay east)	94.510000	29.524600	9.9	9.3	8.4	8.3	8.5	8.6	6.3	5.5	5.2	5.3
Galveston Is (nearshore west)	95.081400	29.106000	17.8	17.9	18.1	18.0	17.9	11.6	11.6	11.8	11.7	11.7
Galveston Is (nearshore mid)	94.947000	29.190600	20.2	20.2	20.4	20.2	20.2	13.3	13.3	13.4	13.4	13.3
Galveston (Pleasure Pier)	94.787800	29.285300	22.2	22.2	22.3	22.2	22.2	15.4	15.4	15.5	15.4	15.4
Bolivar Pen (nearshore west)	94.673700	29.423600	23.0	23.0	23.1	23.0	23.0	17.5	17.5	17.6	17.5	17.5
Bolivar Pen (nearshore mid)	94.593600	29.464600	22.2	22.3	22.4	22.3	22.3	18.0	18	18.1	17.9	17.9
Bolivar Pen (nearshore east)	94.506000	29.499400	21.5	21.6	21.7	21.6	21.6	18.2	18.3	18.5	18.3	18.3
Univ Texas Medical Branch	94.779962	29.317565	10.0	10.0	10.0	9.7	10.1	7.3	7.5	7.5	6.2	6.5

Draft